

Journal of

Tropical Biodiversity and Biotechnology

VOLUME 8 | ISSUE 2 | AUGUST 2023

PUBLISHED BY



UNIVERSITAS GADJAH MADA
FAKULTAS BIOLOGI

IN COLLABORATION WITH



KBI

KONSORSIUM BIOTEKNOLOGI
INDONESIA
INDONESIAN BIOTECHNOLOGY CONSORTIUM

Credits

Editor	Miftahul Ilmi Ardaning Nuriliani Furzani Binti Pa'ee Sri Nopitasari Liya Audinah Annisaa Widyasari Tanti Agustina
Copyeditor and Language Editor	Salwa Shabria Wafi Almaulidio Tazkia Dina Syarifah Rosana
Layout Editor	Salwa Shabria Wafi Muchamad Ulul Azmi
Cover Photo	Dika Sundari
Editorial Board	Prof. Dr. Wibowo Mangunwardoyo Prof. Dr. Budi Setiadi Daryono, M.Agr.Sc. Prof. Dr. Jonathan A. Anticamara Prof. Jean W. H. Yong, Ph.D. Dr. Farid Asif Shaheen Ts. Dr. Kamarul Rahim bin Kamarudin Assoc. Prof. Dr. Wong Wey Lim Dr. Phoon Lee Quen Sukirno, M.Sc., Ph.D. Dr. rer. nat. Andhika Puspito Nugroho Assoc. Prof. Dr. Ruqiah Ganda Putri Panjaitan Dr. Abdul Razaq Chasani Dr. Ratna Stia Dewi Assoc. Prof. Dr. Alona Cuevas Linatoc Assoc. Prof. Madya Ts. Dr. Muhammad Abdul Latiff Bin Abu Bakar Ts. Dr. Siti Fatimah Binti Sabran

Table of Contents

Short Communication

- Essential Oils of *Etilingera acanthodes* A.D. Poulsen, An Endemic Ginger from Sulawesi Island jtbb72117
Hurria Hurria, Anggra Alfian, Muhammad Fajri Ramadhan Muslim Saleh, Heder Djamaludin, Murni Mursyid, Witno Witno, Asri Subkhan Mahulette
- First Report on The Naturalized *Alocasia cucullata* (Araceae) in Java, Indonesia jtbb73456
Arifin Surya Dwipa Irsyam, Muhammad Rifqi Hariri, Asih Perwita Dewi, Rina Ratnasih Irwanto
- Nutritional Contents and Bioactive Compounds among Several Variants of *Dolichos lablab*: Fundamental Facts for Functional Food Development jtbb81339
Elly Purwanti, Feri Eko Hermanto, Wahyu Prihanta, Tutut Indria Permana, I Gusti Ngurah Agung Wirwekananda

Research Articles

- Diversity and Community Structure of Dragonflies (Odonata) in Various Types of Habitat at Lakarsantri District, Surabaya, Indonesia jtbb76690
Muhamad Azmi Dwi Susanto, Nirmala Fitria Firdhausi, Saiful Bahri
- Diversity and Distribution of *Ficus* (Moraceae) in The Karst Ecosystem of Bantimurung Bulusaraung National Park jtbb78811
Yelastri Yelastri, Sulistijorini Sulistijorini, Nina Ratna Djuita
- Butterfly Diversity from Isolated Lowland Area: An Assessment in Langsa Urban Forest, Langsa, Aceh, Indonesia jtbb74610
Herlina Putri Endah Sari, Andri Yusman Persada, Wendy Achmmad Mustaqim, Kartika Aprilia Putri, Imti Yazil Wafa
- Molecular Identification of Several Morphologically Distinct Flowerhorn Fish (Family) Using Mitochondrial *COI* Gene Marker jtbb78459
Dini Wahyu Kartika Sari, Himawan Achmad, Hafit Rahman, Harya Bimasuci
- Isolation and Characterization of Rhizospheric Bacteria Associated with Canna Plant for Production of Maltooligosaccharide Amylase jtbb78346
Rina Dwi Agustiani, Oedjijono Oedjijono, Nanik Rahmani, Nuraeni Ekorwati
- DNA Authentication of Indonesian Leafyfish *Pristolepis grooti* from Kelekar River and Ogan River in South Sumatra Based on *Cytochrome C Oxidase Subunit I (COI)* Gene jtbb74133
Mochamad Syaifudin
- In Silico* and Validation Approaches for Optimum Conditions of *Rattus norvegicus* Target Gene qPCR Primers jtbb71765
Gracia Alice Victoria Pollo, Nyoman Yudi Antara, Firman Alamsyah, Rarastoeti Pratiwi
- Differences in Swim Bladder Histology of *Anguilla bicolor bicolor* at Various Stages of Sexual Maturity jtbb74702
Nur Indah Septriani, Muhammad Ardillah Rusydan, Gizela Aulia Agustin, Nareta Defiani, Fajar Sofyantoro, Ariel Hananya, Dwi Eny Djoko Setyono

- Anti-hypercholesterolemia, Anti-atherogenic, and Anti-hypertension Effects of Red Beetroot (*Beta vulgaris* L.) in Rats Induced by High Fat and Fructose Diet jtbb75914
Alim El-Hakim, Sunarti Sunarti, Lisna Hidayati, Slamet Widiyanto
- The Synergistic Effect of Combination of Pentagamavunone-1 with Diosmin, Galangin, and Piperine in WiDr Colon Cancer Cells: *In vitro* and Target Protein Prediction jtbb80975
Muthi Ikarwati, Hajidah Musyayyadah, Yurananda Magnalia Putri, Ummi Maryam Zulfan, Febri Wulandari, Dyaningtyas Dewi Pamungkas Putri, Edy Meiyanto
- Biostratigraphy and Climate Change in the Late Miocene Age Based on Foraminifera in the Oyo Formation, Oyo River Section, Gunung Kidul, Yogyakarta jtbb81769
Adesti Audina Ulfah, Akmaluddin Akmaluddin, Didit Hadi Barianto
- Autecology of *Nepenthes* spp. in Peat Swamp and Heath Forest Pematang Gadung, West Kalimantan jtbb81351
Nofi Utari, Sulistijorini Sulistijorini, Nunik Sri Ariyanti
- Genetic Identification of Two Mudskipper Species (Oxudercidae: *Periophthalmus*) from Kulon Progo, Special Region of Yogyakarta, Indonesia jtbb78161
Diana Febriyanti, Katon Waskito Aji, Dwi Sendi Priyono, Tuty Arisuryanti
- Detection of *AtRKD4* Gene and Induction of Somatic Embryo in Transformant of *Phalaenopsis amabilis* Carrying 35S::GR::*AtRKD4* jtbb71211
Dika Sundari, Naufal Ghazi Aditya Perdana, Windi Mose, Jose Gutierrez -Marcos, Endang Semiarti
- Combining Moderate and High Resolution of Satellite Images for Characterizing Suitable Habitat for Vegetation and Wildlife jtbb77710
Sheriza Mohd Razali, Zaiton Samdin, Marryanna Lion
- In silico* Determination of Host-Viral Interaction of Apoptotic Mimicry Pathway Proteins During Hepatitis B Viral Pathogenesis jtbb72578
Prachie Sharma, Kamal Rawal, Kapila Kumar

Review Article

- Updated Species Check-list of the Indonesian Stingless Bees (Hymenoptera, Apidae, Apinae, Meliponini) jtbb77160
Manap Trianto, Tuty Arisuryanti, Hari Purwanto, Rosichon Ubaidillah

Short Communications

Essential Oils of *Etilingera acanthodes* A.D. Poulsen, An Endemic Ginger from Sulawesi Island

Hurria¹, Anggra Alfian^{2,3*}, Muhammad Fajri Ramadhan Muslim Saleh^{3,4}, Heder Djameludin⁵, Murni Mursyid¹, Witno^{3,6}, Asri Subkhan Mahulette⁷

1)Department of Pharmacy, Faculty of Health, Universitas Muhammadiyah Palopo, Kota Palopo, 91922

2)Faculty of Engineering, Agriculture and Marine, Universitas Muhammadiyah Palopo, Kota Palopo, 91922

3)Aksi Konservasi Celebica, Kota Palopo, 91926

4)Biology Department, Tadulako University, Kota Palu, 94118

5)Fisheries Product Technology, Faculty of Fisheries and Marine Sciences, Brawijaya University, Malang, 65145

6)Department of Forestry, Andi Djemma University, Palopo 91911, South Sulawesi, Indonesia, Kota Palopo, 91911

7)Department of Agrotechnology, Faculty of Agriculture, Pattimura University, Kota Ambon, 97233

* Corresponding author, email: anggra.alfian@gmail.com

Keywords:

Etilingera acanthodes

Essential oils

GC-MS

Compound

Submitted:

10 January 2022

Accepted:

13 February 2023

Published:

24 May 2023

Editor:

Furzani Binti Pa'ee

ABSTRACT

Etilingera acanthodes A.D. Poulsen is a ginger endemic to Sulawesi, and there is no research on its essential oils. The Essential oil information of *E. acanthodes* is the first reported and has a high novelty. The objective of the study is to analyze the component of *E. acanthodes* essential oils, which are endemic to Sulawesi. The essential oils obtained by hydrodistillation of the leaves, stems, flowers, and rhizomes of *E. acanthodes* A.D. Poulsen. The samples were analyzed by GC-MS method using the Agilent Technologies 7890 Gas Chromatograph with Auto Sampler. Data analysis of essential oils of GC-MS results were determined based on comparing mass spectra from the NIST 2005 v.2.0 library and Wiley 7 library 2003. The oils of *E. acanthodes* contain terpenoids, phenolic, steroids, and other compounds. Phenolic compounds (39.56%) predominate in leaves, other compounds (41.25%) on stems, diterpenes hydrocarbons (77.3%) in flowers, and other compounds (43.5%) and steroids (40.4%) on rhizomes. The five main compounds of *E. acanthodes* are Neophytadiene; (+)-De-O-Methylcentrolbine; Cholest-5-En-3-Ol,23-Ethyl-,(3. Beta.23S)-; 9,12-Octadecadienoic Acid, Phenol, 2-ethyl-. The analysis found several compounds that can be used for industry and medicine in the future.

Copyright: © 2023, J. Tropical Biodiversity Biotechnology (CC BY-SA 4.0)

Etilingera acanthodes A.D. Poulsen, a family of Zingiberaceae, is endemic ginger from Sulawesi. The species is commonly known as “Tikala” in the local community of Central Sulawesi (Kulawi Language) (Poulsen 2012; Pitopang et al. 2019). The fruit of the species is also edible and used in fish dishes and as a flavor enhancer (Pitopang et al. 2019). The distribution of *E. acanthodes* is only known in the mountains at Lore Lindu National Park, around 1000 - 2025 m. Ecology and habitat of *E. acanthodes* in primary lower montane forest, mixed several plants, tend to grow in humid areas and clustered in one population. The genus *Etilingera* is one of the aromatic medicinal plants (Ud-Daula & Basher 2019), which contains essential oils.

The genus *Etilingera* is distributed from India, Indo-China throughout Malaysia to the Pacific Islands and consists of more than 100 species (Poulsen 2012; Poulsen & Docot 2018). In Indonesia, research on essen-

tial oils in the Zingiberaceae family has mostly been carried out in the genus *Curcuma* and *Zingiber*. In contrast, the genus *Etltingera* has not been widely studied. Only *Etltingera elatior* (Torch Ginger, Kecombrang, or Patikala) essential oils have been analyzed by the GC-MS method (Wong et al. 2010). Also, this species has potential medicine-like antioxidants (Juwita et al. 2018), antibacterial properties (Chan et al. 2011), and anti-cancer (Krajarng et al. 2017).

Studies on essential oils in other *Etltingera* species from Sulawesi have not been carried out, one of which is *E. acanthodes*. In Sulawesi, Poulsen (2012) reported \pm 46 *Etltingera* species and new species (*Etltingera tjiasmantoi*) was published in 2020 (Ardiyani et al. 2020). Therefore, the Essential oil information of *E. acanthodes* is the first reported and has a high novelty. The information can also get potential chemical substances such as antimicrobials, antioxidants, and other potencies like other *Etltingera* species (Ud-Daula & Basher 2019).

Essential oils from plants are commonly used in several industries such as perfume, medicine, food enhancements, and flavors. Essential oils can also be used as aromatherapy, antiseptics, animal feed supplements, and other industrial products (Ribeiro-santos et al. 2017). Zingiberaceae is a family that produces essential oils that have benefits for human life.

The research aims to determine the content of *E. acanthodes* essential oils in leaves, stems, flowers, and rhizomes. Information on essential oils content in each part of the plant has a different composition. Apart from that, the research also observed the morphological characteristics of *E. acanthodes*.

Plant materials collected from Mt. Nokilalaki, Lore Lindu National Park, Central Sulawesi. Samples were collected along the climbing route at 1000-2025 m. Fresh samples (leaves, stems, flowers, and rhizomes) were taken to the laboratory to analyze the essential oil components using Gas Chromatography-Mass Spectrometry (GC-MS) method. Also, herbarium specimens were taken for further morphological character analysis. To a certain species, morphological observations were made using living collections in the wild and herbarium specimens (ANG_S_007) and described by Muh. Fajri Ramadhan in Herbarium Celebense. Measurements were made using a ruler and microscope.

Gas chromatography-mass spectrometry (GC-MS) analysis was conducted to obtain data on essential oils component in *E. acanthodes* using the Agilent Technologies 7890 Gas Chromatograph with Auto Sampler. The specifications for the tools used consist of columns in the form of HP Ultra; column length 30 x 0.25 (mm) I.D x 0.25 (μ m) film thickness. *E. acanthodes* oil was injected into the column using a 0.1 μ l GC-MS syringe and carried by helium gas. The column temperature is increased from 80°C (held for 0 minutes) to up to 150°C (held for 1 minute) and ends at 280°C (held for 26 minutes). The mobile phase flow rate is set at 1.2 μ /min, the injector temperature is 250°C, the pressure is 12 kPa, and the injector split ratio is set at 8:1.

Data analysis of essential oil components of GC-MS results is determined based on a comparison of mass spectra from the NIST 2005 v.2.0 library and Wiley 7 library 2003 (Wenqiang et al. 2007; Hossain et al. 2012). The GC-MS analysis result component data were analyzed with the R Stat 3.1.0 software to get the main compounds from each part. Compound grouping based on information on Pubchem NCBI.

The results of the morphological observation indicated that *E. acanthodes* has characteristics stem up to 2 m. Rhizome 1.5-2 cm diameter, 10-20 cm above ground, green-maroon. Leafly shoots up to 2 m- long, with 18-22 leaves. Lingule bilobed, 5 mm long. Lamina sessile, green

upper leaf, red lower leaf. Inflorescent arising from rhizome, up to 20 cm long, many flowers. Staminal tube 10-11 mm long, white; labellum ovate, 10-11 x 9-10 mm, pink. lateral lobes erect, covering the stamen, margin undulating; stamen 6 mm long; filament 0.5-1 x 2-2.5 mm, white; anther pink-white; style 2.5 cm long, glabrous; stigma 1.5-1.8 mm wide (Figure 1)

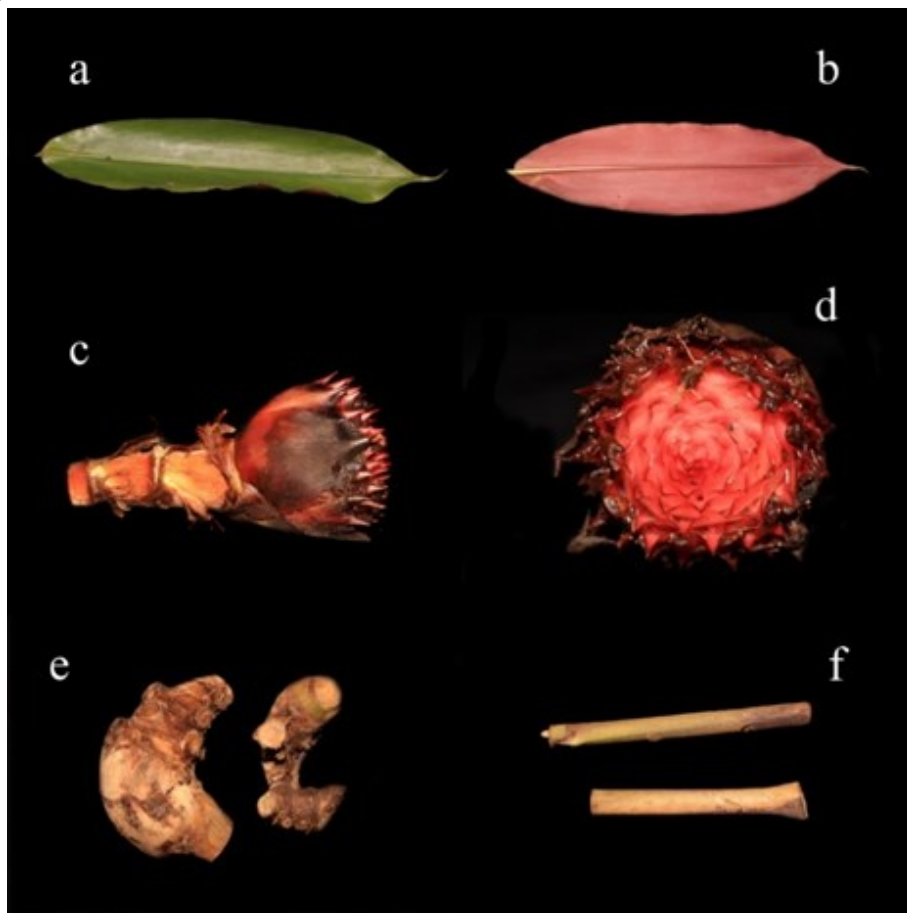


Figure 1. Morphology of *E. acanthodes*. (a) upper surface of leaf, (b) lower surface of leaf, (c) inflorescence, (d) upper view of inflorescence, (e) rhizome, (f) stem

The hydrodistilled oils through GC-MS Analysis obtained data on chemical compound, retention time (RT) and percentage of the essential oils shown in table 1. Retention times were used for preliminary information for the identification of the peak. Primary data at this retention time was used to identify the compound. The GC-MS method is powerful method to identify component of essential oils at the plant. The main compounds are Neophytadiene (10.78% - 33.73%), (+) - De -O-Methylcentrolobine (7.67% - 13.08%), Cholest-5-En-3-Ol, 23-Ethyl-, (3.Beta.23S) - (14.73% - 26.86%), 9,12-Octadecadienoic Acid (1.75% - 21.59%), and Phenol, 2-ethyl- (3.35% - 21.76%), Hexadeconoic Acid (13.03% - 17.77%), (9Z)-9-Tricosene (21.71%), 9-Tricosene (21.32%), and Z-5-Nonadecene (16.9%).

The main compounds in each part of the plant also vary. The main compound in leaves are Neophytadiene (33.73%), Phenol,2-ethyl-(21.76%), and (+)-De-O-Methylcentrolobine (12.96%). The main compounds in stem are 9,12-Octadecadienoic Acid (21.59%), Hexadeconoic Acid (17.77%), and Cholest-5-En-3-Ol, 23-Ethyl-,(3.Beta.23S)- (14.73%). The main compounds in flowers are (9Z)-9-Tricosene (21.71%), 9-Tricosene (21.32%), and Z-5-Nonadecene (16.9%). Cholest-5-En-3-Ol, 23-Ethyl-, (3.Beta.23S)- (26.86%), Hexadeconoic Acid (13.03%), and 9,12-Octadecadienoic Acid (11.34%) are the main component in rhizomes.

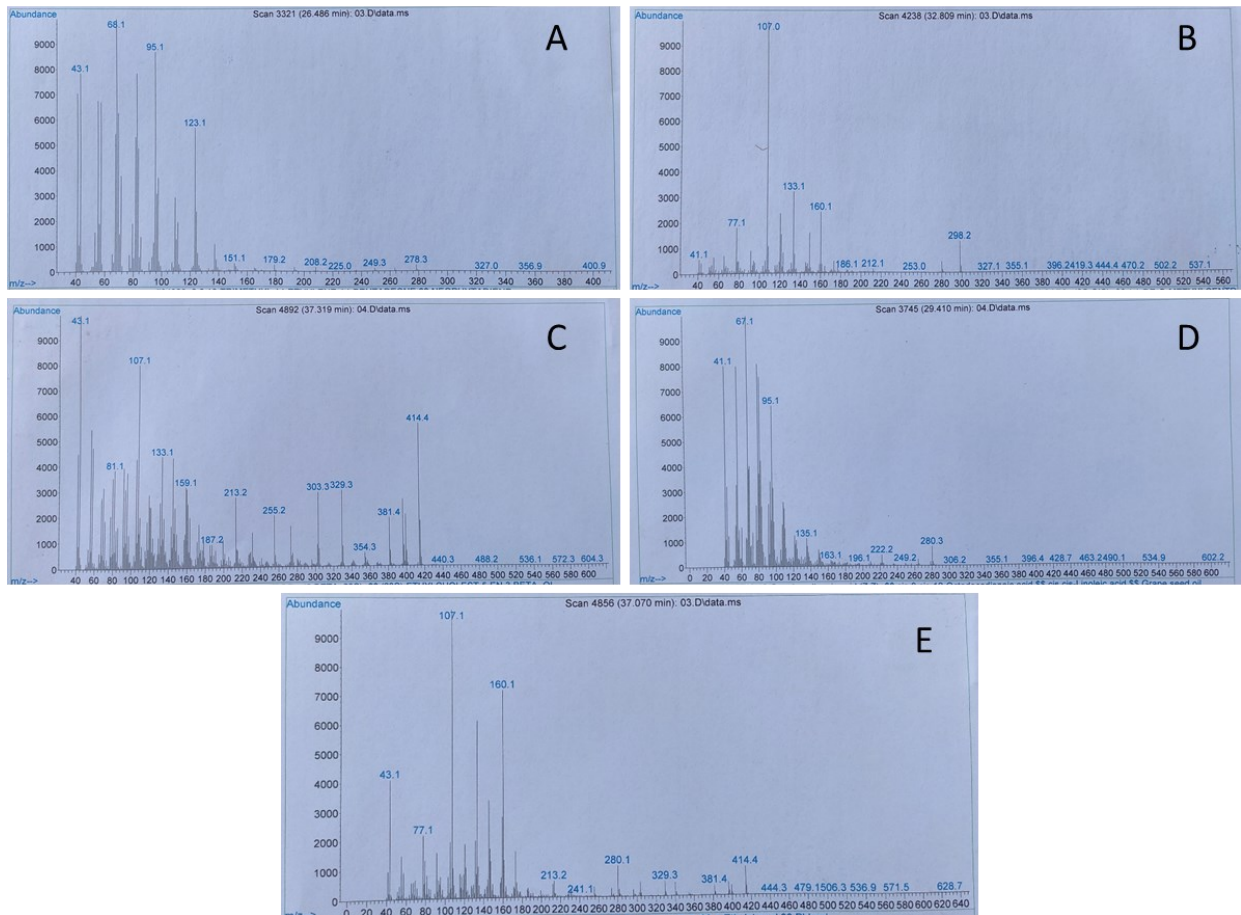


Figure 2. The chromatogram for main components of *E. acanthodes*. (A) Neophytadiene; (B) (+)-De-O-Methylcentrolobine; (C) Cholest-5-En-3-Ol,23-Ethyl-,(3. Beta.23S)-; (D) 9,12-Octadecadienoic Acid, (E) Phenol, 2-ethyl-

The compounds found are grouped into four parts: terpenoids (monoterpene, sesquiterpenes, and diterpenes), phenolic, steroids, and other compounds (Figure 2). Phenolic compounds (39.56%) predominate in leaves, other compounds (41.25%) in stems, diterpene hydrocarbons (77.3%) in flowers, and Other compounds (43.5%) and steroids (40.4%) in rhizomes. The compounds in rhizomes, stems, and leaves are grouped and tend to have similarities. It is due to the growth of stems and leaves that comes from rhizomes (Poulsen 2012). In comparison, flowers have compound characters that are very different from the others. Analysis of the essential oils in the fruit has not been carried out because no fruit was found at sampling in the field. The chemical composition is very different from the *Elingera elatior* species, with terpenoids as the predominant compound (Ud-Daulla & Basher 2019).

There are several exciting compounds to develop their potential in the future. (+)- Alpha-Tocopherol is part of vitamin E (Jilani & Iqbal 2018). *E. acanthodes* contains Gamma-Sitosterol, which has high antioxidant activity and anti-cancer potency (Ambarwati et al. 2019). (Z)-9-tricosene can be used as an effective strategy for housefly management (Kannan et al. 2020). The rhizome of *E. acanthodes* also contains Stigmasterol which has been documented as immunomodulatory with huge therapeutic potential, immune response, and proposed as candidate for anti-cancer agents (Antwi et al. 2017; Kangsamaksin et al. 2017). (Z)-9-tricosene has been used in several studies as a pheromone for house flies in domo traps (Kannan et al. 2020). Information on the essential oils of *E. acanthodes* can be used as an initial guide in developing potential in industry and medicine.

Table 1. Essential oils component of *E. acanthodes* A.D. Poulsen

Chemical Compounds	Retention Times	Percentage (%)			
		Leaves	Stems	Flowers	Rhizomes
Monoterpenes hydrocarbons					
1,2-Dimethyl-3,5-Divinylcyclohexane.	34.264	1.12	-	-	-
Sesquiterpens hydrocarbons					
Tridecene.	28.865	-	-	9.24	-
Ethyl (9Z)-9-Octadecenoate.	29.106	-	-	-	1.58
Pentadecene.	29.975	-	-	2.54	-
Diterpens hydrocarbons					
Neophytadiene.	26.486	33.73	10.78	-	-
Nonadecene.	26.893	-	-	1.78	-
Z-5-Nonadecene.	28.665	-	-	16.9	-
9-Tricosene.	29.782	-	-	21.32	-
(9Z)-9-Tricosene.	29.851	-	-	21.71	-
Pentacosane.	30.713	-	-	1.88	-
Docosene.	31.410	-	-	2.41	-
Bicyclo [10.9.0] eicosane, cis-.	31.582	-	-	9.84	-
Cyclotetracosane.	31.644	-	-	1.49	-
Octacosane.	32.271	-	-	-	1.89
Phenolic					
(+)-D-O-Methylcentrolobine.	33.120	12.96	13.08	0	7.67
(+) - Alpha-Tocopherol.	34.485	2.9	-	-	-
Phenol,2-ethyl.	37.070	21.76	0	0	3.35
(2RS,3RS)-2-T-Butyl-6-Methoxy-4-Phenylsulfonyl-1,2,3,4-Tetrahydrocyclopent[B]Indol-3-OL	36.043	1.94	0	0	0
Steroid					
Cholestan-7-one,8,14-epoxy-(5.alpha.,8.alpha.).	35.788	2.18	-	-	-
Gamma-Sitosterol.	37.450	0.27	2.23	-	-
Stigmasterol.	36.326	-	-	-	2.41
Sitosterol.	37.401	-	-	-	11.13
Cholest-5-En-3-Ol,23-Ethyl-,(3.Beta.23S)-.	37.319	-	14.73	-	26.86
Other compounds					
Hexadecanoic Acid, Ethyl Ester.	27.989	-	1.89	-	1.99
Hexadecanoic Acid.	28.382	-	17.77	-	13.03
9,12-Octadecadienoic Acid.	29.410	-	21.59	1.75	11.34
Hydroxypentadecanoic Acid.	30.865	2.64	-	-	-
p-toluenesulfony-tyrosyl-S-carboxymethylcysteine.	34.257	-	-	-	8.91
1-(1,5-Dimethylhexyl)-10A,12A-Dimethyltetradecahydro-5-H-Cyclopenta [1,2] Phenanthro [1,10A-B] Oxire-5-One.	35.402	1.64	-	-	-
N-(4-Bromophenyl)-2-(4-Chlorophenoxy) Acetamide.	35.567	-	-	-	8.27
Butane, 1,4-Bis [3-(4-Tolyl)].	36.690	11.83	-	-	-
3-Butyl-5-Methyl-1,2,3,8A-Tetrahydroindolizine.	37.416	3.33	-	-	-
Total		96.03	91.58	93.09	98.43

Several *Etlingera* species have been studied and have potential in medicine and bioactivity. *Etlingera wingensis* has the potential as antioxidant and antimicrobial activity on its rhizomes, stems, and leaves (Mahdavi et al. 2017). *Etlingera punicea* rhizome has antimicrobial activity tested on *Staphylococcus aureus*, *Pseudomonas aeruginosa*, *Salmonella Albany*, and fungus *Candida albicans* (Tadtong et al. 2014). *Etlingera brevilabrum* also has bioactivity as antioxidants and antibacterials (Mahdawi et al. 2016). *Etlingera coccinea* and *Etlingera sessilantha*, endemic to Borneo, have antimicrobial activity against *Bacillus cereus*, *Bacillus subtilis*, and

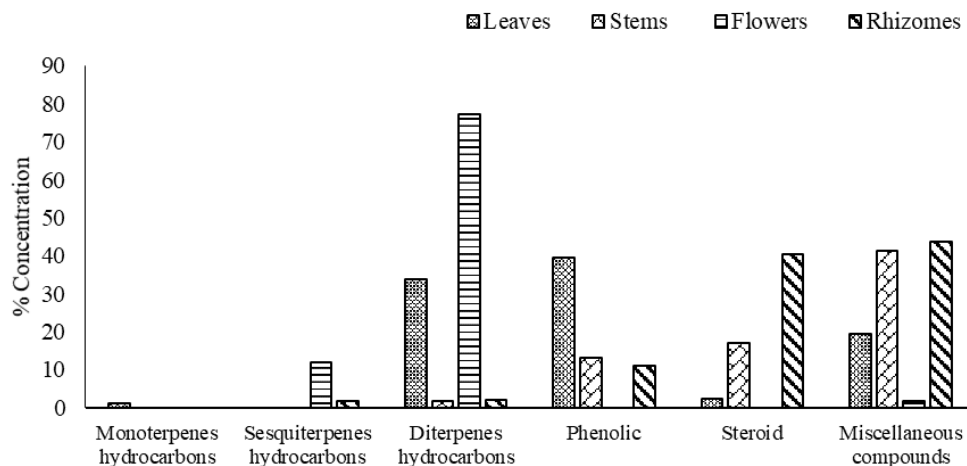


Figure 2. Chemical Composition of the Essential Oils of *E.acnthodes* A.D. Poulsen

Staphylococcus aureus (Daniel-Jambun et al. 2019). *Etlingera pavieana* has potential as an anti-inflammatory effect from rhizome extract and its phenolic compounds (Srisook et al. 2017). *Etlingera pubescens*, endemic to Borneo, can potentially be a bactericidal and cytotoxic activity of a diarylheptanoid (etlingerin) (Daniel-Jambun et al. 2019).

AUTHOR CONTRIBUTION

H., A.A., and M.M., conducted research of essential oils and wrote the manuscript. M.F.R., and W. provide sample from the forest. A.S.M., and H.D. conducted data analysis and supervised the manuscript.

ACKNOWLEDGMENTS

The research was supported by Yayasan Aksi Konservasi Celebica through collaboration funding.

CONFLICT OF INTEREST

The authors declare there is no conflict of interest.

REFERENCES

- Ambarwati, K., Jannah, M. & Adawiyah, A.R., 2019. Analisis gama – sosterol pada ficus carica sebagai prediksi aktivitas apoptosis pada sel hela. *Jurnal Bidang Ilmu Kesehatan*, 9(2), pp.191–195.
- Antwi, A. O. et al., 2017. Stigmasterol inhibits lipopolysaccharide-induced innate immune responses in murine models. *International Immunopharmacology*, 53, pp.105–113. doi: 10.1016/j.intimp.2017.10.018
- Ardiyani, M. et al., 2020. *Etlingera tjiasmantoi* (zingiberaceae), a new species from central Central Sulawesi. *Reinwardtia*, 19(2), pp.103–108. doi: 10.14203/reinwardtia.v19i2.3972
- Chan, E.W. et al., 2011. Antioxidant and antibacterial properties of *Alpinia galanga*, *Curcuma longa*, and *Etlingera elatior* (Zingiberaceae). *Pharmacognosy Journal*, 3(22), pp.54–61. doi: 10.5530/pj.2011.22.11
- Daniel-Jambun, D. et al., 2019. Bactericidal and cytotoxic activity of a diarylheptanoid (etlingerin) isolated from a ginger (*Etlingera pubescens*) endemic to Borneo. *Journal of Applied Microbiology*, 127, pp.59–67. doi: 10.1111/jam.14287
- Hossain, M. A. et al., 2012. Constituents of the essential oil from different brands of *Syzygium caryophyllatum* L. by gas chromatography-mass spectrometry. *Asian Pacific Journal of Tropical Biomedicine*, pp.1446–1449. doi: 10.1016/S2221-1691(12)60435-3

- Jilani, T. & Iqbal, M.P., 2018. Vitamin E deficiency in South Asian population and the therapeutic use of alpha-tocopherol (Vitamin E) for correction of anemia. *Pak J Med Sci.*, 34(6), pp.1571–1575.
- Juwita, T., Puspitasari, I. M. & Levita, J., 2018. Torch ginger (*Etlingera elatior*): a review on its botanical aspects, phytoconstituents and pharmacological activities. *Pakistan Journal of Biological Sciences*, 21 (4), pp.151–165. doi: 10.3923/pjbs.2018.151.165
- Kangsamaksin, T. et al., 2017. Lupeol and stigmasterol suppress tumor angiogenesis and inhibit cholangiocarcinoma growth in mice via downregulation of tumor necrosis factor- α . *Plos One*, 12(12), e0189628.
- Kannan, S., Makam, L. & Kolarath, R., 2020. Evaluation of (Z)-9-tricosene pheromone and food bait for house flies, *Musca domestica* L. (*Diptera: Muscidae*) attraction using Domo trap. *Journal of Entomology and Zoology Studies*, 8(5), pp.1071–1074.
- Krajarng, A., Chulasiri, M. & Watanapokasin, R., 2017. *Etlingera elatior* extract promotes cell death in B16 melanoma cells via downregulation of ERK and Akt signaling pathways. *BMC complementary and alternative medicine*, 17(1), 415. doi: 10.1186/s12906-017-1921-y
- Mahdavi, B., Yaacob, W.A. & Din, L.B., 2017. Chemical composition, antioxidant, and antibacterial activity of essential oils from *Etlingera sayapensis* A.D. Poulsen & Ibrahim Behnam. *Asian Pacific Journal of Tropical Medicine*, 10, pp.819–826. doi: 10.1016/j.apjtm.2017.08.006
- Mahdawi, B. et al., 2016. Chemical composition, antioxidant, and antibacterial activities of essential oils from *Etlingera brevilabrum* Valetton. *Record of Natural Product*, 10, pp.22–31.
- Pitopang, R. et al., 2019. Diversity of Zingiberaceae and traditional uses by three indigenous groups at Lore Lindu National Park, Central Sulawesi, Indonesia. *IOP Conf. Series: Journal of Physics: Conf. Series*, 1242, 012039. doi: 10.1088/1742-6596/1242/1/012039
- Poulsen, A., 2012. *Etlingera of Sulawesi*. Natural History Publications (Borneo), Kota Kinabalu.
- Poulsen, A.D. & Docot, R.V.A., 2018. How many species of etlingera (zingiberaceae) are there in the Philippines? *Edinburgh Journal of Botany*, 76(1), 33–44. doi: 10.1017/S0960428618000240
- Ribeiro-santos, R. et al., 2017. Essential oils for food application: natural substances with established biological activities. *Food Bioprocess Technol*, 11, pp.43–71. doi: 10.1007/s11947-017-1948-6
- Srisook, E. et al., 2017. Anti-inflammatory effect of *Etlingera pavieana* (Pierre ex Gagnep.) R.M.Sm. rhizomal extract and its phenolic compounds in lipopolysaccharide-stimulated macrophages. *Phcog Mag*, 13, pp.230–235. doi: 10.4103/pm.pm
- Tadtong, S. et al., 2014. Antimicrobial activities of essential oil from *Etlingera punicea* rhizome. *J Health Res.*, 23(2), pp.77–79.
- Ud-Daula, A.F.M.S. & Basher, M.A., 2019. Genus *Etlingera* - A review on chemical composition and antimicrobial activity of essential oils. *Journal of Medicinal Plants Research*, 13(7), pp.135–156. doi: 10.5897/JMPR2019.6740
- Wenqiang, G. et al., 2007. Comparison of essential oils of clove buds extracted with supercritical carbon dioxide and other three traditional extraction methods. *Food Chemistry*, 101, pp.1558–1564. doi: 10.1016/j.foodchem.2006.04.009
- Wong, K.C. et al., 2010. Essential oils of *Etlingera elatior* (Jack) R. M. Smith and *Etlingera littoralis* (Koenig) Giseke. *Journal of Essential Oil Research*, 22(5), pp.461–466. doi: 10.1080/10412905.2010.9700372

Short Communications

First Report on The Naturalized *Alocasia cucullata* (Araceae) in Java, Indonesia

Arifin Surya Dwipa Irsyam^{1,2*}, Muhammad Rifqi Hariri³, Asih Perwita Dewi⁴, Rina Ratnasih Irwanto⁵

1)Herbarium Bandungense (FIPIA), School of Life Sciences and Technology (SITH), Institut Teknologi Bandung (ITB), Labtek VC Building, Jl. Let. Jen. Purn. Dr (HC) Mashudi No. 1 Jatinangor, West Java, 45363, Indonesia.

2)Yayasan Botani Tropika Indonesia (Botanika), Jl. Seruni No. 25, Loji, Bogor, West Java, 16117, Indonesia.

3)Research Center for Plant Conservation and Botanic Gardens, National Research and Innovation Agency (BRIN), Jl. Ir. H. Juanda No. 13 Bogor, West Java, 16003, Indonesia.

4)Research Centre for Biology, National Research and Innovation Agency (BRIN), Jl. Raya Jakarta-Bogor Km. 46, Cibinong, West Java, 16911, Indonesia.

5)School of Life Sciences and Technology (SITH), Institut Teknologi Bandung Labtek XI Building, Jl. Ganesha No. 10 Bandung, West Java, 40132, Indonesia.

* Corresponding author, email: arifin@itb.ac.id

Keywords:

Alien

Alocasia

Araceae

Introduced

Java

Submitted:

08 March 2022

Accepted:

25 January 2023

Published:

14 June 2023

Editor:

Ardaning Nuriliani

ABSTRACT

The presence of naturalized *Alocasia cucullata* (Lour.) G.Don (Araceae) in Java is reported for the first time in this paper. The species is an introduced ornamental plant native to India, Sri Lanka, and Indo-China and was only known in cultivation. In this study we collected samples from its naturalized populations in Sukabumi Regency (Cibadak Subdistrict) and Sumedang Regency (Jatinangor and Tanjungsari Subdistricts). The observed population grows along the roadside, coastal, ITB Jatinangor green space area, and palm oil plantation. In nature, *A. cucullata* may spread vegetatively either through root suckers, corms, and stem fragments. The description, distribution map, photographs, and a brief discussion are provided here.

Copyright: © 2023, J. Tropical Biodiversity Biotechnology (CC BY-SA 4.0)

The horticultural trade route of ornamental plants has led to the global spread of foreign species. This trade route has spread invasive species to various parts of the world (Pyšek et al. 2017; Chowdhuri & Deka 2019; Arianoutsou et al. 2021). Recently, the international market for decorative plants has seen a surge in demand, particularly in urban areas. (Necha & Bautista-Baños 2016; Olewnicki et al. 2019; Darras 2020). Therefore, urban areas often become a starting point for the spreading of alien plants species (Mayer et al. 2017). According to Setyawati et al. (2015), about 2000 species of alien plants were recorded in Indonesia, and more than half are alien-cultivated plants, including ornamental species. Many have been naturalized or escaped from cultivation areas and become established in natural or semi-natural habitats (Tjitrosoedirdjo 2005; Tjitrosoedirdjo 2007). This number may increase in the future, considering that the ornamental plant trade is still occurring.

Araceae or arum family is one of the popular groups of flowering plants for cultivation. This family is widely distributed globally, especially in tropical America, mainland Southeast Asia, and Malesia (Boyce 2015; Wilkin & Haigh 2015; Christenhusz et al. 2017). Araceae consists

of around 4000 species grouped into 115 genera, of which 1105 native species occur in Malesia (Boyce & Wong 2012; Wilkin & Haigh 2015). Nine genera of exotic genera were introduced to Malesia, and six genera, such as *Caladium* Vent., *Dieffenbachia* Schott, *Epipremnum* Schott, *Pistia* L., *Syngonium* Shott, and *Xanthosoma* Schott, have become naturalized in the region (Chong et al. 2010; Boyce & Wong 2012; Witt 2017).

A further of the occurrence records of naturalized alien aroids in Indonesia has been published by Mustaqim & Nisyawati (2016) and Irsyam et al. (2021). During a botanical exploration of West Java from 2020 to 2021, we collected a naturalized alien aroid identified as *A. cucullata* (Lour.) G.Don which has not been previously reported in Java. Therefore, our study represents the first record for naturalized alien flora of Java. The description, photograph, and discussion are given below.

Alocasia cucullata (Lour.) G.Don in R.Sweet, Hort. Brit., ed. 3: 631. 1839; Hook.f., Fl. Brit.

India 6: 525. 1893; Boyce, Thai. For. Bull. 36: 7. 2008. – *Arum cucullatum* Lour., Fl. Cochinch 2: 536. 1790. – *Caladium cucullatum* (Lour.) Pers., Syn. Pl. 2: 575. 1807. – *Colocasia cucullata* (Lour.) Schott in H.W.Schott & S.L.Endlicher, Melet. Bot.: 18. 1832. – *Caladium rugosum* Desf., Tabl. École Bot., ed. 3: 386. 1829. – *Colocasia rugosa* Kunth, Enum. Pl. 3: 41. 1841. – *Caladium colocasia* Schott ex Wight, Icon. Pl. Ind. Orient. 3: t. 787. 1844. – *Colocasia cochleata* Miq., Index Seminum (AMD) 1853. 1853. – *Alocasia rugosa* Schott, Oesterr. Bot. Wochenbl. 4: 410. 1854. – *Panzhuyuia omeiensis* Z.Y.Zhu, J. Sichuan Chinese Med. School 4(5): 50. 1985. Figure 1–3

Description. Robust, evergreen herb, up to 65 cm tall. Stems erect, basally branched, with leaf scars. Leaves simple; petiole 23.5–35 cm long, weak, spongy, glabrous, green; petiolar sheath reaching up to ½ way, margin membranous; lamina broadly ovate to cordate, 11.5–25 × 6.5–14.5 cm, base cordate, margin entire, apex acuminate, veins 5–8 pairs, adaxial surface yellowish green to dark green, shiny, glabrous, abaxial surface pale green to yellowish-green, glabrous. Inflorescence solitary, subtended by membranous cataphylls; flowers unisexual; peduncle 12.5–19 cm long, glabrous, yellowish-green to green. Spathe 9 cm long; lower spathe enclosing the spadix, forming a tube with convolute margins, 3.5–6 cm long, glabrous, green; upper spathe boat-shaped, 6.5 cm long, apex mucronate, waxy-glaucous; spadix c. 9.5 cm long; female flower zone cylindrical, basal, c. 1–2 cm long; sterile interstice zone c. 2 cm long, staminodia rhomboidal, c. 3 cm long yellowish-green; male flower zone c. 4–5 cm long, yellow; appendix conical c. 2–3.5 mm long, yellowish-white; male flowers: perianths absent; stamen connate into a synandrium; synandria flat-topped, irregularly rhomboidal, 1–5 mm wide, green; female flowers: perianths absent; ovary 1, styles very short, stigma capitate, white. Fruit not seen.

Distribution. *Alocasia cucullata* is distributed from North East, India (Sikkim) to Taiwan and it is distributed south to Sri Lanka (Boyce 2008). *Alocasia cucullata* is introduced to other tropical countries as an ornamental plant (Hay 1998; Miyake & Yasufo 2005; Boyce 2008; Nauheimer et al. 2012).

Habitat. In this study, the wild populations of *A. cucullata* were found in disturbed areas, watersides, palm oil plantations, and roadsides at 522–885 m a.s.l.

Specimen examined. INDONESIA. JAVA – West Java • Sukabumi Regency, Cibadak Subdistrict, Neglasari, Pasir Randu Palm Oil Plantation, 6°54'51.029"S 106°44'31.3800"E, 10.IV.2021, ASD Irsyam Psrrnd 02

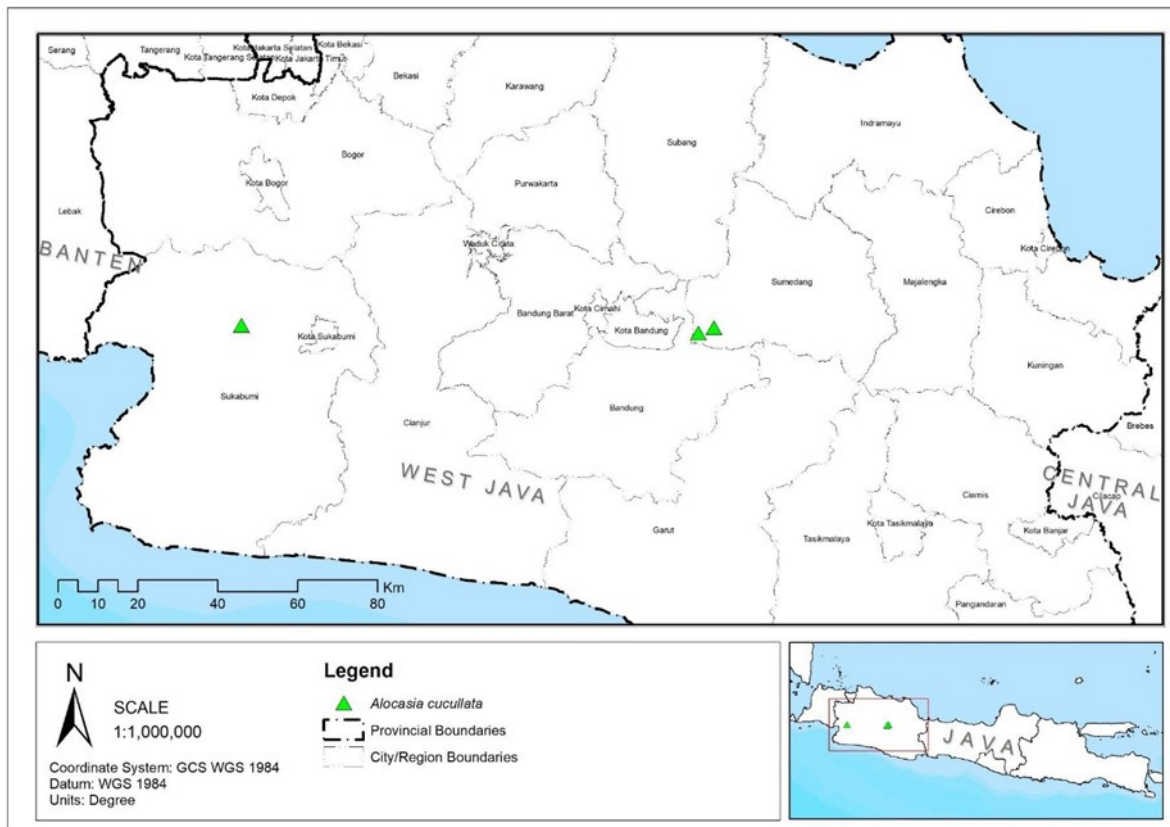


Figure 1. Distribution map of the naturalized *A. cucullata* in Java.

(FIPIA); Sumedang Regency, Jatinangor Subdistrict, ITB Campus, green space area around the lecturer dormitory building, $6^{\circ}55'54.7''\text{S}$ $107^{\circ}46'14.3''\text{E}$, 21.II.2022, *ASD Irsyam 683* (FIPIA); Sumedang Regency, Tanjungsari Subdistrict, Cinanjung, Komplek PPI, $6^{\circ}55'10.9''\text{S}$ $107^{\circ}48'20.7''\text{E}$, 22.II.2022, *ASD Irsyam 684* (FIPIA).

Vernacular names. *Nampu hijau* (Javanese) (Muhyi et al. 2020).

Uses. *Alocasia cucullata* is an ornamental plant that can be used for medicine (Asih et al. 2014). It is used externally as medicine to treat snake bites, abscesses, rheumatism, and arthritis by Chinese people (Boyce 2008). Moreover, Arora (2014) reported that the corm was edible and cooked as a vegetable. In Java, the species has only been cultivated for its ornamental purposes.

Alocasia (Schott) G.Don is a member of Araceae naturally distributed in tropical Asia, Australasia, Malesia, and Melanesia (Mayo et al. 1997). About 57 indigenous species of *Alocasia* occur in Malesia, of which 31 species were found in West Malesia (Hay 1998). In addition, one exotic species, *A. cucullata*, has been widely cultivated and naturalized throughout the tropics, including Malesia (Mayo et al. 1997; Hay 1998; Nauheimer et al. 2012; Truyen et al. 2015). The species is quite commonly grown as an outdoor plant in Java due to its showy leaves.

However, there is no information about naturalized *A. cucullata* on the Java Island. The previous data was obtained only from its cultivation (Nisyawati & Mustaqim 2017; Mustaqim 2019).

In this study, we reported the naturalized *A. cucullata* from Java for the first time. Although *A. cucullata* was previously only known from the western part of Java, it is probable that the species has already spread to other provinces. *Alocasia cucullata* has grown in several locations in West Java Province (Figure 1). It grows in a palm oil plantation and along a waterside at the observation site in Pasir Randu, Cibadak, Suka-

bumi Regency. For this research, the samples were collected from naturalized of *A. cucullata* at two locations in Sumedang Regency, at a green space area around the dormitory building of ITB Jatinangor and on a roadside in Regency Complex PPI Cinanjung-Tanjungsari (Figure 3). *Alocasia cucullata* has become locally abundant in shaded and humid conditions. Previous research revealed that exotic ornamental plants usually had overcome the barrier of introduction by establishing their wild population in green open space areas, arboreta, botanical gardens, and private gardens (Mayer et al. 2017). In 2020, *A. cucullata* was reported in the forest edge of Bantarbolang Nature Reserve, Pemalang, Central Java (Muhyi et al. 2020). However, Muhyi et al. (2020) did not mention whether it was cultivated or naturalized. According to Widodo (personal communication, February 21, 2021), the population of *A. cucullata* from Pemalang, Central Java Province, may result from naturalization.

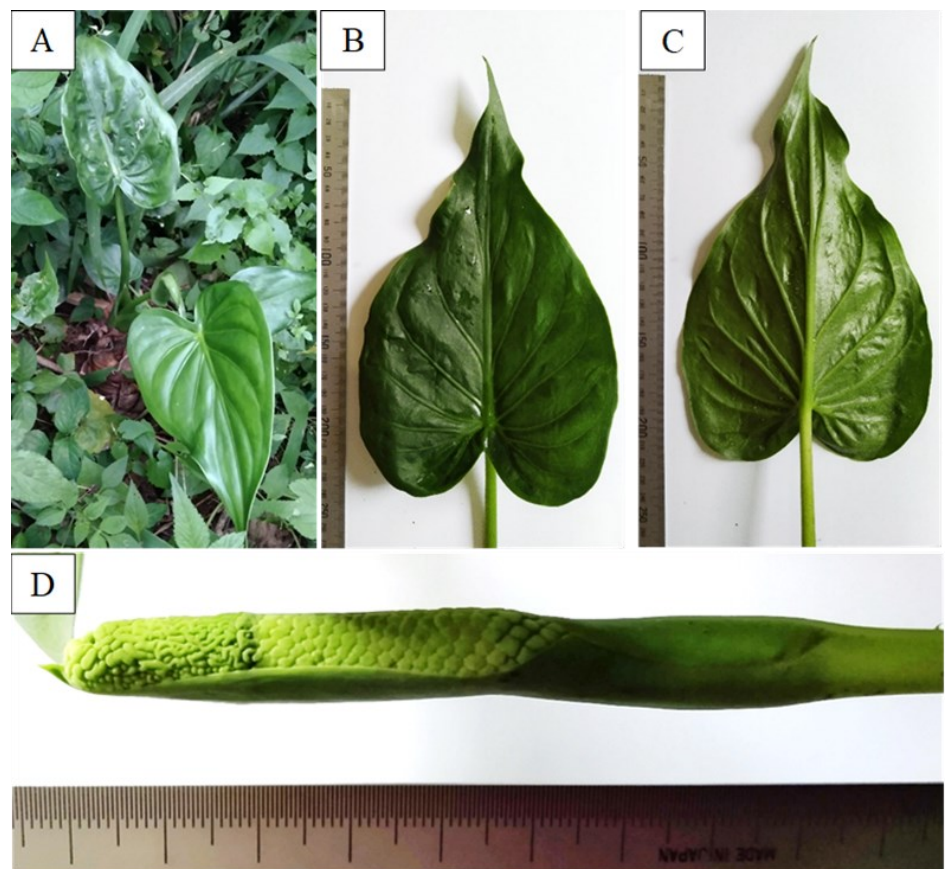


Figure 2. Morphological characters of *A. cucullata*. (A) habit; (B) adaxial leaf surface; (C) abaxial leaf surface; (D) inflorescence.

The history of the first introduction of *A. cucullata* in Java has not been widely known, both in literature and herbarium data. This species is not recorded in the Flora of Java vol. III (Backer & Bahkuizen van den Brink 1968; Mustaqim 2019). Examination of specimens at Herbarium Bogoriense (BO) and Herbarium Bandungense (FIPIA) also showed no *A. cucullata* specimens collected from cultivated or wild populations. The specimen deposited in Herbarium Bogoriense were collected from Chiang Mai Province, Muang Fang, Thailand (BO-1339506) (Figure 4). It is estimated that *A. cucullata* entered Java in the 1970s after the Flora of Java series publication was completed.

During field observations, *A. cucullata* found in Pasir Randu and Cinanjung did not have any inflorescences. *Alocasia cucullata* with inflorescences were observed from one individual at the ITB Jatinangor Campus (Figure 2). Previous researchers also reported that *A. cucullata* rarely

produces inflorescences in the wild (Boyce 2008; Rojas-Sandoval 2019). *Alocasia cucullata* mainly propagates vegetatively through root suckers, rhizomes, and corm fragments (Rojas-Sandoval 2019). According to Boyce (2008) and Fang et al. (2020), the distribution of *A. cucullata* is associated with human disturbance. The naturalized *A. cucullata* in Jatinangor and Cinanjung turned from waste from pruning gardens or other public green spaces. The waste originating from ornamental aroids in the form of vegetative fragments such as tubers, stems, or rhizomes, corms without specific treatment can grow into new individuals near their disposal sites. Other naturalized aroid species such as *Monstera deliciosa* Liebm., *Philodendron hederaceum* (Jacq.) Schott, *Syngonium podophyllum* Schott, and *Xanthosoma sagittifolium* (L.) Schott may spread with a similar mechanism (Martin 2002; Chong et al. 2010; Bhattacharyya 2021; Irsyam et al. 2021).



Figure 3. The wild population of *A. cucullata* in (A) Pasir Randu palm oil plantation, Cibadak, Sukabumi Regency; (B) ITB Campus, Jatinangor, Sumedang Regency; (C) Komp. PPI Cinanjung, Tanjungsari, Sumedang Regency.

The presence of naturalized *A. cucullata* in the wild needs to be closely monitored because it can be invasive and disturb native species. Previous research has shown the species to be invasive in Cuba, Costa Rica, Hawaii, Fiji, the Cook Islands, Micronesia, Palau, and French Polynesia. (Space et al. 2009; Rojas-Sandoval 2019). *Alocasia cucullata* also escape from the Lesser Antilles cultivation area and then became naturalized in St. Lucia (Graveson 2012; Joseph & Abati 2016).



Figure 4. Specimen *A. cucullata* deposited in Herbarium Bogoriense (BO) (Doc. By Asih Perwita Dewi, 2022)

AUTHORS CONTRIBUTION

ASDI and MRH designed the research. ASDI, APD, and MRH collected the plant materials, observed the specimen, and analyzed the data. ASDI, MRH, APD, RRI wrote the original draft and agreed to the final manuscript.

ACKNOWLEDGMENTS

The authors would like to thank the Head of Herbarium Bogoriense, National Research and Innovation Agency (BRIN), for allowing us all to examine the specimens. We also would like to thank Mrs Lia Nuralia, S.S., M.Hum., and the Gutta Percha Research 2021 (BRIN) team for welcoming us to inspect the field in the Sukabumi Regency; Dr Pudji Widodo, M.Sc., for the discussion on the *A. cucullata* in Bantarbolang Nature Reserve, Pemalang, Central Java.

CONFLICT OF INTEREST

The authors declare no competing interests regarding the research or the research funding.

REFERENCES

- Arianoutsou, M. et al., 2021. Alien plants of Europe: introduction pathways, gateways and time trends. *PeerJ*, 9, e11270. doi: 10.7717/peerj.11270.
- Arora, R.K., 2014. *Diversity in Underutilized Plant Species – An Asia-Pacific Perspective*. New Delhi, India: Biodiversity International.
- Asih, N.P.S. et al., 2014. Araceae Berpotensi Obat di Kebun Raya “Eka Karya” Bali. *Prosiding Semnas Biodiversitas*, 3(1), pp.84–87.
- Backer, C.A. & Bakhuizen van den Brink, R.C., 1968. *Flora of Java. Vol. III*, Groningen, The Netherlands: N.V.P. Noordhoff.
- Bhattacharyya, K., 2021. Invasion alert for the alien plant *Xanthosoma sagittifolium* (L.) Schott (Araceae) in the East Bardhaman District of West Bengal, India. *International Journal of Current Research*, 13(6), pp.17698–17701.
- Boyce, P.C., 2008. A review of *Alocasia* (Araceae: Colocasieae) for Thailand, including a novel species and new species records from South-West Thailand. *Thai Forest Bulletin (Botany)*, 36, pp.1–17.
- Boyce, P.C., 2015. Why is ‘Flora Malesiana’ Araceae not currently a practicable undertaking - *Fenestratarum* as an example. *Aroideana*, 38E (1), pp.75–83.
- Boyce, P.C. & Wong, S.Y., 2012. The Araceae of Malesia I: Introduction. *Malayan Nature Journal*, 64(1), pp.33–67.
- Chong, K.Y. et al., 2010. Identity and spread of an exotic *Syngonium* species in Singapore. *Nature in Singapore*, 3, pp.1–5.
- Chowdhuri, T.K. & Deka, K., 2019. Biodiversity and Conservation of Ornamental Crops. In Conservation and utilization of Horticultural Genetic Resources. Singapore: *Springer Nature Singapore*, pp.139–216. doi: 10.1007/978-981-13-3669-0_6.
- Christenhusz, M.J.M. et al., 2017. *Plants of The World: An Illustrated Encyclopedia of Vascular Plants*, Chicago: The University of Chicago Press.
- Darras, A.I., 2020. Implementation of Sustainable Practices to Ornamental Plant Cultivation Worldwide: A Critical Review. *Agronomy*, 10, 1570. doi: 10.3390/agronomy10101570.
- Graveson, R., 2012. *Survey of Ornamental Plants in Resorts and Hotels Saint Lucia, 2012*, Union: Forestry Department.
- Fang, Q. et al., 2020. *Alocasia lihengiae*, a new species of Araceae from Southern Yunnan. *Phytotaxa*, 436(2), pp.97–103. doi: 10.11646/phytotaxa.436.2.1.
- Hay, A., 1998. The genus *Alocasia* (Araceae-Colocasieae) in West Malesia and Sulawesi. *The Gardens' Bulletin Singapore*, 50(2), pp.221–334.
- Irsyam, A.S.D. et al., 2021. Laporan Pertama *Philodendron hederaceum* (Jacq.) Schott ternaturalisasi di Sumatra, Indonesia. *Biologica Samudra*, 3(1), pp.43–53.
- Joseph, P. & Abati, Y., 2016. The flower plants introduced in the Lesser Antilles: Martinique’s example (general summary of the key data and ecosystem impacts). *IOSR Journal of Environmental Science, Toxicology and Food Technology*, 10(8), pp.88–108.
- Martin, T.J., 2002. A Mexican migrant the naturalisation of *Monstera deliciosa* (fruit salad plant) in New Zealand. *Auckland Botanical Society*, 57, pp.151–154.
- Mayer, K. et al., 2017. Naturalization of ornamental plant species in public green spaces and private gardens. *Biological Invasions*, 19, pp. 3613–3627. doi: 10.1007/s10530-017-1594-y.

- Mayo, S.J. et al., 1997. *The Genera of Araceae*, Kew: Royal Botanic Gardens.
- Miyake, T. & Yosufu, M., 2005. Pollination of *Alocasia cucullata* (Araceae) by two *Colocasiomyia* flies known to be specific pollinators for *Alocasia odora*. *Plant Species Biology*, 20, pp.201–208.
- Muhyi, M.D. et al., 2020. Diversity and Evenness of Medicinal Plants in Bantarbolang Nature Reserve Block 19-21, Pemalang, Central Java. *BioEksakta: Jurnal Ilmiah Biologi Unsoed*, 2(1), pp.33–41.
- Mustaqim, W.A. & Nisyawati, 2016. Records of adventive *Syngonium wendlandii* (Araceae) from Universitas Indonesia, Depok, West Java. *Aroideana*, 39(3), pp.23–26.
- Mustaqim, W.A., 2019. Aroids in and around urbanized lowland ecosystem of Jakarta and Bogor, Western Java, Indonesia. *Aroideana*, 42(2), pp.23–36.
- Nauheimer, L. et al., 2012. Giant taro and its relatives: A phylogeny of the large genus *Alocasia* (Araceae) sheds light on Miocene floristic exchange in the Malesian region. *Molecular Phylogenetics and Evolution*, 63(1), pp.43–51. doi: 10.1016/j.ympev.2011.12.011.
- Necha, L.L.B. & Bautista-Baños, S., 2016. Prospects for the Use of Chitosan and Other Alternatives in Ornamental Conservation. In *Chitosan in the Preservation of Agricultural Commodities*. Cambridge: Academic Press, pp.221–249. doi: 10.1016/B978-0-12-802735-6.00008-2.
- Nisyawati & Mustaqim, W.A., 2017. *A Guide to The Urban Plants of Universitas Indonesia: Spermatophyte*, Depok: UI Press.
- Olewnicki, D. et al., 2019. The demand for ornamental plants in Poland after its integration into the EU: a quantitative approach. *Bulgarian Journal of Agricultural Science*, 25(5), pp.932–943.
- Pyšek, P. et al., 2017. Naturalized alien flora of the world: Species diversity, taxonomic and phylogenetic patterns, geographic distribution and global hotspots of plant invasion. *Preslia*, 89(3), pp.203–274. doi: 10.23855/preslia.2017.203.
- Rojas-Sandoval, J., 2019. *Alocasia cucullata* (Chinese taro). Invasive Species Compendium. Wallingford, UK: CABI. doi: 10.1079/ISC.37019438.20203482787.
- Setyawati, T. et al., 2015. *A Guide Book to Invasive Alien Plant Species in Indonesia*, Bogor: Research, Development and Innovation Agency, Ministry of Environment and Forestry.
- Space, J.C. et al., 2009. *Report to the Republic of Palau: 2008 update on Invasive Plant Species*. Hawai'i, USA: Institute of Pacific Islands Forestry.
- Tjitrosoedirdjo, S.S., 2005. Inventory of the invasive alien plant species in Indonesia. *Biotropia*, 25, pp.60–73. doi: 10.11598/btb.2005.0.25.209.
- Tjitrosoedirdjo, S.S., 2007. Notes on the profile of Indonesian invasive alien plant species. *Biotropia*, 14(1), pp.62–68. doi: 10.11598/btb.2007.14.1.25.
- Truyen, D. M. et al., 2015. A note on Aroids Ethnobotany in Hau River, Vietnam. *Tropical Plant Research*, 2(1), pp.58–63.
- Wilkin, P. & Haigh, A., 2015. Araceae. In *The Kew tropical plant families identification handbook Second Edition*. Kew: Kew Publishing, pp.28–29.
- Witt, A., 2017. *Guide to the naturalized and invasive plants of Southeast Asia*, Oxfordshire: CABI.

Short Communications

Nutritional Contents and Bioactive Compounds among Several Variants of *Dolichos lablab*: Fundamental Facts for Functional Food Development

Elly Purwanti^{1*}, Feri Eko Hermanto^{2,3}, Wahyu Prihanta¹, Tutut Indria Permana¹, I Gusti Ngurah Agung Wiwekananda⁴

1)Department of Educational Biology, Faculty of Teacher Training and Education, University of Muhammadiyah Malang, Malang 65144, East Java, Indonesia

2)Faculty of Animal Sciences, Universitas Brawijaya, Malang 65145, East Java, Indonesia

3)Bioinformatics Research Center, Indonesian Institute of Bioinformatics (INBIO Indonesia), Malang 65162, East Java, Indonesia

4) Department of Biology, Faculty of Mathematics and Natural Sciences, Universitas Brawijaya, Malang 65145, East Java, Indonesia

* Corresponding author, email: purwantielly@gmail.com

Keywords:

Antioxidant
Dolichos lablab
functional food
nutritional value
secondary metabolites

Submitted:

15 January 2023

Accepted:

29 March 2023

Published:

03 July 2023

Editor:

Miftahul Ilmi

ABSTRACT

To date, the data describing various nutritional and secondary metabolites content of Lablab beans is incomplete. Therefore, this study evaluated the nutritional value, secondary metabolites, and antioxidant activity of three different variants of Lablab beans, i.e., brown, black, and cream beans. The results showed that the brown Lablab beans had outperformed other variants according to their nutritional value and flavonoid content with outstanding DPPH scavenging activity. However, the black beans also showed good bioactive contents through their total phenolic percentage with decent reducing activity via the FRAP assay. Those who are keen in developing functional food from Lablab beans should consider this data as a reference.

Copyright: © 2023, J. Tropical Biodiversity Biotechnology (CC BY-SA 4.0)

Legumes have provided nutritional value for years, contributing to the development of agriculture and food security (Considine et al. 2017). Not only are they a staple food in several regions of the globe, but legumes also provide valuable nutritional and health benefits (Polak et al. 2015; Piergiovanni 2021). The consumption of legumes has been reported to have protective roles against modern society's health problems, such as diabetes mellitus, hyperlipidemia, and cardiovascular diseases (Polak et al. 2015; Hermanto et al. 2022a; Hermanto et al. 2022b). Furthermore, the bioactive compounds in legumes also provide numerous biological activities to achieve physiological homeostasis (Çakir et al. 2019). Those facts are more than enough to describe the vital role of legumes in developing social health status. There are many species of legumes worldwide, but not all beans are known in the society. One of the underutilized legumes is Lablab beans (*Dolichos lablab*), also known as Koro Komak in Indonesia (Purwanti et al. 2019b). Natively grown in the African continent and Indian subcontinent, Lablab beans have become the primary source of energy due to their rich fibre and carbohydrate contents (Maass et al. 2010; Purwanti et al. 2019a). Moreover, Lablab beans also have superior

environmental adaptation due to their ability to grow in drought areas (Missanga et al. 2021). Their innate nature may benefit the maintenance of food security, particularly in lands with low water supply. Thus, the cultivation of Lablab beans provides a promising means in maintaining primary food stock in dry areas.

Three primary accessions or variants of Lablab beans have been identified in Indonesia (Purwanti et al. 2019b). Those accessions are commonly identified based on the beans' colour, i.e., brown, black, and cream (figure 1). Although other variants may exist, these three are commonly found in several regions in Indonesia, such as East Java (Probolinggo and Madura Island) and West Nusa Tenggara (Purwanti et al. 2019b). The previous study reported the bioactivity of bioactive compounds and nutritional values of Lablab beans (Purwanti et al. 2021; Purwanti et al. 2022). Nevertheless, no report addresses the nutritional differences among the variants of Lablab beans. Lablab beans have numerous bioactivities including antioxidant (Maheshu et al. 2013), antidiabetic (Purwanti et al. 2022), antiviral (Purwanti et al. 2021), antimicrobial (Bai-Ngew et al. 2021), and anti-inflammatory properties (An et al. 2020). These bioactivities make it a promising and excellent candidate for functional food development. The details on the nutritional comparison among Lablab beans will provide a fundamental guideline for determining suitable variants for functional food development, and it will be addressed by this study.

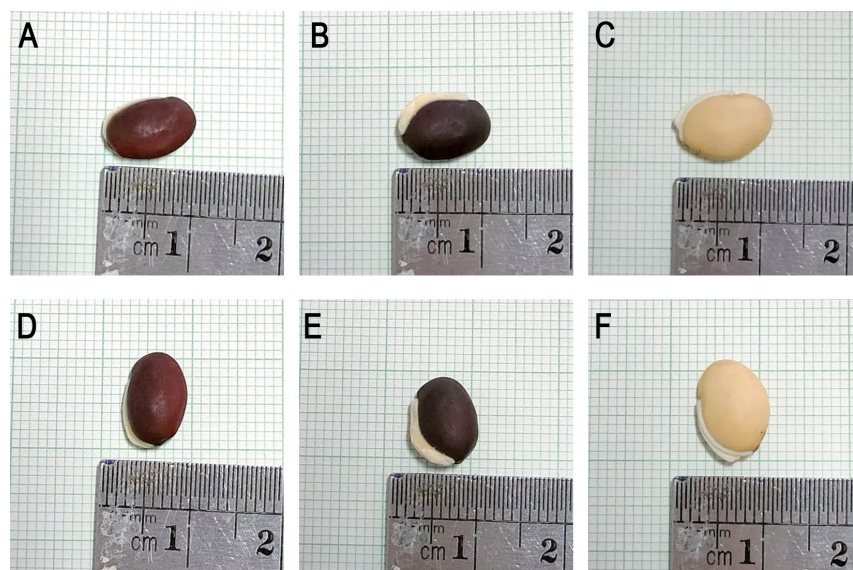


Figure 1. The most popular Lablab beans variant found in Indonesia are brown (A, D), black (B, E), and cream (C, F). The beans have been positioned to obtain the length (A-C) and the width (D-F).

The sample of the beans for this study was obtained from Sumenep, Madura Island, East Java, Indonesia during dry season in 2019. Details of the sample profiles and precise locations are as described in the previous study (Purwanti et al. 2019b). The beans were stored in 4°C until used. The beans were processed as per the extraction method previously mentioned in (Purwanti et al. 2022). Briefly, grounded beans were soaked in 96% ethanol with 3:1 ratio (volume in L and weight in kg) for 24 hours. The soaked beans powder then filtered to obtain the filtrate and homogenate. The filtrate then rotary evaporated to separate solvent and solute followed by freeze drying process to obtain Lablab beans' extract. The extract then processed to the subsequent analysis.

The crude fibre, total protein, and crude fat content were determined according to the previous protocol (Thiex 2009). Amylose and am-

ylpectin content were also measured colorimetrically using a previously described method (McGrance et al. 1998). On the other hand, IKA C2000 Calorimeter System (IKA Works, Germany) was employed to calculate the total calories as per manufacturer's protocol.

To determine the secondary metabolites content, total phenol and total flavonoid was employed. Total flavonoid was performed as per a previous protocol with minor modifications (Pratami et al. 2018). Quercetin was used as the standard flavonoid compound. The extract was dissolved in water, then 50 µL of the dissolved extract was mixed with 10 µL of 5% NaNO₂, followed by the addition of 150 µL of water and 10 µL of 1 M CH₃COONa, consecutively. The sample was then incubated at room temperature for 40 minutes. After incubation, the sample was quantified using a spectrophotometer at 415 nm wavelength. The total flavonoid concentration was described as percent (%) of Quercetin Equivalent (QE) according to the standard curve.

Total phenol was measured according to the previous study with minor modifications (Hyun et al. 2014), with gallic acid as the standard. The sample was diluted in water, and 100 µL of the sample was added to 1 mL of Folin Ciocalteu reagent and incubated for 5 minutes at room temperature with minimum light ambiance. 1 mL of 7.5% Na₂CO₃ was added to the mixture, followed by incubation for 90 minutes in the same condition mentioned beforehand. Upon incubation, the sample was then quantified spectrophotometrically at 725 nm. The total phenol was defined as percentage of Gallic Acid Equivalent (GAE) as per the build standard curve.

The antioxidant activity was measured by DPPH scavenging and Ferric Reducing Antioxidant Potential (FRAP) assays. The method for DPPH scavenging and FRAP reducing power was performed as described in the earlier work (Irshad et al. 2012). All data were analysed by one-way ANOVA followed by Least Significant Difference (LSD) post-hoc analysis. The data was determined as significantly different if the p-value is < 0.05. The data was then visualised as mean ± standard deviation.

All Lablab bean variants have good nutritional content according to the caloric, total fibre, protein, crude fat, amylose, and amylopectin content. The fibre content of black Lablab bean was the highest, with 8% fibre content, followed by the cream and brown variants (table 1). The considerable content of dietary fibre in Lablab beans displayed an immense potential to be developed as a functional food. As commonly known, fibre consumption can improve physiological homeostasis, particularly in relations to lipid and glucose metabolism (Jahan et al. 2020). High fibre content is also suitable for dietary intervention to prevent obesity (Dayib et al. 2020). With regards to total protein content, cream beans had the same protein content as brown beans, while black beans had the lowest content of total proteins (table 1). The high percentage of total protein content in Lablab beans would be valuable as a candidate for functional foods since plant-based protein have broad health benefits, such as antioxidant, antiviral, antidiabetic, and anticancer properties (Maphosa et al. 2017; Liu et al. 2020; Sipahli et al. 2021; Roy et al. 2022; Purwanti et al. 2022). Nevertheless, specific treatment, such as isoelectric preparation, was suggested to obtain a protein isolate with adequate quality and good functional properties (Subagio 2006).

Cream beans have the highest percentage of crude fat among all variants (table 1). The low-fat content of Lablab beans exhibit a great potential as functional food compared to other beans since most legumes contain around 1,5% crude fat total (Etiosa et al. 2017). Low-lipid food

provides more health benefits with deleterious high-energy intake, particularly in areas with high level of famine cases (Delaš 2011; Robson 2013). For instance, West Nusa Tenggara province in Indonesia has the highest occurrence of hunger cases (Mone & Utami 2021). Interestingly, this region also founds a large distribution of Lablab beans (Jayanti et al. 2011). The utilization of Lablab beans to reduce the incidence of famine should be considered. Thus, the low-fat content of Lablab beans displayed their potential as a functional food candidate.

This study also measured the amount of amylose and amylopectin as part of its functional properties and energy source. The black Lablab bean has the highest amylose content, with 15% amylose content, followed by brown and cream (table 1). In contrast, black beans had the lowest amylopectin content compared to the other analysed variants (table 1). Similarly, black beans also had the lowest calorie per gram compared to other variants of Lablab beans (table 1). A food source with high amylopectin induces a better glycemic response, especially during fasting (Singhania & Senray 2012). This starch also provides higher energy intake than low amylopectin sources (Singhania & Senray 2012). Moreover, the increasing ratio of amylopectin/amylose reflects better nutrient digestibility (Gao et al. 2020). A diet containing large portion of amylopectin positively associated with the postprandial insulin response resulted in more efficient nutrient uptake and glucose metabolism (Gao et al. 2020). Therefore, brown and cream beans may become potential candidates as functional food.

This study demonstrated that Lablab beans have been found to have comparable levels of total protein with *Vigna radiata* and *Pisum sativum*, and even higher levels than *Glycine max* and *Lens culinaris* (Singh et al. 2022). In addition, Lablab beans have a favourable nutritional profile with higher dietary fibre and lower fat content compared to *Phaseolus vulgaris*, *L. culinaris*, *P. sativum*, and Edamame (Dhingra et al. 2012; Mullins & Arjmandi 2021; Didinger & Thompson 2021). The amylose content in Lablab beans was higher than *Cicer arietinum* and *G. max* (Tayade et al. 2019). Moreover, the amylose and amylopectin content in Lablab beans also similar with *V. angularis*, a “red pearls” that has good nutrients and hypoglycemic activity (Zhang et al. 2022).

The total phenolic and flavonoid contents evaluation demonstrated that brown beans exhibited the greatest content of flavonoid ($p < 0.01$), while the cream beans had the most negligible flavonoid content (table 2). On the other hand, the phenolic content was highest in black beans compared to other Lablab variants ($p < 0.05$, table 2). This result showed that Lablab beans have many phenolic compounds, with the flavonoid group being the most abundant in brown beans. In other words, the other variants may comprise of other phenolic compounds like phenolic acids, tannins, and other phenolic compounds (Purwanti et al. 2022). The current result was also higher than several edible beans, such as *P. vulgaris*, *P. lunatus*, *V. radiata* and *C. arietinum* (Zhao et al. 2014). Nonethe-

Table 1. The comparison of primary metabolites and nutritional content among Lablab bean variants.

Variant	Fiber (%)	Protein (%)	Crude Fat (%)	Amylose (%)	Amylopectin (%)	Calorie (kcal/g)
Brown	7.02 ± 0.015 ^a	24.91 ± 0.06 ^a	0.36 ± 0.01 ^a	14.41 ± 0.095 ^a	87.18 ± 0.030 ^a	3.86 ± 0.005 ^a
Black	8.16 ± 0.040 ^b	23.43 ± 0.23 ^b	0.45 ± 0.03 ^b	15.46 ± 0.515 ^b	85.79 ± 0.015 ^b	3.83 ± 0.002 ^b
Cream	8.11 ± 0.005 ^c	24.82 ± 0.15 ^a	0.55 ± 0.04 ^c	13.52 ± 0.120 ^c	87.90 ± 0.025 ^c	3.85 ± 0.002 ^a

Note: The data was presented as mean ± standard deviations (n = 3). Different alphabetical notation indicates significant difference with $p < 0.05$ based on LSD test.

less, the total flavonoid contents of Lablab beans were lower compared to *P. sativum*, *C. arietinum*, *V. radiata*, *P. vulgaris*, *P. lunatus*, *L. culinaris*, *Vicia faba*, and *G. max* (Sharma & Giri 2022). Although flavonoids are the most abundant phenolic compounds with various biological activities (Kumar & Pandey 2013), other phenolic compounds, either simple phenols or polyphenols other than flavonoids, have also been reported to have bioactivities to improve physiological homeostasis, mainly through their antioxidant activity (Shahidi & Ambigaipalan 2015; Singh et al. 2017).

The high flavonoid content was positively correlated with antioxidant activity through DPPH scavenging activity, where brown beans had the highest scavenging activity compared to the others (table 2). However, the ferric reducing activity was stronger in variant with higher phenolic contents (table 2). These results were supported by a structure-activity relationship between radical scavenging from different phenolic compounds and the radical scavenging mechanism in DPPH and FRAP assay. Flavonoids have an *ortho*-dihydroxyl structure that plays a role in radical scavenging during DPPH assay by forming an intramolecular hydrogen bond and more stable *ortho*-hydroxyl phenoxy radical during the oxidation process of radical scavenging (Zheng et al. 2010). Alternatively, other phenolic compounds, such as phenolic acids, have *ortho* or *para* position of the hydroxyl group in its benzene ring (Spiegel et al. 2020). Those structural differences influence the radical scavenging mechanism of flavonoids and other phenolic compounds in different antioxidant assay. Hydrogen Atom Transfer (HAT), Single-Electron Transfer followed by Proton Transfer (SET-PT), and Sequential Proton-Loss Electron Transfer (SPLET) are taking place during the DPPH assay. Contrary, SPLET is the main mechanism during the electron transfer enthalpy in the FRAP reaction system (Chen et al. 2020). Ferulic Acid, Hydroxycinnamic Acid, Sinapinic Acid, Coumaric Acid, and Isovanillic Acid are identified phenolic acids in Lablab beans. Also, Rutin and Isoquercetin are flavonoids that also found in Lablab beans (Purwanti et al. 2022). Those compounds were identified in adequate abundance in Lablab beans and may perform as radical scavenger during this study. Nevertheless, future studies are required to compare the secondary metabolites among different variant of Lablab beans to comprehend the phytochemical content differences better. Despite the different mechanisms and types of bioactive compounds in performing the antioxidant activity, it has been displayed that brown and black beans exhibit solid antioxidant properties.

This study shows that all Lablab bean variants have good amount of nutritional value, total phenol and flavonoid contents, and antioxidant activity. Lablab beans have adequate nutritional values surpassed other types of edible beans. Despite having lower flavonoid contents compared to commonly consumed beans, the phenolic compounds in these beans still exhibit superior performance. Finally, the cream variant shows slightly lower nutritional contents and bioactive compound compared to

Table 2. The total flavonoid, phenolic, and antioxidant capacity according to the DPPH scavenging capacity and FRAP analysis.

Variant	Total Flavonoid (%)	Total Phenol (%)	DPPH Scavenging (%)	FRAP ($\mu\text{M FeSO}_4/\text{mg}$)
Brown	26.25 \pm 0.34 ^a	40.56 \pm 0.69 ^a	78.87 \pm 1.59 ^a	1154.58 \pm 4.17 ^a
Black	12.99 \pm 0.31 ^b	45.28 \pm 2.56 ^b	40.01 \pm 0.16 ^b	2398.05 \pm 4.81 ^b
Cream	12.15 \pm 0.06 ^c	40.32 \pm 3.06 ^a	24.53 \pm 0.16 ^c	1061.53 \pm 2.41 ^c

Notes: The data was presented in mean \pm standard deviations (n = 3). Different alphabetical notation indicates significant difference with $p < 0.05$ based on LSD test.

the other analysed Lablab beans. Still, some varieties possess a promising characteristic as a functional food candidate owing to their nutritional value.

AUTHORS CONTRIBUTION

EP designed the research and acquired the project funding, FE collected and analysed the data, WP and TIP wrote the manuscript, and IGNAW performed critical review and revision.

ACKNOWLEDGMENTS

The authors thank the Directorate of Research and Community Service (DPPM), University of Muhammadiyah Malang under PKID research grant scheme in 2022 (Grant No. E.2.a/334/BAA-UMM/IV/2022) for funding this work.

CONFLICT OF INTEREST

There is no conflict of interest raised in this study.

REFERENCES

- An, J.M. et al., 2020. Dolichos lablab L. extracts as pharmanutrient for stress-related mucosal disease in rat stomach. *Journal of Clinical Biochemistry and Nutrition*, 67(1), pp.89–101. doi: 10.3164/jcbtn.20-11.
- Bai-Ngew, S. et al., 2021. Antimicrobial activity of a crude peptide extract from lablab bean (*Dolichos lablab*) for semi-dried rice noodles shelf-life. *Quality Assurance and Safety of Crops & Foods*, 13(2), pp.25–33. doi: 10.15586/qas.v13i2.882.
- Çakir, Ö. et al., 2019. Nutritional and health benefits of legumes and their distinctive genomic properties. *Food Science and Technology*, 39, pp.1–12. doi: 10.1590/fst.42117.
- Chen, J. et al., 2020. Structure-antioxidant activity relationship of methoxy, phenolic hydroxyl, and carboxylic acid groups of phenolic acids. *Scientific Reports*, 10(1), 2611. doi: 10.1038/s41598-020-59451-z.
- Considine, M.J., Siddique, K.H.M. & Foyer, C.H., 2017. Nature's pulse power: legumes, food security and climate change. *Journal of Experimental Botany*, 68(8), pp.1815–1818. doi: 10.1093/jxb/erx099.
- Dayib, M., Larson, J. & Slavin, J., 2020. Dietary fibers reduce obesity-related disorders: mechanisms of action. *Current Opinion in Clinical Nutrition & Metabolic Care*, 23(6), pp.445–450. doi: 10.1097/MCO.0000000000000696.
- Delaš, I., 2011. Benefits and hazards of fat-free diets. *Trends in Food Science & Technology*, 22(10), pp.576–582. doi: 10.1016/j.tifs.2011.08.008.
- Dhingra, D. et al., 2012. Dietary fibre in foods: a review. *Journal of Food Science and Technology*, 49(3), 255. doi: 10.1007/s13197-011-0365-5.
- Didinger, C. & Thompson, H.J., 2021. Defining Nutritional and Functional Niches of Legumes: A Call for Clarity to Distinguish a Future Role for Pulses in the Dietary Guidelines for Americans. *Nutrients*, 13(4), 1100. doi: 10.3390/nu13041100.

- Etiosa, O.R., Chika, N.B. & Benedicta, A., 2017. Mineral and Proximate Composition of Soya Bean. *Asian Journal of Physical and Chemical Sciences*, pp.1–6. doi: 10.9734/AJOPACS/2017/38530.
- Gao, X. et al., 2020. Effects of Dietary Starch Structure on Growth Performance, Serum Glucose–Insulin Response, and Intestinal Health in Weaned Piglets. *Animals*, 10(3), p.543. doi: 10.3390/ani10030543.
- Hermanto, F.E. et al., 2022a. On The Hypolipidemic Activity of Elicited Soybeans: Evidences Based on Computational Analysis. *Indonesian Journal of Chemistry*, 22(6), pp.1626–1636. doi: 10.22146/ijc.75777.
- Hermanto, F.E. et al., 2022b. Understanding hypocholesterolemic activity of soy isoflavones: Completing the puzzle through computational simulations. *Journal of Biomolecular Structure and Dynamics*, in press, pp.1–7. doi: 10.1080/07391102.2022.2148752.
- Hyun, T.K., Kim, H.C. & Kim, J.S., 2014. Antioxidant and antidiabetic activity of *Thymus quinquecostatus* Celak. *Industrial Crops and Products*, 52, pp.611–616. doi: 10.1016/j.indcrop.2013.11.039.
- Irshad, M. et al., 2012. Comparative Analysis of the Antioxidant Activity of Cassia fistula Extracts. *International Journal of Medicinal Chemistry*, 2012, 157125. doi: 10.1155/2012/157125.
- Jahan, K., Qadri, O.S. & Younis, K., 2020. Dietary Fiber as a Functional Food. In *Functional Food Products and Sustainable Health*. Singapore: Springer, pp. 155–167. doi: 10.1007/978-981-15-4716-4_10.
- Jayanti, E.T., Kasiamdari, R.S. & Daryono, B.S., 2011. Morphological Variation and Phenetic Relationship of Hyacinth Bean (*Lablab purpureus* (L.) Sweet) in Lombok, West Nusa Tenggara. *Proceeding ICBB (The International Conference on Bioscience and Biotechnology)*, 1 (1), pp.C9–C15.
- Kumar, S. & Pandey, A.K., 2013. Chemistry and biological activities of flavonoids: an overview. *TheScientificWorldJournal*, 2013, 162750. doi: 10.1155/2013/162750.
- Liu, Y.M. et al., 2020. A Carbohydrate-Binding Protein from the Edible Lablab Beans Effectively Blocks the Infections of Influenza Viruses and SARS-CoV-2. *Cell Reports*, 32(6), 108016. doi: 10.1016/j.celrep.2020.108016.
- Maass, B.L. et al., 2010. Lablab purpureus—A Crop Lost for Africa? *Tropical Plant Biology*, 3(3), pp.123–135. doi: 10.1007/s12042-010-9046-1.
- Maheshu, V., Priyadarsini, D.T. & Sasikumar, J.M., 2013. Effects of processing conditions on the stability of polyphenolic contents and antioxidant capacity of *Dolichos lablab* L. *Journal of Food Science and Technology*, 50(4), pp.731–738. doi: 10.1007/s13197-011-0387-z.
- Maphosa, Y. et al., 2017. *The Role of Legumes in Human Nutrition*, IntechOpen. doi: 10.5772/intechopen.69127.
- McGrance, S.J., Cornell, H.J. & Rix, C.J., 1998. A Simple and Rapid Colorimetric Method for the Determination of Amylose in Starch Products. *Starch - Stärke*, 50(4), pp.158–163. doi: 10.1002/(SICI)1521-379X(199804)50:4<158::AID-STAR158>3.0.CO;2-7.

- Missanga, J.S., Venkataramana, P.B. & Ndakidemi, P.A., 2021. Recent developments in Lablab purpureus genomics: A focus on drought stress tolerance and use of genomic resources to develop stress-resilient varieties. *Legume Science*, 3(3), p.e99. doi: 10.1002/leg3.99.
- Mone, D.M.V. & Utami, E.D., 2021. Determinan Kelaparan di Indonesia Tahun 2015-2019. *Seminar Nasional Official Statistics*, 2021(1), pp.547-556. doi: 10.34123/semnasoffstat.v2021i1.962.
- Mullins, A.P. & Arjmandi, B.H., 2021. Health Benefits of Plant-Based Nutrition: Focus on Beans in Cardiometabolic Diseases. *Nutrients*, 13(2), p.519. doi: 10.3390/nu13020519.
- Piergiovanni, A.R., 2021. Legumes: staple foods used in rituals and festive events of Apulia region (southern Italy). *Food, Culture & Society*, 24(4), pp.543-561. doi: 10.1080/15528014.2021.1884420.
- Polak, R., Phillips, E.M. & Campbell, A., 2015. Legumes: Health Benefits and Culinary Approaches to Increase Intake. *Clinical Diabetes: A Publication of the American Diabetes Association*, 33(4), pp.198-205. doi: 10.2337/diaclin.33.4.198.
- Pratami, D. et al., 2018. Phytochemical Profile and Antioxidant Activity of Propolis Ethanolic Extract from Tetragonula Bee. *Pharmacognosy Journal*, 10(1), pp.128-135. doi: 10.5530/pj.2018.1.23.
- Purwanti, E., Prihanta, W. & Fauzi, A., 2019a. Nutritional Content Characteristics of Dolichos lablab L. Accessions in Effort to Investigate Functional Food Source. *Atlantis Press*, pp. 166-170. doi: 10.2991/iccd-19.2019.45.
- Purwanti, E., Prihanta, W. & Fauzi, A., 2019b. The Diversity of Seed Size and Nutrient Content of Lablab Bean from Three Locations in Indonesia. *International Journal of Advanced Engineering, Management and Science*, 5(6), pp.395-402. doi: 10.22161/ijaems.5.6.7.
- Purwanti, E. et al., 2021. Exploring public health benefits of Dolichos lablab as a dietary supplement during the COVID-19 outbreak: A computational study. *Journal of Applied Pharmaceutical Science*, 11, (2), pp.135-140. doi: 10.7324/JAPS.2021.110217.
- Purwanti, E. et al., 2022. Unfolding Biomechanism of Dolichos lablab Bean as A Dietary Supplement in Type 2 Diabetes Mellitus Management through Computational Simulation. *Research Journal of Pharmacy and Technology*, 15(7), pp.3233-3240. doi: 10.52711/0974-360X.2022.00542.
- Robson, A.A., 2013. Chapter 25 - Preventing the Epidemic of Non-Communicable Diseases: An Overview. In R. R. Watson & V. R. Preedy, eds. *Bioactive Food as Dietary Interventions for Liver and Gastrointestinal Disease*. San Diego: Academic Press, pp. 383-400. doi: 10.1016/B978-0-12-397154-8.00016-6.
- Roy, M. et al., 2022. Evaluation of quality parameters and antioxidant properties of protein concentrates and hydrolysates of hyacinth bean (Lablab purpureus). *Legume Science*, 4(2), p.e128. doi: 10.1002/leg3.128.

- Shahidi, F. & Ambigaipalan, P., 2015. Phenolics and polyphenolics in foods, beverages and spices: Antioxidant activity and health effects – A review. *Journal of Functional Foods*, 18, pp.820–897. doi: 10.1016/j.jff.2015.06.018.
- Sharma, K.R. & Giri, G., 2022. Quantification of Phenolic and Flavonoid Content, Antioxidant Activity, and Proximate Composition of Some Legume Seeds Grown in Nepal. *International Journal of Food Science*, 2022, e4629290. doi: 10.1155/2022/4629290.
- Singh, B. et al., 2017. Phenolic composition and antioxidant potential of grain legume seeds: A review. *Food Research International*, 101, pp.1–16. doi: 10.1016/j.foodres.2017.09.026.
- Singh, N. et al., 2022. Escalate protein plates from legumes for sustainable human nutrition. *Frontiers in Nutrition*, 9, 977986. doi: 10.3389/fnut.2022.977986.
- Singhania, P.R. & Senray, K., 2012. Glycemic response to amylopectin rich starch present in common fasting foods of India. *Nutrition & Food Science*, 42(3), pp.196–203. doi: 10.1108/00346651211228496.
- Sipahli, S. et al., 2021. In vitro antioxidant and apoptotic activity of Lablab purpureus (L.) Sweet isolate and hydrolysates. *Food Science and Technology*, 42, e55220. doi: 10.1590/fst.55220.
- Spiegel, M. et al., 2020. Antioxidant Activity of Selected Phenolic Acids–Ferric Reducing Antioxidant Power Assay and QSAR Analysis of the Structural Features. *Molecules (Basel, Switzerland)*, 25(13), 3088. doi: 10.3390/molecules25133088.
- Subagio, A., 2006. Characterization of hyacinth bean (Lablab purpureus (L.) sweet) seeds from Indonesia and their protein isolate. *Food Chemistry*, 95(1), pp.65–70. doi: 10.1016/j.foodchem.2004.12.042.
- Tayade, R. et al., 2019. Insight Into the Prospects for the Improvement of Seed Starch in Legume—A Review. *Frontiers in Plant Science*, 10, 1213. doi: 10.3389/fpls.2019.01213.
- Thiex, N., 2009. Evaluation of Analytical Methods for the Determination of Moisture, Crude Protein, Crude Fat, and Crude Fiber in Distillers Dried Grains with Solubles. *Journal of AOAC INTERNATIONAL*, 92(1), pp.61–73. doi: 10.1093/jaoac/92.1.61.
- Zhang, L. et al., 2022. Analysis and Research on Starch Content and Its Processing, Structure and Quality of 12 Adzuki Bean Varieties. *Foods*, 11(21), p.3381. doi: 10.3390/foods11213381.
- Zhao, Y. et al., 2014. In vitro antioxidant activity of extracts from common legumes. *Food Chemistry*, 152, pp.462–466. doi: 10.1016/j.foodchem.2013.12.006.
- Zheng, C.D. et al., 2010. DPPH-Scavenging Activities and Structure-Activity Relationships of Phenolic Compounds. *Natural Product Communications*, 5(11), pp.1759–1765. doi: 10.1177/1934578X1000501112.

Research Article

Diversity and Community Structure of Dragonflies (Odonata) in Various Types of Habitat at Lakarsantri District, Surabaya, Indonesia

Muhamad Azmi Dwi Susanto¹, Nirmala Fitria Firdhausi², Saiful Bahri^{2*}

1)Department of Biology, Faculty of Mathematics and Natural Sciences, Universitas Brawijaya, Malang, Indonesia

2)Department of Biology, Faculty of Science and Technology, UIN Sunan Ampel Surabaya, Indonesia

* Corresponding author, email: saifulsi@uinsby.ac.id

Keywords:

Urban area
Aquatic ecosystem

Conservation

Submitted:

29 July 2022

Accepted:

16 January 2023

Published:

03 May 2023

Editor:

Miftahul Ilmi

ABSTRACT

Dragonflies are insects that are very dependent on the existence of freshwater ecosystems. However, the population of dragonflies in urban freshwater ecosystems is at risk due to a number of issues. Consequently, it is essential to carry out research and efforts to preserve dragonflies in urban areas. This study aims to provide information about the diversity and structure of dragonfly communities in various habitat types in the Lakarsantri, Surabaya. Data collection in this study was carried out in the habitat types of ponds, reservoir, river, and rice field in July to September 2021. The study results show there are 22 species from 4 families with a total of 827 individuals. Analysis of the Shannon-Wiener diversity index showed that the highest value of dragonfly diversity was found in a pond, with a value of $H' = 2.40$, and the location with the lowest value was a river, with a value of $H' = 1.77$. At four research locations that have different aquatic ecosystems, the community structure of dragonfly is also different. The composition of the dragonfly community structure at the reservoir location has similarities to a pond, and at a river location, it has similarities to a paddy field. Differences in abiotic factors consisting of light intensity, humidity, and temperature at each study location have a correlation with differences in dragonfly community structure. In addition, the composition of the vegetation at each location is also one of the factors causing differences in the structure of the dragonfly community.

Copyright: © 2023, J. Tropical Biodiversity Biotechnology (CC BY-SA 4.0)

INTRODUCTION

Dragonflies are flying insects essential to the ecosystem's ability to balance its food chain (Tang et al. 2010). Dragonflies are insect predators throughout their life cycle, from nymph to adult (Kandibane et al. 2005) so that they can become natural predators for disease vector insects in urban environments such as flies and mosquitoes (Dalia & Leksono 2014). Dragonflies not only keep the food chain in balance but also serve as a bioindicator of the state of the ecosystem. This is because some species of dragonflies also have a very high sensitivity to changes in environmental quality (Tang et al. 2010; Dolný et al. 2012). If the environment that is the dragonfly's natural habitat is disturbed or damaged, the dragonfly will react (Buczyński et al. 2020).

Dragonflies spend most of their lives in water, namely during their egg and larval phases (Choong et al. 2020) so that the main habitat of

dragonflies cannot be separated from freshwater ecosystems (Tang et al. 2010). Generally, dragonflies can be found in locations that have freshwater ecosystems such as lakes, reservoirs, ponds, or rivers in mountainous or urban areas (Paulson 2009). However, aquatic ecosystems in urban areas have problems that can reduce quality to the point of damaging the environment and waters. Examples of problems that often occur are organic and chemical water pollution from household waste. Furthermore, the growing number of developments harms various wetlands and freshwater bodies. This causes the aquatic ecosystems that should be used as natural habitats for dragonflies to be damaged and their populations to be disrupted. This is also supported by IUCN (2021). Which states that more than a quarter of the total dragonfly species in Southeast Asia are threatened with extinction, due to the destruction of the wetlands, which are the natural habitat of dragonflies. Therefore, research and conservation of the diversity of dragonfly species in urban areas are urgently needed.

The existence of damage and pollution in an urban area can be a major factor affecting the differences in the structure of the dragonfly community in an unspoiled area (Vilenica & Mihaljević 2022). The factors that most influence the community of dragonflies in cities are the presence of polluted aquatic habitats and also the presence of riparian vegetation (Maldonado-Benítez et al. 2022). Research on the community structure of dragonfly in a variety of habitats in urban East Java is still very limited, especially in the city of Surabaya. This research is the first research on the community structure of the dragonfly in various types of habitats in the city of Surabaya, and it was carried out in the Lakarsantri District.

Lakarsantri District is an urban area that still has green open space with various freshwater ecosystems, including rice fields, rivers, ponds, and reservoirs. The existence of various types of aquatic ecosystems has a good chance of developing into a natural habitat for different species of dragonflies. But with population growth and increasing human activities that continue to occur, as well as the absence of dragonfly research on various types of ecosystems in the Lakarsantri District, this research is very important to do. Therefore, the purpose of this study was to ascertain the diversity and community structure of dragonflies in various habitat types in the Lakarsantri District.

MATERIALS AND METHODS

Time and Location Study

Data collection was carried out from July to September 2021. Data collection was carried out once a month during sunny conditions with observation time from 08.00 am to 04.00 pm with rest time from 11.00 am to 01.30 pm. This research was conducted in Lakarsantri District, Surabaya City, East Java, Indonesia. The observation location based on the various types of habitats that can be found in each of the four research locations namely Pond, Reservoir, River, and Rice field (Figure 1) so that each location represented one habitat type (Figure 2).

Data Collection

Data collection used the modified Visual Encounter Survey (VES) technique, which is a direct observation technique. These observations were carried out by tracing all the observation locations determined by noting the variety of dragonfly species and counting the number of each species' individuals that were observed. Observation of dragonflies using the VES method on several habitat types in Lakarsantri District was modified us-

ing the Transect method (Oppel 2006) and Belt Transect (Haritonov & Popova 2011). The transect method was an observation method by following a predetermined straight line and was used at a river research location. While the Belt Transect method involved making observations while traveling along a predetermined circular line and was used at research sites of pond, reservoir, and rice field. The research sites were selected based on the different habitat types from every location and their potential as dragonfly natural habitats (Purposive Random Sampling).

Data was collected by captured dragonflies using a sweeping net, then each body part was documented in detail using a camera. Every dragonfly found is also documented when in the wild for aesthetic purposes. Each individual that has been collected or documented is then

Table 1. Description of research location.

Location	Coordinate point		Description
	Latitude	Longitude	
Pond	S7° 19' 33.8	E112° 40' 25.6	A pond is a body of stagnant water located in cultural heritage areas and near settlements. This location consists of water plants, herbaceous vegetation, and some trees.
Reservoir	S7° 18' 2.3	E112° 39' 40.9	A reservoir is a body of stagnant water that is used as a tourist and fishing spot and is located near settlements. This location consists of herbaceous vegetation and some trees.
River	S7° 19' 13.0	E112° 41' 8.0	A river is a body of water that flows. This location is dominated by grass vegetation.
Rice field	S7° 20' 7.7	E112° 39' 54.2	A rice field is a land that has stagnant waters and a pond as an irrigation system. This location is dominated by rice plants.

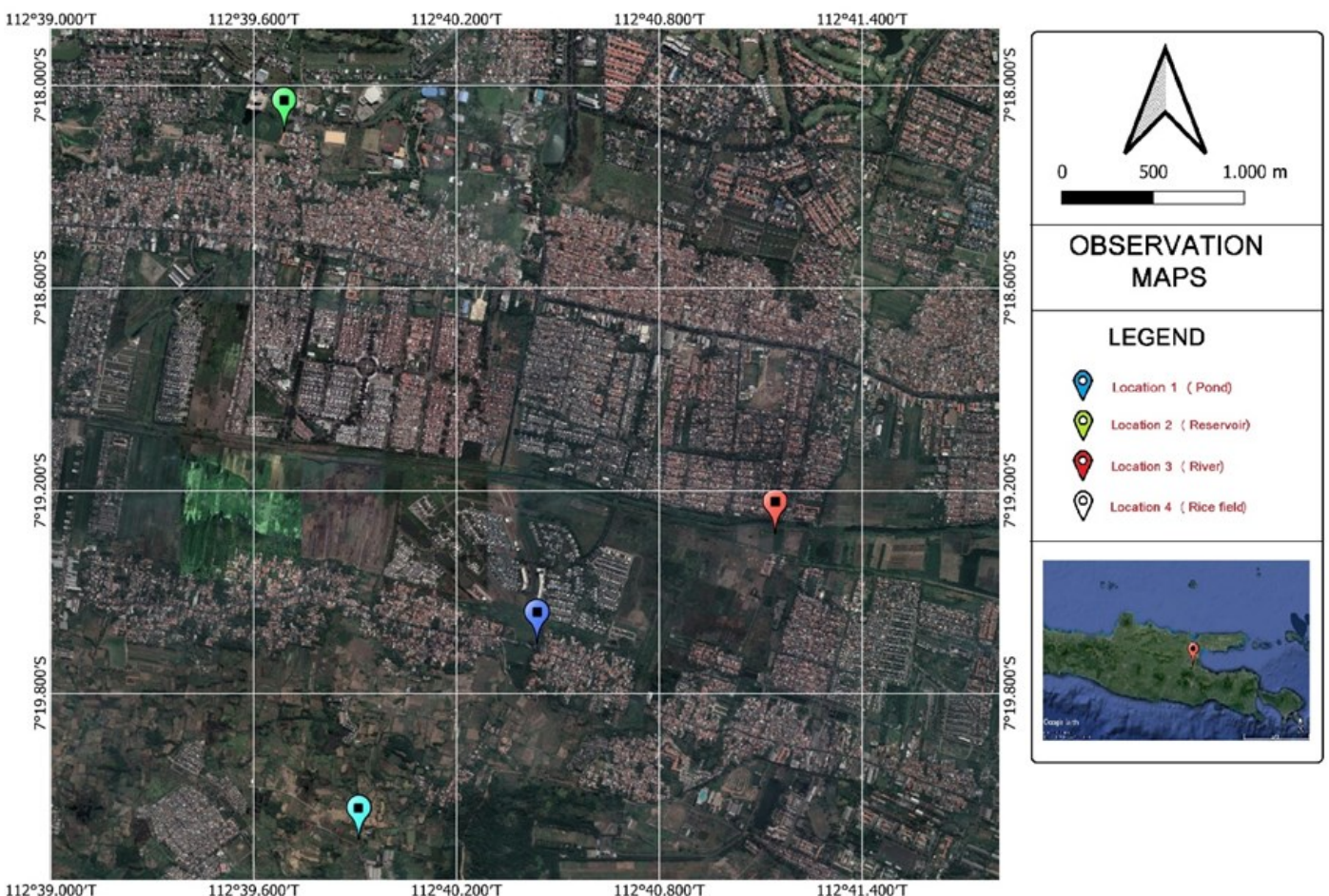


Figure 1. Study location maps.

identified to the species level. Dragonfly species identification was conducted using the morphological feature of each individual according to the identification key including body size, color, pattern, wings venation, and tuft shape. Identification was carried out using an identification manual (Orr 2005; Kalkman & Orr 2013; Orr & Kalkman 2015; Setiyono et al. 2017). This study's data collection included consideration of microclimate elements like light intensity, humidity, and air temperature. The air temperature and humidity factors were measured using a Thermo hygrometer, and the light intensity factor was measured using a light meter. Vegetation data collection was also carried out by identifying the dominant types of plants found at the study site.

Data Analysis

Data obtained was then analysed for the diversity value using the Shannon-Wiener index (Metcalf 1989), evenness index, dominance index (Magurran 2004), relative abundance, and frequency of attendance. With the following formula:

$$H' = \sum \left(\frac{n_i}{N} \ln \frac{n_i}{N} \right)$$

Information:

- H' = Shannon-Wiener diversity index
- n_i = Number of individuals of type i
- N = Number of individuals of all types

$$E = \frac{H'}{\ln S}$$

Information:

- E = Evenness index



Figure 2. Documentation research site (A) Pond, (B) Reservoir, (C) River, (D), Rice field.

H' = Shannon-Wiener diversity index
S = Number of species

$$D = \sum \left(\frac{n_i}{N}\right)^2$$

Information:

D = Dominance index
n_i = Number of individuals of type i
N = Number of individuals of all types

$$RA = \frac{n_i}{N} \times 100\%$$

Information:

RA = Relative abundance
n_i = Number of individuals of type i
N = Number of individuals of all types

$$PF = \frac{\text{Total posts found species } i}{\text{the total of posts}} \times 100\%$$

Information:

PF = Presence frequency

The next analysis was principal component analysis (PCA). This analysis was used to determine the relationship between location of observation with the results of measurements of abiotic factors (environmental) and biotic index (Koneri et al. 2022). PCA analysis using Paleontology Statistical software (PAST 4.03 software). The similarity of dragonfly composition using the UPGMA cluster analysis method (index Bray-Curtis), and the correlation of biotic factors with abiotic factors were analyzed using PAST 4.03. Calculation of the mean and standard deviation using the software of Statistical Program for Social Science (SPSS 24).

RESULTS AND DISCUSSION

Based on observations made on various types of habitats in Lakarsantri District, 22 species from 4 families with a total of 827 individuals were found (Table 2). In the suborder Anisoptera found 15 species of dragonflies from 2 families namely Gomphidae and Libellulidae with a total of 671 individuals. While in the suborder Zygoptera found 7 species from 2 families, namely Coenagrionidae and Platycnemididae with a total of 156 individuals. Most of the dragonfly species that were found, namely 19 species, had a conservation status of Least Concern (LC). However, two species with Data Deficient (DD) conservation status were also found, namely *Neurothemis feralis* and *Pseudagrion nigrofasciatum*, as well as one species with Not Evaluated (NE) conservation status, namely *Zyxomma obtusum*.

The results of this study indicated that dragonflies belonging to suborder Anisoptera had more species and individuals than suborder Zygoptera. Almost all research sites have areas dominated by open habitats with understorey vegetation and some trees, making them suitable habitats for dragonflies of the suborder Anisoptera. Members of the Anisoptera were often found in open habitats to look for food and most of them were flying at a fairly high intensity of sunlight (Kalkman & Orr 2013). In addition, they also have excellent flight abilities leading to a wider range of cruising. Members of Anisoptera can adapt to urban environ-

ments and also with high roaming abilities, the Anisoptera is not very dependent on the availability of food around the waters.

There were fewer members of the suborder Zygoptera in this study than the suborder Anisoptera, which could be because Zygoptera had a higher sensitivity to pollution. This is following (Maldonado-Benítez et al. 2022), who reported that in poor habitat conditions the abundance of Zygoptera was reduced. The presence of aquatic plants and riparian vegetation in the habitat also impacts the presence significantly and abundance of the Zygoptera. Because of the vegetation can be a natural habitat for various small insects that are a source of food for dragonflies. Zygoptera has the ability to fly and a low cruising range makes Zygoptera highly dependent on the availability of food in a location.

Considering the analysis of the study's dragonfly's presence data for frequency, it showed that most of the dragonfly species encountered had the characteristics of their respective natural habitats. So that not all species can be found in all research locations. Of all the species found, there were only four species that had a presence frequency value of 100%, which means that these species were found in all locations of this study (although not always found every month), namely at the pond, reservoir, river, and rice field (Table 1). The four species are *Brachythemis contaminata* (Figure 4-C), *Crocothemis servilia* (Figure 4-E), *Orthetrum sabina* (Figure 4-I), and *Agriocnemis femina* (Figure 3-A). These four species can be found in all locations because these four species have a relatively high tolerance for environmental disturbances or changes. This is in accordance with (Kulkarni & Subramanian 2013; Irawan & Rahadi 2016), who reported that *Brachythemis contaminata* species have low sensitivity to disturbances, therefore, they are still present in contaminated waters. There are several different habitats where *Brachythemis contaminata* species can be found, including riverbanks, lakes, ponds, and other calm waters (Lieftinck 1934; Irawan & Rahadi 2016).



Figure 3. Documentation of suborder Zygoptera (A) *Agriocnemis femina*, (B) *Agriocnemis pygmaea*, (C) *Ceriagrion praetermissum*, (D) *Ischnura senegalensis*, (E) *Pseudagrion rubriceps*, (F) *Copera marginipes* (Photo: Muhamad Azmi Dwi Susanto, 2021).

Table 2. Species richness and abundance.

Taxa	Conservation Status	Presence Frequency (%)	Relative Abundance (%)	Number of individuals					Total
				Pond	Reservoir	River	Rice field		
Gomphidae									
<i>Ictinogomphus decoratus</i> (Selys, 1854)	LC	50	2.18	2	16	0	0	0	18
Libellulidae									
<i>Acisoma panorpoides</i> (Rambur, 1842)	LC	75	2.78	20	1	0	2		23
<i>Brachythemis contaminata</i> (Fabricius, 1793)	LC	100	30.96	107	108	3	38		256
<i>Brachydiplax chalybea</i> (Brauer, 1868)	LC	50	14.51	95	25	0	0	0	120
<i>Crocothemis servilia</i> (Drury, 1770)	LC	100	3.87	10	5	13	4		32
<i>Diplacodes trivialis</i> (Rambur, 1842)	LC	75	1.33	9	1	0	1		11
<i>Macrodiplax cora</i> (Brauer, 1867)	LC	75	3.39	0	13	3	12		28
<i>Neurothemis feralis</i> (Burmeister, 1839)	DD	25	3.02	25	0	0	0		25
<i>Orthetrum sabina</i> (Drury, 1770)	LC	100	7.86	25	14	12	14		65
<i>Pantala flavescens</i> (Fabricius, 1798)	LC	75	3.14	0	4	16	6		26
<i>Potamarcha congener</i> (Rambur, 1842)	LC	75	2.18	5	11	0	2		18
<i>Rhyothemis phyllis</i> (Sulzer, 1776)	LC	50	0.60	3	2	0	0		5
<i>Rhodothemis rufa</i> (Rambur, 1842)	LC	75	1.93	12	2	0	2		16
<i>Thohymis tillarga</i> (Fabricius, 1798)	LC	75	3.14	15	2	0	9		26
<i>Zyxomma obtusum</i> (Albarda, 1881)	NE	25	0.24	2	0	0	0		2
Coenagrionidae									
<i>Agriocnemis femina</i> (Brauer, 1868)	LC	100	6.29	16	21	11	4		52
<i>Agriocnemis pygmaea</i> (Rambur, 1842)	LC	50	1.45	4	8	0	0		12
<i>Ceriagrion praetermissum</i> (Liefstinck, 1929)	LC	25	0.60	5	0	0	0		5
<i>Ischnura senegalensis</i> (Rambur, 1842)	LC	75	1.69	8	2	4	0		14
<i>Pseudagrion nigrofasciatum</i> (Liefstinck, 1934)	DD	25	0.60	5	0	0	0		5
<i>Pseudagrion rubriceps</i> (Selys, 1876)	LC	25	3.87	32	0	0	0		32
Platycnemididae									
<i>Copera marginipes</i> (Rambur, 1842)	LC	25	4.35	36	0	0	0		36
Total Abundance				463	235	62	94		827
Species richness				20	16	7	11		22
Mean ± Standard Deviation				21.80 ± 28.94	14.69 ± 26.00	8.86 ± 5.39	8.55 ± 10.69		

Information: NE (Not Evaluated), DD (Data Deficient) & LC (Least Concern) Source: (IUCN 2022)

Crocothemis servilia Species is present in many different kinds of ecosystems, including ponds, rice fields, rivers, and swamps (Pamungkas 2016). Additionally, species of *Crocothemis servilia* are frequently observed perching on the tips of nearby plants (Setiyono et al. 2017). The *Orthetrum sabina* species can also be found in various types of habitats (Kalita & Ray 2015). According to (Haissoufi et al. 2015), *Orthetrum sabina* species can be found in habitats of lakes, ponds, rice fields, to swamps. And can develop well in non-flowing waters (Pamungkas 2016), to slow-flowing streams (Kumar 1984). Also, the *Agriocnemis femina* species can be discovered in a variety of habitats. that have grass vegetation around puddles (Setiyono et al. 2017). In addition, the *Agriocnemis femina* species can also be found in waters containing aquatic plants such as water hyacinth (Nicolla et al. 2021).

The similarity level of the research locations was analyzed using the Bray-Curtis index. The parameter used is the species composition of dragonflies in each research location. Based on the similarity analysis of the composition of dragonflies, there are two groups: river and rice field, and reservoir and pond (Figure 5). River and rice field have the same level of dragonfly composition similarity; there are six species found in these two locations, namely *Agriocnemis femina*, *Pantala flavescens*, *Macrodiplax cora*, *Crocothemis servilia*, *Orthetrum sabina*, and *Brachythemis contaminata* (Table 2). Whereas in other groups, reservoir and pond have the same



Figure 4. Documentation of suborder Anisoptera (A) *Ictinogomphus decoratus*, (B) *Acisoma panorpoides*, (C) *Brachythemis contaminata* (D) *Brachydiplax chalybea*, (E) *Crocothemis servilia*, (F) *Diplacodes trivialis*, (G) *Macrodiplax cora*, (H) *Neurothemis feralis*, (I) *Orthetrum sabina*, (J) *Pantala flavescens*, (K) *Potamarcha congener*, (L) *Rhyothemis phyllis*, (M) *Rhodothemis rufa*, (N) *Tholymis tillarga* (Photo: Muhamad Azmi Dwi Susanto, 2021).

level of composition similarity; there are 14 species that can be found in these two locations, namely *Agriocnemis femina*, *Agriocnemis pygmaea*, *Ischnura senegalensis*, *Acisoma panorpoides*, *Brachydiplax chalybea*, *Brachythemis contaminata*, *Crocothemis servilia*, *Diplacodes trivialis*, *Orthetrum sabina*, *Potamarcha congener*, *Rhodothemis rufa*, *Rhyothemis phyllis*, *Tholymis tillarga*, and *Ictinogomphus decoratus* (Table 2).

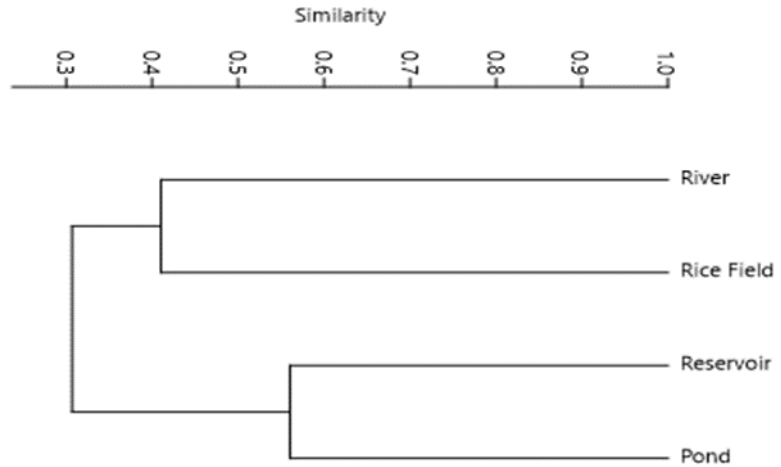


Figure 5. Similarity of dragonfly composition.

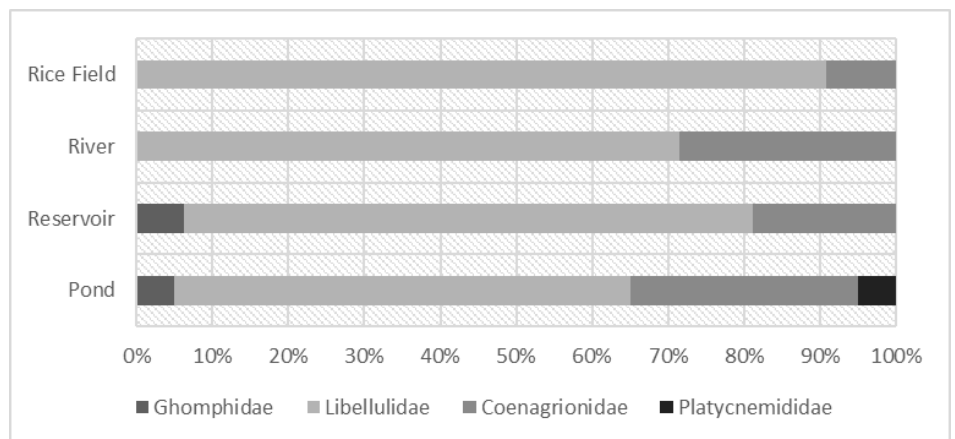


Figure 6. Differences in family composition.

The composition of the dragonfly family found in this study showed that the Libellulidae and Coenagrionidae families could be found in all research locations (Figure 6). Meanwhile, in the Platycnemididae family, it can only be found at the pond location and only one species is found, namely *Copera marginipes* (Figure 3-F). This can be due to the fact that the pond location has a type of aquatic stagnant ecosystem with a closed canopy and there is quite dense vegetation, so that at this location it has characteristics that match the natural habitat of the *Copera marginipes* species. This statement is supported by (Furtado 1974), who reported that *Copera marginipes* species are often found perching on aquatic plants or grasses in stagnant waters such as ponds. *Copera marginipes* species are also often found in habitats with closed canopies (Irawan & Rahadi 2016).

In the Gomphidae family, only one species was found, namely *Ictinogomphus decoratus* (Figure 4-A), and also only found in two locations, namely Pond and Reservoir. This is because at both locations, the members of the Gomphidae family have a stagnant aquatic ecosystem type and have tree vegetation and bamboo vegetation. This statement is supported by (Pamungkas 2016), who reported that the species

Ictinogomphus decoratus can be found in stagnant water habitats. In addition, the species *Ictinogomphus decoratus* is typically observed perched on the ends of dry branches, bamboo, or tree trunks (Rahadi et al. 2013; Setiyono et al. 2017).

Based on the evenness index analysis, the location with the most value is along the river, namely $E = 0.88$, and the lowest is the reservoir, namely $E = 0.45$ (Figure 7). Meanwhile, the highest dominance index is the reservoir with a value of $D = 0.24$ and the lowest is a pond with a value of $D = 0.13$ (Figure 7). The river location has the lowest evenness value because it has species with an abundance that is not much different, namely the species that has the highest number, namely *Pantala flavescens* (16 individuals), and the least *Brachythemis contaminata* and *Macrodiplax cora* with a total of 3 individuals. While the reservoir location has the lowest evenness value as well as the highest dominance value because at this location there is a species that dominates, namely *Brachythemis contaminata* with a total of 108 individuals.

Based on analysis of the Shannon-Wiener index, it shows that the highest value of dragonfly diversity is in a variety of habitats in Lakarsantri, namely at the observation location of Ponds with a value of $H' = 2.40$. Furthermore, at the reservoir location, namely $H' = 1.94$, the rice field location, namely $H' = 1.88$, and at the river observation location the location with the lowest dragonfly diversity index value with a value of $H' = 1.77$ (Figure 7). The difference in species diversity of dragonfly influences vary depending on the observation location, including the habitat type (Perez & Bautista 2020), microclimate (Borisov 2006), and vegetation (Silva et al. 2010).

At the location of the pond, 20 species from 4 families were found with a total of 463 individuals (Table 2). There are 6 species found only in this location, namely *Neurothemis feralis*, *Zyxomma obtusum*, *Ceriagrion*

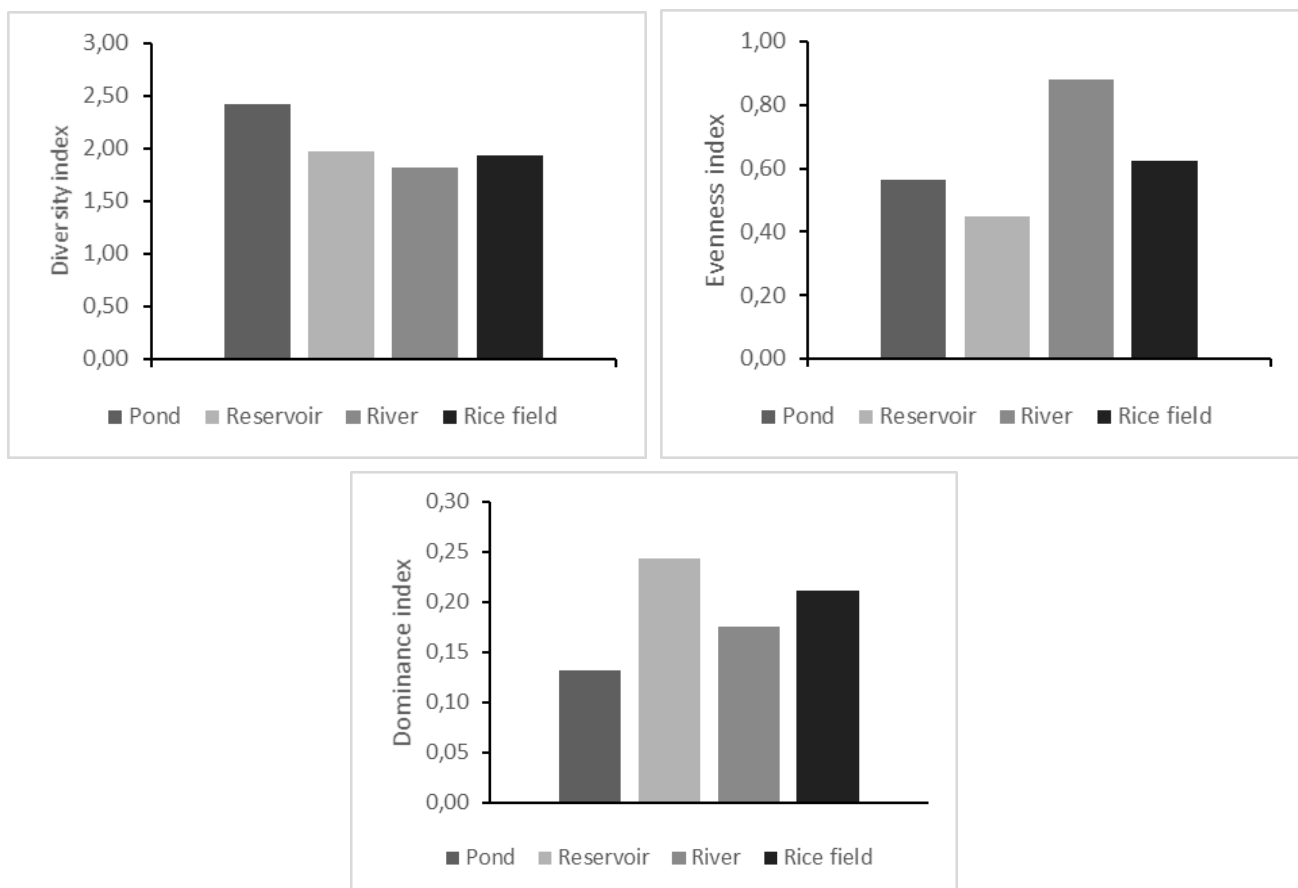


Figure 7. Result of diversity, evenness and dominance index.

praetermissum, *Pseudagrion nigrofasciatum*, *Pseudagrion rubriceps* dan *Copera marginipes*. The pond has the highest diversity index value of any research site (Figure 7), this can be because at this location a variety of vegetation supports the survival of dragonflies. The vegetation factor at the location of the pond is one of the important factors in a natural habitat for the dragonfly community (Nagy et al. 2019). Vegetation conditions are one of the key elements that significantly influences the presence and diversity of dragonfly species in a place. Some dragonfly families also need vegetation such as understory to lay eggs when breeding, especially the Suborder Zygoptera such as Coenagrionidae (Remmers et al. 2017). Additionally, plants along riverbanks are necessary for dragonfly larvae to find food and defend themselves from predators. Adult dragonflies use the vegetation on riverbanks as a perch, a place to sunbathe, and a place to rest (Silva et al. 2010).

There is some vegetation in the pond location, including aquatic plant vegetation, herb, and tree vegetation (Table 3), these three types of vegetation have different dragonfly community structures. The aquatic plant vegetation (*Ipomoea aquatica* and *Eichhornia crassipes*) found species of *Ceriagrion praetermissum*, *Pseudagrion rubriceps*, *Copera marginipes*, *Brachythemis contaminata*, *Rhodothemis rufa*, and *Ischnura senegalensis*. In the herb vegetation found on the banks (*Eleusine indica* dan *Pennisetum* sp.) and around the pond, species *Ischnura senegalensis*, *Agriocnemis pygmaea*, *Agriocnemis femina*, *Diplacodes trivialis*, *Acisoma panorpoides*, *Neurothemis feralis*, and *Orthetrum sabina* and was found. In addition, in the grass (*Eleusine indica*) vegetation which is quite dense at the edge of the pond, the species *Tholymis tillarga* was found. The presence of herbs (*Bambusa* sp.) and tree vegetation (*Ficus benjamina*, *Muntingia calabura*, and *Swietenia macrophylla*) at the pond location can be a factor in the discovery of *Ictinogomphus decoratus* and *Zyxomma obtusum* species in this study.

In addition to the vegetation factor, the pond location also has an open canopy condition and some locations have a closed canopy condition. The canopy is one of the important factors in the composition of the natural habitat of dragonflies. In the natural habitat of dragonflies, the canopy is one component that affects the diversity and abundance of dragonfly food sources, namely small insects (Davis et al. 2011). Some varieties of dragonflies need a canopy to shield them from excessively bright sunlight (Nugrahani et al. 2014). An open canopy at a location increases the light's intensity, which will change the area's air temperature. So that in open canopy conditions, dragonflies are usually used to sunbathe. Meanwhile, the denser canopy condition causes the speed of air temperature and the intensity of sunlight to not be hindered from entering. So in closed canopy conditions, dragonflies are usually used to rest (Paulson 2009).

Table 3. Types of plants at the research site.

No	Type	Plant Species	Pond	Reservoir	River	Rice field
1	Tree	<i>Ficus benjamina</i>	+	-	-	-
2	Tree	<i>Muntingia calabura</i>	+	+	-	-
3	Tree	<i>Swietenia macrophylla</i>	+	-	-	-
4	Herb	<i>Musa paradisiaca</i>	+	+	-	-
5	Herb	<i>Bambusa</i> sp.	+	+	-	-
6	Herb	<i>Pennisetum</i> sp.	++	++	+	-
7	Herb	<i>Eleusine indica</i>	++	+	++	+
8	Herb	<i>Oryza sativa</i>	-	-	-	++
9	Aquatic plant	<i>Ipomoea aquatica</i>	+	+	-	-
10	Aquatic plant	<i>Eichhornia crassipes</i>	+	-	++	-

The river is the research location in this study with the lowest diversity index value (Figure 3), with 7 species from 2 families found with a total of 62 individuals (Table 2). At the location, the river has a flowing water ecosystem type with a very open canopy condition with a sunlight intensity of 32767 lx (Figure 8). So that some species of dragonflies do not have a place to shelter when the sunlight intensity is very high. Therefore, the composition of dragonflies found in open areas mostly has the ability to adapt in places with high sunlight intensity. Species found at this location were *Agriocnemis femina*, *Ischnura senegalensis*, *Orthetrum sabina*, *Macrodiplax cora*, *Pantala flavescens*, *Crocothemis servilia* and *Brachythemis contaminata*.

Sunlight is one of the factors in providing dragonfly flying activity (Goforth 2010). This is because most dragonflies live diurnal and only fly in cloudy sunny conditions or at dusk (Samways 2008). In their natural habitat, dragonflies' activity is primarily influenced by the brightness of the light. Dragonflies will sunbathe and hunt for food at the ideal light intensity, but if the light is too high or too low, they will rest and seek shelter (Corbet 1962). In addition to the intensity of sunlight, which affects the presence and activity of dragonflies at a location are temperature (Schalkwyk et al. 2014) and humidity (Samraoui et al. 1998). Temperature and humidity also determine the activity of dragonflies to locate a place to rest, a time to fly, and a moment to mate (Corbet 1962).

Microclimate differences which include temperature, humidity, and light intensity at each location and time of observation, caused not all species to be found in the three repetitions in each month (Table 4). In addition, the flying ability of each dragonfly can also affect the difference in the presence of dragonflies in each repetition. This is because the roaming ability of each type of dragonfly is different and if it has a high cruising ability, it will have great potential to move locations easily.

In the analysis of this community structure study, there are abiotic factors that influence the community structure of the dragonfly. The sunlight intensity was negatively correlated with diversity index, abundance, and species richness of dragonflies (Figure 9). The intensity of sunlight greatly affects the abundance and species richness of dragonflies, the higher the light intensity, the lower the abundance and species richness. As the results of observations show, the river location, which has the highest sunlight intensity value (Figure 8), has the lowest species richness and abundance, namely 7 species and 62 individuals (Table 2). While the location with the lowest light intensity, namely a pond with an intensity value (Figure 8), has the highest species richness and abundance, namely 20 species and 463 individuals (Table 2). This can be because dragonflies generally have a sensitivity to sunlight intensity that is too high, but some species are resistant to high light intensity.

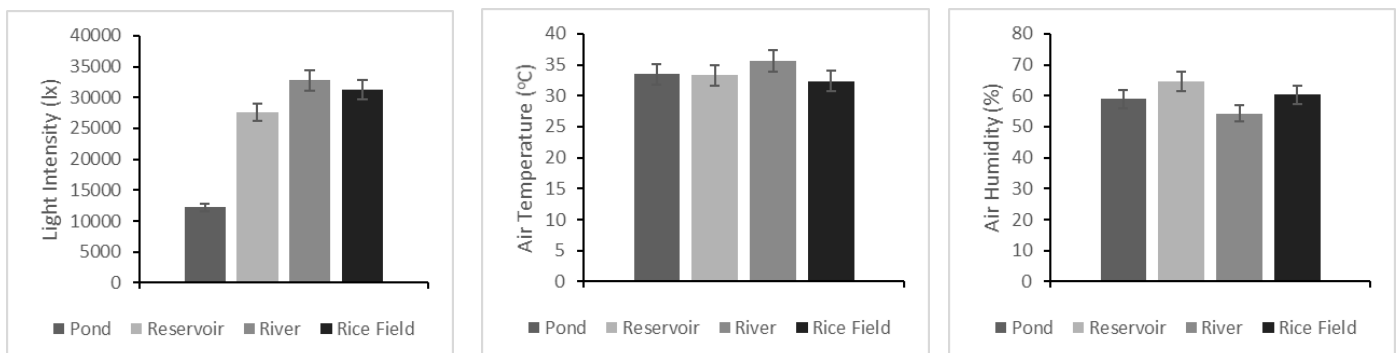


Figure 8. Results of light intensity, air temperature, and air humidity.

Table 4. Presence of species at three months.

Species	July				August				September			
	L1	L2	L3	L4	L1	L2	L3	L4	L1	L2	L3	L4
<i>Ictinogomphus decoratus</i>	√	√	-	-	√	√	-	-	-	√	-	-
<i>Acisoma panorpoides</i>	√	-	-	-	√	-	-	√	√	√	-	-
<i>Brachythemis contaminata</i>	√	√	√	√	√	√	-	√	√	√	-	√
<i>Brachydiplax chalybea</i>	√	√	-	-	√	√	-	-	√	√	-	-
<i>Crocothemis servilia</i>	√	√	√	√	√	√	√	-	√	√	√	√
<i>Diplacodes trivialis</i>	√	-	-	√	-	√	-	-	-	-	-	-
<i>Macrodiplax cora</i>	-	√	√	-	-	√	-	√	-	-	-	-
<i>Neurothemis feralis</i>	√	-	-	-	√	-	-	-	√	-	-	-
<i>Orthetrum sabina</i>	√	√	√	√	√	√	√	√	√	-	√	√
<i>Pantala flavescens</i>	-	√	√	√	-	-	√	-	-	√	-	-
<i>Potamarcha congener</i>	√	√	-	-	-	√	-	√	-	√	-	√
<i>Rhyothemis phyllis</i>	√	√	-	-	-	√	-	-	-	-	-	-
<i>Rhodothemis rufa</i>	√	√	-	-	-	√	-	√	√	-	-	-
<i>Tholymis tillarga</i>	√	√	-	√	√	-	-	-	√	-	-	-
<i>Zyxomma obtusum</i>	√	-	-	-	-	-	-	-	-	-	-	-
<i>Agriocnemis femina</i>	√	√	√	-	√	√	√	√	√	√	√	√
<i>Agriocnemis pygmaea</i>	√	√	-	-	-	-	-	-	-	-	-	-
<i>Ceriagrion praetermissum</i>	√	√	-	-	-	√	-	-	-	√	-	-
<i>Ischnura senegalensis</i>	√	√	√	-	√	√	√	-	√	-	√	-
<i>Pseudagrion nigrofasciatum</i>	√	-	-	-	√	-	-	-	-	-	-	-
<i>Pseudagrion rubriceps</i>	√	-	-	-	√	-	-	-	√	-	-	-
<i>Copera marginipes</i>	√	-	-	-	√	-	-	-	√	-	-	-

The intensity of sunlight has a negative correlation with the diversity index, so an index of sunlight intensity that is too high will cause a low catch of dragonflies. As the observation results show, the location of the river that has the highest sunlight intensity value has the lowest diversity index value, namely $H' = 1.77$ (Figure 7). Meanwhile, the pond location that has the lowest light intensity has the highest diversity index value, namely $H' = 2.40$ (Figure 7). This can be because dragonflies choose to rest and roost to avoid the high intensity of sunlight.

Humidity negatively correlates with the evenness index (Figure 9). This shows that the higher the humidity value, the lower the evenness of the dragonfly. As the observation results show, the results showed that the reservoir location which had the highest humidity value, namely 64.6% (Figure 8), had the lowest evenness index value, namely $E = 0.7$ (Figure 7). Meanwhile, the river location that has the lowest humidity value of 54.33% (Figure 8), has the highest index value of $E = 0.91$ (Figure 7). This can be because most species of dragonflies require sufficient humidity to support their flight activity. If the humidity value is too high, only certain species can survive, so the evenness value is low and a certain species dominance is formed.

The PCA analysis findings regarding the interaction between abiotic and abiotic factors to the structure of the dragonfly community showed that the two axes of the main components made up the total contribution of 95.01% (Figure 10). All variables have almost the same vector length, but the dominance, humidity, and evenness variables have longer vectors, which means that these 3 variables have more varied values than other variables. The light intensity variable (abiotic factor) with the dominance variable (biotic index) has a positive correlation (Figure 10). This shows that the higher the light intensity value, the

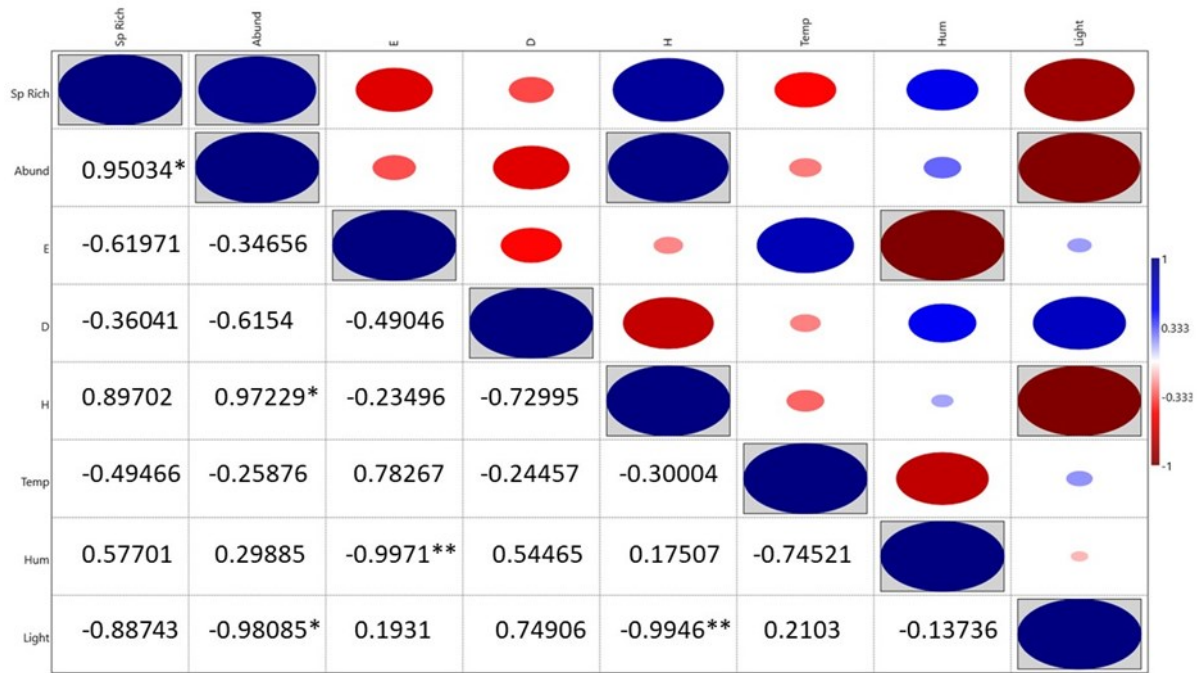


Figure 9. Correlation between biotic and abiotic factors at the research site. Sp rich = Species richness, Abund = Abundance, E = Evenness index, D = Dominance index, H' = Diversity index, Temp = Temperature, Hum = Humidity, and Light = Sunlight intensity. **significant >0.001, *significant 0.01-0.05.

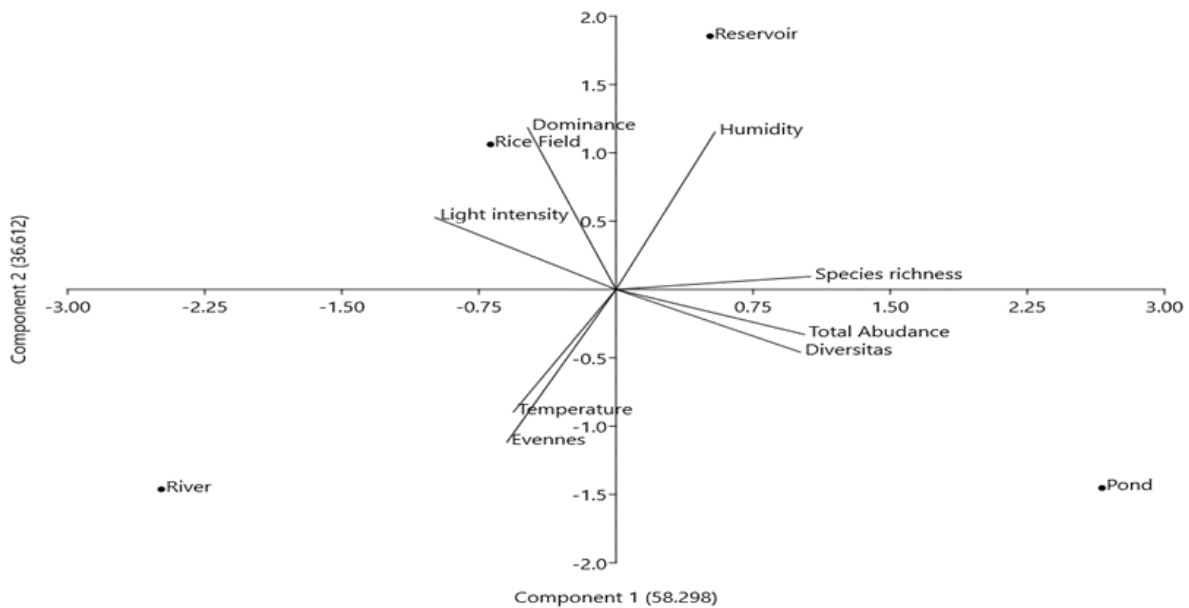


Figure 10. PCA ordinations of four locations.

higher the dominance index will be. This is because only certain species can adapt to high sunlight intensity, so that it will form the dominant of certain species and cause species diversity to be lower. In addition, air temperature also has a positive correlation with evenness index values.

CONCLUSION

The diversity of dragonflies found in various types of habitats in the Lakarsantri Sub-District includes 22 species from 4 families: Gomphidae, Libellulidae, Coenagrionidae, and Platycnemididae. Ponds are the observation sites that have the highest diversity index value, with a value of H' = 2.40, while the river location has the lowest diversity index value, with a

value of $H' = 1.77$. Because of the pond's location in stagnant waters with a variety of vegetation, this location has a composition of the dragonfly community structure that does not change quickly and has the highest diversity value. At the level of similarity in the composition of the dragonfly community structure, the location of the river has similarities to rice fields, while the location of the reservoir has the same level as ponds. This research shows that various aquatic ecosystems in urban areas can become natural habitats for dragonfly communities, especially pond ecosystems. Therefore, the quality of the aquatic environment in urban areas must be maintained so that dragonfly populations are maintained.

AUTHOR CONTRIBUTION

M.A.D.S designed the research, collected and analyzed the data, and wrote the manuscript, N.F.F. designed the research and supervised all the process, S.B designed the research, assisted in manuscript revision and supervised all the process.

ACKNOWLEDGEMENTS

The authors would like to thank the KUTRIK entomology study group. We also thank M. Iqbal Pratama, Ahmad Alfin Romzalis, Najwa Maulidina Putri, Okta Fina Arianti, Fachrul Asaddin Nuri A., and Yudha Ari Setiawan who participated in the field data collection process. Thank to Najmatul Millah, Siti Zulaikha, Satria Febriansyah, and Zainul Muttaqin Sany who have helped in the writing process. Especially thanks to the late Muhibbuddin Abdillah who helped me learn about dragonflies.

CONFLICT OF INTEREST

The authors declare there is no conflict of interest in any part of this research.

REFERENCES

- Borisov, S.N., 2006. Adaptations of dragonflies (Odonata) under desert conditions. *Entomological Review*, 86(5), pp.534–543
- Buczyński, P. et al., 2020. Dragonflies (Odonata) of the city of Lublin (Eastern Poland). *Polish Journal of Entomology*, 89(3), pp.153–180. doi: 10.5604/01.3001.0014.4239.
- Choong, C.Y. et al., 2020. Diversity of Odonata Species at Kangkawat, Imbak Canyon, Sabah. *Journal of Tropical Biology and Conservation*, 17, pp.1–10.
- Corbet, P.S., 1962. *A BIOLOGY OF DRAGONFLIES*, H. F. & G. WITHERBY LTD.
- Dalia, B.P.I. & Leksono, A.S., 2014. Interaksi antara capung dengan arthropoda dan vertebrata predator di kepanjen, kabupaten malang. *Jurnal Biotropika*, 2(1), pp.26–30.
- Davis, A.J., Sutton, S.L. & Brendell, M.J.D., 2011. Vertical distribution of beetles in a tropical rainforest in Sulawesi : the role of the canopy in contributing to biodiversity. *Sepilok Bulletin*, 13(14), pp.59–83.
- Dolný, A. et al., 2012. Aquatic insects indicate terrestrial habitat degradation: changes in taxonomical structure and functional diversity of dragonflies in tropical rainforest of East Kalimantan. *Tropical Zoology*, 25(3), pp.141–157. doi: 10.1080/03946975.2012.717480.
- Furtado, J.I., 1974. The reproductive behaviour of *Copera marginipes* (Rambur) and *C. vittata acutimargo* (Kruger) (Zygoptera: Platycnemididae). *Odonatologica*, 3(3), pp.167–177.

- Goforth, C.L., 2010. Behavioural responses of *Enallagma* to changes in weather (Zygoptera: Coenagrionidae). *Odonatologica*, 39(3), pp.225–234.
- Haissofi, E.M. et al., 2015. Contribution to the knowledge of the Moroccan Odonata, with first records of *Orthetrum sabina*, and an overview of first and last dates for all species. *Odonatologica*, 44(3), pp.225–254.
- Haritonov, A. & Popova, O., 2011. Spatial displacement of Odonata in south-west Siberia. *International Journal of Odonatology*, 14(1), pp.1–10. doi: 10.1080/13887890.2011.568188.
- Irawan, A. & Rahadi, W.S., 2016. *Capung Sumba*, Balai Taman Nasional Manupeu Tanah Daru dan Laiwangi Wanggameti.
- IUCN, 2021. Dragonflies threatened as wetlands around the world disappear - IUCN Red List. viewed June 14, 2022 from <https://www.iucn.org/news/species/202112/dragonflies-threatened-wetlands-around-world-disappear-iucn-red-list>.
- IUCN, 2022. The IUCN Red List of Threatened Species, viewed June 10, 2022 from <https://www.iucnredlist.org/en>.
- Kalita, G.J. & Ray, S.D., 2015. Studies on the diversity and habitat preference of odonates in Deepor Beel Bird Sanctuary , Kamrup , Assam. *Journal of Entomology and Zoology Studies*, 3(2), pp.278–285.
- Kalkman, V.J. & Orr, A.G., 2013. Field Guide to the damselflies of New Guinea Buku Panduan Lapangan Capung Jarum untuk Wilayah New Guinea. *Brachytron*, 16(2), pp.3–118.
- Kandibane, M., Raguraman, S. & Ganapathy, N., 2005. Relative abundance and diversity of odonata in an irrigated rice field of Madurai, Tamil Nadu. *Zoos' Print Journal*, 20(11), pp.2051–2052. doi: 10.11609/jott.zpj.1293.2051-2.
- Koneri, R., Angoy, R.N. & Iahaan, M.J.S., 2022. Species Diversity Of Dragonflies on The Sangihe Islands, North Sulawesi, Indonesia. *Applied Ecology And Environmental Research*, 20(2), pp.1763–1780. doi: 10.15666/aer/2002_17631780.
- Kulkarni, A.S. & Subramanian, K.A., 2013. Habitat and seasonal distribution of Odonata (Insecta) of Mula and Mutha river basins , Maharashtra , India Habitat and seasonal distribution of Odonata (Insecta) of Mula and Mutha river basins , Maharashtra , India. *Journal of Threatened Taxa*, 5(7), pp.4084–4095. doi: 10.11609/JoTT.o3253.4084-95.
- Kumar, A., 1984. Studies on the life history of Indian dragonflies, *Diplacodes trivialis* (Rambur, 1842). *Records of the Zoological Survey of India*, 81(3 & 4), pp.13–22.
- Lieftinck, M., 1934. An Annotated List of the Odonata of Java, With Notes on Their Distribution, Habits and Life-History. *Treubia*, 14 (3).
- Magurran, A.E., 2004. *Ecological Diversity and Its Measurement*, USA: Chapman and Hall.
- Maldonado-Benítez, N., Mariani-Ríos, A. & Ramírez, A., 2022. Effects of urbanization on Odonata assemblages in tropical island streams in San Juan, Puerto Rico. *International Journal of Odonatology*, 25, pp.31–42. doi: 10.48156/1388.2022.1917163.
- Metcalf, J.L., 1989. Biological water quality assessment of running waters based on microinvertebrates communities: History and present status in Europe. *Environ*, pp.101–139.
- Nagy, H.B. et al., 2019. Landscape-scale terrestrial factors are also vital in shaping odonata assemblages of watercourses. *Scientific reports*, 9 (1), pp.1–8. doi: 10.1038/s41598-019-54628-7.

- Nicolla, A.C. et al., 2021. Comparison of Damselfly (Odonata : Zygoptera) diversity in wet dune slack habitat with canopied and non-canopied areas of Gumuk Pasir Parangkusumo , Yogyakarta , Indonesia. In *IOP Conference Series: Earth and Environmental Science*. doi: 10.1088/1755-1315/736/1/012046.
- Nugrahani, M.P. et al., 2014. *Peluit Tanda Bahaya: Capung Indikator Lingkungan Panduan Penilaian Kualitas Lingkungan Melalui Capung*, Yogyakarta: Indonesia Dragonfly Society.
- Oppel, S., 2006. Using distance sampling to quantify Odonata density in tropical rainforests. *International Journal of Odonatology*, 9(1), pp.81–88.
- Orr, A.G., 2005. *Dragonflies of Peninsular Malaysia and Singapore*, Natural History Publication. Kota Kinabalu.
- Orr, A.G. & Kalkman, V.J., 2015. *Field guide to the dragonflies of New Guinea Buku Panduan Lapangan Capung Jarum untuk Wilayah New Guinea*, Brachytron.
- Pamungkas, B.C., 2016. *UNTRING: Dragonflies of Banyuwangi*, Yogyakarta: Indonesian Dragonfly Society.
- Paulson, D., 2009. *Dragonflies and Damselflies of the West*, Princeton University Press.
- Perez, E.S.N. & Bautista, M.G., 2020. Dragonflies in the City: Diversity of Odonates in Urban Davao, Philippines. *Journal of Agricultural Science and Technology A*, 10(1), pp.12–19. doi: 10.17265/2161-6256/2020.01.002.
- Rahadi, W.S. et al., 2013. *Naga terbang Wendit: keanekaragaman capung perairan Wendit, Malang, Jawa Timur*, Indonesia Dragonfly Society.
- Remmers, W. et al., 2017. Elephant (*Loxodonta africana*) footprints as habitat for aquatic Elephant (*Loxodonta africana*) footprints as habitat for aquatic macroinvertebrate communities in Kibale. *African journal of ecology*, 55(3), pp.342–351. doi: 10.1111/aje.12358.
- Samraoui, B. et al., 1998. Postponed reproductive maturation in upland refuges maintains life-cycle continuity during the hot, dry season in Algerian dragonflies (Anisoptera). *International Journal of Odonatology*, 1(2), pp.119–135. doi: 10.1080/13887890.1998.9748100.
- Samways, M.J., 2008. *Dragonflies and damselflies of South Africa*, Pensoft Publishers.
- Schalkwyk, J. Van, Samways, M.J. & Pryke, J.S., 2014. Winter survival by dragonfly adults in the Cape Floristic Region. *International Journal of Odonatology*, 17(1), pp.17–30. doi: 10.1080/13887890.2014.880382.
- Setiyono, J. et al., 2017. *Dragonfly of Yogyakarta*, Yogyakarta: Indonesia Dragonfly Society.
- Silva, D. de paiva, De Marco, P. & Resende, D.C., 2010. Adult odonate abundance and community assemblage measures as indicators of stream ecological integrity: A case study. *Ecological Indicators*, 10 (3), pp.744–752. doi: 10.1016/j.ecolind.2009.12.004.
- Tang, H.B., Wang, L.K. & Hämäläinen, M., 2010. *A photographic guide to the dragonflies of Singapore*, Department of Biological Sciences, National University of Singapore.
- Vilenica, M. & Mihaljević, Z., 2022. Odonata Assemblages in Anthropogenically Impacted Habitats in the Drava River-A Long-Term Study. doi: 10.3390/w14193119.

Research Article

Diversity and Distribution of *Ficus* (Moraceae) in The Karst Ecosystem of Bantimurung Bulusaraung National Park

Yelastri Yelastri¹, Sulistijorini Sulistijorini^{2*}, Nina Ratna Djuita²

1)Plant Biology Graduate Program, Department of Biology, Faculty of Mathematics and Natural Science, IPB University, Jl. Raya Dramaga, Bogor, West Java, 16680, Indonesia.

2)Department of Biology, Faculty of Mathematics and Natural Science, IPB University, Jl. Raya Dramaga, Bogor, West Java, 16680, Indonesia.

* Corresponding author, email: sulistijorini@apps.ipb.ac.id

Keywords:

Conservation

Ficus ecology

keystone species

Principal Component Analysis

Submitted:

02 November 2022

Accepted:

30 January 2023

Published:

12 May 2023

Editor:

Miftahul Ilmi

ABSTRACT

Bantimurung Bulusaraung National Park is an area that has the largest karst ecosystem in Indonesia. Karst is prone to damage and difficult to reuse, so it requires conservation efforts. One of the plant species that can maintain this sustainability is *Ficus* which acts as key species in karst ecosystems. However, at this time the species is experiencing disturbances, one of which is due to the experience of invasive plants that can threaten the existence of *Ficus* because the weeds can colonize habitats and are dominant which can change species diversity. This study aimed to analyze the diversity and distribution of *Ficus*, compare species composition, and analyze environmental factors that affect *Ficus* spp. in Pattunuang Resort and Bantimurung Resort. Vegetation analysis method with nesting plots placed by purposive sampling and supported with environmental and soil data measurements to determine the factors that indicate the habitat preference of *Ficus*. We found 18 plant species of *Ficus* spp. in total. At Resort Pattunuang we found 14 *Ficus* species with the highest abundance being *Ficus sunndaica* (27.55%), while we recorded 15 *Ficus* species at Resort Bantimurung with the highest abundance being *Ficus ampelas* (29.23%). *Ficus* species were uniformly distributed with a relatively high ratio of species composition in both resorts. Principal Component Analysis (PCA) showed that the presence of *Ficus* in Pattunuang Resort is influenced by wind speed, soil temperature, air temperature, soil moisture, soil pH, and air humidity. In Bantimurung Resort, the existence of *Ficus* is influenced by wind speed, soil temperature, soil moisture, and air humidity.

Copyright: © 2023, J. Tropical Biodiversity Biotechnology (CC BY-SA 4.0)

INTRODUCTION

Karst areas cover approximately 12-15% of the world's total land area (Zhao et al. 2014; Zhu et al. 2017; Liu et al. 2020), providing water supply for 25% of the world's water population (Bystriakova et al. 2019). Karst landscapes are formed due to the dissolution of rocks (Waele 2016; Sun et al. 2018), which are dominated by carbonate rocks consisting of calcite as the main mineral (Retnowati et al. 2014). Indonesia, with a land area of around 1.919.440 km², has a karst area of approximately 154.000 km² in total (Cahyadi 2017), or equal to 8% of the total land area of Indonesia. One of these Indonesian karst areas is in South Sulawesi, the largest karst area in Indonesia and the second largest karst area in the

world after China (Achmad & Hamzah 2016). The area is located in Pangkep Regency and Maros Regency with a part of the area included in the Bantimurung Bulusaraung National Park. The area of Bantimurung Bulusaraung National Park is $\pm 437,5$ km² with a karst area of 228 km² which has a geological expanse in the form of a distinctive and unique landscape and landform with the main characteristic of a karst shape that resembling a tower (karst tower). The topographical terrain of this area is the form of rock outcrops, karst caves, sinkholes, and underground rivers (Pepe & Parise 2014).

The diversity of a species is one of the essential things in ecology because it is related to ecosystem function (Zhenming et al. 2020). One of the supporting plants in the ecosystem is a plant originating from the *Ficus* genus (Moraceae), which acts as a key species because it has a major impact on the ecosystem as a food source and animal habitat. In addition, *Ficus* a root system that can store water reserves and can maintain slope, and also has a lush canopy that can absorb CO₂ in the air (Hao et al. 2016; Hendrayana et al. 2021). *Ficus* is a widely distributed pantropical plant with high diversity (Harrison et al. 2012; Wijaya & Defiani 2021). These species can be distinguished from other plant species by their unique fruit called syconium. The fruit is the enlarged part of the receptacle and contains hundreds of tiny flowers (Berg & Wiebes 1992). In addition, the fruit has a hole called an ostiole as an entrance after the compound is released to attract specific pollinators (Harrison & Rasplus 2006). Insects can only pollinate *Ficus* from the Agaonidae, Hymenoptera, and Chalcidoidea families (Serrato et al. 2004; Pothasin et al. 2014; Chiang et al. 2018). *Ficus* has 735 species spread throughout the world (Berg & Corner 2005; Bain et al. 2015), 367 *Ficus* species are found in the Malesiana area, 81 species are found in Sulawesi (Berg & Corner 2005), and 47 species are found in Bantimurung Bulusaraung National Park (Achmad & Hamzah 2016).

Ficus is a plant that is a key species because it can bear fruit throughout the year, so it becomes a food source when natural resources are scarce (Shanahan & Compton 2001; Tello, 2003; Pothasin et al. 2014). However, the existence of *Ficus* in Bantimurung Bulusaraung National Park is experiencing disturbance due to invasive plants threatening the existence of *Ficus* (BKSDAE 2017). Invasive plants can colonize a habitat and become dominant, which can change the composition of species diversity and even cause the extinction of native species unable to compete. These have a sustainable impact on the existence of *Macaca maura*, *Aceros cassidix*, and *Strigocuscus celebensis* as endemic animals of Sulawesi which are protected because *Ficus* is a source of food for these animals (Kinnaird et al. 1996; Dwiyahreni et al. 1999; Labahi 2021). Ecological studies of *Ficus* as a key species are still limited which causes the lack of information to carry out efforts to protect and conserve the species. Conservation of species is essential to consider the status of Bantimurung Bulusaraung National Park, which is currently included in the UNESCO Global Geoparks. Therefore, this study aimed to analyze the diversity and distribution of *Ficus*, compare its species composition, and analyze abiotic factor of habitat preferences of *Ficus* in Pattunuang Resort and Bantimurung Resort.

MATERIALS AND METHODS

Study Site

This research was conducted from January 2022 to June 2022 in the karst ecosystem of Pattunuang Resort and Bantimurung Resort, Bantimurung Bulusaraung National Park, Maros Regency, South Sulawesi

(Figure 1). Bantimurung Bulusaraung National Park has seven resorts. The highest area of the region is in the North Bulusaraung Mountain with an altitude of 1.565 m asl (Bantimurung Bulusaraung National Park Hall (BTNBB) 2016).

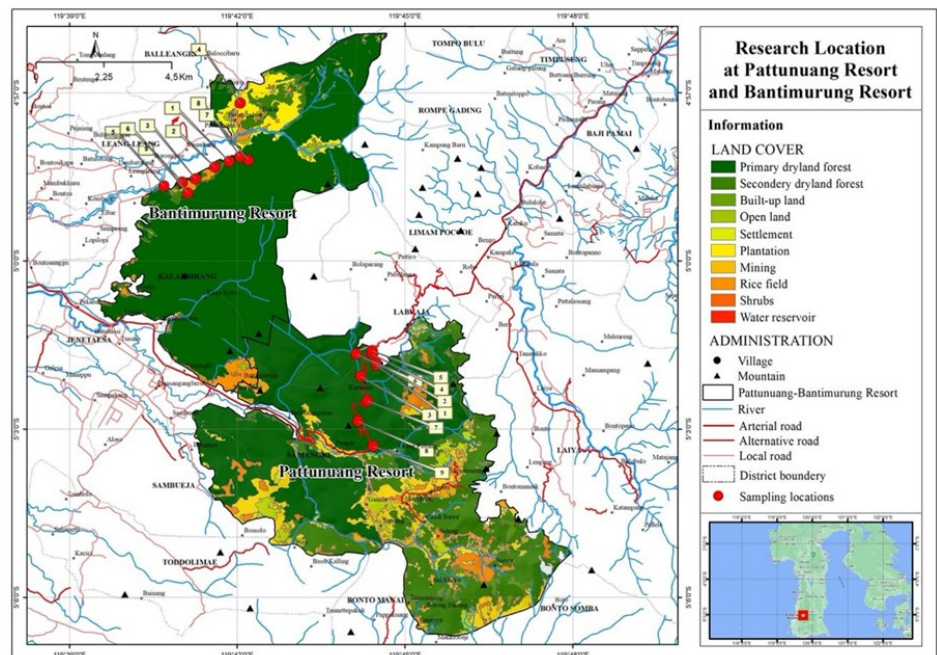


Figure 1. Sampling locations at Pattunuang Resort dan Bantimurung Resort.

Materials and Methods

Vegetation data were collected using the roaming method to determine field conditions and the presence of *Ficus* (Serrato et al. 2004). Each location that is considered representative of the population is made into multilevel square plots which are placed by purposive sampling with an undetermined distance between plots because the sampling is based on the presence of *Ficus* in the field (Tongco 2007). Plot sizes used are 20 m x 20 m for trees, 10 m x 10 m for poles, 5 m x 5 m for saplings, and 2 m x 2 m for seedlings (Mueller-Dombois & Ellenberg 1974). At Pattunuang Resort and Bantimurung Resort, 9 plots were made using the same method.

The collected microclimate data were air humidity, air temperature, light intensity, and wind speed. These microclimate data were measured using a 4 in 1 environmental tester. Collected soil data consisted of soil temperature, soil pH, and soil moisture and were measured using a soil tester. In addition, soil texture identification and chemical analysis were carried out by taking 1 kg of soil samples at each sampling location and then composited and tested in the laboratory for nutrient content and soil texture.

Data Analysis

Ficus spp. was identified based on Flora Malesiana *Ficus* (Berg & Corner 2005). Other plant species were identified in the Flora Malesiana (Flora Malesiana 2022). The accepted species naming system follows the species classification on the Plants of The World (POWO 2022). The calculation of the Important Value Index (INP) with the accumulative parameters of relative density, relative frequency, and relative dominance was following Cox (1978). The calculation of the Summed Dominance Ratio (SDR) by dividing the INP value with the number of parameters that compile the INP (Kusmana 2017). Other calculations of biodiversity index parameters

such as the Shannon-Wiener Diversity Index (H') (Krebs 1989), the Margelaf Wealth Index (R) (Magurran 2004), the Evenness Index (E) (Magurran 1988), and the Dominance Index (C) (Misra 1988) was processed using Past software version 4.03 (Hammer et al. 2001). The species distribution was analyzed using the Morisita Index (Brower et al. 1989) and the vertical distribution of species was analyzed using the Past software version 4.03. Microclimate data were analyzed using Principal Component Analysis with R software version 4.0.4. (Husson et al. 2017).

RESULTS AND DISCUSSION

Species Diversity of *Ficus* spp.

The identification results show that Pattunuang Resort contains as many as 14 species of *Ficus* spp. we found as many as 15 species of *Ficus* at Bantimurung. Berg & Corner (2005) stated that *Ficus* has six subgenera: *Ficus*, *Pharmacosycea*, *Sycidium*, *Sycomorus*, *Urostigma* and *Synoecia* distinguished by basis of the vegetative parts and the exterior of the fruit. There were 1 species of *Ficus* found from the *Ficus* subgenus, 2 species of *Pharmacosycea* subgenus, 5 species of *Sycidium* subgenus, 4 species of *Sycomorus* subgenus, and 6 species of *Urostigma* subgenus (Table 1). The number of *Ficus* individuals observed was 103 individuals from both resorts.

Table 1. Diversity of *Ficus* spp. at Pattunuang Resort and Bantimurung Resort.

Species	Reproduction system	FR (%)	Growth phase	Plant height (m)*
Subgenus <i>Ficus</i>				
<i>Ficus fulva</i> Reinw ex. Blume ^B	Gyno ¹	1,16	Tr	20
Subgenus <i>Pharmacosycea</i>				
<i>Ficus albipila</i> (Miq.) King ^A	Mono ²	2,33	Tr	40
<i>Ficus callosa</i> Willd. ^{AB}	Mono ³	9,30	Tr	45
Subgenus <i>Sycidium</i>				
<i>Ficus ampelas</i> Burm f. ^{AB}	Dioe ⁴	12,79	Tr	15 – 25
<i>Ficus pisifera</i> Wall ex. Voigt ^B	Dioe ⁵	9,30	Tr, Sp	10
<i>Ficus gul</i> K.Schum. & Lauterb. ^{AB}	Dioe ⁶	5,81	Tr, Sp	25
<i>Ficus obscura</i> Blume ^{AB}	Dioe ¹	3,49	Tr, Pl, Sp	8
<i>Ficus subulata</i> Blume ^A	Dioe ¹	4,65	Tr	15
Subgenus <i>Sycomorus</i>				
<i>Ficus fistulosa</i> Reinw ex. Blume ^B	Dioe ⁷	3,49	Sp	10 – 18
<i>Ficus septica</i> Burm.f. ^B	Dioe	1,16	Tr	25
<i>Ficus racemosa</i> L. ^{AB}	Mono ⁹	3,49	Tr	30
<i>Ficus variegata</i> Blume ^{AB}	Dioe ⁸	4,65	Tr	40
Subgenus <i>Urostigma</i>				
<i>Ficus benjamina</i> L. ^{AB}	Mono ¹⁰	3,49	Tr	35
<i>Ficus callophylla</i> Blume ^{AB}	Mono ¹¹	4,65	Tr	25
<i>Ficus drupacea</i> Thunb. ^{AB}	Mono ⁷	8,14	Tr	35
<i>Ficus sumatrana</i> Miq. ^A	Mono ¹¹	2,33	Tr	30
<i>Ficus sundaica</i> Blume ^{AB}	Mono ¹⁰	11,63	Tr	35
<i>Ficus virens</i> Aiton ^{AB}	Mono ¹²	8,14	Tr	35

FR: relative frequency; m: meter; A: Pattunuang Resort; B: Bantimurung Resort; Gyno: gynodioecious; Dioe: dioecious; Mono: monoecious; (1) Shanahan & Compton (2001); (2) Weiblen (2000); (3) Tarachai et al. (2011); (4) Bain et al. (2013); (5) Huang et al. (2019); (6) Wijaya & Defiani (2021); (7) Corlett (2006); (8) Bain et al. (2015); (9) Teixeira et al. (2018); (10) Harrison (2008); (11) Shanahan (2000); (12) Fu et al. (2017); Tr: Tree; Pl: Pole; Sp: Sapling; (*): Berg & Corner (2005).

The recorded growth phase *Ficus* in the study sites are trees, poles, and saplings. The seedling growth phase was not found in the study sites. The relation between the presence of *Ficus* in nature and frugivore is an influential factor in seed distribution. The different sizes of fruit have implications for the frugivorous species that feed on them. *Ficus* fruit is mainly eaten by birds and is placed in the tree canopy so that it is easy to germinate because it is exposed to direct sunlight. In mammals, frugivores with a larger size require more food. In addition, these frugivores travel longer distances. Therefore, *Ficus* seeds are not found close to the tree (Shanahan 2000). Competition with understory plants in obtaining nutrients and sunlight access to the forest floor makes it difficult for *Ficus* to grow and develop (Rodrigues et al. 2018), so the seedling phase is not found.

Most of the recorded *Ficus* species belong to the subgenus *Urostigma*. All species of *Urostigma* are monoecious that live as hemi-epiphytes by starting the life phase in the tree canopy. Species of the subgenus *Urostigma* are easily pollinated because male and female flowers are in the same fruit. Therefore, their presence is found throughout the year. Fruits of the subgenus *Urostigma* are eaten and carried by birds with comprehensive mobility, so *Ficus* of *Urostigma* is found in both resorts except *F. sumatrana* (Berg & Corner 2005). Species from the subgenus *Synoecia* were not found in this study. All species of the subgenus *Synoecia* live as climbers. This can be caused by several factors, such as the ability of the host tree to get sunlight, the frequency of trees suitable for plant development, features of the bark of plants (Berg & Corner 2005), and stagnant development due to shade so that not all trees are suitable for use as a tree host (Harrison 2005).

Distribution of *Ficus* spp. at Pattunuang Resort and Bantimurung Resort

Pattunuang Resort has a hilly topography with less dense vegetation conditions. Some of Sulawesi's endemic animals are in the area, such as *Macaca maura* and *Tarsius fuscus*, so this location is often used as an animal observation area. Bantimurung Resort has a more open land cover and denser vegetation. Bantimurung Resort has several natural attractions, one of which is the famous natural tourist attraction Bantimurung like The Kingdom of Butterfly. *Ficus* INP values that exceeded or equal to 20% are presented in Table 2.

Pattunuang Resort is dominated by *F. sundaica*, *F. callophylla*, and *F. subulata*. *Ficus sundaica* and *F. callophylla* are subgenus *Urostigma* species that are distributed mainly by birds and arboreal mammals, so these species are commonly found in the study site. *Ficus sundaica* and *F. callophylla* live as epiphytes in the tree canopy. Seeds carried by animals are stored in gaps or tree trunks that support growth and development. *Ficus subulata* belongs to the subgenus *Sycidium* and is a common species found in large forest areas. *Ficus subulata* can produce a massive number of fruits. This species can serve as a refuge area and a niche for some frugivores by forming dense branches (Wijaya & Defiani 2021). The three *Ficus* species were found to have tree trunk diameters of more than 50 cm such as *F. benjamina*, *F. callosa*, and *F. variegata* with deep roots. The root system of *Ficus* can maintain the integrity of the slope so that it can act as erosion control (Vannoppen et al. 2017; Chen et al. 2022).

Bantimurung Resort was dominated by *F. ampelas*, *F. virens*, and *F. drupacea*. *Ficus ampelas* belongs to the subgenus *Sycidium*, a species that inhabits primary and secondary forests and is eaten by birds that forage under tree canopies. *Ficus virens* and *F. drupacea* are species from the sub-

Table 2. Composition of *Ficus* spp. at Pattunuang Resort and Bantimurung Resort with INP values that exceeded or equal to 20%.

Location	Growth	Species	KR (%)	FR (%)	DR (%)	INP (%)
PTN	Tree	<i>Ficus sundaica</i>	5,88	7,35	14,32	27,55
		<i>Ficus callophylla</i>	2,35	2,94	18,50	23,79
		<i>Ficus subulata</i>	5,88	5,88	11,26	23,02
BTM	Tree	<i>Ficus ampelas</i>	6,85	8,47	13,90	29,23
		<i>Ficus virens</i>	8,22	10,17	9,93	28,32
		<i>Ficus drupacea</i>	6,85	8,47	8,18	23,51
	Pole	<i>Ficus pisifera</i>	14,71	10,34	14,82	39,87
	Sappling	<i>Ficus pisifera</i>	4,30	7,55	11,67	23,52

PTN: Pattunuang Resort; BTM: Bantimurung Resort; KR: relative density; FR: relative frequency; DR: relative dominance; INP: important index value.

genus *Urostigma*, categorized as potential and high-potential species. They are consumed by animals that forage above and under the tree canopy, so their presence is often found due to having many fruit dispersal agents (Rahayuningsih et al. 2020). *Ficus pisifera* was found to dominate the growth phase of the poles and saplings in Bantimurung Resort. This species has small fruit with a diameter of less than 5 cm. It is consumed by animals that forage under the tree canopy (Cruaud et al. 2012) with mobility that is not too far from where it forages. Possibly this is why the species is only found in Bantimurung Resort only. Various index values that indicate *Ficus* diversity in the Pattunuang Resort and Bantimurung Resort are shown in Figure 2 and Figure 3 respectively.

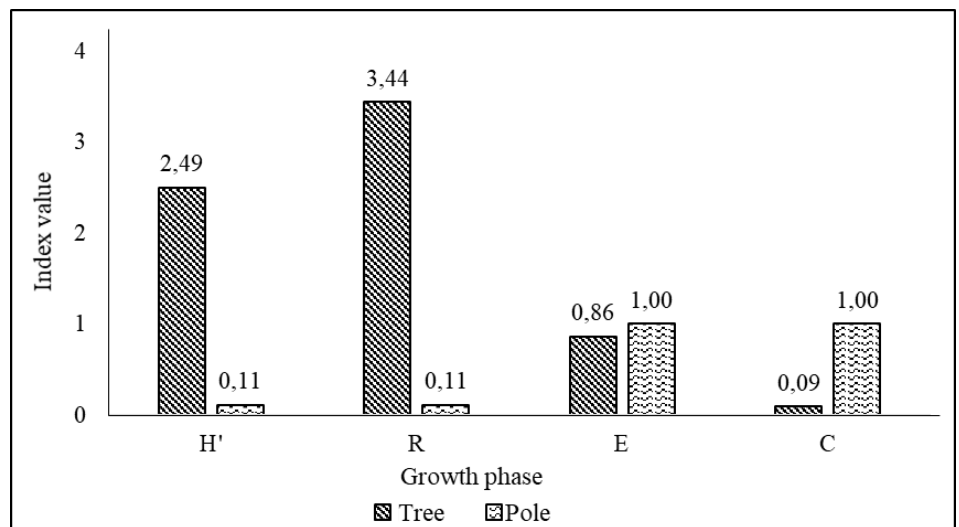


Figure 2. Diversity of *Ficus* spp. at Pattunuang Resort; H': species diversity; R: species richness; E: species evenness; C: species dominance.

The diversity (H') of *Ficus* at Pattunuang Resort for the tree and pole phases is classified as moderate with an index value of more than 1 and less than 3. In contrast, the pole has a low category because the index value is less than 1. Species richness (R) for all growth phases shows a value of less than 3.5 which indicates that the species richness is low. The level of evenness (E) in all growth phases shows a value close to 1, indicating that all species are evenly distributed. The dominance (C) in the tree phase is close to 0, which indicates that there is less concentration of species in the tree growth phase. In contrast, the dominance value of the pole is near to 1, indicating that *Ficus* in the pole phase is the dominant concentration in the Pattunuang Resort.

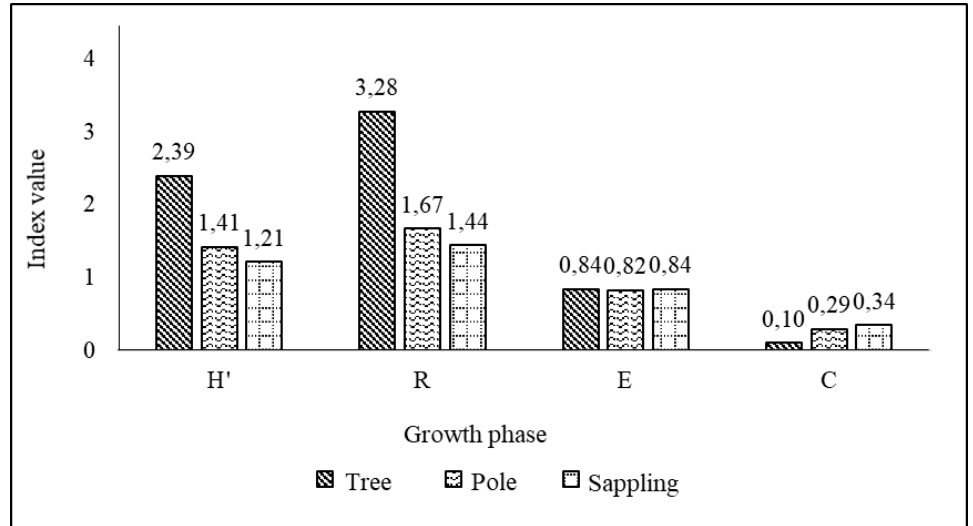


Figure 3. Diversity of *Ficus* spp. at Bantimurung Resort; H': species diversity; R: species richness; E: species evenness; C: species dominance.

The diversity (H') of *Ficus* at Bantimurung Resort for all growth phases is moderate because it has an index value greater than 1 but below 3. Species richness (R) is low because it shows a value of less than 3,5 for all growth phases. The level of evenness (E) in all growth phases shows a value close to 1, indicating that all species are evenly distributed. That is in line with a dominance value close to 0, which indicates no particular dominant growth phases of *Ficus* species in Bantimurung Resort.

Based on the data analysis, it was found that *Ficus* spp. has a uniform distribution pattern in both resorts. The relevant index value are presented in Table 3.

The distribution pattern of *Ficus* spp. has a uniform pattern, shown by the value of the Standardized Morisita Index (Ip) below 0. The distribution with a uniform pattern was also found in the study of [Geekiyana et al. \(2019\)](#), which shows that tree species with non-random distribution patterns found in karst areas are closely related to their edaphic variations. The uniform distribution pattern occurs due to competition between individuals which causes equal or even distribution of space so that there is no tendency to group. In addition, the uniform distribution pattern is associated with a specific pollination system ([Harrison et al. 2012](#)). *Ficus* distribution is often found in the tropics and thrives in the lowlands ([Bain et al. 2015](#)). Bantimurung Bulusaraung National Park with an altitude of 1,565 m asl is similar to the *Ficus* habitat elevation as stated by [Berg and Corner \(2005\)](#) that *Ficus* mainly grows on plains of 1,500 m asl. The vertical distribution of *Ficus* was found evenly along the elevation gradient of the sampling locations at both resorts. The distribution can be seen in Figure 4.

In the field, exploration results found *Ficus* at an altitude of 35 – 334 m asl (Figure 4). *Ficus* at altitudes 0-100 m asl found 15 species at an altitude of 100-200 m asl, as many as 9 species, at an altitude of 200-300 m asl found 8 species, and at an altitude of 300-400 m asl there were 10 species. *Ficus ampelas* is a species found at an altitude of 36 m asl and is a species found at the lowest location. *Ficus obscura* is a species found at the highest location with an altitude of 334 m asl. *Ficus albipila* and *F. sumatrana* are species found in almost every altitude interval. *Ficus albipila* is a large tree species and is often found because its disperser insects can regularly spread seeds over long distances ([Harrison & Rasplus 2006](#)). *Ficus sumatrana* is a species that has various morphological variations so that it is easy to adapt, including at different altitudes ([Berg & Corner 2005](#)).

Table 3. Composition of *Ficus* spp. at Pattunuang Resort and Bantimurung Resort.

Resort name	Disperse Morisita index (Id)	Uniform index (Mu)	Clumped index (Mc)	Standard Morisita index (Ip)	Distribution pattern
PTN	0,91	0,87	1,22	-0,32	Uniform
BTM	0,86	0,85	1,25	-0,45	Uniform

PTN: Pattunuang Resort; BTM: Bantimurung Resort.

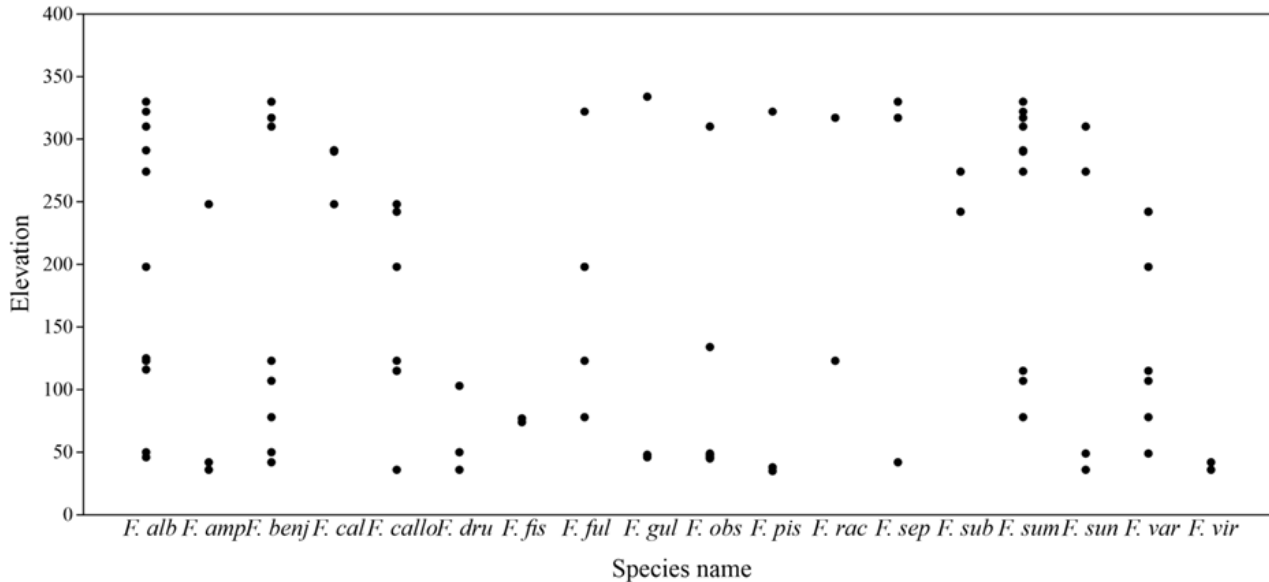


Figure 4. Vertical distribution of *Ficus* spp. at Pattunuang Resort and Bantimurung Resort; F. alb: *F. albipila*; F. amp: *F. ampelas*; F. benj: *F. benjamina*; F. cal: *F. callosa*; F. callo: *F. callophylla*; F. dru: *F. drupacea*; F. fis: *F. fistulosa*; F. ful: *F. fulva*; F. gul: *F. gul*; F. obs: *F. obscura*; F. pis: *F. pisifera*; F. rac: *F. racemosa*; F. sep: *F. septica*; F. sub: *F. subulata*; F. sum: *F. sumatrana*; F. var: *F. variegata*; F. vir: *F. virens*.

Organisms that occupy the same space tend to be dependent on and influence each other so that if there is a disturbance to the organism and its environment, it will affect the community as a whole (Barbour et al. 1987). The studied forest area dominated by karst hills and rocks, makes *Ficus* can only be observed along the observation path. A total of 11 species of *Ficus* spp. was found in both observation resorts, namely *F. ampelas*, *F. benjamina*, *F. callophylla*, *F. callosa*, *F. drupacea*, *F. gul*, *F. obscura*, *F. racemosa*, *F. sundaica*, *F. variegata*, and *F. virens*.

The species similarity at both locations is indicated by the Jaccard similarity index value is 61% which illustrates the similarity of *Ficus* spp. between the two resorts is high based on the criteria by Mueller-Dombois & Ellenberg (2016). The presence of the same species indicates that *Ficus* can occupy ample space and grow well in extreme karst environments. Achmad & Hamzah (2016) found as many as 47 species of *Ficus* spp. scattered throughout the Bantimurung Bulusaraung National Park area and in this study 18 species were found, indicating that the recorded species of *Ficus* spp. in this study is equal to 38% of the total *Ficus* in Bantimurung Bulusaraung National Park.

Habitat Characteristics as Habitat Preference of *Ficus* spp.

Ficus is widely distributed in the tropics, including in the karst ecosystem. The distribution can be influenced by the suitability between environmental conditions (such as light intensity, soil, wind, and humidity) and the character possessed by plant species. The ability to grow well and develop in *Ficus* makes it used as an important species in karst slope

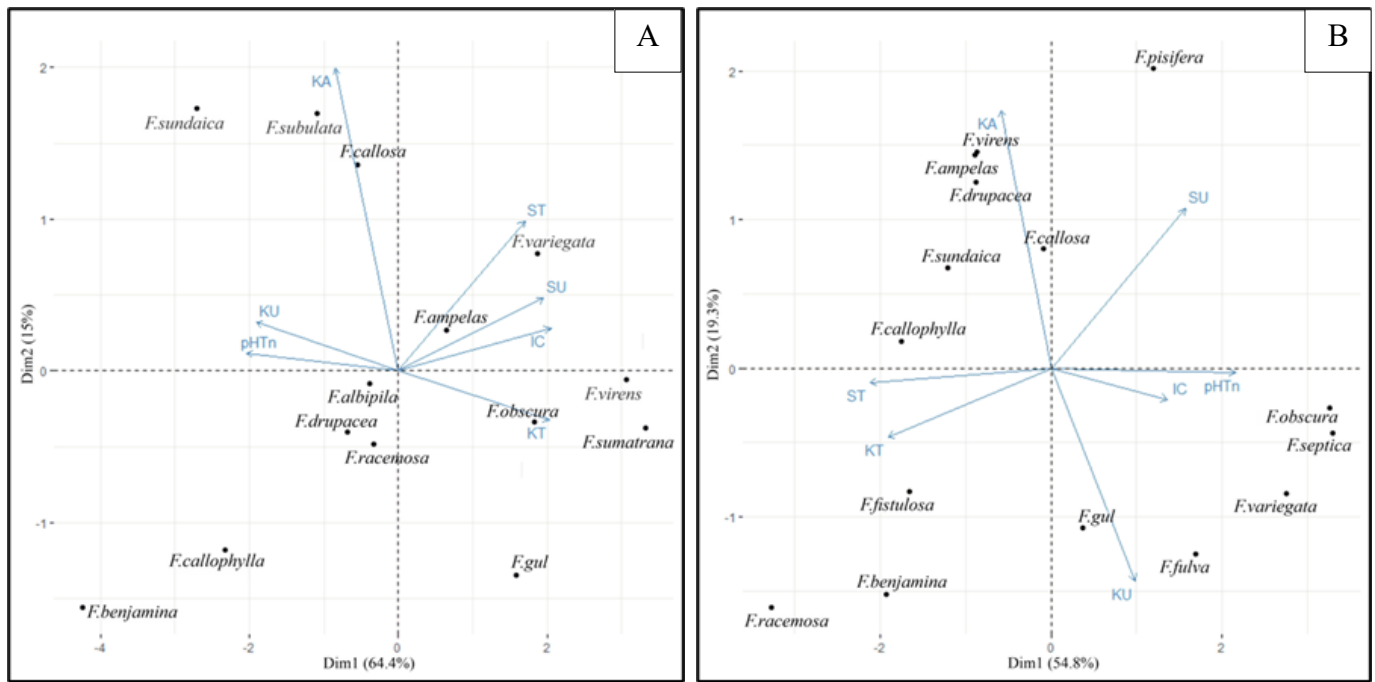


Figure 5. A: Pattunuang Resorts; B: Bantimurung Resorts; IC: light intensity; SU: air temperature; ST: soil temperature; KA: wind velocity; KU: air humidity; pHTn: soil pH; soil moisture.

areas to prevent erosion (Chen et al. 2022). The existence of *Ficus* is often used as an indicator of the process of forest succession because of its flexibility to grow as epiphytes, hemi-epiphytes, and trees, as well as efficient pollination that lasts for a long time, making it considered a pioneer plants (Berg & Corner 2005). PCA results that indicate the relation of environmental characteristics with the presence of *Ficus* spp. can be seen in Figure 5.

Pattunuang Resort (Figure 5A) has an eigenvalue of 4,51 (Dim 1) and 1,05 (Dim 2), respectively. Dim 1 explains 64,4% of data diversity and Dim 2 explains 15% of data diversity. *Ficus sundaica*, *F. drupacea*, *F. racemosa*, *F. callophylla*, *F. benjamina*, *F. gul*, *F. sumatrana*, and *F. virens* are far from vectors of environmental factors, so there are no environmental factors that precisely characterize the existence of the species. In contrast to *F. subulata* and *F. callosa* were influenced by wind speed. Soil temperature and air temperature influence the presence of *F. variegata* and *F. ampelas*. The presence of *F. obscura* is influenced by soil moisture. Air humidity and soil pH influence the presence of *F. albipila*. Bantimurung Resort (Figure 5B) has an eigenvalue of 3,83 (Dim 1) and 1,34 (Dim 2), respectively Dim 1 explains 54,8% and Dim 2 explains 19,3% of data diversity. *Ficus sundaica*, *F. benjamina*, *F. racemosa*, *F. variegata*, *F. septica*, *F. obscura*, and *F. pisifera* are far from vectors of environmental factors. Hence, the existence of these species is not significantly influenced by environmental factors. Wind speed affected the species of *F. virens*, *F. ampelas*, *F. drupacea*, and *F. callosa*. Soil temperature influences the presence of *F. callophylla*. Soil moisture affects *F. fistulosa*. The presence of *F. gul* and *F. fulva* was influenced by air humidity.

Environmental factors that have been grouped into PCA show the results of species based on the seven environmental factors, the majority have a distribution of *Ficus* spp. uniformly distributed species. Various environmental factors play an essential role in the distribution of a plant species (Körner 2007). None of the *Ficus* found in the study site were dominant because the overall INP values of *Ficus* were below 40%. BKS-DAE South Sulawesi has reported that the presence of *Ficus* is threatened

Table 4. The results of the analysis of chemical properties of soil texture.

Parameters	PTN		BTM	
	Value	Criteria*	Value	Criteria*
Soil texture		Clay loam		Clay loam
Soil pH [±]	6,43	Slightly acid	6,55	Slightly acid
C-Org (%)	1,73	Low	1,57	Low
N-Total (%)	0,17	Low	0,11	Low
Rasio C/N	10	Low	14	Medium
P ₂ O ₅ Olsen (ppm)	9,81	Low	12,48	Medium
Ca (cmol _c /kg)	5,63	Medium	4,95	Low
Mg (cmol _c /kg)	1,69	Medium	1,06	Medium
K (cmol _c /kg)	0,47	Medium	0,28	Low
Na (cmol _c /kg)	0,18	Low	0,11	Low
SO ₄ (ppm)	25,32	Low	24,19	Low
KTK (cmol _c /kg)	23,95	Medium	19,69	Medium
KB (%)	33	Low	33	Low

PTN: Pattunuang Resort; BTM: Bantimurung Resort; ±: measurement data in field; *: criteria fo assessing the results of soil analysis according to [Eviati & Sulaeman \(2009\)](#).

by invasive species. *Spathodea campanulata* is an invasive species in Bantimurung Bulusaraung National Park ([BKSDAE 2017](#)). That species can grow and spread significantly through the production of up to 1.000 seeds per fruit and having the ability to develop vegetatively by stolons. The results of the composite soil analysis are shown in Table 4.

The analysis showed that the soil conditions were not significantly different at the two resorts. The two resorts criteria for different soil nutrients are the C/N ratio, P₂O₅, Ca, and K content. Karstification is a long-term phenomenon that affects the heterogeneity of nutrients along the topography of the karst ecosystem ([Geekiyanage et al. 2019](#)) so that some pathways in carbonate rocks result in faster soil leaching, causing reduced nutrient availability ([Zhang et al. 2007](#)). On the other hand, soil nutrient elements with medium and low criteria can indicate the presence of allelopathic compounds caused by invasive species. Lack of nutrients can lead to deficiencies in plants, making them unproductive ([Osman 2013](#)).

Conservation Strategy of *Ficus* spp. as Key Species of Karst Ecosystem in Bantimurung Bulusaraung National Park

Bantimurung Bulusaraung National Park has three main ecosystem types: karst ecosystems, non-dipterocarp rainforest ecosystem, and low mountain ecosystems. This type of ecosystem describes a high diversity and abundance of plant as reported by [Achmad & Hamzah \(2016\)](#). The peculiarities and uniqueness of the karst ecosystem store the potential that can be developed as an object and natural tourist attraction. All this potential is in the utilization zone known as The Seven Wonder ([BTNBB 2016](#)). Karst can be degraded due to geological activities, climate, and utilization, so vegetation is considered necessary to prevent damage.

Conservation of natural resources is a continuous conservation and protection activity that is carried out so that ecological processes are maintained. Conservation is carried out to deal with the biodiversity crisis ([Heywood & Iriondo 2003](#)). Based on the International Union for Conservation of Nature shows that all *Ficus* species found in this study have Least Concern conservation status ([IUCN 2022](#)), which means all species have been evaluated except *F. pisifera* and *F. callosa* which do not has a conservation status because it has not been evaluated (Table 5).

Table 5. Conservation status of *Ficus* spp. at Pattunuang Resort and Bantimurung Resort.

No.	Species	SDR (%)	Conservation status	Last reviewed
1	<i>Ficus sundaica</i>	8,05	Least Concern	2019
2	<i>Ficus pisifera</i>	7,84	-	-
3	<i>Ficus subulata</i>	7,67	Least Concern	2018
4	<i>Ficus variegata</i>	5,62	Least Concern	2018
5	<i>Ficus callosa</i>	5,50	-	-
6	<i>Ficus callophylla</i>	5,28	Least Concern	2018
7	<i>Ficus virens</i>	5,19	Least Concern	2018
8	<i>Ficus drupacea</i>	4,98	Least Concern	2018
9	<i>Ficus ampelas</i>	4,97	Least Concern	2018
10	<i>Ficus fistulosa</i>	4,52	Least Concern	2018
11	<i>Ficus albipila</i>	3,17	Least Concern	2019
12	<i>Ficus racemosa</i>	3,16	Least Concern	2018
13	<i>Ficus sumatrana</i>	3,14	Least Concern	2018
14	<i>Ficus gul</i>	2,49	Least Concern	2018
15	<i>Ficus benjamina</i>	2,30	Least Concern	2018
16	<i>Ficus obscura</i>	2,02	Least Concern	2018
17	<i>Ficus septica</i>	1,55	Least Concern	2018
18	<i>Ficus fulva</i>	1,42	Least Concern	2018

SDR: summed dominance ratio.

Ficus spp. at Pattunuang Resort and Bantimurung Resort show the highest dominance of 8% based on the Summed Dominance Ratio (SDR) value derived from the accumulated values of relative density, relative frequency, and relative dominance (Table 5). The SDR value illustrates the amount of control of a species over other species in the community (Kusmana 2017). Although *Ficus* is not a dominating species, its presence in the karst ecosystem has a significant role in maintaining the balance of the ecosystem. One of them is to provide food for protected animals such as *Macaca maura*, *Tarsius fuscus*, *Aceros cassidix*, *Ailurops ursinus*, and *Cervus timorensis* (Shanahan & Compton 2001).

Ficus is a threatened species due to the presence of *Spathodea campanulata* as an invasive species in the karst area of Bantimurung Bulusaraung National Park (BKSDAE 2017), making it necessary to conserve even though it is still listed in the IUCN Red List with Least Concern (LC) status. This is in line with the Bantimurung Bulusaraung National Park Long Term Management Plan 2016-2025 to realize the ideal governance of the area, maintain the karst ecosystem and its biodiversity, and improve ecosystem functions (BTNBB 2016). The study of *Ficus* diversity and distribution that has been carried out in this study provides information about efforts to achieve this. Conservation activities have implications for maintaining ecological processes, genetic diversity, and sustainable use of species and ecosystem.

CONCLUSIONS

There are 18 species of *Ficus* spp. found at Pattunuang Resort and Bantimurung Resort. Pattunuang Resort and Bantimurung Resort have a diversity index classified as moderate because the value of H' is more than 1 and less than 3. *Ficus* spp. uniformly distributed in both resorts. Comparison of the species composition of *Ficus* spp. classified as high in both Resorts with an IS_j value of 61%. Environmental factors affecting *Ficus* presence in Pattunuang Resort are wind speed, soil temperature, air temperature, soil moisture, soil pH, and air humidity. The presence of *Ficus* in Bantimurung Resort is influenced by wind speed, soil temperature, soil moisture, and air humidity.

AUTHOR CONTRIBUTIONS

In this research, Y, S, and RND designed research; Y has been tasked with sampling and observing the existence of *Ficus* and its ecological character in the field, data analysis, and manuscript writing. S and NRD supervised the identification process in the laboratory, data analysis, manuscript writing, and editing

ACKNOWLEDGMENTS

The authors would like to express their deepest gratitude to Lembaga Pengelola Dana Pendidikan (LPDP)/ Indonesian Endowment Fund for Education under The Ministry of Finance of Republic of Indonesia for the funding of this research.

CONFLICT OF INTEREST

There is no conflict of interest in this research.

REFERENCES

- Achmad, A. & Hamzah, A.S., 2016. *Database karst Sulawesi Selatan*. Makassar: Badan Lingkungan Hidup Daerah Provinsi Sulawesi Selatan.
- Bain, A., Harrison, R.D. & Schatz, B., 2013. How to be an ant on figs. *Acta Oecologica*, 1–12. doi: 10.1016/j.actao.2013.05.006.
- Bain, A., Tzeng, H., Wu, W. & Chou, L., 2015. *Ficus* (Moraceae) and fig wasps (hymenoptera: chalcidoidea) in Taiwan. *Bot Stud.*, 56(11), pp.1–12. doi: 10.1186/s40529-015-0090-x.
- Balai Konservasi Sumber Daya Alam dan Ekosistem (BKSDAE), 2017. *Tumbuhan alien menggerogoti ekosistem karst TN Bantimurung Bulusaraung* viewed 10 February 2022, from <http://ksdae.menlhk.go.id/info/2681/tumbuhan-alien-menggerogoti-ekosistem-karst-tn-bantimurung-bulusaraung.html>.
- Balai Taman Nasional Bantimurung Bulusaraung (BTNBB), 2016. *Rencana pengelolaan jangka panjang TN Bantimurung Bulusaraung periode tahun 2016 s/d 2025*. Maros: Direktorat Konservasi Sumber Daya Alam dan Ekosistem
- Barbour, M.G., Burk, J.H. & Pitts, W.D., 1987. *Methods of sampling the plant community*. San Fransisco: Benjamin/Cummings Publishing.
- Berg, C.C. & Corner, E.J.H., 2005. Moraceae: ficeae. In *Flora malesiana series I Volume 17, Part 2*. Belanda: The National Herbarium of Netherlands.
- Berg, C.C. & Wiebes, J.T., 1992. *African fig trees AND figs wasps*, Netherland: Koninklijke Nederlandse Akademie van Wetenschappen.
- Brower, J.E., Zar, J.H. & Ende, C.N.V., 1989. *Field and laboratory method for general ecology fourth edition*, USA: McGraw-Hill.
- Bystriakova, N. et al., 2019. A preliminary evaluation of the karst flora of Brazil using collections data. *Sci Rep.*, 9, pp.1–13. doi: 10.1038/s41598-019-53104-6.
- Cahyadi, A., 2017. Pengelolaan kawasan karst dan peranannya dalam siklus karbon di Indonesia. *Seminar Nasional Perubahan Iklim di Indonesia*, pp.1–14.
- Chen, Y. et al., 2022. Root tensile strength of terrace hedgerow plants in the karst trough valleys of SW China: Relation with root morphology and fiber content. *Int Soil Water Conserv Res*, 10(4), pp.677–686. doi: 10.1016/j.iswcr.2022.01.008.
- Chiang, Y.P. et al., 2018. Adaptive phenology of *Ficus subpisocarpa* and *Ficus caulocarpa* in Taipei, Taiwan. *Acta Oecologica*, 90, pp.35–45. doi: 10.1016/j.actao.2017.11.013.

- Corlett, R.T., 2006. Figs (*Ficus*, Moraceae) in urban Hong Kong, south China. *Biotropica*, 38(1), pp.116–121. doi: 10.1111/j.1744-7429.2006.00109.x.
- Cox, G.W., 1978. *Laboratory manual of general ecology*, New York: WMC Brown.
- Cruaud, A. et al., 2012. An extreme case of plant-insect codiversification: figs and fig-pollinating wasps. *Syst Biol.*, 61(6), pp.1029–1047. doi:10.1093/sysbio/sys068.
- Dwiyahreni, A.A. et al., 1999. Diet and activity of the bear cuscus, *Ailurops ursinus*, in North Sulawesi, Indonesia. *J Mammal.*, 80(3), pp.905–912. doi: 10.2307/1383259.
- Eviati & Sulaeman, 2009. Analisis Kimia Tanah, Tanaman, Air dan Pupuk. In *Petunjuk Teknis Edisi 2*. Bogor: Balai Penelitian Tanah.
- Flora Malesiana, 2022. *Flora Malesiana*, viewed 1 March 2022, from <https://floramalesiana.org/new/>.
- Fu, R.H. et al., 2017. Development of fifteen polymorphic microsatellite markers for *Ficus virens* (Moraceae). *Appl Plant Sci.*, 5(1), 1600101. doi: 10.3732/apps.1600101.
- Geekiyange, N. et al., 2019. Plant ecology of tropical and subtropical karst ecosystems. *Wiley Biotropica*, 51(5), pp.626–640. doi: 10.1111/btp.12696.
- Hammer, Ø., Harper, D.A.T. & Ryan, P.D., 2001. PAST: Paleontological statistic software package for education and data analysis. *Palaeontol Electron.*, 4(1), pp. 1–9.
- Hao, G.Y., Cao, K.F., & Goldstein, G., 2016. Hemiepiphytic trees: *Ficus* as a model system for understanding hemiepiphytes. In *Tropical Tree Physiol.* Switzerland: Springer, Cham, pp.3–24. doi: 10.1007/978-3-319-27422-5_1.
- Harrison, R.D., 2005. Fig and the diversity of tropical rainforest. *BioScience*, 55(12), pp.1053–1064.
- Harrison, R.D., 2008. Adaptive significance of phenological variation among monoecious hemi-epiphytic figs in Borneo. *Symbiosis*, 45, pp.83–90.
- Harrison, R.D. & Rasplus, J.Y., 2006. Dispersal of fig pollinators in Asian tropical rain forests. *Journal of Tropical Ecology*, 22, pp.631–639. doi: 10.1017/S0266467406003488.
- Harrison, R.D. et al., 2012. Evolution of fruit traits in *Ficus* subgenus *Sycomor* (Moraceae): To what extent do frugivores determine seed dispersal mode? *PLoS ONE*, 7(6), e38432. doi: 10.1371/journal.pone.0038432.
- Hendrayana, Y. et al., 2021. Distribution and association of *Ficus* spp. in the shrubs area of Gunung Ciremai National Park Indonesia. *IOP Conf. Ser.: Earth Environ. Sci.*, 819, 012078. doi: 10.1088/1755-1315/819/1/012078.
- Heywood, V.H. & Iriondo, J.M., 2003. Plant conservation: old problems, new perspectives. *Biol Conserv.*, 113(3), pp.321–335. doi: 10.1016/S0006-3207(03)00121-6.
- Huang, Y.T. et al., 2019. Fruiting phenology and nutrient content variation among sympatric figs and the ecological correlates. *Bot. Stud.*, 60, 27. doi: 10.1186/s40529-019-0275-9.
- Husson, F. et al., 2017. *FactoMineR: Multivariate Exploratory Data Analysis and Data Mining*, viewed 17 June 2022 from <https://CRAN.R-project.org/package=FactoMineR>.
- International Union for Conservation of Nature (IUCN), 2022. *The IUCN Red List of Threatened Species*, viewed 1 May 2022, from <https://www.iucnredlist.org/>.

- Kinnaird, M.F., O'Brien, T.G. & Suryadi, S., 1996. Population fluctuation in sulawesi red-knobbed hornbills: tracking figs in space and time. *Am Ornithol Union.*, 113(2), pp.431–440. doi: 10.2307/4088909.
- Körner, C., 2007. The use of altitude in ecological research. *Trends Ecol Evol.*, 15(11), pp.513–514. doi: 10.1016/j.tree.2007.09.006.
- Krebs, C.J., 1989. *Ecological methodology*, New York: Harper Collins.
- Kusmana, C., 2017. *Metode survey dan interpretasi data ekologi*, Bogor: Bogor Agricultural University.
- Labahi, P.A., 2021. Behavior of sulawesi black monkey (*Macaca maura*): a case study of attacking behavior in agricultural plants. *IOP Conf. Ser.: Earth Environ. Sci.*, 788, 012089. doi: 10.1088/1755-1315/788/1/012089.
- Liu, Y. et al., 2020. An assessment of soil's nutrient deficiencies and their influence on the restoration of degraded karst vegetation in Southwest China. *Forests*, 11(8), 797. doi: 10.3390/f11080797.
- Magurran, A.E., 2004. *Measuring biological diversity*, USA: Blackwell.
- Magurran, A.E., 1988. The Commonness, and Rarity, of Species. In *Measuring Biological Diversity*. United Kingdom: TJ International, Padstow, Cornwall.
- Misra, K.C., 1988. *Manual of plant ecology second edition*, New York: Oxford and IBH Pub. Co.
- Mueller-Dombois, D. & Ellenberg, H., 1974. *Aims and methods of vegetation ecology*, USA: John Wiley & Sons, Inc. doi: 10.2307/213332.
- Mueller-Dombois, D. & Ellenberg, H., 2016. *Ekologi vegetasi: tujuan dan metode*, Jakarta: LIPI Pr, pp.1–638.
- Osman, K.T., 2013. *Soils: principles, properties and management*, Springer Dordrecht, pp.129–159. doi: 10.1007/978-94-007-5663-2.
- Pepe, M. & Parise, M., 2014. Structural control on development of karst landscape in the salento peninsula (Apulia, se Italy). *Acta Carsologica*, 43(1), pp.101–114. doi: 10.3986/ac.v43i1.643.
- Plant of the world (POWO), 2022. *Plant of the world*, viewed 1 March 2022, from <https://powo.science.kew.org/>.
- Pothasin, P., Compton, S.G. & Wangpakapattanawong, P., 2014. Riparian *Ficus* tree communities: the distribution and abundance of riparian fig tree in Northern Thailand. *PLoS ONE*, 9(10), e108945. doi: 10.1371/journal.pone.0108945.
- Rahayuningsih, M., Kurniawan, F.H. & Kartijono, N.E., 2020. The potential of *Ficus* species as frugivorous feed on Gentong Hill, Mount Ungaran, Indonesia. *For Ideas.*, 26(2), pp.540–548.
- Retnowati, A. et al., 2014. Environmental ethics in local knowledge responding to climate change: an understanding of seasonal traditional calendar pranoto mongso and its phenology in karst area of Gunung Kidul, Yogyakarta, Indonesia. *Procedia Environ Sci.*, 20, pp.785–794. doi: 10.1016/j.proenv.2014.03.095.
- Rodrigues, P.M.S. et al., 2018. Effects of soil on vegetation structure and plant diversity in different savanna and tropical forest habitats. *J Plant Ecol.*, 11(2), pp.226–236. doi: 10.1093/jpe/rtw135
- Serrato, A., Ibarra-Manríquez, G. & Oyama, K., 2004. Biogeography and conservation of the genus *Ficus* (Moraceae) in Mexico. *Journal of Biogeography*, 31, pp.475–485. doi: 10.1046/j.0305-0270.2003.01039.x.
- Shanahan, M. & Compton, S. G., 2001. Vertical stratification of figs and fig-eaters in a Bornean lowland rain forest: How is the canopy different? *Plant Ecol.*, 153(1–2), pp.121–132. doi: 10.1023/A:1017537707010.

- Shanahan, M.J., 2000. *Ficus Seed Dispersal Guilds: Ecology, Evolution and Conservation Implications*. The University of Leeds.
- Sun, S. et al., 2018. Karst development mechanism and characteristics based on comprehensive exploration along Jinan Metro, China. *Sustainability*, 10(10), 3383. doi: 10.3390/su10103383.
- Tarachai, Y. et al., 2011. Diversity of figs and their pollinators in Chiang Mai Province, Thailand. *Chiang Mai J Sci*, 38(4), pp.638–647.
- Teixeira, S.P. et al., 2018. Morphological diversity and function of the stigma in *Ficus* species (Moraceae). *Acta Oecologica*, 90, pp.117–131. doi: 10.1016/j.actao.2018.02.008.
- Tello, J.G., 2003. Frugivores at a fruiting *Ficus* in south-eastern Peru. *J Trop Ecol.*, 19, pp.717–721. doi: 10.1017/S0266467403006114.
- Tongco, M.D.C., 2007. Purposive sampling as a tool for informant selection. *Ethnobotany research and applications*, 5, pp.147–158. doi: 10.17348/era.5.0.147-158.
- Vannoppen, W. et al., 2017. How do root and soil characteristics affect the erosion-reducing potential of plant species? *Ecol Eng.*, 109, pp. 186–195. doi: 10.1016/j.ecoleng.2017.08.001.
- Waele, J.D., 2016. Karst processes and landforms. In *International Encyclopedia of Geography: People, the Earth, Environment and Technology*. John Wiley & Sons. doi: 10.1002/9781118786352.wbieg0968.
- Weiblen, G.D., 2000. Phylogenetic relationships of functionally dioecious *Ficus* (Moraceae) based on ribosomal DNA sequences and morphology. *Am J Bot.*, 87(9), pp.1342–1357. doi: 10.2307/2656726.
- Wijaya, I.M.S. & Defiani, M.R., 2021. Diversity and distribution of figs (*Ficus*: Moraceae) in Gianyar District, Bali, Indonesia. *Biodiversitas*, 22(1), pp.233–246. doi: 10.13057/biodiv/d220129.
- Zhang, W. et al., 2007. The heterogeneity and its influencing factors of soil nutrients in peak-cluster depression areas of karst region. *Agric Sci China.*, 6(3), pp.322–329. doi: 10.1016/S1671-2927(07)60052-2.
- Zhao, J. et al., 2014. The soil biota composition along a progressive succession of secondary vegetation in a karst area. *PLoS ONE*, 9(11), e112436. doi: 10.1371/journal.pone.0112436.
- Zhenming, Z., Xianfei, H. & Yingying, L., 2020. Species composition and diversity of plants at different successional stages in small catchments of karst areas. *Pakistan J Bot.*, 52(2), pp.551–556. doi: 10.30848/PJB2020-2(33).
- Zhu, X. et al., 2017. Humus soil as a critical driver of flora conversion on karst rock outcrops. *Sci Rep.*, 7, 12611. doi: 10.1038/s41598-017-13060-5.

Research Article

Butterfly Diversity from Isolated Lowland Area: An Assessment in Langsa Urban Forest, Langsa, Aceh, Indonesia

Herlina Putri Endah Sari^{1*}, Andri Yusman Persada¹, Wendy Achmmad Mustaqim^{1,2}, Kartika Aprilia Putri¹, Imti Yazil Wafa³

1)Department of Biology, Faculty of Engineering, Universitas Samudra, Langsa, Aceh 24416, Indonesia

2)Forum Pohon Langka Indonesia, Bogor, West Java, Indonesia

3)Sahabat Kupu-Kupu Indonesia, Komunitas Penggiat Kupu-kupu, Malang, East Java, Indonesia

* Corresponding author, email: herlinaputriendahsari@unsam.ac.id

Keywords:

conservation
diversity
lowland urban forest
Sumatra
urban butterfly

Submitted:

12 May 2022

Accepted:

02 February 2023

Published:

17 May 2023

Editor:

Ardaning Nuriliani

ABSTRACT

Langsa Urban Forest (LUF) is a 10-ha of the isolated urban forest in Langsa, Aceh, which is maintained to preserve urban biodiversity such as the butterfly. No recent study has been done in this area on butterfly biodiversity including the diversity and plant's potential for host and food plant sources. A one-month survey in July 2021 using the standard walk method on four transects was conducted. There are 36 species recorded during this study including 5 families, with Nymphalidae as the most abundant family and *Leptosia nina* as the most abundant species. Shannon-Wiener diversity index was used for this recent research with the value of H' 1.78–2.78 and the Evenness index with scale 0.66–0.94. Most of the species have broad geographical ranges, with 3 of them restricted to the Indomalayan realm. There are 117 plants were recorded which 33 species supposed as host and food plants divided into 26 as host plants, 11 as food plants, and 4 for both. No specific plants threatened the collected butterflies, but it's important since providing diversity data.

Copyright: © 2023, J. Tropical Biodiversity Biotechnology (CC BY-SA 4.0)

INTRODUCTION

Butterflies (Papilionoidea) comprise *c.* 17,000 species worldwide, with *c.* 2,000 of them found in Indonesia (Peggie & Amir 2006), with all known 7 families occurring i.e Papilionidae, Hedyliidae, Hesperidae, Lycaenidae, Nymphalidae, Pieridae and Riodinidae (Kawahara & Breinholt 2014; EOL 2022), and is the most studied group among insects (Panjaitan et al. 2020). Butterflies are very important in ecosystems because of their role in plants' pollination (Peggie & Amir 2006), and as a component of food webs. Meanwhile, the larvae are often categorized as pests (Nair et al. 2014; Panjaitan et al. 2020). Oftentimes, butterflies are appreciated for their beauty, and therefore, often used as a subject to optimize ecotourism (Subahar & Yuliana 2010; Kurnianto et al. 2016).

The presence of butterflies usually depends on the availability of plants (Curtis et al. 2015), either as host plants for larva to eat or as food plants for the adult butterfly to forage on (Subahar & Yuliana 2010), and

their interaction sometimes can be specific (New 1997; Peggie & Amir 2006). The more specific interaction, the more butterflies become susceptible to disturbances in the environment, so they can act as environment bioindicators (Swaay et al. 2012). Several studies have shown that butterfly diversity will increase with the high diversity of plants, whereas areas with low diversity of plants have low butterfly diversity (Vu et al. 2015; Widhiono 2015).

Langsa Urban Forest (LUF) is an isolated urban forest that is mainly used for ecotourism in Langsa, Aceh, the northernmost province in Sumatra. In general, biological explorations in this province are limited. Several studies on butterflies in Aceh have been carried out, for example, Banda Aceh (Alfida et al. 2016), Aceh Jaya (Yusuf et al. 2018), Aceh Besar (Akla et al. 2018), and Subulussalam (Suwarno et al. 2019), but no study dealing with butterflies has been done in Langsa Urban Forest (LUF). In this study, we investigate the diversity, host and food plants, distribution, also conservation of butterflies in LUF, an isolated urban forest on the eastern side of Aceh Province. The data from LUF is important to complete information about butterfly diversity in one of the poorly explored areas in Indonesia, and the conservation and development plan of LUF as ecotourism.

MATERIALS AND METHODS

Study Area

LUF is located in Paya Bujok Seulemak Village, Langsa Baro District, Langsa City (4°29'25" N 97°56'44" E), and at an elevation of around 7 m asl (Figure 1 and 2). It is a ±10 hectare green area mainly used for ecotourism, with a remnant natural forest fragment at some parts. Air temperature range from 30–32°C and humidity at 50–60%. In this forest, there are some natural stands of trees mostly dipterocarps, including the Endangered *Shorea pauciflora* King, and understorey to forest floor vegetation. LUF was recently converted to a tourism resort, which is based on the Qanun of Langsa City No. 16 in the Year 2015, it is aimed to preserve, harmonize and balance the urban ecosystem of Langsa, covering environmental, social, and cultural elements.

Field survey and data collection

Four transects were laid in four selected sites in LUF, each representing a different type of habitat: forested areas (1, 2) and open areas (3, 4) (Figure 2). Location 1 consists of trees and is dominated by herbs such as *Asystasia gangetica*. Location 2 is dominated by trees and covered by leaf litter. Location 3 as an open area is dominated by understorey vegetation i.e *Axonopus compressus*, *Ageratum conyzoides*, etc. Location 4 is an open area and filled with flowering plants, including *Melastoma malabathricum* and *Bougainvillea glabra*.

Butterflies were recorded once a week in July 2021 from 09.00 to 15.00 GMT+7, preferably during good weather. Data collection was done using a modification of the standard walk method (Pollard & Yates 1993; Swaay et al. 2012), with each station placed 150 m distant. The observations were made along the transects of 10 m width. When needed, specimens were collected to facilitate identification. Identification was done using morphological and photographs comparison to relevant literature including Braby (2004), Peggie and Amir (2006), Baskoro et al. (2018), and Iqbal et al. (2021).

Plant species data are also recorded and used to analyse the potential source of the host or foodplant. The plants' uses were compiled according to data from our field surveys and literature (Subahar & Yuliana 2010; Rusman et al. 2016; Kunte et al. 2021a; Kunte et al. 2021b). Geo-

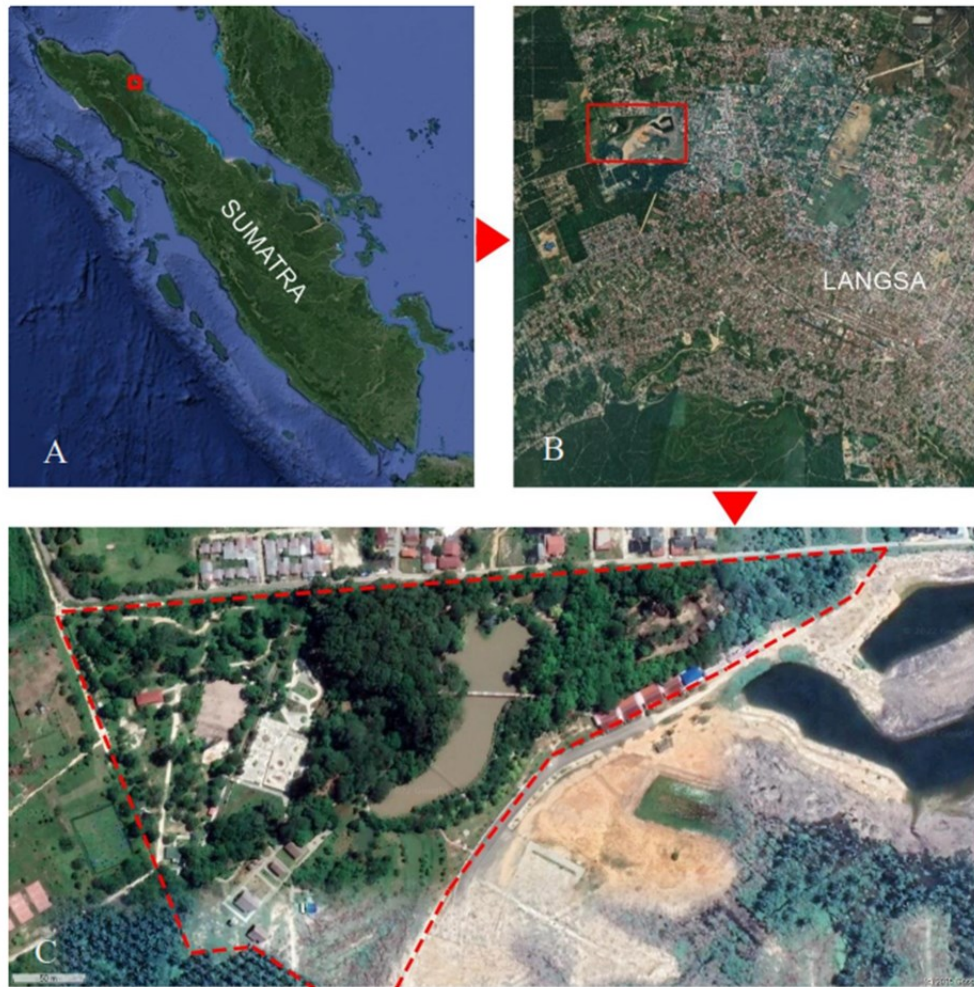


Figure 1. Map of Langsa Urban Forest: Sumatra (A), Langsa (B), and LUF (C) (Terra Incognita software 2022).



Figure 2. Map of butterfly inventory in LUF (Google Earth software 2021) and photographs of four stations: forested areas (1, 2) and open areas (3, 4).

graphical distribution analysis was done according to six zoogeographical regions (24 subregions) from Wallace (1876), and species distribution data were obtained from the literature (Braby 2004; Larsen et al. 2007; Morgun & Martin 2012; Hitchings & Campbell 2016; Hardy & Lawrence 2017; Rosmidi 2017; Yong et al. 2018; Domine & de la Cruz 2020; Echude et al. 2020; Nayak 2020; Rahman & Maryati 2020; Manzoor et al. 2020; Iqbal et al. 2021; Kunte et al. 2021a; Kunte et al. 2021b; GBIF 2022) (see Appendix). The conservation status of butterflies and plants were adapted from IUCN Red List (2022).

Data analysis

The recorded butterflies are listed and discussed. To categorise the diversity of butterflies in LUF, we calculate the diversity index (H') according to Krebs (1999) as the following formula:

$$H' = \sum_{i=1}^s (p_i) (\log 2 p_i)$$

To analyse the spatial distribution, we calculate the evenness index following Magurran (2004) as the following formula:

$$J' = H' / \ln S$$

The diversity index results can be classified into low (<1), medium (1-3), and high (>3). The evenness index ranges between 0 and 1, with 1 being the maximum value (Krebs 1999). Photographs were taken using a digital camera. The plate of representative species was prepared using photo editing software, each species with both ventral and dorsal sides. A scale is also included for each photograph.

RESULTS AND DISCUSSION

Results

There are 36 species belonging to 5 families of butterflies recorded from LUF, with Nymphalidae being the largest family with 17 species (47.2%), followed by Lycaenidae with 6 species (16.67%), Pieridae with 5 species (13.89%), and the lowest from Papilionidae and Hesperidae, each with 4 species (11.11%) (Figure 3).

A total of 143 butterfly species were collected, most of them from Nymphalidae and the fewest individuals from Hesperidae. At the species level, *Leptosia nina* has the highest number of individuals (36), followed by *Mycalasis mineus* (14) and *Hypolimnas bolina* (10). Ten species (27.8%) were only recorded from a single individual (Table 1).

Quantitative approaches indicate good results in the presence of butterflies in LUF. Using the diversity index, it is shown that all four sites support medium diversity, as shown by H's value of 1.78–2.78. This finding is also supported by the Evenness Index which shows a range of 0.66–0.94, which means that out of four sites, three of them show a very even distribution (Table 2).

A plant inventory in four selected sites yielded 117 species (24 families) with 33 species (20 families) of them being the potential host or food plants (Table 3). Based on observations, found 33 species (20 families) could be used as hosts and food plants for butterflies. There are 26 species of plants that can be used as host plants, 11 species as food plants, and 4 species as both. The recorded plants' habitus range from herbs, shrubs, trees, liana, and palms, with some species, being aliens.

Discussion

Species diversity

The number of species found comprised c. 4% of the total butterflies known in Sumatra (890 species) (Widjaja et al. 2014). With 36 species,

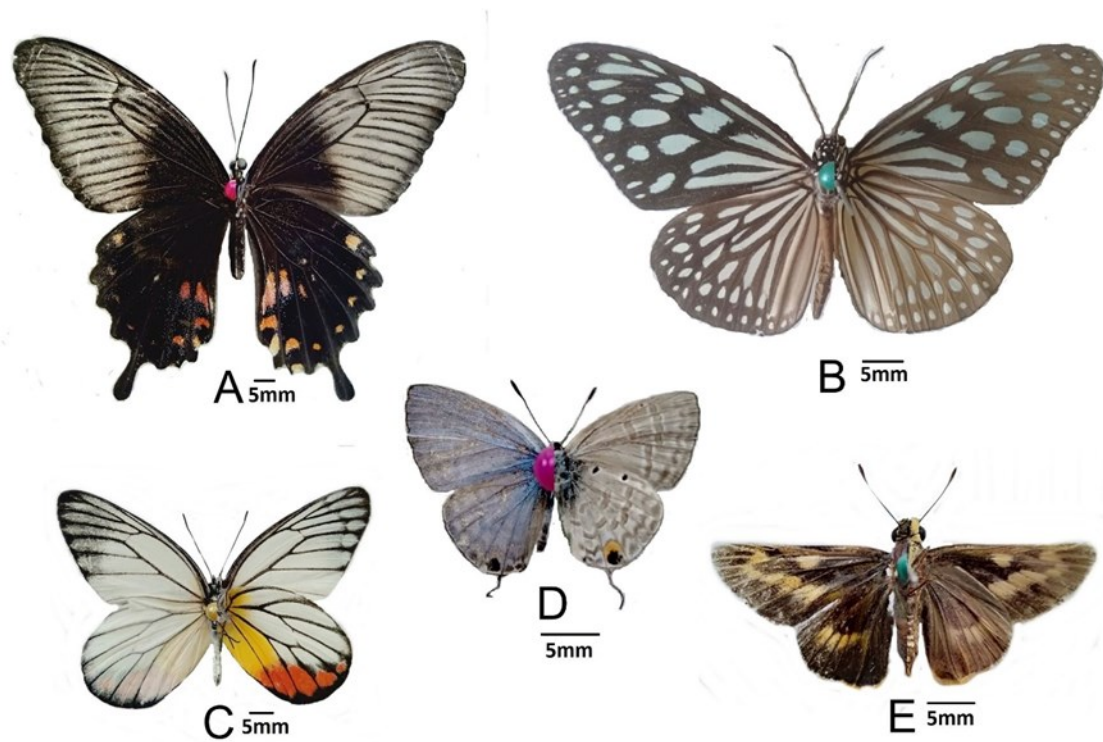


Figure 3. Representatives of each butterfly family in Langsa Urban Forest, Aceh, Indonesia: (A) Papilionidae (*Papilio polytes*), (B) Nymphalidae (*Ideopsis vulgaris*), (C) Pieridae (*Delias hyparete*), (D) Lycaenidae (*Catochrysops panormus*), and (E) Hesperidae (*Cephrènes acalle*).

which likely increased if further studies were conducted, LUF has either a higher or lower number of species compared to other areas in Aceh, e.g. 31 species in Pulau Raya Aceh Jaya (Yusuf et al. 2018), 30 species in City Garden Banda Aceh (Suwarno et al. 2018), 25 species in Soraya Research Station, Subulussalam (Suwarno 2019), and 18 species in BNI Banda Aceh Urban Forest (Alfida et al. 2016), but lower than in Brayeun River, Aceh Besar with 51 species (Akla et al. 2018). It is interesting, however, because Pulau Raya and Soraya Research Station are both natural ecosystems. The difference maybe is caused by other factors but is worthy of further investigation.

Compared to other urban parks outside Aceh, the position of LUF is also quite remarkable as it has more than twice the number of species in a 99-ha Angke Kapuk Nature Tourism Park, North Jakarta (13 species) (Ruslan et al. 2019) with the dominant plant only from Acanthaceae family and is close, although lower, to a 50ha urban ecosystem of Universitas Negeri Medan (43 species) (Siregar & Simatupang 2017), where found 6 families of plants similar to those in LUF, i.e Rutaceae, Rubiaceae, Melastomataceae, Acanthaceae, Euphorbiaceae and Moraceae, but 7 other plants families not found in LUF.

The diversity indexes from all sites are categorized as medium, with the highest index being Station 4. This condition is due to the support of flowering plants which can act as food plants (54.54%) for butterflies. Butterflies are very active visiting many different nectar plants as food plants. Butterfly diversity increase when the habitat is suitable for nectar plant as food plant as well as host plants (Nacua 2016; Rusman et al. 2016; Thakur & Chaudhuri 2017).

The taxonomic grouping of species shows a similar pattern to any previous local-scale research in Indonesia, in which the Nymphalidae usually become the dominant family (Leo et al. 2016; Panjaitan et al. 2020). This situation is not surprising as Nymphalidae is the largest fam-

Table 1. List of butterfly species in Langsa Urban Forest, Aceh, Indonesia.

Family/Subfamily/Species	Number of individu per site				Total	IUCN Conservation Status
	1	2	3	4		
PAPILIONIDAE						
Papilioninae						
<i>Graphium agamemnon</i> (Linnaeus, 1758)	-	-	1	-	1	NE
<i>Papilio polytes</i> Linnaeus, 1758	1	2	-	-	3	NE
<i>Papilio demoleus</i> Linnaeus, 1758	-	-	-	2	2	NE
<i>Papilio memnon</i> Linnaeus, 1758	-	2	-	1	3	NE
NYMPHALIDAE						
Danainae						
<i>Euploea midamus</i> (Linnaeus, 1758)	-	1	-	-	1	NE
<i>Ideopsis vulgaris</i> (Butler, 1874)	-	1	-	2	3	LC
Limenitidinae						
<i>Athyma perius</i> (Linnaeus, 1758)	1	-	2	-	3	NE
<i>Lexias pardalis</i> (Moore, 1878)	2	1	-	-	3	NE
<i>Neptis hylas</i> (Linnaeus, 1758)	1	-	-	-	1	NE
<i>Neptis clinia</i> Moore, 1872	1	1	1	-	3	NE
Nymphalinae						
<i>Junonia orithya</i> (Linnaeus, 1758)	-	-	1	1	2	LC
<i>Junonia hedonia</i> (Linnaeus, 1764)	1	1	-	1	3	NE
<i>Junonia atlites</i> (Linnaeus, 1763)	-	1	-	-	1	NE
<i>Junonia almana</i> (Linnaeus, 1758)	-	-	2	-	2	LC
<i>Hypolimnas bolina</i> (Linnaeus, 1758)	-	3	3	4	10	NE
Satyrinae						
<i>Elymnias hypermnestra</i> (Linnaeus, 1763)	1	-	-	-	1	NE
<i>Melanitis phedima</i> (Cramer, [1780])	1	-	1	1	3	NE
<i>Mycalesis mineus</i> (Linnaeus, 1758)	1	4	8	1	14	NE
<i>Mycalesis janardana</i> Moore, 1857	1	4	-	-	5	LC
<i>Mycalesis perseus</i> (Fabricius, 1775)	2	-	4	-	6	NE
<i>Ypthima horsfieldi</i> Moore, 1884	-	1	-	1	2	NE
PIERIDAE						
Coliadinae						
<i>Eurema hecabe</i> (Linnaeus, 1758)	-	-	2	1	3	NE
<i>Eurema sp.</i> Hübner, 1818	1	1	1	1	4	NE
Pierinae						
<i>Delias hyparete</i> (Linnaeus, 1758)	-	-	-	1	1	NE
<i>Appias olferna</i> Swinhoe, 1890	-	-	4	-	4	NE
<i>Leptosia nina</i> (Fabricius, 1793)	22	9	1	4	36	NE
LYCAENIDAE						
Theclinae						
<i>Arhopala kinabala</i> Druce, 1895	-	1	-	-	1	NE
<i>Flos apidanus</i> Cramer, [1777]	1	2	1	-	4	NE
<i>Rapala manea</i> (Hewitson, 1863)	-	-	-	1	1	NE
Polyommatainae						
<i>Catochrysops panormus</i> (C. Felder, 1860)	-	-	1	1	2	NE
<i>Zizina otis</i> (Fabricius, 1787)	-	-	4	2	6	LC
<i>Zizula hylax</i> (Fabricius, 1775)	-	-	1	1	2	LC

Table 1. Contd.

Family/Subfamily/Species	Number of individu per site				Total	IUCN Conservation Status
	1	2	3	4		
HESPERIDAE						
Hesperinae						
<i>Caltois bromus</i> (Leech, 1844)	1	-	-	-	1	NE
<i>Cephrenes acalle</i> (Höpffer, 1874)	-	-	-	3	3	NE
<i>Pelopidas conjuncta</i> (Herrich-Schäffer, 1869)	-	-	1	1	2	NE
<i>Potanthus sp.</i> Scudder, 1872	-	1	-	-	1	NE
Total number of individu	38	36	39	30	143	
Total number of species	15	17	17	19		

Table 2. Diversity and Evenness index of butterflies in Langsa Urban Forest, Aceh, Indonesia.

Station	Number of species	Number of individuals	Number of host plants	Number of food plants	H'		Evenness Index
					Value	Category	Value
1	15	38	16	4	1.78	medium	0.66
2	17	36	4	1	2.52	medium	0.89
3	17	39	8	5	2.39	medium	0.84
4	19	30	12	6	2.78	medium	0.94

Table 3. List of plant diversity that used by butterfly as host plant and food plant.

Family/Species	Station				Occurrence / conservation status of native	Butterfly species association*
	1	2	3	4		
ACANTHACEAE						
<i>Asystasia gangetica</i> (L.) T.Anderson	√	-	√	√	Alien	HP: <i>H. bolina</i> , <i>J. hedonia</i> , <i>J. orythya</i> *
<i>Rostellularia sp.</i>	-	-	-	√	-	FP: <i>J. hedonia</i> , <i>E. hecabe</i>
APOCYNACEAE						
<i>Alstonia scholaris</i> (L.) R.Br.	√	-	-	-	Native/LC	FP: <i>P. polytes</i> , <i>J. atlites</i> , <i>D. hyparete</i> , <i>Rapala sp.</i> , <i>Euploea sp.</i>
ARECACEAE						
<i>Arenga pinnata</i> (Wurmb.) Merr.	-	-	√	-	Native/NE	HP: <i>E. hypermnestra</i>
<i>Cyrtotachys renda</i> Blume	√	-	-	√	Native/NE	HP: - FP: -
<i>Hyophorbe lagenicaulis</i> (L.H.Bailey) H.E.Moore	√	-	-	√	Alien	HP: <i>E.hypermnestra</i> *
ARISTOLOCHIACEAE						
<i>Thottea sp.</i>	-	√	-	√	-	HP: -
ASTERACEAE						
<i>Ageratum conyzoides</i> L.	-	-	√	√	Alien	FP: -
<i>Emilia sonchifolia</i> (L.) DC.	-	-	√	√	Native/NE	FP: -
<i>Synedrella nodiflora</i> (L.) Gaertn	-	-	√	-	Alien	FP: -
COMBRETACEAE						
<i>Terminalia catappa</i> L.	√	-	-	-	Native/LC	HP: <i>Arhopala sp.</i> , <i>F. apidanus</i> , <i>Rapala sp.</i>

Table 3. Contd.

Family/Species	Station				Occurrence / conservation status of native	Butterfly species association*
	1	2	3	4		
DIPTEROCARPACEAE						
<i>Hopea</i> sp.	-	√	-	-	-	HP: <i>Arhopala</i> sp.
EUPHORBIACEAE						
<i>Macaranga tanarius</i> (L.) Müll.Arg.	√	-	-	√	Native/LC	HP: - FP: -
FABACEAE						
<i>Alysicarpus vaginalis</i> (L.) DC.	√	-	-	-	Native/NE	HP: <i>Z. otis</i>
<i>Bauhinia purpurea</i> L.	-	-	√	-	Alien	HP: <i>Eurema</i> sp.
<i>Mimosa pudica</i> L.	√	-	√	-	Alien	HP: <i>J. orithya</i> , <i>E. hecabe</i> , <i>Zizina Otis</i> , <i>Zizula hylax</i> FP: <i>J. lmanac</i> , <i>Eurema</i> sp.
LAURACEAE						
<i>Litsea</i> sp.	√	-	√	-	-	HP: -
MAGNOLIACEAE						
<i>Magnolia × alba</i> (DC.) Figlar	√	-	-	-	Native/NE	HP: <i>G. agamemnon</i>
MELASTOMACEAE						
<i>Melastoma malabathricum</i> L.	-	√	-	√	Native/NE	HP: <i>J. atlites</i> , <i>E. hypermnestra</i>
MORACEAE						
<i>Ficus benghalensis</i> L.	√	-	-	√	Alien	HP: <i>Euploea</i> sp.
<i>Streblus asper</i> Lour.	-	√	-	-	Native/LC	HP: <i>Euploea</i> sp.
MUSACEAE						
<i>Musa × paradisiaca</i> L.	-	-	-	√	Native/NE	HP: -
MYRTACEAE						
<i>Syzygium cumini</i> (L.) Skeels	√	-	-	-	Native/LC	HP: <i>F. apidanus</i> , <i>Arhopala</i> sp.
NYCTAGINACEAE						
<i>Bougainvillea glabra</i> Choisy	-	-	-	√	Alien	FP: <i>P. polytes</i> , <i>J. almana</i> , <i>D. hyparete</i>
PHYLLANTHACEAE						
<i>Phyllanthus niruri</i> L.	-	-	√	-	Native/NE	HP: <i>A. perius</i>
POACEAE						
<i>Axonopus compressus</i> (Sw.) P.Beauv.	√	-	√	√	Alien	HP: <i>Melanitis</i> sp., <i>Mycalesis mineus</i> *, <i>Mycalesis perseus</i> *, <i>Mycalesis</i> sp.
<i>Bambusa vulgaris</i> Schrad. ex J.C.Wendl.	√	-	-	-	Native/NE	HP: <i>Melanitis</i> sp., <i>Caltoris</i> sp., <i>Potanthus</i> sp.
<i>Paspalum conjugatum</i> P.J.Bergius	√	-	-	-	Native/LC	HP: -
<i>Imperata cylindrica</i> (L.) P.Beauv.	-	-	√	√	Native/NE	HP: -
<i>Saccharum officinarum</i> L.	√	-	-	√	Alien	HP: <i>Melanitis</i> sp., <i>P. conjuncta</i>
RUBIACEAE						
<i>Ixora javanica</i> (Blume) DC.	-	√	-	-	Native/LC	FP: <i>P. demoleus</i> , <i>P. memnon</i> , <i>P. polytes</i> , <i>P. conjuncta</i> , <i>G. agamemnon</i>
<i>Neolamarckia cadamba</i> (Roxb.) Bosser	√	-	-	-	Alien	HP: -
RUTACEAE						
<i>Citrus × limon</i> (L.) Osbeck	-	-	-	√	Alien	HP: <i>P. polytes</i> *, <i>P. demoleus</i> , <i>G. agamemnon</i>
Total species per station	17	5	11	16		

Note: HP: host plant; FP: food plant; -: no data; *: direct observation

ily with perhaps 650 species or 34.21% of all known butterflies (Widjaja 2014). On the other hand, the lowest number of species was recorded from the inconspicuous family of Hesperidae and is also similar to other areas in Indonesia, such as Baluran National Park (6.35%), Sangehe Island (0.64%), Talaud Island (3.12%) and Landsfill Balai Gadang (4.54%) (Leo et al. 2016; Koneri & Nangoy 2019; Muhelni & Anwar 2020).

Technical issues may also contribute to the low number of certain families. In LUF, the number of swallowtail butterflies from Papilionoidea is only four species, similar to those of Hesperidae. Our result may be underestimated as species from this family usually fly fast and are hard to observe or even captured, for instance, *Graphium* (Betts & Wootton 1988). Other studies, even in the vegetation-rich ecosystems also yielded a low number of this family, e.g. Baluran National Parks comprised c. 1.58% (Leo et al. 2016).

Species distribution

Most of the species in LUF have broad geographical distributions with 19 subregions from five zoogeographical regions, i.e. Palearctic, Ethiopian, Oriental Region, Australian, and Neotropical (Appendix). Most of the species are distributed in Oriental and Australian regions. Only three species are distributed in five regions, four species in four regions, seven species in three regions, fifteen species in two regions, and seven species in one region (Oriental Region). These numbers show that the geographic distributions of the species are considerably broad.

Three species occupy five regions, *Papilio demoleus* (Morgun & Martin 2012; Yong et al. 2018), *Hypolimnas bolina* and *Eurema* sp., while the species with four regions is *Junonia orithya* (Biricik 2011), *Eurema hecabe*, *Zizina otis* and *Zizula hylax*. A large proportion of species also can be found in the Australian region (80,55%), followed by Palearctic (36,11%), Ethiopian (19,44%), and Neotropical (8,33%). In the Oriental region, three species restricted to the Indomalayan realm, LUF butterflies are also found in India (83,33%), followed by Ceylon (77,78%), and Indo-China (69,44%).

Host and food plants

The population dynamics of butterflies in certain areas are influenced by the vegetation, in part, related to the presence of host and food plant species (Curtis et al. 2015; Suwarno et al. 2018; Panjaitan et al. 2020). Butterfly abundance is influenced by plant species found in the ecosystem. The abundance and richness of butterflies depend on abundance and richness of plants species (Yamamoto et al. 2007; Subahar & Yuliana 2010, Hantson & Baz 2011; Panjaitan et al. 2020) with generalist butterfly has a higher number than a specialist butterfly in the ecosystem (Hantson & Baz 2011).

In LUF, around 28.20% of the recorded plants are either hosts or food plants, or partly both. The most common plant species found as hosts and food plants belong to Poaceae (15.15%), followed by the Arecaceae, Asteraceae, and Fabaceae families (all 9.09%), and other 14 families represented by 1 species (3.03%). Many plant families in LUF have been previously reported as important groups for butterflies.

Poaceae, used by 4 butterfly genera from Hesperidae and Nymphalidae as host plants in LUF, there are *Melanitis*, *Mycalesis*, *Caltoris* dan *Potanthus*. This was also reported by Leo et al. (2016) and Peggie and Amir (2006), Poaceae are widely used as host plants by Hesperidae and Nymphalidae, while Asteraceae and Fabaceae for the Nymphalidae (Peggie & Amir 2006). Therefore, it is not surprising that many Nym-

phalidae species were recorded in LUF. Besides that, Fabaceae is also an important source of nectars for adult butterflies, especially for Lycaenidae (Rusman et al. 2016), yielding the diverse species of Lycaenidae found in station 3 where the family is also diverse.

Conservation

According to the IUCN Red List (2022), the conservation status of the five evaluated species is all of Least Concern (LC), while the others are Not Evaluated (NE). Least Concern species have a lower risk of extinction, but some of them are slow declines, so it is important to monitor these species to prevent them from becoming threatened in the future (IUCN 2022). Despite the medium diversity we found, the LUF did not support the conservation of threatened species. Furthermore, according to the regulation from the Indonesian Ministry of Environment and Forestry No. 106 in the year 2018, there are also no protected butterflies. This implies that the conservation effort in the future should be an ecosystem-level approach since the use of flagship species (see Verissimo et al. 2011) is considered inapplicable.

On a local scale, however, some species are only found once during the study. Those types of species need further attention, especially in efforts to avoid local extinction. To make sure that the species will sustain, some strategies can be implemented by the local stakeholders, for example by making sure that the presence of food or host plants is also maintained. A focus should be made on the native plant species to maintain the original ecosystem interaction.

The presence of alien plants, especially those that are used as a source of food or host plants, a yet-unknown role in the diversity of butterflies in LUF. This group of plants has been known to negatively impact the butterfly species richness (Gallien et al. 2017) but has positive impacts on the butterfly species in another research (Mukherjee et al. 2015). Out of 33 food and or host plants, 11 of them are alien species, which is considered a large proportion. Those alien plants such as *Asystasia gangetica* and *Mimosa pudica* can be used as host or food plants, i.e. *J. orithya*, *J. almana*, *J. hedonia*, *H. bolina*, *E. hecabe*, *Z. otis*, and *Z. hylax*. As no data on the food and or host plant partition between the native vs alien species are available, further studies are encouraged to ensure the alien plant's role in the LUF ecosystem. The conservation status of the plant is also important as described before that some of the least concern species are slow declines. This information is necessary to make sure that the plants used as food and or host plants are available to maintain the existence of butterflies. This type of effort would be useful to create a conservation action plan in LUF.

CONCLUSION

The current study revealed 36 species of butterflies in an isolated lowland urban forest of Langsa, Aceh, Indonesia. The pattern of species composition more or less follows a common pattern in other areas of Indonesia with Nymphalidae being the most species-rich family. The vegetation in LUF also supports the butterfly diversity by providing sources of food, host, or both, from 33 species or 28.20 percent of all known species. Further studies are needed to support the idea of making LUF a conservation site for urban butterflies, e.g. year-long monitoring of butterflies and food and or host plant species traits. These types of studies will gain a better understanding of the biology of butterflies in this area and also could serve as important references for future conservation.

AUTHORS CONTRIBUTION

H.P.E.S. designed the research and supervised all the processes, A.Y.P collected and analysed butterfly diversity data and wrote the manuscript, W.A.M collected and analysed plant data and wrote the manuscript, K.A.P collected butterflies, I.Y.W. analysed butterfly species and wrote the manuscript. All authors agreed on the final version of the manuscript.

ACKNOWLEDGMENTS

The authors thanked the management of Langsa Urban Forest, Aceh Province, who provided permission for research. The author also thanked Agusti Randi who assisted with plant identification.

CONFLICT OF INTEREST

The authors declare that they hold no competing interests and no funding applied.

REFERENCES

- Akla, N. et al., 2018. Keragaman kupu-kupu di Sungai Brayeun, Kabupaten Aceh Besar. *Jurnal Bioleuser*, 2(3), pp.69-71. doi: 10.24815/jobioleuser.v2i3.14962
- Alfida, Hanum, U., & Eliyanti., 2016. Kupu-kupu (Rhopalocera) di kawasan Hutan Kota BNI Banda Aceh. *Jurnal Biotik*, 4(2), pp.117-127. doi: 10.22373/biotik.v4i2.2906
- Baskoro, K., Kamaludin, N., & Irawan, F., 2018. *Lepidoptera Semarang Raya*. Semarang: Departemen Biologi Universitas Diponegoro.
- Betts, C.R. & Wootton, R.J., 1988. Wing shape and flight behaviour in butterflies (Lepidoptera: Papilionoidea and Hesperioidea): a preliminary analysis. *Journal of Experimental Biology*, 138, pp.271-288. doi: 10.1242/jeb.138.1.271
- Biricik, M. 2011., First record of *Junonia orithya* (Linnaeus, 1758) (Lepidoptera: Nymphalidae) in Turkey. *Zoology in the Middle East*, 53(1), pp.130-132. doi: 10.1080/09397140.2011.10648871
- Braby, M., 2004. *The Complete field guide to butterflies of Australia*. Australia: CSIRO Publishing.
- Curtis, R. J. et al., 2015. Butterfly abundance is determined by food availability and is mediated by species traits. *Journal of Applied Ecology*, 52(6), pp.1676-1684. doi: 10.1111/1365-2664.12523
- Domine, A.F.S., & dela Cruz, N.B., 2020. Checklist of butterflies and moth in Andanan Watershed Forest Reserve, Philippines. *Journal of Ecosystem Sciences and Eco-Governance*, 2(2), pp.42-50.
- Echude, D. et al., 2020. Checklist and comparison of butterfly species in zoological and botanical garden, University of Nigeria, Nsukka, Enugu State, Nigeria. *Journal of Biological Research & Biotechnology*, 18(1), pp.1071-1077. doi: 10.4314/br.v18i1.1
- EOL., 2022. Encyclopedia of Life Butterflies Papilionoidea, viewed August 2022, from <https://eol.org/pages/854>.
- Gallien, L. et al., 2017. Invasive plants threaten the least mobile butterflies in Switzerland. *Diversity and Distributions*, 23(2), pp.185-195. doi:10.1111/ddi.12513.
- GBIF., 2022. GBIF Home Page, viewed January 2022, from <https://www.gbif.org/>.
- Hantson, S., & Baz, A., 2011. Seasonal change in nectar preference for a mediterranean butterfly community. *Journal of The Lepidopterists' Society*, 67(2), pp.134-142. doi: 10.18473/lepi.v67i2.a5

- Hardy, P.B., & Lawrence, J.M., 2017. *Field Guide to Butterflies of the Philippines*. UK: Siri Scientific Press.
- Hitchings, V., & Campbell, O., 2016. A record of the great eggfly *Hypolimnas bolina* (Linnaeus, 1758) from Masirah Island, Oman and a summary of previous records from Arabia. *Tribulus*, 24, pp.109-114.
- Iqbal, M. et al., 2021. *Kupu-kupu (Lepidoptera: Rhopalocera) di Sumatera*. Palembang: Kelompok Pengamat Burung Spirit of South Sumatera.
- IUCN., 2022. The IUCN red list of threatened species. Version 2021-3, viewed October 2021, from <https://www.iucnredlist.org/>.
- Kawahara, A.Y., & Breinholt, J.W., 2014. Phylogenomics provides strong evidence for relationships of butterflies and moths. *Proceedings of The Royal Society B*. doi: 10.1098/rspb.2014.0970
- Koneri, R. & Nangoy, M. J., 2019. Butterfly community structure and diversity in Sangihe Islands, North Sulawesi, Indonesia. *Applied Ecology and Environmental Research*, 17(2), pp.2501-2517. doi:10.15666/aer/1702_25012517
- Krebs, C.J., 1999. *Ecological methodology*. Canada: Benjamin Cummings.
- Kunte, K., Sondhi, S., & Roy, P., 2021a. Butterfly of India: Nectar Plants. Indian Foundation for Butterflies, India, viewed September 2021, from <http://www.ifoundbutterflies.org/nectar-plants/2/plantae>.
- Kunte, K., Sondhi, S., & Roy, P., 2021b. Butterfly of India: Larval Host Plants. Indian Foundation for Butterflies, India, viewed September 2021, from <https://www.ifoundbutterflies.org/larval-host-plants/2/Plantae>.
- Kurnianto, A.S. et al., 2016. The potential of butterflies in tourism diversification product: case study at Coban Rais Waterfall, Batu, East Java. *Journal of Indonesian Tourism and Development Studies*, 4(3), pp.115-122. doi: 10.21776/ub.jitode.2016.004.03.04.
- Larsen, T.B. et al., 2007. Bobiri butterfly sanctuary in Ghana-discovering its butterflies. *Metamorphosis*, 18(3), pp.88-126.
- Leo, S. et al., 2016. Butterflies of Baluran National Park, East Java, Indonesia. *Seminar Nasional Masyarakat Biodiversitas Indonesia*. doi: 10.13057/psnmbi/m20209
- Magurran, A. E., 2004. *Measuring biological diversity*. Australia: Blackwell Publishing.
- Manzoor, M., Khan, S. W., & Shah, S. A., 2020. An annotated checklist of butterflies at elevated protected areas of Pakistan. *Journal of Bioresource Management*, 7(1), pp.41-52. doi: 10.35691/JBM.0202.0119.
- Morgun, D. V. & Wiemers, M., 2012. First record of The Lime Swallowtail *Papilio demoleus* Linnaeus, 1758 (Lepidoptera, Papilionidae) in Europe. *The Journal of Research on the Lepidoptera*, 45, pp.85-89. doi: 10.5962/p.266485
- Muhelni, L. & Anwar, H., 2020. The diversity of butterfly in Air Dingin Landfills, Balai Gadang, Padang City. *Berita Biologi*, 19(2), pp.207-213. doi: 10.14203/beritabiologi.v19i2.3788.
- Mukherjee, S. et al., 2015. *Lantana camara* and butterfly abundance in an urban landscape: benefits for conservation or species invasion? *Ekologia*, 34(4), pp. 309-328. doi: 10.1515/eko-2015-0029.
- Nacua, E.A., 2016. Occurance of Butterflies in a mini-urban garden in Universidad de Manila (UDM) including short-distance migration analysis. *Journal of Entomology and Zoology Studies*, 4(4), pp.86-91. doi: [dx.doi.org/10.22271/j.ento](https://doi.org/10.22271/j.ento)

- Nair, V.A., Mitra, P., & Aditya, S., 2014. Studies on the diversity and abundance of butterfly (Lepidoptera: Rhopalocera) fauna in and around Sarojini Naidu college campus, Kolkata, West Bengal, India. *Journal of Entomology and Zoology Studies*, 2(4), pp.129-134. doi: dx.doi.org/10.22271/j.ento
- Nayak, A., 2020. A checklist of butterfly fauna of Bankura Town, West Bengal, India. *Journal of Threatened Taxa*, 12(13), pp.16868-16878. doi: 10/11609/jott.4882.12.13.16868-16878
- New, T.R., 1997. *Butterfly conservation*. Melbourne: Oxford University Press Australia.
- Panjaitan, R. et al., 2020. Diversity of butterflies (Lepidoptera) across rainforest transformation system in Jambi, Sumatra, Indonesia. *Biodiversitas*, 21(11), pp.5119-5127. doi: 10.13057/biodiv/d211117.
- Peggie, D. & Amir, M., 2006. *Practical guide to the butterflies of Bogor Botanical Garden*. Cibinong: Bidang Zoologi LIPI.
- Pollard, E. & Yates, T.J., 1993. *Monitoring butterflies for ecology and conservation*. London: Chapman and Hall.
- Qanun Kota Langsa., 2015. Qanun Kota Langsa tentang Pengelolaan Ruang Terbuka Hijau. https://jdihn.go.id/files/505/QANUN_KOTA_LANGSA_NOMOR_16_TAHUN_2015_TENTANG_PENGELOLAAN_RTH_KOTA_LANGSA1.pdf
- Rahman, A.A.A., & Maryati, M., 2020. Checklist of butterflies (Lepidoptera: Papilionoidea and Hesperioidea) in Gunung Pulai Forest Reserve, Johor. *IOP Conference Series: Earth and Environmental Science*. doi: 10.1088/1755-1315/736/1/012058.
- Rosmidi, F. et al., 2017. Checklist of butterflies in Pulau Perhentian and Pulau Bidong, Terengganu. *Journal of Sustainability Science and Management*, 12(1), pp.40-48.
- Ruslan, H., Andayaningsih, D., & Camin, Y. R., 2019. Biodiversitas kupu-kupu (Lepidoptera: Papilionoidea) di Kawasan Taman Wisata Alam Angke Kapuk Jakarta Utara. *Prosiding Seminar Nasional Perhimpunan Biologi Indonesia XXV*.
- Rusman, R., Atmowidi, T., & Peggie, D., 2016. Butterflies (Lepidoptera: Papilionoidea) of Mount Sago, West Sumatra: diversity and flower preference. *Hayati Journal of Bioscience*, 23, pp.132-137. doi: 10.4308/hjb.23.3.132
- Siregar, E.H. & Simatupang, H., 2017. Inventarisasi kupu-kupu di Universitas Negeri Medan. *BioLink*, 4(1), pp.63-68. doi: 10.31289/biolink.v4i1.968
- Subahar, T.A.S., & Yuliana, A., 2010. Butterfly diversity as a data base for the development plan of butterfly garden at Bosscha Observatory, Lembang, West Java. *Biodiversitas*, 11(1), pp.24-28. doi: 10.13057/biodiv/d110106
- Suwarno et al., 2018. Diversity and abundance of butterfly (Lepidoptera Rhopalocera) in the City Garden of Banda Aceh, Indonesia. *Ecology, Environment and Conservation*, 24(3), pp.1009-1017.
- Suwarno, S. et al., 2019. Mud-puddling behaviour of butterflies in the Soraya research station, district of Subulussalam, Aceh, Indonesia. *The 3rd International Conference on Natural and Environmental Sciences*, 364, pp.1-5. doi: 10.1088/1755-1315/364/1/012027.
- Swaay, C. et al., 2012. *Manual for butterfly monitoring*. Wageningen: Butterfly Conservation UK and Butterfly Conservation Europe.
- Thakur, D.C. & Chaudhuri, A., 2017. Eco-ethology study of butterfly species found in set up garden in an urban area, Kolkata, India. *Journal of Entomology and Zoology Studies*, 5(3), pp.1900-1909. doi: dx.doi.org/10.22271/j.ento

- Verissimo, D., MacMillan, D. C., & Smith, R. J., 2011. Toward a systematic approach for identifying conservation flagships. *Conservation Letters*, 4, pp.1-8. doi: 10.1111/j.1755-263X.2010.00151.x.
- Vu, L.V. et al., 2015. Butterfly diversity and habitat variation in a disturbed forest in northern Vietnam. *The Pan-Pacific Entomologist*, 91 (1), pp.29-38. doi: 10.3956/2014-91.1.029
- Wallace, A.R., 1876. *The geographical distribution of animals, Vols 1*. New York: Harper & Brothers.
- Widjaja, E.A. et al., 2014. *Kekinian keanekaragaman hayati Indonesia*. Jakarta: LIPI Press.
- Widhiono, I., 2015. Diversity of butterflies in four different forest types in Mount Slamet, Central Java, Indonesia. 2015. *Biodiversitas*, 16(2), pp.196-204. doi: 10.13057/biodiv/d160215
- Yamamoto, N., Yokoyama, J., & Kawata, M., 2007. Relative resource abundance explains butterfly biodiversity in island communities. *PNAS*, 104(25), pp 10524-10529. doi: 10.1073/pnas/0701583104
- Yong, S., Teruel, R., & Breto, D., 2018. Occurrence of the Lime Swallowtail *Papilio demoleus* Linnaeus, 1758 (Lepidoptera: Papilionidae) in Western Cuba. *Ecologica Montenegrina*, 18, pp.15-17. doi: 10.37828/em.2018.18.2
- Yusuf, M. et al., 2018. Keanekaragaman dan distribusi kupu-kupu di Pulau Raya, Kabupaten Aceh Jaya, Provinsi Aceh. *Jurnal Bioleuser*, 2(2), pp.54-58. doi: 10.24815/JOBIOLEUSER.V2I2.14887

APPENDIX

Family / Subfamily / Species	Distribution	Data Source
PAPILIONIDAE		
Papilioninae		
<i>Graphium agamemnon</i> (Linnaeus, 1758)	Oriental: Indian, Ceylon, Indo-China, Indo-Malayan Australian: Austro-Malayan, Polynesia, Australian	GBIF (2022) Iqbal et al. (2021) Nayak (2020)
<i>Papilio polytes</i> Linnaeus, 1758	Oriental: Indian, Ceylon, Indo-China, Indo-Malaya Australian: Austro-Malayan Palearctic: Manchurian	Domine and dela Cruz (2020) GBIF (2022) Hardy and Lawrence (2017) Iqbal et al. (2021) Manzoor et al. (2020) Nayak (2020) Rosmidi (2017)
<i>Papilio demoleus</i> Linnaeus, 1758	Neotropical: Antilean Oriental: Indian, Ceylon, Indo-China, Indo-Malayan Australian: Austro-Malayan, Australian Ethiopian: West Africa Palearctic: Europe, Mediteranian	Echude et al. (2020) GBIF (2022) Hardy and Lawrence (2017) Iqbal et al. (2021) Manzoor et al. (2020) Morgun and Martin (2012) Nayak (2020) Yong et al. 2018
<i>Papilio memnon</i> Linnaeus, 1758	Oriental: Indian, Ceylon, Indo-China, Indo-Malayan Australian: Austro-Malayan, Australian Palearctic: Manchurian	GBIF (2022) Hardy and Lawrence (2017) Iqbal et al. (2021) Nayak (2020) Rahman and Maryati (2020) Rosmidi (2017)
NYMPHALIDAE		
Danainae		
<i>Euploea midamus</i> (Linnaeus, 1758)	Oriental: Indian, Ceylon, Indo-Malayan	GBIF (2022) Hardy and Lawrence (2017) Iqbal et al. (2021) Kunte et al. (2021)
<i>Ideopsis vulgaris</i> (Butler, 1874)	Oriental: Indo-Malayan	GBIF (2022) Hardy and Lawrence (2017) Iqbal et al. (2021)
Limnitiidinae		
<i>Athyma perius</i> (Linnaeus, 1758)	Oriental: Indian, Ceylon, Indo-China, Indo-Malayan	GBIF (2022) Hardy and Lawrence (2017) Iqbal et al. (2021)
<i>Lexias pardalis</i> Moore, 1878	Oriental: Indian, Indo-China, Indo-Malayan	GBIF (2022) Hardy and Lawrence (2017) Iqbal et al. (2021) Kunte et sl. (2021) Rahman and Maryati (2020)
<i>Neptis hylas</i> (Linnaeus, 1758)	Oriental: Indian, Ceylon, Indo-China, Indo-Malayan Australian: Austro-Malayan Palearctic: Manchurian	GBIF (2022) Iqbal et al. (2021) Hardy and Lawrence (2017) Manzoor et al. (2020) Nayak (2020) Rahman and Maryati (2020)
<i>Neptis clinia</i> Moore, (1872)	Oriental: Indian, Ceylon, Indo-China, Indo-Malayan	GBIF (2022) Hardy and Lawrence (2017) Iqbal et al. (2021)

APPENDIX Contd.

Family / Subfamily / Species	Distribution	Data Source
Nymphalinae		
<i>Junonia orithya</i> (Linnaeus, 1758)	Oriental: Indian, Ceylon, Indo-China, Indo-Malayan Australian: Austro-Malayan, New Zealand, Australia Ethiopian: East Africa, West Africa, South Africa, Malagasy Palearctic: Europe, Mediteranian	GBIF (2022) Hardy and Lawrence (2017) Iqbal et al. (2021) Larsen et al. (2007) Manzoor et al. (2020) Nayak (2020)
<i>Junonia hedonia</i> (Linnaeus, 1764)	Oriental: Indo-Malayan Australian: Austro-Malayan, Polynesian, Australian	Domine and dela Cruz (2020) GBIF (2022) Hardy and Lawrence (2017) Iqbal et al. (2021) Rahman and Maryati (2020)
<i>Junonia atlites</i> (Linnaeus, 1763)	Oriental: Indian, Ceylon, Indo-China, Indo-Malayan Australian: Australian	GBIF (2022) Hardy and Lawrence (2017) Iqbal et al. (2021) Nayak (2020)
<i>Junonia almana</i> (Linnaeus, 1758)	Oriental: Indian, Ceylon, Indo-China, Indo-Malayan Australian: Austro-Malayan Palearctic: Manchurian	GBIF (2022) Hardy and Lawrence (2017) Iqbal et al. (2021) Nayak (2020) Rahman and Maryati (2020)
<i>Hypolimnas bolina</i> (Linnaeus, 1758)	Neotropical: Mexican, Antillean Oriental: Indian, Ceylon, Indo-China, Indo-Malayan Australian: Austro-Malayan, Polynesian, New Zealand, Australian Ethiopian: West Africa, East Africa, Malagasy Palearctic: Mediteranian	GBIF (2022) Domine and dela Cruz (2020) Hardy and Lawrence (2017) Hitchings and Campbell (2016) Iqbal et al. (2021) Nayak (2020) Rosmidi (2017)
Satyrinae		
<i>Elymnias hypermnestra</i> (Linnaeus, 1763)	Oriental: Indian, Ceylon, Indo-China, Indo-Malayan Australian: Austro-Malayan	GBIF (2022) Iqbal et al. (2021) Nayak (2020) Rosmidi (2017)
<i>Melanitis phedima</i> (Cramer, 1780)	Oriental: Indian, Ceylon, Indo-China, Indo-Malayan Australian: Austro-Malayan Palearctic: Manchurian	GBIF (2022) Hardy and Lawrence (2017) Iqbal et al. (2021) Nayak (2020)
<i>Mycalesis mineus</i> (Linnaeus, 1758)	Oriental: Indian, Ceylon, Indo-China, Indo-Malayan Australian: Austro-Malayan	GBIF (2022) Domine and dela Cruz (2020) Hardy and Lawrence (2017) Iqbal et al. (2021) Nayak (2020) Rahman and Maryati (2020)
<i>Mycalesis janardana</i> Moore, 1857	Oriental: Indo-Malayan Australian: Austro-Malayan	GBIF (2022) Hardy and Lawrence (2017) Iqbal et al. (2021)
<i>Mycalesis perseus</i> (Fabricius, 1775)	Oriental: Indian, Ceylon, Indo-Malayan Australian: Austro-Malayan, Polynesian, Australian	GBIF (2022) Hardy and Lawrence (2017) Iqbal et al. (2021) Rahman and Maryati (2020)
<i>Ypthima horsfieldi</i> Hübner, 1819	Oriental: Indo-Malayan	GBIF (2022) Iqbal et al. (2021) Rahman and Maryati (2020)

APPENDIX Contd.

Family / Subfamily / Species	Distribution	Data Source
PIERIDAE		
Coliadinae		
<i>Eurema hecabe</i> (Linnaeus, 1758)	Oriental: Indian, Ceylon, Indo-China, Indo-Malayan Australian: Austro-Malayan, Polynesian, Australian Ethiopian: West Africa, East Africa, South Africa Palearctic: Europe, Manchurian	Domine and dela Cruz (2020) GBIF (2022) Hardy and Lawrence (2017) Iqbal et al. (2021) Larsen et al. (2007) Manzoor et al. (2020) Nayak (2020) Rahman and Maryati (2020)
<i>Eurema sp.</i> Hübner, 1818	Neotropical: Chilean, Brazilian, Mexican, Antillean Oriental: Indian, Ceylon, Indo-China, Indo-Malayan Australian: Austro-Malayan, Polynesian, Australian Ethiopian: West Africa, East Africa, South Africa, Malagasy Palearctic: Europe, Manchurian	GBIF (2022)
Pierinae		
<i>Delias hyparete</i> (Linnaeus, 1758)	Oriental: Indian, Ceylon, Indo-China, Indo-Malayan Australian: Austro-Malayan	GBIF (2022) Hardy and Lawrence (2017) Iqbal et al. (2021)
<i>Appias olferna</i> Swinhoe, 1890	Oriental: Indian, Ceylon, Indo-China, Indo-Malayan Australian: Australian	Braby (2004) GBIF (2022) Hardy and Lawrence (2017) Iqbal et al. (2021)
<i>Leptosia nina</i> (Fabricius, 1793)	Oriental: Indian, Ceylon, Indo-Malayan Australian: Austro-Malayan	GBIF (2022) Domine and dela Cruz (2020) Hardy and Lawrence (2017) Iqbal et al. (2021) Nayak (2020) Rahman and Maryati (2020)
LYCAENIDAE		
Theclinae		
<i>Arhopala kinabala</i> (H.H. Druce, 1895)	Oriental: Indo-Malayan	Iqbal et al. (2021)
<i>Flos apidanus</i> (Cramer, [1777])	Oriental: Indian, Indo-Malayan Australian: Austro-Malayan	GBIF (2022) Hardy and Lawrence (2017) Iqbal et al. (2021) Kunte et al. (2021)
<i>Rapala manea</i> (Hewitson, [1863])	Oriental: Indian, Ceylon, Indo-China, Indo-Malayan Australian: Austro-Malayan	GBIF (2022) Hardy and Lawrence (2017) Iqbal et al. (2021) Nayak (2020)
Polyommatainae		
<i>Catochrysops panormus</i> (C. Felder, 1860)	Oriental: Indian, Ceylon, Indo-China, Indo-Malayan Australian: Australian	GBIF (2022) Hardy and Lawrence (2017) Iqbal et al. (2021)
<i>Zizina otis</i> (Fabricius, 1787)	Oriental: Indian, Ceylon, Indo-China, Indo-Malayan Australian: Austro-Malayan, Polynesian, Australian Ethiopian: West Africa, South Africa Palearctic: Manchurian	GBIF (2022) Hardy and Lawrence (2017) Iqbal et al. (2021) Kunte et al. (2021)

APPENDIX Contd.

Family / Subfamily / Species	Distribution	Data Source
<i>Zizula hylax</i> (Fabricius, 1775)	Oriental: Indian, Ceylon, Indo-China, Indo-Malayan Australian: Austro-Malayan, Polynesian, Australian Ethiopian: West Africa, East Africa, South Africa, Malagasy	GBIF (2022) Hardy and Lawrence (2017) Iqbal et al. (2021) Larsen et al. (2007)
HESPERIDAE		
Hesperinae		
<i>Caltoris bromus</i> Leech, 1894	Oriental: Indo-China, Indo-Malayan Australian: Austro-Malayan Palearctic: Manchurian	GBIF (2022) Hardy and Lawrence (2017) Iqbal et al. (2021)
<i>Cephrenes acalle</i> Höpffer, 1874	Oriental: Indian, Ceylon, Indo-Malayan Australian: Austro-Malayan	GBIF (2022) Hardy and Lawrence (2017) Iqbal et al. (2021)
<i>Pelopidas conjuncta</i> (Herrich-Schäffer, 1869)	Oriental: Indian, Ceylon, Indo-Malayan Australian: Austro-Malayan	GBIF (2022) Hardy and Lawrence (2017) Iqbal et al. (2021)
<i>Potanthus sp.</i> Scudder, 1872	Oriental: Indian, Ceylon, Indo-China, Indo-Malayan Australian: Austro-Malayan Palearctic: Manchurian	GBIF (2022) Hardy and Lawrence (2017)

Research Article

Molecular Identification of Several Morphologically Distinct Flowerhorn Fish (Family) Using Mitochondrial *COI* Gene Marker

Dini Wahyu Kartika Sari^{1,3*}, Himawan Achmad^{2*}, Hafit Rahman², Harya Bimasuci³

1)Genetics and Fish Breeding Laboratory, Department of Fisheries, Faculty of Agriculture, Universitas Gadjah Mada, Yogyakarta, Indonesia

2)Fish Quarantine and Inspection Agency Yogyakarta, Ministry of Marine Affairs and Fisheries, Republic of Indonesia

3)Biotechnology Research Center, Universitas Gadjah Mada, Yogyakarta, Indonesia

* Corresponding author, email: dini.sari@ugm.ac.id, himz0008@gmail.com

Keywords:

Cichlid

COI

DNA barcoding

Flowerhorn

Mitochondria

phylogenetics

Submitted:

18 October 2022

Accepted:

27 February 2023

Published:

22 May 2023

Editor:

Ardaning Nuriliani

ABSTRACT

Flowerhorn fish has been known as a breed of fish produced by artificial hybridization between several cichlid fish. Other ornamental cichlid fish generally known to be crossed to make flowerhorn variant includes *Amphilophus citrinelus*, *Amphilophus labiatus*, *Vieja melanurus*, and *Amphilophus trimaculatus*. Our study identified a variety of flowerhorn samples with distinct morphotypes, dubbed as Cencu (LH1CC), Kamfa (LH2KF), Thai Silk (LH3TS), Kirin (LH4KR), Parrot (LH5PR), and Vieja (LH6VJ) using mtDNA *COI*-based DNA barcoding. Molecular analysis and phylogenetics showed that all sample had 0% genetic divergence and conspecific with *A. trimaculatus* sequence. Hence, we concluded that despite having varied morphotypes, all flowerhorn samples were identified as *A. trimaculatus* and were a variation of flowerhorn from *A. trimaculatus* lineage. The findings should be used as a precaution as the fish is identified as an invasive species.

Copyright: © 2023, J. Tropical Biodiversity Biotechnology (CC BY-SA 4.0)

INTRODUCTION

Ornamental fish has been one of the most prominent live fish commodities in the ornamental market. The global market valuation for ornamental fish is estimated at more than US\$ 10 billion, with over 2500 species being traded and more than 60% are freshwater fish (Dey et al. 2016). Among the freshwater fish breed and marketed as ornamental fish, flowerhorn fish is popular as aquarium fish especially in Southeast Asia (Mutia et al. 2007; Nico et al. 2007; Ng 2016).

Flowerhorn fish is considered as a hybrid individual, being a cross between different species and breeds of Neotropical cichlids that originated in Central America, such as Parrot cichlid, *Amphilopus labiatus*, *A. citrinelus*, *Amphilophus trimaculatus*, and *Vieja melanurus* (Nico et al. 2007; McMahan 2010). It is a popular aquarium fish known to be bred with various other cichlid species to produce individuals with specific desirable characteristics. The fish were divided into numerous types in the market based on morphological traits such as body color, pattern, and the presence of a head hump. The flowerhorn varieties were dubbed with various names such as Kamfa, Nakeemix, Golden base, Zhen zhu (Cencu) (Gonzales-Plasus et al. 2022).

Flowerhorn fish is a medium-sized fish with adult size around 35 cm (Magalhães et al. 2017), had vivid coloration and is often characterized by its head protuberance or nuptial hump and has black horizontal markings on their body (Than et al. 2019). Flowerhorn fish have been traded and distributed throughout Asia, the Americas, and Europe as decorative aquarium fish. The fish trade was particularly high in the Southeast Asia (Sandford 2007), with many aquarium owners and traders specially breed and contesting their fish. The flowerhorn itself is not a fish naturally found in local environment. In light of this, releasing the fish into nearby rivers, lakes, and waterways could potentially introduce an invasive species that endangers the aquatic habitat there (Mutia et al. 2007).

The invasive characteristics of flowerhorn fish derived from its hardiness and high-adaptability, making it a prominent competitor to the local fish community. The fish has been known as highly aggressive, omnivorous, adaptable and can rapidly breed in natural environment due to its parental brood care trait (Knight 2010). It is also predatory especially to juveniles and smaller fish, hence not only putting ecological pressure through resource competition but also through predation of the endemic fish (Hilgers et al. 2018). Cases of flowerhorn presence in local environment have been documented in the Southeast Asia region, such as in Malaysia (Ahmad et al. 2020), Thailand (Nico et al. 2007), and the Philippines (Guerrero 2014).

The flowerhorn fish is also widely circulated and traded in Indonesia as ornamental fish, marketed as “Louhan fish”, and is also considered a non-native and invasive species (Sentosa & Hediarto 2019). There have been several studies documenting the invasion of flowerhorn fish in local water system and natural lakes in Indonesia. The presence of flowerhorn varieties has been reported in Cirata reservoir in West Java (Wahyuni et al. 2014), Sermo Reservoir in Yogyakarta (Ariasari et al. 2018), Lake Toba in North Sumatra (Sinambela et al. 2021), and Lake Maninjau in West Sumatera (Samir et al. 2021). The fish was also reportedly introduced to Malili Lake system and Lake Poso in South Sulawesi where they severely impacted the population of endemic species through predation and competition (Herder et al. 2012; Sentosa & Wijaya 2012; Herder et al. 2022).

The Indonesian Government through Ministry of Fisheries and Marine Affairs have regulated distribution and banned several invasive species in the Minister Regulation No. 19/2020 which dictates that about 75 species of animals including fish, invertebrates, and amphibia were prohibited from distribution and entry in Indonesian territory (KKP 2020). The regulation was erected to control the circulation of potentially invasive species, and mitigate the introduction of non-native species that could harm endemic ecosystems. The list from the regulation includes several cichlid species such as *Cichlasoma trimaculatum*, now valid as *Amphilophus trimaculatus* (Fricke et al. 2022), *Amphilophus labiatus*, *Amphilopus citrinellus*, and *Mayaheros urophthalmus*, which are usually cross-bred as flowerhorn varieties.

Flowerhorn breeding usually resulted in many morphological variations, and the designated species of the fish itself can be unclear resulting of generations of hybridization. Varied morphological forms and external characteristics would hinder identifying flowerhorn fish. Hence, relying exclusively on morphological analysis for identification is generally inadequate. A further step is needed to identify flowerhorn fish, especially in molecular level.

Molecular identification of cichlid fish using DNA barcoding method have been previously conducted with overall success (van der Bank

2019), and even successfully identify closely related species such as species of *Oreochromis* and *Coptodon* using *COI* marker (Panprommin et al. 2019). Mitochondrial *COI* gene marker has been widely used as universal barcode for fish identification and can be used for identification and monitoring of invasive species in general (Nagarajan et al. 2020). In Indonesia, DNA barcoding using *COI* marker has been successfully used to identify invasive *Amphilophus* cichlid species in Brantas River (Amin et al. 2019), which further assert that *COI* gene is generally robust for identification of cichlid fish. This study aimed to identify flowerhorn fish with various morphological types that were part of the ornamental fish trade. DNA barcoding method using *COI* marker was employed to ascertain the species of the distributed flowerhorn fish in Yogyakarta area.

MATERIALS AND METHODS

Sample Processing

Samples were collected in 2019 and 2020 during annual invasive species mapping held by Fish Quarantine Station in Yogyakarta. Six fish samples were obtained from various ornamental fish shops and patrons of the Yogyakarta Fish Quarantine Station. The fish samples were given sample voucher corresponding to their trade names: LH1CC (Cencu), LH2KF (Kamfa), LH3TS (Thai Silk), LH4KR (Kirin), LH5PR (Parrot), and LH6VJ (Vieja). Sample materials were taken by anesthetizing the fish followed by aseptically cutting 1 cm² of the caudal fin. DNA was extracted using FavorPrep Tissue Genomic DNA Extraction Mini Kit (Favorgen) with the steps according to the manufacturer's manual.

PCR Amplification

DNA barcoding was used to further identify each specimen by amplifying the *COI* gene using PCR. The PCR reaction were prepared using MyTaq PCR mix (Bioline), containing Taq DNA polymerase, dNTPs, MgCl₂ and buffer. Primer pair used in this study was COX1 F (TCA CAC GTT GAT TTT TCT CGA CT) and COX1 R (AAT AAG CGC GTG TGT CAA CG), self-developed using Primer 3 Plus software (Rozen & Skaletsky 2000). PCR process consisted of one cycle of pre-denaturation step at 94°C for 3 minutes, followed by 35 cycles of denaturation step at 94°C for 1 minutes, annealing at 50°C for 30 seconds, and extension at 72°C for 1 minute, and a final extension step at 72°C for 5 minutes.

Amplified DNA was checked using gel electrophoresis with 1% agarose in 1X TBE. The gel was run in Mupid EXu Submarine Electrophoresis System at 10 V for 20 minutes and visualized using UV Transilluminator. Samples were sequenced by sequencing facility at 1st Base Asia (Singapore) using a sanger sequencing method.

Sequence Analysis

Raw sequences were processed post-sequencing before being aligned and analyzed. Sequences were checked and edited using BioEdit 7.2 (Hall 1999), and subsequently aligned using ClustalW 2.1 algorithm (Larkin et al. 2007). Nucleotide BLAST by NCBI was used for sequence identification. Phylogenetic analysis was conducted using MEGA11 software (Tamura et al. 2021). Tree-based analysis was performed using a Neighbor-Joining (NJ) method. The NJ phylogenetic tree was produced by bootstrap method with 1000 replicates to find the consensus tree. *COI* sequence of *Andinoacara rivulatus* (MT505734) was added as an outgroup. Pairwise genetic distances were calculated using Kimura-2 Parameter (K2P) using DnaSP ver.6 (Rozas et al. 2017).

RESULTS AND DISCUSSION

Results

Molecular Identification with BLAST Analysis

DNA sequences were amplified from partial *COI* gene. The sequences were compared to other *COI* genes in the GenBank database using BLAST algorithm. The result was selected and confirmed by higher percent identity score (95 - 100%), which concede with higher similarity from the GenBank sequences. Thus, 100% percent identity score would be interpreted as the sample and comparison sequence being the same species.

The NCBI BLAST and BOLD analysis results (Table 1) showed that all samples had 100% identity with *Amphilophus trimaculatus* (GenBank: MN888505; BOLD: MT975935). The BLAST results also had 100% query cover and zero e-value, meaning each queried sequence was fully aligned with the GenBank reference sequence with zero error value.

Table 2 shows the results of other congeneric and intergeneric species. *Amphilophus lyonsi* (MG936655) and *Amphilophus citrinellus* (MG496077) had the highest BLAST percent identity at 95.73% and 95.41%, respectively, followed by *Amphilophus labiatus* (JQ667489) at 95.40. The top two congeneric related species, according to BOLD species identifier, are *A. lyonsi* (DQ11919) and *A. citrinellus* (JN024798). The results indicated that the *COI* sequences from the six specimens were homologous to the *COI* DNA sequence of *Amphilophus trimaculatus*.

Table 1. Results of NCBI BLAST and BOLD Species Identifier based on *COI* sequence from the six flowerhorn samples.

No	Sample	GenBank Asc. no.	BLAST					BOLD		
			Species	Percent Identity	Query Cover	e-value	Top Similar	Species	Similarity	Top Similar
1	LH1CC	OQ3713 22	<i>Amphilophus trimaculatus</i>	100%	100%	0	MN888505	<i>Amphilophus trimaculatus</i>	100%	MT975935
2	LH2KF	OQ3713 23	<i>Amphilophus trimaculatus</i>	100%	100%	0	MN888505	<i>Amphilophus trimaculatus</i>	100%	MT975935
3	LH3TS	OQ3713 24	<i>Amphilophus trimaculatus</i>	100%	100%	0	MN888505	<i>Amphilophus trimaculatus</i>	100%	MT975935
4	LH4KR	OQ3713 25	<i>Amphilophus trimaculatus</i>	100%	100%	0	MN888505	<i>Amphilophus trimaculatus</i>	100%	MT975935
5	LH5PR	OQ3713 26	<i>Amphilophus trimaculatus</i>	100%	100%	0	MN888505	<i>Amphilophus trimaculatus</i>	100%	MT975935
6	LH6VJ	OQ3713 27	<i>Amphilophus trimaculatus</i>	100%	100%	0	MN888505	<i>Amphilophus trimaculatus</i>	100%	MT975935

Table 2. Top five related species results from BLAST and BOLD identification.

No	BLAST					BOLD		
	Species	Percent Identity	Query Cover	e-value	Asc. Number	Species	Similarity	Asc. Number
1	<i>Amphilophus lyonsi</i>	95.73%	99%	0	MG936655	<i>Amphilophus lyonsi</i>	95.73%	DQ119199
2	<i>Amphilophus citrinellus</i>	95.41%	99%	0	MG496077	<i>Amphilophus citrinellus</i>	95.55%	JN024798
3	<i>Amphilophus labiatus</i>	95.41%	99%	0	JQ667489	<i>Amphilophus labiatus</i>	95.52%	Unpublished
4	<i>Parachromis managuensis</i>	93.53%	100%	0	KU692739	<i>Amphilophus astorquii</i>	95.52%	Unpublished
5	<i>Panamius panamensis</i>	93.35%	99%	0	MG937088	<i>Amphilophus chancho</i>	95.52%	Unpublished

Pairwise Distance Analysis

Pairwise distance analysis estimates the evolutionary divergence between compared sequences. Analysis was conducted using Kimura 2-parameter (K2P) model. Results from pairwise distance analysis is presented in table 3 with percentage K2P values. Samples were compared with sequences derived from BLAST result and additional *Vieja* genus: *Vieja maculicauda* (MG496249), *Vieja fenestrata* (HM379818), and *Vieja melanura* with the valid name *V. melanurus* (MZ379719) for further comparison

Based from distance analysis, intraspecific genetic distance value was at 0.00%. Distance value of 4.95 – 21.25% showed inter-generic distance. All samples showed 0.00% genetic distance with *Amphilophus trimaculatus* sequence. Samples higher genetic divergence from the *Amphilophus* and *Vieja* genus sequences with 4.95% pairwise distance value and 13.52 – 14.29% value compared to the outgroup. It can be inferred that the six samples belong to the same taxonomic group as *Amphilophus trimaculatus* sequence.

Phylogenetic Tree Analysis

Tree analysis was conducted using Neighbor-Joining method. The tree was drawn to scale, with branch lengths in the same units as those of the evolutionary distances used to infer the phylogenetic tree (K2P). A total of 12 aligned and trimmed sequences were used to make the phylogenetic tree, each comprised of 634 bp. Six *COI* sequences were derived from our samples presented with coded label, while the rest were sequences derived from GenBank for comparison. All trees were rooted using out-group *Andinoacara rivulatus* sequence. Evolutionary distance was calculated using Kimura 2-parameters on all trees with 1000 bootstrap replicates. Phylogenetic tree is presented in Figure 1.

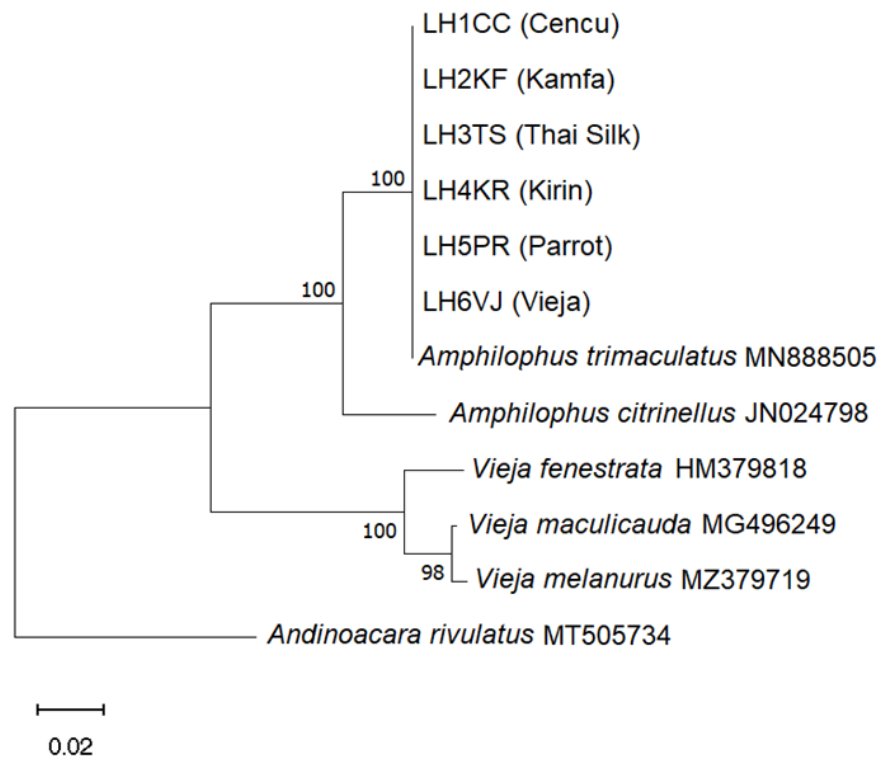


Figure 1. Phylogenetic analysis results using Neighbor-Joining (NJ). Bar represents calculated genetic distance based on the number of base substitutions for each site. Numbers on the branches indicated bootstrap support. Samples were coded with “LH-“ prefix followed by a number and 2 letters of morphotype code.

Table 3. Genetic distance between samples and compared sequences (percentage of K2P).

No	Species	1	2	3	4	5	6	7	8	9	10	11
1	LH1CC (Cencu)											
2	LH2KF (Kamfa)	0.00										
3	LH3TS (Thai_Silk)	0.00	0.00									
4	LH4KR (Kirin)	0.00	0.00	0.00								
5	LH5PR (Parrot)	0.00	0.00	0.00	0.00							
6	LH6VJ (Vieja)	0.00	0.00	0.00	0.00	0.00						
7	<i>Amphilophus trimaculatus</i>	0.00	0.00	0.00	0.00	0.00	0.00					
8	<i>Amphilophus citrinellus</i>	4.95	4.95	4.95	4.95	4.95	4.95	4.95				
9	<i>Vieja maculicauda</i>	13.52	13.52	13.52	13.52	13.52	13.52	13.52	14.18			
10	<i>Vieja fenestrata</i>	13.90	13.90	13.90	13.90	13.90	13.90	13.90	13.95	3.93		
11	<i>Vieja melanura</i>	14.29	14.29	14.29	14.29	14.29	14.29	14.29	14.96	0.95	3.58	
12	<i>Andinoacara rivulatus</i>	19.36	19.36	19.36	19.36	19.36	19.36	19.36	20.50	21.25	20.82	21.25

The phylogenetic tree indicated that all six samples formed a distinct grouping with the *Amphilophus trimaculatus* sequence. *Amphilophus* and *Vieja* genera made a separate group from the sample sequences, thus inferred that they are genetically distant from *Amphilophus trimaculatus* group. The topology strongly suggests that all samples were the same species and classified as *Amphilophus trimaculatus* despite morphological difference.

Discussion

Flowerhorn, a hybrid breed of several cichlids has been known to have unclear taxonomic status. Morphological distinctions have led to the rise of several "variants" of flowerhorn that were circulated in the market such as "Zhen zhu" or "Cencu" variant with pearly-white scale coloration, "Golden base" variant characterized by yellow-colored body, and "Kamfa" variety with larger head bump. It is considered almost impossible to identify the original cichlid species used to make flowerhorn hybrid, let alone designate the taxonomic status. Hence, this study used molecular identification using *COI* gene in an effort to shed some light on the phylogenetics and taxonomic position of flowerhorn cichlid.

The family of Cichlidae or cichlid fishes was known to be highly adaptable and resilient to environmental changes. Previous work by van Rijssel et al. (2021) elucidated how a species of cichlid (*Haplochromis pyrrhocephalus*) showed morphological adaptation responses to environmental perturbation, which the morphological changes transcended species-exclusive characteristics. Such natural morphological adaptation remains unclear whether it was from hybridization, phenotypical plasticity or evolution. In case of flowerhorn species, morphological differences were exclusively artificial as a result of selective hybridization. There is currently limited evidence that the flowerhorn morphology would change when the fish was released outside the aquarium environment. However, in spite of hobbyists' beliefs that domestication is able to tame the rapaciousness of flowerhorn, it is scientifically proven that flowerhorns can survive and thrive in natural environment, which accounts to their invasive capability (Mutia et al. 2007; Herder et al. 2012)

Previous studies such as Shirak et al. (2009) used partial sequence of mitochondrial *COI* to identify native and introduced cichlid fishes. Since then, the *COI* gene has also been used to identify and map invasive cichlid fish species in aquatic environment (Pèlèbè et al. 2021) and investigate the genetic diversity of the designated invasive species (De la Ossa-Guerra et al. 2020). Partial sequence of *COI* gene was also successfully amplified in this study and yielded 650 bp of nucleotide sequence for mo-

lecular identification. The main idea of the molecular identification process was to verify whether the flowerhorn aquarium specimens found in this study belonged to which cichlid species that were deemed invasive species, to which the culture and translocation are regulated by The Indonesian government.

Molecular identification process was initially performed by using NCBI BLAST and BOLD species identifier algorithm to investigate the percent identity between *COI* genes of the six specimens to other *COI* sequences in GenBank. The results showed that all sequences had 100% similarity with *Amphilophus trimaculatus* sequence, and to a lesser extent *Amphilophus citrinellus* and *A. labiatus*.

Further comparison with pairwise distance analysis showed that all six specimens had zero genetic divergence with *A. trimaculatus* sequence, while higher divergence was shown with *Amphilophus* with 4.95% genetic distance. The genetic distance with *Vieja* genus showed higher divergence at 13.52 - 14.29%. *Vieja* genus was also used as comparison since some members of the genus were often used as parent for cross-breeding flowerhorn fish (Nico et al. 2007). *Andinoacara rivulatus* or Green Terror fish, another possible parent breed for flowerhorn variant, was used as outgroup and showed 19.36% genetic distance compared to the specimens. The results of genetic distance exhibited homologous *COI* gene sequences from the six specimen and *A. trimaculatus*.

Phylogenetic analysis showed the six flowerhorn specimens clustered into one clade alongside *A. trimaculatus* sequence, while the other genus formed their own clade. The samples also indicated being the same haplotype as the *A. trimaculatus* sequence, being in the same end-point of the branch. The trees topology and phylogenetic position further assert that the flowerhorn samples can be identified as *A. trimaculatus*.

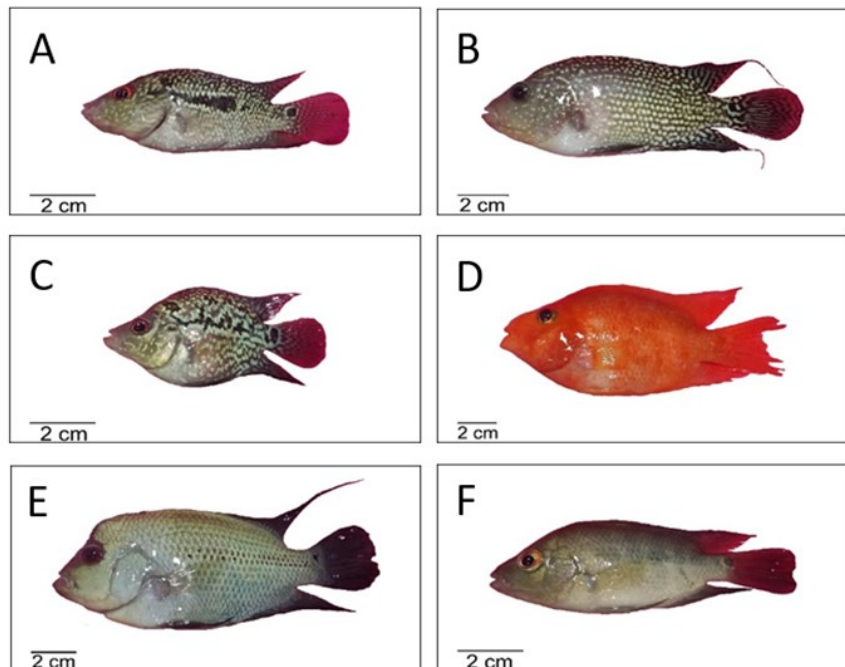


Figure 2. Samples with different morphotypes: (A) Cencu - LH1CC, (B) Kamfa - LH2KF, (C) Thai Silk - LH3TS, (D) Kirin - LH4KR, (E) Parrot - LH5PR, (F) Vieja - LH6VJ.

It is interesting to note that among morphologically distinct samples, especially dubbed as variants of flowerhorn species (Figure 2) such as Zhen Zhu, Kamfa, Parrot, Vieja, Kirin, and Thai Silk, molecular analysis classified them as one clade alongside *A. trimaculatus* with 0% genetic

divergence, while genus with potential parentage showed > 4% divergence as in the *Amphilopus* genus. Previous study by Wang et al. (2015) found that K2P genetic divergence among congeneric farmed freshwater fish averaged 5%, while conspecific divergence averaged 0.34%. The result is similar to this study, with intraspecific divergence is 0% and interspecific divergence being 4.95%.

Red devil fish (*Amphilopus labiatus*) and Midas cichlid (*Amphilopus citrinelus*) were known as potential cross to obtain specific variety of flowerhorn fish, as well as *A. trimaculatus* (Three spotted cichlid). Other cichlid fish such a *Cichlasoma festae*, now valid as *Mesoheros festae* (Guayas cichlid), and another hybrid cichlid called Blood Parrot cichlid were also suggested as cross-breeding material to create flowerhorn fish (Rahmati-Holasoo et al. 2015). However, it can be assumed based on the genetic divergence analysis that the parental lineage for the specimens could be *A. trimaculatus*.

The results of this study were entirely based on comparison and analysis between mitochondrial *COI* gene. It is generally accepted that mitochondrial inheritance in animals is uniparental, particularly in the matrilineal lineage. The cellular mitochondrion is inherited through the mitochondria of the oocyte, hence the mitochondrial genes would reflect the maternal origin of the individual (Sato & Sato 2013). The result of the species being closely related to *A. trimaculatus* in the molecular analysis may only reflect the maternal lineage of specimens.

We could not identify the parental hybrid by using just mitochondrial *COI* sequence for analysis, however our findings still raised a question regarding to the status of the flowerhorn specimen being a hybridized fish in this study. All samples were not collected from only one flowerhorn breeding facility, rather they came from various shops and patrons of The Fish Quarantine Station in Yogyakarta. Despite varied source and morphology, the mtDNA *COI* sequences from all six specimens did not exhibit polymorphism and had consistent genetic divergence value.

We also assume that the parental linkage is exclusively maternal. Although, the case of heteroplasmy or paternal leakage has been known to occur in hybridized fish. For instance, previous work by Morgan et al. (2013) found indication of paternal leakage in mitochondrial DNA of hybridized Scombrid fish. However, we took the general assumption that heteroplasmy or parental leakage does not occur in our *COI* sequence by the absence of double peaks and consistently similar nucleotide sequence between the sample sequences. Presence of double peaks in the nucleotide sequence of the *COI* region is an indicator of parental leakage in mitochondrial sequence (Rodríguez-Pena et al. 2020).

Phylogenetic analysis of mtDNA *COI* strongly suggested that the specimens were monophyletic with 100% similarity and 0% genetic divergence from *A. trimaculatus* sequence. All samples had identical *COI* sequence, despite being collected from various sources. Morphological differences were vastly distinctive between samples, despite molecular analysis found all to be one species of *A. trimaculatum*. Clear morphological distinction with the parent species was indeed a trait of hybridized fish (Selz et al. 2014; Pauers et al. 2018). In our case, different morphological variation of flowerhorns breed despite all specimen being conspecific with *A. trimaculatus* would infer that flowerhorn specimens in this study were solely bred from a flowerhorn variation of *A. trimaculatus* origin as opposed to being a hybrid or cross-bred from different cichlid species. However, regarding the verification of the fish being hybrid, our findings were inconclusive since mitochondria *COI* gene is inherited mat-

rilineally. The *COI* gene can be reliably used to identify and delineate cichlid species, but in the case of hybridization and hemiplasy, an integrative procedure is preferred (Breman et al. 2016). A more complex approach such as using *RAG1* nuclear gene (Kim et al. 2020), combination between mtDNA and nuclear *RFR3* gene marker (Qu et al. 2018), or multi-locus gene analysis with mitochondrial control region gene, nuclear gene, and microsatellite loci (Willis et al. 2012) or similar approach should be considered for future study to identify both parental hereditary components within their genome

The results of this analysis however did not diminish the fact that each specimen has the potential to be an invasive species if released in natural environment. The species of *Amphilophus trimaculatus* (previously named *Cichlasoma trimaculatum*) has been known as an invasive fish and their breed has been previously reported to invade local ecosystems in Indonesia, such as Lake Matano in Sulawesi (Nasution & Dina 2019). The fish was also reported as being invasive in Lake Sempor in Central Java (Hedianto et al. 2014) where the *A. trimaculatus* flowerhorn species dominated overall fish catch in the lake. Previously mentioned study also reported that fish is unpopular for consumption and fetch low price in the market compared local commodities like barb (*Barbonymus goniotus*), ceba fish (*Puntius binotatus*), and lunjar fish (*Rasbora argyrotaenia*). Nasution et al. (2022) reported *A. trimaculatum* population is relatively abundant in the littoral zone of Lake Mahalona, Sulawesi, consisted of up to 21.34% from the total population structure despite being an alien species. Reports outside Indonesia included India's Lake Chenai (Daniel et al. 2020) and River Cauvery (Kumar et al. 2020) where the fish exhibited predatory behavior and may deter predation by having spiny dorsal fins. The potential for flowerhorn fish to become an invasive species should be considered in the aquarium trade; as a result, fish distributors and owners should check the regulations and avoid releasing the fish into the local environments.

CONCLUSIONS

The flowerhorn fish samples with distinct morphological characteristics had homologous mtDNA *COI* sequence, and were conspecific to *Amphilophus trimaculatus* sequence according to phylogenetic and distance analysis. It is assumed that based on mtDNA *COI* all flowerhorn samples were bred from flowerhorn parents with *A. trimaculatus* origin. Further study should investigate the hybridization of different flowerhorn fish to confirm whether the fish were bred from different species parentals using other DNA markers, such as nuclear genes, microsatellites, or a combined approach. Our findings should also be used as precaution for the flowerhorn's potential as invasive fish species for being in the lineage of *A. trimaculatus*, a previously known invasive species.

AUTHOR CONTRIBUTION

D.W.K.S. designed the research, performed experiments, analyzed the data, and wrote the manuscript; H.A. and H.R collected the samples and analyzed data; H.B analyzed the data and wrote the manuscript.

ACKNOWLEDGMENT

This work was partly supported by Ministry of Marine Affairs and Fisheries Republic of Indonesia and partly supported by Faculty of Agriculture UGM under the grant number 1505/PN/PT/2020. We thank Rohana Hidayati, Ayu Luthfiah Purnamasari, and Shabrina Arysandi for technical assistance.

CONFLICT OF INTEREST

Authors declare that there is no conflict of interest.

REFERENCES

- Ahmad, A.K. et al., 2020. Preliminary Study on Invasive Fish Species Diffusion in Selected Malaysian Freshwater Ecosystems. *Pakistan Journal of Biological Sciences*, 23, pp.1374-1379. doi: 10.3923/pjbs.2020.1374.1379
- Amin, M.H.F. et al., 2019. DNA barcoding of invasive freshwater fish reveals two species of *Amphilophus* from two dams in Brantas stream, East Java, Indonesia. *Eco. Env. & Cons.*, 25, pp.141-145.
- Ariasari, A., Helmiati, S. & Setyobudi, E., 2018. Food preference of red devil (*Amphilophus labiatus*) in the Sermo Reservoir, Kulon Progo Regency. *IOP Conf. Ser.: Earth Environ. Sci.*, 139. doi: 10.1088/1755-1315/139/1/012018
- Breman, F.C. et al., 2016. Testing the potential of DNA barcoding in vertebrate radiations: the case of the littoral cichlids (Pisces, Perciformes, Cichlidae) from Lake Tanganyika. *Mol Ecol Resour*, 16, pp.1455-1464. doi: 10.1111/1755-0998.12523
- Daniel, N. et al., 2020. Report on the occurrence of invasive alien fish, *Cichlasoma trimaculatum* *Cichlasoma trimaculatum* (Günther, 1867) at freshwater Lake of Chennai. *Journal of Entomology and Zoology Studies*, 8(4), pp. 2418-2420
- De la Ossa-Guerra, L.E., Santos, M.H., & Artoni, R.F., 2020. Genetic Diversity of the Cichlid *Andinoacara latifrons* (Steindachner, 1878) as a Conservation Strategy in Different Colombian Basins. *Front. Genet.*, 11(815), pp.1-9. doi: 10.3389/fgene.2020.00815
- Dey, V.K., 2016. The global trade in ornamental fish. *Infofish International*, 4, pp.52-55.
- Fricke, R., Eschmeyer, W.N., & van der Laan, R., 2022. 'Eschmeyer's catalog of Fishes: Genera, Species, References', in *California Academy of Sciences*, viewed 26 February 2023 from <http://researcharchive.calacademy.org/research/ichthyology/catalog/fishcatmain.asp>
- Gonzales-Plasus, M., Plasus, L.N. & Mecha, NJMF., 2022. Baseline study on the freshwater ornamental fish industry in Palawan. *The Palawan Scientist*, 14(1), pp.11-21
- Guerrero III, R.D., 2014. Impacts of Introduced Freshwater Fishes in the Philippines (1905-2013): A Review and Recommendations. *Philippine Journal of Science*, 143(1), pp.49-59.
- Hall, T.A., 1999. BioEdit: A User-Friendly Biological Sequence Alignment Editor and Analysis Program for Windows 95/98/NT. *Nucleic Acids Symposium Series*, 41, pp.95-98.
- Hedianto, D.A. et al., 2014. Parameter Populasi Ikan Lohan (*Cichlasoma trimaculatum*, Gunther 1867) di Waduk Sempor, Jawa Tengah. *Jurnal Penelitian Perikanan Indonesia*, (20)2, pp.81-88. doi: 10.15578/jppi.20.2.2014.81-88
- Herder, F. et al., 2022. More Non-Native Fish Species than Natives, and an Invasion of Malawi Cichlids, in Ancient Lake Poso, Sulawesi, Indonesia. *Aquatic Invasions*, 17(1), pp.72-91. doi: 10.3391/ai.2022.17.1.05.
- Herder, F. et al., 2012. Alien invasion in Wallace's Dreamponds: records of the hybridogenic "flowerhorn" cichlid in Lake Matano, with an annotated checklist of fish species introduced to the Malili Lakes system in Sulawesi. *Aquatic Invasions*, 7(4), pp.521-535. doi: 10.3391/AI.2012.7.4.009

- Hilgers, L. et al., 2018. Alien attack: trophic interactions of flowerhorn cichlids with endemics of ancient Lake Matano (Sulawesi, Indonesia). *Evolutionary Ecology Research*, 19, pp.575-590
- Kementerian Kelautan & Perikanan (KKP), 2020. 'PERMEN KKP No.19/PERMEN-KP/2020', viewed 10 October 2021, from <https://jdih.kkp.go.id/peraturan/4cae6-19-permen-kp-2020-larangan-jenis-ikan-berbahaya-dan-merugikan-otentifikasi.pdf>
- Kim, P., Han, J. & An, S.L., 2020. Genetic identification of species and natural hybridization determination based on mitochondrial DNA and nuclear DNA of genus *Zacco* in Korea. *Mitochondrial DNA Part A*, 31(6), pp.221-227. doi: 10.1080/24701394.2020.1777994
- Knight, J.D.M., 2010. Invasive ornamental fish: a potential threat to aquatic biodiversity in peninsular India. *J Threat Taxa.*, 2, pp.700-704. doi: 10.11609/JoTT.o2179.700-4
- Tamura, K., Stecher, G., & Kumar, S., 2021. MEGA11: Molecular Evolutionary Genetics Analysis Version 11. *Molecular Biology and Evolution*, 38(7), pp.3022-3027. doi: 10.1093/molbev/msab120
- Kumar, L. et al., 2020. Risk analysis of non-native three-spot cichlid, *Amphilophus trimaculatus*, in the River Cauvery (India). *Fish Manag Ecol*, 28, pp.158-166. doi: 10.1111/fme.12467
- Larkin, M.A. et al., 2007. Clustal W and Clustal X version 2.0. *Bioinformatics*, 23, pp.2947-2948.
- Magalhães, A.L.B. et al., 2017. Small size today, aquarium dumping tomorrow: sales of juvenile non-native large fish as an important threat in Brazil. *Neotropical Ichthyology*, 15(4), pp.1-10. doi: 10.1590/1982-0224-20170033
- McMahan C.D., Geheber A.D. & Piller, K.R., 2010. Molecular systematics of the enigmatic Middle American genus *Vieja* (Teleostei: Cichlidae). *Molecular Phylogenetics and Evolution*, 57, pp.1293-1300, doi: 10.1016/j.ympev.2010.09.005
- Morgan, J.A.T. et al., 2013. Hybridisation, paternal leakage and mitochondrial DNA linearization in three anomalous fish (Scombridae). *Mitochondrion*, 13(6), pp.852-861. doi: 10.1016/j.mito.2013.06.002
- Mutia M. et al., 2007. Review of the Ornamental Fish Industry: Production Marketing Trends, Technological Developments, and Risks. *Fish for the People: a Southeast Asian Fisheries Development Center*, pp.1-20.
- Nagarajan, M., Parambath, A.N. & Prabhu, V.R., 2020. DNA Barcoding: A Potential Tool for Invasive Species Identification. In: *DNA Barcoding and Moleccular Phylogeny - Second Edition*. Cham, Switzerland: Springer Nature Switzerland, pp.31-43. doi: 10.1007/978-3-030-50075-7_3.
- Nasution, S.H. & Dina, R., 2019. Population structure and gonadal maturity stage of endemic and alien fish dominant species in Lake Matano, South Sulawesi. *IOP Conf. Ser. Earth Environ. Sci*, 380. doi:10.1088/1755-1315/380/1/012012
- Nasution, S.H., Muchlis, A.M. & Cinnawara, H.T., 2022. The abundance of alien fish species flowerhorn (*Cichlasoma trimaculatum* (Gunther, 1867) in its fishing ground area at Lake Mahalona, South Sulawesi. *IOP Conf. Ser.: Earth Environ. Sci.*, 1036. doi:10.1088/1755-1315/1036/1/012103
- Ng, C., 2016. The ornamental freshwater fish trade in Malaysia: The collection, breeding and marketing of ornamental fishes is a sizable industry. *Utar Agriculture Science Journal*, 2(4), pp.7-18.

- Nico, L.G., Beamish, W.H. & Musikasinthorn, P., 2007. Discovery of the invasive Mayan Cichlid fish *Cichlasoma urophthalmus* (Günther, 1862) in Thailand, with comments on other introductions and potential impacts. *Aquatic Invasions*, 2, pp.197–214. doi: 10.3391/ai.2007.2.3.7
- Panprommin, D., Soontornpravit, K. & Pangeson, T., 2019. Comparison of three molecular methods for species identification of the family *Cichlidae* in Kwan Phayao, Thailand. *Mitochondrial DNA Part A*, 30 (1), pp.184–190. doi: 10.1080/24701394.2018.1472248
- Pauers, M.J. et al., 2018. Selection, hybridization, and the evolution of morphology in the Lake Malaŵi endemic cichlids of the genus *Labotropheus*. *Scientific Reports*, 8(15842), pp.1–10. doi:10.1038/s41598-018-34135-x
- Pèlèbè, R.O.E. et al., 2021. Molecular Identification of an Invasive *Sarotherodon* Species from the Atchakpa Freshwater Reservoir (Ouémé River Basin, Benin) and Comparison within *S. melanotheron* Using *COI* Markers. *Diversity*, 13(7), 297. <https://doi.org/10.3390/d13070297>
- Qu, M. et al., 2018. Genetic diversity within grouper species and a method for interspecific hybrid identification using DNA barcoding and *RYR3* marker. *Molecular Phylogenetics and Evolution*, 121, pp.46–51. doi:10.1016/j.ympev.2017.12.031
- Rahmati-Holasoo, H., et al., 2015. Polycystic liver in flower horn fish, hybrid cichlid. *Journal of Fish Disease*, 38(3), pp. 325–328 doi: 10.1111/jfd.12245.
- Raja, K. et al., 2019. Present and future market trends of Indian ornamental fish sector. *International Journal of Fisheries and Aquatic Studies*, 7(2), pp.06–15.
- Rodríguez-Pena, E. et al., 2020. High incidence of heteroplasmy in the mtDNA of a natural population of the spider crab *Maja brachydactyla*. *PloS one*, 15(3), e0230243. <https://doi.org/10.1371/journal.pone.0230243>
- Rozas, J. et al., 2017. DnaSP 6: DNA Sequence Polymorphism Analysis of Large Datasets. *Mol. Biol. Evol.*, 34, pp.3299–3302. doi: 10.1093/molbev/msx248
- Rozen, S. & Skaletsky, H.J., 2000. Primer3 on the WWW for general users and for biologist programmers. In *Bioinformatics Methods and Protocols: Methods in Molecular Biology*. Totowa, NJ: Humana Press, pp.365–386. doi: 10.1385/1-59259-192-2:365
- Samir, O. et al., 2021. Introduced fish species and their characters in Lake Maninjau, West Sumatra. *IOP Conf. Ser.: Earth Environ. Sci.*, 789. doi: 10.1088/1755-1315/789/1/012024.
- Sandford, G., 2007. An Illustrated Encyclopedia of Aquarium Fish. In Singapore: Quantum Publishing
- Sato M. & Sato K., 2013. Maternal inheritance of mitochondrial DNA by diverse mechanisms to eliminate paternal mitochondrial DNA. *Biochimica et Biophysica Acta*, 1833(8), pp.1979–1984. doi:10.1016/j.bbamcr.2013.03.010.
- Selz, O.M., et al., 2014. Relaxed trait covariance in interspecific cichlid hybrids predicts morphological diversity in adaptive radiations. *J. Evol. Biol.*, 27, pp.11–24. <https://doi.org/10.1111/jeb.12283>
- Sentosa, A.A. & Hediando, D.A., 2019. Sebaran Louhan yang Menjadi Invasif di Danau Matano, Sulawesi Selatan. *LIMNOTEK Perairan Darat Tropis di Indonesia*, 26(1), pp.1–9. doi: 10.14203/limnotek.v26i1.255

- Sentosa, A.A. & Wijaya, D., 2012. Community structure of introduced fish in Lake Batur, Bali. *Berita Biologi*, 11(3), pp.329-337.
- Shirak, A., et al., 2009. DNA Barcoding of Israeli Indigenous and Introduced Cichlids. *The Israeli Journal of Aquaculture – Bamidgeh*, 61(2), pp.83-88.
- Sinambela, M. et al., 2021. Fish Diversity In Lake Toba. *Proceedings of Sixth Postgraduate Bio Expo 2021*. Medan State University.
- Than, A.A., Aung, N.N. & Myint, K.M.M., 2019. Investigation of the growth rate of *Cichlasoma* sp. (Gunther, 1867) rearing with different diets in aquaria. *University Research Journal*, 11(4), pp.1-12.
- van der Bank, F.H., 2019. A DNA barcoding study of seven cichlid species from southern Africa reveals their phylogenetic relationships. *African Journal of Aquatic Science*, 44(3), pp.291-293. doi: 10.2989/16085914.2019.1628703
- van Rijssel, J.C., et al., 2021. Rapid Evolutionary Responses in Cichlids: Genetics of Adaptation, Morphology, and Taxonomic Implications. In: *The Behavior, Ecology, and Evolution of Cichlid Fishes*. Dordrecht, The Netherlands: Springer Nature B.V., pp.247-283. doi: 10.1007/978-94-024-2080-7_8.
- Wahyuni, S., Sulistiono, & Affandi, R., 2014. Distribusi secara spasial dan temporal ikan di Waduk Cirata, Jawa Barat. *Jurnal Bumi Lestari*, 14 (1), pp.74-84.
- Wang, Q. et al., 2015. DNA barcoding analysis of commercial freshwater fish species cultured in china. *The Israeli Journal of Aquaculture – Bamidgeh*, 67, pp.1-6. doi: 10.46989/001c.20699
- Willis, S.C. et al., 2012. Simultaneous delimitation of species and quantification of interspecific hybridization in Amazonian peacock cichlids (genus *Cichla*) using multi-locus data. *BMC Evolutionary Biology*, (12)96, pp.1-24. doi:10.1186/1471-2148-12-96

Research Article

Isolation and Characterization of Rhizospheric Bacteria Associated with Canna Plant for Production of Maltooligosaccharide Amylase

Rina Dwi Agustiani^{1,3}, Oedjijono^{1*}, Nanik Rahmani², Nuraeni Ekowati¹

1) Faculty of Biology, University of Jenderal Soedirman, Jalan dr. Soeparno 63 Purwokerto 53122, Indonesia.

2) Center for Applied Microbiology Research, Research Institute for Life and Environmental Sciences, National Research and Innovation Agency (BRIN), Cibinong, Bogor 16911, Indonesia.

3) Department of Biology, Faculty of Science and Technology, International Women University, Bandung 40173, Indonesia.

* Corresponding author, email: oedjijono@unsoed.ac.id

Keywords:

Amylolytic bacteria

Canna

Maltooligosaccharides

16S rDNA gene

Submitted:

13 October 2022

Accepted:

30 January 2023

Published:

26 May 2023

Editor:

Miftahul Ilmi

ABSTRACT

The objectives of the study were to isolate amylolytic bacteria from the rhizosphere and plant tissue of *Canna edulis* Ker., as well as litter; to know oligosaccharide compounds produced from starch hydrolyzed by the bacterial enzymes, and to identify the amylolytic bacteria based on phenetic and 16S rRNA gene sequences. From the rhizosphere, Canna plant tissue, and litters obtained thirty-two amylolytic bacterial isolates. Eight isolates (TH6, TH7, T5, T10, D2, D3, A3, S1) produced high clear zone diameters ranging from 18-30 mm; especially an isolate T10, which was consistent in producing a total clear zone diameter of 20 mm. The hydrolysate of starch hydrolysed by the T10 amylase resulted in three oligosaccharide compounds maltotriose, maltotetraose, and maltopentose. The amylase activity of isolate T10 was optimal at a temperature of 40°C and pH at 0.801 U/mL. The isolate T10 was identified as a species member of *Bacillus toyonensis* based on phenotypic characterization and 16S rDNA gene sequencing analysis with a similarity value of 99.93%.

Copyright: © 2023, J. Tropical Biodiversity Biotechnology (CC BY-SA 4.0)

INTRODUCTION

Oligosaccharides are members of an essential group of carbohydrates. Macromolecules with short-chain polysaccharide sugars of 2 to 20 saccharide units. Functional oligosaccharides such as galactooligosaccharide (GOS), fructooligosaccharide (FOS), and maltooligosaccharide (MOS) are well-known prebiotics owing to their ability to selectively stimulate beneficial bacteria in the intestines, particularly bifidobacterial species (Zhao et al. 2017). Developing oligosaccharide products is one of the businesses with high economic value. Plants such as Canna contain much starch, one of the crucial ingredients (substrate) to produce oligosaccharides enzymatically. Canna plants (*Canna edulis* Ker.) contain high levels of carbohydrates, mainly starch (93.3%), which consists of amylose (33.48%) and amylopectin (59.82%) (El-Fallal et al. 2012). Starch is hydrolysed into smaller oligosaccharides by α -amylase, one of the most important commercial enzymes (Jang et al. 2020).

The starch-processing industry has exploited amylase as a substitute for acid hydrolysis in producing starch hydrolysis. Amylase acts as a biocatalyst for the hydrolysis of starch into simpler carbohydrates, such

as glucose, maltose, and dextrin (Divakaran et al. 2011; Abdalla et al. 2021). Amylolytic bacteria are producers of amylase that can be used as biocatalysts in the starch hydrolysis process (Ding et al. 2021) to produce various maltooligosaccharide products, such as maltotriose, maltotetraose, maltopentaose, and maltohexaose (Pan et al. 2017).

Canna plants and its surrounding, including the rhizosphere and plant tissues, can be sources of isolating amylolytic bacteria. The high starch content in canna tubers makes them a suitable substrate for growing various bacteria, especially amylolytic bacteria. The bacteria isolated from starch-rich sources generally have the potential to produce amylase with high activity (Hellmuth & van den Brink 2013). In addition, the rhizosphere is known as the most diverse microbial habitat concerning species richness and community size. The interaction between plant roots and microorganisms is intensive around the rhizosphere, because the plants secrete exudates containing carbohydrates, amino acids, and other nutrients utilized by bacteria for growth. On the contrary, rhizospheric bacteria can produce proteins and enzymes that are important for the biological function of host plants (Afifah et al. 2018).

Bacteria, fungi, plants, and animals play an important role in utilizing polysaccharides. Members of the genus *Bacillus* were known to produce various enzymes, such as amylase that have been used in many industries, such as fermentation, textiles, paper, medicine, and sugar (Gupta et al. 2003). They are derived mainly from *Bacillus licheniformis* and *B. amyloliquefaciens*. Moradi et al. (2014) found several bacterial isolates producing high amylolytic enzymes, which were subsequently identified as *Bacillus cereus*, *B. amyloliquefaciens*, *B. licheniformis*, and *Paenibacillus lautus*. Luo et al. (2021) isolated *Bacillus toyonensis* P18, a group of Gram-positive bacteria belonging to the *Bacillus cereus* group and often used as probiotics or biocontrol agents. The bacterium has also been known to be treated as a probiotic for preventing microbial diseases in crops or improving the immune response of animals (Santos et al. 2018).

The objectives of the study were to isolate amylolytic bacteria from rhizosphere and plant tissue of Canna, as well as litter; to know oligosaccharide compounds produced from hydrolysate of starch hydrolysed by the bacterial enzymes; and to identify the selected amylolytic bacteria based on 16S rRNA gene sequences.

MATERIALS AND METHODS

Sample Collection and Location of Sampling

Samples were taken from the rhizosphere and parts of Canna plant (*C. edulis* Ker.) including tubers, stems, leaves, tissue, as well as litter growing in two places, namely in the forest and the community gardens around the Perhutani Forest West Banyumas, Central Java, Indonesia. The coordinates of the former are S 07°20.846 'E 109°06.410 and the latter is S 07 °20.812 'E 109°05.92 (Figure 1).

Isolation, Screening, and Morphological Characterization of Amylolytic Bacteria

Plant tissues and litter were cleaned with running water, then cut into 1 cm long pieces and separated according to the plant part. The sample pieces were immersed in 70% alcohol for 1 minute, then in 1% sodium hypochlorite solution for 3 minutes, after which they were soaked again using 70% alcohol for 1 minute, and rinsed with sterile distilled water three times (Duan et al. 2021, with modification). The sterile samples were placed on sterile tissue papers and then crushed using a mortar and one gram of each sample was diluted with 9 mL of sterile distilled water,

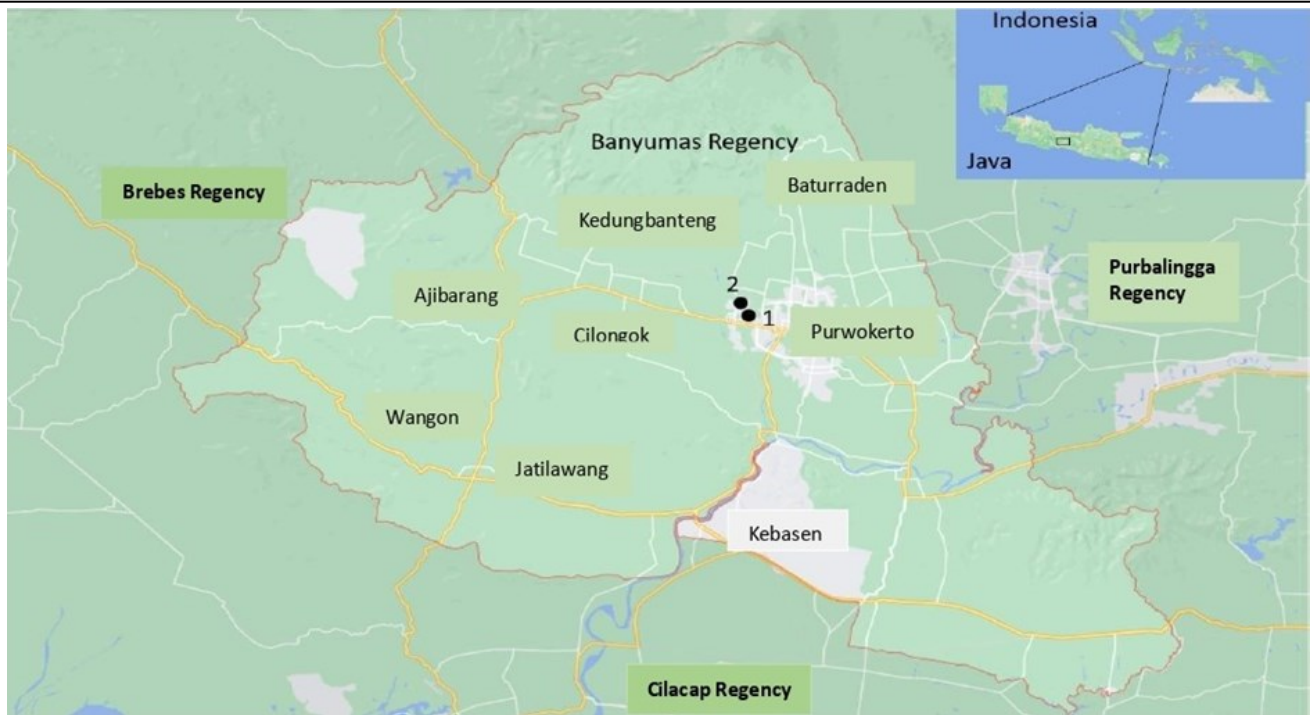


Figure 1. A map of Banyumas Regency and sampling sites: (1) the Perhutani Forest KPH West Banyumas, Central Java, (2) Community gardens around the Perhutani Forest KPH West Banyumas, Central Java.

and then serial dilutions were made up to 10^{-7} .

One gram of *Canna* rhizospheric soil was put into a 20 mL of nutrient broth (NB) medium containing 1% soluble starch (Merck) in a 100 mL Erlenmeyer flask. The solution was then homogenized in an agitation speed shaker machine at 150 rpm and incubated for 24 hours at 30 °C. The amount of 1 mL of the solution was diluted with 9 mL of sterile distilled water, and then serial dilutions were made up to 10^{-7} .

One mL from each series of dilutions was inoculated onto nutrient Agar (NA) medium containing 1% soluble starch using a pour plate method. The plates were then incubated for 24 hours at 30 °C. Each growing bacterial colony was then inoculated onto an NA medium containing 1% soluble starch and purified using a streak quadrant method.

The number of 0.5L of bacterial cultures aged 24 hours at 30°C growing on NB medium containing 1% soluble starch was spot inoculated onto NA medium containing 1% commercial soluble starch, then incubated for 72 hours at 30°C. The growing colonies were flooded with iodine solution, and the clear zones formed around the colonies were observed and measured in their diameter (Vijayalakshmi et al. 2012). The isolates having high diameter clear zones were selected and tested for their enzyme production. The colonial and cell morphology of the isolated bacteria were characterized using conventional methods (Smibert & Krieg 1981).

Phenetic and Phylogenetic Characterizations of the Selected Bacterium

Phenetic characterizations of the selected bacterium (producing high diameter clear zones and maltooligosaccharide enzyme) including colony morphology, cell morphology, and biochemistry, were conducted by conventional methods (Smibert & Krieg 1981). Biochemical tests were also conducted using the API 50CHB kit.

The 16S rDNA gene was amplified by polymerase chain reaction (PCR) technique using a pair of primers (9F: 5'GAGTTT-GATCCTCCTGGCTCAG-3') 1510R: 5'GGCTACCTTGTTACGA-3')

(Yopi et al. 2017). The obtained bands were stained and visualized by UV Transilluminator. The sequence was confirmed via 1st BASE Sequencing, Malaysia. The 16S rDNA nucleotide sequences were analyzed by nucleotide BLAST (Basic Local Alignment Search Tool) search in the Gene Bank of National Center for Biotechnology Information (NCBI) or BLAST for amino acid analysis (Zhuang et al. 2012). The phylogenetic tree was constructed using a neighbour-joining algorithm in MEGA 6.0 software (De-Moraes-Russo & Selvatti 2018).

Analysis of The Hydrolysis Products by A Thin-Layer Chromatography Method (Rahmani et al. 2013)

An amount of 2 mL of each 24 h old bacterial culture (four selected isolates) was inoculated into a 200 mL flask containing 20 mL of NB medium plus 1% (w/v) starch solution, pH 6 (50 mM acetate buffer) and incubated at 30 °C for 24 h. The culture was sampling every 24 hour and then centrifugated, and the supernatant obtained was tested for its amylolytic activity.

The hydrolytic activity of amylase in a substrate solution was carried out at 30°C in 50 mM acetate buffer, pH 6, containing 0.5% of commercial starch. The enzyme-substrate ratio (v/v) was 1:1 and the reaction times were in hours (0, 1, 2, 3, 4, 24). Reactions were carried out in 2 mL Eppendorf containing 1 mL of reaction mixture in a Deep Well Maximizer (Bioshaker M-BR-022UP, Taitec Japan).

A Thin Layer Chromatography (TLC) of maltooligosaccharide products was carried out on silica gel 60F₂₅₄ plates (Merck Art 20-20 cm) and eluent using a solvent mixture of n-butanol:acid:water (12:6:6, v/v/v). Spots formed were visualized by spraying the sugar colours (0.5 g α -diphenylamine, 25 mL acetone, 2.5 mL phosphate acid, 0.5 mL aniline). All samples were applied in equal quantities (4 μ L). Glucose (Sigma-Aldrich, U.S.A), maltose (M2), maltotriose (M3), maltotetraose (M4), maltopentaose (M5), maltohexaose (M6), and maltoheptaose (M7) (Megazyme) were used as standards.

Crude Enzyme Production and Amylase Activity at Different Fermentation Time

An amount of 2 mL of the 24 h old bacterial cultures (isolate T10) was inoculated into a 200 mL flask containing 20 mL of NB medium plus 1% (w/v) starch solution, pH 6 (50 mM acetate buffer), and incubated at 30 °C for five days. The culture was sampled every 24 hours and then centrifuged and the supernatant obtained was tested for its amylase activity.

The enzyme reaction was conducted as above when measuring amylase activity using a DNS method (Miller 1959). The absorbance of the solution was measured using a spectrophotometer at a wavelength of 540 nm. The enzyme activity (U/mL) was calculated based on the equation:

$$\text{enzyme activity} = \frac{c \times d \times 1000}{t \times mw} \text{ U/mL}$$

Where c: amylase concentration; d: dilution; t: incubation time; mw: molecular weight.

A standard curve used D-Glucose at various concentrations. One unit of amylase activity is defined as the amount of enzyme that liberates one μ mol of D-Glucose per minute under the experimental condition given.

Effect of pH and Temperature on Enzyme Activity of the Selected Isolate

The optimal pH of the enzyme activity was done at pH ranges of 3.0-10.0 under standard assay conditions. Various buffers (0.05M) used were sodi-

um acetate (pH 3.0-6.0), sodium phosphate (6.0-8.0), Tris-HCL (pH 7.0-9.0), and Glycine-NaOH (pH 8.0-10.0). The enzyme reactions were incubated at 40°C for 30 min in the presence of 0.5% (w/v) starch solution (Merck)). The effect of temperatures on enzyme activity was conducted at temperatures ranging from 30-90 °C in 50 mM acetate buffer at optimum pH for 30 min. Amylase activity was assayed by DNS method (Miller 1959).

RESULTS AND DISCUSSION

Isolation and An Amylytic Assay of Bacteria Isolated from The Rhizosphere and Plant Tissue of Canna, and Litter

The results of the study found 32 bacterial isolates growing on NA medium supplemented with 1% soluble starch, with details: 11 isolates were from the rhizosphere of the Canna growing in the forest, 12 isolates from the rhizosphere of the Canna growing in the people's gardens around the forest, four isolates from the leave tissue of the Canna growing in the people's gardens around the forest, three isolates from the roots of the Canna growing in the people's gardens around the forest, and two isolates were from the litters of the Canna in the gardens of the residents around the forest (Table 1).

The ability of the bacteria to grow and produce clear zones in the medium indicates that those bacteria were capable of producing amylase. The more amylase is released, the wider clear zones are produced due to the degradation of amyllum in the medium, resulting in enhancing the amylytic index (Ginting et al. 2021). The research results showed that eight isolates of TH6, TH7, T5, T10, D2, D3, A3, and S1 showed high total clear zone diameters (mm) of 18, 18, 18, 20, 18, 30, 18, and 18, respectively (Table 1). The consistency of the bacterial isolates, resulting in the total clear zone diameter, was shown by the isolates TH6, T10, D3, A3, and S1, while the other isolates tended to reduce or lose their amylytic activity (Figure 2). Based on the ability of isolates to produce a clear zone diameter ≥ 18 mm and consideration of source representatives, five isolates (TH6, T10, D3, A3, and S1) were selected for further testing, namely their ability to hydrolyze starch. Hasanah et al. (2020) reported that bacterial isolates having an amylytic index of more than 9 mm were potentials to produce amylase. According to Ochoa-Solano & Olmos-Soto (2006), bacterial isolates produce clear zones two or three times the diameter of the colony are potential enzyme producers.

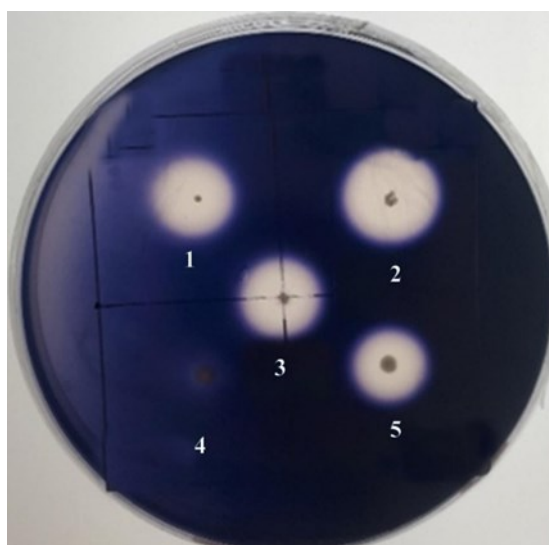


Figure 2. The amylytic zones produced by bacterial isolates of: (1) T10, (2) D3, (3) A3, (4) TH6, and (5) S1 on a NA medium + 1% soluble starch.

Table 1. Sources, number, and total clear zone diameter of amylolytic bacteria isolated from the rhizosphere, plant tissues of Canna, and litter.

Source of bacterial isolates	Isolate code	Total clear zone diameter (mm)
Rhizospheres of the Canna plants growing in the forest	TH1	16
	TH2	15
	TH3	17
	TH4	16
	TH5	16
	TH6	18
	TH7	18
	TH8	17
	TH9	17
	TH10	16
	TH11	16
Rhizospheres of the Canna plants growing in the people's gardens around the forest	T1	15
	T2	16
	T3	16
	T4	16
	T5	18
	T6	17
	T7	15
	T8	15
	T9	15
	T10	20
	T11	17
	T12	16
Leaves of the Canna plant tissue growing in the people's gardens around the forest	D1	16
	D2	18
	D3	30
	D4	15
Roots of the Canna plant tissue growing in the people's gardens around the forest	A1	17
	A2	16
	A3	18
Litters of the Canna plant from the gardens of the residents around the forest	S1	18
	S2	16

A high number of amylolytic bacteria isolated from the rhizosphere of Canna was by [Vaseekaran et al. \(2010\)](#), who stated that bacteria isolated from starch-rich materials have better potential to produce amylase. [Vijayalakshmi et al. \(2012\)](#) found *Bacillus subtilis* KC3 isolated from the rhizosphere of *Euphorbia hirta* produced a maximum halo zone of 23 mm on a Starch Agar medium. [Gebreyohannes \(2015\)](#) reported that 16 bacterial isolates from soils could produce clear zones of 3-22 mm on starch agar plates. [Ginting et al. \(2021\)](#) found thermophilic bacteria of *Bacillus* sp. L3 and *B. caldotenax* L9 from a marine hydrothermal produces high amylolytic indexes of 3.04 and 3.52, respectively. The clear zone formed results from breaking starch compounds into simple compounds; the wider the clear zone formed, the higher the amylolytic activity ([Zubaidah et al. 2019](#)).

The characteristics of colonial morphology of the 34 isolates were rough, dry, bright, and pink; cells were Gram-positive, rod shape, motile, and had endospores. The endospore position of isolates D1-D4 and S1-S2 was in terminal, while isolates of TH1-TH11, T1-T12, and D1-D4 had endospores in the centre. All isolates were able to hydrolyse starch and produce lecithinase (Table 2). Those characteristics indicated that the bacteria were members of the genus *Bacillus*. According to [Logan & De](#)

Table 2. Morphological and physiological properties of the bacteria isolated from Canna plants and their surrounding.

Characteristics	Isolate code				
	TH1-TH11	T1-T12	D1-D4	A1-A3	S1-S2
Colonial morphology on NA Agar	Rough, dry, bright, and Pink	Rough, dry, bright and pink	Rough, dry, bright and pink	Rough, dry, bright and pink	Rough, dry, bright, and pink
Gram reaction	+	+	+	+	+
Cell shape	Rod	Rod	Rod	Rod	Rod
Motility	+	+	+	+	+
Presence of spore	+	+	+	+	+
Position of spore	Centre	Centre	Terminal	Centre	Terminal
Starch hydrolysis	+	+	+	+	+
Lecithinase production	+	+	+	+	+

Vos (2009), the main characteristics of the genus *Bacillus* are cells rod-shaped, straight or slightly curved, occurring singly and in pairs, some in chains, form endospores, Gram-positive or Gram-negative, motile, aerobes or facultative anaerobes, and mostly isolated from soil.

Identification of The Selected Isolate of T10 Based on Phenetic and Phylogenetic Characteristics

Based on the ability of the selected isolate to produce malto-oligosachharides of maltotriose, maltotetraose, and maltopentaose (Method 3.3); further characterization of the isolate T10 was conducted. The isolate had colonial morphology of irregular with undulate edges, opaque, cream-coloured, and had a granular texture. The cells formed endospores, facultatively anaerobic, Gram-positive, rod-shaped, motile, and occurring singly or in chains (Table 2, Table 3, Figure 3). These characteristics include biochemistry, physiology, and nutrition, indicating that isolate T10 was similar to those typical of the species *Bacillus cereus*. This species is a species complex within the genus *Bacillus*, with members including *B. anthracis*, *B. thuringiensis*, *B. mycoides*, and *B. toyonensis* (Luo et al. 2021).

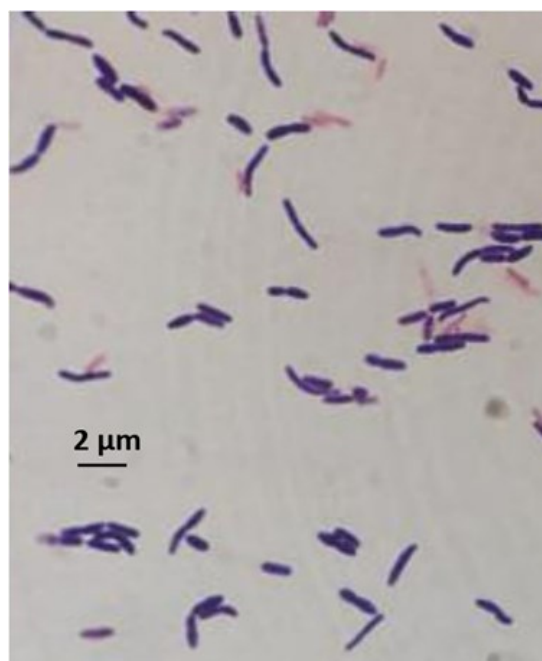


Figure 3. The appearance of bacterial cells isolate T10 under a microscope with a magnification of 1000x. The cells appear single or in chains.

Table 3. Phenotypic characterization of the isolate T10.

Characteristics	Isolate T10
Cell length (μm)	3.00 - 4.00
Egg-yolk lecithinase	+
Anaerobic growth	+
Rhizoid colony	-
Parasporal crystal	-
Growth temperature range ($^{\circ}\text{C}$)	10 - 45
Optimal growth temperature ($^{\circ}\text{C}$)	35
Salinity tolerance range (%NaCl)	≤ 4
API 50CHB	
Glycerol	-
D-Ribose	+
D-Mannose	+
Methyl- α D-glucopyranoside	+
Amygdalin	+w
Arbutin	+
Salicin	+
Cellobiose	-
D-saccharose	+
D-trehalose	+
Starch	+
Glycogen	+
D-turanose	+

The electrophoresis visualization of the PCR product showed that the DNA of T10 produced a single band with a size of 1500 kb (Figure 4). The results of comparing the 16S rRNA gene sequence of isolate T10 and nucleotide sequences in the GeneBank (<http://blast.ncbi.nlm.nih.gov/>) showed that the bacterium is closely related to species members of the genus *Bacillus*. The BLAST analysis showed that isolate T10 had a similarity of 99.3% with either *Bacillus toyonensis* SPa09NA, *B. toyonensis* PZ-48, or *B. toyonensis* SMP1. The phylogenetic tree was constructed using Neighbor-Joining, Model Maximum Composite Likelihood, and 1000x Bootstrapping. A dendrogram resulted from MEGA10 program showed that isolate T10 joined *B. toyonensis* SX04NA, *B. toyonensis* Spa09NA, *B. toyonensis* SMP1, *B. toyonensis* PZ-48, *B. toyonensis* BCT-7112, and *B. toyonensis* l3aM to form a separate cluster (Figure 5). Hence, isolate T10 was identified as the species member of *B. toyonensis* based on the phenetic and phylogenetic characteristics.

B. toyonensis strain BCT-7112^T was first isolated in 1966 in Japan from a survey designed to obtain naturally occurring microorganisms as pure cultures in the laboratory for use as probiotics in animal nutrition (Jiménez et al. 2013). This strain was first identified as *B. cereus* var. *toyoi*, and it has been used as the active ingredient of the preparation TOYOCERIN, an additive for animal nutrition (e.g. swine, poultry, cattle, rabbits and aquaculture). Agamennone et al. (2019) isolated *B. toyonensis* strain VU-DES13 from the gut of the soil-dwelling springtail *Folsomia candida*, which was highly resistant to penicillin and inhibited the growth of a variety of pathogenic microorganisms. Its secondary metabolite clusters produce siderophores, bacteriocins, and nonribosomal peptide synthetases. Wang et al. (2021) reported that *Bacillus toyonensis* XIN-YC13 produced a novel antibiotic, toyoncin, with antimicrobial activity against *B. cereus* and *Listeria monocytogenes*. This antibiotic exerts bactericidal activity and induces cell membrane damage.

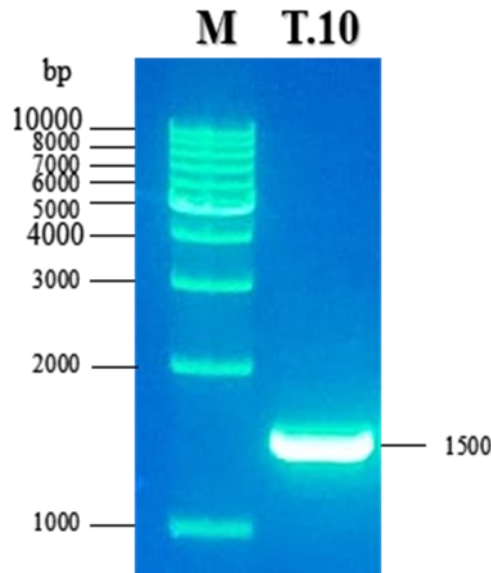


Figure 4. An electropherogram of the amplified 16S rRNA gene of isolate T10 with a size of 1500 bp. Marker (M): 1 kb DNA ladder.

Analysis of Hydrolysed Products by The Selected Bacterial Amylases Using a TLC Method

Starch hydrolysis products were assayed by oligosaccharide profile analysis on the amylase-hydrolyzed samples from the fourth isolates (T10, D3, A3, and S1) qualitatively. The results of TLC analysis showed that isolate T10 produced three bands, namely maltotriose (M3), maltotetraose (M4), and maltopentaose (M5), isolate S1 produced two bands, namely maltotriose (M3) and maltotetraose (M4), while two amylases of the isolates D3 and A3 were unable to hydrolyze starch (Figure 6).

Based on the TLC chromatogram, the starch degraded by T10 amylase resulted in malto-oligosaccharides of maltotriose, maltotetraose, and maltopentaose. Amylases can break down starch polymer bonds into shorter oligosaccharides or simple sugar molecules (Putri et al. 2012). The results showed that amyolytic bacteria with high amyolytic indexes (AI) did not correlate with their ability to degrade amyllum. The isolate T10, with its total diameter lower than isolate D3, showed a higher ability to break down starch polymer bonds into shorter or oligosaccharides. The results of this study proved that a high AI value is only sometimes accompanied by the high ability of the amylase to break down starch polymer bonds. The ability of the T10 amylase to produce the maltooligosaccharides was similar to the amylase of *Bacillus circulans* GRS 313 isolated from soil that also produced maltotriose, maltotetraose, and maltopentaose (Dey et al. 2002). On the contrary, Rahmani et al. (2013) found maltose and maltotriose produced by amylase of *Brevibacterium* sp. using black potato starch as substrate, while amylase of *Bacillus subtilis* strain SDP1 isolated from rhizosphere of Acacia produces maltotriose and maltotetraose (Ozturk et al. 2014). Furthermore, Abdul-Manas et al. (2014) reported that amylase of an alkaliphilic *Bacillus lehensis* G1 could degrade oligosaccharides by producing maltooligosaccharides with a higher degree of polymerization than maltoheptaose observed on thin-layer chromatography and high-performance liquid chromatography analyses.

Crude Enzyme Production of a Selected Isolate and Measurement of its Amylase Activity at Different Culture Incubations

Based on the ability of the fourth selected amyolytic bacteria to produce different types of hydrolysed product, isolate T10 was further assayed for

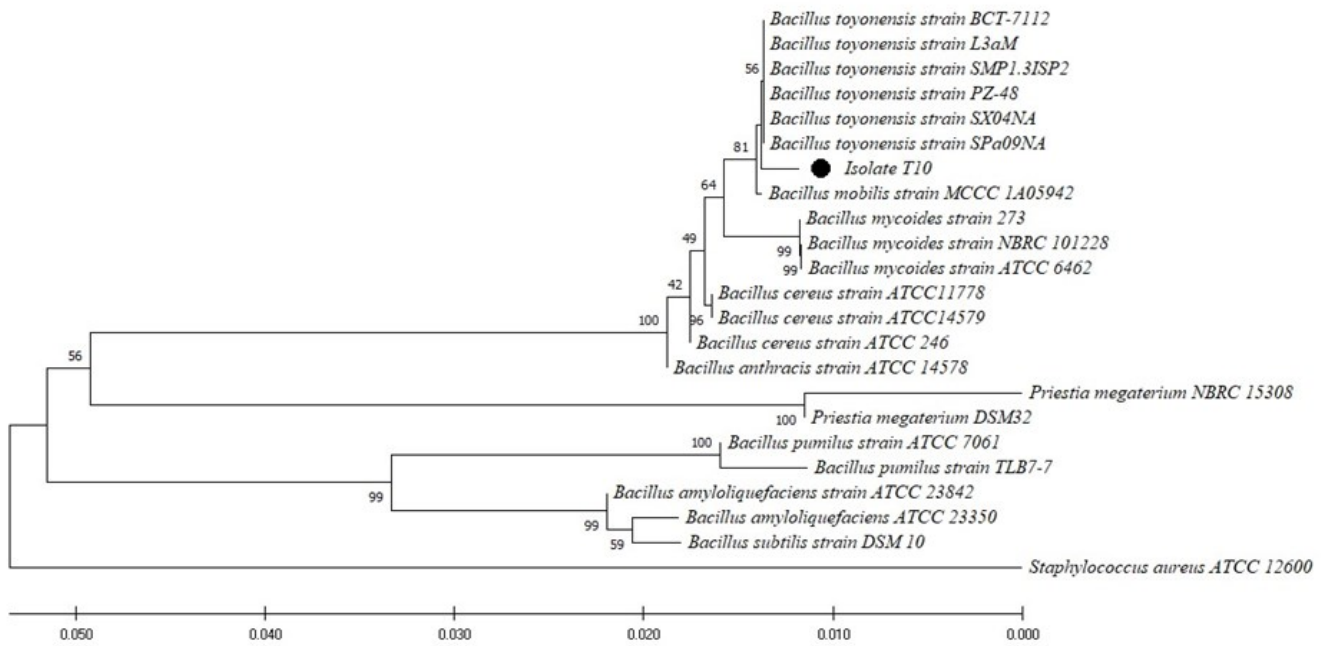


Figure 5. A phylogenetic tree showing the relationship between strain T10 isolated from rhizospheres of *Canna* (*C. edulis*) and several species members of the genus *Bacillus* on the basis of 16S rRNA gene sequence reconstructed based on Neighbor-Joining, Model Maximum Composite Likelihood, and 1000x Bootstrapping. The analysis used a MEGA10 program and *Staphylococcus aureus* ATCC 12600 as an outgroup.

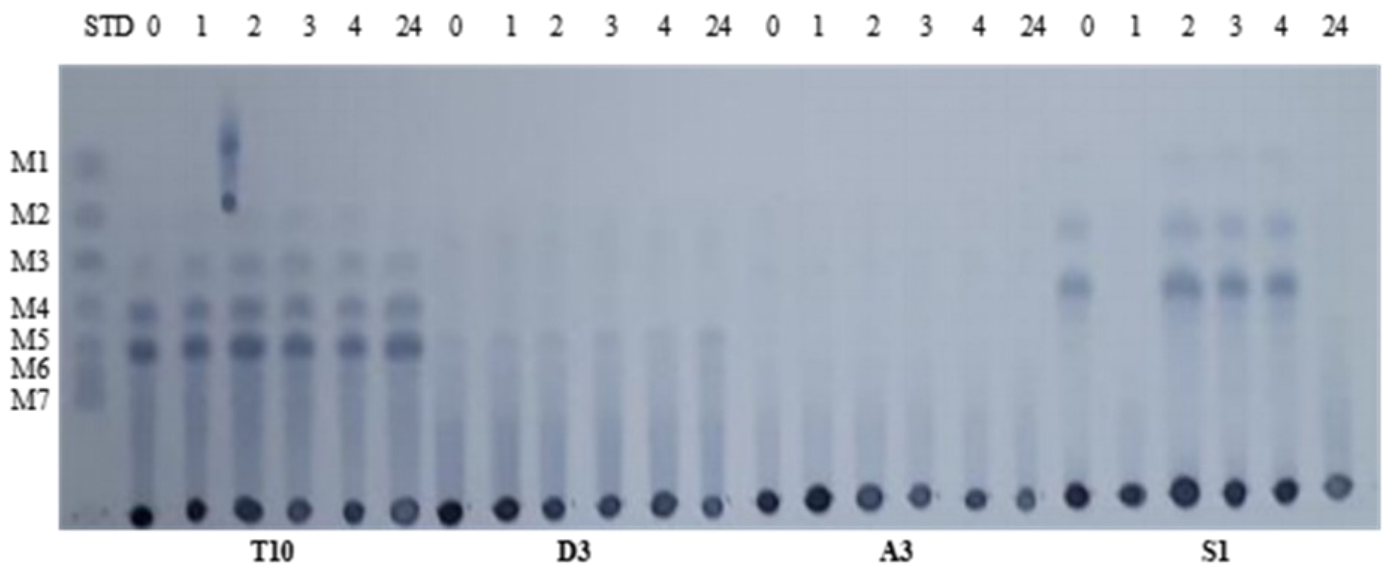


Figure 6. The product profile of starch hydrolyzed by amylase of the amylolytic bacteria (T10, D3, A3, and S1) using a TLC method with reaction times (hours): of 0, 1, 2, 3, 4, and 24 at 30°C. The Standards (STD): monosaccharide (M1), maltose (M2), maltotriose (M3), maltotetraose (M4), maltopentaose (M5), maltohexaose (M6) and maltohepta (M7).

its optimal amylase activity at different incubation times. The results showed that incubation times affected the amylase activity of isolate T10 carried out in a 0.5% starch solution at 30°C in 50 mM acetate buffer of pH 6. The amylase activity of T10 was optimal during incubation 1-3 days ranging from 0.546-0.717 U/mL and the highest amylase activity was found at 24 hr incubation of 0.717 U/mL (Figure 7). The results also showed that amylase activity decreased after 72 h of incubation. The amylase activity value at day 0 is quite high, this might be due to the measurement of the enzyme activity using the DNS method, in which reduc-

ing sugar formed from a carbon source (starch) is used by bacteria for the initial stages of growth; then, the bacteria will use the carbon source for the production of enzymes.

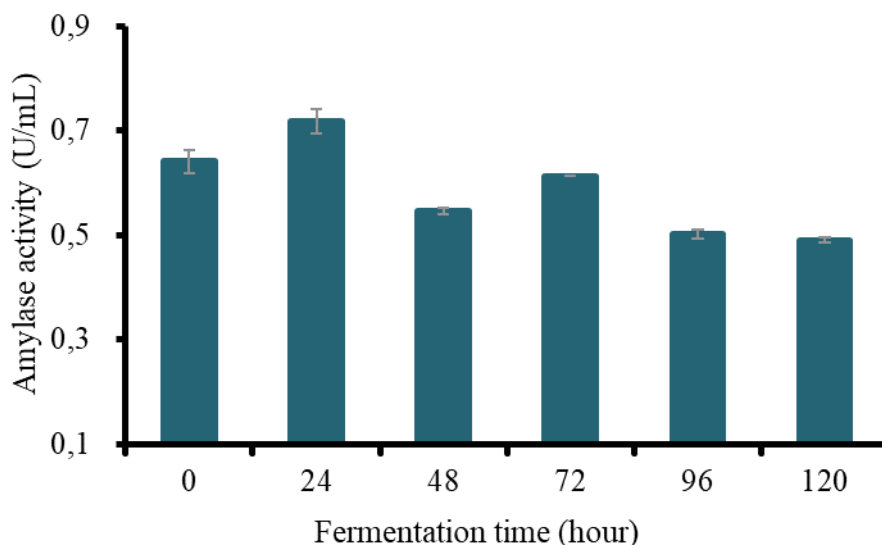


Figure 7. Amylase activity of T10 at different incubation times.

The amylase activity of *Bacillus cereus* KN isolated from Ranu Ngebel and incubated for three days was 0.016 U/mL, while strain G20 isolated from Ranu Grati was lower at about 0.0001 U/mL (Nisa et al. 2021). Luang et al. (2019) found *Bacillus* sp. 3.5AL2 isolated from soils of the unexplored Nasinuan Forest, Thailand and incubated for three days exhibiting amylase activity of 1.97 U/mg protein at the optimal conditions of 60°C and pH 7.0 after 30 min incubation with 1% starch in 0.05 M phosphate buffer. Gebreyohannes (2015) reported that the amylase activity of *Bacillus* spp. decreased after 48 h incubations due to the suppression and accumulation of other byproducts in the fermentation medium and also depletion of nutrients.

Enzyme Characterization: The Effect of pH and Temperature Against Enzyme Activity of The Selected Isolate

The effects of pH's on the amylase activity of isolate T10 showed that optimum conditions were in sodium acetate buffer pH 6 with an amylase activity of 0.262 U/mL and in sodium phosphate buffer pH 7 with an amylase activity of 0.341 U/mL (Figure 8). The optimal pH of isolate T10 was by Naidu et al. (2019) for *Paenibacillus* sp. D9 that its optimal pH for amylase activity is in the neutral range (pH 6-8). The increase in pH beyond these values resulted in a decline in enzyme activity. Any change in pH causes a change in the enzyme's active site (Lim & Oslan 2021). Bajpai et al. (2015) reported that the optimal pH for amylase activity of *Haloferax* sp. HA10 was at pH 7.0. According to Asgher et al. (2007), each enzyme has an optimal pH to work most actively, and the optimal pH of amylase is varied from pH 3.8 to 9.5 depending on the type of enzyme and the source. Behal et al. (2016) reported an amylase produced by *Bacillus* sp. AB04 had optimal activity at pH 8. Moreover, the enzyme is stable in neutral to alkaline (pH 7-10).

The amylase activity of isolate T10 was observed at temperatures ranging from 30-90°C at pH 7.0. Amylase activity of the T10 isolate tended to be optimum at 40°C with an activity value of 0.801 U/mL (Figure 9). A similar finding was also reported by Sivaramakrishnan et al. (2006) for several species of *Bacillus* sp., *B. subtilis*, *B. stearothermophilus*, *B.*

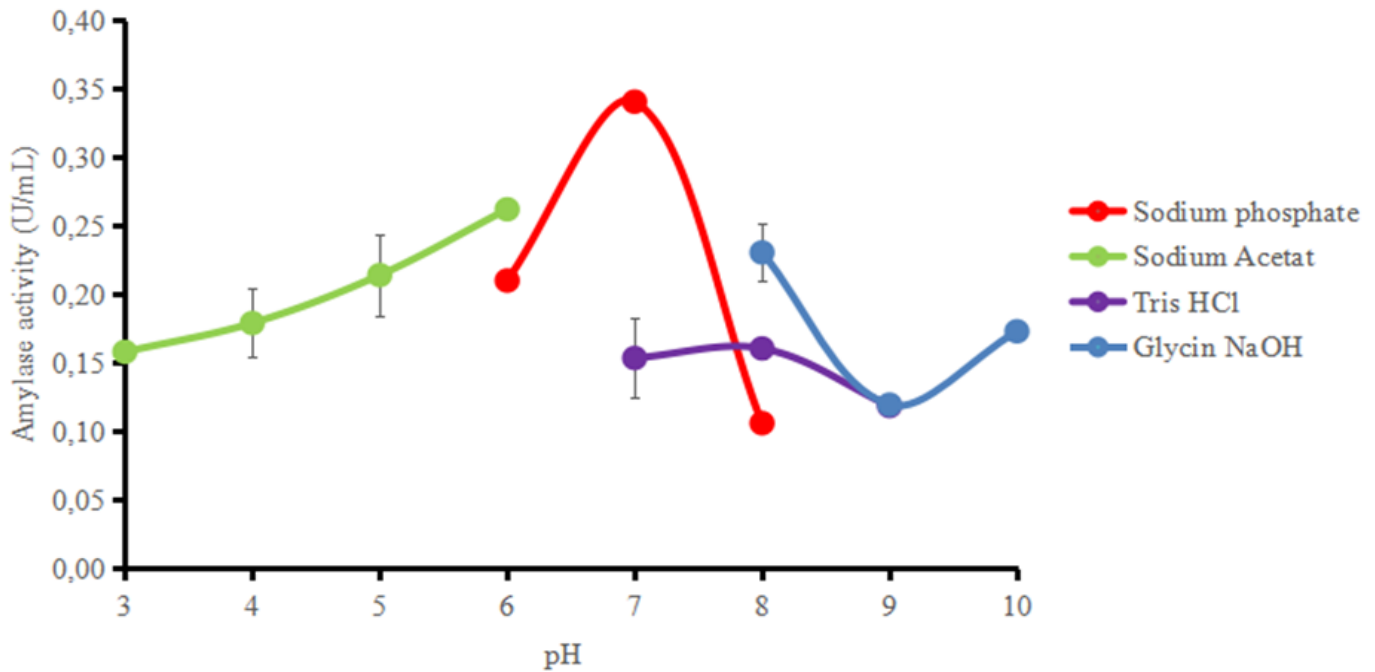


Figure 8. Amylase activity of T10 at different pH and buffers.

licheniformis, and *B. amiloliquefaciens* have optimum temperatures of 37-60°C. Gebreyohannes (2015) found that the maximum amylase activity of *Bacillus* spp. was 40°C and *Streptomyces* spp. at 37°C, used 4% starch concentration at a neutral pH and an incubated for 48 h. The crude enzyme of *Bacillus* sp. AB04 showed maximum activity at pH 8 with an optimum temperature of 40° C with more than 75% activity in range of 50 - 80° C (Behal et al. 2016). The results showed that either pH or temperature significantly affected the enzyme activity of the T10 amylase which was optimum at pH 7.0 and a temperature of 40°C.

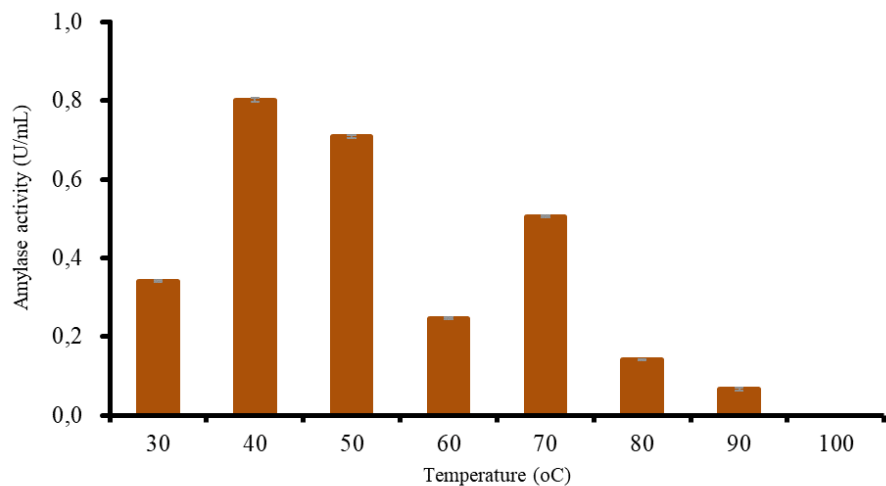


Figure 9. Amylase activity of isolate T10 at different temperatures.

The differences in the pH and temperature characteristics of enzyme activity indicated that enzymes are specific, depending on the species that produces them. A decrease or increase in temperature can affect the secretion of extracellular enzymes by changing the physiology of the cell membrane (Rahmani et al. 2018). The optimum temperature is the temperature that causes chemical reactions at the most incredible speed (Subagiyo et al. 2017). The results showed that after reaching the optimum condition, it was seen that the activity of the T10 amylase de-

creased. High temperatures can cause enzymatic reactions to decrease because enzyme proteins undergo conformational changes so that protein molecules will experience denaturation (Yufinta et al. 2018).

The production of a specific maltooligosaccharide in high yield through the enzymatic hydrolysis of starch is of considerable commercial interest. This has been achieved on an industrial scale after discovering a suitable maltooligosaccharide-forming amylase (MFA_{ses}). Moreover, several studies have tried to improve existing methods by increasing the yields of M3 and M5. These studies have included efforts to find new wild-type strains producing MFA_{ses}, construct novel systems to achieve large-scale MFA_{ses} expression, and immobilize MFA_{ses} for stability and productivity (Ben-Ali et al. 2006). MFA_{ses} from *Bacillus toyonensis*, a novel M5-amylase, seems promising for the manufacture of high M5 syrups from starch and may apply to starch processing technologies due to their particular activity, unique substrate specificity, and endo-type action pattern (Pan et al. 2017).

CONCLUSIONS

It can be concluded that amounts of 32 amylolytic bacteria were isolated from rhizosphere and plant tissue of *Canna edulis*, as well as litter; the selected amylolytic bacterial isolate of T10 was capable of hydrolysing starch by producing maltotriose (M3), maltotetraose (M4) and maltopentaose (M5); and the identity of the selected isolate T10 belonged to a species member of *B. toyonensis* based on phenotypic and phylogenetic characterizations.

AUTHORS CONTRIBUTION

RNA designed, collected, and analysed the research data, O, NR and NE supervised all the process, and re-wrote the manuscript.

ACKNOWLEDGMENTS

We would like to thank the Research Center for Biotechnology (BRIN) and International Women University (IWU) for funding this research.

CONFLICT OF INTEREST

The author declares that there is no conflict of interest in this research.

REFERENCES

- Abdalla, M. et al., 2021. One-pot production of maltoheptaose (DP7) from starch by sequential addition of cyclodextrin glucotransferase and cyclomaltodextrinase. *Enzyme and Microbial Technology*, 149 (6), 109847. doi: 10.1016/j.enzmictec.2021.109847
- Abdul-Manas, N.H. et al., 2014. The characterization of an alkali-stable maltogenic amylase from *Bacillus lehensis* G1 and improved maltooligosaccharide production by hydrolysis suppression. *PLoS ONE*, 9(9). doi: 10.1371/journal.pone.0106481
- Afifah, N., Putri, D.H. & Irdawati, 2018. Isolation and identification of endophytic bacteria from the Andalas plant stem (*Morus macroura* Miq.). *Bioscience*, 2(1), pp.72-75.
- Agamennone, V. et al., 2019. Genome annotation and antimicrobial properties of *B. toyonensis* VU-DES13, isolated from the *Folsomia candida* gut. *Entomologia Experimentalis et Applicata*, 167, pp:269-285. doi: 10.1111/eea.12763.
- Asgher, M. et al., 2007. A thermostable α -amylase from moderately thermophilic *Bacillus subtilis* strain for starch processing. *J Food Eng.*, 79, pp.950-955.

- Bajpai, B., Chaudhary, M. & Saxena, J., 2015. Production and characterization of α -Amylase from an extremely halophilic archaeon, *Haloferax* sp. HA10. *Food Technol Biotechnol.*, 53(1), pp.11-17, doi: 10.17113/ftb.53.01.15.3824
- Ben-Ali, M. et al., 2006. Thermostability enhancement and change in starch hydrolysis profile of the maltohexaose-forming amylase of *Bacillus stearothermophilus* US100 strain. *Biochemical Journal*, 394(1), pp.51-56. doi: 10.1042/BJ20050726
- Behal, A. et al., 2016. Characterization of alkaline α - amylase from *Bacillus* sp. AB 04. *IJAB*, 8(1), pp.80-83.
- De-Moraes-Russo, C.A. & Selvatti, A.P., 2018. Bootstrap and rogue identification tests for phylogenetic analyses. *Molecular Biology and Evolution*, 35(9), pp.2327-2333. doi: 10.1093/molbev/msy118.
- Dey, G. et al., 2002. Purification and characterization of maltooligosaccharide-forming amylase from *Bacillus circulans* GRS 313. *Journal of Industrial Microbiology and Biotechnology*, 28(4), pp.193-200. DOI: 10.1038/sj/jim/7000220.
- Ding, N. et al., 2021. Carbohydrate-binding module and linker allow cold adaptation and salt tolerance of maltopentaose-forming amylase from marine bacterium *Saccharophagus degradans* 2-40T. *Frontiers in Microbiology*, 12(7), pp.1-14. doi: 10.3389/fmicb.2021.708480.
- Divakaran, D., Chandran, A. & Pratap-Chandran, R., 2011. Comparative study on production of α -amylase from *Bacillus licheniformis* strains. *Brazilian Journal of Microbiology*, 42(4), pp.1397-1404. doi: 10.1590/S1517-83822011000400022.
- Duan, Y. et al., 2021. Isolation, identification, and antibacterial mechanisms of *Bacillus amyloliquefaciens* QSB-6 and its effect on plant roots. *Frontiers in Microbiology*, 12, 746799. doi:10.3389/fmicb.2021.746799.
- El-Fallal, A. et al., 2012. Starch and microbial α -amylases: from concepts to biotechnological applications. In *Carbohydrates-Comprehensive Studies on Glycobiology and Glycotechnology*. Intech Open Science, pp.459-488. doi: 10.5772/51571
- Gebreyohannes, G., 2015. Isolation and optimization of amylase producing bacteria and actinomycetes from soil samples of Maraki and Tewedros campus, University of Gondar, North West Ethiopia. *African Journal of Microbiology Research*, 9(31), pp.1877-1882.
- Ginting, E.L. et al., 2021. Isolation and identification of thermophilic amyolytic bacteria from Likupang Marine Hydrothermal, North Sulawesi, Indonesia. *Biodiversitas*, 22(6), pp.3326-3332. doi: 10.13057/biodiv/d220638.
- Gupta, R. et al., 2003. Microbial α -amylases: A biotechnological perspective. *Process Biochemistry*, 38(11), pp.1599-1616. doi: 10.1016/S0032-9592(03)00053-0.
- Hasanah, U. et al., 2020. Amylolytic activity of bacterial strains isolated from sago pulp of the traditional sago industry in Palopo, South Sulawesi. *AIP Conference Proceedings* 2231, 040073 (2020), <https://doi.org/10.1063/5.0002487>.
- Hellmuth, K. & van-den Brink, J.M., 2013. Microbial production of enzymes used in food applications. In *Microbial Production of Food Ingredients, Enzymes and Nutraceuticals*. Woodhead Publishing Limited. doi: 10.1533/9780857093547.2.262.

- Jang, E.Y. et al., 2020. Amylase-producing maltooligosaccharide provides potential relief in rats with loperamide-induced constipation. *Evidence-Based Complementary and Alternative Medicine*, 2020, 5470268. doi: 10.1155/2020/5470268.
- Jiménez, G. et al., 2013. Description of *Bacillus toyonensis* sp. nov., a novel species of the *Bacillus cereus* group, and pairwise genome comparisons of the species of the group by means of ANI calculations. *Systematic and Applied Microbiology*, 36(6), pp.383-391. doi: 10.1016/j.syapm.2013.04.008.
- Lim, S.J. & Oslan, S.N., 2021. Native to designed: Microbial α -Amylases for industrial applications. *PeerJ*, 9, pp.1-30. doi: 10.7717/peerj.11315.
- Logan, N.A. & De Vos, P., 2009. Genus I. Bacillus Cohn 1872. In *Bergey's Manual of Systematic Bacteriology Second Edition Volume Three The Firmicutes*. Springer, Springer Dordrecht Heidelberg London New York. pp.21-127. doi: 10.1007/b92997.
- Luang-In, V. et al., 2019. Isolation and identification of amylase-producing bacteria from soil in Nasinuan community forest, Maha Sarakham, Thailand. *Biomedical & Pharmacology Journal*, 12(3), pp.1061-1068.
- Luo, J-c. et al., 2021. Characterization of a deep sea *Bacillus toyonensis* isolate: genomic and pathogenic features. *Frontiers in Cellular and Infection Microbiology*, 11, 629116. doi: 10.3389/fcimb.2021.629116.
- Miller, G.L., 1959. Use of dinitrosalicylic acid reagent for determination of reducing sugar. *Analytical Chemistry*, 31(3), pp.426-428. doi: 10.1021/ac60147a030
- Moradi, M. et al., 2014. Screening and isolation of powerful amylolytic bacterial strains. *International Journal of Current Microbiology and Applied Sciences*, 3(2), pp.758-768.
- Naidu, K. et al., 2019. Purification and characterization of α -amylase from *Paenibacillus* sp. D9 and *Escherichia coli* recombinants. *Biocatalysis and Biotransformation*, 38(1), pp.24-34. doi: 10.1080/10242422.2019.1628738.
- Nisa, I.K. et al., 2021. The potential of amylase enzyme activity against bacteria isolated from several lakes in East Java, Indonesia. *Biodiversitas*, 22(1), pp.42-49.
- Ochoa-Solano, J.L. & Olmos-Soto, J., 2006. The functional property of Bacillus for Shrimp feeds. *Food Microbiology*, 23(6), pp.519-525, doi: 10.1016/j.fm.2005.10.004.
- Ozturk, H.U. et al., 2014. A maltooligosaccharides producing α -amylase from *Bacillus subtilis* SDP1 isolated from rhizosphere of *Acacia cyanophylla* Lindley. *Food Biotechnology*, 28(4), pp.309-332. doi: 10.1080/08905436.2014.963600.
- Pan, S. et al., 2017. Maltooligosaccharide-forming amylase: Characteristics, preparation, and application. *Biotechnology Advances*, 35(5), pp.619-632. doi: 10.1016/j.biotechadv.2017.04.004.
- Putri, W.D.R. et al., 2012. Isolation and characterization of amylolytic lactic acid bacteria during growol fermentation, an Indonesian traditional food. *Jurnal Teknologi Pertanian*, 13(1), pp.52-60.
- Rahmani, N. et al., 2013. Production of maltooligosaccharides from black potato (*Coleus tuberosus*) starch by α -amylase from a marine bacterium (*Brevibacterium* sp.). *Microbiology Indonesia*, 7(3), pp.129-136. doi: 10.5454/mi.7.3.6.

- Rahmani, N. et al., 2018. Xylanase and feruloyl esterase from actinomycetes cultures could enhance sugarcane bagasse hydrolysis in the production of fermentable sugars. *Bioscience Biotechnology and Biochemistry*, 82(5), pp.904–915. doi: 10.1080/09168451.2018.1438169.
- Santos, F.D.S. et al., 2018. *Bacillus toyonensis* improves immune response in the mice vaccinated with recombinant antigen of bovine herpesvirus type 5. *Benef. Microbes*, 9(1), pp.133–142. doi: 10.3920/BM2017.0021.
- Sivaramakrishnan, S. et al., 2006. α -Amylase from microbial sources: An overview on recent developments. *Food Technol. Biotechnol.*, 44(2), pp.173–184.
- Smibert, R.M. & Krieg, N.R., 1981. General Characterization. In *Manual Methods for General Bacteriology*. American Society for Microbiology, Washington.
- Subagiyo, Djarod, M.S.R. & Setyati, W.A., 2017. Potensi ekosistem mangrove sebagai sumber bakteri untuk produksi protease, amilase, dan selulase. *Jurnal Kelautan Tropis*, 20(2), pp.106–111.
- Vaseekaran, S., Balakumar, S. & Arasaratnam, V., 2010. Isolation and identification of a bacterial strain producing thermostable α -amylase. *Tropical Agricultural Research*, 22(1), pp.1–11. doi: 10.4038/tar.v22i1.2603.
- Vijayalakshmi et al., 2012. Isolation and characterization of *Bacillus subtilis* KC3 for amylolytic activity. *International Journal of Bioscience, Biochemistry and Bioinformatics*, 2(5), pp.336–341. doi: 10.7763/IJBBB.2012.V2.128.
- Wang, J. et al., 2021. Toyoncin, a novel leaderless bacteriocin that is produced by *Bacillus toyonensis* XIN-YC13 and specifically targets *B. cereus* and *Listeria monocytogenes*. *Applied and Environmental Microbiology*, 87(12), e00185–21. doi: 10.1128/AEM.00185–21.
- Yopi et al., 2017. Isolation and characterization of mannanase, xylanase, and cellulase from marine bacteria *Bacillus* sp. *Biofarmasi Journal of Natural Product Biochemistry*, 15(1), pp.15–20. doi: 10.13057/biofar/f150103.
- Yufinta, C.P., Julyantoro, P.G.S. & Pratiwi, M.A., 2018. Pengaruh penambahan *Bacillus* sp. terhadap kelulushidupan pasca larva udang *Vannamei* (*Litopenaeus vannamei*) yang terinfeksi vibriosis. *Current Trends in Aquatic Science*, 1(1), pp.89–95.
- Zhao, C. et al., 2017. Functional properties, structural studies and chemo-enzymatic synthesis of oligosaccharides. *Trends in Food Science and Technology*, 66, pp.135–145. doi: 10.1016/j.tifs.2017.06.008.
- Zhuang, Y., Zhou, X. & Wang, S., 2012. Gapped BLAST and PSI-BLAST: a new generation of protein database search programs. *Plant Systematics and Evolution*, 298(7), pp.3389–3402. doi: 10.2503/jjshs.58.977.
- Zubaidah, A. et al., 2019. Screening bakteri selulolitik dan amilolitik pada rumen sapi sebagai kandidat probiotik pada budidaya ikan secara *in vitro*. *Jurnal Riset Akuakultur*, 14(4), pp.261–271.

Research Article

DNA Authentication of Indonesian Leaffish *Pristolepis grooti* from Kelekar River and Ogan River in South Sumatra Based on *Cytochrome C Oxidase Subunit I (COI)* Gene

Mochamad Syaifudin^{1*}, Evitry Tamaria Gultom¹, Marini Wijayanti¹

1)Aquaculture Study Program, Department of Fisheries, Faculty of Agriculture, Sriwijaya University. Jl. Raya Palembang-Prabumulih KM.32 Indralaya, Ogan Ilir, South Sumatra, Indonesia. 30662.

* Corresponding author, email: msyaifudin@fp.unsri.ac.id

Keywords:

Cytochrome c Oxidase Subunit I (COI) gene
Kelekar River
Indonesian leaffish
Ogan River
phylogenetics

Submitted:

15 April 2022

Accepted:

16 February 2023

Published:

31 May 2023

Editor:

Ardaning Nuriliani

ABSTRACT

Indonesian leaffish *Pristolepis grooti*, an endemic species, are distributed in the region of Sumatra, Riau, Bangka Belitung and Kalimantan. However, there has been a decline in the population recently. This research purposed to investigate the mitochondrial DNA *cytochrome c oxidase subunit I (COI)* gene, the genetic distance, the genetic tree of the leaffish and characterize the chemical physics of water of its habitat in the Kelekar River Muara Enim Regency and the Ogan River, Ogan Ilir Regency. The method used in species authentication was DNA isolation, amplification using PCR (Polymerase Chain Reaction) and sequencing of *COI* gene. The size of the *COI* mtDNA gene fragment was 704 bp (PM 1, PM 4, PP 2 and PP 4) and 723 bp (PM 2, PM 3, PP 1 and PP 3). A cryptic diversity of the species *P. grooti* is found based on the genetic distance value of 4.5-6%, both in the Kelakar and Ogan Rivers. The phylogenetic tree of the leaffish of this study formed 2 separate sub-clusters with a bootstrap value of 50%. The properties of water qualities in the two rivers included temperatures 28.3-31.8°C, pH 5.6-8.3, dissolved oxygen 4.82-10.89 mg L⁻¹, alkalinity 10-28 mg L⁻¹ CaCO₃, water transparency 16-45 cm, ammonia 0.47-0.70 mg L⁻¹, water current 0.17-0.30 m s⁻¹ and TDS 7-44 mg L⁻¹.

Copyright: © 2023, J. Tropical Biodiversity Biotechnology (CC BY-SA 4.0)

INTRODUCTION

The Indonesian leaffish *Pristolepis* sp., known locally as sepatung is one of the indigenous fishes in Indonesia. It is distributed in the Kelekar River South Sumatra (Muslim et al. 2019), the Ogan River, Ogan Ilir Regency, and the Musi River, Palembang (Emawati et al. 2017), also in the Kampar River (Riau), Borneo, Bangka and Belitung (Kottelat & Whitten 1993). The leaffish is a family group of *Pristolepidae* commonly found in flooded swamp waters and has high economic value. Currently, Fishbase reported 8 species recognized species in this genus, two of which are *Pristolepis grooti* known as Indonesian leaffish and *P. fasciata* known as Malayan leaffish (Froese & Pauly 2019) which also lives in the territory of Indonesia. The phenotypic diversity of the two species in nature makes it difficult to determine the phenotypic comparison of the two types of fish, furthermore, the two species possibly exist in the same water (Muslim et al. 2019). *P. grootii* has been reported as one of dominants species (C=0.05-

0.014) in Kelekar floodplain, Ogan Ilir Regency (Muslim & Syaifudin 2022). Identification and characterization of leaffish are essential, as they are related to the adaptability, cultivation techniques and conservation of the leaffish in its natural habitat, which is still very limited, so thus it is important to apply a relatively easy and more accurate method to identify the species using the molecular technique, relatively. One of which is through DNA barcoding by using mitochondrial DNA that matches the target for analysis on various species-level target genes (Masters et al. 2007). The samples of leaffish for DNA barcoding were taken from the Kelekar River, Muara Enim Regency and the Ogan River in Pemulutan, Ogan Ilir Regency.

Cytochrome C oxidase subunit 1 (COI) is one of the genes in the mitochondrial genome (mtDNA), which is precisely used as a barcode. This molecular technique can be used for determining genetic analysis systematically and at the taxonomic level of species, populations and also plays a role in the selection process of fish genetic diversity. The application of DNA barcoding has been conducted on several aquatic organisms i.e. *Hemibagrus nemurus* (Syaifudin et al. 2017), *flatfish* from Vietnam (Truong et al. 2020), snake-skin gourami, blue gourami (Syaifudin et al. 2019), *Pristolepis fasciata* from Malaysia (Noikotr 2019) striped snakehead, catfish *Mystus singaringan* (Pramono et al. 2019), and ocellated snakehead (Syaifudin et al. 2020). In this study, the application of DNA barcodes has an important role in determining COI gene sequences as a taxonomic tool to reveal the genetics authentication of species among Indonesian leaffish from the Kelekar and the Ogan River in South Sumatra.

MATERIALS AND METHODS

Materials

Indonesian leaffish (Figure 1) and water samples were taken from two locations (Figure 2) i.e. Kelekar River in Segayam Village, Muara Enim Regency (given the PM code) and the leaffish from the Ogan River in Pemulutan District, Ogan Ilir Regency at sampling coordinates 3°03'17" S 104°46'32" E (given the PP code). Four individuals were taken from each river. All specimens were collected in the wild and determined morphologically in situ by visual observation based on manual identification (Saainin 1984). The length of leaffish from the Kelekar River ranged from 6.6-10.9 cm and weighed of 4.37-34.12 g while the leaffish from the Ogan River measures 11.5-13.5 cm in length and 28.66-50.53 grams of weight. Fin samples were put into a 1.5 ml tube with a 96% ethanol solution, then stored in a freezer at -20°C until DNA isolation was carried out.

Methods

DNA Isolation

The total genome of the leaffish DNA was isolated using the extraction kit of Genomic DNA (GeneAid) as described in the protocol. The DNA was extracted in six stages, i.e. the preparation of specimens, the lysis of cell, RNase addition, DNA precipitation, cleaning and DNA dissolution. The extracted DNA of fin samples were stored in a freezer (-20 °C), until the electrophoresis process was carried out to check DNA integrity and PCR (Polymerase Chain Reaction).

DNA Amplification

DNA genome was amplified using Polymerase Chain Reaction (PCR) to target a 655 bp of *COI* gene with primer pairs of FishF2 (forward)-5' TCGACTAATCATAAAGATATCGGCAC 3' dan FishR2 (reverse)-5'



Figure 1. Indonesian leaf fish (*Pristolepis grooti*).

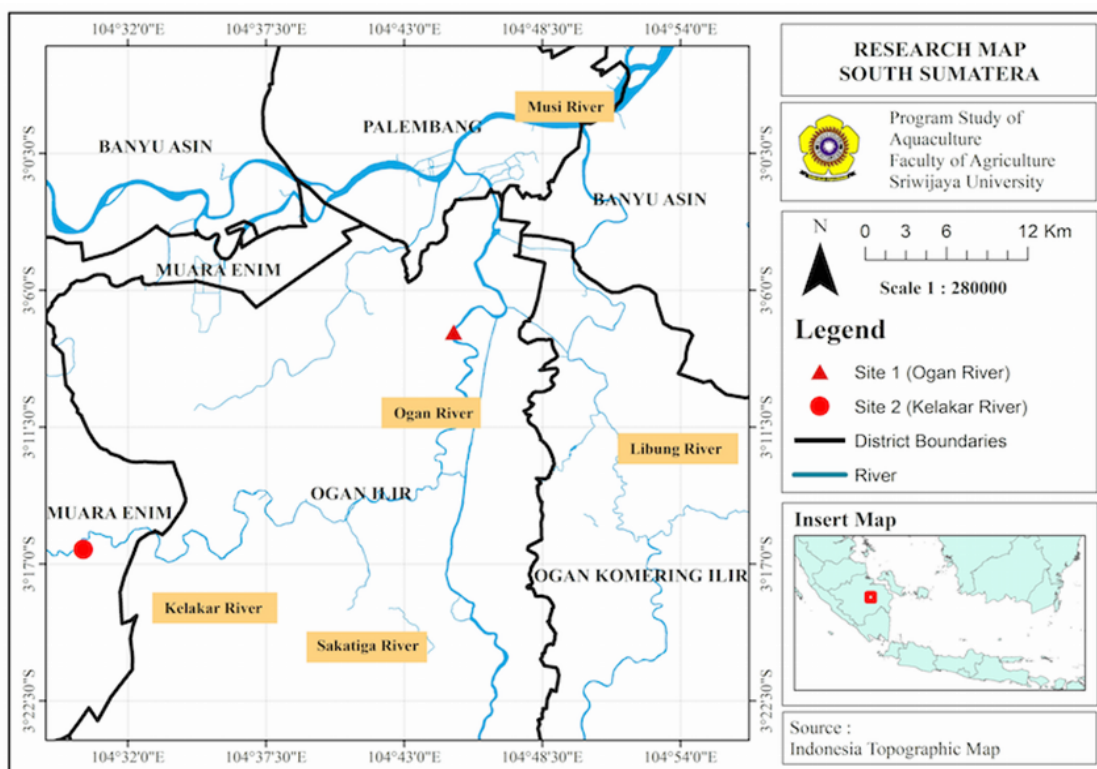


Figure 2. Map of research locations in the Kelakar and Ogan River.

ACTTCAGGGTGACCGAAGAATCAGAA 3' (Ward et al. 2005). PCR was performed in a final volume of 50 μ L. Each reaction contained 17 μ L ddH₂O, 25 μ L My Taq Red Mix, 10 μ L Fish R2 primer (10 pmol/ μ L), 10 μ L Fish F2 primer (10 pmol/ μ L) and 6 μ L DNA template. DNA amplification was carried out in stages: initiation cycle at 94 °C for 1 minute in 1 cycle, denaturation at 94 °C for 30 seconds, annealing at 52 °C for 30 seconds, extension or elongation at 72 °C for 15 seconds in 35 cycles and post extension 72 °C for 4 minutes in 1 cycle. Furthermore, the PCR product was visualized by electrophoresis of 1% agarose gel in 75 voltage for 35 minutes. The size of the DNA from the PCR was measured using a 1 kb DNA marker. The PCR products were sequenced bi-direction with both primers through the services of PT Genetics Science (Jakarta).

Water Quality

Water qualities were measured three times at each location during the

study. The parameters observed i.e. temperature ($^{\circ}\text{C}$), water transparency (cm), dissolved oxygen (mg L^{-1}), pH, ammonia (mg L^{-1}), total alkalinity (mg L^{-1}), total dissolved solid/TDS (mg L^{-1}) and water current (m s^{-1}).

Data Analysis

The *COI* gene sequences in fasta format are then aligned using MEGA X software, then continue to BLAST (Basic Local Alignment Search Tool) for determining the homology of a DNA sequence with the data in NCBI (National Center for Biotechnology Information). Furthermore, all sequences were aligned to analyze the genetic distance and phylogenetic tree, including a sequence of *Oreochromis niloticus* (GenBank: KM438528) from Stirling collection as an outgroup. The phylogenetic tree was constructed using the Neighbor-Joining (NJ) method and the Maximum Composite Likelihood model on MEGA software X Version (Kumar et al. 2018; Stecher et al. 2020) and the genetic distance was analyzed using the Pairwise Distance method (Kimura 1980).

RESULTS AND DISCUSSION

DNA Authentication

The amplified DNA of the *COI* gene of leaffish was electrophoresed using 1% agarose gel, showing a size of 704 bp for PM 1, PM 4, PP 2 and PP 4 samples code and 723 bp for PM 2, PM 3, PP 1 and PP 3. All sequences of PCR product have been submitted in Barcode of Life Database Identification (BOLD-ID) under the accession number BOLD:ADO0531 and BOLD:ADN7493. The *COI* gene sequence of the leaffish is analyzed through nucleotide BLAST on the website of the National Center for Biotechnology Information (www.ncbi.nlm.nih.gov) for comparison with other species in the GenBank database. The percentages of nucleotide similarity of the leaffish were presented in Table 1.

Nine individuals of *P. grooti* were barcoded successfully using *COI* gene with universal primer followed (Ward et al. 2005) at annealing temperature optimization of 52°C for 30 seconds in 35 cycles of PCR. Annealing temperature in the PCR used to usually calculated from $T_m-5^{\circ}\text{C}$ to $T_m+5^{\circ}\text{C}$ (Muladno 2010). The table 1 indicated that the *COI* nucleotide sequences of the leaffish (*P. grooti*) had the highest identity of around 95.29%-96.13% with *P. fasciata* from Malaysia (accession code KT001055.1), then 94.70-95.85 to *P. fasciata* from Vietnam (accession code MH721176.1). The smallest percentage of similarity (87.48% - 89.22%) was *P. rubripinnis* from India (MG9234001, MG923399.1, MG923396.1).

There was none of the leaffish from the Kelekar River and the Ogan River 100% similar to other fish samples or the same species in GenBank (Table 1). *Pristolepis grooti* is very similar to *P. fasciata*, with slight differences in the presence of $3\frac{1}{2}$ rows (*fasciata*: $4\frac{1}{2}$ rows) of scales separating dorsal fin mid spines from lateral line scales; ventral fin that does not reach the anal canal, coloration, and profile of the top of the head towards the nape which is more convex (*fasciata*: tends to be straight) (Weber & Beaufort. 1936).

Based on data from meristic measurements of leaffish (*Pristolepis* sp.) from the Kelekar River and Ogan River, the leaffish had a total length between 12.7 cm - 13.5 cm. Table 2 Indicated the dorsal fins have 12-13 hard spines and 13-16 soft rays (D.XIII.15-16), 3-8 anal fins, 12-14 soft rays of pectoral fins (P. 12-14), 1 hard spine, 5 soft rays of ventral fins, 12-14 soft rays of caudal fins (C. 12-14). Research by (Muslim et al. 2019) on an Indonesian leaffish *Pristolepis grootii*, the dorsal fin has 13 hard spines and 15-16 soft rays (D.XIII.15-16), the anal fin consists of 3

Table 1. The similarity percentage of nucleotides of leaffish *P. grooti* from the Kelekar and Ogan rivers.

No.	Code	Description	Query cover (%)	Identity (%)	Accession	Origin
1.	PM 1	<i>Pristolepis fasciata</i>	91	95.62	KT001055.1	Malaysia
			94	95.28	MH721176.1	Vietnam
2.	PM 2	<i>P. fasciata</i>	91	95.29	KT001055.1	Malaysia
			95	94.70	MH721176.1	Vietnam
3.	PM 3	<i>P. fasciata</i>	91	95.62	KT001055.1	Malaysia
			93	95.39	MH721176.1	Vietnam
4.	PM 4	<i>P. fasciata</i>	92	95.29	KT001055.1	Malaysia
			96	94.96	MH721176.1	Vietnam
5.	PP 1	<i>P. fasciata</i>	87	96.13	KT001055.1	Malaysia
			92	95.85	MH721176.1	Vietnam
6.	PP 2	<i>P. fasciata</i>	91	95.96	KT001055.1	Malaysia
			94	95.72	MH721176.1	Vietnam
7.	PP 3	<i>P. fasciata</i>	91	95.96	KT001055.1	Malaysia
			94	95.72	MH721176.1	Vietnam
8.	PP 4	<i>P. fasciata</i>	91	95.96	KT001055.1	Malaysia
			95	95.32	MH721176.1	Vietnam
9.	All samples	<i>P. rubripinnis</i>	94-99	87.48-88.91	MG9234001	India
					MG923399.1	
					MG923396.1	

Table 2. Meristic parameter between *P. grooti* and *P. fasciata*.

Character	Sample		Species	
	Kelekar River	Ogan River	<i>P. grooti</i>	<i>P. fasciata</i>
Dorsal fins	DXII-XIII.13-16	DXII-XIII.13-15	DXIII.15-16	D.XII-XIII.13-14
Ventral fins	V.I.5	V.I.5	V.I.5	V.1.5
Pectoral	P.12-14	P.12-14	P.13-14	P.12
Caudal	C.12-14	C.12-14	C.13-14	-
Anal	AIII.7-8	AIII.7-8	AIII.7-8	A.III.7-8
Source			(Muslim et al. 2019)	(Sukmono & Margaretha 2017)

hard spines and 7-8 soft rays (A.III.7-8). As for the pectoral fins, there are no hard spines with 13-14 soft rays (P.13-14), the ventral fin has 1 hard spine and 5 soft rays (V.I.5) and the caudal fin which all consists of 13-14 soft rays (C.13-14). While the Malayan leaffish *Pristolepis fasciata* has dorsal meristic characteristics consisting of 12-13 hard spines and 13-14 soft rays (D.XII-XIII.13-14), anal fin consists of 3 hard spines and 7-8 soft rays (A.III.7-8), pectoral fins consist of 12 soft rays (P.12), ventral fins consist of 1 hard spine and 5 soft rays (V.I.5) (Sukmono & Margaretha 2017). The meristic showed overlapping measurements between the two species, except the soft rays number in dorsal fins of *P. grooti* is slightly higher than *P. fasciata*. Molecularly, there was 94.70 – 96.13% identity based on nucleotide sequences of *COI* gene between *P. grooti* and *P. fasciata*. Determining the homology level of a sequence with other species sequences in GenBank data can be explained by the value of max score and total score, query coverage approaching 100%, E-value approaching 0 and percentage identity approaching 100% (Tindi et al. 2017).

Genetic Distance and Phylogenetics

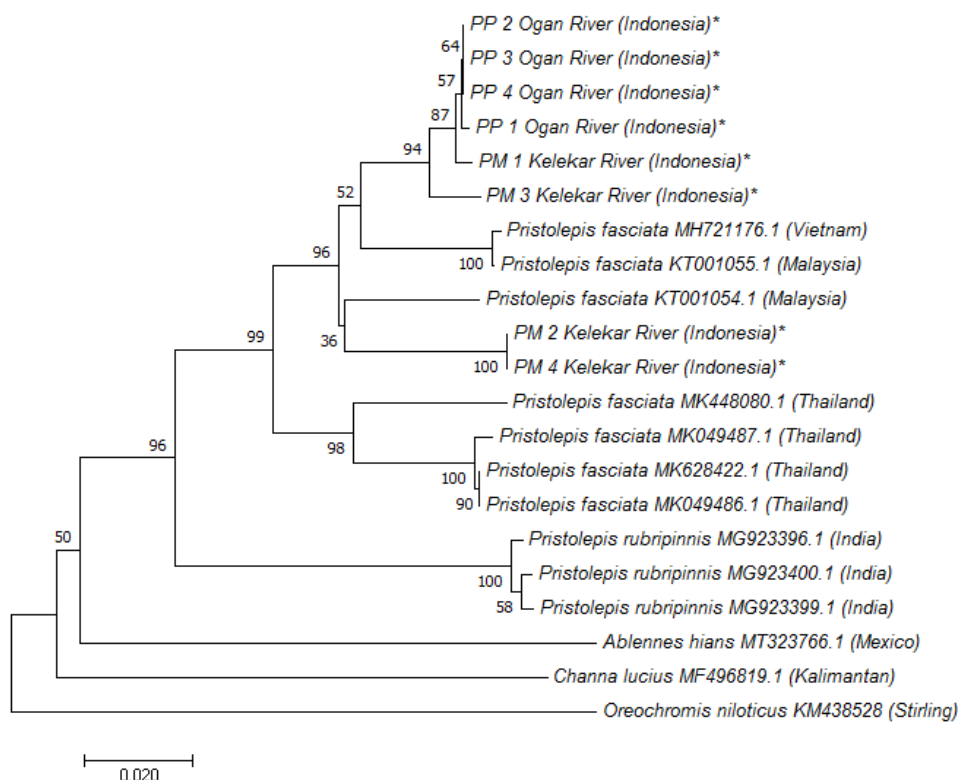
The genetic distance of the leaffish from the Kelekar and the Ogan River with other species in the GenBank data was presented in Table 3.

The genetic distance of the leaffish *P. grooti* from both rivers showed a range of 1.6-8.4% with *P. fasciata* from Genbank database. Sam-

ples PP 2, PP 3, PP 4, PM 1 have a genetic distance of 0.016 (1.6%) against PM3 and 0.045 (4.5%) to PM 4. The genetic distance of samples PM 1, PM 3, PP 2, PP 3 and PP 4 was 0.047 (4.7%) to *P. fasciata* from Malaysia (KT001055.1) and 0.049 (4, 9%) from Vietnam (MH721176.1).

The genetic distance within population from Kelekar or Ogan River is around 4.5-6%. This finding showed cryptic diversity of the fish species. Cryptic species are taxa which are distinguished by unique genetic differences, distinctive ecological preferences and the complete or practically complete absence of morphological discrepancies (Bączkiewicz et al. 2017). Therefore, they can be distinguished with the use of molecular methods, as it has been done for sea cucumbers (Muliani et al. 2020), triplophysa (Wang et al. 2020), and Asian bronze featherback (Lavoué et al. 2020).

The genetic construction of the leaffish from the Kelekar River and the Ogan River is presented in Figure 3. The genetic tree of the leaffish consisted of four clusters, namely first cluster of research samples from the Kelekar, Ogan River and *Pristolepis fasciata* from Vietnam (accession code: MH721176.1) and Malaysia (KT001055.1, KT001054.1) with bootstrap value of 91%. There were three sub clusters of the first cluster. Samples PP1, PP2, PP3, PP4, PM1 and PM3 were in separate sub cluster from PM2 and PM4 (bv= 91). The second cluster was a group of *P. fasciata* from Thailand (MK448080.1, MK049487.1, MK628422, and MK 049486.1) (bv=98), the third cluster was *P. rubripinnis* from India, while the fourth cluster was an outgroup of *O. niloticus* (KM438528). The phylogenetic of the leaffish of this study formed 2 separate sub-clusters consisting of the first sub-cluster, namely PP 2, PP 3, PP 4, PP 1, PM 1 and



PP 1, PP 2, PP3, and PP4 from Ogan River, PM1, PM2, PM4 from Kelekar River, *P. fasciata* KT001055 (Malaysia), *P. fasciata* MH721176 (Vietnam), *P. fasciata* KT001054 (Malaysia), *P. fasciata* MK628422 (Thailand), *P. fasciata* MK049486 (Thailand), *P. fasciata* MK049487 (Thailand), *P. fasciata* MK448080 (Thailand), *P. rubripinnis* MG923396 (India), *P. rubripinnis* MG923400 (India), *P. rubripinnis* MG923399 (India), *Channa lucius* MF496819 (Kalimantan), *Ablennes hians* MT323766 (Mexico), *Oreochromis niloticus* KM438528 (Stirling).

Figure 3. The genetic tree of the leaffish from the Kelekar and Ogan River.

Table 3. The genetic distance of the leaffish from the Kelekar and Ogan River.

Species Name	1	2	3	4	5	6	7	8	9	10	11	12	13	14	15	16	17	18	19	20
1 PM 3 Sungai Kelekar (Indonesia)*																				
2 PP 4 Sungai Ogan (Indonesia)*	0.016																			
3 PP 2 Sungai Ogan (Indonesia)*	0.016	0.000																		
4 PP 3 Sungai Ogan (Indonesia)*	0.016	0.000	0.000																	
5 PM 1 Sungai Kelekar (Indonesia)*	0.016	0.004	0.004	0.004																
6 PP 1 Sungai Ogan (Indonesia)*	0.018	0.002	0.002	0.002	0.006															
7 PM 2 Sungai Kelekar (Indonesia)*	0.045	0.057	0.057	0.057	0.060	0.057														
8 PM 4 Sungai Kelekar (Indonesia)*	0.045	0.057	0.057	0.057	0.060	0.057	0.000													
9 <i>P. fasciata</i> KT001055 (Malaysia)	0.047	0.043	0.043	0.043	0.047	0.041	0.055	0.06												
10 <i>P. fasciata</i> MH721176 (Vietnam)	0.049	0.045	0.045	0.045	0.049	0.043	0.057	0.06	0.002											
11 <i>P. fasciata</i> KT001054 (Malaysia)	0.055	0.047	0.047	0.047	0.051	0.045	0.055	0.06	0.066	0.064										
12 <i>P. fasciata</i> MK628422 (Thailand)	0.076	0.072	0.072	0.072	0.072	0.074	0.086	0.09	0.076	0.078	0.080									
13 <i>P. fasciata</i> MK049486 (Thailand)	0.076	0.072	0.072	0.072	0.072	0.074	0.086	0.09	0.076	0.078	0.080	0.000								
14 <i>P. fasciata</i> MK049487 (Thailand)	0.080	0.076	0.076	0.076	0.076	0.078	0.090	0.090	0.076	0.078	0.084	0.004	0.004							
15 <i>P. fasciata</i> MK448080 (Thailand)	0.084	0.080	0.080	0.080	0.080	0.082	0.084	0.084	0.086	0.088	0.068	0.051	0.051	0.055						
16 <i>P. rubripinnis</i> MG923396 (India)	0.129	0.117	0.117	0.117	0.117	0.115	0.136	0.14	0.117	0.115	0.117	0.123	0.123	0.119	0.127					
17 <i>P. rubripinnis</i> MG923400 (India)	0.129	0.121	0.121	0.121	0.121	0.119	0.136	0.136	0.117	0.115	0.121	0.123	0.123	0.119	0.127	0.004				
18 <i>P. rubripinnis</i> MG923399 (India)	0.129	0.121	0.121	0.121	0.121	0.119	0.136	0.14	0.117	0.115	0.121	0.123	0.123	0.119	0.127	0.008	0.004			
19 <i>Channa lucius</i> MF496819 (Kalimantan)	0.164	0.164	0.164	0.164	0.164	0.162	0.164	0.164	0.170	0.168	0.166	0.179	0.179	0.179	0.177	0.177	0.181	0.183		
20 <i>Ablemes hians</i> MT323766 (Meksiko)	0.173	0.160	0.160	0.160	0.160	0.162	0.173	0.173	0.179	0.177	0.177	0.170	0.170	0.168	0.172	0.177	0.181	0.181	0.189	
21 <i>Oreochromis niloticus</i> KM438528 (Stirling)	0.201	0.203	0.203	0.203	0.201	0.201	0.185	0.185	0.187	0.185	0.197	0.189	0.189	0.191	0.201	0.197	0.197	0.197	0.21	0.216

PM 3 with *P. fasciata* from Vietnam (MH721176) and Malaysia (KT001055) and the second sub-cluster, namely PM 2 and PM 4 with *P. fasciata* from Malaysia (KT001054) with a bootstrap value of 50%.

The genetic distance indicated that *P. grootii* differed genetically more than 3% than *P. fasciata*, genetically. The smaller the value of genetic distance denotes that the species is more related to other species and has a close relationship, while the greater the value of genetic distance indicates that the species is increasingly divergent. If the genetic distance is more than 3%, it indicates that in the group there are species that are different from other members, on the contrary, if the genetic distance value is equal to or less than 3%, it indicates that the group or cluster still comes from one species or the same species (Wong & Hanner 2008).

The construction of the phylogenetic relationship between species or related taxa was supported by the availability of a sequence database in many species (Hedrick 2005). However, when only one *COI* gene is used, a gene tree is produced, and it will not describe the broad evolutionary history of a group of species (Rubin et al. 2012). The genetic tree of all specimens of *P. grootii* in this study was separated from *P. fasciata* Thailand, but showed an indefinite cluster with the specimen from Malaysia and Vietnam. *P. fasciata* from Malaysia and Vietnam were located between two clusters of samples PP1, PP2, PP3, PP4, PM1, PM3 and PM2 and PM4 with low bootstrap value (bv=50). Bootstrapping is used to make inferences and evaluate the robustness of the tree (Holmes 2003). The data is relatively stable when the bootstrap value is greater than 70% (Lemey et al. 2009) relatively. Furthermore, *P. grootii* of this study also indicated different sub-cluster between Kelekar and Ogan River, where PM2 and PM4 from Kelekar River were separated from PM1 and PM3 (bv=91), where they belong to the same sub-cluster to PP1, PP2, PP3 and PP4 (originally from Ogan River). The proximity of the leaffish of the Kelekar and the Ogan River is interconnected because the Kelekar River flows into the Ogan River and empties into the Musi River (Wijaya 2001). The high similarity and genetic relationship of the leaffish are in line with the high level of diversity of these fish species that inhabit the Sunda shelf which consists of interconnected islands of Sumatra, Kalimantan, Java, Bangka

Table 4. Water quality measurements in the Kelekar and the Ogan River.

Water Quality	Kelekar River	Ogan River	Water quality standards
pH (Unit)	5.6-7.2	6.9-8.3	6-9 (Central Government 2001)
Temperature (°C)	28.3-31.8	30.8-31.5	25-32 (Central Government 2001)
Water current (m s ⁻¹)	0.17-0.30	0.19-0.21	0.25-0.5 (Supartiwi 2000)
Dissolved oxygen (DO) (mg L ⁻¹)	4.82-6.93	6.92-10.89	>4 (Central Government 2001)
Water transparency (cm)	16-20	41-45	30-60 (Cholik et al. 1991)
TDS (mg L ⁻¹)	7-11	24-44	<1000 (Central Government 2001)
Ammonia (mg L ⁻¹)	0.47-0.70	0.52-0.61	<0.2 (Central Government 2021)
Total alkalinity (mg L ⁻¹)	10-18	24-28	5-500 (Effendi 2003)

Belitung, which are dominated by fish that inhabit peatlands and fresh-water, especially those that are endemic (Hubert et al. 2008), so that mating occurs in the distribution of the leaffish, geographically.

Water Quality

The water quality of the habitat of the leaffish in Kelekar and Ogan River was presented in Table 4. the pH value of Kelekar and Ogan River ranged 5.6-8.3, temperature values of 28.3-31.8°C, dissolved oxygen was between 4.82-10.89 mg L⁻¹, total dissolved solid (TDS) was about 7-44 mg L⁻¹. The water transparency value was approximately 16-40 cm, while the total alkalinity was about 10-28 mg L⁻¹. Mutagenic substances in the Reservoir 1 in the Canela National Forest have been altering the genetic integrity of the aquatic organisms that may be a threat for that aquatic ecosystem (Bühler et al. 2014). Furthermore, pollutants present in Madin Reservoir water were genotoxic and cytotoxic to *C. carpio* (Pérez-Coyotl et al. 2017).

Water pH media, dissolved oxygen and TDS in Kelekar and Ogan River were in accordance with the water quality standard class II for fishing activities, mainly for fish to grow and reproduce (Government Implementation of Environmental Protection and Management. 2021). The value of ammonia (NH₃) was 0.47-0.70 mg L⁻¹. This range was higher than required for fish production in freshwater based on the quality standard for grades 2 (< 0.2 mg/L (Central Government 2021). In this study, water current ranges from 0.17 to 0.30 m s⁻¹, indicated that the Kelekar River was classified as a slow current, while the Ogan River (0.19-0.21 m s⁻¹) was categorized as a slow current and water current of 0.25-0.5 m s⁻¹ was at medium current (Supartiwi 2000). The water transparency value was approximately 16-40 cm, while the optimal value for water transparency required for the growth of freshwater fish is around 30-60 cm (Cholik et al. 1991). The total alkalinity was about 10-28 mg L⁻¹ and still supports the survival of the leaffish. The total value of good alkalinity in waters is between 5-500 mg L⁻¹ CaCO₃ (Effendi 2003).

CONCLUSIONS

This investigation utilizes the COI barcode for the molecular authentication of endemic fish *P. grooti* from Southern Sumatra. These results indicated the leaffish had the highest identity to *P. fasciata* from Malaysia (KT001055) with different percentages of each sample ranging from 95.29 to 96.13%. The genetic tree supported that *P. grooti* in this study was separated from *P. fasciata* in Thailand, but showed an indefinite cluster with the specimen from Malaysia and Vietnam.

AUTHOR CONTRIBUTION

The study was designed by MSF. ETG and MW were conducted the laboratory works. The data was analysed by MSF and ETG. All the authors wrote original draft, edited and approved the manuscript.

ACKNOWLEDGMENTS

The authors would like to express greatest appreciation to the Head of Aquaculture and Basic Fisheries Laboratory in Fisheries Department. We also sincerely thank to the Head of Plant Physiology Laboratory at Faculty of Agriculture, Sriwijaya University for granting us access to the laboratory facilities.

CONFLICT OF INTEREST

The authors state that the research was created in the absence of any commercial or financial matters that could be a potential conflict of interest.

REFERENCES

- Bączkiewicz, A. et al., 2017. DNA barcoding, ecology and geography of the cryptic species of *Aneura pinguis* and their relationships with *Aneura maxima* and *Aneura mirabilis* (Metzgeriales, Marchantiophyta). *PLoS ONE*, 12(12), e188837. doi: 10.1371/journal.pone.0188837.
- Bühler, D. et al., 2014. Genetic damage induced by water pollutants in the freshwater fish *Hyphessobrycon luetkenii* (Characidae) in a reservoir of the Canela National Forest, Brazil. *Journal of Freshwater Ecology*, 29(2), pp.295–299. doi: 10.1080/02705060.2013.879539.
- Cholik, F., Artati & Arifudin, R., 1991. *Water Quality Management of Fish Pond*, Direktorat Jenderal Perikanan, Jakarta.
- Central Government, 2001. *PP No. 82.: Peraturan Pemerintah Republik Indonesia Tentang Pengelolaan Kualitas Air dan Pengelolaan Pencemaran Air*, Jakarta.
- Central Government, 2021. *Government Regulation of Republic of Indonesia No. 22, 2021: Government Implementation of Environmental Protection and Management.*, Indonesia.
- Effendi, H., 2003. *Water Quality Study for Water Resources and Environmental Management*, Yogyakarta: Kanisius.
- Emawati, Y., Aida, S.N.A. & Juwaini, H., 2017. Reproductive biology of leaf fish, *Pristolepis grootii* Blkr. 1852 (Nandidae) in the Musi River. *Iktiologi Indonesia*, 9(1), pp.13–24.
- Froese, R. & Pauly, D., 2019. Species of *Pristolepis*. *FishBase*.
- Hedrick, P.W., 2005. *Genetics of Populations* Third., Jones and Bartlett.
- Holmes, S., 2003. Bootstrapping Phylogenetic Trees: Theory and Methods. *Statistical Science*, 18(2), pp.241–255. doi: 10.1214/ss/1063994979.
- Hubert, N. et al., 2008. Identifying Canadian freshwater fishes through DNA barcodes. *PLoS ONE*, 3(6), e2490. doi: 10.1371/journal.pone.0002490.
- Kimura, M., 1980. A simple method for estimating evolutionary rate of base substitutions through comparative studies of nucleotide sequences. *J Mol Evol*, 15, pp.111–120.
- Kottelat, M. & Whitten, A.J., 1993. *Freshwater Fishes of Indonesian and Sulawesi*, Periplus Editions Limited.
- Kumar, S. et al., 2018. MEGA X: Molecular Evolutionary Genetics Analysis across computing platforms. *Molecular Biology and Evolution*, 35, pp.1547–1549.

- Lavoué, S. et al., 2020. Genetic evidence for the recognition of two allopatric species of Asian bronze featherback *Notopterus* (Teleostei, Osteoglossomorpha, Notopteridae). *Zoosystematics and Evolution*, 96 (2), pp.449–454. doi: 10.3897/zse.96.51350.suppl2.
- Lemey, P., Selemi, M. & Vandamme, A.M., 2009. *The Phylogenetic Handbook: A Practical Approach to Phylogenetic Analysis and Hypothesis Testing*, Cambridge-UK: Cambridge University Press.
- Masters, J.C. et al., 2007. Phylogenetic relationships among the lorisoidea as indicated by craniodental morphology and mitochondrial sequence data. *American Journal of Primatology*, 69(1), pp.6–15. doi: 10.1002/ajp.20322.
- Muladno, 2010. *Genetic Engineering Technology*, Bogor: IPB Press.
- Muliani, D.R. et al., 2020. Characteristics of Crassostrea Oyster Cytochrome Oxidase Subunit I (COI) Gene as Species Identity In Delta Cimanuk, West Java. *Jurnal Moluska Indonesia*, 4(1), pp.8–16.
- Muslim, M. et al., 2019. Introduction to know the leaf fish (*Pristolepis grootii*), a species native to Indonesia, a candidate commodity for aquaculture. *Jurnal Akuakultur Sungai dan Danau*, 4(2), pp.40–45. doi: 10.33087/aquaculture.v4i2.52.
- Muslim, M. & Syaifudin, M., 2022. Biodiversity of Freshwater Fish in Kelekar Floodplain Ogan Ilir Regency in Indonesia. *Journal of Tropical Biodiversity and Biotechnology*, 7(1), jtbb67494. doi: 10.22146/jtbb.67494.
- Noikotr, K., 2019. *Pristolepis fasciata* Voucher FNP014 Cytochrome C Oxidase Subunit I (COI) Gene, Partial cds; Mitochondrial. *Biology, Ramkhamhaeng University, Bangkok, Thailand.*, viewed January 3, 2022, from <https://www.ncbi.nlm.nih.gov/nuccore/1607272014>
- Pramono, et al. 2019. Genetic characteristics of Senggarangan fish (*Mystus singarngan*) from Klawing River, Brantas River and Thailand as basis of conservation and domestication. *AAFL Bioflux*, 12 (4), pp.996–1004.
- Pérez-Coyotl, I. et al., 2017. DNA damage and cytotoxicity induced on common carp by pollutants in water from an urban reservoir. Madín reservoir, a case study. *Chemosphere*, 185, pp.789–797. doi: 10.1016/j.chemosphere.2017.07.072.
- Rubin, B.E.R., Ree, R.H. & Moreau, C.S., 2012. Inferring phylogenies from RAD sequence data. *PloS one*, 7(4), e33394. doi: 10.1371/journal.pone.0033394.
- Saanin, H. 1984. *Taxonomy and Fish Identification Keys Volume 1 and 2*, Jakarta: Bina Cipta
- Sukmono, T. dan Margaretha, M., 2017. *Ikan Air Tawar di Ekosistem Bukit Tigapuluh (Freshwater Fishes of the Bukit Tigapuluh Ecosystem)*, Jambi Indonesia: Yayasan Konservasi Ekosistem Hutan Sumatera dan Frankfurt. Zoological Society.
- Stecher, G. et al., 2020. Molecular Evolutionary Genetics Analysis (MEGA) for macOS. *Molecular Biology and Evolution*, 37, pp.1237–1239.
- Supartiwi, E.N., 2000. *Characteristics of the phytoplankton and periphyton communities as indicators of the environmental quality of the Cujung River, West Java*, Bogor: IPB Press.
- Syaifudin, M. et al., 2017. DNA authentication of asian redtail catfish *Hemibagrus nemurus* from Musi and Penukal River, South Sumatra Indonesia. *Genetics of Aquatic Organisms*, 1(December), pp.43–48. doi: 10.4194/2459-1831-v1.

- Syaifudin, M. et al., 2019. DNA barcoding of snakeskin gourami *Trichogaster pectoralis* and blue gourami *Trichogaster trichopterus* based on cytochrome c oxidase subunit i (COI) gene. *IOP Conference Series: Earth and Environmental Science*, 348, 012031. doi: 10.1088/1755-1315/348/1/012031.
- Syaifudin, M. et al., 2020. DNA barcodes and phylogenetic of striped snakehead and ocellated snakehead fish from South Sumatra, Indonesia. *Biodiversitas*, 21(3), pp.1227–1235. doi: 10.13057/biodiv/d210350.
- Tindi, M. et al., 2017. DNA Barcode dan analisis filogenetik molekuler beberapa jenis bivalvia asal perairan Sulawesi Utara berdasarkan gen COI. *Jurnal Pesisir Dan Laut Tropis*, 5(2), p.32. doi: 10.35800/jplt.5.2.2017.15050.
- Truong, O.T., Pham, P.T. & Dang, B.T., 2020. The 3rd International Conference on Sustainable Agriculture and Environment. In *Species Diversity and Molecular Phylogeny Of Perciformes in Mekong Delta, Vietnam*. Ho Chi Minh: Nong Lam University.
- Wang, T. et al., 2020. DNA barcoding reveals cryptic diversity in the underestimated genus *Triplophysa* (Cypriniformes: Cobitidae, Nemacheilinae) from the northeastern Qinghai-Tibet Plateau. *BMC Evolutionary Biology*, 20, 151. doi: 10.1186/s12862-020-01718-0.
- Ward, R.D. et al., 2005. DNA barcoding Australia's fish species. *Philosophical transactions of the Royal Society of London. Series B, Biological sciences*, 360(1462), pp.1847–57. doi: 10.1098/rstb.2005.1716.
- Weber, M. & Beaufort., L.F. de, 1936. *The Fishes of The Indo-Australian Archipelago VII: 479-80.*, E.J. Brill. Leiden.
- Wijaya, F., 2001. *Optimizing the use of production factors in the cultivation of catfish (Pangasius pangasius) with cage systems (in the waters of the Ogan River and Kelekar River, OKI Regency, South Sumatra)*, Bogor.
- Wong, E.H.K. & Hanner, R.H., 2008. DNA barcoding detects market substitution in North American seafood. *Food Research International*, 41(8), pp.828–837. doi: 10.1016/j.foodres.2008.07.005.

Research Article

In Silico and Validation Approaches for Optimum Conditions of *Rattus norvegicus* Target Gene qPCR Primers

Gracia Alice Victoria Pollo¹, Nyoman Yudi Antara², Firman Alamsyah³, Rarastoeti Pratiwi^{1*}

1)Faculty of Biology, Universitas Gadjah Mada, Yogyakarta, 55281, Indonesia

2)Faculty of Health, Universitas Kader Bangsa, Palembang, 30129, Indonesia

3)Center for Medical Physics and Cancer Research, CTECH Laboratories EDWAR TECHNOLOGY, Tangerang, 15320, Indonesia

* Corresponding author, email: rarastp@ugm.ac.id

Keywords:

experimental validation
in silico

oligonucleotide

qPCR primer

SYBR Green I

Submitted:

31 December 2021

Accepted:

07 March 2023

Published:

05 June 2023

Editor:

Ardaning Nuriliani

ABSTRACT

Gene expression analysis using the qPCR method requires an oligonucleotide pair to prime the amplification process. Supporting the widely used qPCR method, variety of qPCR reagents and primer options are available. This infers to the importance of *in silico* and laboratory experimental validation approach considering SYBR Green optimum annealing temperature to validate the most suitable primer for prior use. Several genes are suspected to be involved in the BM-MSCs migration and differentiation into Cancer-associated Fibroblast Cells in *Rattus norvegicus*. This article aims to provide *in silico* analysis with the case of the suspected genes namely actin alpha-2 smooth muscle (*ACTA2*), fibroblast activation protein (*FAP*), hypoxanthine phosphoribosyltransferase-1 (*HPRT1*), platelet-derived growth factor subunit B (*PDGFB*), phosphoinositide-3-kinase regulatory subunit-1 (*PIK3R1*), and vascular cell adhesion molecule-1 (*VCAM1*) qPCR primer with qPCR and electrophoresis validation. The procedure used in this approach was *in silico* analysis of primer from published articles and newly designed primer. The analysis was done with Primer-BLAST for gene specificity, Primer-Dimer, OligoCalc for hairpin formation, BLAST Nucleotide for identical sequence screening, and Clustal Omega for product length validation. Experimental validation was done using qPCR for optimal annealing temperature, priming ability, amplicon specificity, and electrophoresis for product length validation. This assessment resulted in *in silico* and laboratory experimental validation of *ACTA2*, *FAP*, *HPRT1*, *PDGFB*, *PIK3R1*, and *VCAM1* primer pairs producing suitable amplicon for qPCR using *Rattus norvegicus* cDNA with SYBR annealing temperature range of 60-65°C with three mM MgCl₂. The primer pairs can be used for further qPCR analysis under similar conditions and the procedure stated can be used as starting point for qPCR Primer preparation accounting for fluorophore optimum annealing temperature.

Copyright: © 2023, J. Tropical Biodiversity Biotechnology (CC BY-SA 4.0)

INTRODUCTION

A molecular approach such as qPCR has been the vastly used method (Luna et al. 2012; Canh et al. 2020; Caselli et al. 2021). This approach has been applied to various gene expression analyses (Fiechter et al. 2021; Sharma et al. 2021), pathological detection (Caselli et al. 2021), and

microbial detection (Luna et al. 2012; Cuevas-Ferrando et al. 2021). Broad options for qPCR reagent are offered (Petrovan et al. 2020; Brown et al. 2021; Kang et al. 2021) with broad options of analysis object present (Luna et al. 2012; Fiechter et al. 2021).

A variety of qPCR reagents having different reaction conditions can affect the annealing of primer, where a pair of oligonucleotides is required to prime the amplification process (Sato et al. 2021). Research showed that even SYBR Green I was used by several different manufacturers, there would still be variations in the amplification (Hargreaves et al. 2013). MgCl₂ concentration is known to give a slight change in annealing temperature. Annealing temperatures from the same set of primer can affect amplification (Hargreaves et al. 2013). The prediction that can be done for primer can give the researchers chance to bypass designing primer pairs with the unintended annealing possibility (Johnston et al. 2019). Most available primers on published articles share a wide range of melting temperatures. It presents challenges in using those primers with the possible different reagents (Vogels et al. 2020; Yang et al. 2020; Langlois et al. 2021). Prior to qPCR primers application, *in silico* (Vanneste et al. 2018; Covey 2021) and laboratory experimental approach (Trigo et al. 2021) are essential in validating the most suitable primer.

Several suspected genes are involved in the BM-MSCs migration and differentiation into cancer associated fibroblast (CAF) cells in *Rattus norvegicus* breast tumour. A chemoattractant gene, *PDGFB*, is involved in that migration (Camorani et al. 2017). Genes such as *PIK3R1* (Jiménez et al. 2000) and *VCAM1* (Hu et al. 2012) are involved in cellular migration signalling process. *ACTA2* and *FAP* are the genes expressing CAFs molecular markers (Costa et al. 2018). Prior to relative gene expression analysis on *Rattus norvegicus* gene expression, qPCR primer for *ACTA2*, *FAP*, *HPRT1*, *PDGFB*, *PIK3R1*, and *VCAM1* had been analyzed. Due to the specificity of SYBR efficacy to function, this article shares the evidence about the analyzed qPCR primers producing suitable primer pairs for SYBR Green I with three mM of MgCl₂.

MATERIALS AND METHODS

Materials

In silico materials used were Google Scholar search engine, National Center for Biotechnology Information (NCBI) database, and software tool (Primer3, Primer-Blast, Primer-Dimer, OligoCalc, Nucleotide Blast, Clustal Omega). Laboratory experimental validation materials used were *Rattus norvegicus* cDNA (ethical clearance: No. 00029/04/LPPT/IV/2018), nuclease-free water (Thermo Scientific Water Nuclease-Free R0581), qPCR reagent (Bioline SensiFAST SYBR No-ROX Kit BIO-98005), qPCR primer (synthesized by Integrated DNA Technologies (IDT)), agarose powder, Tris-Boric-EDTA (TBE) buffer (1st BASE – 10X TBE Buffer BUF-3010-10X1L), DNA Ladder (Smobio Excel-Band™ 50 bp DNA Ladder DM1100), microtube (Biologix), qPCR tube (Biorad – 0.2 mL 8-tube PCR strips without caps, low profile, white – TLS0851), qPCR tube lid (BioRad – 0.2 mL flat PCR tube 8-cap strips optical, ultra-clear – JH95290002), micropipette tip (Biologix), and parafilm (Parafilm “M” Roll Size Four in x 125 ft – P7793 – 1EA).

Methods

Primer sequences for all targeted genes were searched in related published articles throughout Google Scholar Search Engine and articles citing the curated mRNA database accession numbers in National Center for Biotechnology Information (NCBI) database. This was accessed

through NM_031004.2 for *ACTA2* mRNA sequence, NM_138850.1 for *FAP* mRNA sequence, NM_012583.2 for *HPRT1* mRNA sequence, NM_031524.1 for *PDGFB* mRNA sequence, NM_013005.2 for *PIK3R1* mRNA sequence, and NM_012889.2 for *VCAM1* mRNA sequence. The decision of unsuitable primer was based on Primer3 analysis, particularly on melting temperature outside the favourable melting temperature range by the manufacturer, which was 60-65°C. The suitable primer sets went through further procedures for *in silico* analysis. Primer pairs from published articles with unsuitable results were decided to be designed based on the database. The analyzed primers were then synthesized and underwent laboratory experimental validation.

In silico design and analysis

A. Primer3

Primer design was done using Primer3 as suggested by the Bioline SYBR qPCR kit. This bioinformatics tool was accessed through <http://frodo.wi.mit.edu/primer3/>. Primer set sequences from published articles were submitted for analysis. The FASTA sequences of the stated accession numbers were used as the primer design template. The product size range used was 80-200 bp as suggested. Primer T_m preferences were set in accordance with the qPCR kit's recommendations. The minimum primer T_m was set to 60.0°C. The optimal primer T_m was set to 62.5°C as the median point. The maximum primer T_m was set to 65.0°C. The maximum primer T_m difference was set to 1°C.

B. Primer Blast

Primer specificity was analyzed using PrimerBLAST (Ye et al. 2012). This bioinformatics tool was accessed through <https://www.ncbi.nlm.nih.gov/tools/primer-blast/>. The designed primer set sequences in the 5'-3' direction were submitted. The organism's name was specified for the targeted organism sample. Other parameters were left unedited because the primer set sequences were already determined as this approach was used for analyzing gene specificity. The primer set was determined as gene-specific when the primer set was only specific to the desired gene.

C. Primer Dimer

The possibility of primer dimer formation was analyzed by using Primer Dimer by Primer Suite. Primer Dimer's website was accessed at <http://www.primer-dimer.com/>. The forward and reverse primer sequences were submitted in FASTA format. Paired analysis was used for dimer possibility formation screening between forward and reverse primers. Result output option of 'Dimer Structure Report' was chosen for the predicted most stable dimer formation.

D. Primer Hairpin

The possibility of primer hairpin formation was analyzed by using OligoCalc through <http://biotools.nubic.northwestern.edu/OligoCalc.html>. Primer set sequences were submitted separately. The separate input was done due to the hairpin formation being a self-complementary formation, thus the analyses were done separately.

E. Nucleotide Blast

Primer specificity validation was done by using BlastNucleotide through https://blast.ncbi.nlm.nih.gov/Blast.cgi?PROGRAM=blastn&PAGE_TYPE=BlastSearch&LINK_LOC=blasthome. Forward and reverse pri-

mer sequences were submitted separately. The reverse primer sequence underwent 'Reverse-Complement' formatting through https://www.bioinformatics.org/sms/rev_comp.html before submission. The sample organism was then used to filter the result for organism specificity.

F. Clustal Omega

Primer product length validation was done by using 'Clustal Omega'. This alignment tool was accessed through <https://www.ebi.ac.uk/Tools/msa/clustalo/>. The 'DNA' option was chosen as the sequence type. Fasta sequences of the primer set and similar sequences from Blast Nucleotide were submitted. The primer set sequences were validated to be conserved with the reference target sequences. The number of nucleotides covered from forward primer to reverse primer was counted and validated to the expected amplicon length.

In-lab validation

A. Primer annealing temperature optimization

Primer annealing temperature optimization was done by using CFX96 Touch Real-Time PCR System. The reaction consisted of 5 µL SYBR Green reagents, 3.2 µL nuclease-free water, 0.4 µL 10 µM forward primer, 0.4 µL 10 µM reverse primer, 1 µL cDNA (25 ng of the corresponding RNA) of *Rattus norvegicus*, Sprague Dawley Strain. The reaction was carried out as stated in the manufacture's protocol. Gradient temperatures used for annealing temperature optimization were 61.0; 61.8; 62.6; 63.6; and 64.8°C, each with two replicate reactions. These two replications for each temperature aimed for result reproducibility.

B. Electrophoresis

Electrophoresis was needed to be done for amplicon length validation as bioinformatically estimated. The 2% electrophoresis gel was prepared with 1x TBE as solvent and running buffer. DNA ladder (5 µL) was loaded into the gel well. The 5 µL amplified samples with 1 µL loading dye were loaded into the gel well. The electrophoresis process was done by using 110 V for 25 minutes. The gel was then visualized using a UV transilluminator.

RESULTS AND DISCUSSION

Results

ACTA2 Primer

The analyzed primers from published articles were considered unsuitable for favourable temperature ranges. Primer design targeted for *ACTA2* using NM_031004.2 sequence resulting in various primer sets. One set of the resulting primers were 5'-GCCATCATGCGTCTGGACTT-3' for forward primer and 5'-CTCACGCTCAGCAGTAGTCACG-3' for reverse primer. The calculated melting temperature was 63.53°C for forward primer and 63.57°C for reverse primer. The melting temperature difference was 0.04°C. The GC contents of the primer set were 55% for forward primer and 59.09% for reverse primer. The gene specificity analysis resulted in specific targeting of *ACTA2* mRNA of *Rattus norvegicus* mRNA database (Figure 1a). It showed no possibility of an unintended priming site on the other genes in the targeted animal sample. The specific *ACTA2* primer pair was further analyzed for primer dimer. The analysis showed a possibility of primer dimer formation at the end of reverse with two hydrogen bonds (Figure 1b). The subsequent analysis processes were still carried on considering overall results that needed to

be determined. Primer hairpin possibilities analysis showed that both forward and reverse primers had no possibilities for primer hairpin formation. The primer set has two identical sequences for both primer sequences which were NM_031004.2 for the *Rattus norvegicus* curated *ACTA2* mRNA sequence and BC158550.1 for *Rattus norvegicus* *ACTA2* cDNA clone. The sequence alignment showed that the forward primer and reverse primer confine amplification to produce 102 bp amplicon which conformed to primer design information.

Products on target templates				
>NM_031004.2 Rattus norvegicus actin alpha 2, smooth muscle (Acta2), mRNA				
product length = 102				
Forward primer	1	GCCATCATGCGTCTGGACTT	20	
Template	583	602	
Reverse primer	1	CTCACGCTCAGCAGTAGTCACG	22	
Template	684	663	

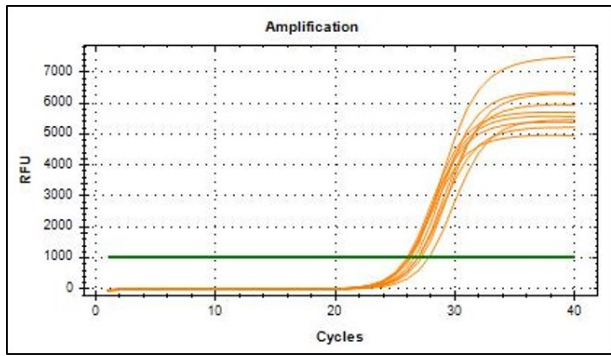
(a) Analysis for *ACTA2* Primer Set Specificity

>>>	- - - - -	<<<
	Reverse vs Reverse: -5.06 kcal/mol	
	- - - - -	
	5'> CTCACGCTCAGCAGTAGTCACG >3'	
	3'< GCACTGATGACGACTCGCACTC <5'	
>>>	- - - - -	<<<

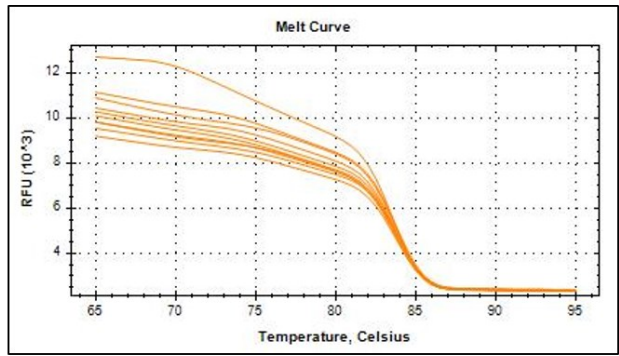
(b) Analysis for Potential *ACTA2* Primer Dimer Formation

Figure 1. Bioinformatic Primer Analysis Results for *ACTA2* Primer. (a) Analysis result from Primer-Blast (<https://www.ncbi.nlm.nih.gov/tools/primer-blast/>) showed primer specificity to *ACTA2* mRNA. (b) Analysis result from PrimerDimer (<http://www.primer-dimer.com/>) showed low indication of Primer Dimer Formation with two hydrogen bonds.

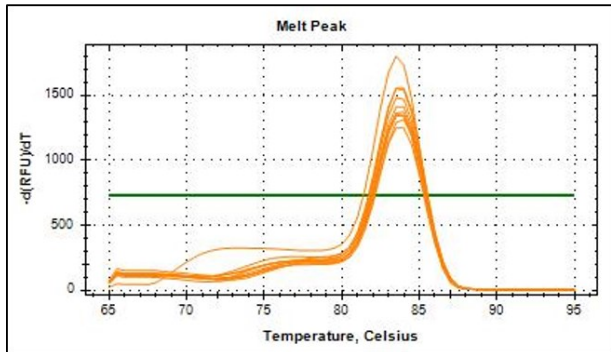
The designed and bioinformatically analyzed primer set was further analyzed for its reliability using qPCR, electrophoresis, and NTC analysis. In general, the amplification chart showed that this primer could prime amplification (Figure 2a). The qPCR amplification result was followed by the qPCR melt curve and melt peak results. It showed that *ACTA2* primer amplification resulted in one specific dissociation (Figure 2b) and melt peak (Figure 2c) indicating specific priming for all annealing temperatures used. The temperature which produced the lowest Ct value indicated the most compatible temperature for *ACTA2* primer to anneal by having the appropriate condition to anneal resulting in higher amplicon products. The optimal annealing temperature for *ACTA2* primer was considered as 61°C due to the lowest Ct value produced (Figure 2g). The qPCR products of *ACTA2* primer with the annealing temperature of 61°C were then used for electrophoresis-based product length validation. The visualized amplicon length corresponded to the DNA ladder of 100 bp (Figure 2h). It validated the bioinformatic analysis of the primer resulting in a 100 bp amplicon. The NTC reaction was run for *ACTA2* primer and the amplification chart (Figure 2d), melt curve (Figure 2e), and melt peak (Figure 2f) showed that there was no possibility of amplification of primer dimer. These overall results suggested that this primer set can be used for subsequent gene expression analysis.



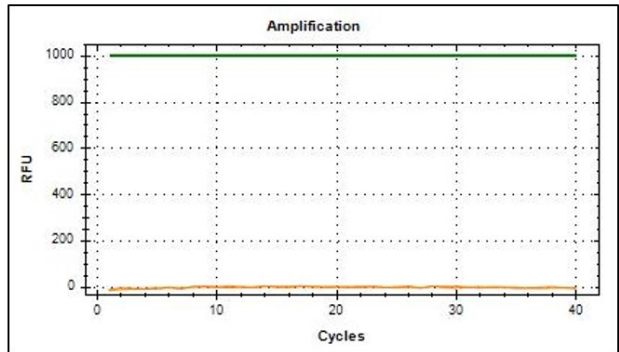
(a) Amplification Plot of ACTA2 Primer Annealing Temperature Optimization



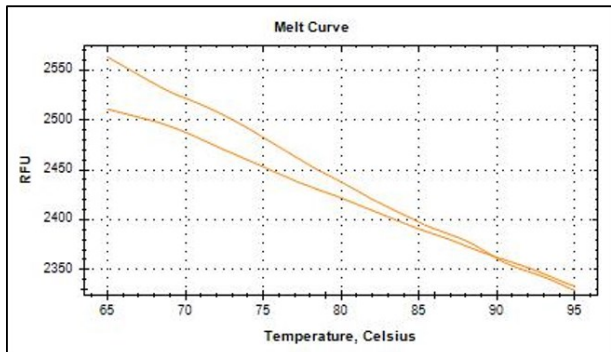
(b) Melt Curve of ACTA2 Primer Annealing Temperature Optimization



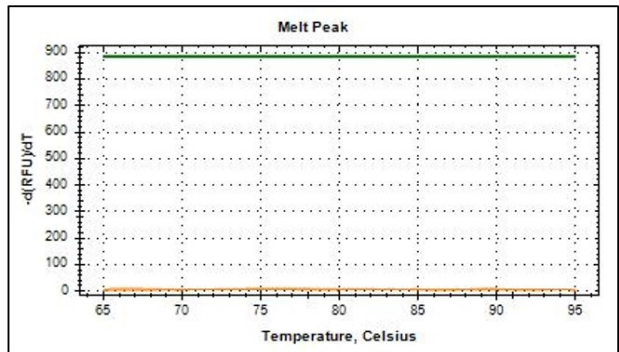
(c) Melt Peak of ACTA2 Primer Annealing Temperature Optimization



(d) Amplification Plot of ACTA2 Primer NTC



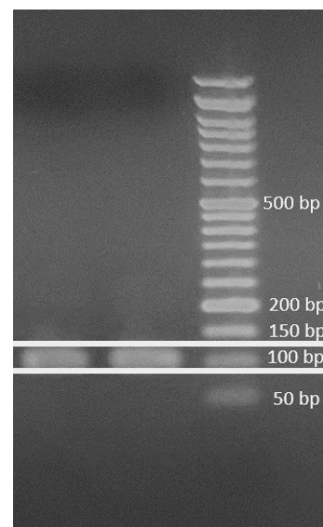
(e) Melt Curve of ACTA2 Primer NTC



(f) Melt Peak of ACTA2 Primer NTC

<i>ACTA2</i>				
Temperature (°C)	Ct1	Ct2	Ct Average	Ct Difference
64.8	27.22	27.85	27.535	0.63
63.6	26.95	27.02	26.985	0.07
62.6	26.33	26.63	26.48	0.3
61.8	26.21	26.18	26.195	0.03
61	26.05	26.16	26.105	0.11

(g) Ct Value of ACTA2 Primer Annealing Temperature Optimization



(h) Electrophoresis Validation on Product Length of ACTA2 Primer

Figure 2. Experiment Validation using qPCR and Electrophoresis for *ACTA2* Primer. Results from qPCR run showed (a) successful amplification process, (b) specific dissociation of amplicons, (c) specific melt peak of amplicons, with no primer-dimer evident based on (d) no amplification, (e) no dissociation and (f) no melt peak from NTC reaction, (g) temperature gradient qPCR run showed the optimum annealing temperature with lowest Ct detected, (h) electrophoresis run showed specific amplicon with targeted length.

FAP Primer

Primer for *FAP* was screened throughout the published articles and then analyzed. The primer pair selections did not fit the bioinformatic criteria. Thus, qPCR primer for *FAP* was decided to be designed and screened for matching criteria. The suitable resulted in primer pair was 5'-TGTTTCATCCCTAGCCCTTGC-3' for forward primer and 5'-TGTTGGGAGGCCCATGAAT-3' for reverse primer. The calculated melting temperatures were 63.56°C for forward primer and 63.59°C for a reverse primer with the melting temperature difference of 0.03°C. The GC content for each primer was 52.38% for forward primer and 52.63% for reverse primer. The primer pair produced a 124 bp amplicon based on bioinformatic analysis on NM_138850.1. The accession number of NM_138850.1 is the accession number of *Rattus norvegicus* fibroblast activation protein alpha (*FAP*) mRNA. The primer pair was analyzed as specific to the target gene (Figure 3a). The primer pair was analyzed for primer dimer possibility. There was a possibility of primer dimer formation in two forward primer sequences with two hydrogen bonds at the end of the sequences (Figure 3b). Throughout the primer selections, both from reference articles and designed primers, this primer pair had the least possible primer dimer formation with no hairpin formation possibility. The primer pair was analyzed manually through nucleotide alignment and showed the product length was 124 bp corresponding to Primer3 and Primer Blast results.

```

Products on target templates
>XM_039104226.1 PREDICTED: Rattus norvegicus fibroblast activation protein, alpha (Fap), transcript variant X2, mRNA

product length = 124
Forward primer 1   TGTTTCATCCCTAGCCCTTGC 21
Template        2036 ..... 2056

Reverse primer 1   TGTTGGGAGGCCCATGAAT 19
Template        2159 ..... 2141

>XM_039104225.1 PREDICTED: Rattus norvegicus fibroblast activation protein, alpha (Fap), transcript variant X1, mRNA

product length = 124
Forward primer 1   TGTTTCATCCCTAGCCCTTGC 21
Template        2036 ..... 2056

Reverse primer 1   TGTTGGGAGGCCCATGAAT 19
Template        2159 ..... 2141

>NM_138850.1 Rattus norvegicus fibroblast activation protein, alpha (Fap), mRNA

product length = 124
Forward primer 1   TGTTTCATCCCTAGCCCTTGC 21
Template        1891 ..... 1911

Reverse primer 1   TGTTGGGAGGCCCATGAAT 19
Template        2014 ..... 1996
    
```

(a) Analysis for *FAP* Primer Set Specificity

```

>>> - - - - - <<<
      Forward vs Forward: -3.86 kcal/mol
      - - - - -
      5'> TGTTTCATCCCTAGCCCTTGC >3'
           ||
           3'< CGTTCCCGATCCCTACTTTGT <5'
>>> - - - - - <<<
    
```

(b) Analysis for Potential *FAP* Primer Dimer Formation

Figure 3. Bioinformatic Primer Analysis Results for *FAP* Primer. (a) Analysis result from Primer-Blast (<https://www.ncbi.nlm.nih.gov/tools/primer-blast/>)

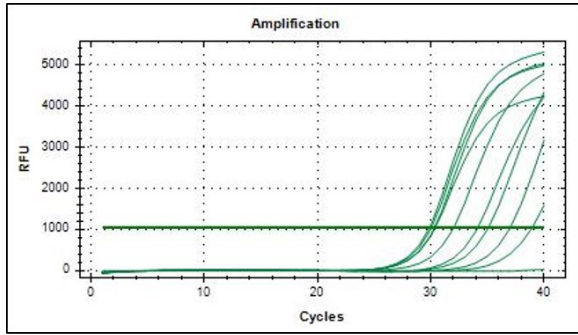
showed primer specificity to *FAP* mRNA. (b) Analysis result from PrimerDimer (<http://www.primer-dimer.com/>) showed low indication of Primer Dimer Formation with two hydrogen bonds.

The selected primer pair was then tested for amplification priming ability with qPCR machine with annealing temperature optimization. The amplification chart showed that the primer pair could amplify the cDNA template (Figure 4a). The primed amplification with various annealing temperatures showed a slight difference in amplicon dissociation seen in the melt curve chart (Figure 4b) across annealing temperatures. The melt peak chart showed that the annealing temperature conditions of 61.0 and 61.8°C resulted in two possible amplicons. The otherwise happened to amplify with the annealing temperature condition of 62.6; 63.6; and 64.8°C. The three annealing temperature conditions resulted in one possible amplicon (Figure 4c). The lowest C_q value resulted from 61.0°C (Figure 4g) which might result in the optimal priming condition being refused to be one of the primer option considerations. It is because this annealing temperature has the possibility of facilitating the amplification for two amplicons rather than one specific amplicon. This can be seen by the two melt peaks in the melt peak curve. The possible annealing temperature for this primer pair was 63.6°C with the highest precision for annealing temperature producing one possible amplicon. The amplicon with one melt peak from annealing temperature of 63.6°C resulted in one electrophoresis visualization band in between 100 and 150 bp marker bands referring to a specific amplicon length of 124 bp (Figure 4h). The primer dimer validation was done by running the NTC reaction with this primer. The amplification (Figure 4d), melt curve (Figure 4e), and melt peak (Figure 4f) charts showed that there was no possibility of primer-dimer and hairpin formation based on NTC reaction.

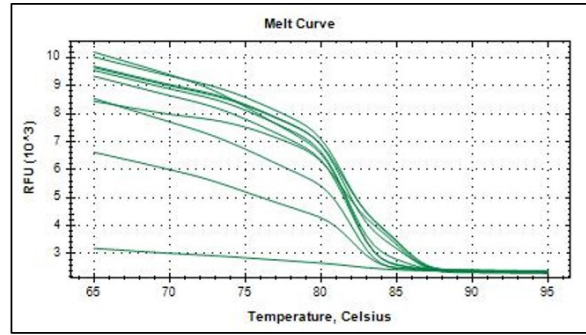
HPRT1 Primer

The primer pair of *HPRT1* from (Landry et al. 2019) matched the NM_013005.2 sequence. The sequence of this primer was 5'-CTCATGGACTGATTATGGACAGGAC-3' for forward primer and 5'-GCAGGTCAGCAAAGAACTTATAGCC-3' for reverse primer. The melting temperature for this primer pair was 63.12°C for forward primer and 63.63°C for a reverse primer with a 0.51°C difference. The GC contents for this primer set were 48% for both forward and reverse primer. This primer was specific for *Rattus norvegicus*. *HPRT1* mRNA produces 123 bp amplicon (Figure 5a). Primer dimer formation analysis resulted in two hydrogen bonds formation possibilities on the reverse primers (Figure 5b). Hairpin formation analysis revealed that both forward and reverse primer could not form a hairpin structure. The screening in the *Rattus norvegicus* gene database revealed that both submitted sequence of the primer set was identical to NM_013005.2 and several similar sequences. The sequences were simultaneously aligned which validates the priming site of primers. The result revealed that the primer set confined the targeted amplification to produce a 123 bp amplicon.

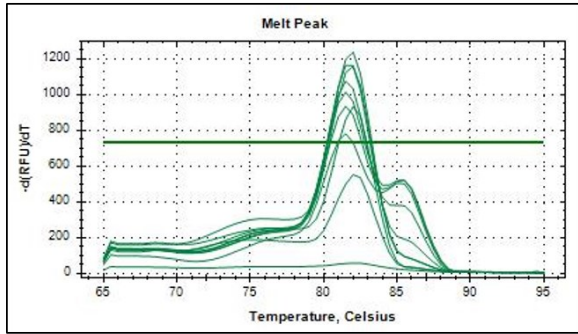
The resulting amplification data showed that the designed primer set was able to prime amplification on every annealing temperature used (Figure 6a). The overall amplification using this primer set can be said to be specific based on the specific melt curve (Figure 6b) and melt peak (Figure 6c) obtained. The lowest Ct value of two qPCR technical replicate reactions and average Ct value was produced by amplification with the annealing temperature of 62.6°C (Figure 6g). The amplification results using 62.6°C annealing temperature was used for electrophoresis. The amplicon visualization band resided between 100 and 150 bp (Figure



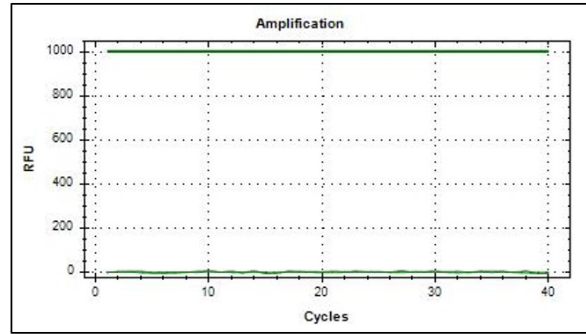
(a) Amplification Plot of *FAP* Primer Annealing Temperature Optimization



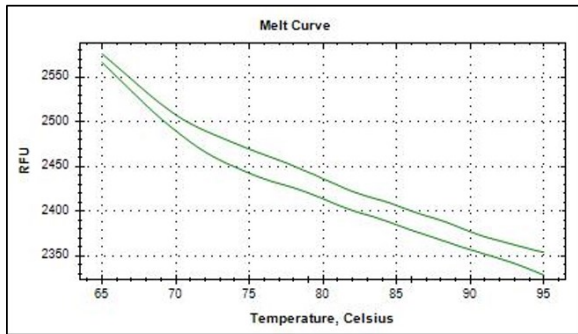
(b) Melt Curve of *FAP* Primer Annealing Temperature Optimization



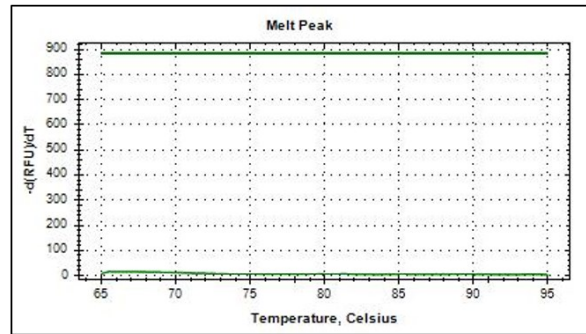
(c) Melt Peak of *FAP* Primer Annealing Temperature Optimization



(d) Amplification Plot of *FAP* Primer NTC



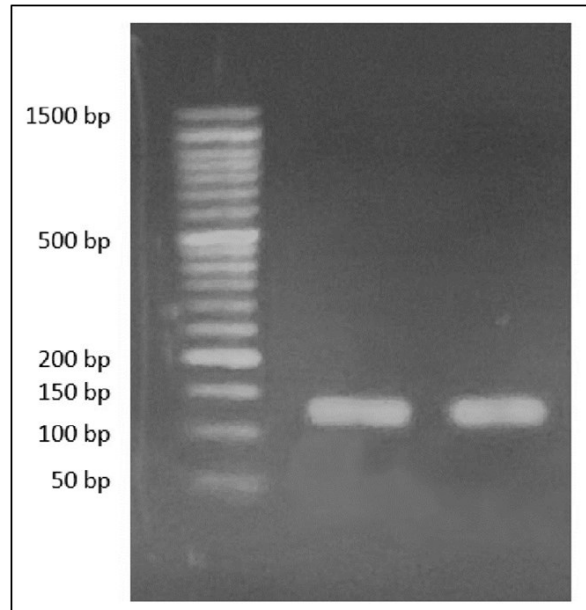
(e) Melt Curve of *FAP* Primer NTC



(f) Melt Peak of *FAP* Primer NTC

Temperature (°C)	<i>FAP</i>			
	Ct1	Ct2	Ct Average	Ct Difference
64.8	37.02			
63.6	34.14	32.04	33.09	2.1
62.6	38.94	35.08	37.01	3.86
61.8	30.31	30.37	30.34	0.06
61	29.89	30.05	29.97	0.16

(g) Ct Value of *FAP* Primer Annealing Temperature Optimization



(h) Electrophoresis Validation on Product Length of *FAP* Primer

Figure 4. Experiment Validation using qPCR and Electrophoresis for *FAP* Primer. Results from qPCR run showed (a) successful amplification process, (b) specific dissociation of amplicons, (c) specific melt peak of amplicons, with no primer-dimer evident based on (d) no amplification, (e) no dissociation and (f) no melt peak from NTC reaction, (g) temperature gradient qPCR run showed the optimum annealing temperature with lowest Ct detected, (h) electrophoresis run showed specific amplicon with targeted length.

6h). This implied that the amplicon length corresponds to the designed primer product length of 123 bp. The NTC analysis showed that there was no possibility of primer-dimer and hairpin formation based on amplification (Figure 6d), melt curve (Figure 6e), and melt peak (Figure 6f) charts.

```

Products on target templates
>XM_039099447.1 PREDICTED: Rattus norvegicus hypoxanthine phosphoribosyltransferase 1 (Hprt1), transcript variant X1, mRNA

product length = 123
Forward primer 1 CTCATGGACTGATTATGGACAGGAC 25
Template 313 ..... 337

Reverse primer 1 GCAGGTCAGCAAAGAACTTATAGCC 25
Template 435 ..... 411

>NM_012583.2 Rattus norvegicus hypoxanthine phosphoribosyltransferase 1 (Hprt1), mRNA

product length = 123
Forward primer 1 CTCATGGACTGATTATGGACAGGAC 25
Template 179 ..... 203

Reverse primer 1 GCAGGTCAGCAAAGAACTTATAGCC 25
Template 301 ..... 277
    
```

(a) Analysis for *HPRT1* Primer Set Specificity

```

>>> - - - - - <<<
      Forward vs Reverse: 0.46 kcal/mol
      - - - - -
      5'> CTCATGGACTGATTATGGACAGGAC >3'
              ||
              3'< CCGATATTCAAGAAACGACTGGACG <5'
>>> - - - - - <<<
    
```

(b) Analysis for Potential *HPRT1* Primer Dimer Formation

Figure 5. Bioinformatic Primer Analysis Results for *HPRT1* Primer. (a) Analysis result from Primer-Blast (<https://www.ncbi.nlm.nih.gov/tools/primer-blast/>) showed primer specificity to *HPRT1* mRNA. (b) Analysis result from PrimerDimer (<http://www.primer-dimer.com/>) showed low indication of Primer Dimer Formation with two hydrogen bonds.

***PDGFB* Primer**

The suitable *PDGFB* primer was from Lee et al. (2016) with 5'- ACCAC-TCCATCCGCTCCTTT-3' for forward primer and 5'- TGTGCTCGGGTCATGTTCAA-3' for reverse primer. The calculated melting temperature was 63.22°C for forward primer and 63.69°C for a reverse primer with a 0.47°C difference. The GC contents for both primers were 55 and 50% respectively. The primer pair can be said to be specific with no unintended possible amplicon (Figure 7a). The primer pair was possibly two hydrogen bonds at the 3' end of forward and reverse primer (Figure 7b). The hairpin formation possibility for both forward and reverse primer was none. The primer pair alignment with similar sequences from Nucleotide Blast resulted in 100 bp amplicon.

The amplification chart (Figure 8a) showed that the primer pair could prime the amplification of the cDNA template resulting in specific dissociation (Figure 8b) and one peak of melt peak chart (Figure 8c). The Ct values indicated that the optimal annealing temperature was 62.6°C (Figure 8g). The specific targeting of primer was validated with one visualization in electrophoresis, parallel to 100 bp marker band (Figure 8h). The NTC results from the amplification plot (Figure 8d), melt curve (Figure 8e), and melt peak (Figure 8f) charts showed that there was no possibility of primer-dimer and hairpin formation.

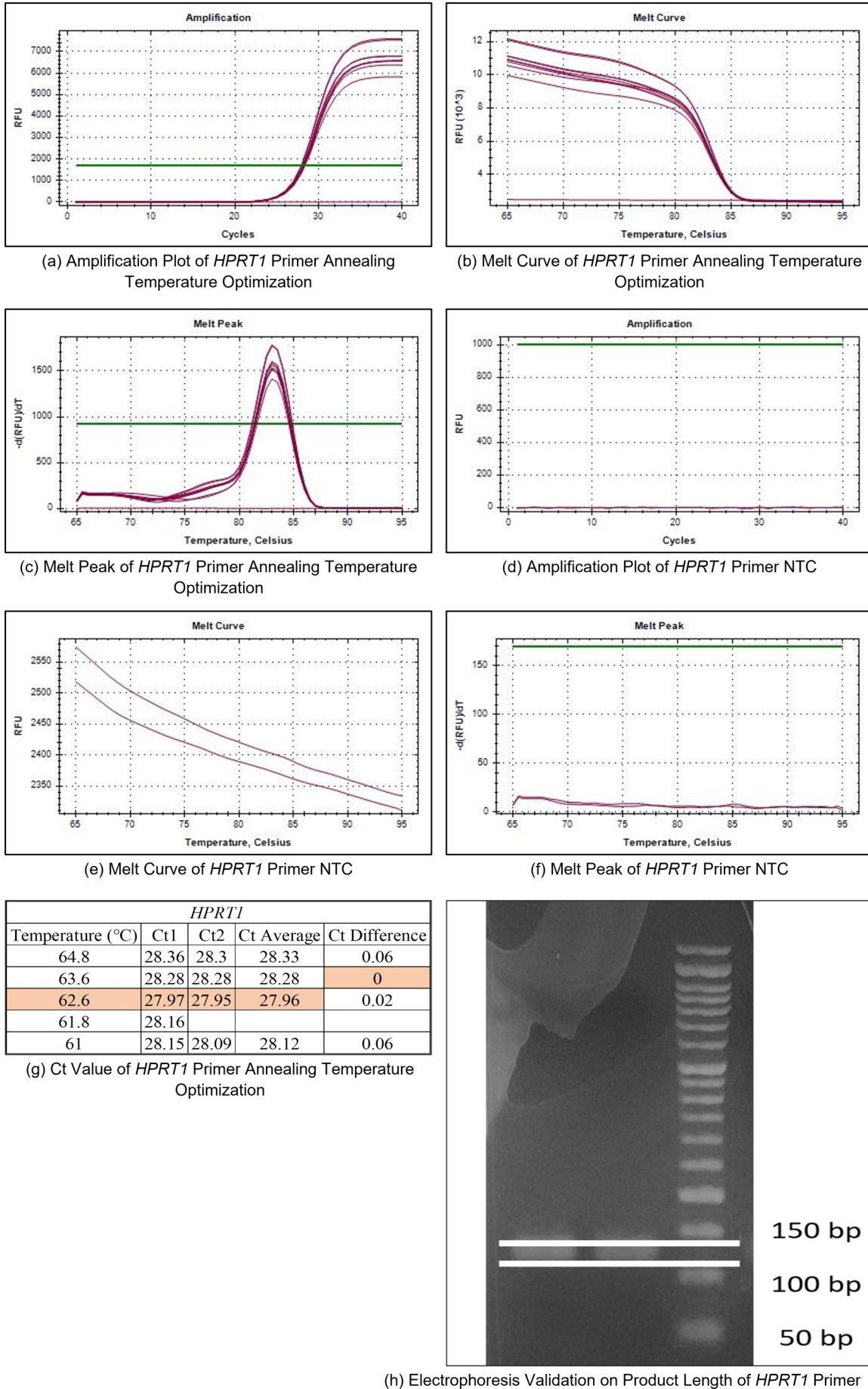


Figure 6. Experiment Validation using qPCR and Electrophoresis for *HPRT1* Primer. Results from qPCR run showed (a) successful amplification process, (b) specific dissociation of amplicons, (c) specific melt peak of amplicons, with no primer-dimer evident based on (d) no amplification, (e) no dissociation and (f) no melt peak from NTC reaction, (g) temperature gradient qPCR run showed the optimum annealing temperature with lowest Ct detected, (h) electrophoresis run showed specific amplicon with targeted length.

```

Products on target templates
>XM_039078420.1 PREDICTED: Rattus norvegicus platelet derived growth factor subunit B (Pdgfb), transcript variant X1, mRNA

product length = 96
Forward primer 1  ACCACTCCATCCGCTCCTTT  20
Template       41  ..... 60

Reverse primer 1  TGTGCTCGGGTCATGTTCAA  20
Template       136 ..... 117

>NM_031524.1 Rattus norvegicus platelet derived growth factor subunit B (Pdgfb), mRNA

product length = 100
Forward primer 1  ACCACTCCATCCGCTCCTTT  20
Template       499 ..... 518

Reverse primer 1  TGTGCTCGGGTCATGTTCAA  20
Template       598 ..... 579
    
```

(a) Analysis for *PDGFB* Primer Set Specificity

```

>>> - - - - - <<<
      Forward vs Reverse: 1.89 kcal/mol
      - - - - -
      5'> ACCACTCCATCCGCTCCTTT >3'
           ||
           3'< AACTTGTACTGGGCTCGTGT <5'
>>> - - - - - <<<
    
```

(b) Analysis for Potential *PDGFB* Primer Dimer Formation

Figure 7. Bioinformatic Primer Analysis Results for *PDGFB* Primer. (a) Analysis results from Primer-Blast (<https://www.ncbi.nlm.nih.gov/tools/primer-blast/>) showed primer specificity to *PDGFB* mRNA. (b) Analysis result from PrimerDimer (<http://www.primer-dimer.com/>) showed low indication of Primer Dimer Formation with two hydrogen bonds.

PIK3R1 Primer

A suitable *PIK3R1* primer was found in an article from Cai et al. (2019). The primer sequences were 5'-CGAAAACACAGAAGACCAATACTCA-3' for forward primer and 5'-TCCCTCGCAATAGGTTCTCG-3' for reverse primer. The calculated melting temperatures were 61.71°C for forward primer and 62.54°C for a reverse primer with a 0.83°C difference. The GC contents were 40% for forward primer and 55% for reverse primer. The Primer Blast result showed that this primer pair was specific to its target gene (Figure 9a). The possibility of primer dimer formation could occur on the 3' end of reverse primers with two hydrogen bonds (Figure 9b). The hairpin formation possibility was not possible for each primer. The alignment of the primer pair with a similar sequence showed that the primer produces 122 bp amplicon.

The amplification chart showed that the primer pair was able to prime the qPCR amplification (Figure 10a) with one possible specific amplicon due to one specific dissociation (Figure 10b) and one melt peak (Figure 10c) produced. The optimal temperature was 62.6°C as the lowest Ct value was from 62.6°C annealing temperature (Figure 10g). The electrophoresis result showed that the amplicon was in between the 100 and 150 bp suggesting that the amplicon has the targeted amplicon length of 122 bp (Figure 10h). The NTC analysis showed that there was no possibility of primer-dimer and hairpin formation based on amplification plot (Figure 10d), melt curve (Figure 10e), and melt peak (Figure 10f) charts.

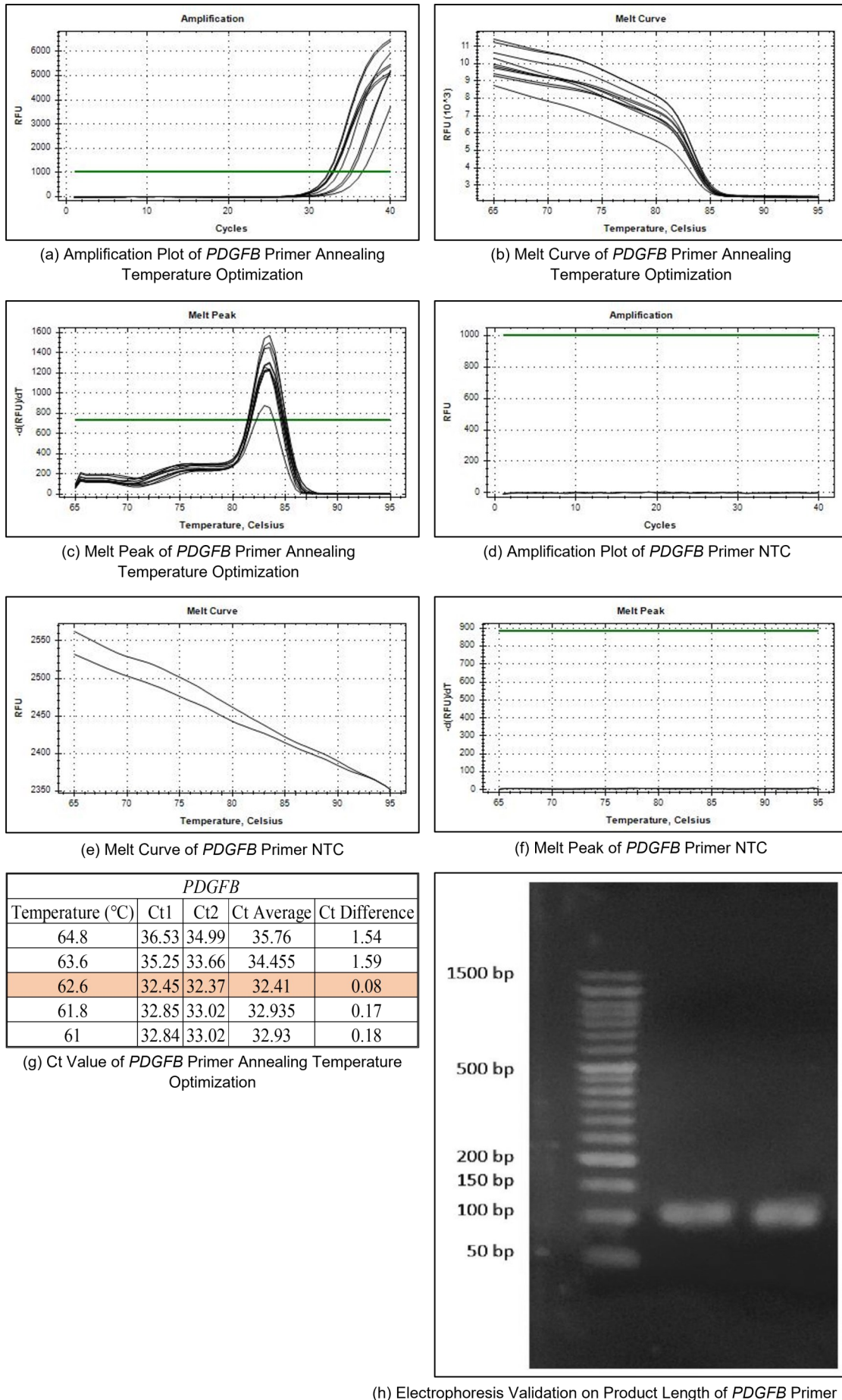


Figure 8. Experiment Validation using qPCR and Electrophoresis for *PDGFB* Primer. Results from qPCR run showed (a) successful amplification process, (b) specific dissociation of amplicons, (c) specific melt peak of amplicons, with no primer-dimer evident based on (d) no amplification, (e) no dissociation and (f) no melt peak from NTC reaction, (g) temperature gradient qPCR run showed the optimum annealing temperature with lowest Ct detected, (h) electrophoresis run showed specific amplicon with targeted length.

```

Products on target templates
>NM_013005.2 Rattus norvegicus phosphoinositide-3-kinase regulatory subunit 1 (Pik3r1), mRNA

product length = 122
Forward primer 1  CGAAAAACACAGAAGACCAATACTCA  25
Template        2373  ..... 2397

Reverse primer 1  TCCCTCGCAATAGGTTCTCG  20
Template        2494  ..... 2475

>XM_008760659.3 PREDICTED: Rattus norvegicus phosphoinositide-3-kinase regulatory subunit 1 (Pik3r1), transcript variant X3, mRNA

product length = 122
Forward primer 1  CGAAAAACACAGAAGACCAATACTCA  25
Template        2819  ..... 2843

Reverse primer 1  TCCCTCGCAATAGGTTCTCG  20
Template        2940  ..... 2921

>XM_006231868.4 PREDICTED: Rattus norvegicus phosphoinositide-3-kinase regulatory subunit 1 (Pik3r1), transcript variant X2, mRNA

product length = 122
Forward primer 1  CGAAAAACACAGAAGACCAATACTCA  25
Template        1927  ..... 1951

Reverse primer 1  TCCCTCGCAATAGGTTCTCG  20
Template        2048  ..... 2029
    
```

(a) Analysis for *PIK3R1* Primer Set Specificity

```

>>> - - - - - <<<
      Reverse vs Reverse: -3.64 kcal/mol
- - - - -
5'> TCCCTCGCAATAGGTTCTCG >3'
      ||
      3'< GCTCTGGATAACGCTCCCT <5'
>>> - - - - - <<<
    
```

(b) Analysis for Potential *PIK3R1* Primer Dimer Formation

Figure 9. Bioinformatic Primer Analysis Results for *PIK3R1* Primer (a) Analysis result from Primer-Blast (<https://www.ncbi.nlm.nih.gov/tools/primer-blast/>) showed primer specificity to *PIK3r1* mRNA. (b) Analysis result from PrimerDimer (<http://www.primer-dimer.com/>) showed low indication of Primer Dimer Formation with two hydrogen bonds.

VCAM1 Primer

Fasta sequence of NM_012889.2 was used for the *VCAM1* primer design template. One set of the resulting primers was 5'-TTGGGGATTCCGTTGTTCTG-3' for forward primer and 5'-TGTAGCCCCTTCATCCCTCA-3' for reverse primer. The calculated melting temperatures were 63.10°C for forward primer and 62.86°C for a reverse primer with a 0.24°C difference. The GC contents were 50% for forward primer and 55% for reverse primer. It was then analyzed for gene specificity, resulting in specific targeted to desired *VCAM1* mRNA sequence. This primer set 116 bp amplicon without showing the possibility of unintended priming site on other genes in the same sample animal (Figure 11a). The primer dimer analysis showed a possibility of primer dimer at the end of primers with two hydrogen bonds (Figure 11b). The primer hairpin analysis showed that both forward and reverse primers had no possibilities for primer hairpin formation. The identical sequence was then aligned showing that the forward primer and reverse primer confine amplification to produce 116 bp amplicon.

The amplification chart showed that the primer pair could amplify the cDNA samples (Figure 12a). The melt curve chart showed one specific dissociation (Figure 12b) and the melting peak showed one peak (Figure 12c) indicating one amplicon being amplified. The lowest average Ct value was using 61°C but with 0.88°C difference being the highest. The annealing temperature resulted in the slightly higher Cq and the

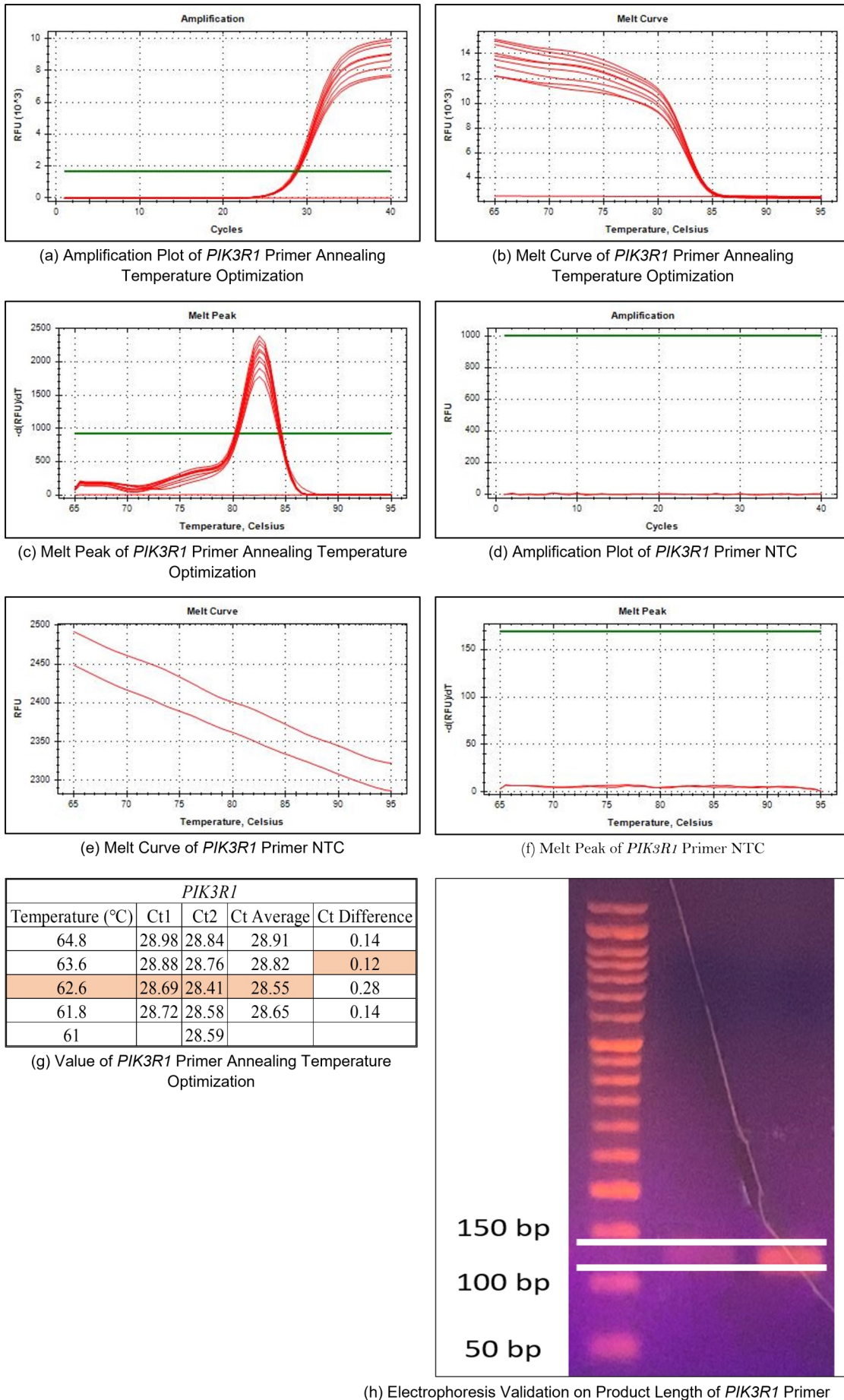


Figure 10. Experiment Validation using qPCR and Electrophoresis for *PIK3R1* Primer. Results from qPCR run showed (a) successful amplification process, (b) specific dissociation of amplicons, (c) specific melt peak of amplicons, with no primer-dimer evident based on (d) no amplification, (e) no dissociation and (f) no melt peak from NTC reaction, (g) temperature gradient qPCR run showed the optimum annealing temperature with lowest Ct detected, (h) electrophoresis run showed specific amplicon with targeted length.

lower difference was 61.8°C (Figure 12g). Based on melt peak and electrophoresis, the analysis showed one band between 100 and 150 bp corresponding to predicted amplicon length (Figure 12h). The NTC results showed that there was no indication of primer-dimer and hairpin formation based on amplification plot (Figure 12d), melt curve (Figure 12e), and melt peak (Figure 12f) charts.

```

Products on target templates
>NM_012889.2 Rattus norvegicus vascular cell adhesion molecule 1 (Vcam1), mRNA

product length = 116
Forward primer  1      TTGGGGATTCCGTTGTTCTG  20
Template        1037  ..... 1056

Reverse primer  1      TGAGCCCTTCATCCCTCA  20
Template        1152  ..... 1133
    
```

(a) Analysis for VCAM1 Primer Set Specificity

```

>>> ----- <<<
      forward vs reverse: -2.29 kcal/mol
-----
      5'> TTGGGGATTCCGTTGTTCTG >3'
              ||
              3'< ACTCCCTACTTCCCCGATGT <5'
>>> ----- <<<
    
```

(b) Analysis for Potential VCAM1 Primer Dimer Formation

Figure 11. Bioinformatic Primer Analysis Results for VCAM1 Primer. (a) Analysis result from Primer-Blast showed primer specificity to VCAM1 mRNA (<https://www.ncbi.nlm.nih.gov/tools/primer-blast/>). (b) Analysis result from PrimerDimer (<http://www.primer-dimer.com/>) showed low indication of Primer Dimer Formation with two hydrogen bonds.

Discussion

Here we reported the qPCR primer sequence and validation approach for *ACTA2*, *FAP*, *HPRT1*, *PDGFB*, *PIK3R1*, and *VCAM1* for the reagent condition of SYBR Green I and 3 mM MgCl₂. This study provided evidence of bioinformatic analytical approach, experimental validation, and tested qPCR primer set for published primer pairs (*HPRT1*, *PDGFB*, and *PIK3R1*) and newly designed genes (*ACTA2*, *FAP*, and *VCAM1*). SYBR Green I can be reliably used in relative quantitative if primers are properly constructed (Ferreira et al. 2006). MgCl₂ can affect the primer priming process. Thus, we made an *in-silico* attempt to predict suitable primer and laboratory work for validation. The bioinformatic analysis results suggested sequences with the highest possibility and suitability. The laboratory experimental validation results indicated that the analyzed primer quality in functioning and suitability with qPCR reagent and reaction condition is quite adequate.

The factors accounted for in this *in silico* analysis were: a) primer melting temperature; b) T_m difference between forward and reverse primer; c) primer GC content; d) primer specificity; e) Hairpin possibility; and f) Dimer formation possibility. Based on the reagent requirement, primer T_m was determined to be within the range of 60-65°C T_m. The comparison was made against the database. The least suitable primer pairs were eliminated (data is not shown). The value of melting temperature was used as the annealing temperature as stated by the manufacture protocol.

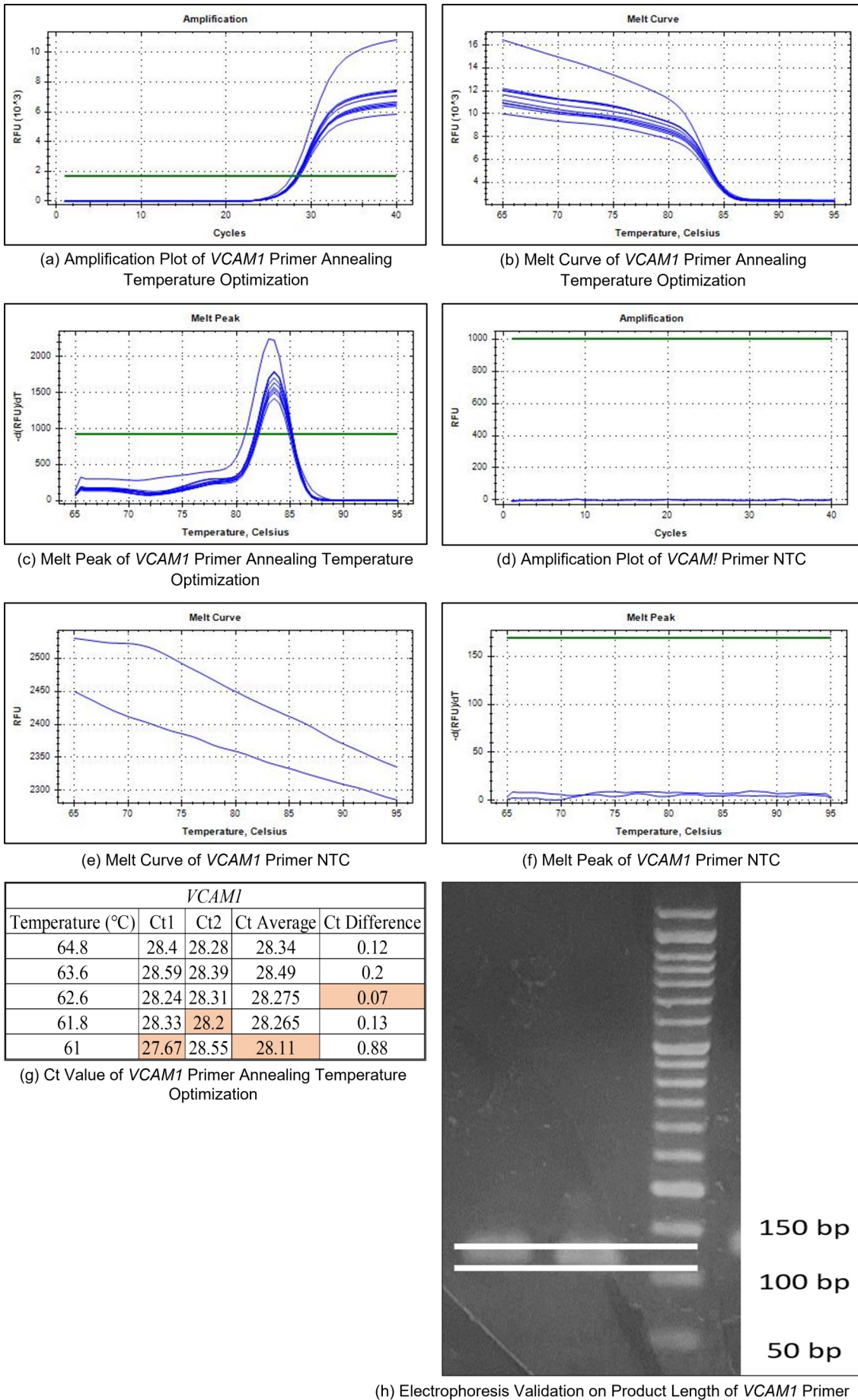


Figure 12. Experiment Validation using qPCR and Electrophoresis for *VCAM1* Primer. Results from qPCR run showed (a) successful amplification process, (b) specific dissociation of amplicons, (c) specific melt peak of amplicons, with no primer-dimer evident based on (d) no amplification, (e) no dissociation and (f) no melt peak from NTC reaction, (g) temperature gradient qPCR run showed the lower optimum annealing temperature, (h) electrophoresis run showed specific amplicon with targeted length.

The technical run of every qPCR reaction follows the manufacture protocol that specifies the temperature of cycling steps such as pre-denaturation, denaturation, and extension, except for annealing temperature. Primer melting temperature was determined within the range of 60–65°C based on reagent requirement. The melting temperature was used as annealing temperature as stated by the manufacturer. According to (Fittipaldi et al. 2010), a high annealing temperature is advantageous in facilitating the dye-binding specificity with DNA. This evades both reaction inhibition of PCR and the formation of primer dimer. As the consideration of using melting temperature as annealing temperature, optimal primer melting temperature was set to the median of the suggested annealing temperature range. This was based on the consideration of statistical normal distribution. The resulting analyzed melting temperature used as annealing temperature was between 61.71–63.69°C. These temperatures were in corresponded to GC content. Primer GC content was chosen to be 40–50% to ensure the strength of the annealing mechanism between primer and template. This is because the hydrogen bond between GC is more stable than AT (Ouldrige et al. 2013).

The melting temperature difference was chosen to have a maximum of 1°C difference in facilitating a parallel annealing starting point. This can maximize two amplicons to be produced by the end of each cycle as the annealing process occurs simultaneously. The small melting temperature difference in annealing temperature aims to avoid unintended primer annealing in each cycle (Hashish et al. 2021). The analyzed melting temperature differences ranged from 0.03 to 0.84°C.

Primer Blast was used to screen the specificity of pre-existing (both from published articles and newly designed) primers against the gene database. Primer specificity was selected to eliminate the possibility of quantifying the wrong amplicon target. Mispriming could occur due to homologous regions and random mismatches, resulting in amplification of non-intended targets (Ye et al. 2012). The specificity screening results showed no indication of mispriming at homologous regions and arbitrary mismatch. Thus, the primer sequences were expected to be specific to the genes of interest.

Primer dimer and hairpin formation possibility was used in selecting the least possible formation and eliminating the greater possible formation present. In all the above dimer formation possibility analysis attempts, the least dimer possibility was that two hydrogen bonds occurred at the 3' primer sequence. Thornton & Basu (2011) stated that primer dimer with 3' complementary matches more than two base pairs should be avoided. The primer pairs in this article have the least complementary possible formation of two bp. With numerous attempts to find the least possible dimer formation, all the primer sequences showed the least possible dimer formation corresponding to the previous statement. Hairpin formation can also affect amplification. This is due to their loop size and complementarity in the 3' end. The formation of loop and complementarity may elevate the possibility of self-complementary amplification. This can result in declining amplification efficiency (Singh et al. 2000). Each of the primer pair sets showed no indication of hairpin formation.

The alignment approach was done to address primer localization and ensuring the amplicon length. The alignment result confirmed the specificity of amplicon length and localization. The adequate possible primer localization site is on the conserved regions. This is due to the possibility of the high level of variation found in the sequence may elevate the degenerate site thus increasing the potential of primer-dimer (Brodin et al. 2013).

Laboratory experimental validation covered amplification chart,

melt curve chart, melt peak chart, C_q value of annealing temperature optimization, amplicon visualization band on electrophoresis, and NTC analysis. The amplification charts showed that primer could prime amplification. Melt curve and melt peak charts showed the specificity of the amplicon, with no detection of amplicon at a lower temperature. Electrophoresis validation results indicated that the amplicon was the targeting amplicon based on the amplicon visualization band. The NTC result showed no possibility of primer-dimer and hairpin formation which validates the melt curves with no peak at a lower temperature. The qPCR showed good specification due to one dissociation peak on the melt peak curve and one visualization band on electrophoresis. This indicates that using this sequence (and potentially any type of sequence) was suitable with the chemical reagent specifically SYBR Green I fluorophore and three mM of MgCl₂. In addition, to ensure qPCR primer before use in gene expression analysis, NTC reaction was tested to see the possible formation of hairpin and primer dimer. All data from each primer pair shows no indication of either hairpin or primer dimer formation.

The amplification chart showed the amplification curve based on exponential fluorescence emission. The results from all primer pair sets showed that the primers could proceed with the priming process, leading to the amplification of templates. Thus, the generated fluorescence emission in an exponential manner is the outcome of the exponential amplification of primer priming in the chain reaction (Goda et al. 2015).

The annealing temperature results varied in variable temperature points. This is due to various factors. Aside from the fact that annealing temperature is dependent on primer sequence (inherent properties), the annealing temperature must be in the range of the efficient temperature range of chemical reagent mode of work, including the suitability to SYBR Green I reagent with buffer including MgCl₂. The reagent used in this approach was Biorline SYBR Green I. Thus, it is an important approach to closely look at the annealing temperature required by the manufacture. Thornton & Basu (2011) explained that primer GC content has a control on the melting temperature of primer. The annealing temperature is usually 3 to 5°C above the melting temperature.

Aside from the GC-controlled annealing temperature of primer, the qPCR reaction may be affected by the mode of action of SYBR Green I. There is an optimal temperature for SYBR. Thornton & Basu (2011) specifically mentioned that optimal qPCR primer melting temperature using SYBR Green fluorophore was between 62 and 67°C, with an optimal melting temperature of 63°C. This is correlated with the bioinformatically analyzed primer melting temperature and the instruction of manufacture (Biorline). The optimal temperature for each primer pair set was determined based on the lowest C_q value obtained across the annealing temperature range (Gaby & Buckley 2017). The results showed that the *ACTA2* and *FAP* had the most suitable annealing temperature of 61°C. The primer pair sets of *HPRT1*, *PDGFB*, and *PIK3R1* had the most suitable annealing temperature of 62.6°C. Meanwhile, *VCAM1* primer pair set had the most considerable annealing temperature of 61.6°C. The validation of temperature covering annealing temperature of 61-65°C showed that optimal annealing temperatures were below the calculated melting temperature. The results suggest that the optimal annealing temperature is inconsistent with the inherent GC content factor in the primer. This is due to the evidence that the higher the GC content of the primers, the lower the annealing temperatures were and vice versa. The results showed that it is more likely that the higher melting temperature differences are coherent with the higher suitable validated annealing tem-

perature. Although this evaluation has not been explored further, the cause of this phenomenon remains unclear.

A melt curve was also run as suggested by (Thornton & Basu 2011) for the purpose of detecting secondary products for taking thoughtful conclusions. As stated by (Gregory et al. 2012), dissociation curves were used to analyze a single amplicon generated in each run by each primer pair. The increase in temperature leads to the denaturation of amplicon, resulting in single-stranded DNA. This occurrence gives rise to fluorophore dissociation, causing the fluorescence emission to plummet (Ahmed et al. 2017). The results showed one descending fluorescence in the melt curve of each amplification of each primer pair set. This excludes the *FAP* amplicon melt curve with the additional descending fluorescence in the lower annealing temperature.

The primer pairs indicated specificity based on the melt charts showing one peak. Based on a preliminary experiment by Ririe et al. (1997), melting peak count correlates with electrophoresis results. This is due to the dissociation of PCR products with the accounted factor of GC ratio, length, and sequence. Melt peak analysis delivers higher certainty referring to the fluorescence obtained during qPCR acquired from the targeted product (Ririe et al. 1997). The melt curve profile was then plotted in the negative derivative of fluorescence vs temperature. This represents the peak at which the dissociation event occurs (Vulchi et al. 2021). Corresponding to melt curve results, the melting peak from every single primer pair was one specific melt peak excluding the melting peak for the *FAP* primer pair set with additional lower annealing temperature melt peak.

Gel electrophoresis was done for amplicon identity validation. One band in electrophoresis indicates one type of amplicon. This is because the generation of one band is caused by the same amplicon length with the same molecular weight (Ririe et al. 1997). The results showed that the amplicon generated from each primer pair set of the most suitable annealing temperature has the corresponding product length as bioinformatic analysis. It suggests that the amplicon is specific and the primer pair sets were able to prime specified regions representing the targeted cDNA.

There are two purposes of no template control (NTC) reaction analysis: to assess a) the presence of contamination in the reaction solution (cross-contamination during reaction setup stated by (Su et al. 2020)) and b) primer-dimer formation (Taylor et al. 2010; D'haene et al. 2010). In this case, the NTC was used to check the primer-dimer formation possibility before gene expression qPCR analysis. This is important for ensuring primer quality and minimizing unexpected bias due to primer-dimer. A melt curve was also run as suggested by Thornton & Basu (2011) to detect secondary products. In testing primer quality control, an NTC reaction was generated by replacing the template with molecular grade water (Alonso et al. 2018). These NTCs experiments were done as stated in Taylor et al. (2010), with two technical replicate reactions.

In the possibility of primer dimer formation, the formation may be detected in qPCR NTC reaction (Morinha et al. 2020) by no Cq value being detected (Cheung et al. 2021). Although no amplicon detected in NTC, if the presence of an additional melt peak detected from the melt curve, it means nonspecific products are being amplified (Thornton & Basu 2011). All data from NTC reactions of each primer pair set shows no indication of either hairpin or primer dimer. This is based on the results of the amplification plot, melt curve, and melt peak charts. These

results correspond to bioinformatic analysis of primer-dimer and primer hairpin formation possibilities with no noteworthy indication of hairpin formation.

Double-strand DNA can be detected using SYBR Green I. This molecule can bind to double-strand DNA. Once it is intercalated to dsDNA, the fluorescence occurs to be detected. When single-strand DNA is present, weaker fluorescence occurs at 520 nm (Wang et al. 2019). When double-strand DNA is present, the stronger fluorescence is emitted. The previous study showed that the fluorescence intensity change is close to the chromophore lifetime change. That finding explains the SYBR Green I quenching dynamic in solution. It is important to underline that the function of fluorescence decay is sensitively impacted by the distribution of chromophore molecule conformers, reflecting the presence of different types of interactions with other molecules (Dragan et al. 2012).

With the storing condition of SYBR (mentioned below), this article ensures the quality of SYBR Green I used. The SYBR Green I reagent was stored in a plastic-based storage. This storing system was considered because plastic-based storage does not adsorb SYBR Green I, thus maintaining fluorescence ability. The SYBR Green I stock solution is also stored in a plastic tube enclosed with foil wrapping as light protection. The storage condition used for SYBR Green I was in -20°C which ensures its stability during storage (Bourzac et al. 2003). Thus, the results may be convinced to be reliable because the SYBR Green I and MgCl_2 condition are ensured to be reliable with the maintained conditions.

MgCl_2 concentration contained in the mix, as stated in Bioline Manufacture's protocol was 3 mM. Thornton & Basu (2011) explained that GC content has a control on the melting temperature of primer. The annealing temperature is usually 3 to 5°C above the melting temperature. In the practical run, specific salt buffer and MgCl_2 concentration can modify primer melting temperature. MgCl_2 can stabilize nucleic acid duplex stability (Nakano et al. 1999). Primer melting temperature can be affected by Mg^{2+} associated with primer GC content (Von Ahsen et al. 2001). The reality that reagents are offered varies with the additional consideration of various unique buffer content ratios. It may alter the MgCl_2 optimal concentration and annealing temperature required (Tajima et al. 2001).

The bioinformatics prediction and experimental validation evidences showed the primer pair sets were suitable with SYBR Green I and three mM of MgCl_2 . This might indicate that these sequences can be used for the following analysis. This can be done especially with the chemical reagent of SYBR Green I with three mM of MgCl_2 , in ensuring the priming of amplification process. The explained procedures also could be used for qPCR primer bioinformatic prediction and validation assessment approach. This is beneficial when the optimum temperatures of SYBR Green I and qPCR primer sequences are considered.

minima veniam, quis nostrum exercitationem ullam corporis suscipit laboriosam, nisi ut aliquid ex ea commodi consequatur? Quis autem vel eum iure reprehenderit qui in ea voluptate velit esse quam nihil molestiae consequatur.

CONCLUSION

The primer pair sequences for *ACTA2*, *FAP*, *HPRT1*, *PDGFB*, *PIK3R1*, and *VCAM1* stated above have been analyzed to produce a suitable amplicon for qPCR using *Rattus norvegicus* cDNA with SYBR Green I, annealing temperature range of $60-65^{\circ}\text{C}$ with three mM MgCl_2 and this approach can be useful for consideration in qPCR primer preparation.

AUTHORS CONTRIBUTION

G.P. contributed in methodology, collected and analyzed the data and wrote the manuscript, N.A. and F.A. conceived the conceptualization of experimental design and methodology, R.P. supervised all the process.

ACKNOWLEDGMENTS

We would like to thank Endah Sri Palupi, Retno Wahidah and Daniel Saputra Wahyudi for providing help in the cDNA sample preparation.

CONFLICT OF INTEREST

The authors declare that there is no conflict of interest.

REFERENCES

- Ahmed, F.E. et al., 2017. Role of Melt Curve Analysis in Interpretation of Nutrigenomics' MicroRNA Expression Data. *Cancer Genomics and Proteomics*, 14(6), pp.469–481. doi: 10.21873/cgp.20057.
- Alonso, G.C. et al., 2018. A Quest to Find Good Primers for Gene Expression Analysis of *Candida albicans* from Clinical Samples. *Journal of Microbiological Methods*, 147, pp.1–13. doi: 10.1016/j.mimet.2018.02.010.
- Bourzac, K.M., LaVine, L.J. & Rice, M., 2003. Analysis of DAPI and SYBR Green I as Alternatives to Ethidium Bromide for Nucleic Acid Staining in Agarose Gel Electrophoresis. *Journal of Chemical Education*, 80(11), pp.1292–1296. doi: 10.1021/ed080p1292.
- Brodin, J. et al., 2013. A Multiple-Alignment based Primer Design Algorithm for Genetically Highly Variable DNA Targets. *BMC Bioinformatics*, 14, 255. doi: 10.1186/1471-2105-14-255.
- Brown, J.R. et al., 2021. Comparison of SARS-CoV-2 N Gene Real-time RT-PCR Targets and Commercially Available Mastermixes. *Journal of Virological Methods*, 295, 114215. doi: 10.1016/j.jviromet.2021.114215.
- Cai, W. et al., 2019. MicroRNA-24 Attenuates Vascular Remodeling in Diabetic Rats through PI3K/Akt Signaling Pathway. *Nutrition, Metabolism and Cardiovascular Diseases*, 29(6), pp.621–632. doi: 10.1016/j.numecd.2019.03.002.
- Camorani, S., Hill, B.S. & Fontanella, R., et al. 2017. Inhibition of BM-MSCs Homing Towards TNBC Microenvironment Using an Anti-PDGFR β Aptamer. *Theranostics*, 7(14), pp.3595–3607
- Canh, V.D. et al., 2020. Application of Capsid Integrity (RT-)qPCR to Assessing Occurrence of Intact Viruses in Surface Water and Tap Water in Japan. *Water Research*, 189, 116674. doi: 10.1016/j.watres.2020.116674.
- Caselli, E. et al., 2021. Looking for More Reliable Biomarkers in Breast Cancer: Comparison Between Routine Methods and RT-qPCR. *PLoS ONE*, 16(9), e0255580. doi: 10.1371/journal.pone.0255580.
- Cheung, H.W. et al., 2021. A Duplex qPCR Assay for Human Erythropoietin (EPO) Transgene to Control Gene Doping in Horses. *Drug Testing and Analysis*, 13(1), pp.113–121. doi: 10.1002/dta.2907.
- Costa, A. et al., 2018. Fibroblast Heterogeneity and Immunosuppressive Environment in Human BC. *Cancer Cell*, 33(3), pp.463–479.e10.
- Covey, S.D., 2021. An Adaptable Dry Lab for SYBR Based RT-qPCR Primer Design to Reinforce Concepts in Molecular Biology and Nucleic Acids. *Biochemistry and Molecular Biology Education*, 49(2), pp.262–270. doi: 10.1002/bmb.21446.

- Cuevas-Ferrando, E. et al., 2021. Platinum Chloride-based Viability RT-qPCR for SARS-CoV-2 Detection in Complex Samples. *Scientific Reports*, 11, 18120. doi: 10.1038/s41598-021-97700-x.
- D'haene, B., Vandesompele, J. & Hellemans, J., 2010. Accurate and Objective Copy Number Profiling using Real-Time Quantitative PCR. *Methods*, 50(4), pp.262–270. doi: 10.1016/j.ymeth.2009.12.007.
- Dragan, A.I. et al., 2012. SYBR Green I: Fluorescence Properties and Interaction with DNA. *Journal of Fluorescence*, 22(4), pp.1189–1199. doi: 10.1007/s10895-012-1059-8.
- Ferreira, I.D., do Rosario, V.E. & Cravo, P.V.L., 2006. Real-time Quantitative PCR with SYBR Green I Detection for Estimating Copy Numbers of Nine Drug Resistance Candidate Genes in *Plasmodium falciparum*. *Malaria Journal*, 5(1). doi: 10.1186/1475-2875-5-1.
- Fiechter, R.H. et al., 2021. IL-12p40/IL-23p40 Blockade with Ustekinumab Decreases the Synovial Inflammatory Infiltrate through Modulation of Multiple Signaling Pathways Including MAPK-ERK and Wnt. *Frontiers in Immunology*, 12, 611656. doi: 10.3389/fimmu.2021.611656.
- Fittipaldi, M., Codony, F. & Morato, J., 2010. Comparison of Conventional Culture and Real-Time Quantitative PCR using SYBR Green for Detection of *Legionella pneumophila* in Water Samples. *African Journals Online*, 36(4), pp.417–424. doi: 10.4314/wsa.v36i4.58411.
- Gaby, J.C. & Buckley, D.H., 2017. The Use of Degenerate Primers in qPCR Analysis of Functional Genes Can Cause Dramatic Quantification Bias as Revealed by Investigation of nifH Primer Performance. *Microbial Ecology*, 74(3), pp.701–708. doi: 10.1007/s00248-017-0968-0.
- Goda, T., Tabata, M. & Miyahara, Y., 2015. Electrical and Electrochemical Monitoring of Nucleic Acid Amplification. *Frontiers in Bioengineering and Biotechnology*, 3(29). doi: 10.3389/fbioe.2015.00029.
- Gregory, S.M. et al., 2012. Latent Kaposi's Sarcoma-Associated Herpesvirus Infection of Monocytes Downregulates Expression of Adaptive Immune Response Costimulatory Receptors and Proinflammatory Cytokines. *Journal of Virology*, 86(7), pp.3916–3923. doi: 10.1128/jvi.06437-11.
- Hargreaves, S.K., Roberto, A.A. & Hofmockel, K.S., 2013. Reaction- and Sample-specific Inhibition Affect Standardization of qPCR Assays of Soil Bacterial Communities. *Soil Biology and Biochemistry*, 59, pp.89–97. doi: 10.1016/j.soilbio.2013.01.007.
- Hashish, A. et al., 2021. Development and Validation of Two Diagnostic Real-Time PCR (Taqman) Assays for the Detection of *Bordetella avium* from Clinical Samples and Comparison to the Currently Available Real-Time Taqman PCR Assay. *Microorganisms*, 9, 2232. doi: 10.3390/microorganisms9112232.
- Hu, Y. et al., 2012. Glioma Cells Promote the Expression of VCAM-1 on BM-MSCs: a Possible Mechanism for Their Tropism Toward Gliomas. *Journal of Molecular Neuroscience*, 48(1), pp.127–135.
- Jiménez, C. et al., 2000. Role of the PI3K Regulatory Subunit in the Control of Actin Organization and Cell Migration. *The Journal of Cell Biology*, 151(2), pp.249–261.
- Johnston, A.D. et al., 2019. PrimerROC: Accurate Condition-Independent Dimer Prediction using ROC Analysis. *Scientific Reports*, 9, 209. doi: 10.1038/s41598-018-36612-9.

- Kang, S.J. et al., 2021. Comparison of Seven Commercial TaqMan Master Mixes and Two Real-Time PCR Platforms Regarding the Rapid Detection of Porcine DNA. *Food Science of Animal Resources*, 41(1), pp.85–94. doi: 10.5851/KOSFA.2020.E80.
- Landry, N.M., Rattan, S.G. & Dixon, I.M.C., 2019. An Improved Method of Maintaining Primary Murine Cardiac Fibroblasts in Two-Dimensional Cell Culture. *Scientific Reports*, 9, 12889. doi: 10.1038/s41598-019-49285-9.
- Langlois, V.S. et al., 2021. The Need for Robust qPCR-based eDNA Detection Assays in Environmental Monitoring and Species Inventories. *Environmental DNA*, 3(3), pp.519–527. doi: 10.1002/edn3.164.
- Lee, S.B. et al., 2016. Ethyl Acetate Fraction of *Amomum xanthioides* Exerts Antihepatofibrotic Actions via the Regulation of Fibrogenic Cytokines in a Dimethylnitrosamine-Induced Rat Model. *Evidence-based Complementary and Alternative Medicine*, 2016, 6014380. doi: 10.1155/2016/6014380.
- Luna, G.M. et al., 2012. A New Molecular Approach based on qPCR for the Quantification of Fecal Bacteria in Contaminated Marine Sediments. *Journal of Biotechnology*, 157(4), pp.446–453. doi: 10.1016/j.jbiotec.2011.07.033.
- Morinha, F., Magalhães, P. & Blanco, G., 2020. Different qPCR Master Mixes Influence Telomere Primer Binding within and between Bird Species. *Journal of Avian Biology*, 51(2), e02352. doi: 10.1111/jav.02352.
- Nakano, S.I. et al., 1999. Nucleic Acid Duplex Stability: Influence of Base Composition on Cation Effects. *Nucleic Acids Research*, 27(14), pp.2957–2965. doi: 10.1093/nar/27.14.2957.
- Ouldrige, T.E. et al., 2013. DNA Hybridization Kinetics: Zippering, Internal Displacement and Sequence Dependence. *Nucleic Acids Research*, 41(19), pp.8886–8895. doi: 10.1093/nar/gkt687.
- Petrovan, V. et al., 2020. Evaluation of Commercial qPCR Kits for Detection of SARS-CoV-2 in Pooled Samples. *Diagnostics*, 10(7), 472. doi: 10.3390/diagnostics10070472.
- Ririe, K.M., Rasmussen, R.P. & Wittwer, C.T., 1997. Product Differentiation by Analysis of DNA Melting Curves during the Polymerase Chain Reaction. *Analytical Biochemistry*, 245(2), pp.154–160. doi: 10.1006/abio.1996.9916.
- Sato, H. et al., 2021. Downregulation of Mitochondrial Biogenesis by Virus Infection Triggers Antiviral Responses by Cyclic GMP-AMP Synthase. *PLoS Pathogens*, 17(10), e1009841. doi: 10.1371/journal.ppat.1009841.
- Sharma, A. et al., 2021. Comparative Transcriptomic and Molecular Pathway Analyses of HL-CZ Human Pro-Monocytic Cells Expressing SARS-CoV-2 Spike S1, S2, NP, NSP15 and NSP16 Genes. *Microorganisms*, 9(6), p.1193. doi: 10.3390/microorganisms9061193.
- Singh, V.K. et al., 2000. The Effect of Hairpin Structure on PCR Amplification Efficiency. *Molecular Biology Today*, 1(3), pp.67–69.
- Su, Q., Sena-Esteves, M. & Gao, G., 2020. Titration of Recombinant Adeno-Associated Virus (rAAV) Genome Copy Number Using Real-Time Quantitative Polymerase Chain Reaction (qPCR). *Cold Spring Harbor Protocols*, 2020(5), pp.158–161. doi: 10.1101/pdb.prot095646.
- Tajima, K. et al., 2001. Diet-Dependent Shifts in the Bacterial Population of the Rumen Revealed with Real-Time PCR. *Applied and Environmental Microbiology*, 67(6), pp.2766–2774. doi: 10.1128/AEM.67.6.2766-2774.2001.

- Taylor, S. et al., 2010. A Practical Approach to RT-qPCR-Publishing Data that Conform to the MIQE Guidelines. *Methods*, 50(4), pp.S1–S5. doi: 10.1016/j.jymeth.2010.01.005.
- Thornton, B. & Basu, C., 2011. Real-Time PCR (qPCR) Primer Design Using Free Online Software Received. *Biochemistry and Molecular Biology Education*, 39(2), pp.145–154. doi: 10.1002/bmb.20461.
- Trigo, B.B. et al., 2021. *In Silico* and *In Vitro* Evaluation of Primers for Molecular Differentiation of Leishmania Species. *Brazilian Journal of Veterinary Parasitology*, 30(1), e022020. doi: 10.1590/s1984-296120201078.
- Vanneste, K. et al., 2018. Application of Whole Genome Data for In Silico Evaluation of Primers and Probes Routinely Employed for the Detection of Viral Species by RT-qPCR using Dengue Virus as a Case Study. *BMC Bioinformatics*, 19(1), 312. doi: 10.1186/s12859-018-2313-0.
- Vogels, C.B.F. et al., 2020. Analytical Sensitivity and Efficiency Comparisons of SARS-CoV-2 RT-qPCR Primer-Probe Sets. *Nature Microbiology*, 5(10), pp.1299–1305. doi: 10.1038/s41564-020-0761-6.
- Von Ahsen, N., Wittwer, C.T. & Schütz, E., 2001. Oligonucleotide Melting Temperatures under PCR Conditions: Nearest-Neighbor Corrections for Mg²⁺, Deoxynucleotide Triphosphate, and Dimethyl Sulfoxide Concentrations with Comparison to Alternative Empirical Formulas. *Clinical Chemistry*, 47(11), pp.1956–1961. doi: 10.1093/clinchem/47.11.1956.
- Vulchi, R., Daane, K.M. & Wenger, J.A., 2021. Development of DNA Melt Curve Analysis for the Identification of Lepidopteran Pests in Almonds and Pistachios. *Insects*, 12(6), 553. doi: 10.3390/insects12060553.
- Wang, H. et al., 2019. An Exonuclease-assisted Fluorescence Sensor for Assaying Alkaline Phosphatase based on SYBR Green I. *Molecular and Cellular Probes*, 45, pp.26–30. doi: 10.1016/j.mcp.2019.04.002.
- Yang, T., Liu, J. & Chen, J., 2020. Compared with Conventional PCR Assay, qPCR Assay Greatly Improves the Detection Efficiency of Predation. *Ecology and Evolution*, 10(14), pp.7713–7722. doi: 10.1002/ece3.6494.
- Ye, J. et al., 2012. Primer-BLAST: A Tool to Design Target-Specific Primers for Polymerase Chain Reaction. *BMC Bioinformatics*, 13, 134. doi: 10.1186/1471-2105-13-134.

Research Article

Differences in Swim Bladder Histology of *Anguilla bicolor bicolor* at Various Stages of Sexual Maturity

Nur Indah Septriani^{1*}, Muhammad Ardillah Rusydan¹, Gizela Aulia Agustin¹, Nareta Defiani¹, Fajar Sofyantoro¹, Ariel Hananya², Dwi Eny Djoko Setyono³

1) Faculty of Biology, Universitas Gadjah Mada, Yogyakarta, Indonesia 55281

2) PT. Delos Teknologi Maritim, Jl. Salak No.38, RT.6/RW.2, Guntur, Kecamatan Setiabudi, Kota Jakarta Selatan Daerah Khusus Ibukota Jakarta 12980

3) National Research and Innovation Agency (BRIN) Gunungkidul, Yogyakarta, Indonesia 55861

* Corresponding author, email: nurindahseptriani@ugm.ac.id

Keywords:

silver eel
yellow eel
gas gland
mucosa
submucosa

Submitted:

17 May 2022

Accepted:

19 January 2023

Published:

09 June 2023

Editor:

Ardaning Nuriliani

ABSTRACT

The current study observed the histological differences of the swim bladder of the tropical eel, *Anguilla bicolor bicolor*, as an adaptation resulting from hydrostatic change. A total of 15 eels were collected from Pasir Puncu, Keburuhan, Purworejo and Segara Anakan, Cilacap, Indonesia in June 2017, September 2020, and April 2021. The eels were grouped into 4 stages based on the silvering stage and sex, namely: yellow undifferentiated, yellow female, silver male, and silver female. The average length and body weight of yellow undifferentiated eels were 255.07 ± 45.91 mm and 13.66 ± 8.5 g, respectively; for yellow female, the values were 374.35 ± 41.51 mm and 56.5 ± 12.02 g; for silver male, the values were 432.43 ± 15.15 mm and 140.29 ± 13.85 g; and for silver female were 702 ± 0.00 mm and 545 ± 11.31 g. The present study successfully recorded the histological structure of the swim bladder of *A. bicolor bicolor* in silver male and silver female stages. Silver males and females displayed a greater significant development of the swim bladder than yellow stages in the gas gland, mucosa, and submucosa layers. These results suggest that an increase in the gas gland thickness allows a greater contribution from gas to gas secretion, the mucosa exerts a mechanical effect on the newly formed gas bubbles, and the submucosa thickness reduces gas conductivity from the swim bladder wall.

Copyright: © 2023, J. Tropical Biodiversity Biotechnology (CC BY-SA 4.0)

INTRODUCTION

Eels (Anguillidae, *Anguilla*) are a facultative catadromous fish, with juveniles living in estuaries, rivers, and lakes, while the adult stage migrates to marine environments for reproduction (Tesch 2003). The life cycle of freshwater eels is divided into 5 stages, namely leptocephalus larvae, glass eel post-larvae, elver young eel, non-mature adult yellow eel, and migratory adult silver eel (Bertin 1956; Cresci 2020; Hatakeyama et al. 2022; Van Wichelen et al. 2022). Upon sexual maturation, the eels undergo physiological and morphological changes to help them undertake the long and difficult oceanic migration to offshore spawning sites. Eels usually display changes in morphological and physiological characters that include an increase in eye diameter (Pankhurst 1982; Beullens et al. 1997), changes in the integumentary structure and colour (Pankhurst & Lythgoe 1982), changes in retinal sensitivity to adapt to dark environments (Pankhurst & Lythgoe 1983; Bowmaker et al. 2008), lateral line

differentiation (Zacchei & Tavolaro 1988), gastrointestinal degeneration (Pankhurst & Sorensen 2011), changes in osmoregulatory processes (Righton et al. 2012), and swim bladder modification (Yamada et al. 2001) used as a volume gas exchange regulator during swimming (Smith & Croll 2011).

The swim bladder of *Anguilla* is classified as physostomous in the glass eel stage and is supplied and discharged through the pneumatic duct (Prem et al. 2000). However, the swim bladder behaves more like physoclistous fish during the metamorphosis process from yellow to silver phase (Pelster 2013). Research on changes in swim bladder at the developmental stage of *Anguilla rostrata* has been previously reported, revealing that the concentration of crystal guanine deposition within the swim bladder in American eels increased 1.5 times with gonadal maturity (Kleckner 1980a; Kleckner 1980b) and increasing acid secretion in gas gland during silvering process (Drechsel et al. 2022). Another study revealed that the length and luminal diameter of the rete mirabile capillaries in the silver eel stage of *A. rostrata* are higher than that of the yellow stage (Yamada et al. 2001). In addition, the GSI value of *A. rostrata* is lower than 3.5 and producing 5 times more gas compared to yellow eels (Yamada et al. 2001), allowing *A. rostrata* to migrate and lay eggs in deeper waters (Schneebauer et al. 2021). Swim bladders of Japanese eels *Anguilla japonica* start to develop in rivers or in shallow seawater before entering the open sea, once they are in the open sea, the swim bladder characteristics become stable (Tesch 2003). The previous study also assumed that swim bladder function would be improved compared to the yellow eels during their spawning migration experience in high hydrostatic pressure (Pelster 2015; Schneebauer et al. 2021; Drechsel et al. 2022).

Research on swim bladders in tropical eels is very limited, and given the theory that tropical eels have closer spawning grounds than temperate eels (Aoyama et al. 2003), it's possible that changes in swim bladder characteristics are less obvious. The current study aimed to observe the histological structure of the swim bladder of the tropical eel *Anguilla bicolor bicolor* as the consequence of adaptation to environmental hydrostatic change to spawn in the open sea. The results of this study are expected to provide the baseline information for sustainable conservation of tropical eels by differentiating the histological structure of the swim bladder between the yellow and silver stages, as well as males and females.

MATERIALS AND METHODS

Sampling Location and Staging

Live eels were collected with *wurru* (traditional baited trap) from Segara Anakan, Cilacap, Indonesia, (Figure 1A) in June 2017 and with fishing gear (Maguro, Lieyuwang 5000, Danyil, and Deco) from Pasir Puncu, Kaburuhan, Purworejo, Indonesia, (Figure 1B) in September 2020 and April 2021. The map figures were constructed using QGIS software. Individuals were identified through morphological characters (Ege 1939) and grouped into four stages based on gonad maturity and sex (Melia et al. 2006; Sugeha, et al. 2009; Geffroy & Bardonnnet 2016; Arai & Abdul Kadir 2017). The four stages are yellow undifferentiated, yellow female, silver male, and silver female. Yellow eels present partial melanization at the tip of the pectoral fins and yellow color on the belly, while silver eels present full melanization at the tip of the pectoral fins and metallic hue on the belly (Okamura et al. 2007).

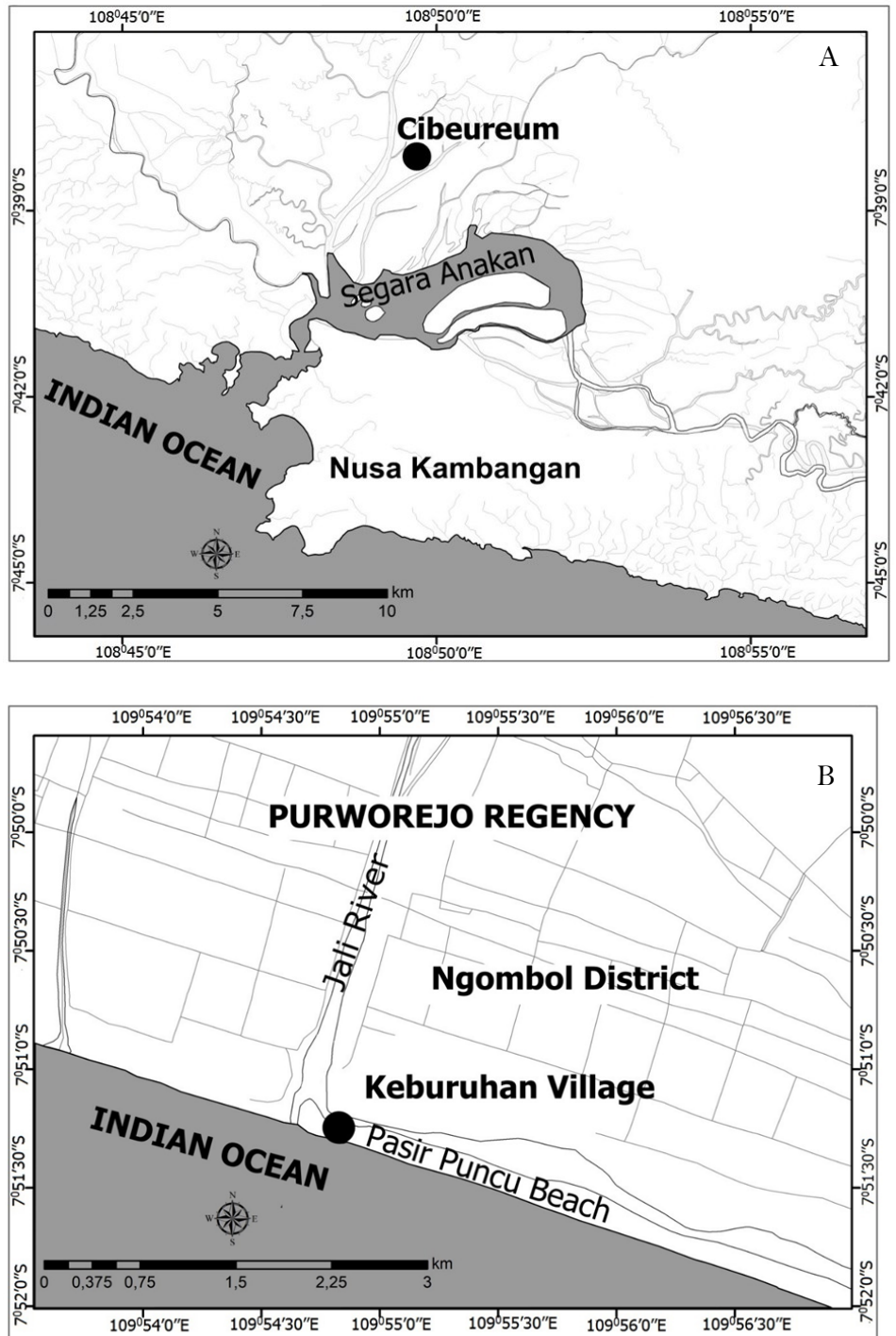


Figure 1. The map shows the study area in (A) Segara Anakan and (B) Pasir Puncu, Indonesia.

Morphometric Measurements

Live eels were transported to the Laboratory of Animal Structure and Development, Faculty of Biology, Universitas Gadjah Mada, Indonesia, where they were anaesthetized and euthanized with 100 ppm MS222, following animal welfare policies of The Integrated Research and Testing Laboratory (No. 00117/04/LPPT/II/2017), to acquire their external and internal biometrics.

Morphological measurements included total length (TL), horizontal eye diameter (HED), vertical eye diameter (VED), and pectoral fin length (PFL). These measurements were carried out using a digital caliper (Taffware SH 20) with an accuracy of 0.01 mm. Body weight (BW) was determined using a digital weighing scale to the nearest 0.01 g. BW

of less than 100 g, swim bladder weight (SBW), and gonadal weight (GW) were determined using a digital jewelry scale (8028-series) to the nearest 0.001 g. TL, EDV, EDH, GW, BW, and PFL values were used to measure the following:

$$\text{Gonadosomatic Index (GSI)} = 100 \text{ GW BW}^{-1}$$

$$\text{Eye Index (EI)} = 100\pi \text{ TL}^{-1} [0.25 (\text{HED} + \text{VED})]^2 \text{ (Pankhurst 1982)}$$

$$\text{Pectoral fin index (PFI)} = 100 \text{ PFL TL}^{-1} \text{ (Hagihara et al. 2012; Huyen et al. 2022)}$$

$$\text{Swim bladder Index (SBI)} = \text{SBW BW}^{-1} \text{ (Hagihara et al. 2012; Huyen et al. 2022)}$$

Histological Preparation

The swim bladders of *A. bicolor bicolor* were prepared following the standard paraffin method (Layton et al. 2018). Initially, the swim bladders were extracted from the body, fixed with Bouin's solution overnight, and washed with 70% alcohol. The next step was tissue dehydration using graded ethanol followed by immersion in toluene or xylene EMSURE® solution to purify the tissue (Wolfe 2019).

When the tissue was ready, it was infiltrated with paraffin (Leica Surgipath®, Leica Biosystem Richmond, Inc. USA). Sections were trimmed into 6 slides from every sample with a thickness of 5 µm using a microtome (MICROM HM310®). Afterwards, the tissue was stained with hematoxylin eosin (HE) dye consisting of hematoxylin Ehrlich, eosin 2%; and Mallory acid fuchsin (MAF) dye consisting of Mallory (aniline blue and orange blue), phosphomolybdic acid (PMA) 1%, and acid fuchsin. Tissue observation was carried out using a Leica ICC50® microscope to observe the gas glands, the mucosa, and submucosa layers with 10 x 10 and 40 x 10 magnifications. The thickness of the gas gland, mucosa, and submucosa layers were measured to the nearest µm using the Image J software, and the data are presented as Gas Gland Index (GGI), Mucosa Index (MI) and Submucosa Index (SMI) (Schneider et al. 2012).

Histological Measurements

To differentiate the maturation levels and adaptation to hydrostatic environment, histological differences were examined. The histological structures of the swim bladders were analyzed descriptively, qualitatively, and quantitatively by comparing the swim bladder index. Histological observations were carried out based on the thickness of gas gland cells (GG), mucosa (M), and submucosa (SM) layers of the undifferentiated yellow, yellow eels, silver males, and silver females. The GGI, MI, and SMI were measured as in Yamada et al. (2004) as follows:

$$\text{Gas Gland Index (GGI)} = 100 \text{ GG TL}^{-1}$$

$$\text{Mucosa Index (MI)} = 100 \text{ M TL}^{-1}$$

$$\text{Submucosa Index (SMI)} = 100 \text{ SM TL}^{-1}$$

GGI, MI, and SMI were calculated from 1-6 slides for each sample, and every slide was measured from 5 directions as replications.

Data Analysis

The collected data were analysed using the Kruskal-Wallis test and the pairwise comparison test with a confidence level of 95%. All statistical analyses were conducted using the SPSS software version 24.0 (SPSS Inc., Chicago, IL, USA).

RESULTS AND DISCUSSION

As shown in Table 1, eels obtained from Pasir Puncu (n=8) belonged to yellow undifferentiated, yellow female, and silver male. Meanwhile, the

Segara Anakan eels (n=7) only consisted of the silver male and female. In this study, the total length and body weight of female silver is higher than male silver eel. This also supports previous research that mature female *A. bicolor bicolor* is larger in size than male *A. bicolor bicolor* (Arai & Abdul Kadir 2017).

The sizes (total length and body weight) of silver stage (male and female) were significantly larger ($p < 0.05$) than those of yellow undifferentiated. Meanwhile, the sizes of yellow undifferentiated and yellow female were not significantly different. Additionally, the total length and body weight of the silver stages were not significantly different from those of the yellow stage of females (Figure 2).

The statistical analyses results showed that GSI, EI, and PFI of silver males were significantly higher than those of yellow undifferentiated, while SBI did not show significant differences among the four categories (Figure 3).

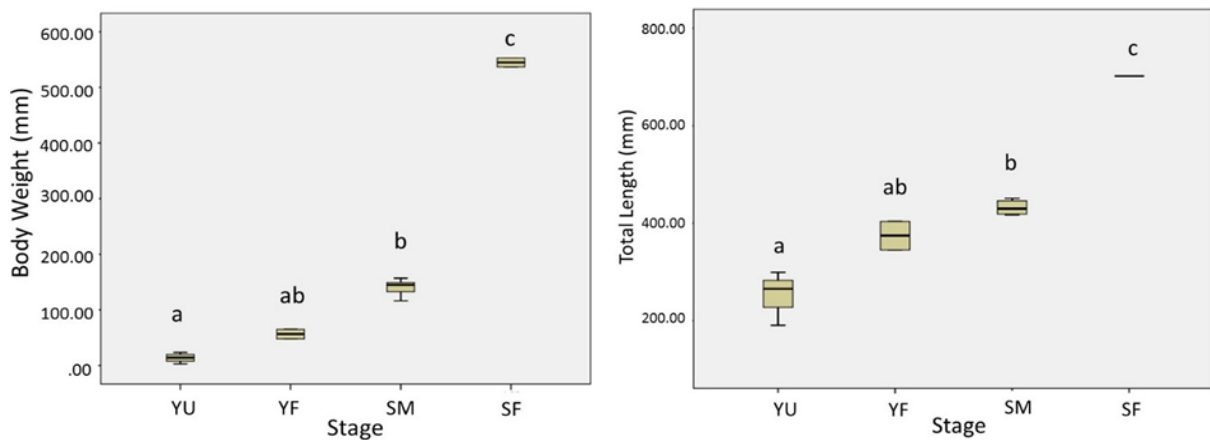


Figure 2. Total length and body weight of eels (*A. bicolor bicolor*); YU - yellow undifferentiated; YF - yellow females; SM - silver males; SF - silver female; different letters on the bar indicate significant differences between stages.

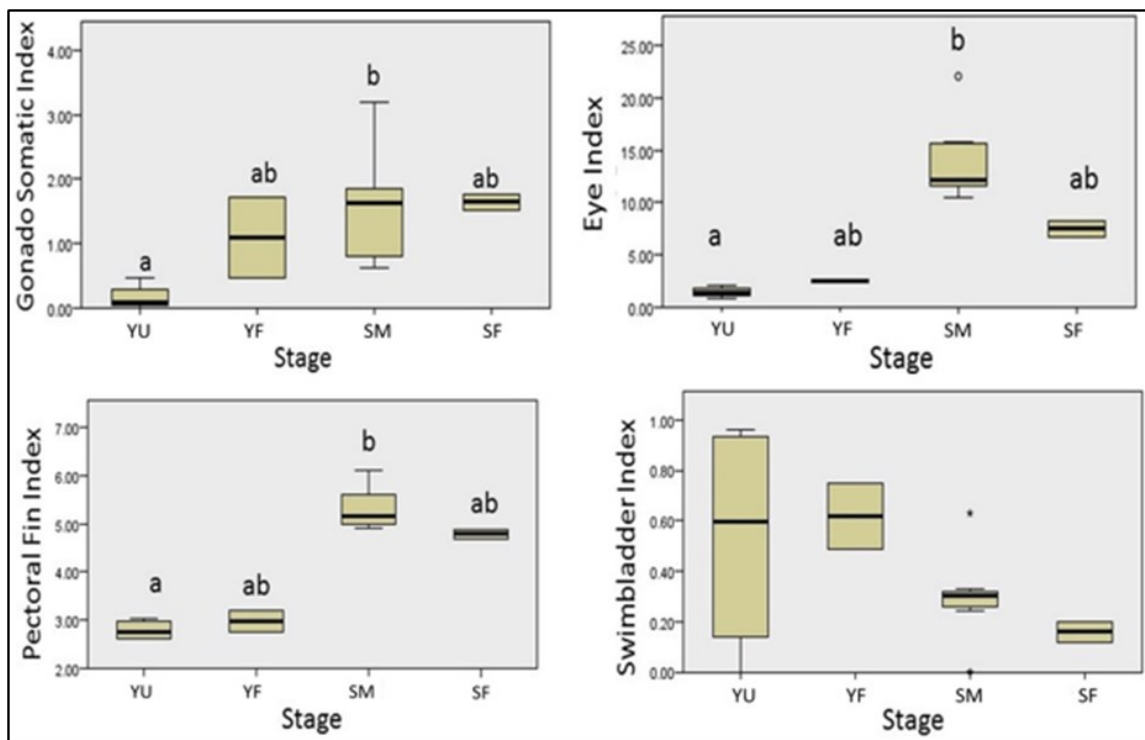


Figure 3. Gonadosomatic index (GSI), eye index (EI), pectoral fin index (PFI), swim bladder index (SBI) of *A. bicolor bicolor*; YU - yellow undifferentiated; YF - yellow female; SM - silver male; SF - silver female; different letters on the bar indicate significant differences between stages.

Table 1. Total length, body weight, stage, and sex of *A. bicolor bicolor* collected from Segara Anakan and Pasir Puncu.

Specimen No.	Total length (mm)	Weight (g)	Sampling location	Sampling date	Stage and sex	TL ± SD and W ± SD
1	264.49	23.4	Pasir Puncu	April 2021	yellow undifferentiated	255.07 ± 45.91 mm and 13.66 ± 8.50 g
2	266.1	12.45				
3	299.18	15.88				
4	190.52	2.92				
5	345	48	Pasir Puncu	September 2020	yellow female	374.35 ± 41.51 mm and 56.5 ± 12.02 g
6	403.7	65				
7	430	157	Pasir Puncu	September 2020	silver male	432.43 ± 15.15 mm and 140.29 ± 13.85 g
8	418	150				
9	450	145				
10	451	148.23	Segara Anakan	June 2017	silver male	432.43 ± 15.15 mm and 140.29 ± 13.85 g
11	442	133.75				
12	419	131.76				
13	417	116.27				
14	702	537	Segara Anakan	June 2017	silver female	702 ± 0.00 mm and 545 ± 11.31 g
15	702	553				

As shown in Figure 4 a-h, the swim bladder consists of 3 layers, 1) the gas gland layer (GG) containing cuboidal epithelium, gas gland cells, and blood vessels, 2) the mucosa layer (M) in the form of smooth muscle, and 3) the submucosa layer comprising dense connective tissue. MAF staining shows collagen fibers (CF) as blue, while blood vessels in *rete mirabile* (RM) and GG (Figure 4e and h) were stained as purple. The epithelium of gas gland in the yellow undifferentiated stage is cuboidal in shape and not folded, whereas in the yellow female and silver stages, the epithelium is folded. The epithelial cells size in the silver stage are longer. There are blood vessels (BV) in the lamina propria located in the basal of the gas gland layer at the yellow stage, while at the silver stage, blood vessels are found abundantly in between the gas gland cells. Higher developmental stage results in thicker mucosa and submucosa layers, which consists of connective tissue that regulate gas permeability (Morris & Albright 1975).

The GGI range was between 0.45 ± 0.08 and 1.18 ± 0.23 in yellow undifferentiated eels, between 0.96 ± 0.15 and 1.12 ± 0.3 in yellow females, between 1.05 ± 0.27 and 2.92 ± 0.67 in silver males, and from 2.06 ± 0.36 to 2.12 ± 0.79 in silver females (Table 2). The highest GGI (2.37 ± 0.77) was observed in silver male, while the lowest (0.73 ± 0.32) was found in the yellow undifferentiated (Table 2). These results are lower compared to those of Japanese eel, in which the GGI can reach up to 10 (Yamada et al. 2004).

The GGI and SMI of yellow stages (undifferentiated and female) were significantly lower than those of silver stages (male and female), but not between the same color stages. While the MI was significantly different between the first three stages, this was not the case between silver stages (Figure 5).

The silvering process of freshwater eels has been reported to be accompanied by increased body size and GSI to support egg ripening and increased swimming capabilities to prepare for oceanic migrations to spawning locations (Durif et al. 2006). Compared to the males, female eels tend to maximize their body weight and length to maximize fecundity (Wenner & Musick 1974; Vøllestad & Jonsson 1986; Helfman et al. 1987). The EI of *A. bicolor bicolor* in this study also showed 3 folds growing trend in females with increasing sexual maturity from yellow to sil-

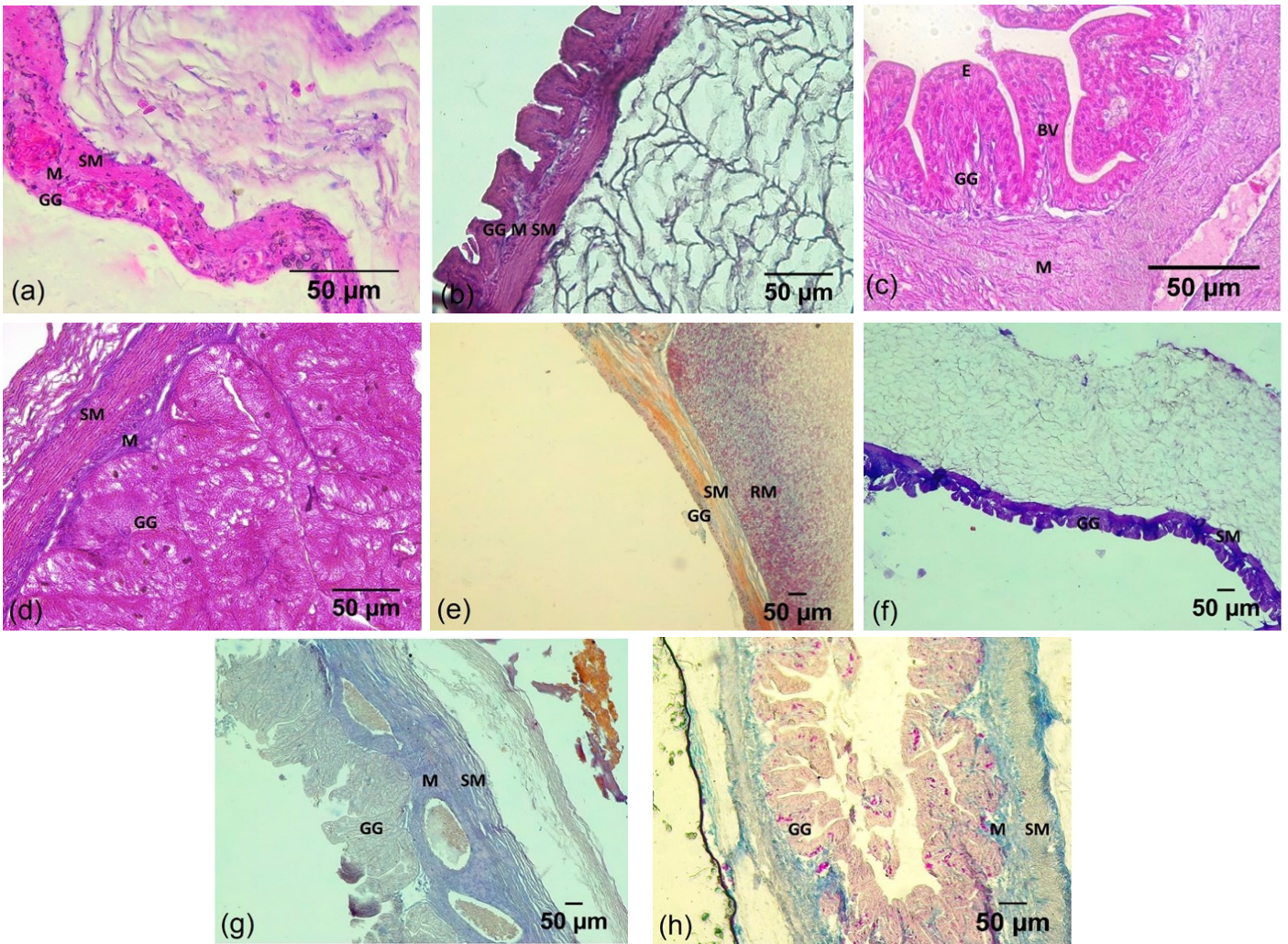


Figure 4. Histology of the swim bladder of *A. bicolor bicolor*: (a) yellow undifferentiated; (b) yellow female; (c) silver male; (d) silver female, (a-d with HE staining, 400x magnification); (e) yellow undifferentiated; (f) yellow female; (g) silver male; (h) silver female (e-h with MAF staining 100x magnification); BV - blood vessel; E - epithelium; GG - gas gland; M - mucosa; SBL - swim bladder lumen; SM - submucosa; RM - rete mirabile.

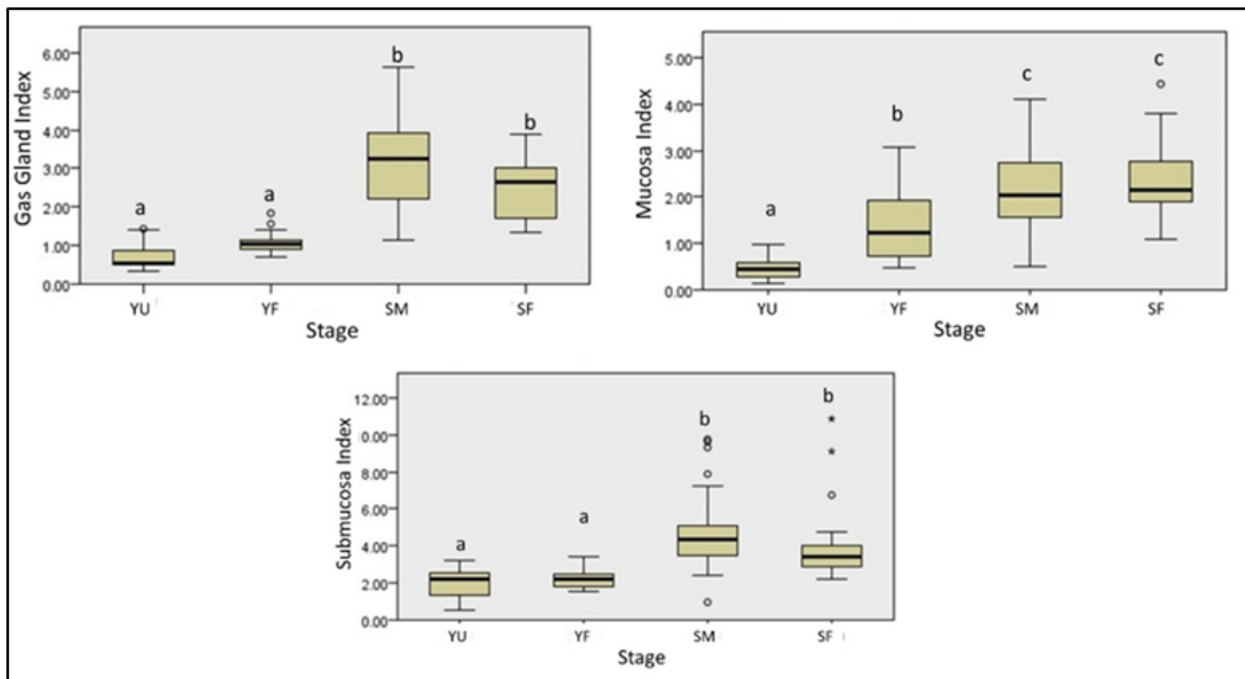


Figure 5. The gas gland, mucosa, and submucosa indices of the swim bladder of *A. bicolor bicolor*. YU - yellow undifferentiated; YF - yellow female; SM - silver male; SF - silver female; different letters on the bar indicate significant differences between stages.

Table 2. Gonadosomatic index (GSI), eye index (EI), pectoral fin index (PFI), swim bladder index (SBI), gas gland index (GGI), mucosa index (MI), and submucosa index (SMI) of *A. bicolor bicolor* collected from Segara Anakan and Pasir Puncu, Indonesia.

Stage	Mean ±SD						
	GSI	EI	PFI	SBI	GGI	SMI	MI
Yellow undifferentiated (n=4)	0.16 ± 0.21	1.42 ± 0.53	2.79 ± 0.22	0.72 ± 0.38	0.73 ± 0.32	0.45 ± 0.23	1.72 ± 0.74
Yellow female (n=2)	1.09 ± 0.88	2.50 ± 0.23	2.97 ± 0.31	0.62 ± 0.18	1.04 ± 0.11	1.11 ± 0.81	2.21 ± 0.41
Silver male (n=7)	0.70 ± 0.91	14.14 ± 4.04	5.34 ± 0.45	0.35 ± 0.14	2.37 ± 0.77	1.76 ± 0.80	4.16 ± 1.35
Silver female (n=2)	1.65 ± 0.18	7.48 ± 1.06	4.79 ± 0.13	0.16 ± 0.06	2.09 ± 0.04	2.18 ± 0.02	4.04 ± 0.10

ver stages. The increased diameter of the eyes in the silver stage also indicates an enhanced ability to adapt to dark environments such as their deep spawning grounds. An increase in PFI might also indicate that pectoral fins function as power stabilizers to avoid predators (Hagihara et al. 2012).

Based on histological observations, silver stages (male and females) had significantly thicker layers of swim bladder than other stages as shown by the histological result (Figure 3) and measurements (Figure 5). These data suggested that an increase in the thickness of the gas gland allows a greater contribution of gas to gas secretion, and that the submucosa thickness reduces gas conductivity from swim bladder wall (Yamada et al. 2001; Yamada et al. 2004). Mucosa layer contains bundle sheets of smooth muscles that play an important role in the mechanical movement of the swim bladder and are closely associated with gas glands (Fänge 1958).

The results of the current study are in line with the previous study (Marshall 1972), demonstrating that deep-sea fish swim bladders have a gas gland thickness larger than that of shallow sea fish, allowing increased gas secretion. Our study also showed that GGI and SMI of Indonesian eels were lower than those of temperate eels, indicating that temperate eels might migrate deeper than tropical eels.

In the present study, a significant and sudden increase of the gas gland thickness and mucosa thickness were observed at silver stages. It is hypothesized that these changes would allow for a shift in the behavior from a benthic, shallow water life in riverine environments to a deep oceanic migration and distant spawning locations. Similar changes were also evident in silver Japanese eels with GSI > 3.5 (Yamada et al. 2001). The early stage silver eels completed the development of swim bladders while still residing in riverine environments prior to commencement of their spawning migrations (Yamada et al. 2001).

CONCLUSIONS

The current study highlighted the difference in the histological structure of the *A. bicolor bicolor* swim bladder from four sexual maturity developmental stages: yellow undifferentiated, yellow female, silver male, and silver female. Similar to temperate eels such as *A. japonica* and *A. rostrata*, the tropical species *A. bicolor bicolor* also displayed thickening of the gas gland, mucosa, and submucosa layers at the mature silver stage. Furthermore, silver females and males showed no significant differences in the

thickness of the swim bladders, suggesting a similar spawning ground habitat.

AUTHOR CONTRIBUTION

N.I.S. and D.E.D.S. designed the research. M.A.R., G.A.A., N.D., and A.H. collected the data. N.I.S. and F.S. analyzed the data and wrote the manuscript. N.I.S. and D.E.D.S. supervised all the processes.

ACKNOWLEDGEMENTS

The authors would like to thank Chinthaka Anushka Hewavitarane Ph.D. and Dr. Senny Helmiati for comments on the manuscript and to the Faculty of Biology, Universitas Gadjah Mada for supporting this research through the Merdeka Belajar Kampus Merdeka (MBKM) 2021 grant.

CONFLICT OF INTEREST

The authors declare that there is no conflict of interest.

REFERENCES

- Aoyama et al., 2003. Short-Distance spawning migration of tropical freshwater eels. *Biological Bulletin*, 204, pp.104–108. doi: 10.2307/1543500
- Arai, T. & Abdul Kadir, S.R., 2017. Opportunistic spawning of tropical anguillid eels *Anguilla bicolor bicolor* and *A. bengalensis bengalensis*. *Scientific Reports*, 7, pp.1–17. doi: 10.1038/srep41649
- Bertin, L., 1956. *Eels, a biological study*, London: Cleaver-Hume Press Ltd.
- Beullens, K. et al., 1997. Sex differentiation, changes in length, weight and eye size before and after metamorphosis of European eel (*Anguilla anguilla* L.) maintained in captivity. *Aquaculture*, 153(1–2), pp.151–162. doi: 10.1016/S0044-8486(97)00019-7
- Bowmaker, J.K. et al., 2008. Eel visual pigments revisited: The fate of retinal cones during metamorphosis. *Visual Neuroscience*, 25(3), pp.249–255. doi: 10.1017/S0952523808080152.
- Cresci, A., 2020. A comprehensive hypothesis on the migration of European glass eels (*Anguilla anguilla*). *Biological Reviews*. 95(5), pp.1273–1286. doi:10.1111/brv.12609.
- Drechsel, V. et al., 2022. Aquaporin expression and cholesterol content in eel swim bladder tissue. *Journal of Fish Biology*, 100, pp.609–618. doi: 10.1111/jfb.14973
- Durif, C. et al., 2006. Impact of silvering stage, age, body size and condition on reproductive potential of the European eel. *Marine Ecology Progress Series*, 327, pp.171–181. doi: 10.3354/meps327171.
- Ege, V., 1939. *A revision of the genus Anguilla Shaw, a systematic, phylogenetic and geographical study (Dana-Report No. 16)*., Carlsberg Foundation; C.A. Reitzels Forlag; Oxford University Press; Bianco Luno.
- Fange, R., 1958. Structure and function of the gas bladder in *Argentina silus*. *Quarterly Journal of Microscopical Science*, 99(1), pp.95–96. doi: 10.1242/jcs.s3-99.45.95
- Geffroy, B. & Bardonnnet, A., 2016. Sex differentiation and sex determination in eels: consequences for management. *Fish and Fisheries*, 17(2), pp.375–398. doi: 10.1111/faf.12113.
- Hagihara, S. et al., 2012. Morphological and physiological changes of female tropical eels, *Anguilla celebesensis* and *Anguilla marmorata*, in relation to downstream migration. *Journal of Fish Biology*, 81(2), pp.408–426. doi: 10.1111/j.1095-8649.2012.03332.x.

- Hatakeyama, R. et al., 2022. Developmental features of Japanese eels, *Anguilla japonica*, from the late leptocephalus to the yellow eel stages: an early metamorphosis to the eel-like form and a prolonged transition to the juvenile. *Journal of Fish Biology*, 100(2), pp.454–473. doi:10.1111/jfb.14956.
- Helfman, G. et al., 1987. Reproductive ecology of the American eel. In *Common strategies of anadromous and catadromous fishes*. American Fisheries Society, Symposium 1, Bethesda, Maryland, pp.42–56. ISBN 0-913235-42-3
- Huyen, K.T. et al. 2022. Morphological characteristics and population structure of Marbled Eel (*Anguilla marmorata*) in Thua Thien Hue, Vietnam. *Journal of Applied Animal Research*, 50, pp.54–60. doi: 10.1080/09712119.2021.2018326
- Kleckner, R.C., 1980a. Swim bladder volume maintenance related to initial oceanic migratory depth in silver-phase *Anguilla rostrata*. *Science*, 208(4451), pp.1481–1482. doi: 10.1126/science.7384792.
- Kleckner, R.C., 1980b. Swimbladder wall guanine enhancement related to migratory depth in silver phase *Anguilla rostrata*. *Comparative Biochemistry and Physiology Part A: Physiology*, 65(3), pp.351–354. doi: 10.1016/0300-9629(80)90041-9.
- Layton, C., Bancroft, J. & Suvarna, S., 2018. Fixation of tissues. In *Bancroft's Theory and Practice of Histological Techniques E-Book*. Amsterdam: Elsevier, p. 40.
- Marshall, N., 1972. Swim bladder organization and depth ranges of deep-sea teleosts. *Symposium of the Society of Experimental Biology*, 26, pp.261–272.
- Melia, P. et al., 2006. Age and growth of *Anguilla anguilla* in the Camargue lagoons. *Journal of Fish Biology*, 68(3), pp.876–890. doi: 10.1111/j.0022-1112.2006.00975.x.
- Morris, S.M. & Albright, J.T., 1975. The ultrastructure of the swimbladder of the toadfish, *Opsanus tau* L. *Cell and Tissue Research*, 164(1). doi: 10.1007/BF00221697.
- Okamura, A. et al., 2007. A silvering index for the Japanese eel *Anguilla japonica*. *Environmental Biology of Fishes*, 80(1), pp.77–89. doi: 10.1007/s10641-006-9121-5.
- Pankhurst, N.W., 1982. Relation of visual changes to the onset of sexual maturation in the European eel *Anguilla anguilla* (L.). *Journal of Fish Biology*, 21(2), pp.127–140. doi: 10.1111/j.1095-8649.1982.tb03994.x.
- Pankhurst, N. W., & Lythgoe, J. N. 1982. Structure and colour of the integument of the European eel *Anguilla anguilla* (L.). *Journal of Fish Biology*, 21(3), pp. 279–296. doi:10.1111/j.1095-8649.1982.tb02833.x
- Pankhurst, N.W. & Lythgoe, J.N., 1983. Changes in vision and olfaction during sexual maturation in the European eel *Anguilla anguilla* (L.). *Journal of Fish Biology*, 23(2), pp.229–240. doi: 10.1111/j.1095-8649.1983.tb02898.x.
- Pankhurst, N.W. & Sorensen, P. W., 2011. Degeneration of the alimentary tract in sexually maturing European *Anguilla anguilla* (L.) and American eels *Anguilla rostrata* (LeSueur). *Canadian Journal of Zoology*, 62(6), pp.1143–1149. doi: 10.1139/z84-165
- Pelster, B., 2013. The swimbladder. In *Eel Physiology*. Enfield: CRCPress), pp. 44–67.
- Pelster, B., 2015. Swimbladder function and the spawning migration of the European eel *Anguilla anguilla*. *Frontiers in Physiology*, 5, 486. doi: 10.3389/fphys.2014.00486.

- Prem, C. et al., 2000. Swim bladder gas gland cells produce surfactant: in vivo and in culture. *American Journal Physiology Regulatory Integrative Comparative Physiology*, 279(6), R2336–R2343. doi: 10.1152/ajpregu.2000.279.6.R2336
- Righton, D.A., Aarestrup, K., & Jellyman, D., 2012. The *Anguilla* spp. migration problem: 40 million years of evolution and two millennia of speculation. *Journal of Fish Biology*, 81, pp.365–386
- Schneebauer, G. et al. 2021. Expression of transport proteins in the rete mirabile of european silver and yellow eel. *BMC Genomic*.86 (822): 1–15. doi: 10.1186/s12864-021-08180-2
- Schneider, C.A., Rasband, W.S. & Eliceiri, K.W., 2012. NIH Image to ImageJ: 25 years of image analysis. *Nature Methods*, 9(7), pp.671–675. doi: 10.1038/nmeth.2089.
- Smith, F.M. & Croll, R.P., 2011. Autonomic control of the swimbladder. *Autonomic Neuroscience*, 165(1), pp.140–148. doi: 10.1016/j.autneu.2010.08.002.
- Sugeha, H.Y., Jatmiko, I., & Muhammad, S., 2009. Sexual development of the tropical short-finned eel *Anguilla bicolor bicolor* of the Segara Anakan Waters, Central Java, Indonesia. *Jurnal Perikanan Universitas Gadjah Mada*, 11(1), pp.108–123. doi: 10.22146/jfs.2988
- Tesch, F.W., 2003. *The Eel, 3rd edn. Ed. by J. E. Thorpe*, Oxford: Blackwell Science.
- Van Wichelen, J. et al., 2022. Glass eel (*Anguilla anguilla* L. 1758) feeding behaviour during upstream migration in an artificial waterway. *Journal of Fish Biology*, 101(4), pp.1047–1057. doi: 10.1111/jfb.15171.
- Vøllestad, L.A. & Jonsson, B., 1986. Life-history characteristics of the European Eel *Anguilla anguilla* in the Imsa River, Norway. *Transactions of the American Fisheries Society*, 115(6), pp.864–871. doi: 10.1577/1548-8659(1986)115<864:LCOTEE>2.0.CO;2.
- Wenner, C.A. & Musick, J.A., 1974. Fecundity and gonad observations of the American Eel, *Anguilla rostrata*, migrating from Chesapeake Bay, Virginia. *Journal of the Fisheries Research Board of Canada*, 31(8), pp.1387–1391. doi: 10.1139/f74-164.
- Wolfe, D., 2019. Tissue processing. In *Suvarna SK, Layton C, Bancroft JD (eds) Bancroft's theory and practice of histological techniques*. London: Elsevier, pp. 73–83. doi: 10.1016/B978-0-7020-6864-5.00006-2.
- Yamada, Y. et al., 2001. Morphological and histological changes in the swim bladder during maturation of the Japanese eel. *Journal of Fish Biology*, 58(3), pp.804–814. doi: 10.1111/j.1095-8649.2001.tb00532.x.
- Yamada, Y. et al., 2004. Monthly changes in the swim bladder morphology of the female Japanese eel *Anguilla japonica* in the coastal waters of Mikawa Bay, Japan. *Ichthyological Research*, 51(1), pp.52–56. doi: 10.1007/s10228-003-0195-1.
- Zacchei, A.M. & Tavolaro, P., 1988. Lateral line system during the life cycle of *Anguilla anguilla* (L.). *Bolletino di zoologia*, 55(1–4), pp.145–153. doi: 10.1080/11250008809386611.

Research Article

Anti-hypercholesterolemia, Anti-atherogenic, and Anti-hypertension Effects of Red Beetroot (*Beta vulgaris* L.) in Rats Induced by High Fat and Fructose Diet

Alim El-Hakim¹, Sunarti², Lisna Hidayati³, Slamet Widiyanto^{4*}

1)Undergraduate Student Faculty of Biology, Universitas Gadjah Mada, Yogyakarta, Indonesia 55281

2)Department of Biochemistry, Faculty of Medicine, Public Health, and Nursing, Universitas Gadjah Mada, Yogyakarta, Indonesia 55281

3)Laboratory of Biochemistry, Faculty of Biology, Universitas Gadjah Mada, Yogyakarta, Indonesia 55281

4)Laboratory of Animal Physiology, Faculty of Biology, Universitas Gadjah Mada, Yogyakarta, Indonesia 55281

* Corresponding author, email: slametbio@ugm.ac.id

Keywords:

atherogenic index
cholesterol
blood pressure
beetroot (*Beta vulgaris* L.)

Submitted:

16 August 2022

Accepted:

30 December 2022

Published:

19 June 2023

Editor:

Ardaning Nuriliani

ABSTRACT

Metabolic syndrome is associated with abnormalities of lipid levels in the blood such as hyperlipidemia. Hyperlipidemia conditions can increase the risk of atherosclerosis and hypertension. Beetroot (*Beta vulgaris* L.) is a plant that contains high antioxidants. Beetroot has the potency to be used as a functional food that can reduce the potential for atherosclerosis and blood pressure. The aim of this study was to examine the effect of beetroot-enriched feed on the cholesterol level, atherogenic index and blood pressure of rats (*Rattus norvegicus* Berkenhout, 1769) induced by high fat and fructose diet. As many as 25 rats were divided into control, hyperlipidemia, and three treatment groups. The hyperlipidemia and treatment groups were induced to become hyperlipidemia using AIN93-M modified high fat and fructose feed for 8 weeks. The treatment groups were followed by intervention with 6, 9, and 12% beetroot enriched feed for 6 weeks. The feed was prepared by mixing beetroot flour in the pellets. Blood pressure, total cholesterol, and HDL level measurement was conducted after hyperlipidemia induction and after the intervention. The data analyzed with one-way ANOVA, DMRT, and T-Test. The results showed that 6% beetroot intervention have the highest increasing of HDL-cholesterol than other groups. The 9% beetroot intervention significantly decrease total cholesterol lower than normal baseline, and 12% beetroot intervention significantly decrease blood pressure than other groups. The atherogenic index of all treatment group was decreased. The 9% beetroot enriched feed was seen as an optimum dose to reduce total cholesterol, atherogenic index and blood pressure and increase HDL-cholesterol.

Copyright: © 2023, J. Tropical Biodiversity Biotechnology (CC BY-SA 4.0)

INTRODUCTION

Modern lifestyle encourages continuous consumption of high-calorie foods. Moreover, the high-calorie consumption in this community is not balanced with regular physical activity. According to WHO in 2016, obesity sufferers reached 13% of the world's population (World Health Organization 2021). Obese people have a high possibility to suffer from hyperlipidemia (Purnell et al. 2018). Hyperlipidemia is a group of disorders characterized by excess lipids in the bloodstream which include cholesterol, phospholipids, and triglycerides (Nelson 2013). Increased levels of

fat in the blood can be caused by unhealthy lifestyles such as eating foods that have high fat levels or foods that contain free radicals. Continuous hyperlipidemia will increase the risk of cardiovascular diseases such as atherosclerosis (Pan et al. 2018).

Atherosclerosis can lead to advanced cardiovascular diseases such as strokes and heart attacks. The chance of someone suffering from atherosclerosis can be calculated by the atherogenic index (Othman et al. 2019). Atherosclerosis is also influenced by blood pressure, if blood pressure increases (hypertension) it will increase the potency of atherosclerosis (Lu et al. 2015).

Hyperlipidemia and obesity give rise to a group of other disorders called metabolic syndromes. Metabolic syndrome is a group of disorders that includes central obesity, decrease high density lipoprotein (HDL) levels, hypertension, increase triglyceride levels and fasting blood sugar levels (Rochlani et al. 2017). Metabolic syndrome, especially the rise of blood pressure is closely related to chronic cardiovascular diseases such as coronary heart disease, stroke, and kidney failure (Scuteri et al. 2005).

Treatment of hyperlipidemia and hypertension still rests on the consumption of drugs that have several side effects such as vision problems, erectile dysfunction, fatigue, and insomnia (Tedla & Bautista 2016). Functional foods exist as a therapeutic solution for a disease with minimal side effects. Functional food is food that is not only digested to meet ordinary nutritional needs but contains ingredients that can play a role in preventing or treating certain diseases (John & Singla 2021). Functional food ingredients that can prevent hypertension and hyperlipidemia are those that contain high antioxidants such as beetroot.

Table beet is a common subspecies of beet which is primary used as vegetables. Beetroot is a temperate crop, thus has optimal growth condition in cold weather (Goldman & Navazio 2008). Based on Fardiaz (2014), cultivation of beetroot in Indonesia is carried out in highlands area such as Lembang, Batu, Kopeng, and Pengalengan. However, in Indonesia beetroot belongs to unpopular vegetables, even though it contains several bioactive compounds such as carotenoid, betaine, flavonoid, and polyphenols that could provide many benefits to its consumer. Betalain, an antioxidant, is the pigment contained in beetroot (Gokhale & Lele 2014).

Previous research showed that ethanol extract from beetroot can reduce cholesterol levels by inhibiting HMGCR activity. The antioxidants contained in beetroot also have the potential to lower blood pressure by inhibiting ACE. These two antioxidant roles could decrease the risk of atherosclerosis (Al-Dosari et al. 2011). Other study concludes that red beet juice consumption has potential effect as cardiovascular protective agent through reducing inflammation and suppressing oxidative stress mechanism (Singh et al. 2015). As a functional food application, semi-finished material like flour is recommended because it is longer to store, easy to mix and easy to apply (Lingling et al. 2018). Therefore, it is important to study the supplementation of beetroot flour by mixing it into food. The aim of this study to evaluate the effects of beetroot enriched feed in total cholesterol, atherogenic index, and blood pressure of rats induced by high fat and fructose diet.

MATERIALS AND METHODS

Feed Preparation

Standard feed was composed of modified AIN93-M. In 100 g standard feed contained 62.10 g corn starch, 14 g casein, 10 g sucrose, 4 g corn oil, 5 g α -cellulose, 3.5 g mineral mixture, 1 g vitamin mixture, 0.18 g DL-

methionine, 0.25 g choline chloride, and 0.008 g tertbutyl- hydroquinone. High fat and fructose feed formulated by Lozano (Lozano et al. 2016) contained 21% of trans fat and 25% of fructose for induction phase (HFFD). Beetroot was obtained from traditional market. The beetroot criteria was a fresh, red, and ripped tubers. The clean beetroot was thinly sliced and then heated in oven (50 °C, 8 hours). The dry beetroot was crumbled by disk mill to become a beetroot flour. Beetroot enriched feed (BEF) contained beetroot flour in various percentage compared to the total weight of feed by modifying the standard feed. BEF contained 6% of beetroot flour for dose 1, 9% for dose 2 and 12% for dose 3.

Animals

Twenty-five male wistar rats (100-120 g, 4 weeks old) were obtained from Faculty of Pharmacy, Universitas Gadjah Mada. The rats were maintained in a standard environment (22- 25 °C and 12 hours light cycle). The rats were acclimatized and fed using standard feed and water *ad libitum* during one-week before beginning the study. Ethics Committee of the Integrated Research and Testing Laboratory, Universitas Gadjah Mada approved all procedures in this study with registration number: 00011/04/LPPT/V/2019.

Experimental Study

The rats were divided into 5 groups: N (normal), HFFD (high-fat fructose diet), HFB1 (high-fat beetroot dose 1), HFB2 (high-fat beetroot dose 2), HFB3 (high-fat beetroot dose 3). The normal group (N) was fed by standard diet for 14 weeks. HFFD group was fed by high fat and fructose feed for 14 weeks. HFB1, HFB2, and HFB3 was fed by high fat and fructose feed for 8 weeks of induction then were given oral feed of BEF6% for HFB1, BEF9% for HFB2, and BEF12% for HFB3 during 6 weeks of treatment. In the all-phase rats was feed *ad libitum*

Lipid Profile and Blood Pressure Analysis

Blood samples were obtained from sinus retro-orbital, before (pre) and after (post) intervention with injected 50 mg ketamine and 50 mg xylazine per kg body weight intramuscular for anesthesia. Total cholesterol and HDL-cholesterol of serum were analysed with DiaSys Diagnostic Systems GmbH. Blood pressure was analysed with CODA Non-invasive Blood Pressure System. Analysis procedure was conducted according to manufacturer's protocol. Atherogenic index (AI) was measured by HDL-cholesterol (HDL.C) and total cholesterol (TC) level calculated using formula: $(TC - HDL.C) / HDL.C$ (Suanarunsawat et al. 2014)

Statistical Analysis

All values are presented as mean \pm standard deviation. One-Way ANOVA, DMRT, and T-test were used to analyse total cholesterol, atherogenic index, and blood pressure between each group.

RESULTS AND DISCUSSION

Feeding high lipid and fructose for eight weeks was carried out to make hyperlipidemia condition. The induction of hyperlipidemia with the addition of fructose will cause oxidative stress so that it reaches hyperlipidemic conditions faster. It is expected that total cholesterol levels will increase, HDL levels will decrease, the atherogenic index will increase, and blood pressure will increase (Hannou et al. 2018).

HDL-Cholesterol

Beetroot-enriched feed intervention gave a significant increase in HDL levels. It is shown by significant different between pre and post-test of HFB1, HFB2, and HFB3 (Figure 1). HFB1, HFB2, and HFB3 groups were recovered the HDL level close to normal group. Based on Figure 1, the HFB2 and HFB3 groups have no significant difference in HDL level compared to normal group in post intervention phase.

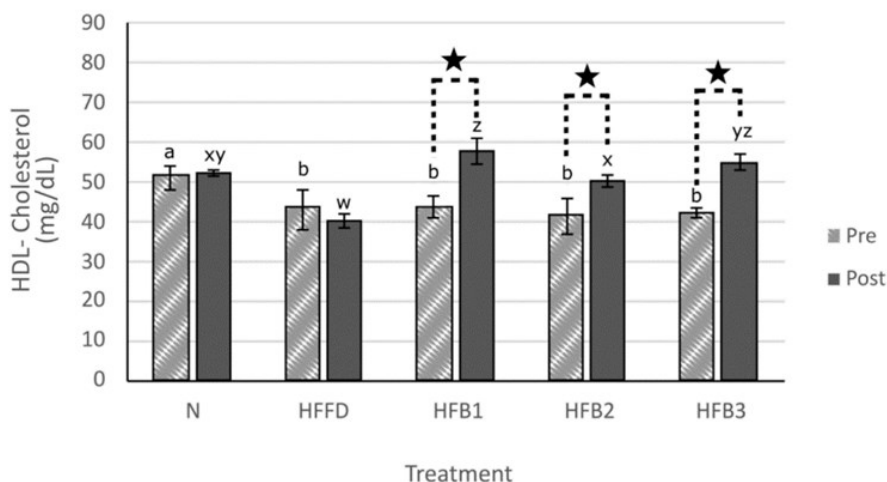


Figure 1. The average of HDL-cholesterol in rats pre and post intervention in Normal (N), High Fat - Fructose Diet (HFFD), High Fat - Fructose and BEF6% (HFB1), High Fat - Fructose and BEF9% (HFB2), High Fat - Fructose and BEF12% (HFB3) treatments.

abwxyz Different letters within the same color bars indicate significant difference between before and after treatment ($p < 0.05$).

Star symbol (★) indicates significant difference between pre- and post-test in the same group.

High consumption of fat in HFFD treatment cause a high cholesterol storage in peripheral tissues. In this condition, HDL act as inducer of cholesterol breakdown in peripheral tissue (Wang et al. 2017). A rise in HDL level in beetroot intervention treatment is consistent with the research of Singh et al. (2015) found that beetroot supplementation could increase HDL levels. Based on Ayala et al. (2014) the increase of HDL levels after high antioxidant food treatment could reduce the lipid deposition in peripheral tissues, the most contributor for rise of HDL levels. The structure of flavonoids has a big impact on antioxidant activity. Hydroxyl group of flavonoids is the most significant determinant to pro-oxidant scavenging mechanism by donating hydrogen and an electron (Santos-Sánchez et al. 2019)

Total Cholesterol

Beetroot-enriched feed intervention gave a significant difference in total cholesterol levels. Based on Figure 2, the group which treated by 6% beetroot enriched feed (HFB1) had total cholesterol levels after intervention which was lower than HFFD treatment but not significantly different, while HFB3 treatment had total cholesterol levels close to normal treatment. HFB2 treatment experienced a significant reduction in total cholesterol and was lower than the normal treatment.

The decrease in total cholesterol levels is due to the content of antioxidant compounds in beetroot such as flavonoids, betalains, and carotenoids (Clifford et al. 2015). Previous study showed that flavonoid compounds such as flavanone, flavone, and isoflavone could decrease total

cholesterol level by cholesterol synthesis inhibition and increase LDL receptor expression (You et al. 2008). A high level of total cholesterol may be caused by free radicals in the blood. Antioxidant compounds in beetroot could have a role as free radical scavengers (Chen et al. 2021).

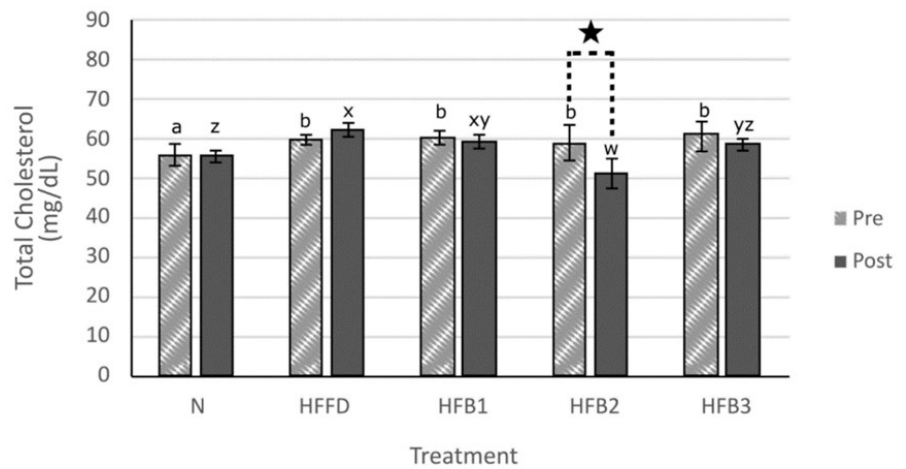


Figure 2. The average of total cholesterol in rats pre and post intervention in Normal (N), High Fat - Fructose Diet (HFFD), High Fat - Fructose and BE-F6% (HFB1), High Fat - Fructose and BEF9% (HFB2), High Fat - Fructose and BEF12% (HFB3) treatments.

abwxyz Different letters within the same color bars indicate significant difference between before and after treatment ($p < 0.05$).

Star symbol (★) indicates significant difference between pre- and post-test in the same group.

Diets enriched with 9% beetroot (HFB2) is better than 6% (HFB1) and 12% (HFB3). Previous study by Nahla et al. (2018) reported that a higher concentration of beetroot ethanol extract increases the antioxidant activity. Carotenoid was the one of antioxidant compound contained in beetroot (Ceclu & Nistor 2020). On another hand several compounds of carotenoid in high concentration has been reported could affect pro-oxidant activities in cell models (Lee et al. 2003).

Atherogenic index

In this study, high fat and fructose diet in induction phase accomplish to increase atherogenic index. Figure 3. shows that atherogenic index of induced group (HFFD, HFB1, HFB2, and HFB3) was significantly increased than normal group. Consumption of a high amount (more than 25% of energy requirement per day) fructose could affect lipid dysregulation, visceral adiposity, and decreased insulin sensitivity. These conditions were associated with cardiovascular disease and type 2 diabetes (Stanhope et al. 2009). Beetroot enriched feed intervention gave a significant difference in the atherogenic index. The group with high fat and fructose feed treatment was then given 6% beetroot enriched feed (HFB1), high fat and fructose then given 9% beetroot enriched feed (HFB2), high fat and fructose then given 12% beetroot enriched feed (HFB3) which has an atherogenic index approaching normal treatment.

A high cholesterol storage in peripheral tissues while a level of HDL is low makes lipid deposition in peripheral tissue cannot be decreased. This condition makes the potency of atherosclerosis increase. Potential of atherosclerosis measured by atherogenic index (Suanarunsawat et al. 2011). In this study beetroot enriched feed could affect the HDL level and total cholesterol. Based on Murphy et al. (2012)

in cardiovascular system, HDL acts as anti-atherogenic agent by preventing and curing the inflammatory of blood vessel peripheral tissue.

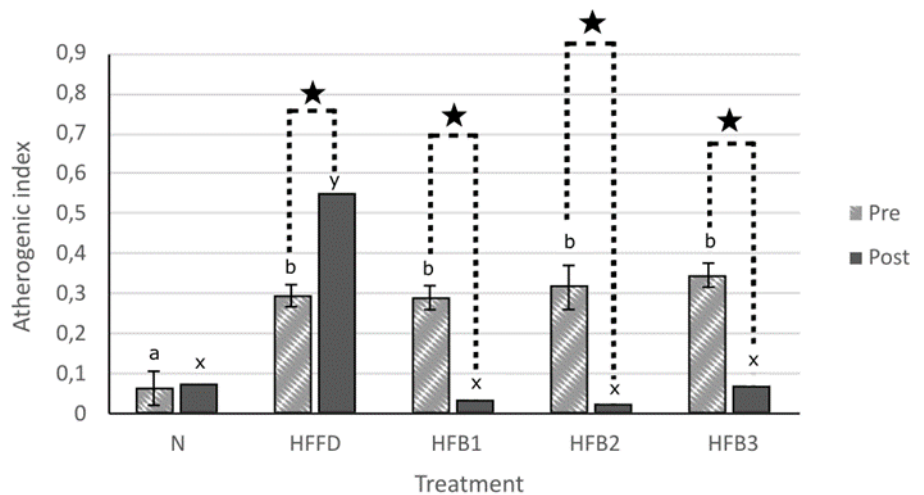


Figure 3. The average of Atherogenic index in rats pre and post intervention in Normal (N), High Fat - Fructose Diet (HFFD), High Fat - Fructose and BEF6% (HFB1), High Fat - Fructose and BEF9% (HFB2), High Fat - Fructose and BEF12% (HFB3) treatments.

^{abxy} Different letters within the same color bars indicates significant difference between before and after treatment ($p < 0.05$).

Star symbol (★) indicates significant difference between pre- and post-test in the same group.

Blood Pressure

Beetroot enriched feed intervention gave a significant difference in blood pressure. The high fat and fructose feed treatment was then treated with 6% and 9% beetroot enriched feed (HFB1 and HFB2) has a blood pressure close to normal group. Based on Figure 4, the blood pressure of 12% beetroot enriched feed intervention group decreased below normal. Post-intervention blood pressure from high lipid treatment was then treated with 9% and 12% beetroot enriched feed (HFB2 and HFB3) experienced a significant reduction.

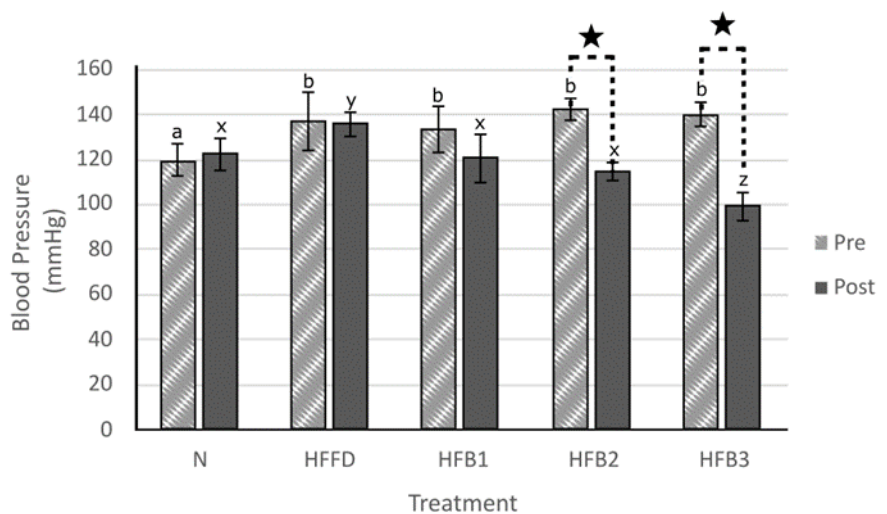


Figure 4. The average of blood pressure in rats pre and post intervention in Normal (N), High Fat - Fructose Diet (HFFD), High Fat - Fructose and BEF6% (HFB1), High Fat - Fructose and BEF9% (HFB2), High Fat - Fructose and BEF12% (HFB3) treatments.

^{abxyz} Different letters within the same color bars indicates significant difference

between before and after treatment ($p < 0.05$)

Star symbol (★) indicates significant difference between pre- and post-test in the same group.

A decrease in blood pressure in the three treatment groups could occur due to the content of antioxidant compounds in beetroot such as carotenoids, phenols, and flavonoids. Previous study reported that antioxidant compounds reduced oxidative stress in the peripheral tissue of blood pressure. Thus, blood pressure decreased significantly (Parik et al. 1996; Murphy et al. 2012; Sorriento et al. 2018). Previous study reported that beetroot antioxidant compound like flavonoids could inhibit angiotensin converting enzyme (ACE) by holding the NADPH oxidation in renin angiotensin aldosterone system (RAAS). A low activity of ACE could affect the arteries vasodilatation and lower blood pressure (Aviram et al. 2004). In this study, a higher dose of beetroot enriched feed given a higher effect to reduce blood pressure.

Correlation analysis

There is a positive correlation between the atherogenic index and blood pressure. Based on Figure 5, an increase in the atherogenic index have implications for an increase in blood pressure. A high level of non-HDL cholesterol and low HDL will cause oxidative stress. Oxidative stress conditions result in damage of blood vessel of peripheral tissue and increased blood pressure (Riccioni et al. 2009). This result is in line with the research Kazemi et al. (2018), which found that the atherogenic index and blood pressure were positively correlated.

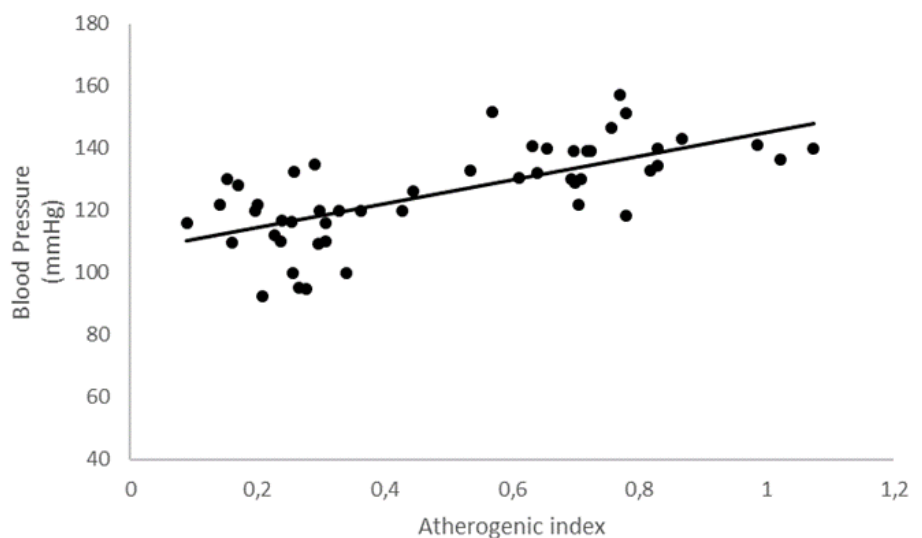


Figure 5. Correlations between atherogenic index and blood pressure ($R^2 = 0.474$)

Based on the simple linear correlation analysis, the atherogenic index affected blood pressure in the moderate level ($R^2 = 0.474$).

Based on this study, beetroot should be promoted as a key component of a healthy lifestyle to control blood pressure and hyperlipidemia. For hypertension and hyperlipidemia sufferer beetroot could be alternative for non-medicine treatment. However, more research about optimal doses for humans, side effects, and proper composition with other ingredients should be conducted in the future.

CONCLUSION

Beetroot enriched feed could decrease total cholesterol, atherogenic index and blood pressure in rats induced by high fat and fructose feed. Intervention of 9% feed enriched beetroot was seen as an optimum dose to reduce total cholesterol, atherogenic index and blood pressure and increase HDL. Atherogenic index and blood pressure have a positive correlation with moderate level.

AUTHORS CONTRIBUTION

A.E.H. collected and analysed the data and wrote the manuscript. S. designed the trial and supervised research process, L.H. analysed the data, S.W. supervised the research process and manuscript.

ACKNOWLEDGMENTS

This study supported by Indonesian Ministry of Research Technology and Higher Education. The data in this article is part of the thesis of Al-im El-Hakim, undergraduate program at the Faculty of Biology UGM.

CONFLICT OF INTEREST

There is no conflict of interest of this study.

REFERENCES

- Al-Dosari, M.S. et al., 2011. Effect of *Beta vulgaris* L. on cholesterol rich diet-induced hypercholesterolemia in rats. *Farmacologia*, 59(5), pp.669-677.
- Aviram, M. et al., 2004. Pomegranate juice consumption for 3 years by patients with carotid artery stenosis reduces common carotid intima-media thickness, blood pressure and LDL oxidation. *Clinical nutrition*, 23(3), pp.423-433. doi: 10.1016/j.clnu.2003.10.002
- Ayala, A., Muñoz, M.F. & Argüelles, S., 2014. Lipid Peroxidation: Production, Metabolism, and Signaling Mechanisms of Malondialdehyde and 4-Hydroxy-2-Nonenal. *Oxidative Medicine and Cellular Longevity*, 2014, 360438. doi: 10.1155/2014/360438
- Ceclu, L. & Nistor, O., 2020. Red beetroot: Composition and health effects - A review. *Journal of Nutritional Medicine and Diet Care*, 6 (043). doi: 10.23937/2572-3278.1510043
- Clifford, T. et al., 2015. The Potential Benefits of Red Beetroot Supplementation in Health and Disease. *Nutrients*, 7(4), pp.2801-2822. doi: 10.3390/nu7042801
- Chen, L. et al., 2021. Beetroot as a functional food with huge health benefits: Antioxidant, antitumor, physical function, and chronic metabolomics activity. *Food science & nutrition*, 9(11), pp.6406-6420. doi: 10.1002/fsn3.2577
- Fardiaz, S., 2014. *Mikrobiologi Pangan I*. Universitas Terbuka
- Gokhale, S.V. & Lele, S.S., 2014. Betalain Content and Antioxidant Activity of *Beta vulgaris*: Effect of Hot Air Convective Drying and Storage. *Journal of Food Processing and Preservation*, 38(1), pp.585-590. doi: 10.1111/jfpp.12006
- Goldman, I.L. & Navazio, J.P., 2007. Table Beet. In *Handbook of Plant Breeding*. NY: Springer, pp.219-238. doi: 10.1007/978-0-387-30443-4_7
- Hannou, S.A. et al., 2018. Fructose metabolism and metabolic disease. *The Journal of clinical investigation*, 128(2), pp.545-555. doi: 10.1172/JCI96702.

- John, R. & Singla, A., 2021. Functional Foods: Components, health benefits, challenges, and major projects. *DRC Sustainable Future: Journal of Environment, Agriculture, and Energy*, 2(1), pp.61-72. doi: 10.37281/drcsf/2.1.7
- Kazemi, T. et al., 2018. Cardiovascular Risk Factors and Atherogenic Indices in an Iranian Population: Birjand East of Iran. *Clinical Medicine Insights: Cardiology*, 20(12), 1179546818759286. doi: 10.1177/1179546818759286
- Lee, J. H., Ozcelik, B. & Min, D. B., 2003. Electron donation mechanisms of β -carotene as a free radical scavenger. *Journal of Food Science*, 68(3), pp.861-865. doi: 10.1111/j.1365-2621.2003.tb08256.x
- Lingling, C. et al., 2018. Preparation of Potato Whole Flour and Its Effects on Quality of Flour Products: A Review. *Grain & Oil Science and Technology*, 1(3), pp.145-150. doi: 10.3724/sp.j.1447.gost.2018.18037
- Lozano, I. et al., 2016. High-fructose and high-fat diet-induced disorders in rats: impact on diabetes risk, hepatic and vascular complications. *Nutrition & Metabolism*, 13, 15. doi: 10.1186/s12986-016-0074-1
- Lu, Y. et al., 2015. Lifestyle and Risk of Hypertension: Follow-Up of a Young Pre-Hypertensive Cohort. *International Journal of Medical Sciences*, 12(7), pp.605-612. doi:10.7150/ijms.12446
- Murphy, A.J. et al., 2012. Anti-atherogenic mechanisms of high-density lipoprotein: Effects on myeloid cells. *Biochimica et Biophysica Acta (BBA) - Molecular and Cell Biology of Lipids*, 1821(3), pp.513-521. doi: 10.1016/j.bbalip.2011.08.003
- Nahla, T.K., Wisam, S.U. & Tariq, N.M., 2018. Antioxidant Activities of Beetroot (*Beta vulgaris* L.) Extracts. *Pakistan Journal of Nutrition: PJN*, 17(10), pp.500-505. doi: 10.3923/pjn.2018.500.505
- Nelson, R.H., 2013. Hyperlipidemia as a Risk Factor for Cardiovascular Disease. *Primary Care: Clinics in Office Practice*, 40(1), pp.195-211. doi: 10.1016/j.pop.2012.11.003
- Othman, Z.A. et al., 2019. Phenolic Compounds and the Anti-Atherogenic Effect of Bee Bread in High-Fat Diet-Induced Obese Rats. *Antioxidants*, 9(1), p.33. doi:10.3390/antiox9010033
- Pan, J. et al., 2018. Prevalence of hyperlipidemia in Shanxi Province, China and application of Bayesian networks to analyse its related factors. *Scientific Reports*, 8, 3750. doi: 10.1038/s41598-018-22167-2
- Parik, T. et al., 1996. Evidence for Oxidative Stress in Essential Hypertension: Perspective for Antioxidant Therapy. *European Journal of Cardiovascular Prevention & Rehabilitation*, 3(1), pp.49-54. doi: 10.1177/174182679600300107
- Purnell, J.Q., 2018. Definitions, Classification, and Epidemiology of Obesity. In *Endotext (Internet)*. South Dartmouth (MA): MDText.com, Inc.
- Riccioni, G. et al., 2009. Relationship between plasma antioxidant concentrations and carotid intima-media thickness: the Asymptomatic Carotid Atherosclerotic Disease in Manfredonia Study. *European Journal of Cardiovascular Prevention & Rehabilitation*, 16(3), pp.351-357. doi:10.1097/HJR.0b013e328325d807
- Rochlani, Y. et al., 2017. Metabolic syndrome: pathophysiology, management, and modulation by natural compounds. *Therapeutic Advances in Cardiovascular Disease*, 11(8), pp.215-225. doi: 10.1177/1753944717711379
- Santos-Sánchez, N.F. et al., 2019. Antioxidant compounds and their antioxidant mechanism. In *Antioxidants*. IntechOpen. doi: 10.5772/intechopen.85270

- Scuteri, A. et al., 2005. The Metabolic Syndrome in Older Individuals: Prevalence and Prediction of Cardiovascular Events: The Cardiovascular Health Study. *Diabetes Care*, 28(4), pp.882–887. doi:10.2337/diacare.28.4.882
- Singh, A. et al., 2015. Beetroot Juice Supplementation Increases High Density Lipoprotein-Cholesterol and Reduces Oxidative Stress in Physically Active Individuals. *Journal of Pharmacy and Nutrition Sciences*, 5(3), pp.179–185. doi: 10.6000/1927-5951.2015.05.03.2
- Sorriento, D. et al., 2018. The Antioxidant Therapy: New Insights in the Treatment of Hypertension. *Frontiers in Physiology*, 9, 258. doi: 10.3389/fphys.2018.00258
- Stanhope, K.L., 2009. Consuming fructose-sweetened, not glucose-sweetened, beverages increases visceral adiposity and lipids and decreases insulin sensitivity in overweight/obese humans. *The Journal of clinical investigation*, 119(5), pp.1322–1334. doi: 10.1172/JCI37385
- Suanarunsawat, T. et al., 2011. Lipid-Lowering and Antioxidative Activities of Aqueous Extracts of *Ocimum sanctum* L. Leaves in Rats Fed with a High-Cholesterol Diet. *Oxidative Medicine and Cellular Longevity*, 2011, 962025. doi: 10.1155/2011/962025.
- Tedla, Y.G., & Bautista, L.E., 2016. Drug Side Effect Symptoms and Adherence to Antihypertensive Medication. *American journal of hypertension*, 29(6), pp.772–779. doi: 10.1093/ajh/hpv185
- Wang, H.H. et al., 2017. Cholesterol and Lipoprotein Metabolism and Atherosclerosis: Recent Advances in Reverse Cholesterol Transport. *Annals of Hepatology*, 16, pp.S27–S42. doi: 10.5604/01.3001.0010.5495
- World Health Organization, 2021, 'Obesity and overweight', in *World Health Organization*, viewed from <https://www.who.int/news-room/fact-sheets/detail/obesity-and-overweight>.
- You, C.L., Su, C.L. & Zhou, C.L., 2008. Study on Effect and mechanisms of *Scutellaria baicalensis* stem-leaf total flavonoid in regulating lipid metabolism. *China J. Chin. Mater. Med.*, 33(9), pp.1064–1066.

Research Article

The Synergistic Effect of Combination of Pentagamavunone-1 with Diosmin, Galangin, and Piperine in WiDr Colon Cancer Cells: *In vitro* and Target Protein Prediction

Muthi Ikawati^{1,2*}, Hajidah Musyayyadah¹, Yurananda Magnalia Putri¹, Umami Maryam Zulfin¹, Febri Wulandari¹, Dyaningtyas Dewi Pamungkas Putri^{1,3}, Edy Meiyanto^{1,2}

1)Cancer Chemoprevention Research Center, Faculty of Pharmacy, Universitas Gadjah Mada, Sekip Utara, Yogyakarta 55281, Indonesia

2)Macromolecular Engineering Laboratory, Department of Pharmaceutical Chemistry, Faculty of Pharmacy, Universitas Gadjah Mada, Sekip Utara, Yogyakarta 55281, Indonesia

3)Department of Pharmacology and Clinical Pharmacy, Faculty of Pharmacy, Universitas Gadjah Mada, Sekip Utara, Yogyakarta 55281, Indonesia

* Corresponding author, email: muthi_ikawati@ugm.ac.id

Keywords:

bioinformatic
curcumin analog
colon cancer
combination
natural compound
Pentagamavunone-1 (PGV-1)

Submitted:

05 January 2023

Accepted:

02 March 2023

Published:

23 June 2023

Editor:

Ardaning Nuriliani

ABSTRACT

Pentagamavunone-1 (PGV-1) is a curcumin analog with a prominent anti-cancer potency *in vitro* and *in vivo* for several cancer types, including colon cancer. Combining PGV-1 with natural compounds such as diosmin, galangin, and piperine can enhance its effectiveness due to their promising chemoprevention properties. We aimed to evaluate the effectiveness of combining PGV-1 with diosmin, galangin, or piperine for colon cancer by using *in vitro* and bioinformatic approaches to predict their target proteins. WiDr cells were used as a model for colon adenocarcinoma (COAD). The cell viability under a single or combination treatment of PGV-1 and diosmin, galangin, or piperine was evaluated using direct counting by the trypan blue exclusion test. SwissTargetProtein, UALCAN, and OncoLnc were utilized to predict target proteins of the compounds in COAD, the expression level of target proteins in COAD, and the survival rate of patients with overexpressed target proteins, respectively. The IC₅₀ values for PGV-1, diosmin, galangin, and piperine were 2.8×10^{-2} µg/mL, 81 µg/mL, 7 µg/mL, and 172 µg/mL, respectively. All the tested natural compounds showed synergistic effects when combined with PGV-1 at low concentrations. Eleven proteins that were overexpressed in COAD were identified as potential targets. Overlapped predicted targets of PGV-1 and galangin or piperine were CDK1, MET, and TOP2A. The high expression of another set of predicted target proteins, SCD, CA9, and SQLE, led to lower survival rates in COAD patients. We concluded that combinations of PGV-1 with natural compounds can synergistically enhance its anti-cancer activity for colon cancer.

Copyright: © 2023, J. Tropical Biodiversity Biotechnology (CC BY-SA 4.0)

INTRODUCTION

Colon cancer is the most newly diagnosed cancer cases globally in 2020 after breast, lung, prostate, and nonmelanoma of skin (Sung et al. 2021). Despite having the highest level of a 5-year survival among the other 18 cancers or cancer groups in Southeast Asia, the survival rates widely vary among countries (Allemani et al. 2018). On the other hand, the

evolving lifestyle including diet may contribute to higher incidence of colon and rectal cancer in young adults (Stoffel & Murphy 2021). Colorectal cancer is in the top four causes of cancer-related death worldwide (Argiles et al. 2020). In the United States alone, colon cancer ranks as the third largest mortality in cancer after breast cancer and lung and bronchial cancer during 2014–2018 (Siegel et al. 2021). The adjuvant treatment by using chemotherapy agents such as 5-fluorouracil (5-FU) and oxaliplatin is involved in the treatment. However, the risk including contraindications, liver and renal dysfunction, and heart failure, have to be monitored and assessed constantly (Argiles et al. 2020). Thus, the advancement in colon cancer treatment as well as the development of highly potent chemotherapy with low side effects is important.

A curcumin analog Pentagamavunon-1 (PGV-1) (Figure 1) has been developed initially to support chemotherapy as a combination agent (co-chemotherapy) for anti-cancer. PGV-1 sensitizes doxorubicin-resistant breast cancer cells (Meiyanto et al. 2014) and synergistically increases the effectiveness of 5-FU in colon cancer cells (Meiyanto et al. 2018). Eventually, PGV-1 itself has been proven as a potent anti-cancer candidate with low side effects and minimal relapse for leukemia, breast adenocarcinoma, cervical cancer, uterine cancer, and pancreatic cancer (Lestari et al. 2019). *In vitro* and *in vivo* assays show that PGV-1 suppresses tumour cell growth and migration via various mechanisms, e.g. metabolic and enzymatic regulation, cell cycle arrest and senescence, and signal transduction, in leukemia (Lestari et al. 2019), breast cancer (Meiyanto et al. 2019; Wulandari et al. 2020; Meiyanto et al. 2021), and colon cancer (Wulandari et al. 2021). Indeed, PGV-1 is a promising anti-cancer candidate.

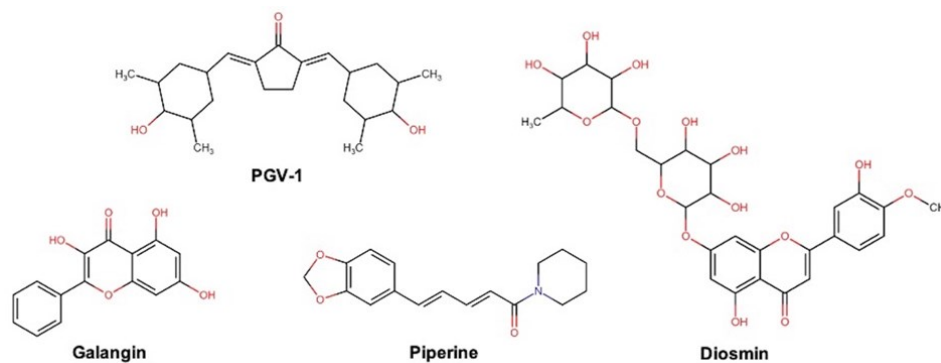


Figure 1. Chemical structures of PGV-1, diosmin, galangin, and piperine (Musyayyadah et al. 2021; Hasbiyani et al. 2021; Endah et al. 2021).

Considering its high cytotoxicity, PGV-1 can be combined with less cytotoxic compounds to lower the PGV-1's dosage but maintain its effectiveness toward cancer cells. Numerous compounds from natural sources have been reported to have cytotoxic activities and are conceivable as combination therapy for colorectal cancer (Rejhova et al. 2018). Recently, combination of PGV-1 with diosmin, galangin, or piperine (Figure 1) presented promising anti-cancer synergisms in triple negative breast cancer cells (Musyayyadah et al. 2021; Hasbiyani et al. 2021; Endah et al. 2021). Diosmin is a methoxy flavonoid that can be found abundantly in *Citrus* sp. (Chen et al. 2020; Utomo et al. 2020) with various pharmacological activities including anti-cancer activity (Zheng et al. 2020) while maintaining its safety (Russo et al. 2018). Another flavonoid that also possesses anti-cancer activities to various cancers is galangin from the rhizome of *Alpinia galanga* (Huang et al. 2020). Additionally, alkaloid piperine found in the most widely used spices, black pepper or other *Piper* species, is also a promising cancer chemoprevention agent

based on its activity on several cancer cell lines (Manayi et al. 2018). Reinforcing the mitotic failure as proven *in vitro*, the bioinformatic analysis confirms that PGV-1 and those above natural compounds target cell cycle protein regulators (Musyayyadah et al. 2021; Hasbiyani et al. 2021; Endah et al. 2021).

Following the combination for breast cancer cells, we further evaluate the PGV-1 combination with diosmin, galangin, or piperine in colon cancer cells. Those three compounds were chosen because of their safety and well-known health beneficial effects. In this study we assessed the synergistic effect of PGV-1 by diosmin, galangin, or piperine in colon cancer cells by a cell viability assay. Thus, their combination with PGV-1 would provide an alternative co-chemotherapy treatment. Further evaluation on PGV-1 and the natural compounds' target proteins that are overexpressed in colon cancer and their effects on patients' survival rate was performed by bioinformatic analysis.

MATERIALS AND METHODS

Materials

PGV-1 with 95% purity was obtained from Cancer Chemoprevention Research Centre (CCRC), Faculty of Pharmacy, Universitas Gadjah Mada (UGM). Diosmin (catalog number #Y0000094), galangin (#282200) and piperine (#P49007) were purchased from Sigma Aldrich (USA). The tested compound was firstly dissolved in dimethyl sulfoxide (DMSO, Sigma) as the stock solution with a concentration of 100,000 μM . The serial dilution was then prepared by diluting the stock in the complete medium with a maximum DMSO concentration of less than 1% in the final concentration. The solution was always prepared freshly before the cell treatment.

Methods

Cell Culture

WiDr cells representing colon adenocarcinoma (COAD) (Chen et al. 1987) as the most common colon cancer were a collection of CCRC, Faculty of Pharmacy, Universitas Gadjah Mada (Wulandari et al. 2021). Cells were cultured in Roswell Park Memorial Institute 1640 (RPMI) medium (Gibco, USA) complemented with 10% fetal bovine serum (FBS) (Gibco, USA) and a final concentration of 50-100 IU/mL penicillin and 50-100 $\mu\text{g}/\text{mL}$ streptomycin (Gibco, USA). The cells were incubated with 5% CO_2 in the 37 °C incubator.

Cell Viability Assay with Direct Counting Method

WiDr cells (1.5×10^4 /well) were distributed into 24-well plates. After reaching about 80% confluency after overnight incubation, the cells were treated with a serial concentration of PGV-1 or natural compounds. Cells were incubated for 24 h and then assayed using the trypan blue exclusion test as modified from previous method (Strober 2015). One part of the cell suspension was mixed with one part of 0.4% trypan blue, incubated for 3 min at room temperature, and the viable cells as unstained cells were counted on the haemocytometer under a microscope. Each concentration was done in triplicate with three times counting for each well. The inhibitory concentration of 50% (IC_{50}) value was calculated by a regression analysis on log concentration versus percentage of cell viability (Musyayyadah et al. 2021). The IC_{50} values were then used as a guide for the combination assay. The combination index (CI) was calculated as described previously (Musyayyadah et al. 2021) by normalizing the percentage of cell viability with respect to the IC_{50} value.

Target Protein Prediction of PGV-1 and Natural Compounds in Colon Cancer

SwissTargetProtein (<http://www.swisstargetprediction.ch>) was used to identify the target proteins (Daina et al. 2019) for PGV-1, diosmin, galangin, and piperine. The UALCAN database (<http://ualcan.path.uab.edu>) was used to access the TCGA dataset for proteins that are overexpressed in colon cancer. To determine overlapping protein targets of the compounds and the overexpressed protein, diagram Venn was utilized using InteractiVenn (<http://www.interactivenn.net>) (Heberle et al. 2015). A MacBook Air with 1,8 GHz Intel Core i5 and 8 GB RAM was used for this analysis.

Expression of Predicted Target Proteins in COAD

UALCAN provides access to the TCGA dataset for the expression of predicted protein targets in normal cells and COAD (Chandrashekar et al. 2017). The collected data from the TCGA dataset was then processed using GraphPad Prism V9. A Hewlett-Packard laptop with AMD Ryzen 3 processor and 4 GB RAM was used for this analysis.

Survival Rate of COAD Patients with Overexpressed Target Proteins

The TCGA dataset for survival rate was accessed using OncoLnc (<http://www.oncolnc.org>) (Anaya 2016). The upper and lower percentiles were both 50:50 to create the optimized result based on the number of samples of COAD patients. All the collected information was prepared using GraphPad Prism V9. The same computer specification as the section above was used for this analysis.

Statistical Analysis

Statistical significance was assayed using GraphPad Prism V9. The parametric test used Student's *t*-test to determine the significance between groups with a 95% confidence level ($p < 0.05$). The normality data was confirmed using the One-Sample Kolmogorov-Smirnov test (Musyayyadah et al. 2021).

RESULTS AND DISCUSSION

Cytotoxicity of PGV-1, Diosmin, Galangin, and Piperine in WiDr Cells

Cytotoxic effect of PGV-1, diosmin, galangin and piperine on WiDr cells was carried out by the direct counting method. Administration of PGV-1 (0.025-2 μ M) or diosmin, galangin, and piperine (10-1,000 μ M) for 24 h showed that all compounds had a dose-dependent cytotoxic activity in WiDr cells (Figure 2). As predicted, PGV-1 showed a remarkable cytotoxic activity with an IC_{50} of 0.08 μ M (Figure 2a). Among the tested natural compounds galangin exhibited the strongest cytotoxicity at IC_{50} of 26 μ M, followed by diosmin and piperine, 133 μ M and 603 μ M, indicating moderate cytotoxicity and not cytotoxic, respectively (Figure 2b, Table 1), based on cytotoxicity classification by World Health Organization (WHO) (Niyibizi et al. 2020).

The Combination Effect of PGV-1 and Diosmin/Galangin/Piperine in WiDr Cells

Based on the IC_{50} values, a combination cytotoxicity test was executed to determine the effect of the natural compounds in increasing PGV-1's effect. One-eighth, quarter, and half of IC_{50} of natural compounds was combined with $\frac{1}{2}$ IC_{50} or IC_{50} of PGV-1. The same direct counting method as the single cytotoxicity assay was employed and the CI was calculated for

Table 1. The IC₅₀ values of PGV-1, diosmin, galangin, and piperine on WiDr cells.

Compound	IC ₅₀
PGV-1	0.08 μM (2.8×10 ⁻² μg/mL)
Diosmin	133 μM (81 μg/mL)
Galangin	26 μM (7 μg/mL)
Piperine	603 μM (172 μg/mL)

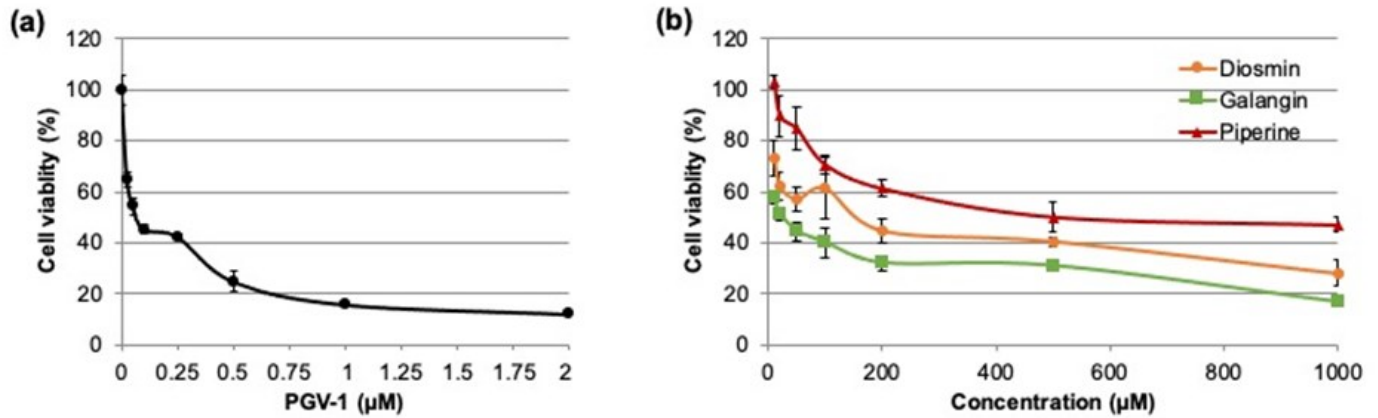


Figure 2. Cytotoxicity of PGV-1 and natural compounds on WiDr cells. Cytotoxicity of PGV-1 (a); diosmin, galangin, and piperine (b). The cell viability was assayed by direct counting and the percentage is presented as average ± SE (*n*=3). The IC₅₀ value was calculated by a regression analysis on log concentration versus percentage of cell viability.

each concentration combination point by normalizing the percentage of cell viability to the respective IC₅₀. CI value of less than 0.9 indicates a synergistic effect (Ikawati & Septisetyani 2018). Even though piperine was not toxic in WiDr cells, almost all the combinations with PGV-1 showed synergistic effects (Figure 3c, Table 2). The combination of PGV-1 and piperine at low concentration resulted in a CI value of 0.2 demonstrating a strong synergy (Table 2). Likewise, all the tested concentrations of galangin gave synergy when combined with low concentration of PGV-1 (Figure 3b, Table 2). Diosmin, on the other hand, showed synergistic effects in all the tested combinations (CI 0.3-0.9) (Figure 3a, Table 2). Taken together, the three tested natural compounds have the ability to inhibit WiDr cell proliferation in combination with PGV-1.

Table 2. The combination index values.

Compound (μM)	Combination index	
	PGV-1 (μM)	
	0.04	0.08
Diosmin		
17	0.5*	0.8*
33	0.5*	0.5*
67	0.6*	0.5*
Galangin		
3	0.7*	1.7
6	0.5*	1.0
13	0.5*	0.9
Piperine		
75	0.2*	0.6*
150	0.4*	0.8*
300	0.7*	1.3

Remark: asterisk indicates synergistic combination.

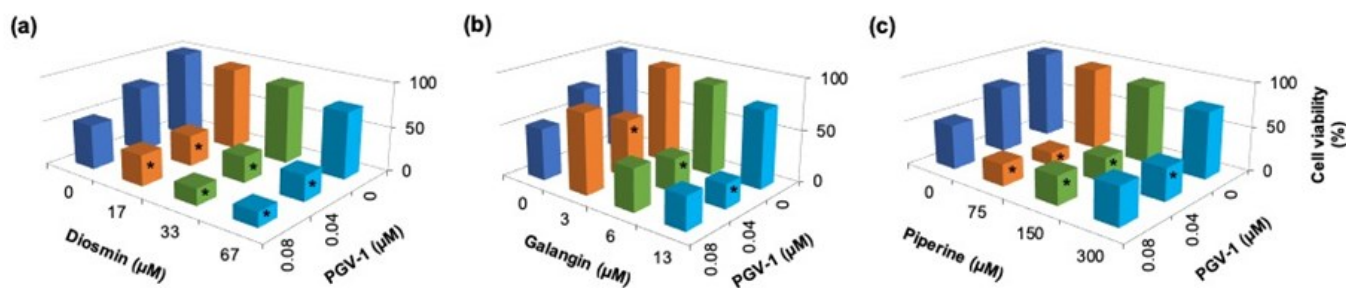


Figure 3. The effect of combination of PGV-1 and diosmin (a), galangin (b), or piperine (c) on WiDr cells. Cells were treated with PGV-1 at $\frac{1}{2}$ or IC_{50} and natural compounds at $\frac{1}{8}$, $\frac{1}{4}$, or $\frac{1}{2}$ IC_{50} in triplicate. The combination index was calculated as previously described by normalizing the percentage of cell viability to the respective IC_{50} value. Asterisk indicates synergistic combination.

Predicted Target Proteins of PGV1 and Diosmin/Galangin/Piperine in Colon Cancer

Predicted target proteins of PGV-1, diosmin, galangin and piperine were explored using the SwissTargetPrediction database ensuing in 100 protein targets from each compound (Figure 4a-c). To find out whether the target proteins of each compound are overexpressed in colon cancer, we searched for overexpressed proteins in the TCGA database using UALCAN, resulting in 300 overexpressed proteins in COAD (Figure 4a-c). To discover the overlap between the PGV-1 and/or each natural compound target protein with the overexpressed protein in COAD, we processed them by using a Venn diagram. Of the 100 predicted compound target proteins, the following proteins are overlapping with overexpressed proteins in COAD: PGV-1: SCD, TOP2A, CDK1, and MET (Figure 4a); diosmin: MMP7, CA9, MMP1, SQLE, and AURKA (Figure 4a); galangin: CA9, MMP3, NEK2, MET, CDK1, and TOP2A (Figure 4b); piperine: AURKA and CDK1 (Figure 4c). A summary of overlapping proteins (11 proteins) can be seen in Table 3.

Expression of Predicted Target Proteins in COAD and the Survival Analysis

To differentiate the expression of the above target proteins in normal cells and cancer cells, we further explored data from the TCGA database. To facilitate access to TCGA, third party websites such as UALCAN were used. We confirmed that the eleven target proteins are significantly overexpressed in COAD when compared to normal cells, all with p values lower than 1×10^{-11} (Figure 5a). Each target protein was then examined for its impact on the patients' survival. From those eleven proteins, we then analysed the effect of high and low expression of the protein in COAD patients. While overexpression 8 of 11 proteins did not negatively

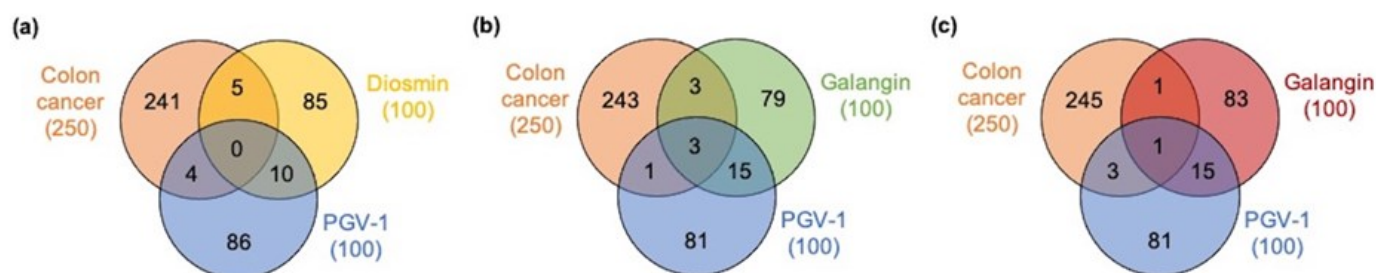


Figure 4. Intercept between overexpressed proteins in colon cancer and target proteins of PGV-1 and diosmin (a), galangin (b), and piperine (c). Predicted target proteins of the compounds was acquired from SwissTargetPrediction. Overexpressed proteins in colon adenocarcinoma were acquired from UALCAN. Venn diagram was created by InteractiVenn.

Table 3. Overlapped target proteins.

Target	Common name	Compound
Cyclin-dependent kinase 1	CDK1*	PGV-1 and galangin/piperine
Hepatocyte growth factor receptor	MET*	PGV-1 and galangin
DNA topoisomerase II alpha	TOP2A*	PGV-1 and galangin
Acyl-CoA desaturase	SCD	PGV-1
Carbonic anhydrase IX	CA9	diosmin, galangin
Serine/threonine-protein kinase Aurora-A	AURKA	diosmin, piperine
Matrix metalloproteinase 7	MMP7	diosmin
Matrix metalloproteinase 3	MMP3	galangin
Matrix metalloproteinase 1	MMP1	diosmin
Squalene monooxygenase	SQLE	diosmin
Serine/threonine-protein kinase NEK2	NEK2	galangin

Remark: asterisk indicates indicates overlapped target protein of PGV-1 and the natural compound.

affect patients' survival rate (data not shown), overexpression of SCD ($p = 0.726$), CA9 ($p = 0.678$), and SQLE ($p = 0.462$) have shown to decrease the survival rate in COAD patients (Figure 5b).

Discussion

We confirmed the high potency of PGV-1 against WiDr colon cancer cells. In this study, we obtained the IC_{50} value of 0.08 μ M, which is lower than those previously reported, 18 μ M (Meiyanto et al. 2018) and 12 μ M (Wulandari et al. 2021). Possibly because of the difference of cell viability assays that were used. In this study we employed a direct counting method rather than an enzymatic colorimetric assay (Aslanturk 2017; Lestari et al. 2019). Nevertheless, the tested natural compounds displayed a similar cytotoxicity profile in WiDr cells as described formerly in 4T1 triple negative breast cancer cells, from the highest to the lowest one is galangin, diosmin, and piperine at the IC_{50} of 120 μ M (Hasbiyani et al. 2021), 389 μ M (Musyayyadah et al. 2021), and 800 μ M (Endah et al. 2021), respectively. Accordingly, the most potent among the tested natural compounds is galangin, followed by diosmin and piperine (Figure 2c). Based on the classification by WHO (Niyibizi et al. 2020), galangin and diosmin are cytotoxic ($IC_{50} < 90 \mu$ g/mL), while piperine is not ($IC_{50} > 90 \mu$ g/mL). Taken together, galangin is the most promising chemoprevention agent among the three tested natural compounds.

Cytotoxic combination assay is a convenient approach to measure the potency of a combination in cancer cells (Avand et al. 2018). In correspondence with the cytotoxicity, the combination assay revealed that galangin shows a solid synergistic effect with low concentration of PGV-1 (Figure 3, Table 2). Each concentration of diosmin also gives synergistic effects in colon cancer cells, similar to the results in breast cancer cells (Musyayyadah et al. 2021). On the contrary to the finding in 4T1 cells (Endah et al. 2021), piperine shows synergism with PGV-1 in WiDr cells, especially at the low concentration of PGV-1. Based on these data, all the three tested natural compounds are promising to be combined with PGV-1.

It is interesting that galangin, diosmin, and piperine act similarly in terms of potentiating of PGV-1 in colon cancer cells despite the different cytotoxic potency. A follow up bioinformatic analysis uncovered that diosmin, galangin, and piperine target the same and different overexpressed proteins in COAD as PGV-1 (Figure 4). Those different protein targets may contribute in resulting a synergistic effect when combined with PGV-1. Most of the overexpressed proteins in COAD that are targets of PGV-1 have roles as catalytic enzymes in degrading extracellular

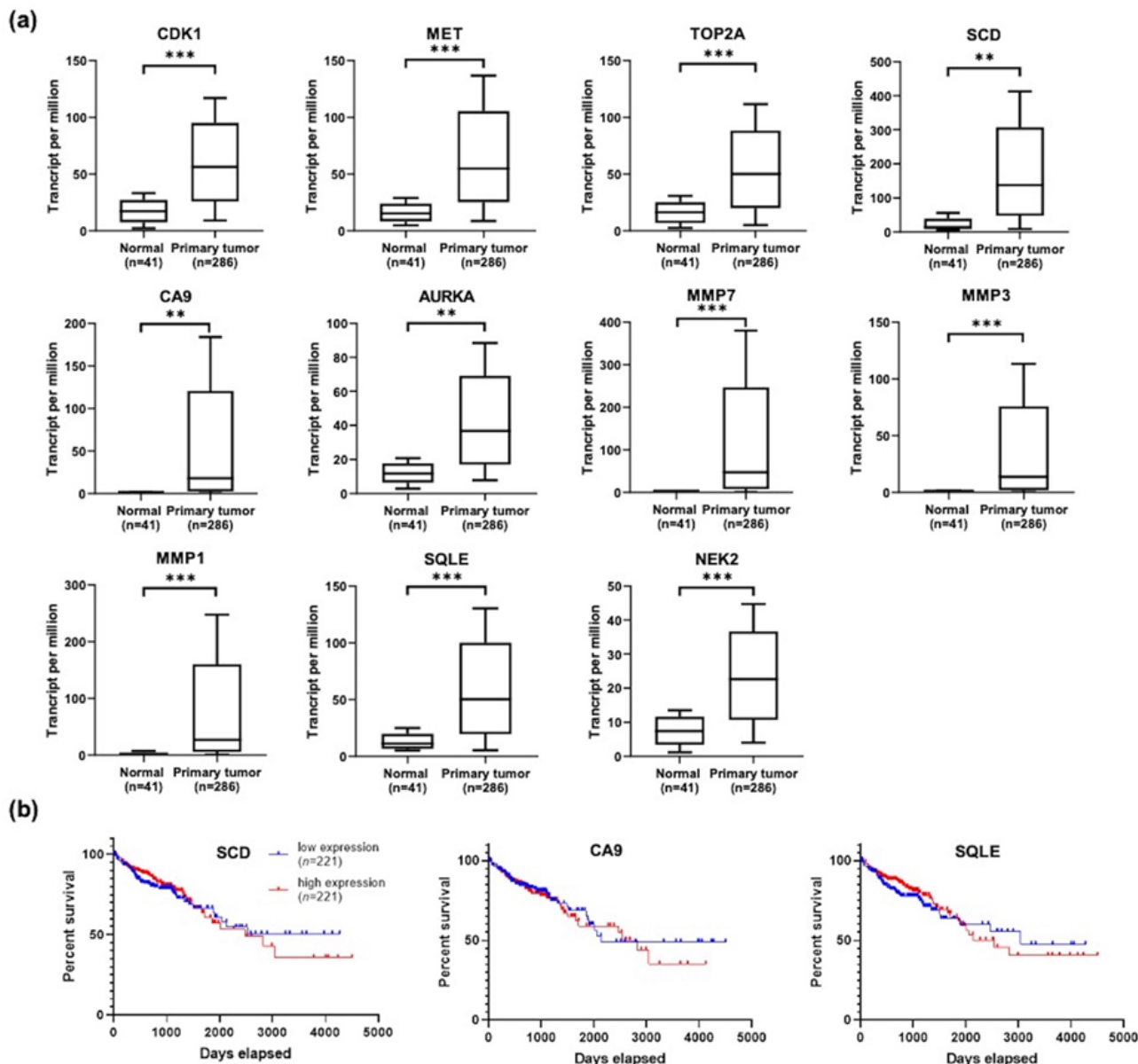


Figure 5. Expression of target proteins in colon cancer (a) and the survival analysis (b). Expression of predicted protein targets was obtained from the TCGA database of UALCAN. Asterisks indicate significant differences between normal and colon adenocarcinoma (**, $p < 0.01$; ***, $p < 0.001$). The percent of survival was analysed by the TCGA dataset accessed via OncoLnc.

matrices and allowing cell migration or invasion, including MMP3, CDK1, AURKA, MMP1, MMP7, MET, SQLE, SCD, and CA9 (Panther Classification System, <http://www.pantherdb.org>). The distinguished effects of galangin are predicted to be caused due to its aim on proteins that are involved in the cell cycle modulation (CDK1 and TOP2A). Meanwhile, diosmin and piperine target proteins that are associated with metabolism (CA9, SQLE) and metastasis (MMP7 and MMP1). Previous studies stated that PGV-1 has a strong antimetastatic activity in colon cancer (Wulandari et al. 2021). Thus, it is worthwhile to further consider the combined effect on metastasis, for example by migration and invasion assay. Additionally, an in silico study by molecular docking can also predict the molecular mechanism of the compounds (Kusuma et al. 2022).

CONCLUSIONS

Among the three tested natural compounds, galangin possesses the highest cytotoxicity in WiDr cells with an IC_{50} of 26 μ M (7 μ g/mL). Nevertheless, based on the combination index, diosmin and piperine also give

synergistic effects, whereas galangin at the concentration of one per eight IC₅₀ exhibits a strongest synergism. Galangin and piperine share predicted protein targets with PGV-1 that are overexpressed in COAD, including CDK1, MET, and TOP2A. On the other hand, the natural compounds also predicted to target proteins that are overexpressed in COAD differently than PGV-1: diosmin targets CA9, AURKA, MMP7, MMP1, and SQLE; galangin targets CA9, MMP3, and NEK2; while piperine targets AUKA. The synergistic effect could also possibly be caused by those different protein targets.

AUTHOR CONTRIBUTION

MI, DDPP, EM designed the study. HM, YMP, UMZ, FW carried out the laboratory works. MI, HM, EM analyzed the data. MI, HM, UMZ wrote the manuscript. EM gave the final approval for the publication. All authors read and approved the final version of the manuscript.

ACKNOWLEDGMENTS

This work was funded by the Indonesian Ministry of Education, Culture, Research and Technology through Penelitian Dasar Unggulan Perguruan Tinggi (PDUPT) 2021 (grant number 6/E1/KP.PTNBH/2021; 006/E4/AK.04.PTNBH/2021; 1623/UN1/DITLIT/DIT-LIT/PT/2021; and 6465/UN1/DITLIT/DIT-LIT/PT/2021 given to MI). The authors thank all members of CCRC Faculty of Pharmacy UGM for their support in this study.

CONFLICT OF INTEREST

The authors declare no conflict of interest regarding the research and the research funding.

REFERENCES

- Allemani, C. et al., 2018. Global Surveillance of Trends in Cancer Survival 2000-14 (CONCORD-3): Analysis of Individual Records for 37513025 Patients Diagnosed with One of 18 Cancers from 322 Population-Based Registries in 71 Countries. *Lancet*, 391(10125), pp.1023-1075. doi: 10.1016/S0140-6736(17)33326-3
- Anaya, J., 2016. OncoLnc: Linking TCGA Survival Data to mRNAs, miRNAs, and lncRNAs. *PeerJ Computer Science*, 2, e67. doi: 10.7717/peerj-cs.67
- Argiles, G. et al., 2020. Localised Colon Cancer: ESMO Clinical Practice Guidelines for Diagnosis, Treatment and Follow-up. *Annals of Oncology*, 31(10), pp.1291-1305. doi: 10.1016/j.annonc.2020.06.022
- Aslanturk, O.S., 2017. In Vitro Cytotoxicity and Cell Viability Assays: Principles, Advantages, and Disadvantages. In *Genotoxicity - A Predictable Risk to Our Actual World*. London: IntechOpen. doi: 10.5772/intechopen.71923
- Avand, A., Akbari, V., & Shafizadegan, S., 2018. In Vitro Cytotoxic Activity of a *Lactococcus lactis* Antimicrobial Peptide Against Breast Cancer Cells. *Iranian Journal Biotechnology*, 16(3), pp.213-220. doi: 10.21859/ijb.1867
- Chandrashekar, D.S. et al., 2017. UALCAN: A Portal for Facilitating Tumor Subgroup Gene Expression and Survival Analyses. *Neoplasia*, 19(8), pp.649-658. doi: 10.1016/j.neo.2017.05.002
- Chen, Q. et al., 2020. Profiling of Flavonoid and Antioxidant Activity of Fruit Tissues from 27 Chinese Local Citrus Cultivars. *Plants*, 9(2), e196. doi: 10.3390/plants9020196

- Chen, T.R. et al., 1987. WiDr is a Derivative of Another Colon Adenocarcinoma Cell Line, HT-29. *Cancer Genetic*, 27(1), pp.125-134. doi: 10.1016/0165-4608(87)90267-6
- Daina, A. et al., 2019. SwissTargetPrediction: Updated Data and New Features for Efficient Prediction of Protein Targets of Small Molecules. *Nucleic Acids Research*, 47(W1), pp.W357-W364. doi: 10.1093/nar/gkz382
- Endah et al., 2021. Piperine Increases Pentagamavunone-1 Anti-cancer Activity on 4T1 Breast Cancer through Mitotic Catastrophe Mechanism and Senescence with Sharing Targeting on Mitotic Regulatory Proteins. *Iranian Journal of Pharmaceutical Research*, 21(1), e123820. doi: 10.5812/ijpr.123820
- Hasbiyani, N.A.F. et al., 2021. Bioinformatics Analysis Confirms the Target Protein Underlying Mitotic Catastrophe of 4T1 Cells Under Combinatorial Treatment of PGV-1 and Galangin. *Scientia Pharmaceutica*, 89(3), e38, doi: 10.3390/scipharm89030038
- Heberle, H. et al., 2015. InteractiVenn: A Web-Based Tool for The Analysis of Sets Through Venn Diagrams. *BMC Bioinformatics*, 16, e169. doi: 10.1186/s12859-015-0611-3
- Huang, H. et al., 2020. Galangin, a Flavonoid from Lesser Galangal, Induced Apoptosis via p53-Dependent Pathway in Ovarian Cancer Cells. *Molecules*, 25(7), e1579. doi: 10.3390/molecules25071579
- Ikawati, M. & Septisetyani, E.P., 2018. Pentagamavunone-0 (PGV-0), A Curcumin Analog, Enhances Cytotoxicity of 5-Fluorouracil and Modulates Cell Cycle in WiDr Colon Cancer Cells. *Indonesian Journal of Cancer Chemoprevention*, 9(1), pp.23-31. doi: 10.14499/indonesianjcanchemoprev9iss1pp23-31
- Kusuma, S.M.W. et al., 2022. Molecular Mechanism of Inhibition of Cell Proliferation: An in Silico Study of The Active Compounds in *Curcuma longa* as An Anticancer. *Journal of Tropical Biodiversity and Biotechnology*, 17(3), jtbb74905. doi: 10.22146/jtbb.74905
- Lestari, B. et al., 2019. Pentagamavunon-1 (PGV-1) Inhibits ROS Metabolic Enzymes and Suppresses Tumor Cell Growth by Inducing M Phase (Prometaphase) Arrest and Cell Senescence. *Scientific Reports*, 9(1), 14867. doi: 10.1038/s41598-019-51244-3
- Manayi, A. et al., 2018. Piperine as a Potential Anti-cancer Agent: A Review on Preclinical Studies. *Current Medicinal Chemistry*, 25(37), pp.4918-4928. doi: 10.2174/0929867324666170523120656
- Meiyanto, E. et al., 2014. Curcumin and Its Analogues (PGV-0 and PGV-1) Enhance Sensitivity of Resistant MCF-7 Cells to Doxorubicin through Inhibition of HER2 and NF-κB Activation. *Asian Pacific Journal of Cancer Prevention*, 15(1), pp.179-184. doi: 10.7314/apjcp.2014.15.1.179
- Meiyanto, E. et al., 2018. Curcumin Analog Pentagamavunon-1 (PGV-1) Sensitizes WiDr Cells to 5-Fluorouracil through Inhibition of NF-κB Activation. *Asian Pacific Journal of Cancer Prevention*, 19(1), pp.49-56. doi: 10.22034/APJCP.2018.19.1.49
- Meiyanto, E. et al., 2019. Anti-proliferative and Anti-metastatic Potential of Curcumin Analogue, Pentagamavunon-1 (PGV-1), Toward Highly Metastatic Breast Cancer Cells in Correlation with ROS Generation. *Advanced Pharmaceutical Bulletin*, 9(3), pp.445-452. doi: 10.15171/apb.2019.053
- Meiyanto, E. et al., 2021. The Target Differences of Anti-Tumorigenesis Potential of Curcumin and its Analogues Against HER-2 Positive and Triple-Negative Breast Cancer Cells. *Advanced Pharmaceutical Bulletin*, 11(1), pp. 88-196. doi: 10.34172/apb.2021.020

- Musyayyadah, H. et al., 2021. The Growth Suppression Activity of Diosmin and PGV-1 Co-Treatment on 4T1 Breast Cancer Targets Mitotic Regulatory Proteins. *Asian Pacific Journal of Cancer Prevention*, 22(9), pp.2929-2938. doi: 10.31557/APJCP.2021.22.9.2929
- Niyibizi, J.B. et al., 2020. Chemical Synthesis, Efficacy, and Safety of Antimalarial Hybrid Drug Comprising of Sarcosine and Aniline Pharmacophores as Scaffolds. *Journal of Tropical Medicine*, 2020, 1643015. doi: 10.1155/2020/1643015
- Rejhova, A. et al., 2018. Natural compounds and combination therapy in colorectal cancer treatment. *European Journal of Medicinal Chemistry*, 144, pp.582-594. doi: 10.1016/j.ejmech.2017.12.039
- Russo, R. et al., 2018. Comparative Bioavailability of Two Diosmin Formulations after Oral Administration to Healthy Volunteers. *Molecules*, 23(9), e2174. doi: 10.3390/molecules23092174
- Siegel, R.L. et al., 2021. Cancer Statistics, 2021. *CA: A Cancer Journal for Clinicians*, 71(1), pp.7-33. doi: 10.3322/caac.21654
- Stoffel, E.M. & Murphy, C.C., 2020. Epidemiology and Mechanisms of the Increasing Incidence of Colon and Rectal Cancers in Young Adults. *Gastroenterology*, 158(2), pp.341-353. doi: 10.1053/j.gastro.2019.07.055
- Strober, W., 2015. Trypan Blue Exclusion Test of Cell Viability. *Current Protocols in Immunology*, 111(1), pp.A3.B.1-A3.B.3. doi: 10.1002/0471142735.ima03bs111
- Sung, H. et al., 2021. Global Cancer Statistics 2020: GLOBOCAN Estimates of Incidence and Mortality Worldwide for 36 Cancers in 185 Countries. *CA: A Cancer Journal for Clinicians*, 71(3), pp.209-249. doi: 10.3322/caac.21660
- Utomo, R.Y. et al., 2020. The Chemopreventive Potential of Diosmin and Hesperidin for COVID-19 and Its Comorbid Diseases. *Indonesian Journal of Cancer Chemoprevention*, 11(3), pp.154-167. doi: 10.14499/indonesianjcanchemoprev11iss3pp154-167
- Wulandari, F. et al., 2020. New curcumin analog, CCA-1.1, synergistically improves the antiproliferative effect of doxorubicin against T47D breast cancer cells. *Indonesian Journal of Pharmacy*, 31(4), pp.244-256. doi: 10.22146/ijp.681
- Wulandari, F. et al., 2021. Curcumin Analogs, PGV-1 and CCA-1.1 Exhibit Anti-migratory Effects and Suppress MMP9 Expression on WiDr Cells. *Indonesian Biomedical Journal*, 13(3), pp.271-280. doi: 10.18585/inabj.v13i3.1583
- Zheng, Y. et al., 2020. Metabolism and Pharmacological Activities of The Natural Health-Benefiting Compound Diosmin. *Food & Function*, 21(10), pp.8472-8492. doi: 10.1039/d0fo01598a

Research Article

Biostratigraphy and Climate Change in the Late Miocene Age Based on Foraminifera in the Oyo Formation, Oyo River Section, Gunung Kidul, Yogyakarta

Adesti Audina Ulfah¹, Akmaluddin^{1*}, Didit Hadi Barianto¹

¹)Department of Geological Engineering, Faculty of Engineering, Universitas Gadjah Mada, Jl. Grafika Bulaksumur No.2, Sleman, Yogyakarta 55284

* Corresponding author, email: akmaluddin@ugm.ac.id

Keywords:

Paleoclimate
Foraminifera
Biostratigraphy
Oyo Formation
Late Miocene

Submitted:

26 January 2022

Accepted:

08 March 2023

Published:

28 June 2023

Editor:

Miftahul Ilmi

ABSTRACT

The date of the paleoclimate event was ascertained using a biostratigraphic analysis. The thickness of the Oyo Formation was measured using measurements with a Jacob stick method, yielding a thickness of 80.8 meters and 23 rock samples. In the Southern Mountains Zone, new result of the age of the upper part of the Oyo Formation by biostratigraphy investigation of the hill Late Miocene (9.79 Ma to 5.78 Ma). Biostratigraphic investigation in the Oyo River revealed 28 species and 9 genera, with two datums. The study area was classified into three biozonations based on the datum found *Globorotalia acostaensis*/M13a/N16 zone, the lower *Globorotalia plesiotumida*/M13b/N17 zone, and the upper *Globigerinoides conglobatus*/M14/N17 zone. The results of a paleoclimate analysis on the Oyo River Section show a general cooling tendency in the study area. Seven paleoclimate zones can be determined from these trends consisting of four warm and three cold zones. Zone I (warm), zone II (cold), zone III (warm), and zone IV (cold) have the coldest peak in the study region in 8.3 Ma, zone V (warm), and zone VI (cold), followed by zone VII (warm). Based on the correlation with other studies (South China Sea, Pacific Ocean, Oyo River, Ngalang River, and Ngioro Section), paleoclimate events in the study area occur globally.

Copyright: © 2023, J. Tropical Biodiversity Biotechnology (CC BY-SA 4.0)

INTRODUCTION

The Late Miocene age period, when the global climate experience a cooling trend, has many fascinating phenomena to investigate (Zachos et al. 2001). The stable oxygen isotope value increased to a maximum of 6.9 million during the Late Miocene, according to Billups (2002). At first, this pattern was thought to increase global ice volume due to a two-step increased benthic foraminiferal $\delta^{18}\text{O}$ values site located on the Atlantic coast of Morocco. Still, after studying the trends associated with cooling the air masses in the Southern Ocean, it was found that after the Middle Pliocene, both the north and south poles were covered in ice. Other changes included the cooling of the ocean, expansion of the Antarctic ice sheet, chunks of ice in the north (predominantly in the North Atlantic), and other changes (Billups 2002). The ratio of oxygen isotopes at 6.8 Ma - 4.8Ma, was used in the study of Rousselle et al. (2013) in the IODP U1338 well in the Pacific Ocean. It is also experiencing a decrease in

temperature. The Middle China paleosol layer between 7.1 Ma - 5.5 Ma shows the dominant winter monsoon. Evidence of hydraulic changes in the South China Sea, changes in vegetation, the average grain size of sediments, and the dominance of mollusk groups that live in dry-cold conditions in China; all support the theory that drying and freezing occurred on the Asian continent at the age of 7 Ma (Holbourn et al. 2018). Significant biological, climatic, and tectonic changes have happened elsewhere, particularly in Asia, Concurrent with advances at both poles. It is, therefore, fascinating to do paleoclimate studies in the Late Miocene.

In Indonesia, the Late Miocene age range also shows a cooling trend by several researchers using foraminifera, nannofossil and isotopes. Van Gorsel & Troelstra (1981) in the Late Miocene to Pliocene age range and Rachmadhan (2019) in the Middle Miocene to Pliocene age range provide evidence of paleoclimate examples utilising foraminifera and Choiriah & Prasetyadi (2020) in the Late Miocene to Early Pliocene age range using nannofossil to determine paleoclimate. The three researchers performed their investigation in the Kendeng Zone. In terms of isotope studies for paleoclimate, one was carried out by Akmaluddin et al. (2010) in the Southern Mountain Zone.

Paleoclimate studies planktonic foraminifera conducted in the Solo River by Van Gorsel & Troelstra (1981) revealed that cooling occurred in the Late Miocene. Rachmadhan (2019), in the Late Miocene age range of the Ngioro Section, there were three paleoclimate climate changes, with a tendency to warm in 8.68 to 6.2 Ma, cooling in 6.2 to 5.72 Ma and cooling in 5.72 to 5.48 Ma. Choiriah & Prasetyadi (2020) in the Kedung Sumber River in the Late Miocene age range also shows a cooling trend.

Akmaluddin et al. (2010) used stable oxygen and carbon isotopes in the Ngalang River in the Oyo Formation in the Late Miocene age range 11 Ma - 9.2. There was a decrease in the stable carbon value and an increase in the stable oxygen value; this is indicated as a cooling trend and coincides with the decline in the Indonesian sea, resulting in a decrease in sea level. However, paleoclimate studies in the Southern Mountains Zone at a younger age range have yet to be carried out, so paleoclimate studies in the upper Oyo Formation have been attempted. One of the locations exposed by Late Miocene sedimentary rocks in the Oyo Formation is in the Oyo River Section, Playen District, Gunung Kidul Regency, Yogyakarta (Figure 1).

Changes in the form of ocean circulation have an impact on basin topography, climate change, and tectonic movements. The flow is affected by a restricted route caused by plate displacement. The walkway is known as a seaway. The Indonesian seaway influences the research area, which results in the closure of the equatorial ocean current system between the Pacific Ocean and the Indian Ocean. The closure of the equatorial ocean current affected temperature changes in Indonesia during the Miocene-Pliocene. Wilson (2008) revealed the closure of the Indonesia seaway, which shows the tectonic movement of the distribution of carbonate rocks in Indonesia, indicating a process of movement of the Australian plate to Eurasia resulted in the closure of the Indonesia seaway (Figure 2).

Biostratigraphic evidence is required to determine when the paleoclimate event occurred. Biostratigraphic studies on planktonic foraminifera were conducted by observing the presence of foraminifera species from foraminifera shells in the form of micro-sized sediment grains discovered after preparation. In contrast, studies on nannofossil were conducted by observing the presence of morphology of nano-sized nannofossil species after smear slides from images. Biostratigraphic research in the Southern Mountain Zone has been carried out by Surono (2009), Akma-

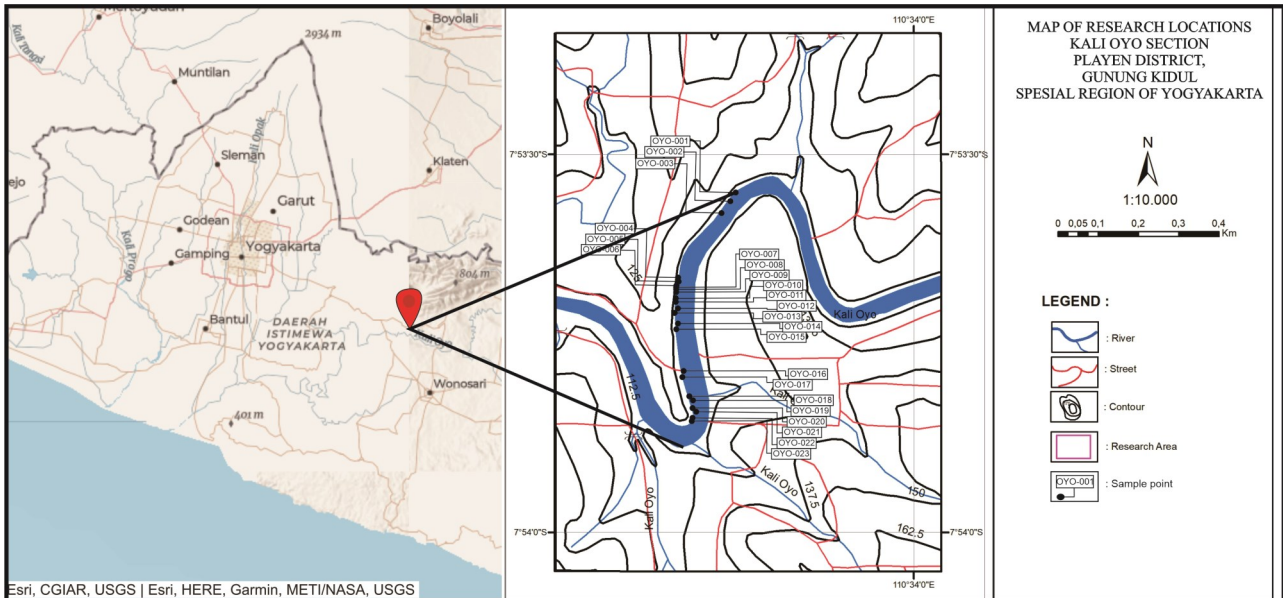


Figure 1. Location of the Research Route in the Oyo River Section, Playen District, Gunung Kidul Regency, Yogyakarta (Badan Informasi Geospasial 2017)

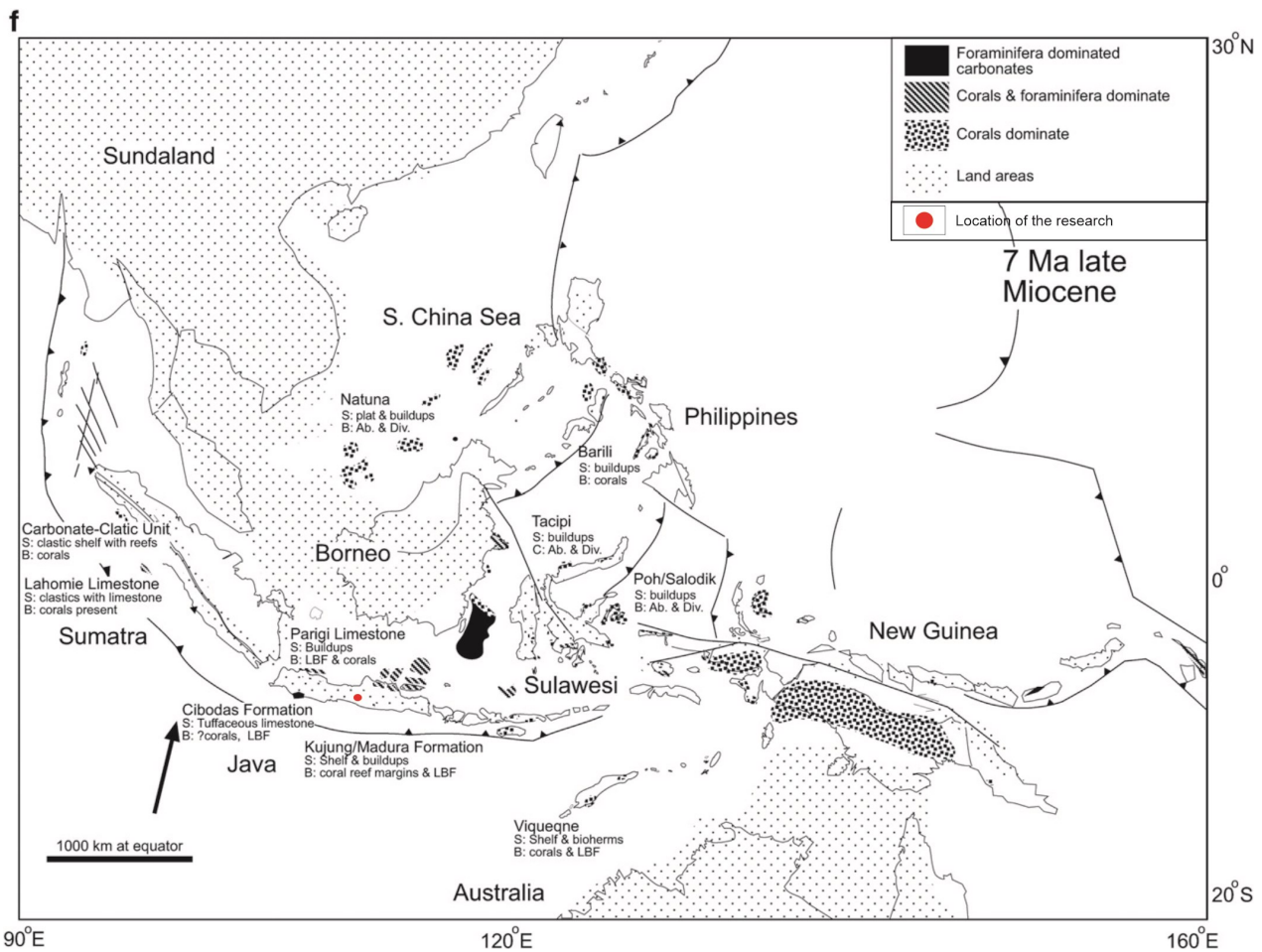


Figure 2. Plate movements during the Late Miocene were based on carbonate development (Wilson 2008).

luddin (2012), and Purbantoro et al. (2020). Surono (2009) using planktonic foraminifera was carried out in the Ngalang River in the Upper Sambipitu Formation during the Early Miocene age (N8), and the Oyo Formation was Early – Middle Miocene (N8-N11). Akmaluddin (2012) in the Ngalang River based on nannofossils from 39 samples, the Early – Middle Miocene Sambipitu Formation (NN2-NN6) and the Late Miocene Oyo Formation (NN8-NN10). In addition, further research on the bound-

aries of the Sambipitu Formation and Oyo Formation on Jalan Ngalang - Gading by [Purbantoro et al. \(2020\)](#) revealed that the Sambipitu Formation is N13-N15 in age, while the Oyo Formation is N14-N16. Despite of several investigations, the upper Oyo Formation has never been the subject of biostratigraphic investigation. Therefore, a thorough biostratigraphic study of the upper Oyo Formation, which represents the Late Miocene age range, is required. This information will then be used to determine when these paleoclimate changes had a place.

Regional Geology

Stratigraphy of the Southern Mountains Zone ([Surono 2009](#)), where Pre-tertiary metamorphic rocks underlie the Southern Mountains Zone. Then on top, they were unconformably deposited sedimentary rocks of the Eocene age, namely the Wungkal Formation and the Gamping Formation. Unconformably deposited in the Kebo Formation and Butak Formation, which are of Late Oligocene – Early Miocene age. The Semilir Formation harmoniously overlays the Kebo-Butak Cluster. Then the Semilir Formation is overlapped in harmony with the Nglanggeran Formation. On top of the Nglanggeran Formation was deposited the Early Miocene Sambipitu Formation, then successively superimposed by the Oyo Formation and the Wonosari Formation on top of Sambipitu Formation. The Oyo Formation is Early Miocene - Middle Miocene, while the Wonosari Formation is Middle Miocene - Late Miocene. Above, the Wonosari Formation is punctuated by the Early Pliocene Kepek Formation.

Based on Figure 3 of the regional geological map ([Surono et al. 1992](#)), the study area is included in the Wonosari Formation. However, this study refers to a research by [Akmaluddin \(2012\)](#), the Oyo Formation includes the research area which its composition is dominated by tuffaceous limestone, tuffaceous marl and well-layered andesitic tuff, with depository and biogenic structures.

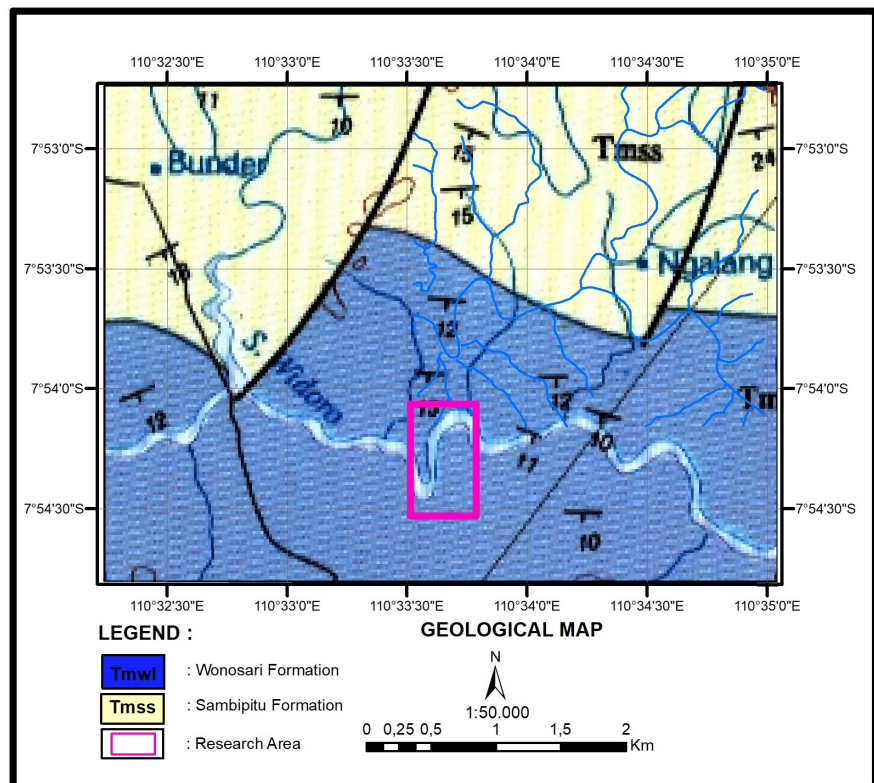


Figure 3. Geological Map of the Study Area, Salatiga Sheet ([Surono et al. 1992](#) in modification).

RESEARCH METHODS

Sampling in the field was carried out by stratigraphic measurements using the Jacob stick method. This study focused on using foraminifera samples due to their abundance and ease of identification also, the depositional environment in shallow oceans made the foraminifera approach more practical. The samples were prepared for planktonic foraminifera weighing 100 grams per sample. Sample preparation was carried out at the Paleontology Laboratory, Gadjah Mada University, starting from mashing the sample, soaking it in a 10% H₂O₂ solution for 1 hour, washing the sampling or sieving it using 3 mesh sizes 16, 30, and 120, then drying the sample using an oven for 4 hours. with a temperature of 70°C. The next stage of determination is identifying the fossils found and counting the number of species obtained. This determination stage refers to Bolli et al. (1989). The determination process was done at the Paleontology Laboratory, Gadjah Mada University, with a 45x magnification binocular microscope. After all, samples had been determined, and biostratigraphic analysis was carried out.

The biostratigraphic analysis uses standard methods by determining the datum based on a species' initial or late appearance. The determination of the datum used refers to Bolli et al. (1989), Blow (1969), and Wade et al. (2011). After the datum was obtained, biostratigraphic zoning was made. The biostratigraphic zone refers to the biozonation of Blow (1969) and Wade et al. (2011).

RESULTS AND DISCUSSION

Research Area Stratigraphy

The Oyo River Section study line's stratigraphic measurements yielded an outcome of 80.8 meters (Figure 4). Sampling was conducted at 1-2 meter intervals beside the empty zone. This investigation yielded 23 samples for biostratigraphic, and paleoclimatic analysis.

The Oyo River Section consists of alternating carbonate sandstones, carbonate tuff sandstones, marl, and limestone, with a laminated top parallel bedding and fine-coarse grain sizes. Tuff nodules are found in several layers (Figure 5). Limestone inserts are found in the middle and bottom of carbonate sandstone lithology at a thickness of 0–5.2 meters. Then, at a thickness of 16.7–20 meters, limestone layers predominate. Two marl strata are 24.9–25.5 meters thick and 30.4–31.3 meters thick. There are alternations of carbonate sandstone limestone layers and carbonate tuff sandstones, with thicknesses ranging from 32.4 to 25.7 meters. There are tuff nodules in several layers, and some have also undergone oxidation. Limestone layers were found between 61.4– 63 meters thick. Carbonate sandstone and limestone alternate with a thickness of 67.5–80.8 meters.

Biostratigraphy

Biostratigraphic analysis of planktonic foraminifera was carried out using a binocular microscope with a magnification of 45x in the study area, which is in the Oyo River Section, Playen District, Gunung Kidul Regency, Yogyakarta. Biostratigraphic analysis of planktonic foraminifera in the study area found rare to moderate foraminifera. From 23 samples, 9 genera and 28 species of planktonic foraminifera were obtained (Figure 6). Two datums were obtained in this study, the first appearance of *Globorotalia plesiotumida* and the first appearance of *Globigerinoides conglobatus*. The Oyo River Section is separated into three zones based on these two datums. The zoning arrangement from old to young (Table 1) includes:

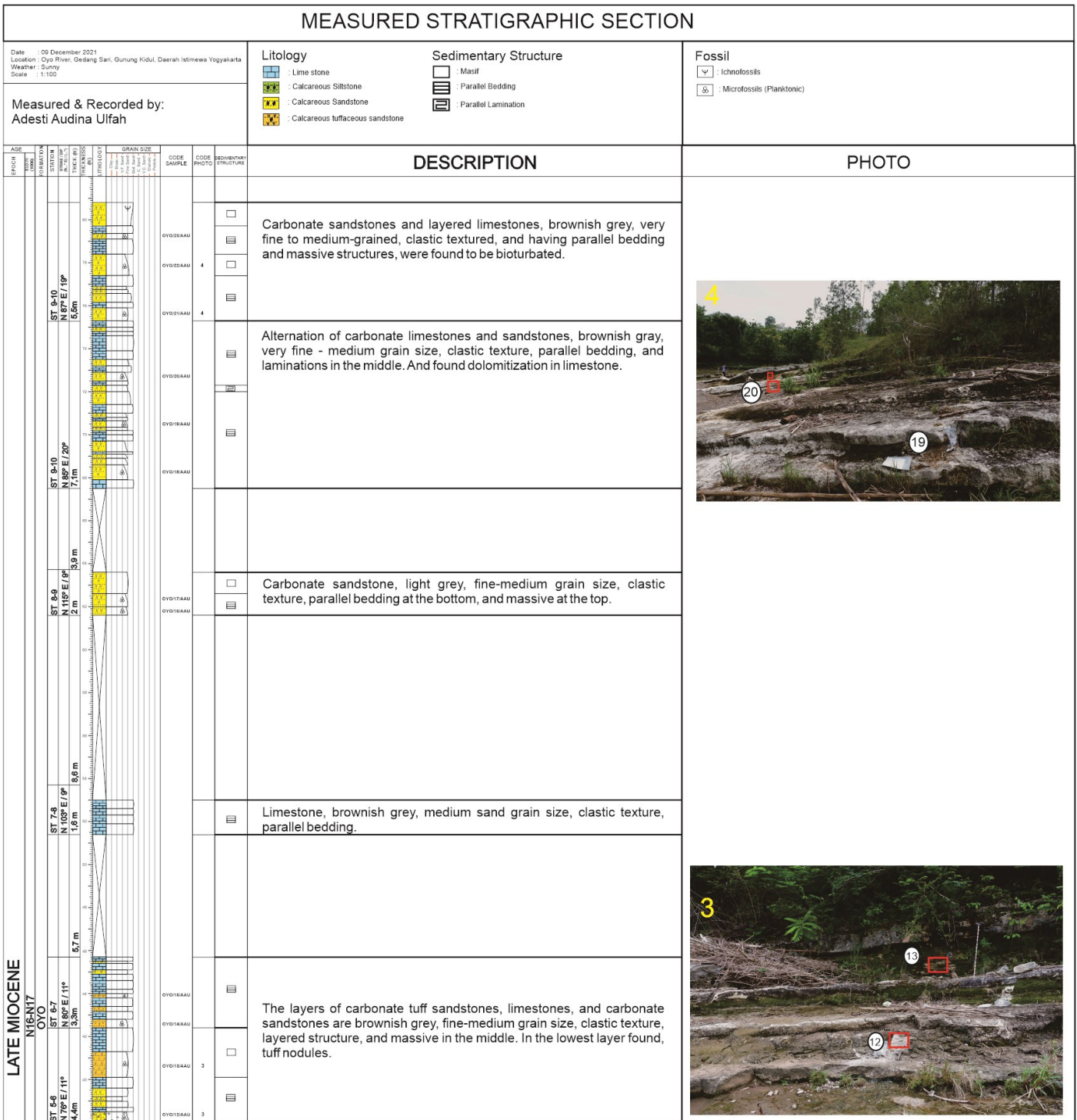


Figure 4. The results of measured stratigraphic measurements on the Oyo River Section with a thickness of 80.8 meters.

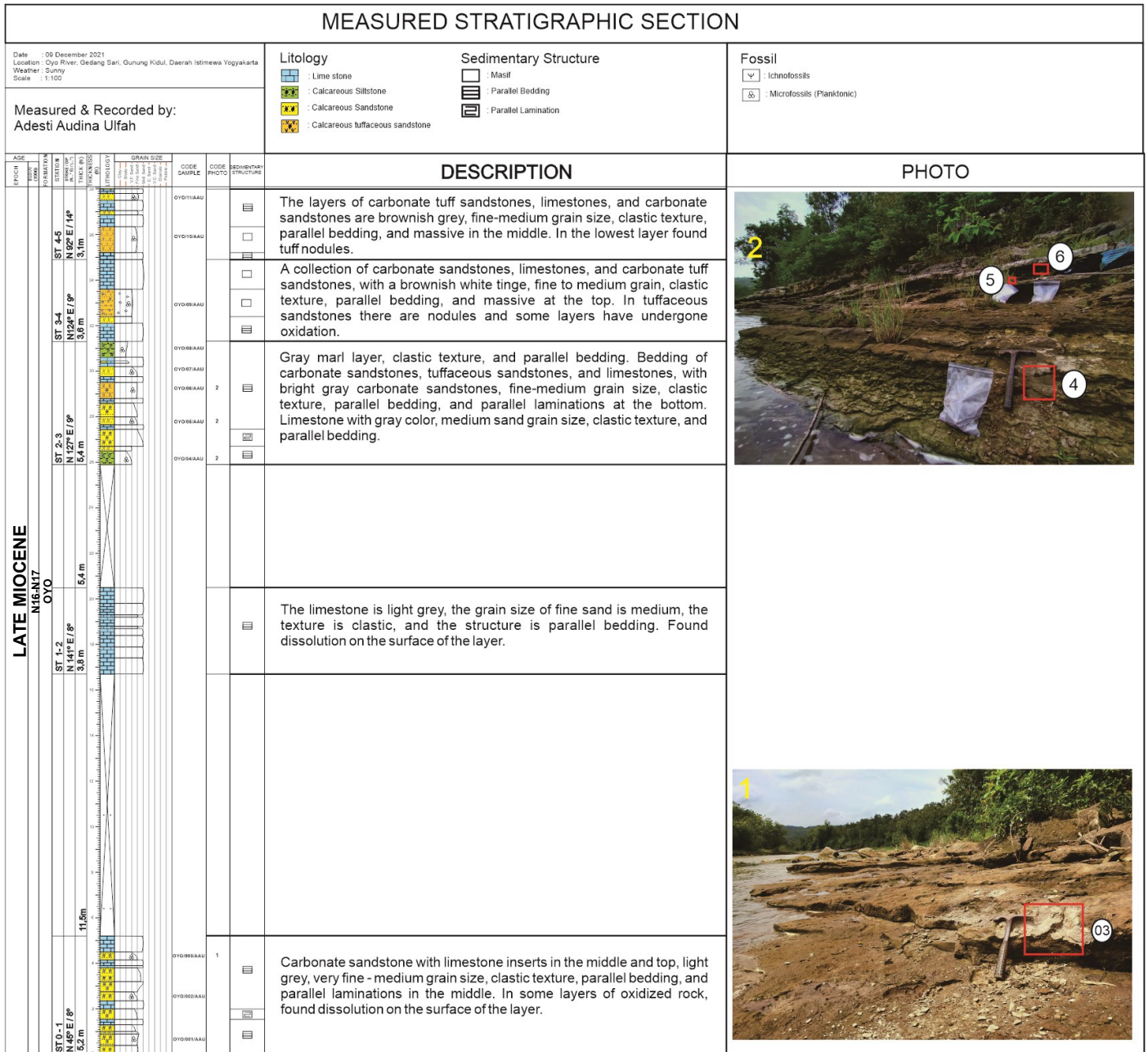


Figure 4. Continued

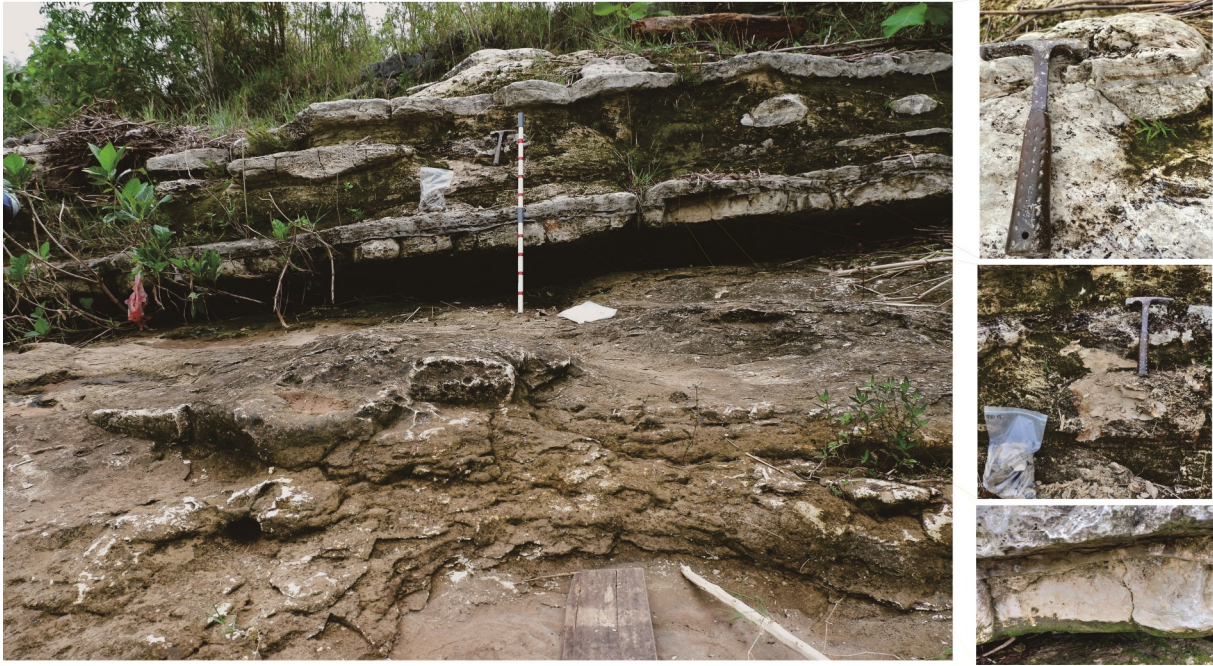


Figure 5. Outcrop photo of carbonate sandstone and limestone on the Oyo River Section with a thickness of 69.2-72 meters with sample code OYO/017/AAU at STA 9-10.

Globorotalia acostaensis / M13a / N16 Zone

The *Globorotalia acostaensis* zone was found in samples OYO/001/AAU – OYO/010/AAU. This zone is characterized by the upper limit of the early appearance of the species *Globorotalia plesiotumida*, while the lower limit is unknown.

Reworked species in this zone are *Globorotalia mayeri* and *Globorotalia fohsi fohsi*. The *Globorotalia acostaensis* zone is by the presence of the *Globigerina venezuelana*, *Globigerinoides bulloideus*, *Globigerinoides quadrilobatus*, *Globorotalia acostaensis*, *Globorotalia humerosa*, *Globorotalia menardii*, *Hastigerina siphonifera*, and *Sphaerodinellopsis seminulina*.

The *Globorotalia acostaensis* zone is equated with the Blow zone (1969) aged N16 (Late Miocene) or in the age range of 9.79 Ma to 8.52 Ma. (Wade et al. 2011). This zone can be compared to the *Globorotalia acostaensis* zone (Blow 1969) or the *Neogloboquadrina acostaensis* zone (M13a) (Wade et al. 2011)

Globorotalia plesiotumida / M13b / N17 Lower Zone

The *Globorotalia plesiotumida* zone was found in sample OYO/011/AAU – OYO/019/AAU. This zone has a lower limit for the early appearance of the species *Globorotalia plesiotumida* and an upper limit for the initial appearance of the species *Globigerinoides conglobatus*.

Reworked species in this zone are *catapsydrax dissimilis* and *Globorotalia fohsi fohsi*. The *Globorotalia plesiotumida* zone is characterized by the presence of the species *Globigerina venezuelana*, *Globigerinoides bulloideus*, *Globigerinoides quadrilobatus*, *Globorotalia acostaensis*, *Globorotalia humerosa*, *Globorotalia menardii*, *Globorotalia plesiotumida*, *Hastigerina siphonifera*, and *Sphaerodinellopsis seminulina*.

The *Globorotalia plesiotumida* zone is equated with the Blow zone (1969) aged N17 Lower (Late Miocene) or in the age range of 8,52 Ma to 6,08 Ma (Wade et al. 2011). This zone can be compared to the *Globorotalia humerosa* zone (Blow 1969), or the *Globorotalia plesiotumida* zone and *Globorotalia languensis* zone (M13b) (Wade et al. 2011).



Figure 6. Assemblages of planktonic foraminifera species in the Oyo River Section (1) *Globigerina venezuelana*, sample OYO/001/AUU; (2) *Pulleniatina obliquiloculata*, sample OYO/007/AA; (3) *Orbulina universa*, sample OYO/004/AUU; (4) *Orbulina bilobata*, sample OYO/002/AAU; (5) *Globoquadrina altispira*, sample OYO/007/AAU; (6) *Globoquadrina dehiscens* sample OYO/006/ AAU; (7) *Hastigerina siphonifera*, sample OYO/001/AAU; (8) *Sphaeroidinellopsis disjuncta*, sample OYO/001/AAU; (9) *Sphaeroidinellopsis seminulina*, sample OYO/004/AAU; (10) *Globigerinoides sacculifer*, sample OYO/006/AAU; (11) *Globigerinoides bulloideus*, sample OYO/006/AAU; (12) *Globigerinoides conglobatus*, sample OYO/020/AAU; (13) *Globigerinoides quadrilobatus*, sampel OYO/003/AAU; (14) *Globigerinoides ruber*, sample OYO/006/AAU; (15) *Globigerinoides trilobus* sample OYO/006/AAU; (16) *Globorotalia acostaensis*, sample OYO/007/AAU; (17) *Globorotalia crassaformis*, sample OYO/006/AAU; (18) *Globorotalia fohsi fohsi*, sample OYO/009/AAU; (19) *Globorotalia humerosa*, sample OYO/004/AAU; (20) *Globorotalia mayeri*, sample OYO/004/AAU; (21) *Globorotalia limbata*, sample OYO/016/AAU; (22) *Globorotalia plesiotumida*, sample OYO/011/AAU; (23) *Globorotalia pseudopima*, sample OYO/002/AAU; (24) *Globorotalia sticula*, sampel OYO/002/AAU; (25) *Catapsydrax dissimilis*, sample OYO/012/AAU. Note: (a) ventral view, (b) dorsal view.

Globigerinoides conglobatus / M14 / N17 Upper Zone

The *Globigerinoides conglobatus* zone was found in sample OYO/020/AAU – OYO/023/AAU. This zone is characterised by the lower boundary of the early emergence of the species *Globigerinoides conglobatus*, while the upper boundary is unknown. No reworked species were found in this zone.

No reworked species were found in this zone. The *Globigerinoides conglobatus* zone is characterised by the presence of the *Globigerina venezuelana*, *Globigerinoides bulloideus*, *Globigerinoides conglobatus*, *Globorotalia acostaensis*, *Globorotalia humerosa*, *Globorotalia menardii*, *Globorotalia plesiotumida*, *Hastigerina siphonifera*.

The *Globigerinoides conglobatus* zone is equated with the Blow zone (1969) aged N17 Upper (Late Miocene) or in the age range of 6,08 Ma to 5,78 Ma (Wade et al. 2011). This zone can be compared to the *Globorotalia humerosa* zone (Blow 1969) or the *Globigerinoides extremus* zone (M14) (Wade et al. 2011).

Paleoclimate

Determination of the paleoclimate in the study area used the method of chamber rotation of *Globorotalia humerosa* and the diameter of the shell *Orbulina universa* and the species *Globigerinoides bulloideus* as warm climate characteristics, with 50 species in each method. Paleoclimate changes in the Oyo River Section, Playen District, Gunung Kidul Regency, Yogyakarta show a cooling trend occurring in the Late Miocene (N16-N17) or the age range 9.79 Ma to 5.78 Ma (Figure 7). The age range obtained is a cross plot of the absolute age of the datum obtained vs. the rock layer thickness measured in the field. From the cooling trend it can be divided into 7 paleoclimate zones (Figure 8) consisting of:

Zone I (Warm)

Zone I includes OYO/001/AAU samples through OYO/003/AAU. This zone is implied as a warmer climate or transition zone towards cold. In this zone, the average diameter of *Orbulina universa* is between 370 µm – 530 µm. In addition, the chamber rotation of *Globorotalia humerosa* has increased in the dextral direction, and the abundance of the warm-characterising species *Globigerinoides bulloideus* has increased. This zone lasts from 9,79 Ma to 9,5 Ma.

Zone II (Cool)

Zone II includes the sample OYO/004/AAU through OYO/006/AAU. This zone is implied as a cold climate. In this zone, the average diameter of *Orbulina universa* is between 424 µm – 499 µm. The chamber rotation of *Globorotalia humerosa* is predominantly sinistral, and the presence of the warm characterising species *Globigerinoides bulloideus* has been reduced in number. This zone extends from 9,5 Ma to 8,75 Ma.

Zone III (Warm/Transition)

Zone III includes the sample OYO/007/AAU through OYO/012/AAU. This zone is implied as a warmer climate or transition zone. In this zone, the average diameter of *Orbulina universa* is between 389 µm – 461 µm. The chamber rotation of *Globorotalia humerosa* has increased in the dextral, and the abundance of the warm-characterising species *Globigerinoides bulloideus* has increased. This zone lasts from 8,75 Ma to 8,45 Ma.

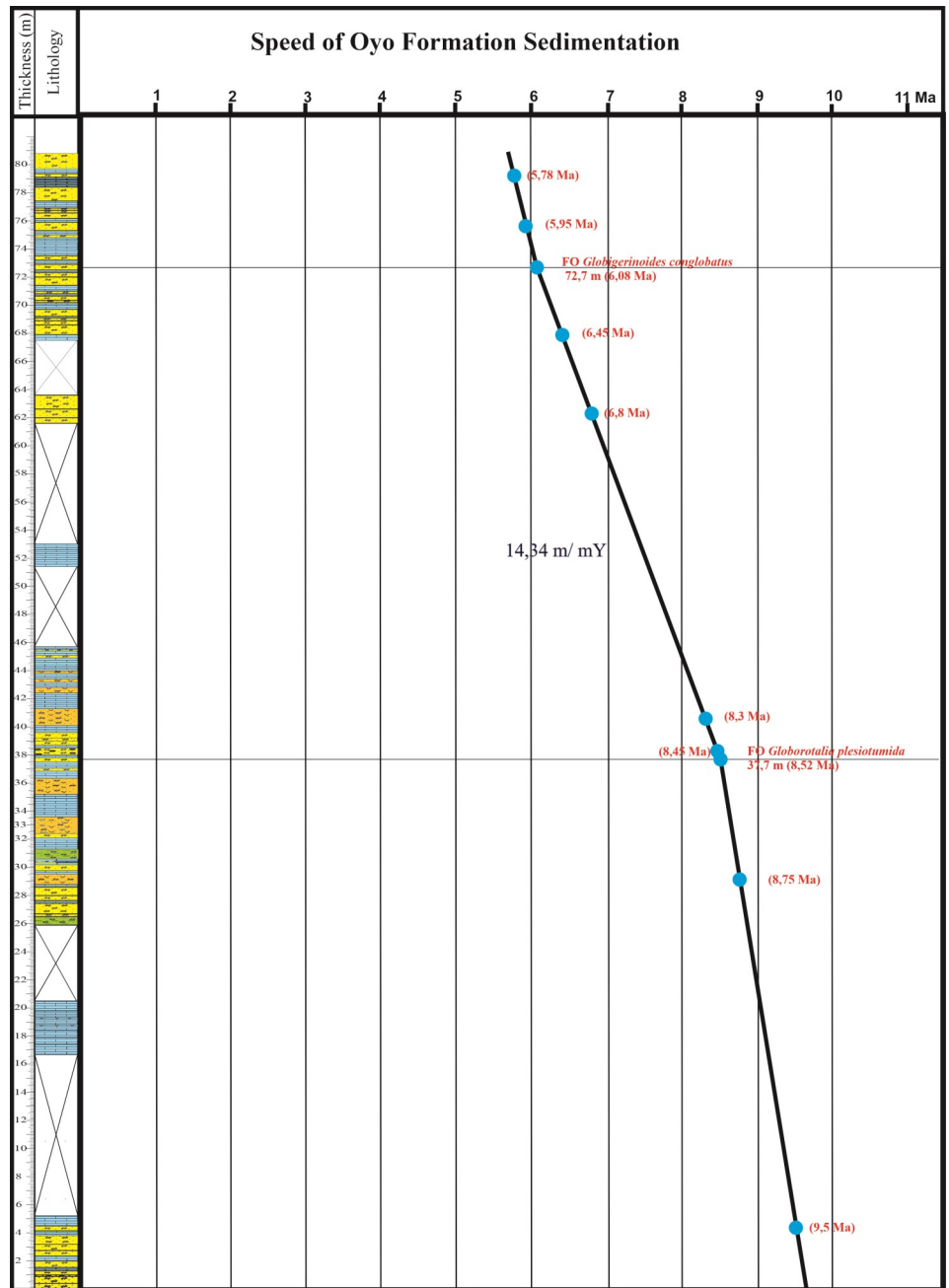


Figure 7. The absolute age of obtained datum vs. rock layer thickness measured in the field in the Oyo River Section. Vertical indicates layer thickness, and horizontal indicates absolute age.

Zone IV (Cool)

Zone IV includes the OYO/013/AAU sample. This zone is implied as a cold climate. In this zone, the average diameter of *Orbulina universa* is 402 μm . The chamber rotation of *Globorotalia humerosa* is predominantly sinistral, and the presence of the warm characterising species *Globigerinoides bulloideus* has been reduced in number. This zone extends from 8,45 Ma to 8,3 Ma.

Zone V (Warm)

Zone V includes OYO/014/AAU samples through OYO/017/AAU. This zone is implied as a warmer climate. In this zone, the average diameter of *Orbulina universa* is between 364 μm – 435 μm . In addition, the chamber rotation of *Globorotalia humerosa* has increased in the dextral direction, and the abundance of the warm-characterising species *Globigerinoides bulloideus* has increased. This zone lasts from 8,3 Ma to 6,8 Ma.

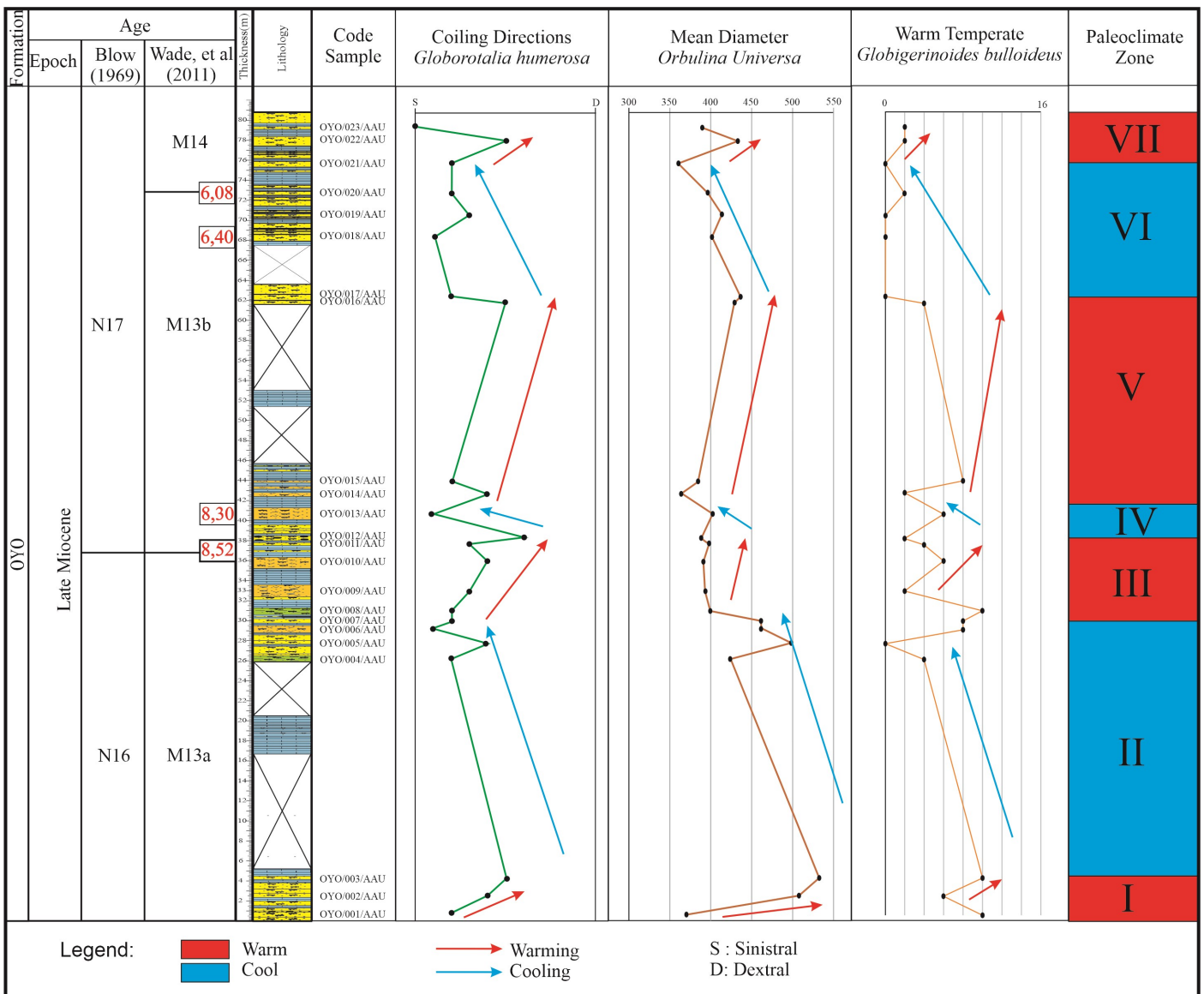


Figure 8. Paleoclimate reconstruction in the study area analysis based on *Globorotalia humerosa* chamber rotation, *Orbulina universa* diameter, and the distinctive species of *Globigerinoides bulloideus*.

Zone VI (Cool)

Zone VI includes the sample OYO/018/AAU through OYO/021/AAU. This zone is implied as a cold climate. In this zone, the average diameter of *Orbulina universa* is between 360 μm - 402 μm. The chamber rotation of *Globorotalia humerosa* is predominantly sinistral, and the presence of the warm characterising species *Globigerinoides bulloideus* has been reduced in number. This zone extends from 6,8 Ma to 5,95 Ma.

Zone VII (Warm)

Zone VII includes the samples OYO/022/ through OYO/023AAU. This zone is implied as a warmer climate or transition zone towards cold. In this zone, the average diameter of *Orbulina universa* is between 389 μm – 433 μm. In addition, the chamber rotation of *Globorotalia humerosa* has increased in the dextral direction, and the abundance of the warm-characterising species *Globigerinoides bulloideus* has increased. This zone lasts from 5,95 Ma to 5,78 Ma.

Discussion

The paleoclimate reconstruction includes the rotation chamber of *Glo-*

borotalia humerosa, the average diameter of *Orbulina universa*, and the warm climate species *Globigerinoides bulloideus*. If the species *Globorotalia humerosa* is found in the left spatial rotation direction, the species lives in a cold climate. Conversely, if it is located in the dextral rotation direction, it indicates that the species lives in an environment with a warm climate. (Jenkins 1967).

Method using the average diameter of *Orbulina universa* species. The larger the diameter of the species indicates that the species lives in an environment with a warm climate, but if the diameter is smaller, the species lives in a cold climate. According to Van Gorsel & Troelstra (1981), *Orbulina universa* species will have a maximum diameter in areas with tropical and subtropical climates.

Then the last method is the species that scharacterise the warm-cold climate, seen from the abundance of the species that scharacterise the warm-cold climate. In this research, the scharacterising species used is *Globigerinoides bulloideus*, which is scharacterised by a scharacterising warm climate (Bicchi et al. 2003). The age of paleoclimate events using the method by (Akmaluddin et al. 2019)

Based on the results of paleoclimate reconstruction using the direction of chamber rotation of *Globorotalia humerosa*, the diameter of *Orbulina universa*, and the characteristic warm species *Globigerinoides bulloideus*, the research area experienced several changes in paleoclimate events. However, if we look at the research area, the overall trend changes are cooling. This change can be seen from the direction of rotation of the chamber *Globrotalia humerosa* to the sinistral direction. In the Range of 8.52 Ma to 6.08 Ma in the study area, there were 3 paleoclimate events: cold, transition, and cold again. There was a change in trend from 8.52 Ma to 8.3 Ma, where there was a cooling trend, then in the age range of 8.3 Ma to 6.8 Ma, which was warmer than the previous trend. It is estimated that this age range is a transition zone. Later paleoclimate trends revealed colder temperatures between 6.8 Ma and 6.08 Ma. Comparisons were made in the study area with existing studies (Figure 9).



Figure 9. The study area is compared with previous researchers in Java, the South China Sea, and the Pacific Ocean (Source: Google Earth).

Compared with research conducted by Holbourn et al. (2018) in the South China Sea using stable oxygen isotopes and carbon from planktonic and benthic foraminifera in the age range of 8.52 Ma to 6.08 Ma, the same trend occurred in the study area. The trend changes from cold, and

then there are a transition or warmer and returns to the cold trend (Figure 10). At 7.7 Ma to 7.2 Ma, based on the existing analysis, the stable oxygen isotope content based on planktonic foraminifera in the South China Sea experiences a warmer or overall trend which can be considered a transition zone before heading to a cooler trend. Although when viewed as a whole in the Range 8.52 Ma to 6.08 Ma in the South China Sea based on data from stable carbon isotopes and stable oxygen isotopes from planktonic and benthic foraminifera, the trend that occurs is dominated by an overall cooling trend.

Rousselle et al. (2013) on the IODP U1338 well in the Pacific Ocean showed a change in trend that occurred in the Late Miocene at 6.8 Ma -5.8 Ma, where there was a decrease in temperature of 1,5°C. The research area in the range of 6.8 Ma – 5.95 Ma is also experiencing a cooling trend, as indicated by the rotation of the *Globorotalia humerosa* shell, which is dominated by sinistral, the average shell diameter of *Orbulina universa* is getting smaller, and the reduced abundance of *Globigerinoides bulloideus* species as a feature of a warm climate.

The study area was compared with the study in Java by Van Gorsel & Troelstra (1981) in the Solo River based on the rotation of the chambers of *Globorotalia menardii* and the diameter of *Orbulina universa*, indicating a change in the cooling trend in the Late Miocene. This trend occurs at the boundaries of N16 and N17 with the species *Globorotalia pleiotumida*. The same thing also happened in the study area. At the boundaries of N16 and N17 or the age range of 8.52 Ma, the study area experienced a change in a cooling trend, indicated by the relatively sinistral rotation of the *Globorotalia humerosa* shell, the smaller the average diameter of the *Orbulina universa*, and reduced species characteristic of *Globigerinoides bulloideus*. Rachmadhan (2019) also conducted a similar study on the Ngioro Section, where at 9.83 Ma – 5.72 Ma, based on planktonic foraminifera, there was a change in trend from cooling, warming, and then cooling. However, in general, the trend was cooling. In a different place, a paleoclimate study conducted by Akmaluddin et al. (2010) in the Ngalang River used stable oxygen and carbon isotopes in the *Globigerinoides sacculifer* shell, showing that there was a temperature change. At

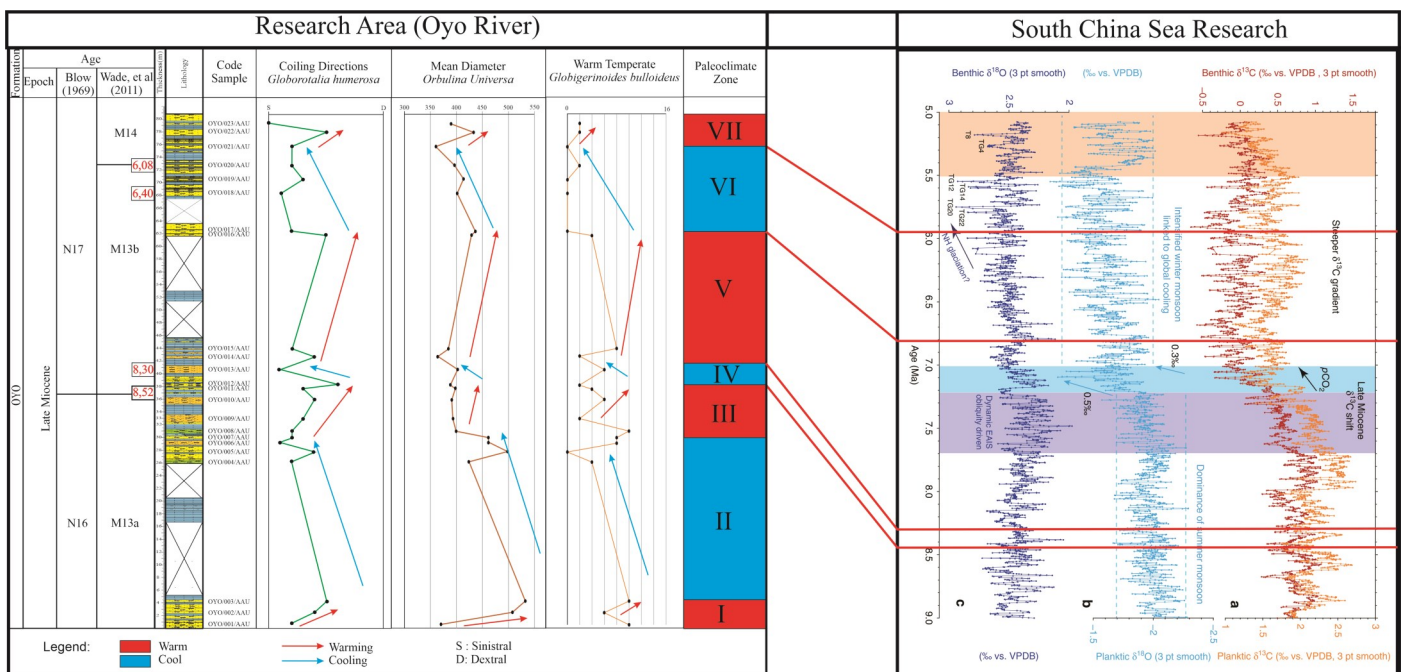


Figure 10. Comparison of the paleoclimate curve of the study area with Holbourn et al. (2018).

9.2 Ma or Late Miocene, this is marked by a decrease in the stable carbon isotope value and an increase in the stable oxygen isotope value, which is indicated as a cooling trend, which coincides with the decline in the Indonesian sea resulting in a decrease in sea level.

Based on a comparison of trends in the study area and other locations (South China Sea, Pacific Ocean, Solo River, Ngalang River, and the Ngioro Section), the paleoclimate in the study area occurs globally. This was initially explained as an increase in global ice volume, but after looking at trends related to the cooling of water masses in the Southern Ocean, cooling in the oceans, expansion of the ice sheet in Antarctica, and ice sheets in the Northern Ocean—hemisphere (predominant in the North Atlantic). The north and south poles were ice-covered after the Middle Pliocene (Billups 2002). Coinciding with the development of ice at both poles, significant ecological, climatic, and tectonic events occurred elsewhere, especially around Asia (Holbourn et al. 2018).

Systematics of Paleontology

Planktonic foraminifera biodiversity was discovered at the Oyo River Section. The samples examined yielded 5 families, 9 genera, and 28 species (Table 2).

CONCLUSION

Based on measured stratigraphic measurements using Jacob's stick method, a thickness of 80.8 meters was obtained. The results of the biostrati-

Table 2. Biodiversity and taxonomy note of foraminifera from Oyo River Section.

Phylum	Class	Order	Family	Genus	Species	
Foraminifera	Globobulimina	Rotaliida	Globigerinidae	Catapsydrax	<i>Catapsydrax dissimilis</i> (Cushman & Bermudez, 1937)	
				Globigerina	<i>Globigerina venezuelana</i> (Hedberg, 1937)	
					<i>Globigerinoides bulloideus</i> (Crescenti, 1966)	
				Globigerinoides	<i>Globigerinoides conglobatus</i> (Brady, 1879)	
					<i>Globigerinoides quadrilobatus</i> (d'Orbigny, 1846)	
				Orbulina	<i>Globigerinoides sacculifer</i> (Brady, 1877)	
					<i>Globigerinoides ruber</i> (d'Orbigny, 1839)	
					<i>Globigerinoides trilobus</i> (Reuss, 1850)	
				Sphaeroidinellopsis	<i>Orbulina bilobata</i> (d'Orbigny, 1846)	
					<i>Orbulina suturalis</i> (Bronnimann, 1951)	
				Catapsydracidae	<i>Orbulina univversa</i> (d'Orbigny, 1839)	
					<i>Sphaeroidinellopsis disjuncta</i> (Finlay, 1940)	
				Globoquadrina	<i>Sphaeroidinellopsis seminulina</i> (Schwager, 1866)	
					<i>Globoquadrina altispira</i> (Chushman & Jarvis)	
				Globorotaliidae	Globorotalia	<i>Globoquadrina dehiscens</i> (Chapman, Parr & Collins, 1934)
						<i>Globorotalia acostaensis</i> (Bolli, 1957)
						<i>Globorotalia crassaformis</i> (Galloway & Wissler, 1927)
<i>Globorotalia fohsi fohsi</i> (Cushman & Ellisor, 1939)						
<i>Globorotalia humerosa</i> (Takayanagi & Saito, 1962)						
<i>Globorotalia limbata</i> (Fornasini, 1902)						
<i>Globorotalia mayeri</i> (Chushman & Ellisor, 1939)						
<i>Globorotalia menardii</i> (Parker, Jones & Brady, 1865)						
<i>Globorotalia plesiotumida</i> (Banner & Blow 1965)						
<i>Globorotalia pertenuis</i> (Beard, 1969)						
Hastigerinidae	Hastigerina	<i>Hastigerina siphonifera</i> (d'Orbigny, 1839)				
Pulleniatinidae	Pulleniatina	<i>Pulleniatina obliquiloculata</i> (Parker & Jones, 1865)				

graphic analysis in the Oyo River Section from 23 samples obtained 9 genera and 28 species. From the analysis, 2 datums were obtained, the initial appearance of *Globorotalia plesiotumida* and *Globigerinoides conglobatus*. From the datum obtained, the study area was divided into 3 biostratigraphic zones, namely the *Globorotalia acostaensis* / M13a / N16 zone in the age range 9.79 Ma – 8.52 Ma, the *Globorotalia plesiotumida* zone M13b / N17 Lower in the age range, 8.52 Ma – 6, 08 mya and Upper M14 / N17 zona *Globigerinoides conglobatus* in the age range 6.08 Ma – 5.78 Ma.

Determination of the paleoclimate in the study area using the chamber rotation method of *Globorotalia humerosa*, the diameter of *Orbulina universa*, and the warm-cold characterising species *Globigerinoides bulloideus*. The research area experienced 7 times the change of paleoclimate events, namely 4 warm and 3 cold zones. However, the paleoclimate change in the study area is experiencing an overall cooling trend when viewed as a whole. Compared to trends in the study area and other locations (South China Sea, Pacific Ocean, Solo River, Ngaling River, and the Ngioro Section), paleoclimate events in the study area occur globally.

AUTHORS CONTRIBUTION

A.A.U. obtained field data, analysed data and created articles for publishing. A. and D.H.B. oversaw all procedures, including data collection, analysis, and paper review.

ACKNOWLEDGMENTS

The researcher wants to express gratitude to everyone who helped carry out this research, from field data gathering to studio and lab analysis. The researcher shows appreciation for the supervising lecturers, the entire Paleontology Laboratory staff, the Department of Geological Engineering, the Faculty of Engineering at Gadjah Mada University, and any other parties who have offered recommendations and guidance on this research. The researcher hopes this research can be expanded in the future and be helpful to many individuals.

CONFLICT OF INTEREST

The authors state that they have no conflicts of interest.

REFERENCES

- Akmaluddin et al., 2010. Miocene warm tropical climate: Evidence based on oxygen isotope in central java, Indonesia. *World Academy of Science, Engineering and Technology.*, 71(11), pp.66–70. doi: 10.5281/zenodo.1063224
- Akmaluddin, 2012. Nannofossils Biostratigraphy Of Miocene Sequences In Southern Mountains, Central Java, Indonesia. *Prosiding Seminar Nasional Kebumihan*, (5), p.11.
- Akmaluddin, A., Agustin, M.V. & Kurniawan A.M., 2019. Stratigraphy and Foraminiferal Biostratigraphy of Sentolo Formation in Sedayu Area: Local Unconformity Identification in Early Pliocene. *Journal of Applied Geology.*, 3(2), pp.32. doi: 10.22146/jag.48596.
- Badan Informasi Geospasial, 2017. Ina Geospasial. viewed 20 October 2021, from <https://tanahair.indonesia.go.id/portal-web>
- Bolli, H.M., Saunders, J.B. & Perch-Nielsen, 1989. *Plankton stratigraphy: volume 1, planktonic foraminifera, calcareous nannofossils and calpionellida* (Vol. 1), Cambridge: Cambridge University Press.

- Bicchi, E., Ferrero, E. & Malgorzata G., 2003. Palaeoclimatic interpretation based on Middle Miocene planktonic Foraminifera: The Silesia Basin (Paratethys) and Monferrato (Tethys) records. *Palaeogeography, Palaeoclimatology, Palaeoecology*, 196(3–4), pp.265–303. doi: 10.1016/S0031-0182(03)00368-7.
- Billups, K., 2002. Late Miocene through early Pliocene deep water circulation and climate change viewed from the sub-Antarctic South Atlantic. *Palaeogeography, Palaeoclimatology, Palaeoecology*, 185(3–4), pp.287–307. doi: 10.1016/S0031-0182(02)00340-1.
- Blow, W. H., 1969. Late Middle Eocene to Recent Planktonic Foraminiferal Biostratigraphy. *Proceedings of the First International Conference on Planktic Microfossils, Micropaleontology (Geneva, 1967)*, 1(1), pp. 199–422.
- Choiriah, S.T. & Prasetyadi, 2020. Paleotemperature Interpretation Based On Calcareous Nannoplankton Of Kedung Sumber River Section, Soko. *Prosiding SEMNAS LPPM*, 2(1), pp.75–83.
- Holbourn et al., 2018. Late Miocene climate cooling and intensification of southeast Asian winter monsoon. *Nature Communications*, 9(1), pp.1–13. doi: 10.1038/s41467-018-03950-1.
- Jenkins, D.G., 1967. Recent Distribution, Origin, and Coiling Ratio Changes in *Globorotalia pachyderma* (Ehrenberg). *Micropaleontology*, 13(2), pp.195. doi: 10.2307/1484670.
- Purbantoro, R., Aini, S.N. & Rizqi, A.H.F., 2020. Konfigurasi Stratigrafi Batas Formasi Sambipitu Dan Oyo Di Jalan Ngalang - Gading, Kecamatan Gedangsari - Playen, Gunung Kidul. *GEODA*, 1(2), pp.81–94.
- Rachmadhan, H.D., 2019. *Biostratigrafi dan Paleoklimat Menggunakan Foraminifera Kecil, Pada Jalur Ngioro Di Cekungan Rembang*. Universitas Gadjah Mada.
- Rousselle et al., 2013. Changes in sea-surface conditions in the Equatorial Pacific during the middle Miocene-Pliocene as inferred from coccolith geochemistry. *Earth and Planetary Science Letters*, 361(4), pp.412–421. doi: 10.1016/j.epsl.2012.11.003.
- Surono, Sudarno, I. & Toha, B., 1992. *Peta geologi lembar Surakarta-Giritontro, Jawa*, Bandung: Pusat Peneliti dan Pengembangan Geologi.
- Surono, 2009. Litostratigrafi Pegunungan Selatan Bagian Timur Daerah Istimewa Yogyakarta dan Jawa Tengah. *Jurnal Geologi dan Sumberdaya Mineral*, 19(3), pp.209–221.
- Van Gorsel, J.T., & Troelstra, S.R., 1981. Late Neogene planktonic foraminiferal biostratigraphy and climatostratigraphy of the Solo River section (Java, Indonesia). *Marine Micropaleontology*, 6(2), pp.183–209. doi: 10.1016/0377-8398(81)90005-0.
- Wade et al., 2011. Review and revision of Cenozoic tropical planktonic foraminiferal biostratigraphy and calibration to the geomagnetic polarity and astronomical time scale. *Earth-Science Reviews*, 104(1–3), pp.111–142. doi: 10.1016/j.earscirev.2010.09.003.
- Wilson, M.E.J., 2008. Global and regional influences on equatorial shallow-marine carbonates during the Cenozoic. *Palaeogeography, Palaeoclimatology, Palaeoecology*, 265(3–4), pp.262–274. doi: 10.1016/j.palaeo.2008.05.012.
- Zachos et al., 2001. Trends, Rhythms, and Aberrations in Global Climate 65 Ma to Present Trends, Rhythms, and Aberrations in Global Climate 65 Ma to Present. *Science*, 292(5517), pp.686–693. doi: 10.1126/science.1059412.

Research Article

Autecology of *Nepenthes* spp. in Peat Swamp and Heath Forest Pematang Gadung, West Kalimantan

Nofi Utari¹, Sulistijorini^{2*}, Nunik Sri Ariyanti²

1)Plant Biology Graduate Program, Department of Biology, Faculty of Mathematics and Natural Sciences, IPB University, Jl. Raya Dramaga, Bogor, West Java, 16680, Indonesia.

2)Department of Biology, Faculty of Mathematics and Natural Sciences, IPB University, Jl. Raya Dramaga, Bogor, West Java, 16680, Indonesia

* Corresponding author, email: sulistijorini@apps.ipb.ac.id

Keywords:

distribution pattern
diversity
population
protected species

Submitted:

16 January 2023

Accepted:

08 March 2023

Published:

07 July 2023

Editor:

Miftahul Ilmi

ABSTRACT

Nepenthes occur in various habitat types in West Kalimantan. But some species are categorized as vulnerable on the IUCN red list. Autecological studies of *Nepenthes* spp. are required for species management and conservation. The study aimed to analyze species diversity, distribution pattern, association, and environmental factors that correlated with *Nepenthes* spp. at peat swamp and heath forest in Pematang Gadung. Data was collected in September 2021 by purposive sampling on 60 plots measuring 3m x 3m in each habitat type. Species diversity was analyzed based on the presence and abundance of species in the plots. The distribution pattern was determined using a standardized Morisita index (I_p). Meanwhile, the association type was determined based on the Jaccard index (JI). Environmental data were analyzed by Canonical Correspondence Analysis (CCA) using Past Version 4.03. This study found six wild species in a peat swamp and four species in a heath forest. The population of *Nepenthes* spp. has clumped distribution pattern with $I_p > 0$. *Nepenthes* spp. are associated with plants such as *Barringtonia racemosa*, *Syzygium* sp., *Nephrolepis biserrata*, and *Camptosperma auriculatum*. The result of CCA revealed that environmental factors in both habitat types affected the presence of each *Nepenthes* species. The air temperature, humidity, soil moisture, and light intensity show different influences on different species.

Copyright: © 2023, J. Tropical Biodiversity Biotechnology (CC BY-SA 4.0)

INTRODUCTION

Nepenthes is the only genus in the family Nepenthaceae. These plants are distributed in Southeast Asia, Seychelles, Madagascar, and Australia (Moran & Clarke 2010). According to Murphy et al. (2020) there were at least 160-180 *Nepenthes* worldwide. *Nepenthes* found in Indonesia consist of 68 species (Mansur 2013). Kalimantan, as a central distribution of *Nepenthes* in Indonesia, has 40 species, and 29 of them are reported as endemic (Dančák et al. 2022).

Nepenthes thrive in lowland tropical rainforest, mountain forest, peat forest, heath forest, limestone mountain, savanna, swamp, and lake (Mansur 2013). *Nepenthes* has leaves that are modified into pitchers as a form of plant adaptation. The pitchers have the function to trap and digest prey (Gilbert et al. 2018; Mithöfer 2022). Pitchers of *Nepenthes* produce 0.2 mL to 1.5 mL of viscous acidic liquid (pH of 3.0-5.5) and contain enzymes to digest the prey, for example, insects (Ravee et al. 2018). *Ne-*

Nepenthes provides ecological advantages such as climate indicator in areas with high annual rainfall, humid, and low soil nutrients (Mansur 2006), absorbing carbon dioxide (CO₂) in the atmosphere (Mansur 2012), supplying nitrogen and phosphorus elements to the soil (Kissinger et al. 2015) and providing food sources for insects (Bauer et al. 2016).

Pematang Gadung Village Forest has a unique ecosystem because it is a swamp forest surrounded by a heath forest. Exploring these habitat types can potentially find endemic and new species of *Nepenthes*. Botanically, the island of Borneo is relatively well-explored in the north (Sabah, Sarawak and Brunei) (Dančák et al. 2022). In contrast, research about *Nepenthes* diversity, especially in peat swamps and heath forests in West Kalimantan, is rarely reported.

An autecological study in Pematang Gadung Village needs to be conducted. Many *Nepenthes* species are threatened due to illegal gold mining activities in this village. This study aimed to analyze *Nepenthes* spp. diversity, distribution pattern, association, and environmental factors that influence the presence of *Nepenthes* spp. in peat swamps and heath forests in Pematang Gadung.

MATERIALS AND METHODS

Study Sites

Study sites located in West Kalimantan at peat swamp (1°56'34.7"S, 110°13'17.6"E in Pematang Gadung Village Forest about 7,004 ha), and heath forest (1°55'18.3"S, 110°16'48.2"E outside the Pematang Gadung Village Forest area, next to a swamp forest) (Figure 1). The study site has an altitude of 2–29 meters above sea level (masl), with flat to sloping (0–8%) topography. Based on climate data from Indonesian Agency for Meteorological, Climatological and Geophysics (BMKG), Pematang Gadung has rainfall of 3,871.2–4,352 mm/year, air temperatures of 23.2–30.3°C, air humidity 68–95% and wind speeds of 0–4 m/s.

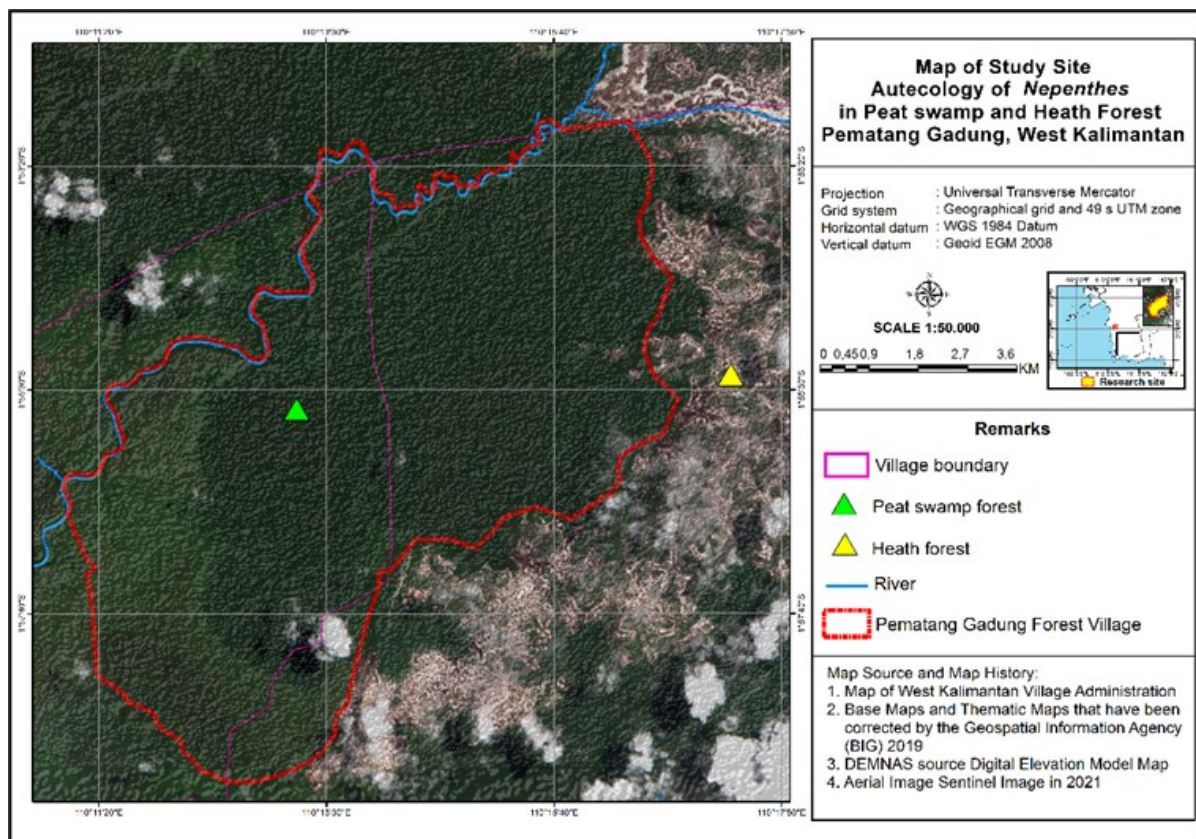


Figure 1. Map of study site in a peat swamp and heath forest Pematang Gadung.

Data Collection

This study was conducted in September 2021. The presence of *Nepenthes* spp. was selected through survey and exploration during the study. Sixty plots of 3m x3m were purposively placed in peat swamps and heath forests. Purposive sampling was chosen for an in-depth investigation to define characteristics for a purpose relevant to the study. Purposive sampling provides a sample that can logically assume to represent the population (Palinkas et al. 2015). The number of *Nepenthes* counted as one individual if more than half of the plant was in the plot. *Nepenthes* were identified using literatures (Cheek & Jebb 2001; Mansur 2006). Meanwhile, the associated plants were observed and identified using (Soepadmo et al. 1995) and websites (<https://powo.science.kew.org/> and <https://www.asianplant.net/>).

Abiotic data collection, including air temperature, humidity, light intensity, and wind speed, was measured using a handheld 4-in-1 environment meter. Soil samples were collected in 1 kg from 10 points of each habitat type at 10–20 cm depth using a sample ring. Then prepared by removing litter residues and plant root debris for physical and chemical analysis.

Data Analysis

The composition of the *Nepenthes* species and the Important value index (IVI) are calculated using the formula (Mueller-Dombois & Ellenberg 1974) as follows:

$$\text{Density} = \frac{\text{No. of individuals of a species}}{\text{Sampling plot area}}$$

$$\text{Relative Density (RD)} = \frac{\text{Density of species}}{\text{Density of all the species}} \times 100\%$$

$$\text{Frekuensi (F)} = \frac{\text{No. of plot of occurrence of species}}{\text{total of plot}}$$

$$\text{Relative Frequency (RF)} = \frac{\text{Frequency of a species}}{\text{frequency of all the species}} \times 100\%$$

$$\text{Important value index (IVI)} = \text{RD} + \text{RF}$$

The Shannon-Wiener formula calculates the diversity index species (H') (Shannon 1948), dominance index (D) is calculated to determine the degree of species dominance (Odum 1993). The evenness index (e) estimates the distribution of individual species within a community (Krebs 1989). The formulas used were as follows:

$$H' = -\sum \left(\frac{n_i}{N} \right) \ln \left(\frac{n_i}{N} \right)$$

$$D = \sum_{i=1}^n \left(\frac{n_i}{N} \right)^2$$

$$e = \left(\frac{H'}{\ln S} \right)$$

Where: n_i is the number of individual species, N represents the number of individuals of the whole species, and S represents the number of species.

The distribution pattern of *Nepenthes* was analyzed using a Standardized Morisita Index (I_p) (Krebs 1989). Using the formulas:

$$I_d = n \left[\frac{\sum x^2 - \sum x}{(\sum x)^2 - \sum x} \right]; M_u = \frac{\sum \chi^2_{0.975-n} + \sum x_i}{\sum x_i - 1}; M_c = \frac{\sum \chi^2_{0.0255-n} + \sum x_i}{(\sum x_i) - 1}$$

$$\text{If } I_d \geq M_c \geq 1, I_p = 0.5 + 0.5 \left(\frac{I_d - M_c}{n - M_c} \right)$$

$$\text{If } I_d > M_c > 1, I_p = 0.5 \left(\frac{I_d - M_c}{M_c - 1} \right)$$

$$\text{If } 1 > I_d > M_u, I_p = -0.5 \left(\frac{I_d - M_u}{M_u - 1} \right)$$

$$\text{If } 1 > M_u > I_d, I_p = -0.5 + 0.5 \left(\frac{I_d - M_u}{M_u} \right)$$

Where: I_d is the Morisita index, n is the number of observation plots, x is the number of *Nepenthes* individuals in plots, M_u is the uniformity index, $\chi^2_{0.975}$ is the chi-square table with a confidence interval of 97.5%, M_c is the clumping index, $\chi^2_{0.0025}$ is the chi-square table with a confidence interval of 2.5%.

Association analysis was determined using a 2x2 contingency table, and the degree of association was calculated using the Jaccard index (JI) (Mueller-Dombois & Ellenberg 1974). Using the formula:

$$JI = \frac{a}{(a+b+c)}$$

Where a: a is the number of plots found *Nepenthes* and others species, b is the number of plots found *Nepenthes*, c is the number of plots found others species.

Canonical Correspondence Analysis (CCA) using Past software version 4.03 was used to examine the correlation between environmental conditions and the existence of *Nepenthes* (Hammer et al. 2001).

RESULTS AND DISCUSSION

Habitat Characteristics of *Nepenthes*

Peat swamp forest is characterized by relatively dense canopy cover, wet soils, low light intensity, and rich leaf litter on the forest floor. Peat swamp is naturally often waterlogged and the water surface and peat surface are highly acidic (Page et al. 1999; Tanjung et al. 2020). The Pematang Gadung Village Forest area is a coastal peat dome located between the Pawan and Pesaguhan Rivers. The floral composition of the peat swamp forest consists of *Aglaia rubiginosa* (Hiern) Pannell, *Baccaurea* sp., *Combretocarpus rotundatus* (Miq.) Danser, *Cratoxylum glaucum* Korth., *Diospyros* spp., *Pandanus* spp., and *Syzygium* spp. In this area, *Gonyostylus bancanus* (Miq.) Kurz was also found. This species is a peat swamp endemic plant, categorized as an endangered species.

In contrast, heath forest has low canopy cover with high light intensity, located close to illegal gold mining sites. The forest floor is covered with white quartz sand; trees have small trunk sizes with tight branches (Whitten et al. 1987). The trees commonly found in this area include *Baeckea frutescens* L., *Cratoxylum glaucum* Korth., *Melaleuca cajuputi* Maton & Sm. ex R. Powell, *Rhodomyrtus tomentosa* (Aiton) Hassk, and *Tristaniopsis obovata* Benn. Ferns and Cyperaceae species are also found, such as *Dicranopteris linearis* (Burm.f.) Underw. and *Scleria biflora* Roxb.

Nepenthes thrive in peat swamps and heath forests, growing in the ground or climbing a host tree. Generally, *Nepenthes* are vines or subscandent scrubs that grow and attach to adjacent trees using looped tendrils. We did not find differences in *Nepenthes* habits in either peat swamp or heath forest.

Species Richness

We recorded four species from the heath forest, *Nepenthes ampullaria* Jack, *Nepenthes gracilis* Korth., *Nepenthes mirabilis* (Lour.) Druce, and *Nepenthes rafflesiana* Jack. These species are also found in peat swamp forest and we recorded two other species from this forest, *Nepenthes bicalcarata* Hook.f. and *Nepenthes x hookeriana* Lindl. (Figure 2). *N. bicalcarata* is an endemic species to Borneo. The latest species is a hybrid of *N. ampullaria* and *N. rafflesiana* (Clarke 2001). *N. bicalcarata* has never been reported to be found in Ketapang Regency (Sunardi & Mansur 2021), so it is the first report of *N. bicalcarata* from Ketapang Regency. *N. reinwardtiana* Miq. can be found in a peat swamp and heath forests (Rantau et al. 2019; Wulandari et al. 2020) but has not been found in this study. *N. reinwardtiana* prefers to grow in open areas (Hariyadi 2013). Nevertheless, degradation in the heath forest due to illegal gold mining may cause this species to be absent at the study site.



Figure 2. *Nepenthes* spp. found in Pematang Gadung Village Forest, West Kalimantan (A) *N. ampullaria*; (B) *N. bicalcarata*; (C) *N. gracilis*; (D) *N. mirabilis*; (E) *N. rafflesiana*; (F) *N. x hookeriana*

Diversity and Distribution Pattern of *Nepenthes* spp.

The most common species found in the peat swamp forest Pematang Gadung Village are *N. ampullaria*. This species, with a density value of 3,370 ind/ha, is predominant since it has the highest (IVI 115.13%) in the peat swamp forest (Table 1). Generally, *N. ampullaria* is abundant in humid conditions, with high water availability and shaded areas (Moran et al. 2003; Nurhadi et al. 2018). This kind of condition is found in Pematang Gadung Village Forest.

Furthermore, a community of *Nepenthes* in the heath forest was dominated by *N. gracilis*, (4,241 ind/ha, IVI 170.36%) (Table 1). This species thrives in heath forest probably because heath forest in Pematang Gadung has lower canopy cover and higher light intensity (479–1987 lux) than in peat swamp forest. *N. gracilis* prefers to grow in conditions with high light intensity. According to Armanda, et al. (2020), *N. gracilis*

Table 1. Density and IVI of *Nepenthes* spp. in peat swamp and heath forest.

Site	Species	D (ind/ha)	RD (%)	RF (%)	IVI (%)
Peat swamp	<i>N. ampullaria</i>	3,370	64.31	50.82	115.13
	<i>N. bicalcarata</i>	148	2.83	4.92	7.74
	<i>N. gracilis</i>	130	2.47	3.28	5.75
	<i>N. mirabilis</i>	296	5.65	8.20	13.85
	<i>N. rafflesiana</i>	1,222	23.32	31.15	54.47
	<i>N. x hookeriana</i>	74	1.41	1.64	3.05
Heath	<i>N. ampullaria</i>	56	1.18	2.78	3.95
	<i>N. gracilis</i>	4,241	89.80	80.56	170.36
	<i>N. mirabilis</i>	37	0.78	2.78	3.56
	<i>N. rafflesiana</i>	389	8.24	13.89	22.12

Remarks: D: density; RD: relative density; RF: relative frequency; IVI: important value index

dominates in heath forests because this species is often more adaptable than others.

N. ampullaria and *N. rafflesiana* prefer to thrive in shaded habitats with high soil moisture. We found these species more abundant in the peat swamp forest compared to the heath forest. In this study, we reported that *N. bicalcarata* was found in peat swamps. The density of *N. bicalcarata* in peat swamp forests is poor (148 ind/ha). In contrast, *N. bicalcarata* is not found in heath forests, probably due to high temperatures. *N. bicalcarata* grow optimally at 18–29°C (Mansur 2006).

N. x hookeriana was rarely found in the peat swamp forest (74 ind/ha, IVI 3.05%) and absent in the heath forest. This species is usually found in limited quantities among the parent species. *N. mirabilis* in the heath forest has the lowest density (37 ind/ha); it might be due to competition with the other species, primarily the dominant species, *N. gracilis*.

Diversity of *Nepenthes* in the peat swamp forest of Pematang Gadung is slightly higher compared with the heath forest. The diversity of *Nepenthes* is categorized as medium ($H' = 1.04$) in the peat swamp forest and low ($H' = 0.39$) in the heath forest (Figure 3a). This data is supported by the values of the dominance and evenness index (Figure 3b, 3c). High diversity, evenness, and density of species in the community indicate the availability of niches, so it is important to maintain their sustainability (Benayas et al. 1999). To avoid their extinction and ensure the availability of genetic material for development efforts, ex-situ conservation and cultivation are necessary.

High dominance index (0.81) makes *Nepenthes* diversity low in heath forests (Figure 3b). A high dominance value indicates that the habitat has low species diversity with an uneven number of species distribution. However, the dominant species with a high IVI score need conserving to maintain species composition. Decreasing species diversity will reduce competition between species and increase competition for each species. *Nepenthes* in peat swamp and heath forest is categorized as having an uneven distribution of the number of species with a value of $(e) \leq 0.50$ (Figure 3c). Diversity and low evenness in the community caused by species dominance may indicate competition for resources and limited niches to occupy (Wilsey & Polley 2004).

Nepenthes spp. have a clumped distribution pattern ($I_p > 0$) in both peat swamp and heath forest of Pematang Gadung (Table 2). These results are in line with reports from previous studies elsewhere (Payung et al. 2021; Apriyanto et al. 2021). *Nepenthes* tends to be clumped and thrive in forests with acidic soils that are nutrient-poor and seasonally wet (Damit et al. 2017).

Table 2. Distribution pattern of *Nepenthes* spp. in peat swamp and heath forest.

Species	Peat swamp		Heath	
	Ip	Distribution Pattern	Ip	Distribution Pattern
<i>N. ampullaria</i>	0.52	Clumped	0.58	Clumped
<i>N. bicalcarata</i>	0.73	Clumped	-	-
<i>N. gracilis</i>	0.51	Clumped	0.50	Clumped
<i>N. mirabilis</i>	0.64	Clumped	0.03	Clumped
<i>N. rafflesiana</i>	0.53	Clumped	0.55	Clumped
<i>N. x hookeriana</i>	0.50	Clumped	-	-

Remarks: Ip: standardized Morisita index value

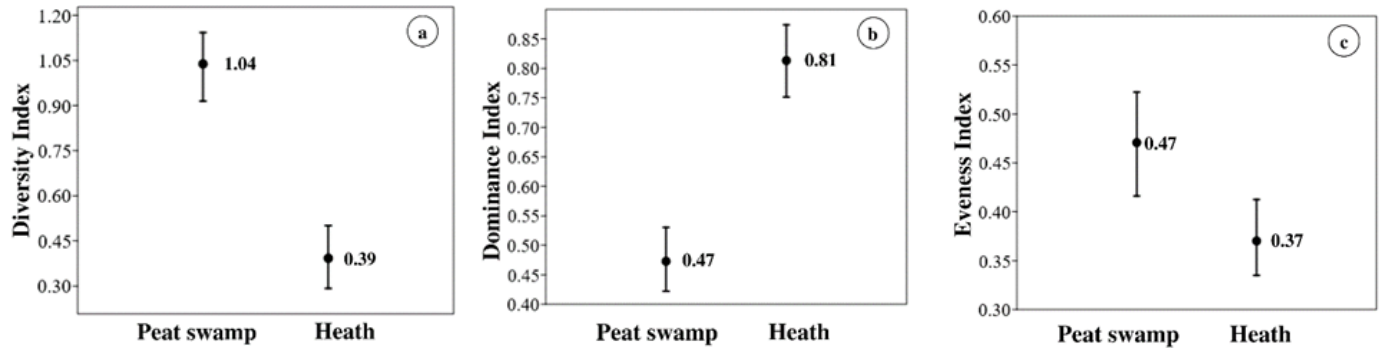


Figure 3. (a) Diversity index value; (b) Dominance index; (c) Evenness index; bar line in graph shows error bar.

Clumped distribution occurs due to generative reproduction supported by environmental conditions. When released and carried by the wind, *Nepenthes* seeds that are thread-shaped with thin wings will fall not far from the *Nepenthes* parent. It is because trees near the *Nepenthes* can restrict the movement of their seeds. Vegetative reproduction in *Nepenthes* also caused clumped distribution patterns. Vegetative reproduction in *Nepenthes* with developing basal shoots that arise from axillary buds along stems at ground level (Lam et al. 2020).

***Nepenthes* spp. Association with other Plants**

Associations influence the occurrence of each species in its habitat. *Nepenthes* spp. in peat swamps and heath forests may have a positive association with a plant species and negative association with the other (Table 3). Positive associations between species indicate differences in resource use and non-competitive interactions between species, while negative associations occur due to competition that can inhibit the presence and abundance of other species (Maire et al. 2012; Sritharan et al. 2021). The positive association between *Nepenthes* species and other plants indicates that these plants can be a climbing tool for *Nepenthes*. In addition, other plants also contribute litter to the pitchers of *N. ampullaria*, which is a semi-detritivorous species.

N. mirabilis tends to coexist with *Barringtonia racemosa* in peat swamp forests (JI 0.60). *N. mirabilis* also associates with other species in peat swamp forests, such as *Poikilospermum suaveolens*. This species was found in plots with low canopy cover, where light can reach the forest floor. In this study, *N. mirabilis* often occupied open areas close to river, whereas *N. ampullaria* did not thrive in these niches. Habitat specification occurs to avoid competition with dominant species (Calatayud et al. 2020). Therefore, associations in species with low abundance suggest that the species may not compete with dominant species for the same resources.

The endemic species, *N. bicalcarata* is positively associated with *Antidesma coriaceum*. *Antidesma coriaceum* is often found in plots where *N.*

Table 3. Chi-square (χ^2) statistic and association index of *Nepenthes* spp. with other plants in peat swamp and heath forest.

<i>Nepenthes</i> -other plant	Chi-square (χ^2)	Association type	JI
<i>N. ampullaria</i> - <i>Macaranga caladiifolia</i> Becc. ¹	4.76	Positive	0.34
<i>N. ampullaria</i> - <i>Tetrameristra glabra</i> Miq. ¹	4.01	Positive	0.13
<i>N. ampullaria</i> - <i>Cratoxylum glaucum</i> Korth. ¹	5.43	Negative	0.07
<i>N. ampullaria</i> - <i>N. rafflesiana</i> ¹	23.32	Negative	0.08
<i>N. ampullaria</i> - <i>Syzygium</i> sp. ²	29.49	Positive	0.50
<i>N. bicalcarata</i> - <i>Antidesma coriaceum</i> Tul. ¹	19.32	Positive	0.33
<i>N. bicalcarata</i> - <i>Simaba borneensis</i> (Noot.) Feuillet ¹	8.82	Positive	0.25
<i>N. gracilis</i> - <i>Nephrolepis hirsutula</i> (G.Forst.) C.Presl ¹	6.59	Positive	0.40
<i>N. gracilis</i> - <i>Curculigo latifolia</i> Dryand.ex W.T.Aiton ¹	4.83	Positive	0.11
<i>N. gracilis</i> - <i>Cratoxylum glaucum</i> Korth. ²	22.76	Negative	0.45
<i>N. gracilis</i> - <i>N. mirabilis</i> ²	13.98	Negative	0.02
<i>N. gracilis</i> - <i>N. rafflesiana</i> ²	9.22	Negative	0.15
<i>N. mirabilis</i> - <i>Barringtonia racemose</i> (L.) Spreng. ¹	34.74	Positive	0.60
<i>N. mirabilis</i> - <i>Poikilospermum suaveolens</i> (Blume) Merr. ¹	4.70	Positive	0.17
<i>N. mirabilis</i> - <i>Nephrolepis biserrata</i> (Sw.) Schott ²	28.97	Positive	0.50
<i>N. mirabilis</i> - <i>Scleria biflora</i> Roxb. ²	4.14	Positive	0.10
<i>N. rafflesiana</i> - <i>Cratoxylum glaucum</i> Korth. ¹	10.82	Positive	0.39
<i>N. rafflesiana</i> - <i>Sandoricum koetjape</i> Merr. ¹	4.46	Positive	0.11
<i>N. rafflesiana</i> - <i>Pternandra rostrata</i> (Cogn.) M.P.Nayar ¹	6.51	Negative	0.05
<i>N. rafflesiana</i> - <i>Baeckea frutescens</i> L. ²	7.37	Positive	0.25
<i>N. rafflesiana</i> - <i>Willughbeia</i> sp. ²	5.68	Positive	0.18
<i>N. x hookeriana</i> - <i>Campnosperma auriculatum</i> (Blume) Hook.fil. ¹	29.49	Positive	0.50
<i>N. x hookeriana</i> - <i>Stemonurus secundiflorus</i> Blume ¹	9.15	Positive	0.17

Remarks: Chi-square table 3.84; 1: peat swamp; 2: heath; JI: Jaccard Index

bicalcarata thrive. This species was also found to be used as a climbing tool for *N. bicalcarata*. This report supports previous information on *N. bicalcarata* in West Kalimantan (Sunardi & Mansur 2021).

Nepenthes spp. exhibited negative associations with some plants. *Cratoxylum glaucum* is a common tree in a peat swamp and heath forest, which has negative associations with *N. ampullaria* and *N. gracilis*. We assume that the dominant species compete for the same resources in these niches. Negative associations in forest communities are found in the most common species with a wide distribution and low habitat specificity (Sritharan et al. 2021). *N. rafflesiana* and *C. glaucum* tends to be found in the same plot, suggesting no competition between both species. In addition, *N. rafflesiana* is not a dominant species in peat swamp forests, so it is unlikely to compete with *C. glaucum*. *Nepenthes* abundance and vegetation composition influence the associations that occur within habitats. *N. ampullaria* in heath forest associated with *Syzygium* sp. This species grows on the forest floor under the shade of *Syzygium* sp. Meanwhile, *N. mirabilis* is associated with *Nephrolepis biserrata* and *Scleria biflora*. This result is aligned with the report from Hidayat et al. (2018) that *N. mirabilis* is often found growing together with Cyperaceae and ferns.

Dominant species of *Nepenthes* are negatively associated with some other *Nepenthes*. It indicates that the dominant species found in peat swamp (*N. ampullaria*) and heath (*N. gracilis*) tend to compete for nutrients and insect prey. Therefore, different *Nepenthes* species were rarely found in the same plot at the research location.

Correlation between Environment Factor Affecting the Abundance of *Nepenthes* spp.

Air temperature and air humidity are essential factors for *Nepenthes* growth. The measurements of environmental factor in peat swamp forest show that the average air temperature is 24.8 °C with an average air humidity of 81.3%. Meanwhile, the average air temperature in the heath forest is higher at 29.8 °C with an air humidity of 73.8%. *Nepenthes* growth in air temperature ranges from 23°C–31°C (Mansur 2006), with air humidity ranging from 67–90% (Nainggolan et al. 2020).

Precipitation is one of the environmental factors affecting the existence of *Nepenthes*. *Nepenthes* is predominantly found in the rainfall range between 3500–4000 mm/year (Sartika et al. 2017). Ketapang Regency rainfall for 2020–2021 ranges from 3871.2–4352 mm/year. Heavy rainfall also supports the availability of water in both habitat types, which can support the growth of *Nepenthes*.

Based on CCA analysis, environmental factors correlate with the presence of *Nepenthes* spp. in peat swamps (Figure 4a) and heath forests (Figure 4b). In peat swamp forest, showed a positive correlation between *N. mirabilis* and *N. gracilis* to light intensity. Both species in the study site are often found in open canopy cover with the light intensity reaching to forest floor. The existence of *N. rafflesiana* is influenced by the air temperature. *N. ampullaria* and *N. bicalcarata* are affected by air humidity. Meanwhile, *N. x hookeriana* had a low correlation with air humidity.

The CCA ordination graph in the heath forest suggests that soil temperature, air temperature, and light intensity are highly correlated with *N. gracilis*. This species can thrive in heath forest with high light intensity from 479–1987 lux, high air temperature of 29.8 °C and soil temperature from 27–30°C. Meanwhile, *N. ampullaria* is influenced by high soil moisture, similar to conditions in peat swamp forests that are often waterlogged. *N. rafflesiana* has a low correlation with environmental factors in the heath forest. This species is generally found in shaded areas, but some individuals are found in open areas.

The results of soil fertility analysis in the *Nepenthes* habitat showed that the nutrient content and pH were low, with 2.9 in the peat swamp forest and 3 in the heath forest. *Nepenthes* spp. in the peat swamp forest grows on soil with a silty loam texture, while in the heath forest, *Nepenthes* spp. grows on sandy soil. The high percentage of sand fraction in the heath forest causes the soil's capacity to bind water significantly lower. Low porosity impacts the ability of nutrients to be released from soil colloids due to infiltration. The percentage of soil texture fraction, sand, dust, and clay also affected the nutrient content.

In the peat swamp forest, the C-organic content is categorized as very high at 40.14% due to the high organic matter contained in the peat soil. Total N in peat soil is relatively high at 1.67%. However, most of it is contained in lipoproteins, so it cannot be utilized directly by plants. Meanwhile, the C-organic content in heath forest is high at 3.3%, with a low total N content of 0.15%. Cation exchange capacity was very high at 171.32 in the peat swamp and low at 11.18 in the heath forest. Both habitats had low base saturation values of <20%.

Study results on habitat characteristics of *Nepenthes* are essential data in species management and necessary for conservation purposes. *Nepenthes* is a protected plant species under Law Number 5 of 1990 and Minister of Environment and Forestry Regulation on Permen LHK/P.20 Year 2018. *N. ampullaria*, *N. gracilis*, *N. mirabilis*, and *N. rafflesiana* as the least concern (LC) species by IUCN. In contrast, endemic species *N. bicalcarata* is categorized as vulnerable (VU) (Schnell et al. 2000). Five spe-

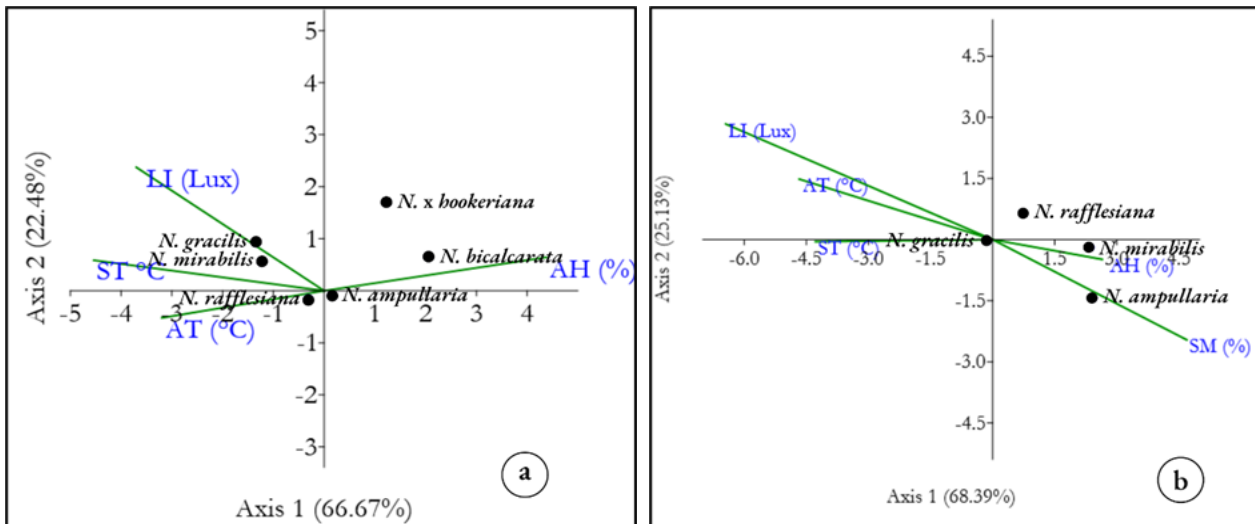


Figure 4. Correlation between environmental factors and the existence of *Nepenthes* spp. (a) peat swamp forest; (b) heath forest. AH: air humidity; AT: air temperature; LI: light intensity; SM: soil moisture; ST: soil temperature.

cies of *Nepenthes* excluding *N. x hookeriana* are also listed as restricted for all trade activities.

N. bicalcarata requires special attention in conservation. This species found in small quantities with a density of 142 ind/ha. Based on IUCN, the annotation of this species needs updating, and its population is considered unspecified. Consequently, further exploration and data collection of *N. bicalcarata* is required. The distribution of *N. bicalcarata* only covers the western and northern parts of Borneo (including Malaysia and Brunei Darussalam). Over the last 30 years, peat swamp forest was converted into oil palm plantations and has decimated 60% of the *N. bicalcarata* population in Borneo (Clarke et al. 2018).

Nepenthes spp. in the Pematang Gadung is threatened by illegal gold mining activities. In-situ conservation of *Nepenthes* species should be implemented in Pematang Gadung Forest Village by restricting forest clearing, illegal logging, and mining area occupation. Monitoring activities of *Nepenthes* spp. discovery points in study site is also crucial. Ex-situ conservation through captive breeding and cultivation techniques, both conventional and tissue culture, can be applied by considering the characteristics of the *Nepenthes*' habitat.

CONCLUSIONS

Based on the results of autecological studies, the population of *Nepenthes* in peat swamp and heath forest has clumped distribution and are often found close to other plants like *Barringtonia racemosa* and *Syzygium* sp. The factors that most influence the presence of *N. gracilis* include light intensity, air temperature, and soil temperature. Meanwhile, the presence of *N. ampullaria* is affected by high soil moisture. The Pematang Gadung Forest has a high potential for *Nepenthes* due to the presence of an endemic species of *N. bicalcarata*. Accordingly, conservation activities are very important to be carried out in this forest to maintain the existing diversity of *Nepenthes*.

AUTHOR CONTRIBUTION

NU, S, and NSA designed research; NU has been tasked with sampling and observing the existence of *Nepenthes* spp. and its autecological factors in the field, data analysis, and manuscript writing. S and NSA supervised the identification process in the laboratory, data analysis, manuscript writing, and editing

ACKNOWLEDGMENTS

We want to convey our deepest appreciation and gratitude to the Indonesia Endowment Fund for Education (LPDP) for supporting this research.

CONFLICT OF INTEREST

There is no conflict of interest in this research

REFERENCES

- Apriyanto, T., Rafdinal, R. & Minsas, S., 2021. Density and spread pattern of carnivore plant (*Nepenthes* spp.) in the area of Sebomban Hill Bonti District, Sanggau. *Jurnal Biologi Tropis*, 21(3), pp.956–964. doi: 10.29303/jbt.v21i3.2839.
- Armanda, Anggraeni & Wahyuni, T., 2020. Populasi dan karakterisasi fenotip kantong semar (*Nepenthes* spp.) di Taman Keanekaragaman Hayati Hutan Pelawan Kabupaten Bangka Tengah, Provinsi Kepulauan Bangka Belitung. *Media Konservasi*, 25(1), pp.89–97. doi: 10.29244/medkon.25.1.89-97.
- Bauer, U., Rembold, K. & Grafe, T.U., 2016. Carnivorous *Nepenthes* pitcher plants are a rich food source for a diverse vertebrate community. *Journal of Natural History*, 50(7–8), pp.483–495. doi: 10.1080/00222933.2015.1059963.
- Benayas, J.M.R. et al., 1999. Conservation Ecology : Commonness and Rarity : Theory and Application of a New Model to Mediterranean Montane Grasslands. *Conservation Ecology*, 3(1), pp.1–16.
- Calatayud, J. et al., 2020. Positive associations among rare species and their persistence in ecological assemblages, *Nature Ecology and Evolution*, 4(1), pp.40–45. doi: 10.1038/s41559-019-1053-5.
- Cheek, M., & Jebb, M., 2001. *Flora Malesiana Series I (Seed Plants)*, Netherlands: National Herbarium Nederland.
- Clarke, C., 2001. *Nepenthes of Sumatera and Peninsular Malaysia*, Kota Kinabalu: Natural History Publication.
- Clarke, C., Cross, A.T & Rice, B., 2018. Conservation of carnivorous plants. In: *Carnivorous Plants: Physiology, Ecology and Evolution*. London, UK: Oxford University Press.
- Cross, A.T. et al., 2020. Conservation of carnivorous plants in the age of extinction. *Global Ecology and Conservation*, 24, e01272. doi: 10.1016/j.gecco.2020.e01272.
- Damit, A., Nilus, R. & Suleiman, M., 2017. Population structure and dispersion pattern of *Nepenthes* along the Kaingaran Trail of Mount Trus Madi , Sabah , Borneo. *Sepilok Bulletin*, 25 & 26 (November 2018), pp.1–11.
- Dančák, M. et al., 2022. First record of functional underground traps in a pitcher plant: *Nepenthes pudica* (Nepenthaceae), a new species from North Kalimantan, Borneo. *PhytoKeys*, 201, pp.77–97. doi: 10.3897/phytokeys.201.82872.
- Gilbert, K.J. et al., 2018. Keeping an eye on coloration : ecological correlates of the evolution of pitcher traits in the genus *Nepenthes* (Caryophyllales). *Biological Journal of the Linnean Society*, 123(2), pp.321–337. doi: 10.1093/biolinnean/blx142.
- Hammer, Ø., Harper, D.A.T., & Paul, D.R., 2001. Past: Paleontological Statistics Software Package for Education and Data Analysis. *Palaeontologia Electronica*, 4(1), pp.4–9
- Hidayat, S. et al. 2018. Habitat of *Nepenthes* spp. in the area of Sampit Botanic Gardens, Central Kalimantan, Indonesia. *Biodiversitas*, 19(4), pp.1258–1265. doi: 10.13057/biodiv/d190411.

- Hariyadi, 2013. Inventarisasi tumbuhan kantong semar (*Nepenthes* spp.) di Lahan Gambut Bukit Rawi, Kalimantan Tengah. *Biospecies*, 6(1), pp.24–27.
- Kissinger et al., 2015. Analisis fungsi *Nepenthes gracilis* Korth. terhadap lingkungan hutan kerangas. *Jurnal Hutan Tropis*, 3(1), pp.61–66. doi: 10.20527/jht.v3i1.4166
- Krebs, C.J., 1989. *Ecological Methodology*, New York: Harper & Row.
- Lam, W.N. et al., 2020. *The Pitcher Plants (Nepenthes Species) of Singapore*, Singapore: Lee Kong Chian Natural History Museum, National University of Singapore.
- Maire, V. et al., 2012. Habitat filtering and niche differentiation jointly explain species relative abundance within grassland communities along fertility and disturbance gradients. *New Phytologist*, 196(2), pp.497–509. doi: 10.1111/j.1469-8137.2012.04287.x.
- Mansur, M., 2006. *Nepenthes Kantong Semar yang Unik*. Jakarta: Penebar Swadaya.
- Mansur, M., 2012. Laju penyerapan CO₂ pada kantong semar (*Nepenthes gymnamphora* Nees) di Taman Nasional Gunung Halimun Salak. Jawa Barat, *Jurnal Teknik Lingkungan*, 13(1), pp.59–65. doi: 10.29122/jtl.v13i1.1405.
- Mansur, M., 2013. Tinjauan tentang *Nepenthes* (Nepenthaceae) di Indonesia. *Berita Biologi*, 12(1), pp.1–7. doi: 10.14203/beritabiologi.v12i1.512.
- Mithöfer, A., 2022. Carnivorous plants and their biotic interactions. *Journal of Plant Interactions*, 17(1), pp.333–343. doi: 10.1080/17429145.2022.2038710.
- Moran, J.A. & Clarke, C.M., 2010. The carnivorous syndrome in *Nepenthes* pitcher plants: Current state of knowledge and potential future directions. *Plant Signaling and Behavior*, 5(6), pp.644–648. doi: 10.4161/psb.5.6.11238.
- Moran, J.A., Clarke, C.M. & Hawkins, B.J., 2003. From carnivore to detritivore? isotopic evidence for leaf litter utilization by the tropical pitcher plant *Nepenthes ampullaria*. *International Journal of Plant Sciences*, 164(4), pp.635–639. doi: 1058-5893/2003/16404-0014.
- Mueller-Dombois, D. & Ellenberg, H., 1974. Aims and methods of vegetation ecology. *Geogr Rev.* 66(1),114. doi:10.2307/213332.
- Murphy, B. et al., 2020. A phylogenomic analysis of *Nepenthes* (Nepenthaceae). *Molecular Phylogenetics and Evolution*, 144, 106668. doi: 10.1016/j.ympev.2019.106668.
- Nainggolan, L., Gultom, T. & Silitonga, M., 2020. Inventory of pitcher plant (*Nepenthes* sp.) and its existence in North Sumatra Indonesia. *Journal of Physics: Conference Series*, 1485, 012013. doi: 10.1088/1742-6596/1485/1/012013.
- Nurhadi, A., Linda, R. & Mukarlina, 2018. Keanekaragaman jenis kantong semar (*Nepenthes* spp.) di Kawasan Taman Wisata Alam Banning Kabupaten Sintang Kalimantan Barat. *Jurnal Protobiont*, 7(3), pp.111–117. doi: 10.26418/protobiont.v7i3.29853.
- Odum, E.P., 1993. *Dasar-dasar Ekologi*, Yogyakarta: Gadjah Mada University Pr.
- Page, S.E. et al., 1999. Interdependence of peat and vegetation in a tropical peat swamp forest. *Philosophical Transactions of The Royal Society B Biological Sciences*, 354(1391), pp.1885–1897. doi: 10.1098/rstb.1999.0529.

- Palinkas, L.A. et al., 2015. Purposeful Sampling for Qualitative Data Collection and Analysis in Mixed Method Implementation Research. *Adm Policy Ment Health*, 42(5), pp.533-544. doi: 10.1007/s10488-013-0528-y.
- Payung, I., Ekariana & Elfrida., 2021. Pola penyebaran tumbuhan kantong semar (*Nepenthes*) di Kawasan Hutan Sultan Daulat Kota Subulussalam Provinsi Aceh. *Jurnal Jeumpa*, 8(1), pp.525-531. doi: 10.33059/jj.v8i1.4005.
- Rantau, G., Ekyastuti, W. & Ekamawanti, H. A., 2019. Keanekaragaman jenis *Nepenthes* spp. di hutan kerangas Desa Sejahtera Kabupaten Kayong Utara. *Jurnal Hutan Lestari*, 9(3), pp. 395-404. doi: 10.26418/jhl.v9i3.44353.
- Ravee, R., Salleh, F. I. M. & Goh, H. H., 2018. Discovery of digestive enzymes in carnivorous plants with focus on proteases. *PeerJ*, 6, e4914. doi: 10.7717/peerj.4914.
- Sartika, Setiawan, A. & Master, J., 2017. Populasi dan pola penyebaran kantong semar (*Nepenthes gracilis*) di Rhino Camp Resort Sukaraja Atas Kawasan Taman Nasional Bukit Barisan Selatan (TNBBS), *Jurnal Sylva Lestari*, 5(3), pp.12-21. doi: 10.23960/jsl3512-21.
- Schnell et al., 2000. *Nepenthes bicalcarata*. The IUCN Red List of Threatened Species 2000: e.T39624A10252393, (24 September 2022). Assesible at <https://www.iucnredlist.org/species/39624/10252393>
- Sritharan, M.S. et al., 2021. Spatial associations between plants and vegetation community characteristics provide insights into the processes influencing plant rarity. *PLoS ONE*, 16(12), e0260215 doi: 10.1371/journal.pone.0260215.
- Shannon, C.E., 1948. A mathematical theory of communication. *Bell Syst Tech J.* 27(4), pp.623-656. doi:10.1002/j.1538-7305.1948.tb00917.x.
- Soepadmo, E. & Wong, K.M., 1995. *Tree Flora of Sabah and Sarawak, Volume 1*. Sabah Forestry Department, Forest Research Institute Malaysia, Sarawak Forestry Department, Malaysia.
- Sunardi, S. & Mansur, M., 2021. Kelimpahan, asosiasi dan ancaman habitat *Nepenthes bicalcarata* Hook.f. di Cagar Alam Mandor Kalimantan Barat. *Buletin Kebun Raya*, 24(2), pp.66-75. doi: 10.14203/bkr.v24i2.734.
- Tanjung, R.H.R. et al., 2020. Characteristics of peatland chemicals and their association with the diversity of dominant plants in Papua. *IOP Conference Series: Earth and Environmental Science*, 575, 012082. doi: 10.1088/1755-1315/575/1/012082.
- Whitten et al., 1984. *Ecology ecosystem of Sumatra*, Yogyakarta: UGM Press.
- Wilsey, B.J. & Polley, H.W., 2004. Realistically low species evenness does not alter grassland species-richness-productivity relationships. *Ecology*, 85(10), pp.2693-2700. doi: 10.1890/04-0245.
- Wulandari, R.J., Sumaryono, M. & Suhardiman, A., 2020. Population distribution patterns of *Nepenthes reinwardtiana* Miq. in Kerangas Forest of Teluk Adang Nature Reserve, Paser Regency. *Jurnal Penelitian Kehutanan Wallacea*, 9(1), p.23. doi: 10.18330/jwallacea.2020.vol9iss1pp23-30.

Research Article

Genetic Identification of Two Mudskipper Species (Oxudercidae: *Periophthalmus*) from Kulon Progo, Special Region of Yogyakarta, Indonesia

Diana Febrianti¹, Katon Waskito Aji¹, Dwi Sendi Priyono², Tuty Arisuryanti^{1*}

1)Laboratory of Genetics and Breeding, Faculty of Biology, Universitas Gadjah Mada, Jl. Teknik Selatan, Sekip Utara, Yogyakarta 55281

2)Laboratory of Animal Systematics, Faculty of Biology, Universitas Gadjah Mada, Jl. Teknik Selatan, Sekip Utara, Yogyakarta 55281

* Corresponding author, email: tuty-arisuryanti@ugm.ac.id

Keywords:

COI
DNA barcoding
cryptic diversity
mudskipper
genetic variation

Submitted:

03 October 2022

Accepted:

13 March 2023

Published:

12 July 2023

Editor:

Ardaning Nuriliani

ABSTRACT

Mudskippers are commonly cryptic species, making identification based solely on morphological characteristics challenging. This study used the DNA barcoding method to identify mudskipper species based on the *COI* mitochondrial gene. The analysis revealed two distinct species, *P. kalolo* (20 samples) and *P. argenteolineatus* (3 samples) with high GC contents ranging from 42.94-45.2%. The genetic divergence analysis of *P. kalolo* showed that they divided into two clades, while *P. argenteolineatus* is divided into three clades with two of the clades (C and D) still conspecific groups, and those two clades with clade E exhibit a genetic distance greater than 3.5%, suggesting the presence of cryptic species. These findings provide valuable insights into the intraspecific genetic diversity of mudskippers in Indonesia, which could have essential implications for conservation efforts and highlight the potential of DNA barcoding as a powerful tool for the identification of cryptic species. Further research combining molecular and morphological identification could lead to a more comprehensive understanding of species identification and help address the challenges posed by cryptic species.

Copyright: © 2023, J. Tropical Biodiversity Biotechnology (CC BY-SA 4.0)

INTRODUCTION

Mudskippers are oxudercine gobies of the family Oxudercidae, sub family Oxudercinae (Nelson et al. 2016; Kuang et al. 2018; McCraney et al. 2020). It is found in the Indo-West Pacific and tropical Western Africa (Jaafar & Murdy 2017; Froese & Pauly 2022). *Periophthalmus* is the most diverse mudskipper genus, with 19 valid species (Froese & Pauly 2022). In Indonesia, eleven species of this genus have been identified in Sumatera, Java, Kalimantan, Lesser Sunda, West Papua, Moluccas, and Sulawesi (Pormansyah et al. 2019). The genus *Periophthalmus* inhabits a wide variety of intertidal and supratidal environments, including unvegetated mud banks, open tidal mudflats, mangrove forests, and freshwater swamps (Baeck et al. 2008; Larson 2008; Polgar & Crosa 2009; Polgar et al. 2010; Polgar & Bartolino 2010; Takita et al. 2011).

The members of the genus *Periophthalmus* are well adapted to an amphibious lifestyle, exhibiting morphological and physiological adaptations such as aerial vision and olfaction, enhanced ammonia tolerance,

terrestrial locomotion via pectoral fins, and greater immunological protection against pathogens (You et al. 2018). The versatility of the fish is further reflected in the variety of pelvic fin morphologies, which suggest their adaptability to both terrestrial and aquatic environments (Hidayat et al. 2022). In addition to their unique adaptations, mudskipper fish have the potential as a source of food, as they are rich in carbohydrates, lipids, proteins, and well-balanced amino acids (Duggal et al. 2020; Mahadevan et al. 2021). Moreover, they play an important role as filter feeders and potential indicators of environmental contamination (Sangur et al. 2021).

The taxonomic classification of members within the family Oxudercidae (previously known as Gobiidae) is often hindered by their morphological similarities, presenting significant difficulties in species identification (Thacker 2003). This phenomenon has been observed in mudskippers of the genus *Boleophthalmus* and *Periophthalmus*, with numerous reports of cryptic species (Chen et al. 2014; Polgar et al. 2014; Arisuryanti et al. 2018; Aji & Arisuryanti 2021; Rha'ifa et al. 2021). Using traditional morphological methods alone has proven to be insufficient in accurately identifying *Periophthalmus* species, as evidenced by several misidentifications such as *Periophthalmus walailakae* with *Periophthalmodon schlosseri* (1), *Periophthalmus takita*, Jaafar & Larson, 2008 with *Periophthalmus novaeguineensis* Eggert, 1935 (2), and *Periophthalmus variabilis* Eggert, 1935 with *Periophthalmus novemradiatus* Hamilton, 1822 (3) (Murdy 1989; Jaafar et al. 2006; Jafaar & Larson 2008; Jaafar et al. 2009). To overcome these limitations, the incorporation of molecular approaches, such as DNA barcoding, into the taxonomic classification process is crucial. DNA barcoding is a fast and accurate technique that utilizes short DNA sequences to identify species. The cytochrome oxidase subunit I (*COI*) mitochondrial gene is a commonly used marker in animal DNA barcoding due to its rapid evolutionary rate, lack of introns, and high copy number, making it an effective tool for identifying numerous animal taxa and cryptic species (Hebert et al. 2003b; Imtiaz et al. 2017; Roesma et al. 2020).

Pasir Mendit Beach in Kulon Progo, Special Region of Yogyakarta, Indonesia is a unique and valuable ecosystem, encompassing both a tourism and conservation area with dense mangroves and muddy terrain. It is located near the coastline of Yogyakarta, close to Muara Bogowonto and Baros Beach, the habitats for several species of mudskipper (Arisuryanti et al. 2018; Aji & Arisuryanti 2021). Despite its significance, the genetic information of the mudskipper populations in Pasir Mendit Beach is yet to be explored. Therefore, this study aimed to identify mudskippers from Pasir Mendit Beach in Kulon Progo, Special Region of Yogyakarta, Indonesia using the mitochondrial gene of *COI* as a DNA barcoding marker.

MATERIALS AND METHODS

Sample Collection

Twenty-three samples of mudskippers (code MSP) were collected from Pasir Mendit Beach, Special Region of Yogyakarta, using a hand net in November 2019 (Figure 1). The collected specimens were thoroughly cleaned and documented (as shown in Figure 2). The samples were placed in a ziplock bag and stored in an icebox, and transported to the Laboratory of Genetics and Breeding at the Faculty of Biology, Universitas Gadjah Mada. The samples were preserved in 99% ethanol and stored at -20°C until utilized for DNA extraction. Given the difficulties in accurately identifying mudskipper species based on morphological characteristics, this study exclusively relied on molecular identification methods. Specifically, Nucleotide BLAST analysis (<https://blast.ncbi.nlm.nih.gov>)

and BOLD (https://www.boldsystems.org/index.php/IDS_OpenIdEngine) of the *COI* gene sequences for each sample code to verify the species of mudskipper.



Figure 1. Map of mudskipper sampling locations in Pasir Mendit Beach, Kulon Progo, Special Region of Yogyakarta.

DNA Extraction

The complete DNA genomic samples were isolated from muscle tissue on the pectoral fins above the back area of the gills using the kit (DNeasy Blood and Tissue kit from QIAGEN, Valencia, CA, USA) following the manufacturer's protocols.

DNA Amplification, Electrophoresis and Sequencing

A partial *COI* mitochondrial gene was amplified using a pair of primers, FishF2 (5'-TCGACTAATCATAAAGATATCGGCAC-3') and FishR2 (5'-ACTTCAGGGTGACC GAAGAATCAGAA-3') (Ward et al. 2005), in a Biorad T100 Thermal-Cycler. The amplification reaction was carried out in a 50 μ L volume, containing 10-100 ng of genomic DNA, 25 μ L of MyTaq HS Red Mix kit (Bioline), 1 mM of $MgCl_2$, 0.6 μ M of each primer (FishR2 and FishR2), and 11 μ L of ddH₂O. To test the effectiveness of DNA amplification, a negative control was added by removing the DNA template from the reaction mixture. The PCR was set up in 35 cycles of reaction for 2 minutes of pre-denaturation at 95°C, 15 seconds of denaturation at 95°C, 30 seconds of annealing at 50°C, 30 seconds of extension at 72°C and 5 minutes of final extension at 72°C (Arisuryanti et al. 2020).

The PCR products were run on a 1% agarose gel electrophoresis at 100 volts for 25 minutes, with Florosafe (Bioline) for staining and Tris-acetate EDTA (TAE) 1X as buffer. The visualization was carried out using UV light. Each amplification sample was delivered to First Base

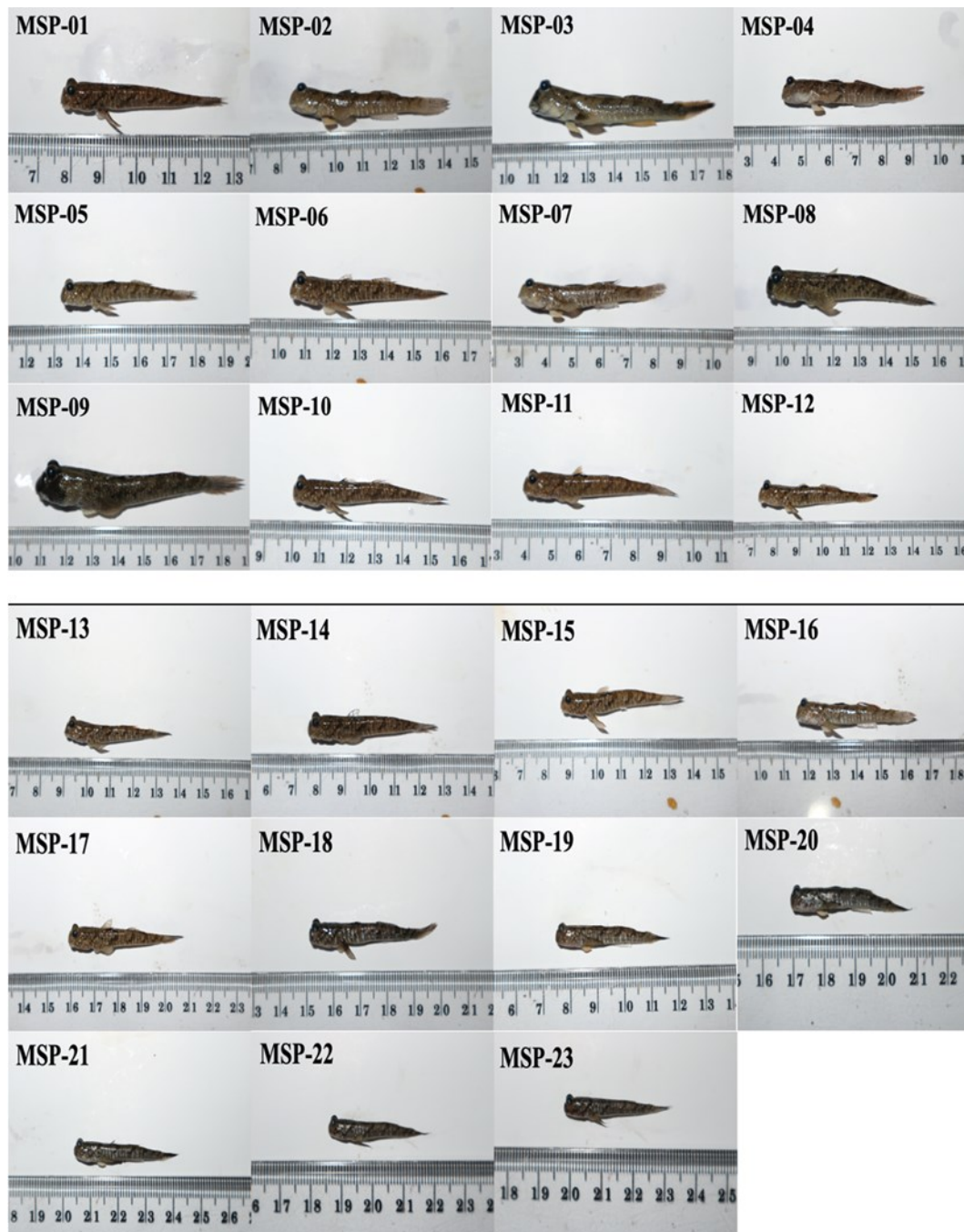


Figure 2. Mudskipper fish collected from Pasir Mendit Beach, Special Region of Yogyakarta.

(Malaysia) via PT Genetika Science in Jakarta for purification and sequencing in forward and reverse directions utilizing the Big Dye Terminator (Applied Biosystems) and the Genetic Analyzer ABI 3730xl.

Sequence Editing

The consensus sequence was constructed and edited using GeneStudio software and validated using the SeqMan and EditSeq menus in the DNASTAR software (DNASTAR Inc., Madison, USA). During this process, the chromatograms were carefully inspected for any ambiguous bases or stop codons.

Sequence Identification

The sequence of mudskipper species was identified using the Nucleotide BLAST analysis available on the NCBI website (<https://blast.ncbi.nlm.nih.gov/Blast.cgi>) and the BOLD Identification Engine menu on the BOLD website (<https://v3.boldsystems.org/index.php/>

IDS_OpenIdEngine). The similarity of the sample and the query cover were used to estimate the species of the mudskipper fish compared to the data available in GenBank and BOLD.

COI Sequence Alignment

The mudskipper *COI* sequences were aligned using the Mesquite v.3.70 software on the Opal menu (Maddison & Maddison 2021) and the MEGAX software on the ClustalW menu (Kumar et al. 2018).

Intrapopulation and Intraspecies Analysis

The focus of the intrapopulation analysis was to determine the nucleotide composition of each species of mudskipper within the population. In addition, the intraspecies analysis expands the investigation by comparing the nucleotide composition, genetic distance, and phylogenetic relationship across different populations.

Nucleotide Composition & Genetic Distance

The MEGAX program was used to compute the *COI* nucleotide composition. The genetic distance was examined using the Kimura-2 parameter model and summarized in a Neighbor-Joining (NJ) tree, which is a commonly used methodology in DNA barcoding research (Hebert et al. 2003a)

Phylogenetic Relationship

The MEGAX software (Kumar et al. 2018) was used to assess the phylogenetic tree reconstruction using the Neighbor-Joining and Maximum Likelihood methods with 1,000 bootstraps, as well as the BEAST program for Bayesian Inference method (Suchard et al. 2018). The Bayesian Information Criterion (BIC) developed in jModelTest 2.1.10 was used to find the optimal evolutionary model (Darriba et al. 2012). The best sequence substitution model on the Bayesian Inference Criterion is HKY with gamma (HKY + G). The posterior probabilities distribution was estimated using the method of Markov chain Monte Carlo (MCMC) over 10^7 generations using a 1,000-generation sampling frequency.

RESULTS AND DISCUSSION

Result

Species Verification

We successfully amplified the *COI* mitochondrial gene from twenty-three mudskipper fish samples collected from Pasir Mendit Beach, yielding a fragment length of 700 bp (Figure 3). Sequence editing using GeneStudio software resulted in consensus sequences ranging from 675 to 702 bp with translated amino acids numbering from 225 to 234. Our analysis of the genetic similarity of the samples to reference species in GenBank and BOLD showed that 20 out of 23 samples had a similarity range of 99.27 to 100% to *P. kalolo*, while the remaining three samples had a similarity range of 99.69 to 99.85% to *P. argenteolineatus*. The genetic similarity of the samples to their conspecific references is presented in Table 1. The *COI* sequences of *P. argenteolineatus* has been deposited in GenBank under accession number OQ804359-OQ804361 whereas the *COI* sequences of *P. kalolo* has been deposited in GenBank under accession number OQ804373-OQ804392.

We performed alignment of the *COI* mitochondrial gene of *P. kalolo* and *P. argenteolineatus* collected from Pasir Mendit Beach which produced consensus sequences of 666 bp for each species. These consensus se-

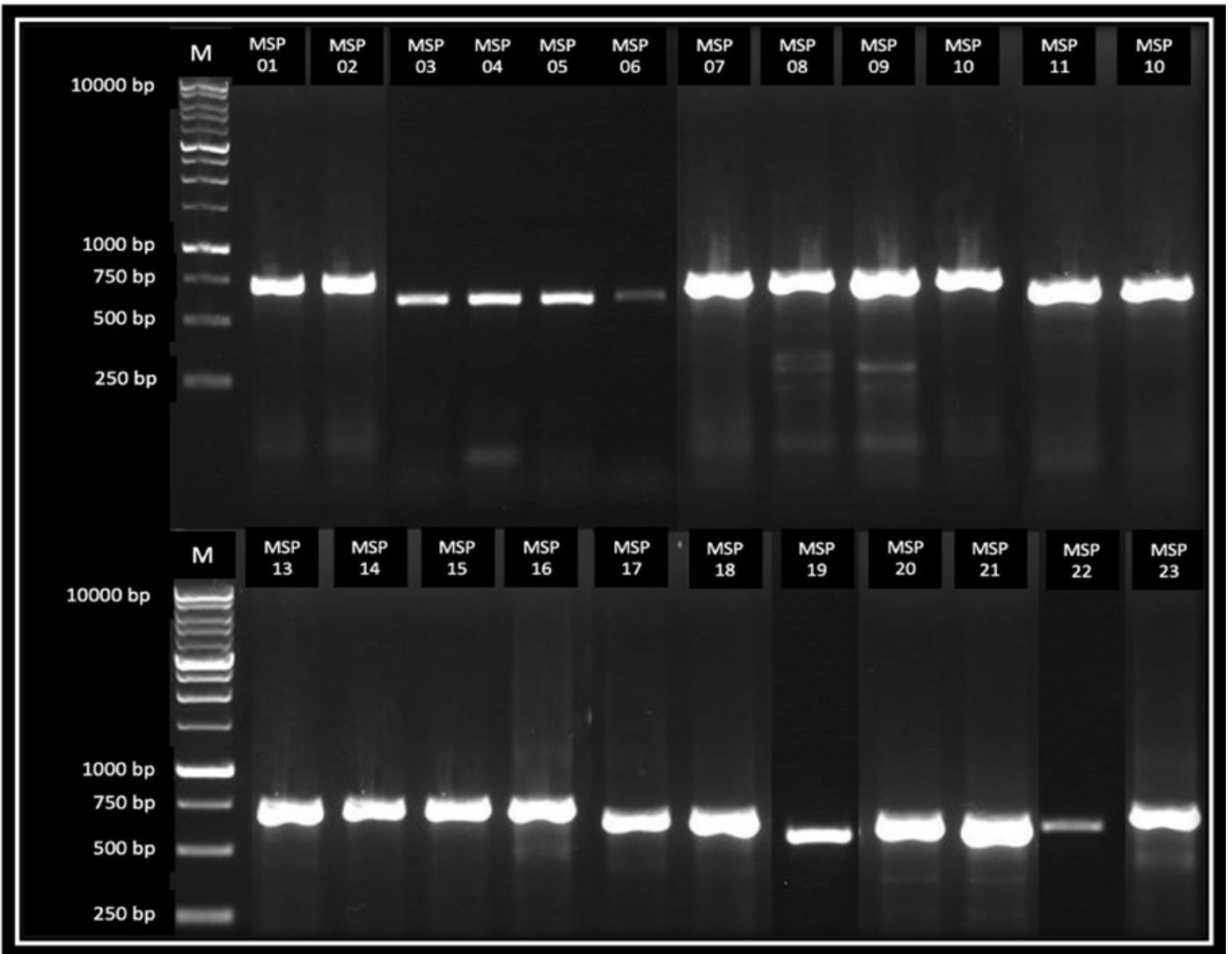


Figure 3. The PCR amplification results of the *COI* mitochondrial gene from the mudskipper samples collected from Pasir Mendit Beach. The samples were run on 1% agarose gel electrophoresis and identified by the sample codes MSP 01 to 23. A 1 kb DNA ladder (GENEAID) was included as a reference marker, labeled as "M" on the figure.

quences were then used to perform intrapopulation analysis for each species. In addition, we also conducted intraspecies analysis, using *COI* sequences of mudskippers from Pasir Mendit Beach and other Indonesian regions recorded in GenBank and BOLD, yielding fragment lengths of 624 bp for *P. kalolo* and 579 bp for *P. argentilineatus*. To understand the evolutionary relationships of the two species, we aligned the sequences from Pasir Mendit Beach with those from other locations in Indonesia documented in GenBank, as well as with the *COI* sequence of *Boleophthalmus boddarti* (accession number KU692377) as an outgroup. The resulting aligned sequences (579 bp) were then used to construct a phylogenetic tree.

For intrapopulation analysis, we analyzed a total of 20 samples of *P. kalolo* and 3 samples of *P. argentilineatus* from Pasir Mendit. Our results showed that the average nucleotide composition of *P. kalolo* consisted of 30.81% thymine (T), 26.99% cytosine (C), 24.31% adenine (A), and 17.89% guanine (G), with variations ranging from 0 to 0.9%, 0 to 1.05%, 0 to 0.30%, and 0 to 0.45%, respectively. In comparison, the average nucleotide composition of 3 samples of *P. argentilineatus* was 31.88% (T), 25.83% (C), 24.92% (A), and 17.37% (G), with variations ranging from 0 to 0.15%, 0 %, 0 to 0.3%, and 0 to 0.45%. We found that the A+T content

Table 1. Identification of species based on database of GenBank using BLAST and BOLD.

No	Sample Code	GenBank/BOLD Species Identified	Similarity (%)	Query Cover (%)	Expect Value	Accession Number	References
1	MSP-01	<i>Periophthalmus kalolo</i>	99.85	97	0.0	MZ614851	Aji and Arisuryanti (2021)
2	MSP-02	<i>Periophthalmus kalolo</i>	99.85	97	0.0	MZ614852 MZ614847 MZ614843	Aji and Arisuryanti (2021)
3	MSP-03	<i>Periophthalmus argentilineatus</i>	99.85	100	0.0	MW514019 MW514017	Rha'ifa et al. (2021)
4	MSP-04	<i>Periophthalmus kalolo</i>	99.85	100	0.0	MZ614854 MZ614848 MZ614842	Aji and Arisuryanti (2021)
5	MSP-05	<i>Periophthalmus kalolo</i>	99.71	99	0.0	MZ614854 MZ614848 MZ614844 MZ614842	Aji and Arisuryanti (2021)
6	MSP-06	<i>Periophthalmus kalolo</i>	99.85	99	0.0	MZ614851	Aji and Arisuryanti (2021)
7	MSP-07	<i>Periophthalmus kalolo</i>	99.85	97	0.0	MZ614846	Aji and Arisuryanti (2021)
8	MSP-08	<i>Periophthalmus argentilineatus</i>	99.85	93	0.0	KU692746 KU692745	Dahrudin et al. (2017)
9	MSP-09	<i>Periophthalmus argentilineatus</i>	99.69	92	0.0	KU692746 KU692745	Dahrudin et al. (2017)
10	MSP-10	<i>Periophthalmus kalolo</i>	100	97	0.0	MZ614849	Aji and Arisuryanti (2021)
11	MSP-11	<i>Periophthalmus kalolo</i>	99.71	97	0.0	MZ614854 MZ614848 MZ614844 MZ614842	Aji and Arisuryanti (2021)
12	MSP-12	<i>Periophthalmus kalolo</i>	100	100	0.0	MZ614843	Aji and Arisuryanti (2021)
13	MSP-13	<i>Periophthalmus kalolo</i>	99.56	97	0.0	MZ614854 MZ614848 MZ614844 MZ614842	Aji and Arisuryanti (2021)
14	MSP-14	<i>Periophthalmus kalolo</i>	100	97	0.0	MZ614843	Aji and Arisuryanti (2021)
15	MSP-15	<i>Periophthalmus kalolo</i>	100	97	0.0	MZ614845	Aji and Arisuryanti (2021)
16	MSP-16	<i>Periophthalmus kalolo</i>	100	98	0.0	MZ614846	Aji and Arisuryanti (2021)
17	MSP-17	<i>Periophthalmus kalolo</i>	99.85	97	0.0	MZ614854 MZ614848 MZ614844 MZ614842	Aji and Arisuryanti (2021)
18	MSP-18	<i>Periophthalmus kalolo</i>	100	97	0.0	MZ614851	Aji and Arisuryanti (2021)
19	MSP-19	<i>Periophthalmus kalolo</i>	99.71	99	0.0	MZ614854 MZ614848 MZ614844 MZ614842	Aji and Arisuryanti (2021)
20	MSP-20	<i>Periophthalmus kalolo</i>	100	97	0.0	MZ614846	Aji and Arisuryanti (2021)
21	MSP-21	<i>Periophthalmus kalolo</i>	99.71	98	0.0	MZ614854 MZ614848 MZ614844 MZ614842	Aji and Arisuryanti (2021)

Table 1. Contd.

No	Sample Code	GenBank/BOLD Species Identified	Similarity (%)	Query Cover (%)	Expect Value	Accession Number	References
22	MSP-22	<i>Periophthalmus kalolo</i>	99.27	98	0.0	MZ614854 MZ614848 MZ614844 MZ614842	Aji and Arisuryanti (2021)
23	MSP-23	<i>Periophthalmus kalolo</i>	99.85	97	0.0	MZ614854 MZ614848 MZ614844 MZ614842	Aji and Arisuryanti (2021)

in both *P. kalolo* and *P. argentilineatus* was higher than the G+C content.

We conducted an intraspecies analysis of *P. kalolo* samples from Pasir Mendit Beach and other locations in Indonesia, revealing average nucleotide composition of 30.48% thymine (T), 27.03% cytosine (C), 25.00% adenine (A), and 17.48% guanine (G), with differences ranging from 0-1.12%, 0.16-1.28%, 0.16-0.48%, and 0.16-0.64%, respectively. The A+T content varied from 54.97 to 56.09%, while the G+C content varied from 43.91 to 45.03%. The highest A+T composition was found in samples from Baros Beach (MZ614843, MZ614847), Bogowonto (MT439602, MT439601), and Cilacap (KU692753), while the highest G+C composition was detected in a sample from Baros Beach (MZ614841). Additionally, we identified the highest number of similarities in nucleotide composition among samples from several Indonesian locations including Pasir Mendit Beach (MSP-12, MSP-14), Baros Beach (MZ614843, MZ614847), Bogowonto (MT439602, MT439601), and Cilacap (KU692753).

Our intraspecies analysis revealed variations in the composition of nucleotides T, C, A, and G within the *P. argentilineatus*. These variations ranged from 0-1.21% for T, 0.17-1.21% for C, 0-0.52% for A, and 0-0.52% for G. Interestingly, *P. argentilineatus* displayed a higher A+T composition than G+C, with A+T ranging from 56.99 to 57.86% and G+C ranging from 42.14 to 43.01%. The highest A+T composition was observed in samples collected from Pasir Mendit Beach (MSP-03), Baros Beach (MZ606685), and Bogowonto (MT439598), while the highest G+C composition was recorded in samples from Baros Beach (MZ606680, MZ606682). In addition, we also identified the highest number of similarities in nucleotide composition among specimens sourced from various locations, such as Pandeglang (KU692745, KU692746), Bogowonto (MT439599), Baros Beach (MZ606684, MZ606686).

The resulting phylogenetic tree revealed that *P. kalolo* species was divided into two separate clades, supported by high bootstrap values of 100% (NJ), 99% (ML), and a posterior probability of 1 (BI). Meanwhile, *P. argentilineatus* was separated into three clades with values of bootstrap 99% (NJ), 95% (ML), and 1 in the posterior probability (BI) value for the separation of clade C and clade D. The bootstrap values between clade D and clade E were 100% (NJ), 99% (ML), and 1 (BI) for posterior probability. The phylogenetic tree reconstruction is presented in Figure 4.

Our genetic distance analysis of *P. kalolo* samples from Pasir Mendit Beach compared to other *P. kalolo* documented in BOLD and GenBank from other Indonesian regions yielded an average genetic distance of 1.90% (ranging from 1.30 to 2.63%) between Clade A and Clade B (Table 2). On the other hand, in *P. argentilineatus*, the lowest average genetic distance was found within clade C and clade D at 2.50% (1.94–

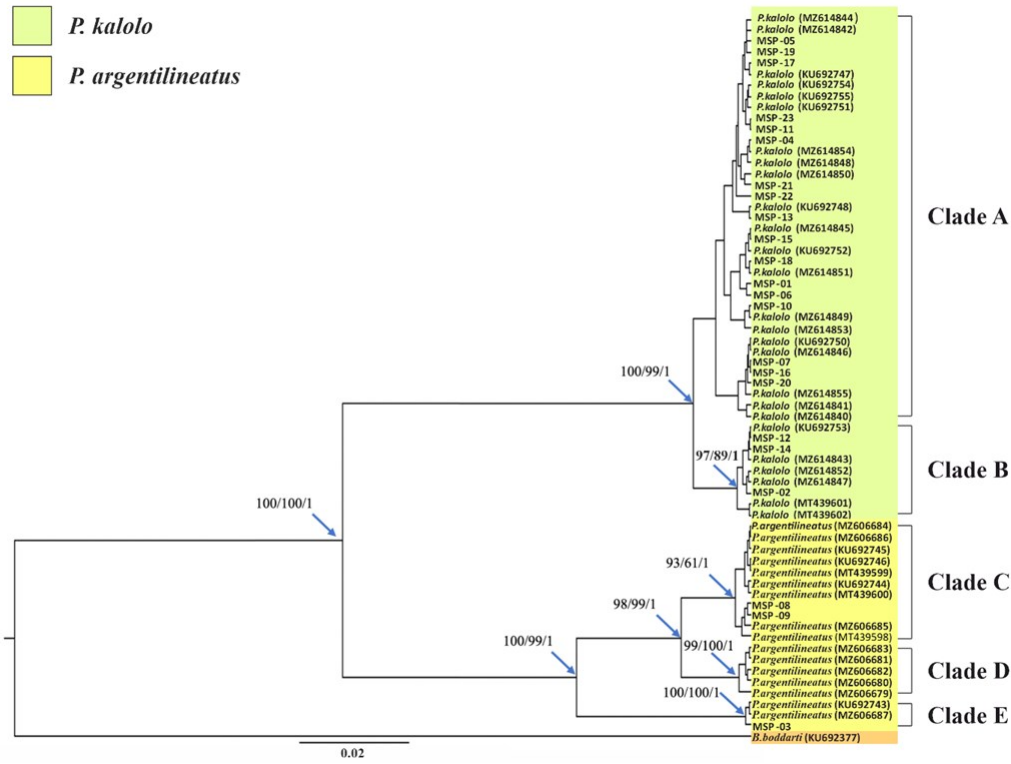


Figure 4. Phylogenetic tree reconstruction based on Neighbor-Joining (NJ), Maximum-Likelihood (ML), Bayesian Inference (BI) topology of two *Periophthalmus* species and an outgroup based on *COI* gene sequences (579 bp). The node represented the number bootstrap (NJ and ML) and Bayesian Posterior Probability (Bayesian Inference).

2.84%), while the highest was between clade E and clade C at 6.01% (5.62–6.38%) (Table 3). The average genetic distance between clade E and clade D was 5.53% (5.24–5.81%).

Table 2. The percentage of the intraspecies genetic distance between *P. kalolo* from Pasir Mendit Beach and other places in Indonesia from GenBank and BOLD data.

	Clade A	Clade B
Clade A		
Clade B	1.90 (1.30–2.63)	

Table 3. The percentage of the intraspecies genetic distance between *P. argentineatus* from Pasir Mendit Beach and other places in Indonesia from GenBank and BOLD data.

	Clade E	Clade C	Clade D
Clade E			
Clade C	6.01 (5.62–6.38)		
Clade D	5.53 (5.24–5.81)	2.50 (1.94–2.84)	

Discussion

DNA barcoding has emerged as a robust tool in the field of taxonomy, enabling the rapid and accurate identification of species. By combining genetic distance and phylogenetic tree approaches, this method has been extensively validated across a wide range of taxa (Ude et al. 2020; Wang et al. 2021; Sachithanandam et al. 2022). The present study applied DNA barcoding to identify of mudskipper species, utilizing the *COI* mtDNA gene. We compared our sequences with those from NCBI GenBank and BOLD database and discovered that the 23 mudskipper samples in this study belonged to two distinct species, *P. kalolo* (20 samples) and *P. argentilineatus* (3 samples). According to Triandiza and Maduppa (2018), the most similar GenBank sequence is characterized by the same maximum and total score, query coverage close to 100%, E value close to 0, and percentage of identity or similarity close to 100%. Based on that criterion, all mudskipper samples in this study showed greater similarity to the sequence of both species in GenBank.

We observed that the nucleotide composition analysis of the *COI* gene in both species of mudskippers revealed GC contents ranging from 42.94–45.2%. This result is consistent with the study by Ward et al. (2005) which discovered a total GC content *COI* ranging from 42.2–47.1%. Additionally, we found a T>C>A>G nucleotide composition pattern of the *COI* gene that was comparable to studies in other fish families (Bingpeng et al. 2018; Kombong & Arisuryanti 2018; Wu et al. 2018; Linh et al. 2018; Aji & Arisuryanti 2021).

Our phylogenetic tree reconstruction, based on mitochondrial *COI* sequences from various locations, including Pasir Mendit Beach, revealed the existence of two distinct clades in *P. kalolo* and three distinct clades within *P. argentilineatus*. We found that *P. kalolo* samples from Bogowonto were in the same clade as samples from Baros Beach (MZ614852, MZ614847), Cilacap (KU692753), but in a different clade compared to samples from Baros Beach (MZ614840–42, MZ614844–46, MZ614848–49, MZ614850–51, MZ614853–54), Tulungagung (KU692750, KU692751, KU692751, KU692755, KU692747, KU692748), and other samples from Cilacap (KU692754). These results are consistent with previous research by Arisuryanti et al. (2018) and Aji and Arisuryanti (2021). Additionally, we also observed that *P. argentilineatus* from Baros Beach (MZ606684–86) were in the same clade as samples from Pandeglang (KU692744–46) and samples from Bogowonto (MT4359598–600), separated from the clade with *P. argentilineatus* from Baros Beach (MZ606687) and a sample from Tukad Bilukpoh, Jembrana Bali (KU692743) (Dahrudin et al. 2017; Aji & Arisuryanti 2021). We evaluated the robustness of our phylogenetic tree by assessing bootstrap and posterior probability values. We found that the formation of the clades in both *P. kalolo* and *P. argentilineatus* had high values of bootstrap and posterior probability, demonstrating the robustness of these clades. According to Apriliyanto and Sembiring (2016), if the bootstrap value in methods of Neighbor-Joining and Maximum Likelihood is closer to 100% and the posterior probability value in the Bayesian Inference method is close to 1, then the formation of the clades is considered robust. Our results meet this criterion, further supporting the reliability and accuracy of our phylogenetic tree reconstruction.

Our analysis revealed a genetic divergence of 1.90% (ranging from 1.30 to 2.63%) in two distinct clades of *P. kalolo*. This value is fall within the intraspecies genetic distance threshold of 3.5% proposed by Zemlak et al. (2009), indicating that *P. kalolo* samples from different Indonesian locations belong to the same species (conspecific). This finding aligns

with previous studies by Arisuryanti et al. (2018) and Aji and Arisuryanti (2021), which also found no significant genetic differentiation among *P. kalolo* populations in Indonesia. In contrast, the genetic distance analysis of *P. argenteolineatus* revealed a more complex picture. Our finding indicates that *P. argenteolineatus* is divided into two conspecific groups, clades C and D, while one group (clades E) exhibited a genetic distance greater than 3.5%. This result is consistent with previous studies (Arisuryanti et al. 2018; Rha'ifa et al. 2021; Aji & Arisuryanti 2021) that have suggested the presence of cryptic species in *P. argenteolineatus* in Indonesia. These results support the clade formation observed in the phylogenetic tree.

Interestingly, we did not observe a clear clades separation by geographical region in the phylogenetic tree, suggesting a lack of geographical structuring in the populations of *P. kalolo* and *P. argenteolineatus*. This lack of geographical structure was particularly evident in clade E, where the sample MSP-03 from Pasir Mendit Beach was grouped with a sample from Baros Beach (MZ606687) and a sample from Tukad Bilukpoh, Jembrana, Bali (KU692743). The distance between Pasir Mendit Beach to Tukad Bilukpoh is more than 400 km, and we assume that there should be little or no gene flow between them. We hypothesize that this result could be attributed to geological events that allowed for the dispersion and gene flow between the remote populations, such as variations in sea level or oceanic currents (Miller et al. 2005; García-De León et al. 2018). Additionally, it is important to note that the lack of clear separation by geographical region in the phylogenetic tree may be influenced by the small sample size of some populations. Future studies with larger sample sizes may be needed to better understand the patterns of genetic diversity and geographic structuring in these two species.

CONCLUSIONS

Our study demonstrates the effectiveness of DNA barcoding in identifying and differentiating mudskipper species. Through analysis of the *COI* mtDNA gene, we were able to identify two distinct species of mudskippers, *P. kalolo* and *P. argenteolineatus*, and assess their genetic diversity and relationships. The high GC content and nucleotide composition pattern observed in the *COI* gene were consistent with other fish families. Our phylogenetic tree analysis revealed the existence of two distinct clades in *P. kalolo* and three in *P. argenteolineatus*, with the robust formation of these clades. Genetic divergence analysis indicated that *P. kalolo* samples from different Indonesian locations are conspecific, while *P. argenteolineatus* is divided into two conspecific groups (clades C and D) and one group with greater genetic distance (clade E), suggesting the presence of cryptic species. These findings provide valuable insights into the evolutionary history of mudskippers and highlight the potential of DNA barcoding as a powerful tool for species identification and conservation.

AUTHOR CONTRIBUTION

T.A. was in charge of planning, designing, supervising the entire research process and reviewed the initial manuscript and revised the final manuscript. D.F. worked in a laboratory (samples collections, DNA extraction, amplification using a PCR technique, electrophoresis using agarose gel, analysis of data, and writing of the manuscript). KWA and DSP guide the laboratory work, data analysis and writing the manuscript.

ACKNOWLEDGMENTS

We would like to thank the Head of the Laboratory of Genetics and

Breeding for granting permission and facilitating this research. This research was supported by RTA Program with the Grant Number 5722/UN1.P.III/Dit-Lit/PT.01.05/2022

CONFLICT OF INTEREST

The authors declare that they have no conflicts of interest. The authors are responsible for the article's content and writing.

REFERENCES

- Aji, K.W. & Arisuryanti, T. 2021. Molecular identification of mudskipper fish (*Periophthalmus* spp.) from Baros Beach, Bantul, Yogyakarta. *Journal of Tropical Biodiversity and Biotechnology*, 6(3), jtbb66391. doi:10.22146/jtbb.66391
- Aprilyanto, V. & Sembiring, L. 2016. *Filogenetika Molekuler: Teori dan Aplikasi*. Innosain.
- Arisuryanti, T., Hasan, R.L., & Koentjana, J.P., 2018. Genetic identification of two mudskipper species (Pisces: Gobiidae) from Bogowonto Lagoon (Yogyakarta, Indonesia) using *COI* mitochondrial gene as a DNA barcoding marker. *AIP Conference Proceedings*, 2002, 020068. doi: 10.1063/1.5050164
- Arisuryanti, T., Firdaus, N.U.N., Hakim, L., 2020. Genetic characterization of striped snakehead (*Channa striata* Bloch, 1793) from Arut River, Central Kalimantan inferred from *COI* mitochondrial gene. *AIP Conference Proceedings*, 2260, 020001. doi: 10.1063/5.0015905
- Baeck, G.W., Takita, T. & Yoon, Y.H., 2008. Lifestyle of Korean mudskipper *Periophthalmus magnuspinnatus* with reference to a congeneric species *Periophthalmus modestus*. *Ichthyological Research*, 55, pp.43–52. doi: 10.1007/s10228-007-0009-y
- Bingpeng, X. et al., 2018. DNA barcoding for identification of fish species in the Taiwan Strait. *PloS one*, 13(6), e0198109. doi: 10.1371/journal.pone.0198109
- Chen, H., et al., 2014. Cryptic species and evolutionary history of the *Boleophthalmus pectinirostris* complex, along the northwestern Pacific coast. *Acta Hydrobiologica Sinica*, 38(1), pp.75-86. doi: 10.7541/2014.10
- Dahrudin, H. et al., 2017. Revisiting the ichthyodiversity of Java and Bali through DNA barcodes: taxonomic coverage, identification accuracy, cryptic diversity and identification of exotic species. *Molecular Ecology Resources*, 17(2), pp.288-299. doi: 10.1111/1755-0998.12528
- Darriba, D. et al., 2012. jModelTest 2: more models, new heuristics and parallel computing. *Nature methods*, 9(8), pp.772-772. doi:10.1038/nmeth.2109
- Duggal, R. et al., 2020. Study of Variation in Nutrient Content of Mudskipper *Boleophthalmus dussumieri* Collected from Gujarat And Maharashtra State, India. *Uttar Pradesh Journal of Zoology*, 41(22), pp.24-30.
- Froese, R. & Pauly, D., 2022, 'FishBase' in *World Wide Web electronic publication*, viewed 13 February 2022, from <http://www.fishbase.org>, version (08/2022).
- García-De León, F.J. et al., 2018. Role of oceanography in shaping the genetic structure in the North Pacific hake *Merluccius productus*. *PLoS One*, 13(3), e0194646. doi: 10.1371/journal.pone.0194646

- Hebert, P.D. et al., 2003a. Biological identifications through DNA barcodes. *Proceedings of the Royal Society of London. Series B: Biological Sciences*, 270(1512), pp.313-321. doi: 10.1098/rspb.2002.2218
- Hebert, P.D., Ratnasingham, S., & Ward, JR. 2003b. Barcoding Animal Life: Cytochrome C Oxidase Subunit 1 Divergences among Closely Related Species. *Proceedings of The Royal Society*, 270, pp.96-99. doi: 10.1098/rsbl.2003.0025
- Hidayat, S. et al., 2022, March. The Morphologies of Mudskipper Pelvic Fins in Relation to Terrestrial and Climbing Behaviour. In *Proceedings of the Zoological Society*, 75(1), pp.83-93. Springer India. doi: 10.1007/s12595-021-00422-1
- Imtiaz, A. et al., 2017. Progress and potential of DNA barcoding for species identification of fish species. *BIODIVERSITAS*, 18(4), pp.1394-1405. doi: 10.13057/biodiv/d180415
- Jaafar, Z. & Larson, H.K., 2008. A new species of mudskipper, *Periophthalmus takita* (Teleostei: Gobiidae: Oxudercinae), from Australia, with a key to the genus. *Zoological Science*, 25(9), pp.946-952. doi: 10.2108/zsj.25.946
- Jaafar, Z. & Murdy E.O., 2017. *Fishes Out of Water: Biology and Ecology of Mudskippers*. CRC Press.
- Jaafar, Z., Lim, K.K. & Chou, L.M., 2006. Taxonomical and morphological notes on two species of mudskippers, *Periophthalmus walailakae* and *Periophthalmodon schlosseri* (Teleostei: Gobiidae) from Singapore. *Zoological Science*, 23(11), pp.1043-1047. doi: 10.2108/zsj.23.1043
- Jaafar, Z., Perrig, M. & Chou, L.M., 2009. *Periophthalmus variabilis* (Teleostei: Gobiidae: Oxudercinae), a valid species of mudskipper, and a re-diagnosis of *Periophthalmus novemradiatus*. *Zoological Science*, 26(4), pp.309-314. doi: 10.2108/zsj.26.309
- Kombong, C.B.S. & Arisuryanti, T., 2018. The 16S and COI Mitochondrial DNA Nucleotide Composition of Stripped Snakehead (*Channa striata* Bloch, 1793) from Lake Sentani, Jayapura, Papua. *UGM Journal of Fish*, 20(2), pp.57-62. doi: 10.22146/jfs.35551
- Kuang, T. et al., 2018. Phylogenomic analysis on the exceptionally diverse fish clade Gobioidi (Actinopterygii: Gobiiformes) and data-filtering based on molecular clocklikeness. *Molecular Phylogenetics and Evolution*, 128, pp.192-202. doi: 10.1016/j.ympev.2018.07.018
- Kumar, S. et al., 2018. MEGA X: Molecular Evolutionary Genetics Analysis across Computing Platforms. *Molecular Biology and Evolution*, 35(6), pp.1547-1549. doi: 10.1093/molbev/msy096
- Larson, H. K. 2008. Weber's mudskipper *Periophthalmus weberi*: new record for the Daly River. *Northern Territory Naturalist*, 20, pp.19-21. doi: 10.5962/p.295507
- Linh, N.M. et al., 2018. DNA barcoding application of mitochondrial COI gene to identify some fish species of family Gobiidae in Vietnam. *Vietnam Journal of Marine Science and Technology*, 18(4), pp.443-451. doi: 10.15625/1859-3097/13662
- Maddison, W.P. & Maddison, D.R., 2021. *Mesquite: a Modular System for Evolutionary Analysis*, viewed 13 February 2023, from <https://mesquiteproject.org>.
- Mahadevan, G. et al., 2021. Nutritional evaluation of elongate mudskipper *Pseudapocryptes elongatus* (Cuvier, 1816) from Diamond Harbor, West Bengal, India. *Natural Product Research*, 35(16), pp.2715-2721. doi: 10.1080/14786419.2019.1666388

- McCraney, W.T., Thacker, C.E. & Alfaro, M.E., 2020. Supermatrix phylogeny resolves goby lineages and reveals unstable root of Gobiaria. *Molecular phylogenetics and evolution*, 151, 106862. doi: 10.1016/j.ympcv.2020.106862
- Miller, K.G. et al., 2005. The Phanerozoic record of global sea-level change. *science*, 310(5752), pp.1293-1298. doi: 10.1126/science.11164
- Murdy, E.O., 1989. A taxonomic revision and cladistic analysis of the oxudercine gobies (Gobiidae: Oxudercinae). *Records of the Australian Museum, Supplement*, 11(August 1989), pp.1-93.
- Nelson, J.S., Grande, T.C. & Wilson, M.V., 2016. *Fishes of the World*. John Wiley & Sons.
- Polgar, G. & Bartolino, V., 2010. Size variation of six species of oxudercine gobies along the intertidal zone in a Malayan coastal swamp. *Marine Ecology Progress Series*, 409, pp.199-212. doi: 10.3354/meps08597
- Polgar, G. & Crosa, G., 2009. Multivariate characterization of the habitats of seven species of Malayan mudskippers (Gobiidae: Oxudercinae). *Marine Biology*, 156, pp.1475-1486. doi: 10.1007/s00227-009-1187-0
- Polgar, G. et al., 2014. Phylogeography and demographic history of two widespread Indo-Pacific mudskippers (Gobiidae: *Periophthalmus*). *Molecular Phylogenetics and Evolution*, 73, pp.161-176. doi: 10.1016/j.ympcv.2014.01.014
- Polgar, G., Sacchetti, A. & Galli, P., 2010. Differentiation and adaptive radiation of amphibious gobies (Gobiidae: Oxudercinae) in semi-terrestrial habitats. *Journal of Fish Biology*, 77, pp.1645-1664. doi: 10.1111/j.1095-8649.2010.02807.x
- Pormansyah et al., 2019. A review of recent status on Mudskippers (Oxudercine Gobies) in Indonesian Waters. *Oceanography and Fisheries*, 9(4), 555769. doi: 10.19080/OFOAJ.2019.09.555769
- Rha'ifa, F.A. et al., 2021. DNA Barcode of Barred Mudskipper (*Periophthalmus argentilineatus* Valenciennes, 1837) from Tekolok Estuary (West Nusa Tenggara, Indonesia) and Their Phylogenetic Relationship with Other Indonesian Barred Mudskippers. *Journal of Tropical Biodiversity and Biotechnology*, 6(2), 59702. doi: 10.22146/jtbb.59702
- Roesma, D.I. et al., 2020. Phylogenetic analysis of transparent gobies in three Sumatran lakes, Inferred from mitochondria Cytochrome Oxidase I (*COI*) gene. *BIODIVERSITAS*, 21(1), pp.43-48. doi: 10.13057/biodiv/d210107
- Sachithanandam, V. et al., 2022. DNA barcode and phylogenetic analysis of Serranidae Fish (subfamily: Epinephelinae) from a Tropical Island Ecosystem of the Indian Ocean. *Thalassas: An International Journal of Marine Sciences*, 38, pp.843-853. doi.org/10.1007/s41208-022-00427-3
- Sangur, K. et al., 2021. Mudskipper as an indicator species for lead, cadmium and cuprum heavy metal pollution in the Mangrove, Ambon, Indonesia. *Journal of Ecological Engineering*, 22(4), pp.1-9. doi: 10.12911/22998993/134077
- Suchard, M.A. et al., 2018. Bayesian phylogenetic and phylodynamic data integration using BEAST 1.10. *Virus Evolution*, 4(1), vey016. doi: 10.1093/ve/vey016

- Takita, T., Larson, H. K. & Ishimatsu, A., 2011. The natural history of mudskippers in northern Australia, with field identification characters. *The Beagle, Records of the Museums and Art Galleries of the Northern Territory*, 27, pp.189–204. doi: 10.5962/p.287482
- Thacker, C.E., 2003. Molecular phylogeny of the gobioid fishes (Teleostei: Perciformes: Gobioidi). *Molecular phylogenetics and evolution*, 26(3), pp.354-368. doi: 10.1016/S1055-7903(02)00361-5
- Triandiza, T. & Maduppa, H., 2018. Aplikasi Analisa Morfologi dan DNA Barcoding pada Penentuan Jenis Kepiting Porecelain (*Pisidia* sp.) yang Berasal dari Pulau Tunda, Banten. *Jurnal Sumberdaya Akuatik Indopasifik*, 2(2), pp.81-90.
- Ude, G.N. et al., 2020. DNA barcoding for identification of fish species from freshwater in Enugu and Anambra States of Nigeria. *Conservation Genetics Resources*, 12, pp.643-658. doi: 10.1007/s12686-020-01155-7
- Wang, Y. et al., 2021. DNA barcoding for identification of fishes in Xiangjiaba reservoir area in the downstream section of the Jinsha river. *Conservation Genetics Resources*, 13, pp.201-208. doi.org/10.1007/s12686-021-01196-6
- Ward, R.D. et al., 2005. DNA barcoding Australia fish species. *Philosophical Transactions of The Royal Society B*, 360, pp.1847-1857. doi: 10.1098/rstb.2005.1716
- Wu, R. et al., 2018. DNA barcoding of the family Sparidae along the coast of China and revelation of potential cryptic diversity in the Indo-West Pacific oceans based on COI and 16S rRNA genes. *Journal of Oceanology and Limnology*, 36(5), pp.1753-1770. doi: 10.1007/s00343-018-7214-6
- You, X. et al., 2018. Mudskippers and their genetic adaptations to an amphibious lifestyle. *Animals*, 8(2), 24. doi: 10.3390/ani8020024
- Zemlak, T.S. et al., 2009. DNA barcoding reveals overlooked marine fishes. *Molecular Ecology Resources*, 9, pp.237-242. doi: 10.1111/j.1755-0998.2009.02649.x

Research Article

Detection of *AtRKD4* Gene and Induction of Somatic Embryo in Transformant of *Phalaenopsis amabilis* Carrying 35S::GR::*AtRKD4*

Dika Sundari¹, Naufal Ghazi Aditya Perdana², Windi Mose³, Jose Gutierrez-Marcos⁴, Endang Semiarti^{1,2*}

1) Graduate School of Magister Biology, Faculty of Biology, Universitas Gadjah Mada, Yogyakarta, Indonesia

2) Department of Tropical Biology, Faculty of Biology, Universitas Gadjah Mada, Yogyakarta, Indonesia

3) Faculty of Mathematics and Natural Sciences, Universitas Pattimura, Maluku, Indonesia

4) School of Life Science, University of Warwick, England

* Corresponding author, email: endsemi@ugm.ac.id

Keywords:

AtRKD4

embryo gene

Arabidopsis thaliana

Phalaenopsis amabilis

somatic embryo

Submitted:

14 December 2021

Accepted:

14 February 2023

Published:

21 July 2023

Editor:

Ardaning Nuriliani

ABSTRACT

Phalaenopsis amabilis (L.) Blume is a native of Indonesian orchid that plays important role in the breeding of orchid's hybrid worldwide. The high consumer demand causes a decline in the population of orchids for commercial trade. Plant propagation through induction of somatic embryogenesis will be very beneficial, because plants can be obtained in large numbers and uniforms. *AtRKD4* gene is an important gene in the model plant *Arabidopsis thaliana* which functions very early in development stage to initiate embryo formation. The *AtRKD4* gene has been inserted into the *P. amabilis* orchid and several transformants have been obtained. This study goals to determine the integration stability of the *AtRKD4* gene in the transformant genome of *P. amabilis* and to induce somatic embryo formation on transformant orchids. Plantation of leaf explants from *P. amabilis* transformants on hormone-free New Phalaenopsis basic medium induced somatic embryo formation by 20%. Anatomical analysis showed that there is no difference stage between anatomy of somatic embryo development pattern in *P. amabilis* transformant and somatic embryo development pattern of monocot plants in general, four weeks old-somatic embryos were analysed by PCR analysis using *AtRKD4* specific primers that showed the embryos still contained 198 bp fragments of the *AtRKD4* gene. In conclusion, the *AtRKD4* gene is stably integrated in the genome of *P. amabilis* and can continuously induce the formation of somatic embryo from somatic cells of orchid transformants.

Copyright: © 2023, J. Tropical Biodiversity Biotechnology (CC BY-SA 4.0)

INTRODUCTION

Phalaenopsis amabilis (L.) Blume is one of Indonesia's native orchids (Rahayu 2015) and has been designated as one of the national flowers since 1991 (Semiarti 2018). These orchids are often used as brood stock in breeding to produce hybrid orchids with superior traits (Semiarti et al. 2007). In orchids, the morphological character of the flower is the character used as a marker to distinguish plant groups (Pangestu et al. 2014). *P. amabilis* (Figure 1) produces beautiful flowers shaped like a moth and has a uniqueness of the antenna-like structure at the end of its labellum (Semiarti et al. 2011). The high consumer demand causes these orchids to

be widely cultivated and taken from their natural habitat (Rahayu 2015) resulting in over-harvesting for trade/commerce (Semiarti 2018). Germination of orchids from seeds is difficult to do (Mondal et al. 2016) making it ineffective for producing large numbers of seeds (Shekarriz et al. 2014). The right propagation method to produce orchid seeds quickly and in large numbers is needed for both commercial market and orchid conservation.

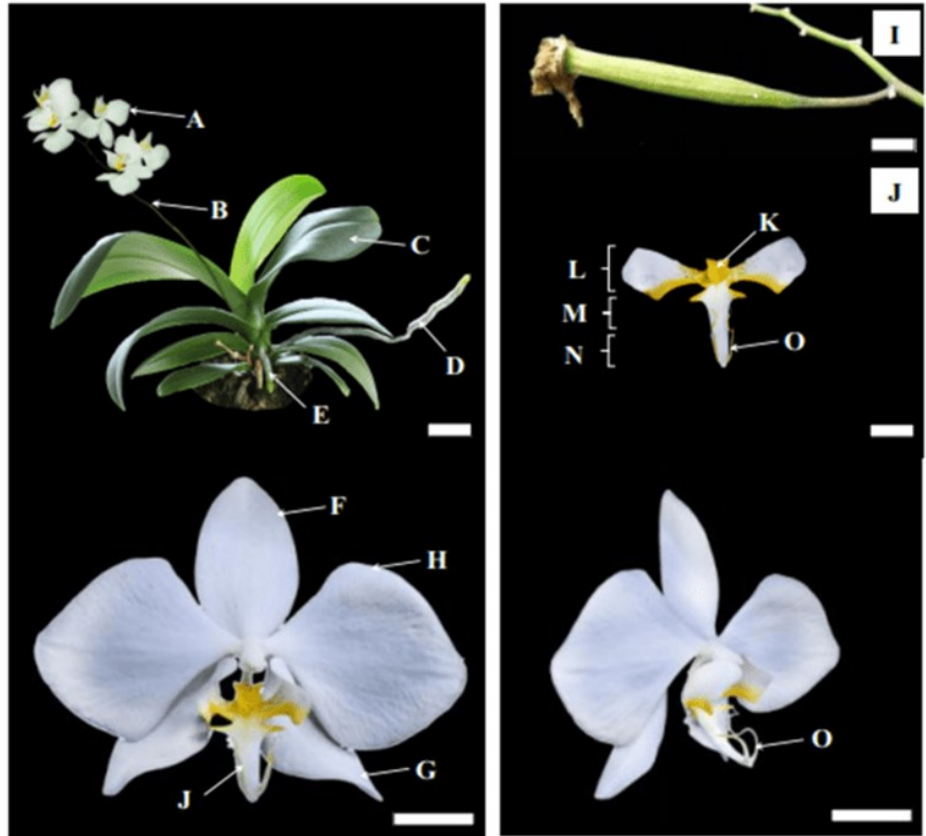


Figure 1. Morphology of *Phalaenopsis amabilis*. (A) flower), (B) flower stalks, (C) leaves, (D) air roots, (E) adhesive roots, (F) dorsal sepallum, (G) lateral sepallum, (H) lateral petallum, (I) fruit, (J) labellum, (K) callus, (L) hipochillium, (M) mesochillium, (N) epichillium, (O) antenna/mouth. Bars: 1 cm.

Somatic embryo formation can be induced with a molecular approach by introducing new traits into the plant genome. One of the genes that induces the change of somatic cells into embryogenic cells is the *RKD4* gene (Setiari et al. 2018) which encodes a protein with the RWP-RK motif (Chardin et al. 2014). The *RKD4* gene has the potential to initiate somatic embryo induction because it can activate other specific genes that have a role in the development of embryo. *RKD4* gene encodes a transcription factor protein with RWP-RK motif in Arabidopsis which expressed in early zygotic embryogenesis and required for embryonic pattern formation (Chardin et al. 2014). This gene encodes a transcription factor protein that expressed very early in zygotic embryogenesis (Waki et al. 2011).

Somatic embryogenesis is one of the methods to produce mass orchid propagation rapidly and efficiently (Hsing et al. 2016). Somatic embryogenesis is a model system to understand physiological, biochemical, and molecular conditions that occur during the development of plant embryo (Karami et al. 2009). Somatic cells contain all of the genetic information to form a functional and complete of new plant (Yang & Zhang 2010). Somatic cells are very unique because they are able to maintain

their developmental plasticity and totipotency in a differentiated state and have ability to differentiate, reproduce, and regenerate into adult plants within appropriate culture conditions (Neelakandan & Wang 2012).

The insertion of the *AtRKD4* gene in orchids has successfully induced ectopic somatic embryo formation in leaves and protocorms (Mose 2019). The somatic embryo has been successfully formed from leaves of the transformant orchids which contain *AtRKD4* gene after induced by DEX. *P. amabilis* transformant plant used in this study carrying T-DNA that contain glucocorticoid induction system (GR). T-DNA also carries the hygromycin phosphotransferase (*HPT*) gene, which is a resistance gene to hygromycin,

The success of genetic transformation was confirmed in the genome of the *Dendrobium phalaenopsis* transformant carrying *35S::GR::AtRKD4* gene by amplifying the *AtRKD4* gene. The construction of T-DNA carrying *35S::GR::AtRKD4* found in plasmid pTA7002. Similar research on the integration detecting of gene carrying *35S::GR::AtRKD4* in the genome of orchid plants has been successfully conducted by Mursyanti et al. (2015) on *Phalaenopsis* hybrid orchids "Sogo Vivien".

The formation of somatic embryos involves a process characterized by a set of morphological changes that direct to plant regeneration. The stability integration of *AtRKD4* gene in the transformant *P. amabilis* genome needs to be studied. This study aims to analyse the stability integration level of *AtRKD4* gene in *P. amabilis* transformants, to compare the morphological and anatomical characters in these orchids, and to maintain the induction of somatic embryos from transformant plants.

MATERIALS AND METHODS

Materials

This study used 18 months old - non transformant (NT) plantlets and transformant (T) plantlets carrying *35S::GR::AtRKD4* construct obtained from our previous research (Mose 2019). The cultures were maintained under continuous light at 20°C. Total sample of 36 explants randomly were divided into 2 groups, transformant dan non transformant, put in 6 Petri dish. Each Petri dish consisted of 6 explants.

Methods

Detection of Stability Integration of *AtRKD4* Gene

Detection of stability integration of *AtRKD4* gene was carried out to confirm the presence of *AtRKD4* gene in the *P. amabilis* genome carrying T-DNA with the construct of *35S::GR::AtRKD4* (Mursyanti et al. 2015) (Figure 2). Detection was carried out by isolating plant genomic DNA, then amplifying the DNA genome with specific primers, there are *HPT* and *AtRKD4* gene. *ACTIN* gene primers were used as positive controls because this gene is a house-keeping gene that owned by most of the plant cells.

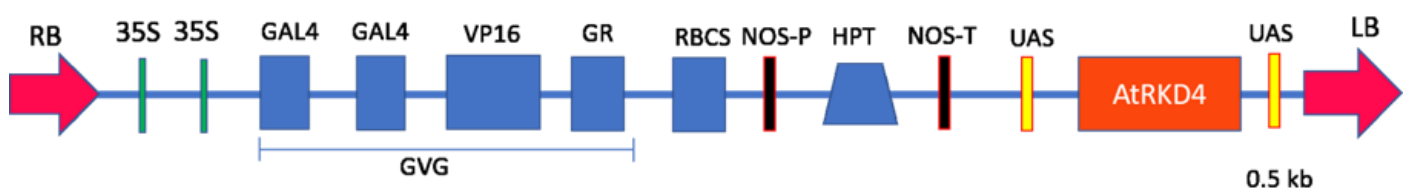


Figure 2. Construction of T-DNA carrying *35S::GR::AtRKD4* found in plasmid pTA7002 (Mursyanti et al. 2015).

Regeneration of Positive Transformant

Plants that were positive in the detection for containing *AtRKD4* gene (transformant plants) were grown on somatic embryo induction media. The media used was *New Phalaenopsis* (NP). The part of the plant used as explants are roots and leaves. Each root and leaf were cut into 3 parts as independent explants. The explants were cultured for eight weeks, maintained the growth, observed carefully whether there was growth of new cells, propagule formation or somatic embryos occurred.

Analysis of Morphological and Anatomical Structure of Somatic Embryos of *P. amabilis* Non-Transformant and Transformant

Morphological analysis was carried out by observing the orchid's growth and compare the morphology between transformant and non-transformant orchid. Morphological analysis was performed by calculating the formation of somatic embryos from *P. amabilis* orchid transformant that maintained on NP0 medium for eight weeks. The DNA genome of the somatic embryos was isolated and amplified with *AtRKD4* primers to detect the stability of the integration of *AtRKD4* genes in the somatic embryos.

Anatomical preparation was conducted by using embedding method according to Sutikno (2016). Explants from somatic embryos were fixed using FAA solution (Formalin: Glacial acetic acid: 70% alcohol) and dehydrated using graded alcohol. Then explants were dealcoholized using alcohol and xylol mixture. The samples were filtered with pure paraffin. The paraffin blocks were cut using microtomes with a size of 10-20 μm . The cut explant samples were given double staining using 1% safranin and 1% fast green, then it was observed by using a light microscope to see the anatomical differences between transformant and non-transformant plants. Anatomical analysis was performed by comparing the stage of anatomical somatic embryo of transformant to non-transformant *P. amabilis*.

RESULTS AND DISCUSSION

Detection the Stability Integration of *AtRKD4* Gene in *Phalaenopsis amabilis* Transformant Plants

Aoyama & Chua (1997) reported that 35S promoter of *cauliflower mosaic virus* (CaMV) is a strong promoter and expressed in almost all tissues in almost all of plant species at various stages of development. GR induction system is one of the gene expression systems that is widely used in plants. In this system, the transcription factor (TF) chimeric GVG contains of yeast GAL4 binding domain (BD), Herpes simplex VP16 activation domain (AD), and glucocorticoid receptor of mice. The presence of a GR domain determines the induction. The chimeric protein GVG in the cytoplasm is bound by a complex of 90 kDa Heat Shock Protein (HSP90) and cannot enter the nucleus without an inducer such as DEX (Picard 1993). After the addition of DEX, the chimeric protein is released and can be localized into nucleus as a transcription factor. Isolated genomic DNA from transformant plants was used as DNA template for detection stability integration of the *AtRKD4* gene in the plant genome by using PCR with specific primers of *AtRKD4* gene.

The PCR process works well with the ACTIN gene amplification in all plants, both transformant dan non transformant. The existence of 198 bp DNA fragments of *AtRKD4* gene and 545 bp DNA fragments of HPT gene indicated the integration of T-DNA in the *P. amabilis* transformants genome, and 114 bp band *ACTIN* supported the results as internal control indicating that the PCR reaction were running well

(Figure 3 lanes 3-10).

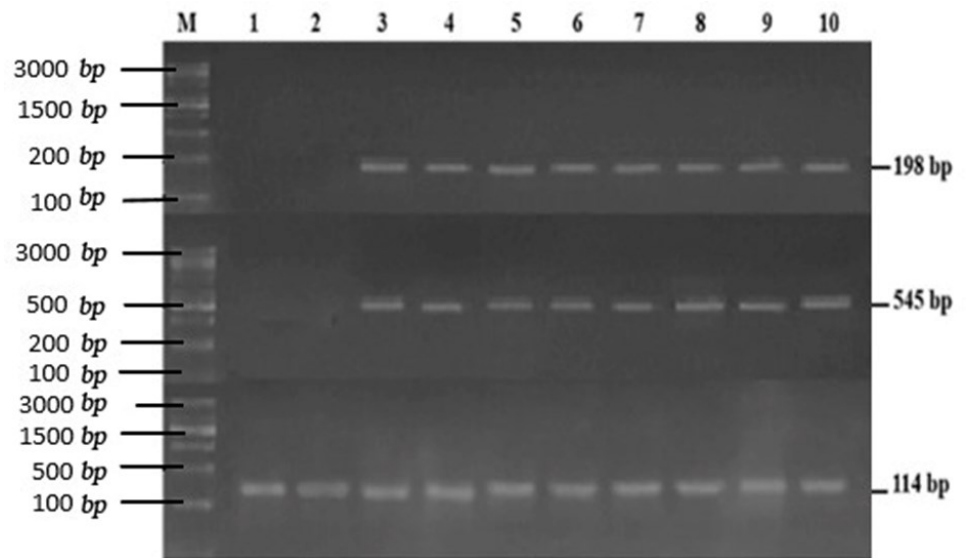


Figure 3. Detection of *AtRKD4* gene stability integration in the *Phalaenopsis amabilis* transformants genome. M: 100 bp GeneRuler markers, Line 1-2: non-transformant *P. amabilis* orchids, and Row 3-10: transformant orchid plants carrying the *35S::GR::AtRKD4* gene. The 114 bp fragments of *ACTIN* gene were amplified from *P. amabilis* non-transformant and transformant plants carrying the *AtRKD4* gene. The 545 bp fragments of *HPT* and 198 bp fragment of *AtRKD4* gene were amplified from *P. amabilis* transformant.

The *ACTIN* as a housekeeping gene which detected almost in all plant cells was used as an internal control. (Semiarti et al. 2007). The *HPT* is the hygromycin resistant gene that used as selection marker of transformants to hygromycin antibiotics. According to Ouwkerk et al. (2001) plants that survived on hygromycin-containing media showed that these plants were resistant to hygromycin. The 545 bp of *HPT* gene was amplified in the *P. amabilis* orchid transformant genome indicating that the plant contained a hygromycin resistant gene. The success of genetic transformation was confirmed by the amplification of the *AtRKD4* in the genome of the *P. amabilis* transformant. Similar research on the detection of *AtRKD4* gene integration in the orchid genome has been successfully carried out by Mursyanti et al. (2015) on the hybrid orchid *Phalaenopsis* “Sogo Vivien” and Setiari et al. (2018) on the *Dendrobium phalaenopsis*.

The morphological characters of *P. amabilis* orchids are shown in the Figure 4. Morphological characters can be observed and measured both qualitatively and quantitatively. Morphological observations of the samples were carried out to determine whether there were differences in the characters of the two plants. The samples have similar morphological characters. There is no significant difference between them. Observation data of *P. amabilis* orchid parameters used independent t-test with $\alpha = 0.05$ to determine the significant difference in growth between the two plants. The following Table 1. showed the parameters observed in plants aged 18 months including number, length, width of leaves and roots.

The data in the Table 1. showed that there are significant differences between non transformant and transformant plants in the growth of length and width of leaves. There is also significant differences between the number of roots of the sample. Meanwhile, in the number of leaves, length and width of roots, there were no significant difference in growth. The average growth of each parameter for 8 weeks can be seen in the following Figure 4.

Table 1. The growth of *Phalaenopsis amabilis* non-transformant and transformant for eight weeks.

Parameter	Average						Sig (2 tailed test)
	Initial Measurement		Growth Difference		Percentage Growth (%)		
	NT	T	NT	T	NT	T	
Number of leaves	4	3.75	0	0	0	0	0.730
Length of leaves (mm)	38.68	24.47	0.86	0.2	2.2	0.8	0.008
Width of leaves (mm)	9.16	8.16	0.59	0	6.5	0	0.001
Number of roots	4	6.5	0	0	0	0	0.032
Length of roots (mm)	27.05	30.34	0.56	1.87	2.1	6.2	0.642
Width of roots (mm)	3.08	3	0.63	0.05	20.5	1.5	0.230

*p < 0.05 means significant difference

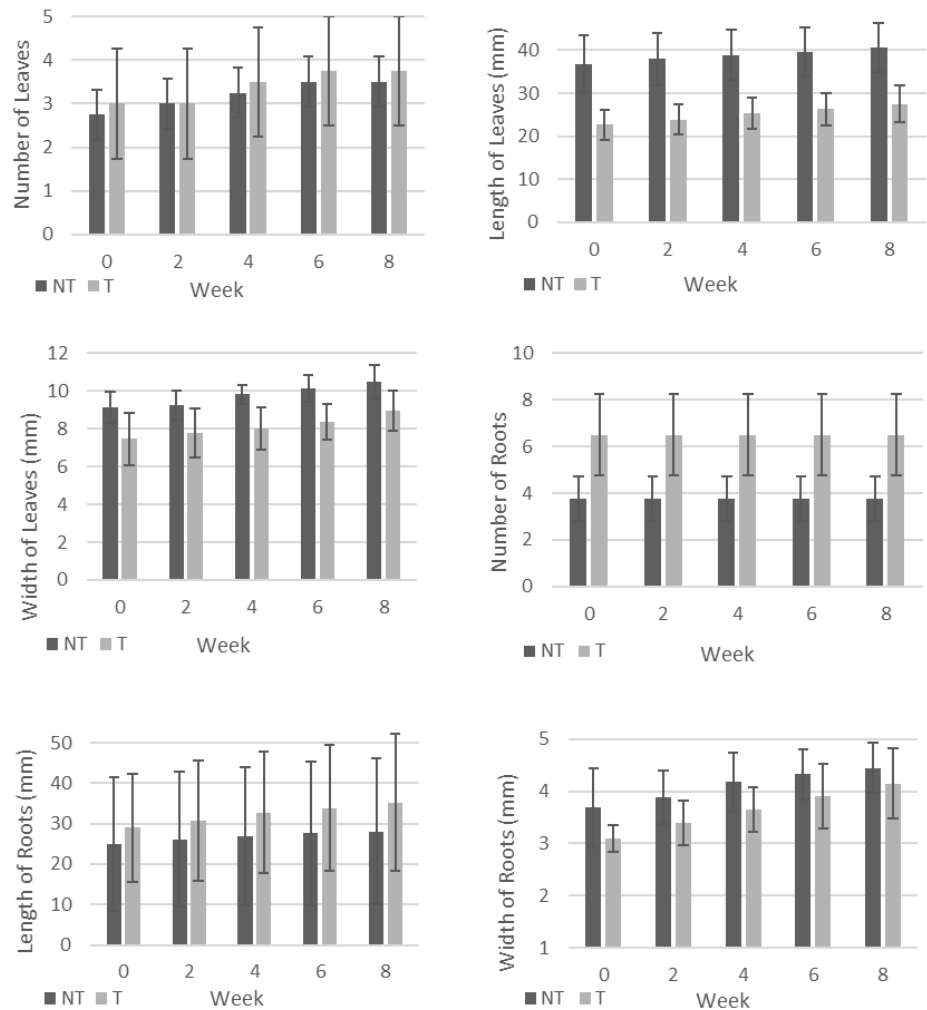


Figure 4. Growth graph of non-transformant (NT) and transformant (T) *P. amabilis* plants carrying construction 35S::GR::*ATRKD4* for 8 weeks.

From the graph, the growth rate in the number of leaves and roots of transformant plant explants was higher than non-transformant plant explants which indicates a higher regeneration ability of transformant plants (Dwiyani et al. 2015). Meanwhile, the root length of the transformant plants was also longer than the non-transformant plants. Based on the growth parameters of leaf length, leaf width, and root width, transformant plants had lower growth performance than non-transformant plants. Auxin in *in vitro* culture is able to make cells in plant tissues undergo a process of division, enlargement, and encourage root formation (Sulasiah et al. 2015). Auxin is a hormone that plays a role in the formation of cell polarity, cell enlargement and elongation, cell

asymmetric division, as well as initiation of root formation (Deo et al. 2010; Gutiérrez-Mora et al. 2012). The addition of auxin in transformant plants will activate the expression of the *AUXIN RESPONSE FACTOR* gene (*ARF7* and *ARF19*). ARF will then act as a transcription factor to activate downstream targets in the form of *LATERAL BOUNDARIES 29 (LBD29)* and *KRYPTONITE (KYP/SUVH4)* genes. *LBD29* and *KYP/SUVH4* are key genes for *in vivo* development and *in vitro* dedifferentiation of *Arabidopsis* cells (Deng et al. 2015).

Induction of somatic embryos from *P. amabilis* transformant using hormone-free medium

The explants used for somatic embryo induction were from 1 year and 6-month-olds *P. amabilis* plantlets cultured on solid hormone free-NP medium for eight weeks. The emergence of propagules from wounded parts of leaf explants of *P. amabilis* transformant indicates that the formation of somatic embryogenesis has initiated. The injury in the middle of the explant aims to trigger the explant response to initiate embryogenesis. The percentage of somatic embryo (SE) emergence increases because of an injury in the middle of the explant. The injury is caused by a response from the uninjured cell near the injured cell that will activate and initiate cell proliferation (Iwase et al. 2011). Orchids transformants grown on NPO medium formed somatic embryos directly from wounded area of the leaves and produced about 20% from the total 5 explants grown in hormone-free NP medium. Von Arnold et al. (2002) added that younger, meristematic explants had a higher ability to induce somatic embryogenesis than differentiated plant cells. Somatic embryo formation began to appear in the second week (Table 2).

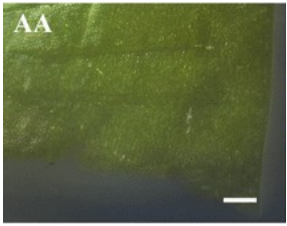

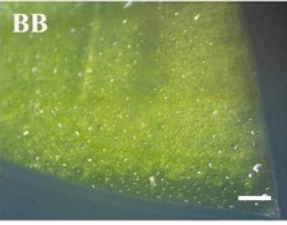
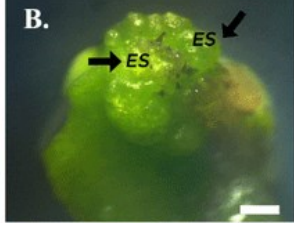
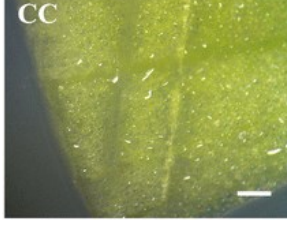

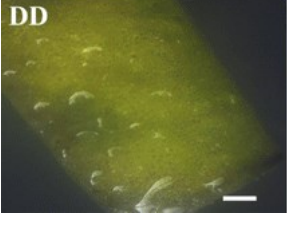
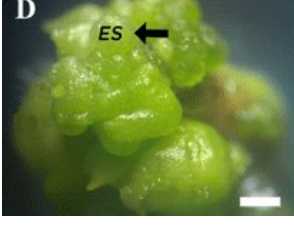
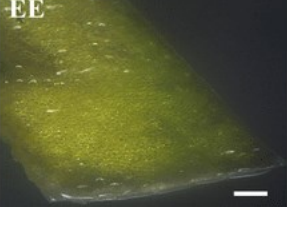

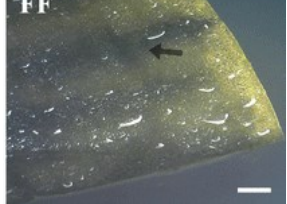

P. amabilis non-transformant did not produced somatic embryos when it cultured on NPO medium. Although it showed the formation chlorosis of explants and then browning after being cultured for 4 weeks. Browning is caused by wounding on the explant when it is being cut. When the plant is injured, a burst of reactive oxygen occurs on the explants which affect the integrity of the membrane (Cascia et al. 2012) and result in loss of cellular compartmentalization of cells. Browning is caused by phenolic compounds in the explants (Di Guardo et al. 2013). The phenolic compounds were caused by wounding act as signaling molecules and promote increased levels of PPO (polyphenol oxidase). In this condition, PPO expression and PPO protein levels are up and cause browning to appear (Deng et al. 2015).

The histological analysis used to see the anatomical structure and origins of the somatic embryos structure that surrounding the embryo (Figure 5).

Steeves and Sussex (1989) stated that the stages of somatic embryo formation begin with the formation of proembryos in the explant epidermal tissue. The proembryo consists of small cells with a large, darker coloured nucleus. Then a globular embryo is formed which is characterized by the enlargement of the proembryo and the formation of a protoderm-like. This structure consists of a layer of cells, organized frequently and tightly. The globular embryo then grows lengthwise and forms a suspensor-like structure at its baseline. Suspensors function for nutrient transport for the embryo, especially in the beginning stages of embryogenesis. The appearance of the suspensors also indicates that the somatic embryos originates from a single cell. The basal structure of the embryo reveals the origin of an embryo. The embryo was derived from a single cell which resembles suspensor in its basal and has been determined since initial division (Horstman et al. 2017). Then, the embryo formed scutellar

notch which mark the conformation of the shoot apical meristem (SAM) and represent the early stages of coleoptile development (Alcantara et al. 2014). Then shoot meristem (sm) is formed from the scutellar notch. The embryo elongated formed a root meristem and two leaf primordia covered with coleoptile which named coleoptilar embryo. Histologically, the somatic embryo development of *P. amabilis* orchids transformant showed that the somatic embryo development pattern is the same as the somatic embryo development pattern of general monocot plants, which includes the stages of proembryo, globular embryo, scutellar embryo, and coleoptilar embryo.

Table 2. Induction of somatic embryos from transformant and non-transformant *P. amabilis* leaf explants.

Week	Non transformant <i>P. amabilis</i>	Transformant <i>P. amabilis</i>
0		
2		
3		
4		
6		
8		

Notes: (A-F) Formation of somatic embryos (SE) of leaf explants from

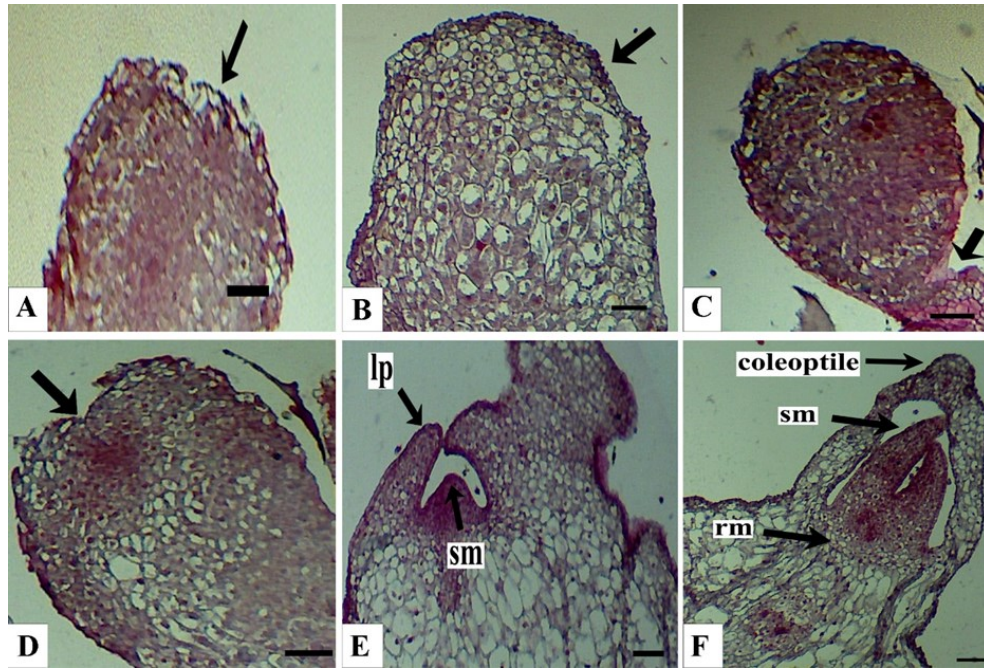


Figure 5. Anatomy of somatic embryos from the leaf explants of *P. amabilis* transformant. (A) The structure resembles to proembryo (arrow) derived from epidermal. (B) Globular embryo, enclosed by protoderm (arrow). (C) Globular embryo with an extended suspensor (arrow) on the basal region. (D) The formation of a scutellar notch in the apical (arrow). Arrows in A, B, and D indicate the position of somatic embryo initiation. Arrow in C indicates an extended suspensor on the basal region of SE. (E) The formation of shoot apical meristem (sam) and leaf primordia (lp). (F) SE contains shoot meristem (sm), leaf primordia (lp), enclosed by coleoptile, and root meristem (rm). Bars = 1000 μ m.

35S::GR::AtRKD4 transformants at the cutting site. (A) SE (arrows) formed from the surface area of the wounding section (B) early stages of somatic embryogenesis starting with formed of proembryo. (C) Proembryo developed into globular embryo. (D) The number of somatic embryos enlarged. (E) The globular embryo developed into a scutellar embryo (F) the embryo begins to form a bud (arrow). (AA-FF) Induction of SE in leaf explants from non-transformant plants. (FF) Arrows indicate browning in explants. (Bars: 5mm)

CONCLUSION

The *AtRKD4* gene is stably integrated in the *P. amabilis* transformants genome. There is no difference between the growth of *P. amabilis* transformant and non-transformant based on the number of leaves and the length and width of the roots. Somatic embryos can be induced directly from leaves of *P. amabilis* transformant cultured on hormone-free NP medium that produced about 20% somatic embryos, but not from non-transformant leaves. There is no significant difference on anatomic characters between somatic embryo of *P. amabilis* transformant and non-transformant plants.

AUTHORS CONTRIBUTION

D.S.: collecting data, preparing, analysing, and writing article from the data. N.G.A.P.: analysing data. W.M.: previous researcher of transformant plant. J.G.M: founder of T-DNA construct. E.S.: advisor of work, analysing, and critical review.

ACKNOWLEDGMENTS

This research was granted by research grants from the Ministry of Research and Technology/ National Agency for Research and Innovation for funding the Master's Thesis Research (PTM) with Contract No. 2011/UN1/DITLIT/DIT-LIT/PT/2020 given to ES and DS.

CONFLICT OF INTEREST

The authors declare that there is no conflict of interest.

REFERENCES

- Alcantara, G.B. et al., 2014. Plant regeneration and histological study of the somatic embryogenesis of sugarcane (*Saccharum* spp.) cultivars RB855156 and RB72454. *Acta Scientiarum - Agronomy*, 36(1), pp.63–72. doi: 10.4025/actasciagron.v36i1.16342.
- Aoyama, T. & Chua, N.H., 1997. A glucocorticoid-mediated transcriptional induction system in transgenic plants. *Plant Journal*, 11(3), pp.605–612. doi: 10.1046/j.1365-313X.1997.11030605.x.
- Von Arnold, S. et al., 2002. Developmental pathways of somatic embryogenesis. *Plant Cell, Tissue and Organ Culture*, 69(3), pp.233–249. doi: 10.1023/A:1015673200621.
- Cascia, G. et al., 2012. Investigation of ascorbate metabolism during induction of storage disorders in pear. *Physiologia Plantarum*, 147(2), pp.121–134. doi: 10.1111/j.1399-3054.2012.01641.x.
- Chardin, C. et al., 2014. The plant RWP-RK transcription factors: Key regulators of nitrogen responses and of gametophyte development. *Journal of Experimental Botany*, 65(19), pp.5577–5587. doi: 10.1093/jxb/eru261.
- Deng, Z. et al., 2015. Molecular cloning, expression profiles and characterization of a glutathione reductase in *Hevea brasiliensis*. *Plant Physiology and Biochemistry*, 96, pp.53–63. doi: 10.1016/j.plaphy.2015.07.022.
- Deo, P.C. et al., 2010. Factors affecting somatic embryogenesis and transformation in modern plant breeding. *The South Pacific Journal of Natural and Applied Sciences*, 28(1), p.27. doi: 10.1071/sp10002.
- Dwiyani, R. et al., 2015. Micropropagation of orchid carrying knotted-like from *Arabidopsis thaliana* (Knat1) gene. *Plant Tissue Culture and Biotechnology*, 25(1), pp.13–20. doi: 10.3329/ptcb.v25i1.24121.
- Di Guardo, M. et al., 2013. A Multidisciplinary Approach Providing New Insight into Fruit Flesh Browning Physiology in Apple (*Malus x domestica* Borkh.). *PLoS ONE*, 8(10), e78004. doi: 10.1371/journal.pone.0078004.
- Gutiérrez-Mora, A. et al., 2012. Plant Somatic Embryogenesis: Some Useful Considerations. In *Embryogenesis*. Mexico. doi: 10.5772/2143.
- Horstman, A., Bemer, M. & Boutilier, K., 2017. A transcriptional view on somatic embryogenesis. *Regeneration*, 4(4), pp.201–216. doi: 10.1002/reg2.91.
- Hsing, H.X. et al., 2016. Efficient and heritable transformation of *Phalaenopsis* orchids. *Botanical Studies*, 57(1), pp.1–12. doi: 10.1186/s40529-016-0146-6.
- Iwase, A. et al., 2011. The AP2/ERF transcription factor WIND1 controls cell dedifferentiation in *Arabidopsis*. *Current Biology*, 21(6), pp.508–514. doi: 10.1016/j.cub.2011.02.020.
- Karami, O., Aghavaisi, B. & Mahmoudi Pour, A., 2009. Molecular aspects of somatic-to-embryogenic transition in plants. *Journal of Chemical Biology*, 2(4), pp.177–190. doi: 10.1007/s12154-009-0028-4.
- Mondal, T., Aditya, S. & Banerjee, N., 2016. Role of plant growth regulators on asexual seed germination and seedling development of *Vanda coerulea* Griff. ex Lindl. an endangered orchid. *Indian Journal of Fundamental and Applied Life Sciences*, 6(3), pp.36–41.

- Mose, W., 2019. *Induksi Embriogenesis Somatik Tanaman Anggrek Phalaenopsis amabilis (L.) Blume dengan Zat Pengatur*. Universitas Gadjah Mada.
- Mursyanti, E. et al., 2015. Induction of Somatic Embryogenesis through Overexpression of ATRKD4 Genes in Phalaenopsis “Sogo Vivien.” *Indonesian Journal of Biotechnology*, 20(1), pp.42–53. doi: 10.22146/ijbiotech.15276.
- Neelakandan, A.K. & Wang, K., 2012. Recent progress in the understanding of tissue culture-induced genome level changes in plants and potential applications. *Plant Cell Reports*, 31, pp.597–620. doi: 10.1007/s00299-011-1202-z.
- Ouwerkerk, P.B. et al., 2001. Glucocorticoid-inducible gene expression in rice. *Planta*, 213, pp.370–378. doi: 10.1007/s004250100583.
- Pangestu, F., Aziz, S.A. & Sukma, D., 2014. Karakterisasi Morfologi Anggrek Phalaenopsis Hibrida Morphological Characterization of Phalaenopsis Hybrid. *Indonesian Horticultural Journal*, 5(1), pp.29–35.
- Picard, D., 1993. Steroid-binding domains for regulating the functions of heterologous proteins in cis. *Trends in Cell Biology*, 3(8), pp.278–280. doi: 10.1016/0962-8924(93)90057-8.
- Rahayu, E.M. Della, 2015. Konservasi anggrek bulan (Phalaenopsis spp.) di Pusat Konservasi Tumbuhan Kebun Raya -LIPI, Bogor. *Prosiding Seminar Nasional Masyarakat Biodiversitas Indonesia*, 1(8), pp.1847–1850. doi: 10.13057/psnmbi/m010816.
- Semiarti, E. et al., 2007. Agrobacterium-mediated transformation of the wild orchid species Phalaenopsis amabilis. *Plant Biotechnology*, 24(3), pp.265–272. doi: 10.5511/plantbiotechnology.24.265.
- Semiarti, E. et al., 2011. Agrobacterium -Mediated Transformation of Indonesian Orchids for Micropropagation. In *Genetic Transformation*. pp. 215–240.
- Semiarti, E., 2018. Orchid biotechnology for Indonesian orchids conservation and industry. In *AIP Conference Proceedings*. pp. 1–6. doi: 10.1063/1.5050118.
- Setiari, N. et al., 2018. Microporopagation of Dendrobium phalaenopsis Orchid Through Overexpression of Embryo Gene AtRKD4. *Journal of Agricultural Science*, 40(2), pp.284–294. doi: 10.1017/S0021859618000163.
- Shekarriz, P. et al., 2014. Coconut Water and Peptone Improve Seed Germination and Protocorm Like Body Formation of Hybrid Phalaenopsis. *Agriculture Science Developments*, 3(10), pp.317–322.
- Steeves, T.A. & Sussex, I.M., 1989. *Patterns in Plant Development* 2nd ed., New York: Cambridge University Press. doi: 10.2307/2484650.
- Sulasiah, A., Tumilisar, C. & Lestari, T., 2015. Pengaruh Pemberian Jenis Dan Konsentrasi Auksin Terhadap Induksi Perakaran Pada Tunas *Dendrobium Sp* Secara in Vitro The Effect of Types and Concentrations of Auxin on Rooting Induction on Dendrobium sp Bud in In Vitro. *Bioma*, 11(1), pp.59–66.
- Sutikno, 2016. *Bahan Ajar Mikroteknik Tumbuhan*, Yogyakarta: Fakultas Biologi Universitas Gadjah Mada.
- Waki, T. et al., 2011. The arabidopsis RWP-RK protein RKD4 triggers gene expression and pattern formation in early embryogenesis. *Current Biology*, 21(15), pp.1277–1281. doi: 10.1016/j.cub.2011.07.001.
- Yang, X. & Zhang, X., 2010. Regulation of somatic embryogenesis in higher plants. *Critical Reviews in Plant Sciences*, 29(1), pp.36–57. doi: 10.1080/07352680903436291.

Research Article

Combining Moderate and High Resolution of Satellite Images for Characterizing Suitable Habitat for Vegetation and Wildlife

Sheriza Mohd Razali^{1*}, Zaiton Samdin^{1,2}, Marryanna Lion³

1)Institute of Tropical Forestry and Forest Products, Universiti Putra Malaysia, 43400 UPM Serdang, Selangor

2)School of Business and Economics, Universiti Putra Malaysia, 43400 UPM Serdang, Selangor

3)Forest Research Institute Malaysia, 52109 Kepong, Selangor

* Corresponding author, email: sheriza@upm.edu.my

Keywords:

High resolution satellite image
wildlife habitat
NDVI

Submitted:

13 September 2022

Accepted:

16 January 2023

Published:

26 July 2023

Editor:

Miftahul Ilmi

ABSTRACT

Combining different resolution of remote sensing satellites becomes a unique approach for vegetation and wildlife habitat assessment study. Remote sensing technology can reach land and water on the Earth's surface, and it can interpret signals from spectral responses. When these techniques are combined with Geographical Information Systems (GIS), land can be monitored in a variety of ways. Meanwhile, changes in land use led to changes in vegetation on the ground, with natural vegetation being removed from natural forests, leaving a degraded forest. This issue was not investigated for assessing habitat suitability for important plantations such as Eucalyptus plantation. Therefore, the study employed remote sensing and Geographical Information System (GIS) to model suitability of habitat to live and to survive in the Eucalyptus plantation. Normalized Difference Vegetation Index (NDVI) and Normalized Difference Water Index (NDWI) derived from a mathematical equation can demonstrate intensity of greenness of green vegetation in particular area and time, and availability of soil moisture, respectively, is very suitable to model the greenness of the area. WorldView-2 satellite image was pre-processed, processed, and classified to produce land use indicator in Sabah Softwoods Berhad plantation majoring Eucalyptus spp. tree planted in Tawau, Sabah. Sentinel and Landsat 8 image were used for vegetation and water stress indicator were downloaded from Land Viewer application. Net Primary Productivity (NPP) at monthly scale was also calculated and ranked the productivity for the suitability mapping. Climatic condition based on monthly precipitation and seasonality derived from ASEAN Specialized Meteorological Centre (ASMC) was employed for ranking its suitability value. In this study, natural forest and oil palm plantation is tested to developed suitability map for vegetation and wildlife habitat to live with. All indicators were ranked 10 to 40 presenting benefit and usefulness of the indicator to vegetation and wildlife in the study area. Then, final classification was made from accumulation of those indicators into 0 to 200 (Not suitable to Highly suitable). The results showed 59.9% of the area classified as moderately suitable, 36.9% highly suitable, 3.2% least suitable and no area was classified as not suitable. This type of study assisted forest managers and policymakers for better managing of their forests for better life of trees and wildlife under their management. The methodology adapted in the study is ecologically sounded and economically viable to be modified and applied in Sustainable Forest Management (SFM) in Malaysia and other tropical forest regions.

Copyright: © 2023, J. Tropical Biodiversity Biotechnology (CC BY-SA 4.0)

INTRODUCTION

Remote sensing technology enables acquisition of satellite image for numerous land monitoring, for example for forest and agricultural lands application. The capable technology of using mathematical equation of multispectral images into vegetation indices for vegetation vigour and risk analysis. The operated technology was based on different satellite resolutions, for example, it has demonstrated with multispectral wavelengths on Landsat Thematic Mapper (TM) and WorldView satellite. The satellites that carry 30-meter and 1.8-meter of cameras, respectively.

WorldView with multispectral range of wavelengths is capable to construct vegetation index build from near-infrared and red bands. These two important wavelengths making WorldView satellite is very beneficial for vegetation study in tropical forest area. In previous study, O'Neil et al. (2020) conducted a study based on vegetation indices for vegetation productivity estimation. At global level, more studies using the indices for land cover change the analysis. A study by Chen et al. (2021), modelled human factor in China pastureland, located in Wulagai River Basin based on the vegetation indices.

Normalized Difference Water Index (NDWI) is an example of index which is a significant index in forest fire study and it is found having good relationship in drought study as demonstrated in Bowyer & Danson (2004) and Razali et al. (2015). Remote sensing is continually showed its capability in above-ground biomass estimation demonstrated in pan-tropical forest (Abbas et al. 2020). Before present, simple ratio shortwave infrared (SWIR) spectral indices were employed for quantifying landscape-level foliar moisture in an ecosystem dominated by *Pinus ponderosa* P. & C. Lawson. However, most studies were using SWIR for estimating foliar moisture in mid- and high-latitude sites (Toomey & Vierling 2005).

Established from information provided, NDVI is a tropical regional index that suitable for the current study proposed. In fact, NDVI has been used a precursor for Leaf Area Index (LAI) and Fraction of Absorbed Photosynthetically Active Radiation (FAPAR) used for carbon assimilation assessment (Nunes et al. 2012). From there on, NDVI was employed with high-resolution Unmanned Aerial Vehicle (UAV) imagery for monitoring species outbreak built from foliar discoloration (Dash et al. 2017). NDWI has a potential in semi-arid land, which it has been modelled in (i) closed and open canopy crops, (ii) semi-arid shrublands, and (iii) boreal conifer forests (Cheng et al. 2006). Generally, NDWI showed good correlations with Equivalent Water Thickness (EWT) tested with AVIRIS, and appeared to provide better estimations of canopy positioned by Moderate Resolution Imaging Spectroradiometer (MODIS) as a moderate resolution satellite image (Cheng et al. 2006).

Application of remote sensing established from different satellite resolution permits various problem solving. This is because there was scarce approach that has been identifying by various agencies managing human-wildlife conflicts in tropical forest region. Central Forest Spine (CFS) or IC-CFS, Improving Connectivity (IC) is a collaborative effort by Malaysian Government and international bodies for developing area with sensitive ecosystem as a results of forest fragmentation. The programs restore the connectivity between three critical landscapes of forest complexes (IC-CFS 2021). The efforts must be continued, and modelling habitat suitability built from low and moderate satellite remote sensing resolution which can be set up in this Eucalyptus plantation landscape.

Specifically, in Malaysia, wildlife habitat creates conflict zone which human frightens and troubles by wildlife nearby their housing area. In that case, it was because natural habitat has been diminished and changed into agricultural land area, i.e palm oil plantation, pineapple, and rubber

plantation. Sabah Softwoods Berhad (SSB) is a company that was experienced in mitigating human wildlife conflicts (Nathan 2016). The company's primary activities are oil palm and tree plantation that make it about 60,000 hectares of land, reported in 2016. The company adopted 7,000 hectares of that area as a reserve land for conservation, meanwhile about 3,000 hectares were earmarked for housing and infrastructure. With the allocation, the company was one of the earliest companies obtained certification for its palm oil operation for Malaysian Sustainable Palm Oil (MSPO) (MPOCC 2022). Elsewhere, in North End of Assateague Island, there are needs for habitat suitability modelling, particularly from the vulnerable to climate change area. Habitat distribution maps play an essential intermediary step towards justifying conservation and planning efforts highlighted by Russ et al. (2022). The company hold down human-elephant conflicts engaged with estimated around two thousand Pygmy elephants that roam the landscape. The elephants get into human activities and the company is using translocation and fencing the plantation.

Human and wildlife conflict is a tough task to handle. Therefore, the objective of the study is to identify as a major criterion in ensuring the security of the wildlife and sufficient land for their lives. This is important to solve the above problem by merging recent advancement of satellite sensor resolution data integrated with climatic data.

MATERIALS AND METHODS

Study Area

To test the site suitability for this study, we examined a plantation area located in Brumas, districts of Tawau, Sabah state. For this study, Softwoods Berhad located at latitude 4°35'36" and longitude 117°45'31" retrieved from Google Map (Figure 1) was chosen. Located at between 200 - 600 m of elevation above sea level, the plantation has luxuriant high disease tolerant tree species. Softwoods Berhad plantation area holds about 18,000 hectares of high demand of *Eucalyptus pellita* and *F. moluccana* tree species. Specifically, *F. moluccana* tree species are planted in the conservation area in the plantation. The plantation is Tanjung Lipat type with clay texture of 25% to 35%. In addition, it is Kumansi type with more than 40% clay. This study adopted from the spirits to see long life of Sungai Umas, Sungai Landau, Sungai Indit and Sungai Umas-Umas in the plantation. Data collected from www.worldweatheronline.com showed monthly temperature with a minimum of 24°C, a maximum of 31°C, and a mean of 28°C recorded in 2016. Meanwhile, data referred from Markos et al. (2018) depicted monthly precipitation of 50 mm recorded in 2014. In the meantime, annual precipitation was collected from Malaysia Meteorological Station as shown in Figure 2.

Methods

The Sentinel and Landsat 8 data were obtained from Land viewer application purchased online. Before that, the image was atmospherically corrected using atmospheric correction wizard, which allows users to execute a variety of atmospheric corrections in the simplest and fastest possible methodology. The wizard automatically in most of the required parameters uses image information and walks the user through each key step. The software's focus application was used to prepare data, and then ATCOR ground reflectance tools were used to analyse atmospheric correction.

A year time series analysis was performed on the NDVI and NDWI data. Inclusion of Sabah's dry and wet seasons. Both satellites' NDVI and

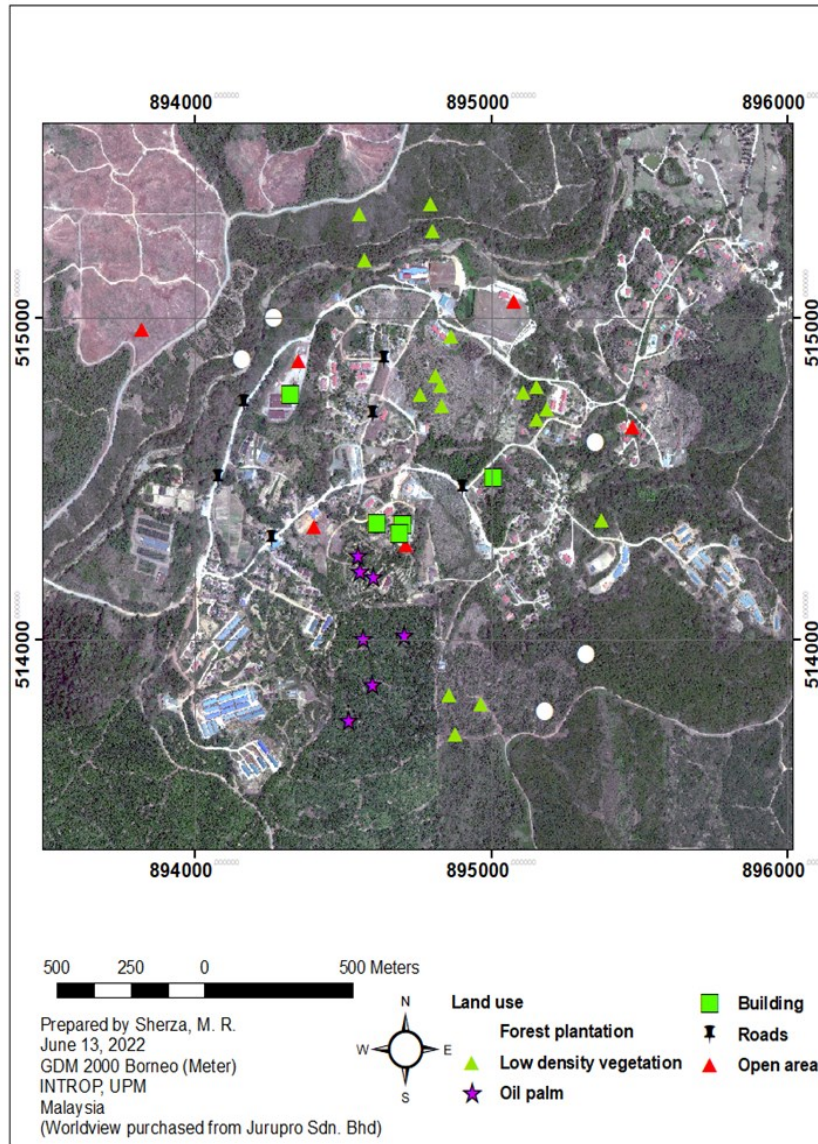


Figure 1. Map of the study area with location of various land uses and land covers.

NDWI were calculated. According to theory, NDVI was calculated using the approach that using the index vegetation status can be identified as healthy and full vegetation coverage between 0.5 and 0.9. The index is very suitable for use in tropical areas as a study by [Braswell et al. \(2003\)](#) discovered that NDVI should not be used in too dry conditions such as Iran and other areas with similar conditions. In the meantime, [Pujiono et al. \(2013\)](#) used NDVI to monitor mangrove forest in Indonesia. A year later [Darmawan & Sofan \(2012\)](#) used the Enhanced Vegetation Index (EVI) and NDVI to detect changes in Indonesia's tropical forest. NDVI was also used to assess vegetation stress in vegetative and agricultural land in India many years ago ([Bhuiyan et al. 2006](#)). The NDVI showed an increasing trend of anthropogenic vegetation change ([Chen et al. 2021](#)). A study by [Rouse et al. \(1973\)](#) was cited.

$$NDVI = (\rho_{NIR} - \rho_{Red}) / (\rho_{NIR} + \rho_{Red}) \dots\dots\dots(1)$$

Meanwhile, NDWI was found very applicable to use in detection of water-stress forest such as in mangrove ([Vidhya et al. 2014](#)). Again, it was applied by [Razali et al. \(2015\)](#) in monitoring vegetation drought in West Malaysia. NDWI measured sensitivity to changes in liquid water content ([Gao 1996](#)). NDWI showed a good relationship with plant stress,

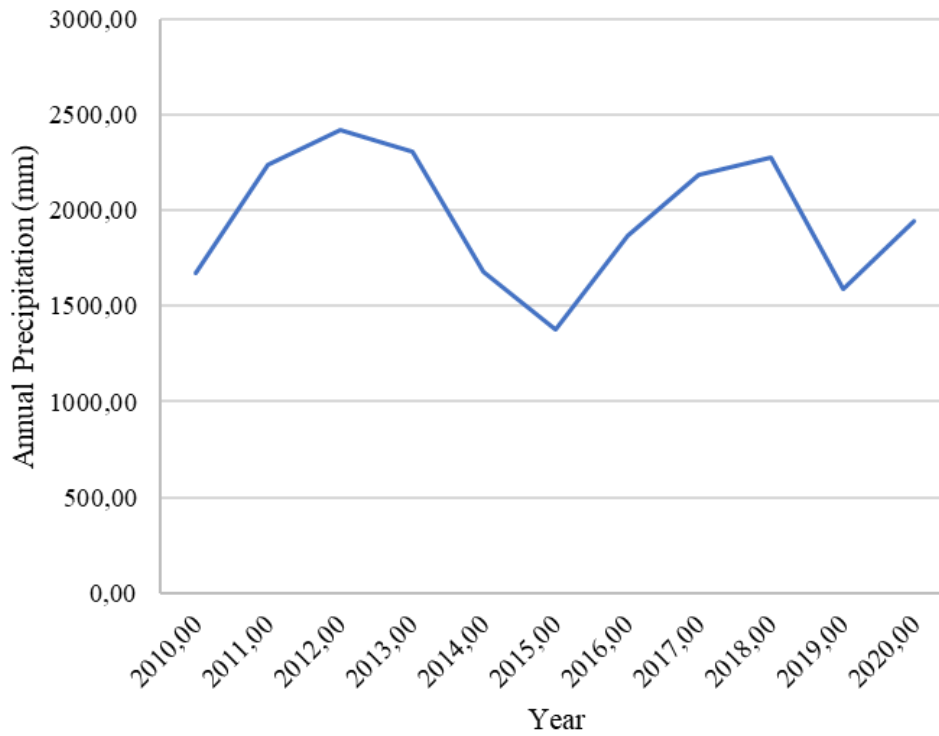


Figure 2. Annual precipitation of Tawau based on data from Malaysia Meteorological Department for 2010 – 2020.

which was used in a study by Vidhya et al. (2014) in classification of mangrove heath status. A recent study of Caturegli et al. (2020) tested NIR at two wavelength of 1240 μm and 2130 μm. The study tested NDWI without water on Bermuda grass in Italy. Based on theory, the index was calculated based on below equation (Gao 1996):

$$NDWI = (\rho_{NIR} - \rho_{SWIR3}) / (\rho_{NIR} + \rho_{SWIR3}) \dots\dots\dots(2)$$

In details, the time series started from June 2017 until April 2022. About 39 samples were collected between the time frames. The study hypothesized that the distribution of Sentinel and Landsat 8 for NDVI and NDWI indices were similar across categories of wet season influenced by Northeast monsoon in Sabah region.

Worldview satellite image for 2016 was derived to calculate NDVI as comparison with the 2021 and 2011 NDVI data. Inadequate spectral properties in Worldview image of shortwave to calculate NDWI for the comparison. This is because the availability for comparison makes use of previous data for related study (Razali & Lion 2021). Overall flowchart of the study is presented below (Figure 3).

Land Use Mapping

The study employed PCI for mapping the land use. Object-based image analysis (OBIA) embedded in Catalyst Professional software, once known as PCI Geomatics is advocated to facilitate the classification. Worldview 2 satellite image was pre-processed by employing Atmospheric Correction (ATCOR) in set up in the software. ATCOR unnecessary enables users to carry out a variety of atmospheric corrections in the most straightforward and available in efficient method. Further efficient way was data preparation, then after that ground reflectance tools will be analysed by the ATCOR. Overall flow of the land use mapping are shown in figure below (Figure 4).

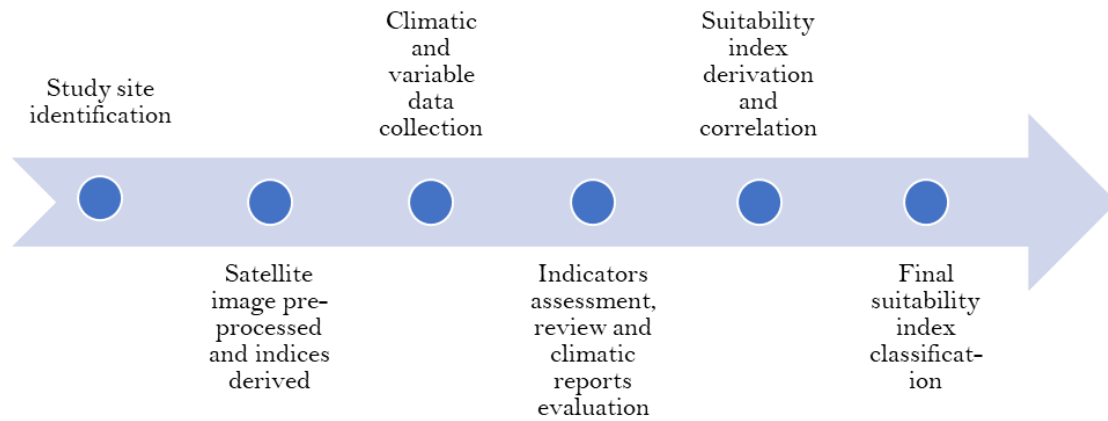


Figure 3. Overall flowchart of the study.

NPP Estimation

The NPP in this study was derived from the GPP, which was based on (Xiao et al. 2004). This is since GPP is the rate of CO₂ fixation via photosynthesis in the forest canopy. As a result, GPP is calculated as follow:

$$GPP = fAPAR \times PAR = \epsilon \times APAR \dots\dots\dots(3)$$

Where, the ϵ is Light Use Efficiency (ϵ), which has long been recognised as important component of the radiation regime for tree growth, incoming photosynthetically active radiation (PAR) ($gMJ^{-1} m^{-2}$) and the fraction of PAR intercepted by foliage (Fraction of photosynthetically active radiation of fAPAR) explained in Xiao et al. (2004).

Moreover, this study estimated PAR from 50% of incoming solar radiation as a result of solar radiation data collected from Sukarno et al. (2017) study. Instruments allocated on rooftop of building on 17 March 2016 as one method adopted for the research. The instruments were installed in Universiti Malaysia Sabah (UMS), in Kota Kinabalu, Sabah. Furthermore, absorbed fraction of photosynthetically active radiation (APAR) (gMJ^{-1}) was derived by combining two aforementioned variables, fAPAR and PAR (Coops et al. 2010). The said components, LUE, [18] was calculated as follows:

$$LUE = 0.8932 + TMonth + 0.0015(PRECIPMonth) - 0.002(GDD) \dots\dots\dots(4)$$

Meanwhile, fAPAR was derived as below:

$$fAPAR = 1.25 \times NDVI - 0.025 \dots\dots\dots(5)$$

An index for vegetation, NDVI determined using red and near-infrared

$$NDVI = (\rho_{NIR} - \rho_{Red}) / (\rho_{NIR} + \rho_{Red}) \dots\dots\dots(6)$$

The equation can be explained as, ρ_{NIR} is the reflectance of the WorldView image at 0.77 – 0.895 nm (Near-infrared band) and ρ_{Red} is the reflectance of the satellite image at 0.63 – 0.690 nm (red band). The NPP ($gCM^{-2} month^{-1}$) was therefore, derived by applying 50% of GPP.

RESULTS AND DISCUSSION

Vegetation and Water Stress Indicator

The study conduct correlation for NDVI and NDWI of the Sentinel and Landsat satellite. From R² values, the NDVI in Sentinel was 0.95, whereas R² for Landsat was 0.99. These results, showed that the NDVI had a

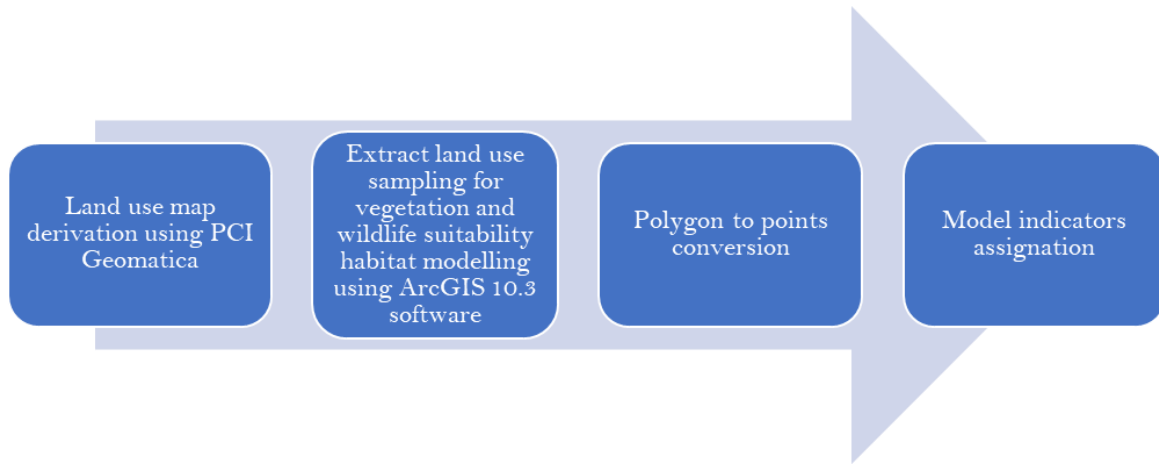


Figure 4. Overall flowchart of land use mapping.

good indicator to predict forest productivity for both satellite, hence, capable at assessing forest health and biomass changes over time. It is potential for drought and post-fire recovery in Eucalyptus forest such as demonstrated by (Caccamo et al. 2011; 2015). NDVI within similar satellite shown relative differences in lower resolution of METOP-A-NOAA-9 and NOAA-9 reported in Trishchenko (2009). The differenced was demonstrated by NIR and red spectral bands of NDVI equation. In a separated study in tropical forest of Peninsular Malaysia, NDVI showed strong correlation with NDWI (Razali et al. 2015) (Figure 5).

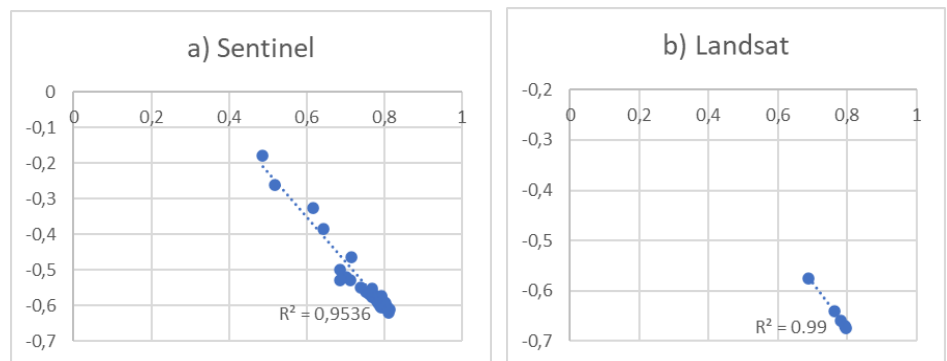


Figure 5. Correlation between NDVI and NDWI Sentinel and Landsat.

It can be seen, based on the two indices, that the NDVI very useful for application in vegetation community is broadleaved and evergreen. Changes on the season scale was also anticipated that higher NDVI values, pursue NDWI to be lower, due to plant capability to maintain water supply for biomass accumulation, hence no water stress was recorded. Some studies define NDWI as Land Surface Water Index (LSWI), whereby as the LSWI served similar indicator. This finding was supported by the LSWI, which showed the fortnightly percentage increase of LSWI and NDVI from the previous fortnight for 2002 and 2005, for a few typical districts of Andhra Pradesh (Chandrasekar et al. 2010). Meanwhile, another study (Penuelas et al. 1997), mentioned Water Index (WI) have good agreement with NDVI (NDVI vs WI, $R^2 = 0.66$) and improved when rationing WI with NDVI ($WI/NDVI=0.71$).

Vegetation and Wildlife Habitat Indicator

NDVI for 2016 that was overlaid with land use map showed $NDVI > 0.8$ is located on Eucalyptus plantation area. Whereas $NDVI > 0.7$ is located on mostly on oil palm plantation. Meanwhile, $NDVI > 0.6$ can be found in Eucalyptus forest plantation but with presence of oil palms fea-

tures (light green colour). The oil palm features have a high agreement with ground data with 100% of accuracy assessment, however, is very uncertain to found oil palm features in Eucalyptus plantation. The features could be misclassified with low growth in the forest plantation. This is making forest plantation has lower NDVI than found in full covered forest. NDVI colour map shown in Figure 6 meanwhile scale and suitability index is tabulated in Table 1.

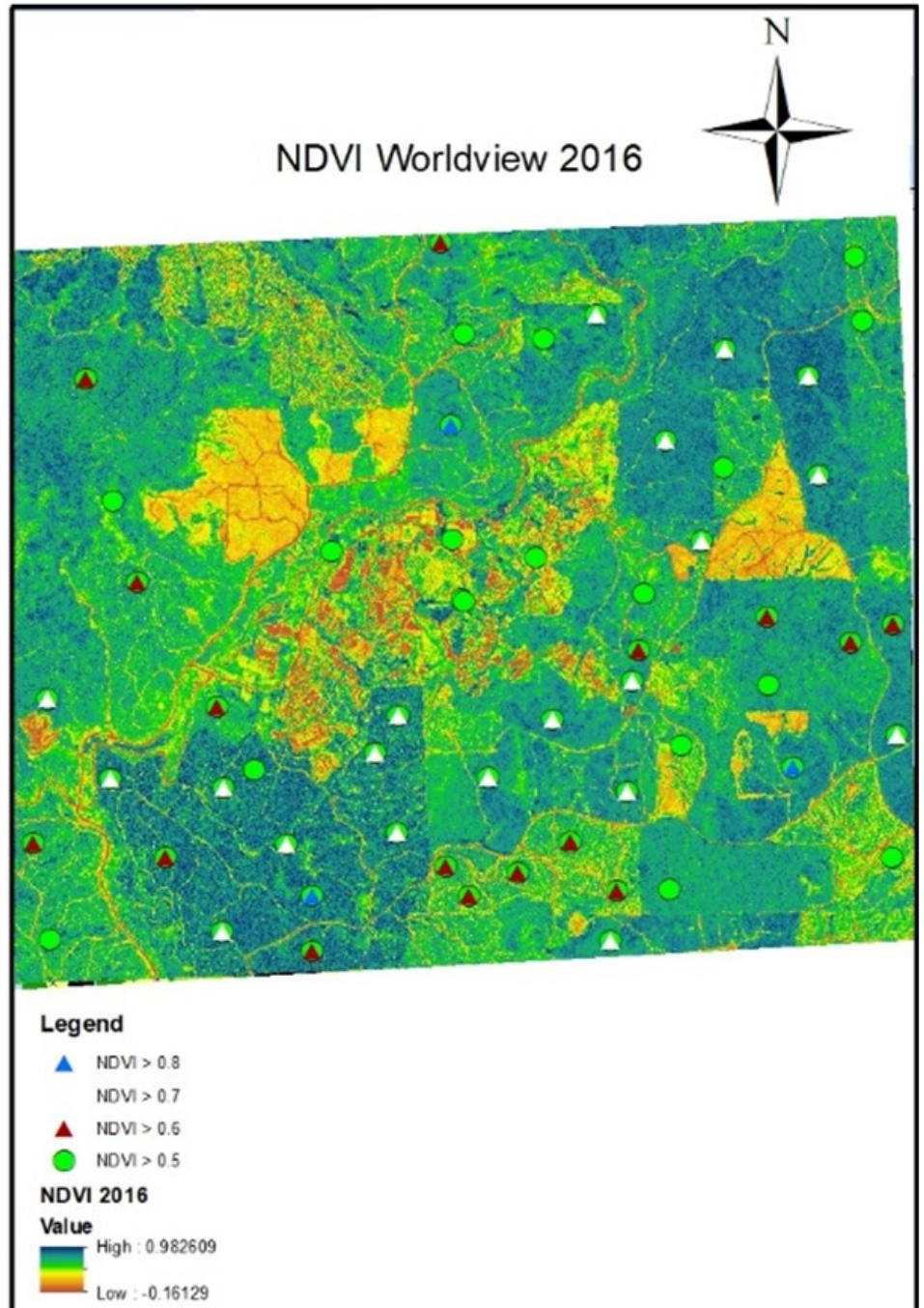


Figure 6. NDVI of the study area.

NDVI range 0 to 0.4 and below was associated with population concentration city as demonstrated in a study by (Potter et al. 2013). Meanwhile, in a mangrove forest with stress environmental condition NDVI was recorded 0.1 to 0.26 (Razali et al. 2019). This is corresponding to stress location due to sand deposition by sand packages that in fact caused poor tidal inundation.

Table 1. NDVI scale and suitability index value for analysis.

NDVI scale	Suitability index
NDVI > 0.8	40
NDVI > 0.7	30
NDVI > 0.6	20
NDVI > 0.5	10

Land Use

The land use accuracy was:

- Producer’s accuracy for Eucalyptus plantation, buildings, low-density vegetation, oil palm, open area and roads were, 100%, 81.25%, 94.12%, 100%, 100% and finally 25%, respectively.
- User’s accuracy was, 94.12%, 61.90%, 100%, 76.92% and finally 80%, respectively.

Each of the class was ranked according to its priority for wildlife to live within the removal of forest to a forest plantation. Higher forest coverage is ranked higher whereas lower forest cover or vegetation cover is ranked as lower (Table 2).

Table 2. Land use type and suitability index.

Land use	Suitability index
Forest plantation	40
Oil palm	30
Low density vegetation	20
Open area/Buildings/Roads	10

The forest plantations were given higher ranking for wildlife habitat suitability because it is associated to primary biodiversity area. According to a study conducted in Eucalyptus plantation in tropical forest of Brazil, forest plantation is the second-growth forest that is becoming dominant components of many tropical forest landscapes (Gardner et al. 2007). Similarly, about 30% of 35% of all amphibian species were confined to primary forests, which recorded in eastern Madagascar according to (Vallan 2002) and, a proportion identical to (Gardner et al. 2007). A recent study, Maliau Basin Conservation Area and Danum Valley Conservation Area, and one mature oil palm plantation were tested for ecosystems energetics. The study concluded that conversion of logged forest into oil palm plantation resulted in the collapse of most energetic pathways (Malhi et al. 2022). Therefore, oil palm was assigned to a suitability index of 30 (Figure 7).

Precipitation

In general, Sabah and Sarawak are influenced by Northeast monsoon which happens on November to April with approximately bringing heavy rain to east coast area, that including Tawau area. In 2015, a study by (Ng et al. 2019) found Tawau recorded 207.0 mm ±92.98 of monthly precipitation. Monthly average for 2010 – 2020 shown in Figure 8 for better evaluating condition of the study area. This making Tawau has higher precipitation than districts of Sabah, namely, Kota Kinabalu, Beaufort, Kudat and Keningau. For additional information, the value similarly recorded by Sandakan area which is located far much northern area. Finally, precipitation rank is shown in Table 3.

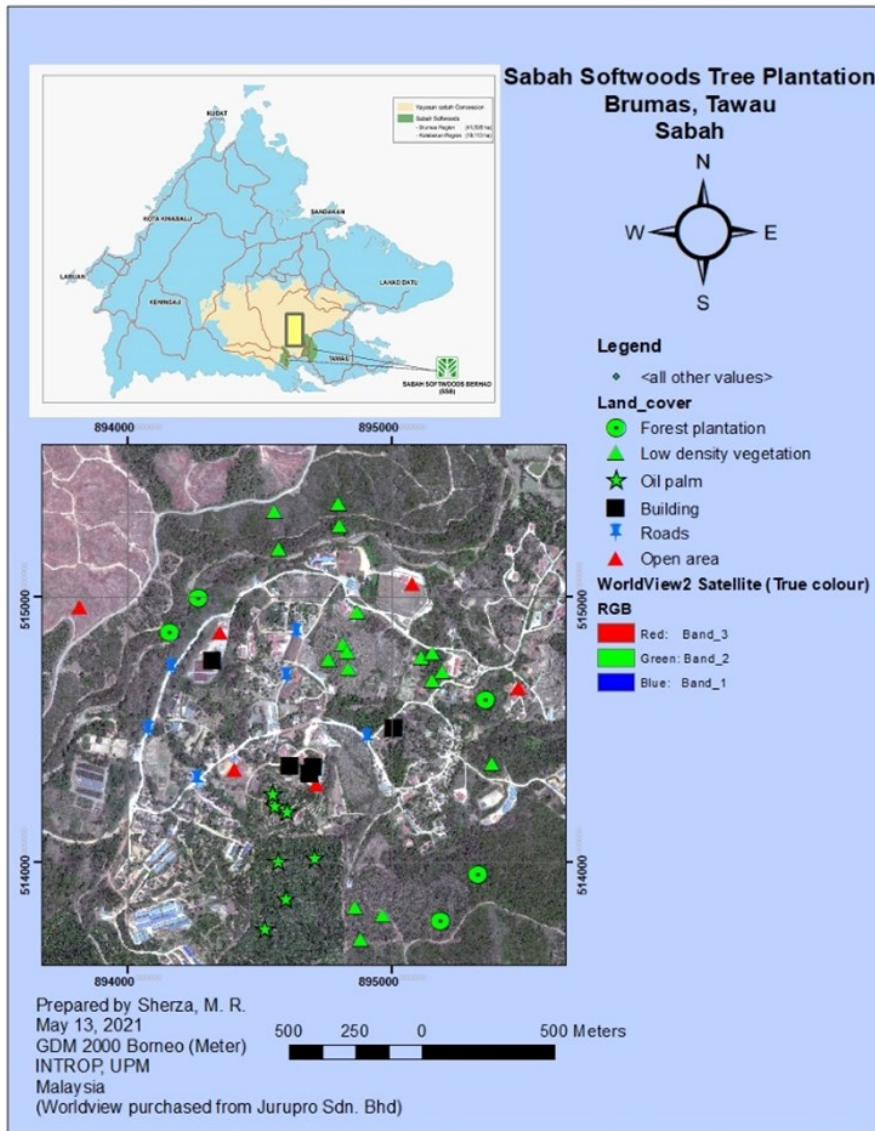


Figure 7. Land use for the study employed for map calculation.

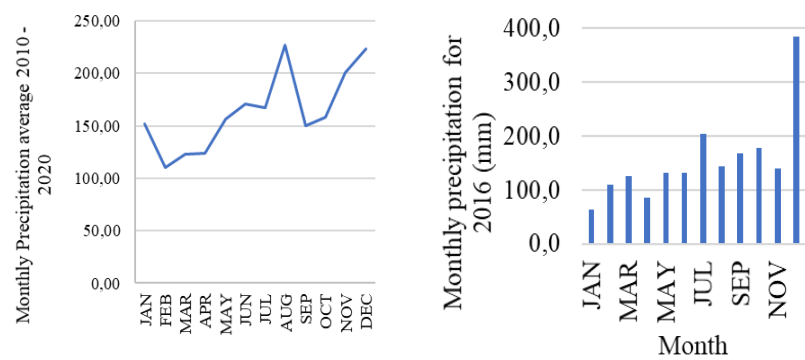


Figure 8. Monthly and annual precipitation for the study area.

Table 3. Mean monthly precipitation and suitability index.

Mean monthly precipitation (mm) of Year 2016, Tawau, Sabah	Suitability index
0 – 80	40
80 – 160	30
160 – 280	20
280 – 340	10

Seasonal

According to a website, www.malaysia.gov.my, Malaysia experiences humid weather throughout the year with the average daily temperature across Malaysia is between 21°C and 32°C. Typically, the Malaysian climate is influenced by the winds blowing from the Indian Ocean (Southwest Monsoon - May to September) and the South China Sea (North-Eastern Monsoon - November to March) (The Malaysian Administrative Modernisation and Management Planning Unit 2016).

Seasonal data was assessed based on ASEAN Specialized Meteorological centre (ASMC) report. The comprehensive report comprising data of ASEAN information on haze situation which rank as in Table 4.

Table 4. Indication of seasonal parameters derived from ASMC report and suitability index.

ASEAN Specialized Meteorological Centre (ASMC) based on Worldview satellite image acquired March 2016	Suitability index
March to May 2020	40
December – January 2016 – 2017	30
September - November 2020	20
Unidentified	10

NPP Productivity

The NPP was interpolated through using instruments in ArcGIS Spatial Analyst to map the proportion of NPP on the ground, as shown in Figure 9.

Estimation of NPP for Pasoh Forest reserve, Peninsular Malaysia was 213.5 gCm⁻² month⁻¹, accepted as a maximum value for tropical forest study (Razali et al. 2015). The proportion was identical to this study of moderate NPP suitability index, 20 (Table 5).

Table 5. Indication of NPP scale and rank value.

NPP scale (650 gCm ⁻² month ⁻¹)	Suitability index
NPP > 500	40
NPP > 300	30
NPP > 200	20
NPP > 100	10

Final Suitability Index

The final index was developed based on accumulation of all indicators suitability index value that was calculated using ArcGIS 10.8 software attribute table. Table 6 showed overall indicators that employed for the index based on below equation:

$$\text{Habitat Wildlife Indicator} = \text{VEG} + \text{LU} + \text{NPP} + \text{PREP} + \text{SEAS}$$

Vegetation and wildlife habitat indicator = VEG

Land use indicator = LU

Net Primary Productivity = NPP

Precipitation indicator = PREP

Season = SEAS

The study was successfully mapping suitability index for vegetation and habitat in Sabah Brumas, Tawau Eucalyptus and oil palm plantation. Habitat and vegetation classification derived after each of the pix-

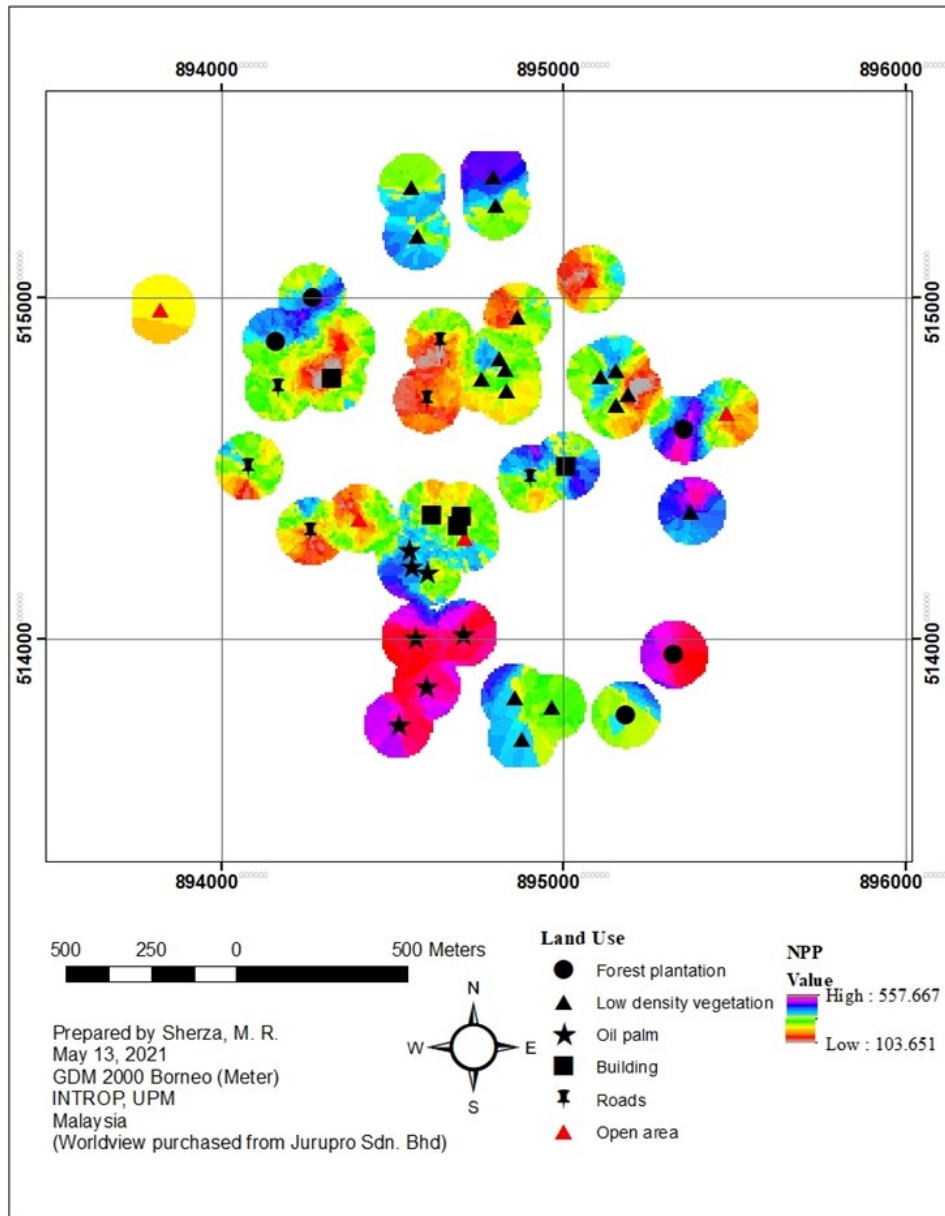


Figure 9. Overall NPP value interpolated on land use layer with points marked showed major area of the land use type.

els accumulated based on its suitability index. An index approaching 200 classified and highly suitable for the wildlife and vegetation to live and to sustain its live for a long term. A value less than 50 indicates as not suitable habitat for wildlife and vegetation to be in the area (Table 7).

Area of the habitat and vegetation classification pixels were classified based on Equal interval and Natural Breaks classifier. Based on the methods, percentage of the area classification derived and shown in Figure 10.

CONCLUSION

The results show the practical use of multispectral index of multiple resolution of satellite image in estimation of vegetation vigor and biomass in Eucalyptus plantation, Sabah, East Malaysia. Land use change has negative impact to wildlife and pursues wildlife conflicts in tropical forest. The research examines how integration of multi-resolution of satellite image may be used to generate a suitable area for wildlife habitat in eucalyptus plantation. Based on Sentinel, Landsat and WorlView-2, the study

Table 6. Indication of accumulation of vegetation and wildlife habitat suitability index.

No.	Indicator/Scale	Description	Suitability index	Source of References
1.	Vegetation and wildlife habitat indicator			Rock/Sand/Snow: Value approaching zero, $0.1 < X < 0.1$
	Biomass			Greenness/Vegetation: Value low positive, $0.1 < X < 0.4$
	NDVI > 0.8	Adequate biomass	40	Tropical rainforest value approaching 1, $X \rightarrow 1$ Hansen et al. (2017)
	NDVI > 0.7	Moderate biomass	30	
	NDVI > 0.6	Low biomass	20	
NDVI > 0.5	Inadequate biomass	10		
2.	Land use indicator			Field observation and author experienced
	Habitat			
	Forest plantation	Natural habitat	40	
	Oil palm	Plantation	30	
	Low density vegetation	Degraded land	20	
	Open area/Buildings/Roads	Infrastructure and non-vegetated land	10	
3.	Net Primary Productivity			NPP evaluated for the plantation is $650 \text{ gCm}^{-2} \text{ month}^{-1}$ (Razali et al. 2022). NPP from WorldView-2 particularly valuable if applied to temporal NDVI data to assess the monthly NDVI for the study area (Razali et al. 2022)
	NPP > 500	Adequate biomass	40	
	NPP > 300	Moderate adequacy biomass	30	
	NPP > 200	Low adequacy biomass	20	
	NPP > 100	Inadequate biomass	10	
4.	Precipitation indicator			200 mm during June and July 350 mm in November and December (climateknowledgeportal.worldbank.org)
	Mean monthly precipitation (mm)			
	280 – 340	High	40	
	160 – 280	Moderate	30	
	80 – 160	Low	20	
	0 – 80	Very low	10	
5.	Seasonal indicator			ASEAN Specialized Meteorological Centre (ASMC) report (2016)
	ASEAN Specialized Meteorological Centre (ASMC)			
	September - November 2020	Wetter	40	
	December – January 2016 - 2017	Wetter than average	30	
	March - May 2020	Wetter and drier effects are averaged	20	
	Unidentified	Unidentified	10	

Table 7. Indication of vegetation and wildlife habitat classification for the study.

Rank	Suitability Index	Habitat & Vegetation classification
1	150 - 200	Highly suitable
2	100 - 150	Moderately suitable
3	50 - 100	Least suitable
4	0 - 50	Not suitable

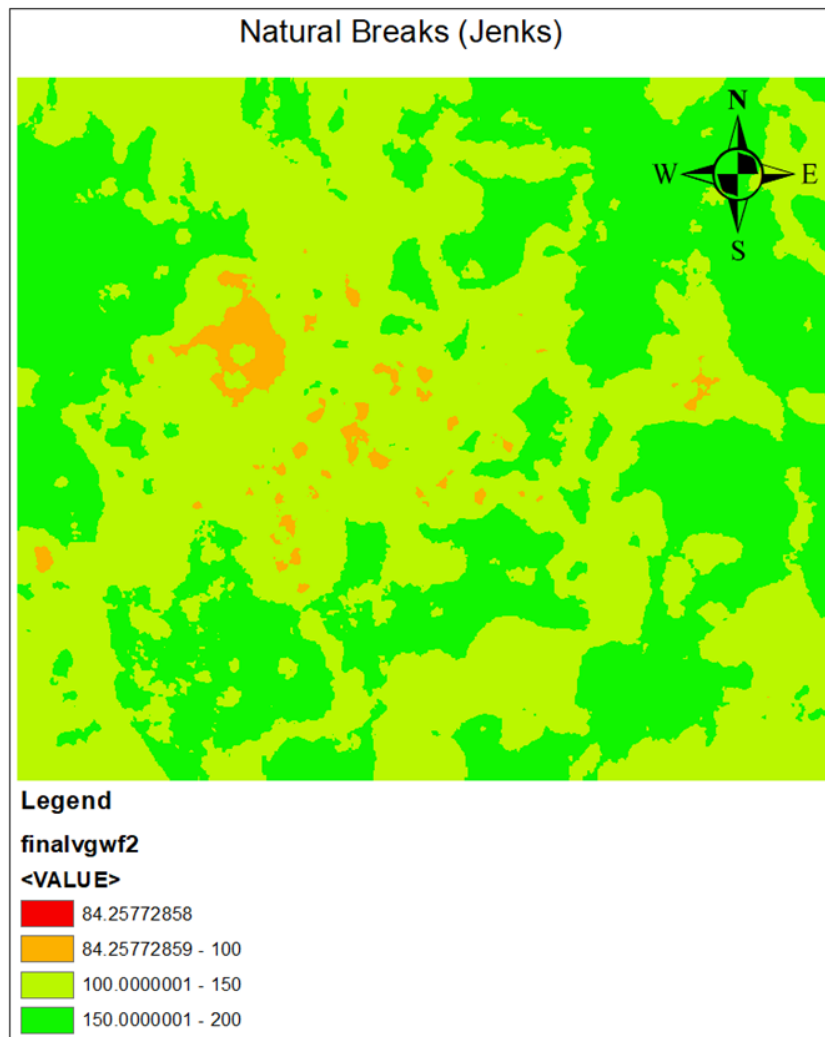


Figure 10. Final index classification for the study area.

found that most of the study area which is about 59.9% was moderately under suitable average habitat for vegetation and wildlife. The variable employed for the study covered land use, climatic condition presented by precipitation, NPP and seasonal variation of the study area showed overview of year 2016 condition of the study area.

Based on the direct approach, the condition of the study area as plantation area is very suitable for natural habitat to live. In addition, considering cost-effective within tropical context, it is also proposed that Landsat data that is free and available can be useful for obtaining land cover and can be economically estimate for larger area. The study suggested a temporal land use change to be conducted in future study to reveal forest-to-oil palm conversion as the primary driver of deforestation.

AUTHOR CONTRIBUTION

S.M.R. designed the methodology that including data collection and analysis which using ArcGIS software. Whereas Z.S. provided research materials and permission for data collection including overall research expenses. M.L. worked on manuscript improvements and given an original idea.

ACKNOWLEDGMENTS

This research was financially supported by the Trans-Disciplinary Fundamental Research Grant Scheme (TRGS 2018-1), Reference code: TRGS/1/2018/UPM/01/2/4 (vote number: 5535803) by Ministry of

Higher Education (MOHE), Malaysia. Sabah Softwoods Berhad, Tawau, Sabah, East Malaysia, also provided the research location, accommodation, and transportation, as well as supporting staff for field work and GPS point collection and data verification.

CONFLICT OF INTEREST

There are no conflicts of interests.

REFERENCES

- Abbas, S. et al., 2020. Approaches of Satellite Remote Sensing for the Assessment of Above-Ground Biomass across Tropical Forests : Pan-tropical to National Scales. *Remote Sens.*, 12(20), 3351. doi: 10.3390/rs12203351
- Bhuiyan, C., Singh, R.P., & Kogan, F.N., 2006. Monitoring Drought Dynamics in the Aravalli Region (India) Using Different Indices Based on Ground and Remote Sensing Data. *International Journal of Applied Earth Observation and Geoinformation*, 8(4), pp.289–302. doi: 10.1016/j.jag.2006.03.002.
- Bowyer, P. & Danson, F.M., 2004. Sensitivity of Spectral Reflectance to Variation in Live Fuel Moisture Content at Leaf and Canopy Level. *Remote Sensing of Environment* 92(3), pp.297–308. doi: 10.1016/j.rse.2004.05.020.
- Braswell, B.H. et al., 2003. A Multivariable Approach for Mapping Sub-Pixel Land Cover Distributions Using MISR and MODIS: Application in the Brazilian Amazon Region. *Remote Sensing of Environment*, 87(2–3), pp.243–256. doi: 10.1016/j.rse.2003.06.002.
- Caccamo, G. et al., 2011. Assessing the Sensitivity of MODIS to Monitor Drought in High Biomass Ecosystems. *Remote Sensing of Environment*, 115(10), pp.2626–39. doi: 10.1016/j.rse.2011.05.018.
- Caccamo, G. et al., 2015. Using MODIS Data to Analyse Post-Fire Vegetation Recovery in Australian Eucalypt Forests. *Journal of Spatial Science*, 60(2), pp.341–52. doi: 10.1080/14498596.2015.974227.
- Caturegli, L. et al., 2020. Effects of Water Stress on Spectral Reflectance of Bermudagrass. *Scientific Reports*, 10, 15055. doi: 10.1038/s41598-020-72006-6.
- Chandrasekar, K. et al., 2010. Land Surface Water Index (LSWI) Response to Rainfall and NDVI Using the MODIS Vegetation Index Product. *International Journal of Remote Sensing*, 31(15), pp.3987–4005. doi: 10.1080/01431160802575653.
- Chen, P. et al., 2021. Vegetation dynamic assessment by ndvi and field observations for sustainability of China's Wulagai river basin. *International Journal of Environmental Research and Public Health*, 18(5), pp.1–20. doi: 10.3390/ijerph18052528.
- Cheng, Y.-B. et al., 2006. Estimating vegetation water content with hyperspectral data for different canopy scenarios: Relationships between AVIRIS and MODIS indexes. *Remote Sensing of Environment*, 105(4), pp.354–366. doi: 10.1016/j.rse.2006.07.005.
- Coops, N. et al., 2010. Estimation of Light-Use Efficiency of Terrestrial Ecosystems from Space: A Status Report. *BioScience*, 60(10), pp.788–797. doi: 10.1525/bio.2010.60.10.5.
- Darmawan, Y. & Sofan, P., 2012. Comparison of the Vegetation Indices to Detect the Tropical Rain Forest Changes Using Breaks for Additive Seasonal and Trend (Bfast) Model. *International Journal of Remote Sensing and Earth Sciences (IJReSES)*, 9(1), pp.21–34. doi: 10.30536/j.ijreses.2012.v9.a1823.

- Dash, J.P. et al., 2017. Assessing very high resolution UAV imagery for monitoring forest health during a simulated disease outbreak. *IS-PRS Journal of Photogrammetry and Remote Sensing*, 131, pp.1–14. doi: 10.1016/j.isprsjprs.2017.07.007.
- Gao, Bo-cai., 1996. NDWI A Normalized Difference Water Index for Remote Sensing of Vegetation Liquid Water from Space. *Remote Sensing of Environment*, 58, pp.257–66.
- Gardner, T.A. et al., 2007. The value of primary, secondary, and plantation forests for a neotropical herpetofauna. *Conservation Biology*, 21 (3), pp.775–787. doi: 10.1111/j.1523-1739.2007.00659.x.
- Hansen, M.C. et al., 2017. Temporal Forest Change Detection and Forest Health Assessment using Remote Sensing. *IOP Conf. Ser.: Earth Environ. Sci.*, 19, 012017. doi: 10.1088/1755-1315/19/1/012017.
- IC-CFS, 2021, 'Introducing the IC-CFS', in *Improving Connectivity in The Centra Forest Spine (CFS)*, viewed 4 January 2022, from <https://www.ic-centralforestspine.com.my>
- Malhi, Y. et al., 2022. Logged tropical forests have amplified and diverse ecosystem energetics. *Nature*, 612, . doi: 10.1038/s41586-022-05523-1.
- Markos, F. et al., 2018. Solar Radiation Resources Under Climate Change Scenarios-A Case Study in Kota Kinabalu, Sabah, Malaysia. *Transactions on Science and Technology*, 5(1), pp.12–24.
- MPOCC., 2022, 'Co-Existing with Elephants - The Sabah Sofywoods Berhad Experience', in *Malaysia Palm Oil Certification Council*, from <https://www.mpocc.org.my/collection-stories-from-the-field/co-existing-with-elephants>.
- Nathan, R., 2016. Human Wildlife Conflict and Evolving Mitigation Methods: Sabah Softwoods Berhad's Experience. *Malaysia Palm Oil Council (MPOC)* 1–2.
- Ng, C.K.C. et al., 2019. Precipitation Trend and Heterogeneity of Sabah, North Borneo. *Sepilok Bulletin*, 28, pp.19–43.
- Nunes, E.L. et al., 2012. Monitoring carbon assimilation in South America's tropical forests: Model specification and application to the Amazonian droughts of 2005 and 2010. *Remote Sensing of Environment*, 117, pp.449–463. doi: 10.1016/j.rse.2011.10.022.
- O'Neil, S. et al., 2020. Wildfire and the Ecological Niche: Diminishing Habitat Suitability for an Indicator Species within Semi-Arid Ecosystems. *Global Change Biology*, 26(11), pp.6296–6312. doi: 10.1111/gcb.15300.
- Potter, C. et al., 2013. Forest production predicted from satellite image analysis for the Southeast Asia region. *Carbon balance and management*, 8, 9. doi: 10.1186/1750-0680-8-9.
- Penuelas, J. et al., 1997. Estimation of Plant Water Concentration by the Reflectance Water Index WI (R900/R970). *International Journal of Remote Sensing*, 18(13), 2869–2875. doi: 10.1080/014311697217396.
- Pujiono, E. et al., 2013. RGB-NDVI Color Composites for Monitoring the Change in Mangrove Area at the Maubesi Nature Reserve, Indonesia. *Forest Science and Technology*, 9(4),171–179. doi: 10.1080/21580103.2013.842327.
- Razali, S.M. et al., 2015. Monitoring Vegetation Drought Using MODIS Remote Sensing Indices for Natural Forest and Plantation Areas. *Journal of Spatial Science*, 61(1), pp.157–172. doi: 10.1080/14498596.2015.1084247.

- Razali, M.R., Nuruddin, A.A. & Lion, M., 2019. Mangrove Vegetation Health Assessment Based on Remote Sensing Indices for Tanjung Piai, Malay Peninsular. *Journal of Landscape Ecology*, 12(2), pp.1–16. doi: 10.2478/jlecol-2019-0008.
- Razali, S. M. & Lion, M., 2021. Eucalyptus Forest Plantation Assessment of Vegetation Health Using Satellite Remote Sensing Techniques. *IOP Conference Series: Earth and Environmental Science*, 918, 012041. doi: 10.1088/1755-1315/918/1/012041.
- Razali, S.M. et al., 2022. Monitoring green biomass utilizing remote sensing techniques for agriculture and forest areas in East Malaysia. *IOP Conference Series: Earth and Environmental Science*, 1064, 012004. doi: 10.1088/1755-1315/1064/1/012004.
- Rouse, J. W. et al., 1973. Monitoring Vegetation Systems in the Great Plains with ERTS. *Third Earth Resources Technology Satellite (ERTS) Symposium*, 1, pp.309–317. doi: citeulike-article-id:12009708.
- Russ, E.R. et al., 2022. Habitat Classification Predictions on an Undeveloped Barrier Island Using a GIS-Based Landscape Modeling Approach. *Remote Sensing*, 14(6). doi: 10.3390/rs14061377
- Sukarno, K. et al., 2017. Comparison of Power Output between Fixed and Perpendicular Solar Photovoltaic PV Panel in Tropical Climate Region. *Advanced Science Letters*, 23(2), pp.1259–1263. doi: 10.1166/asl.2017.8379.
- Toomey, M. & Vierling, L.A., 2005. Multispectral remote sensing of landscape level foliar moisture : techniques and applications for forest ecosystem monitoring. *Canadian Journal of Forest Research*, 1097, pp.1087–1097. doi: 10.1139/X05-043.
- Trishchenko, A.P., 2009. Effects of spectral response function on surface reflectance and NDVI measured with moderate resolution satellite sensors: Extension to AVHRR NOAA-17, 18 and METOP-A. *Remote Sensing of Environment*, 113(2), pp.335–341. doi: 10.1016/j.rse.2008.10.002.
- Vallan, D., 2002. Effects of anthropogenic environmental changes on amphibian diversity in the rain forests of eastern Madagascar. *Journal of Tropical Ecology*, 18(5), pp.725–742. doi: 10.1017/S026646740200247X.
- Vidhya, R. et al., 2014. Improved Classification of Mangroves Health Status Using Hyperspectral Remote Sensing Data. *ISPRS - International Archives of the Photogrammetry, Remote Sensing and Spatial Information Sciences*, XL-8, pp.667–670. doi: 10.5194/isprsarchives-XL-8-667-2014.
- Xiao, X. et al., 2004. Satellite-Based Modeling of Gross Primary Production in an Evergreen Needleleaf Forest. *Remote Sensing of Environment*, 89, pp.519–534. doi: 10.1016/j.rse.2003.11.008.

Research Article

In silico Determination of Host-Viral Interaction of Apoptotic Mimicry Pathway Proteins During Hepatitis B Viral Pathogenesis

Prachie Sharma¹, Kamal Rawal², Kapila Kumar^{1*}

1)Manav Rachna International Institute of Research and Studies, Faridabad, 121003

2)Amity Institute of Biotechnology, Amity University, Noida, 201308

*Corresponding author, email: kapila.fet@mriu.edu.in

Keywords:

Host viral PPI
Apoptotic Mimicry
Hepatitis B Virus
Phosphatidylserine Receptor
HEX 8.0 and ClusPro

Submitted:

28 January 2022

Accepted:

21 February 2023

Published:

31 July 2023

Editor:

Miftahul Ilmi

ABSTRACT

Viruses are the opportunistic pathogens that have developed several elegant strategies to deploy their host systems for a pathogenic invasion. Viral apoptotic mimicry is characterized by the exposure of host cell phospholipid, the phosphatidylserine which marks the host cell for apoptotic activation. The Hepatitis b virus, an enveloped virus has recently been found to interact with Phosphatidylserine (Ptdser) on the host through its large surface protein experimentally. Nonetheless, the employment of apoptotic mimicry during the pathogenesis of HBV has not been determined. Therefore, in the present study, we attempt the *in-silico* exploration of the interaction of the apoptosis initiating receptors activated by Phosphatidylserine Receptors such as TIM3, AXL, MERTK and GAS6 by Hepatitis B Virus L protein. Molecular Docking of Phosphatidylserine Receptor were studied to observe protein – protein interaction against Surface L Protein of Hepatitis B Virus by using online protein interaction software. It was found from the *in-silico* studies that Phosphatidylserine Receptors i.e. TIM3 (PDB: 5F71), AXL (PDB: 5U6B), MERTK (PDB: 2POC) and Gas6 (Growth Arrest Specific protein 6) (PDB: 2C5D) have shown effective binding efficacy against Surface L Protein of Hepatitis B Virus, whereas TIM3 (PDB: F71) and Gas6 (PDB: 2C5D) has shown maximum binding energy with respect to both the software used to analyse the protein-protein docking. This interaction study can form the basis of the experimental attempt in understanding the viral-host protein interaction pattern during hepatitis b viral infection.

Copyright: © 2023, J. Tropical Biodiversity Biotechnology (CC BY-SA 4.0)

INTRODUCTION

Viruses have evolved to invade certain mechanisms of the host over millions of years of co-evolving together. This co-evolution permits the virus to adapt its own biology to attune itself to the host systems so as to exploit them pathogenically (Longdon et al. 2014). Mechanisms such as the phagocytosis, endocytosis, exocytic secretion mediated vesical transport and apoptosis are potentially mechanisms of exploitation by the viruses in general (Miaczynska & Stenmark 2008). Viruses have evolved varied strategies of entering the host cell undetected. Apoptotic mimicry is one such strategy which is significantly utilized by the enveloped viruses without eliciting an immune response (Amara & Mercer 2015). Apoptosis initiation occurs through phosphatidylserine that activates cer-

tain receptors downstream which further activates viral endocytosis (Maginnis 2018). Viruses have evolved varied strategies of entering the host cell undetected. Apoptosis in particular provides an advantage of the viral delivery without the elicitation of the host immune system. It was recently shown that viruses hijack apoptotic recognition and clearance mechanisms to their own advantage (Elliott & Ravichandran 2010). In principle, apoptosis eliminates biochemically abnormal or harmful cells by employing phagocytic cells without eliciting an immune response as well as without perturbing the homeostasis of the surrounding tissues (Arandjelovic & Ravichandran 2015). This process employs well-coordinated and highly regulated successive steps which are highly conserved. The major highlight of this process which makes it a potentiating target for viral exploitation is its active anti-inflammatory mechanisms. There is a mechanism for the recognition of the cells which is distinguished specifically for apoptosis. These cells are provided with phosphatidylserine. It is a negatively charged phospholipid, usually present on the inner leaflet of plasma membrane (Elmore 2007).

Phosphatidylserine (PtdSer) is normally expressed on the inner leaflet of the plasma membrane of living cells. However, PtdSer becomes exposed in necrotic or apoptotic cells, and the exposure of PtdSer allows for phagocytic cells to recognize and remove dead cells. However, during the apoptotic initiation, it gets flipped from inner leaflet of cell membrane to be exposed on the external leaflet of plasma membrane which acts as a signatory molecule marking the host cell for the programmed cell death (Fadok et al. 2001). Phosphatidylserine activates apoptosis through activation of series of receptors such as T-cell immunoglobulin and Mucin domain (TIM-3) and Tyrosine-protein kinase receptor (TYRO 3), AXL as well as MERTK. These are the names of the human receptors. Receptor tyrosine kinase or TAMs family of receptors (Lemke 2017). Both TIM and TAM receptors have been shown to facilitate the mediation of viral entry. Hence during apoptosis, the host cell experiences varied biochemical changes on the membrane which involves redistribution of Ptdser from the inner membrane to outer and membrane blebbing. This characteristic exposure of Ptdser with this blebbing appearance acts as a primary eat me signal which initiates the process of endocytic clearing (Meertens et al. 2012). Axl protein in association with its Gas6 molecule elicits the uptake of these particles. Gas6 acts as a linking molecule between Ptdser and its corresponding receptor (Maginnis 2018). Ptdser receptors have been shown to facilitate viral entry into the host cell for a plethora of enveloped viruses Dengue virus, Zika virus, Ebola virus, West Nile virus and Marburgvirus. While the receptor families of the virus are quite distinct from one another, nonetheless they recognize Ptdser on the viral envelope which thereby mediate viral adherence, endocytosis and initiation of virulent life cycle (Moller-Tank & Maury 2014).

Present investigation deals with the Exploring of Apoptotic Mimicry of Phosphatidylserine Receptor with Surface L Protein of Hepatitis B Virus through *in silico* studies. This mechanism has been hypothesised in the Hepatitis B viral pathogenesis since the discovery of Phosphatidylserine receptor in the viral envelope. The presence of this receptor in other double enveloped viruses such as DENGUE, HIV etc have been shown to employ the pathway of Phosphatidylserine for entering the host cell. The goal was to demonstrate the role of phosphatidylserine receptor in entry of the virus in the host white blood cells. As no preliminary study has been conducted before, therefore before considering *in-vitro* and *in-vivo* studies, we decided to do *in-silico* preliminary study based on which we will plan the experimental studies.

MATERIAL AND METHODS

Structure Modelling of HBV L Surface Protein

Amino acid Sequence of Surface L Protein of HBV was obtained from the NCBI database (<https://www.ncbi.nlm.nih.gov/>) in FASTA format. Protein modelling was done by De novo modelling, where the tertiary structure of protein was determined based on its primary sequence. De novo modelling was performed using I-TASSER database (<https://zhanglab.ccmb.med.umich.edu/I-TASSER/>) (Yang & Zhang 2015). Model validation was done by PROCHECK for Ramachandran Plots (Laskowski et al. 1993) and Protein Structural Analysis (ProSA) to check energy criteria in comparison with known protein structures with similar size (Wiederstein & Sippl 2007).

Selection of Phosphatidylserine Receptor as Ligand

3D structure of Phosphatidylserine receptor families as ligands i.e. TIM3 (PDB: 5F71), AXL (PDB: 5U6B), MERTK (PDB: 2POC) and Gax6 (Growth Arrest Specific protein 6) (PDB: 2C5D) were downloaded from the RCSB protein Data Bank (<https://www.rcsb.org/>). Physicochemical and functional characterization of selected protein molecule was done for the analysis of theoretical isoelectric point (pI), molecular weight, total number of positive and negative residues, extinction coefficient (Gill & von Hippel 1989), instability index (Guruprasad et al. 1990), aliphatic index (IKAI 1980), and grand average hydropathy (GRAVY) by Expasy's ProtParam server (<http://web.expasy.org/protparam/>). Functional characterization of protein was observed by SOSUI server (<https://harrier.nagahama-i-bio.ac.jp/sosui/mobile/>) to identify the transmembrane region and disulfide bonds. To calculate the secondary structural features of the protein sequences, SOPMA server (https://npsa-prabi.ibcp.fr/cgi-bin/npsa_automat.pl?page=/NPSA/npsa_sopma.html) was used (Kyte & Doolittle 1982).

Molecular docking Studies with HBV L Surface Protein

Protein-protein docking was used to dock the selected Phosphatidylserine Receptors as Ligand with homology modelled HBV L Surface Protein. Different servers were used for observing the docking analysis, i.e. HEX 8.0 Docking server and ClusPro server molecular docking.

For validating the efficiency and comparing the binding efficacy of Phosphatidylserine Receptors with HBV L Surface Protein, HEX 8.0 molecular docking server uses modern graphics processor units (GPUs) to accelerate the calculations (Macindoe et al. 2010a). Tool identifies the ligand with the best score and calculate the ligand-receptor Interaction or protein-protein interaction with the lowest free energy value. Following were the parameters used for the docking i.e. correlation type-shape + electrostatic, FFT mode – 3D, Post processing-MM energies, Grid dimension-0.6, receptor range -180, ligand range -180, twist range -360 and distance range. Binding energy were estimated and expressed in KJ mol⁻¹ (Macindoe et al. 2010 b)

ClusPro: It's a known for fast algorithm which is used to filter docking confirmation by simple scoring function and providing structures with good surface complementary. The free energies select complexes with lowest desolvation and electrostatic energies. Energies were given in table with the given downloaded models (Comeau et al. 2004). Cluster scores were obtained from these equations, generated by the server.

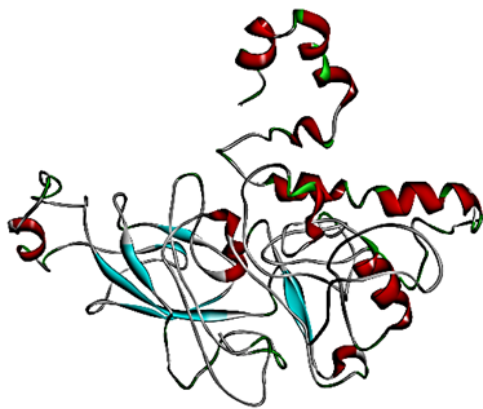
$$E_{\text{Balanced}} = 0.40E_{\text{rep}} + -0.40E_{\text{att}} + 600E_{\text{elec}} + 1.00EDARS$$

$$E_{\text{Electrostatic favoured}} = 0.40E_{\text{rep}} + -0.40E_{\text{att}} + 1200E_{\text{elec}} + 1.00EDARS$$

RESULTS AND DISCUSSION

Apoptotic mimicry is one such strategy which is significantly utilised by the enveloped viruses without eliciting an immune response (Amara & Mercer 2015). Apoptosis initiation occurs through phosphatidylserine that activates certain receptors downstream which further activates viral endocytosis (Maginnis 2018). Apoptotic mimicry is still hypothesized for the Hepatitis B virus. Nonetheless, the Phosphatidylserine has been found experimentally to interact with the large subunit of the surface or envelope protein of the virus (Vanlandschoot & Leroux-Roels 2003). Therefore, for the first time we have attempted to study the plausible interaction between the large subunit of viral surface protein with the downstream receptor proteins activated by phosphatidylserine. 3-D Model structure was validated by PROCHECK (Ramachandran plot) and ProSA to the structural integrity. To check the protein structure validity, ProSA has been used to calculate the overall quality score. Z score indicates the

I.



Predicted 3D Structure of Surface L Protein of Hepatitis B Virus

II.

CLUSTAL O(1.2.4) multiple sequence alignment

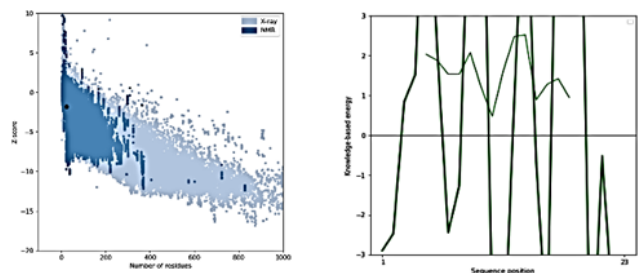
```

AFH7382.1  MCGSSKREKCRSTNLSVFNPLQFPPDQLDPAFGANSNEDQDFNFKDIMPQANQVGV  58
1WZ4_1|Chain  |
-----
AFH7382.1  GAFGDFYPIHGVLGWSPOAGDILATVPVPPPPASTNRQSGRPTFTFSPFLRDSHPQAM  120
1WZ4_1|Chain  |
-----
AFH7382.1  QMNSTAFHQALQDPRIYGLVYFAGGSSSGTLNVPVTIASHSSESSRIGDPAPNENITS  180
1WZ4_1|Chain  |
-----
AFH7382.1  QFLGLLVLQAGFLLTRLLTIQPSLDSWMTSLNFLGDSFVCLQNSQSPYTNISPTSCP  240
1WZ4_1|Chain  |
-----
AFH7382.1  PICQVWMLCRFETFLFLLCLIFLLVLLDYGQMLRVCPLRQSTTTSTGPKCTCTT  300
1WZ4_1|Chain  |
-----
AFH7382.1  PAQNSAFPSCECTEPTGQNTCTPIPISSWAFKYLWEWASVRFSLVLLVPTVQMFVGL  360
1WZ4_1|Chain  |
-----
AFH7382.1  SPTVLSAINRHHYKQPSLVNELSPFIPLLPIFFCLWVYI  400
1WZ4_1|Chain  |

```

Pairwise Sequence Alignment of Surface L Protein of Hepatitis B Virus with 1WZ4

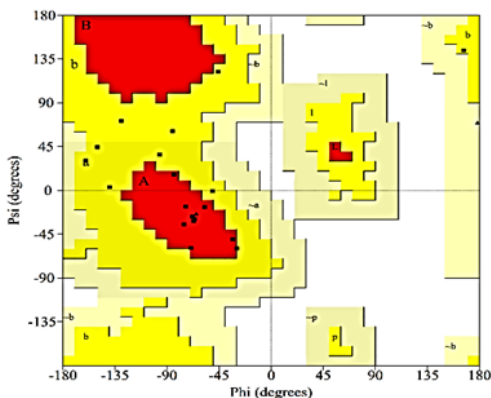
III.



ProSA-Web Z-Score Plot

Local Model Quality

IV.



Ramachandran Plot Analysis

Plot statistics

Residues in most favoured regions [A,B,L]	9	52.9%
Residues in additional allowed regions [a,b,l,p]	8	47.1%
Residues in generously allowed regions [-a,-b,-l,-p]	0	0.0%
Residues in disallowed regions	0	0.0%
Number of non-glycine and non-proline residues	17	100.0%
Number of end-residues (excl. Gly and Pro)	1	
Number of glycine residues (shown as triangles)	3	
Number of proline residues	2	
Total number of residues	23	

Figure 1. Structure analysis and validation of (I.) Predicted 3D structure of Surface L Protein of Hepatitis B Virus by ITASER. (II.) pairwise sequence alignment with 1WZ4 using ClustalW. Where the conserved amino acid residues are elucidated as (*), highly similar residues as (:), and weakly similar residues as (.). (III.) ProSA-Z-Score Plot shows the Overall model quality and Local model quality. (IV.) Ramachandran Plot analysis of 3D Structure of Surface L Protein of Hepatitis B Virus, where the red region defines most favorable area of residues; the yellow region is additionally allowed; and generously allowed residues in the light-yellow region.

overall model quality and our predicted 3D structure has revealed -1.82 Z-score which falls within the values range of the known proteins determined by X-ray (light blue) and NMR (dark blue) as shown in Figure 1 (III). Plot of Local model quality has revealed single residue energies that contains large fluctuations and was of limited value for model evaluation as shown in Figure 1 (III). Ramachandran Plot of modeled protein represents 52.9% of the total residues in the most favored regions and 47.1 % in additionally allowed regions which indicates a good quality model (Figure 1 (IV)). Physiochemical and Secondary structural features of Phosphatidylserine Receptors were studied by standardized methods. Physiochemical characterization was done by ExPasy's ProtParam to observe the isoelectric point and has revealed less than 7 which signifies the acidic character that become useful for the development of buffer system as purification by isoelectric focusing. Instability index smaller than 40 indicates the stability of protein, whereas TIM3 found to be stable with index 26.59 as compared to other receptors as shown in Table 1. Aliphatic index (AI) which is a relative volume of a protein occupied by aliphatic side chain (A, V, I, and L) found to be significant in receptors that are regarded as positive factor for the increase of thermal stability of globular protein (Table 1). Total Sum of hydropathy values of all amino acid divided by the number of residues in the sequence were calculated by grand average hydropathy value as given in Table 1.

SOPMA server was used to predict the secondary structure of the Phosphatidylserine Receptors. This was found from the study that amino acid lies in the alpha helix, extended strand with beta turn and random coil as given in Table 2.

Molecular docking studies were performed among the HBV L Surface Protein (Figure 2) and Phosphatidylserine Receptors to observe the protein-protein interaction by two docking server i.e. Hex 8.0 and

Table 1. Physiochemical characterization of Phosphatidylserine receptor computed using ExPasy's ProtParam tool.

Physiochemical characterization/ PDB	TIM3 (PDB: 5F71)	AXL (PDB: 5U6B)	MERTK (PDB: 2POC)	Gax6 (PDB: 2C5D)
Theoretical isoelectric point (pI)	5.04	5.74	5.91	5.32
Molecular weight	24556.06	127393.54	152785.18	125689.32
-R	26	150	161	128
+R	22	132	141	92
Instability index	26.59	45.44	44.36	45.52
Aliphatic index	84.86	88.27	104.04	94.89
Grand average hydropathy (GRAVY)	-0.137	-0.174	0.048	-0.052

Table 2. Secondary structural of features of Phosphatidylserine receptor by SOPMA

Secondary structure feature	TIM3 (PDB: 5F71)	AXL (PDB: 5U6B)	MERTK (PDB: 2POC)	Gax6 (PDB: 2C5D)
Alpha helix	5.50%	50.62	49.60%	19.72%
3 ₁₀ helix	0.00%	0.00%	0.00%	0.00%
Pi helix	0.00%	0.00%	0.00%	0.00%
Beta bridge	0.00%	0.00%	0.00%	0.00%
Extended strand	37.16%	13.19	14.90%	30.19%
Beta turn	4.59%	7.58	8.82%	9.24%
Bend region	0.00%	0.00%	0.00%	0.00%
Random coil	52.75%	28.61	26.68%	44.66%
Ambiguous states	0.00%	0.00%	0.00%	0.00%
Other states	0.00%	0.00%	0.00%	0.00%

ClusPro. Binding affinity of Phosphatidylserine Receptors with HBV L Surface Protein were studied by the Hex 8.0 software, which is an interactive molecular graphics program that reads molecular coordinate files and displays *in silico* interaction with varied representations and color schemes. This tool also identifies the ligand with the best score and calculates its ligand-receptor interaction with the lowest free energy value. From the interaction this was found that TIM3 as shown maximum binding affinity among the other receptors i.e. $-699.13 \text{ KJ mol}^{-1}$, as far as the MERTK (PDB: 2POC) was concerned it has shown very less binding energy with the HBV L Surface Protein as shown in Table 3 (Figure 3).

Table 3. Docking of Phosphatidylserine receptors as ligand with Surface L Protein of Hepatitis B Virus obtained through Hex 8.0.0 Software

E Value (KJ mol ⁻¹)	TIM3 (PDB: F71)	AXL (PDB: 5U6B)	MERTK (PDB: 2POC)	Gax6 (PDB: 2C5D)
Surface L Protein of Hepatitis B Virus	-699.13	-178.18	-42.80	-551.44

HBV L Surface Protein and Phosphatidylserine Receptors were uploaded on ClusPro online server and has predicted 10 best structures from Piper based on the FFT-based rigid docking program. Binding energies obtained on the basis of balance and electrostatic favored coefficients that were given in Table 4. Models of balance and electrostatic favored coefficients were downloaded as given in Figure 4. From their binding energies among the other Phosphatidylserine Receptors, Gax6 (PDB: 2C5D) has shown maximum binding energy against HBV L Surface Protein, whereas TIM3 has also shown effective binding efficacies against HBV L Surface Protein as shown in Table 4 (Figure 4). As it has been reported in previous studies that HBV which has established its chronic infection has shown cross talk between HBV or other viruses and major cellular components such as c-FLIP in a variety of biological conditions (Lee et al. 2022). This signifies that it can form the basis of the experimental attempt in understanding the viral-host protein interaction pattern during hepatitis b viral infection for the discovery of druggable target.

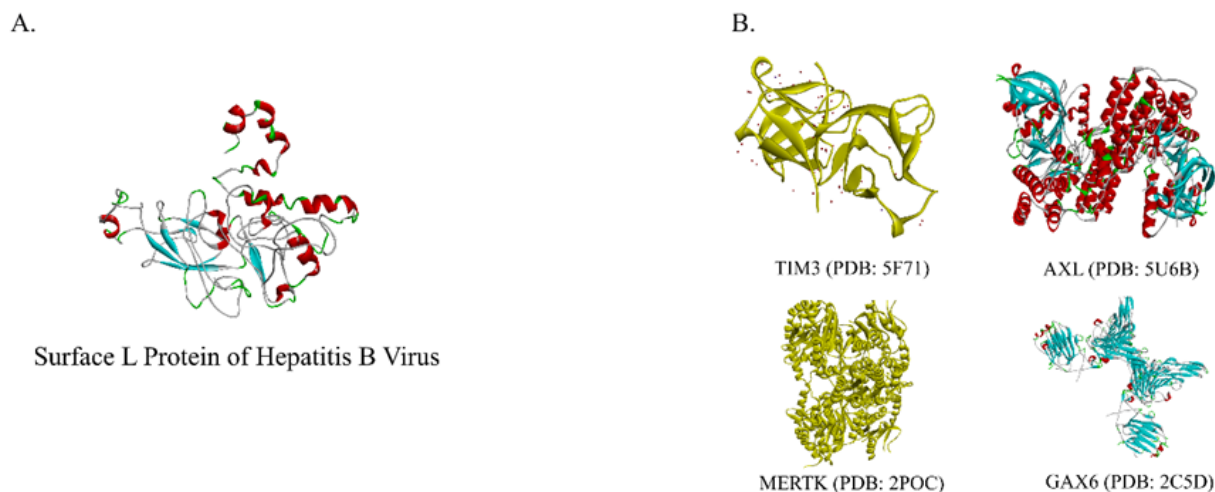


Figure 2. Structure of Receptor (A.) Surface L Protein of Hepatitis B Virus as a target and (B.) Phosphatidylserine receptors as a ligand for Protein-Protein Interaction

Table 4. Binding energies of Phosphatidylserine receptors as ligand with Surface L Protein of Hepatitis B Virus obtained through ClusPro automated server.

Cluster	TIM3 (PDB: 5F71)		AXL (PDB: 5U6B)		MERTK (PDB: 2POC)		Gax6 (PDB: 2C5D)	
	Bal	Elect	Bal	Elect	Bal	Elect	Bal	Elect
Surface L Protein of Hepatitis B Virus	-1388.1	-1466.7	-1524.8	-1551.1	-1385.9	-1367.2	-1537.3	-1614.5

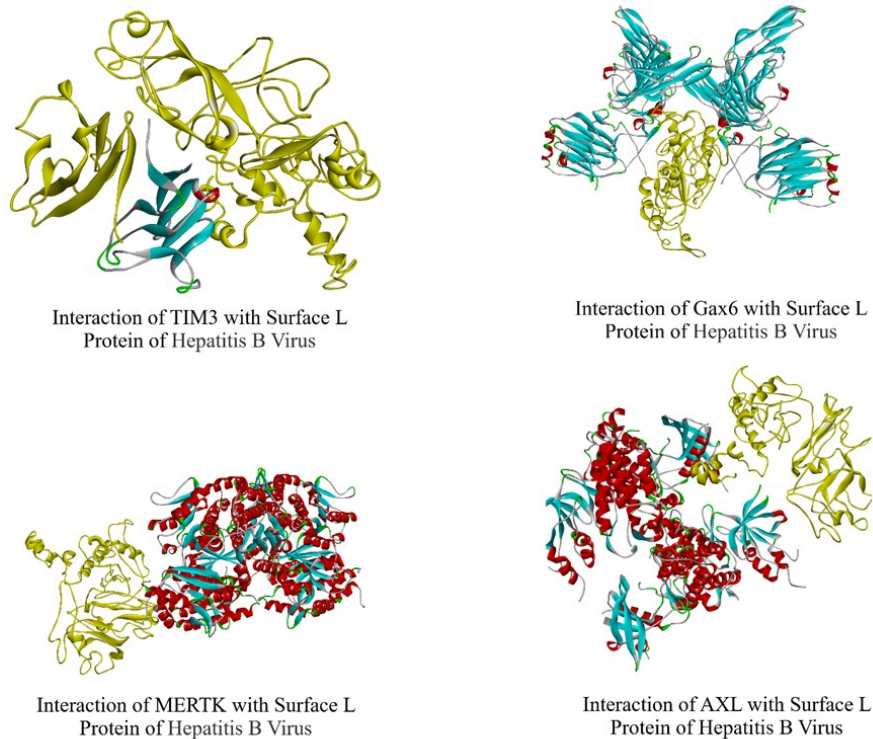


Figure 3. Molecular docking interaction of Phosphatidylserine receptor families as ligands i.e. TIM3 (PDB: 5F71), AXL (PDB: 5U6B), MERTK (PDB: 2POC) and Gas6 (Growth Arrest Specific protein 6) (PDB: 2C5D) with amino acids of Surface L Protein of Hepatitis B Virus showing Protein-Protein Interaction obtained through Hex 8.0.0 Software

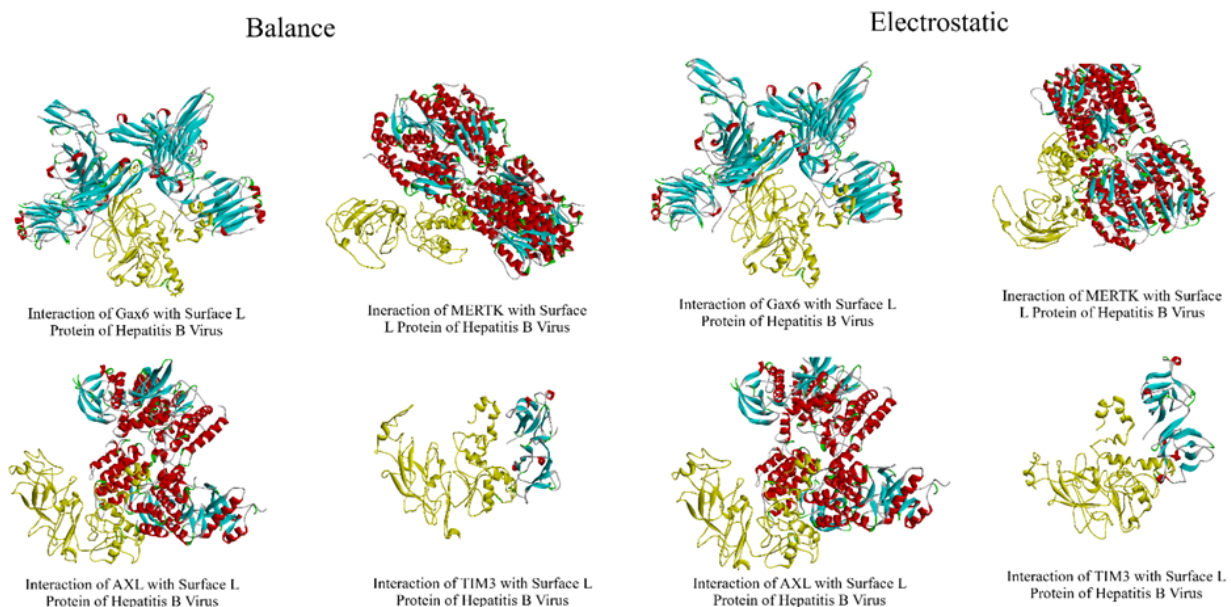


Figure 4. Molecular docking interaction of Phosphatidylserine receptor families as ligands i.e. TIM3 (PDB: 5F71), AXL (PDB: 5U6B), MERTK (PDB: 2POC) and Gas 6 (Growth Arrest Specific protein 6) (PDB: 2C5D) with amino acids of Surface L Protein of Hepatitis B Virus showing Protein-Protein Interaction obtained through ClusPro Software.

CONCLUSION

In this study, the authors observed that Phosphatidylserine receptors such as TIM3, GAS6, MERTK, and AXL interacted against the Surface L Protein of Hepatitis B Virus. 3D structures of Surface L Protein of Hepatitis B Virus were modelled using I-TASSER software and has been validated through PROCHECK and ProSA. Physiochemical and secondary structure prediction of Phosphatidylserine receptor families i.e. TIM3 (PDB: 5F71), AXL (PDB: 5U6B), MERTK (PDB: 2POC) and Gas6 (Growth Arrest Specific protein 6) (PDB: 2C5D) were found to be stable, alpha helix and extended strand with beta turn. From molecular docking studies using HEX 8.0 and ClusPro, it was found that TIM3 (PDB: 5F71) and Gas6 (Growth Arrest Specific protein 6) (PDB: 2C5D) has shown highest negative binding energies against Surface L Protein of Hepatitis B Virus. From the above investigation we can provide the first glimpse of plausible apoptotic mimicry as employed by the virus during the hepatitis b pathogenesis. This in turn has broadened the horizon of hepatitis b viral research by attempting to elucidate interaction possibilities of the pathway which are still elusive experimentally. This is *in-silico* demonstration of the plausible interaction may facilitate the basis of the future experimental confirmation of the pathway thereby entailing the investigation of novel therapeutic targets that hinders the virus prior to entering the host cell.

AUTHOR CONTRIBUTION

P.S. Designed the research, performed all the process and wrote the manuscript. K.K. Supervised all the work. K.R. Co-supervised all the work

ACKNOWLEDGEMENT

There is no acknowledgement to be addressed.

CONFLICT OF INTEREST

Authors declare no conflict of interest.

REFERENCES

- Amara, A. & Mercer, J., 2015. Viral apoptotic mimicry. *Nature Reviews Microbiology*, 13(8), pp.461–469. doi: 10.1038/nrmicro3469.
- Arandjelovic, S. & Ravichandran, K.S., 2015. Phagocytosis of apoptotic cells in homeostasis. *Nature immunology*, 16(9), pp.907–917. doi: 10.1038/ni.3253
- Comeau, S.R. et al., 2004. ClusPro: a fully automated algorithm for protein-protein docking. *Nucleic acids research* 32(Web Server issue), pp.W96–W99. doi: 10.1093/nar/gkh354
- Elliott, M.R. & Ravichandran, K.S., 2010. Clearance of apoptotic cells: implications in health and disease. *The Journal of cell biology*, 189(7), pp.1059–1070. doi: 10.1083/jcb.201004096.
- Elmore, S., 2007. Apoptosis: a review of programmed cell death. *Toxicologic pathology* 35(4), pp.495–516. doi: 10.1080/01926230701320337.
- Fadok, V.A. et al., 2001. Loss of Phospholipid Asymmetry and Surface Exposure of Phosphatidylserine Is Required for Phagocytosis of Apoptotic Cells by Macrophages and Fibroblasts. *Journal of Biological Chemistry*, 276(2), pp.1071–1077. doi: 10.1074/jbc.M003649200.
- Gill, S.C. & von Hippel, P.H., 1989. Calculation of protein extinction coefficients from amino acid sequence data. *Analytical Biochemistry*, 182(2), pp.319–326. doi: 10.1016/0003-2697(89)90602-7

- Guruprasad, K., Reddy, B.V.B. & Pandit, M.W., 1990. Correlation between stability of a protein and its dipeptide composition: a novel approach for predicting in vivo stability of a protein from its primary sequence. *Protein Engineering, Design and Selection*, 4(2), pp.155–161. doi: 10.1093/protein/4.2.155.
- IKAI, A., 1980. Thermostability and Aliphatic Index of Globular Proteins. *The Journal of Biochemistry*, 88(6), pp.1895–1898.
- Kyte, J. & Doolittle, R.F., 1982. A simple method for displaying the hydrophobic character of a protein. *Journal of Molecular Biology*, 157(1), pp.105–132. doi: 10.1016/0022-2836(82)90515-0
- Laskowski, R.A. et al., 1993. PROCHECK: a program to check the stereochemical quality of protein structures. *Journal of Applied Crystallography*, 26(2), pp.283–291. doi: 10.1107/S0021889892009944.
- Lee, A.R. et al., 2022. Interaction between the Hepatitis B Virus and Cellular FLIP Variants in Viral Replication and the Innate Immune System. *Viruses*, 14(2). doi: 10.3390/v14020373.
- Lemke, G., 2017. Phosphatidylserine Is the Signal for TAM Receptors and Their Ligands. *Trends in biochemical sciences*, 42(9), pp.738–748. doi: 10.1016/j.tibs.2017.06.004.
- Longdon, B. et al., 2014. The evolution and genetics of virus host shifts. *PLoS pathogens*, 10(11), e1004395. doi: 10.1371/journal.ppat.1004395.
- Macindoe, G. et al., 2010. HexServer: an FFT-based protein docking server powered by graphics processors. *Nucleic Acids Research*, 38 (Web Server issue), pp.W445–W449. doi: 10.1093/nar/gkq311
- Maginnis, M.S., 2018. Virus-Receptor Interactions: The Key to Cellular Invasion. *Journal of molecular biology*, 430(17), pp.2590–2611. doi: 10.1016/j.jmb.2018.06.024.
- Meertens, L. et al., 2012. The TIM and TAM families of phosphatidylserine receptors mediate dengue virus entry. *Cell host & microbe*, 12 (4), pp. 544–557. doi: 10.1016/j.chom.2012.08.009.
- Miaczynska, M. & Stenmark, H. 2008. Mechanisms and functions of endocytosis. *The Journal of cell biology*, 180(1), pp.7–11. doi: 10.1083/jcb.200711073.
- Moller-Tank, S. & Maury, W., 2014. Phosphatidylserine receptors: enhancers of enveloped virus entry and infection. *Virology*, 468–470, pp.565–580. doi: 10.1016/j.virol.2014.09.009.
- Vanlandschoot, P. & Leroux-Roels, G., 2003. Viral apoptotic mimicry: An immune evasion strategy developed by the hepatitis B virus? *Trends in immunology*, 24, pp.144–147. doi: 10.1016/S1471-4906(03)00026-7.
- Wiederstein, M. & Sippl, M.J., 2007. ProSA-web: interactive web service for the recognition of errors in three-dimensional structures of proteins. *Nucleic Acids Research*, 35(suppl_2), pp.W407–W410. doi: 10.1093/nar/gkm290.
- Yang, J. & Zhang, Y., 2015. I-TASSER server: new development for protein structure and function predictions. *Nucleic acids research*, 43 (W1), pp.W174–W181. doi: 10.1093/nar/gkv342.

Review Article

Updated Species Check-list of the Indonesian Stingless Bees (Hymenoptera, Apidae, Apinae, Meliponini)

Manap Trianto^{1,2}, Tuty Arisuryanti³, Hari Purwanto^{4*}, Rosichon Ubaidillah⁵

1)Graduate Student of Doctor Biology, Faculty of Biology, Universitas Gadjah Mada. Jl. Teknika Selatan, Sekip Utara, Bulaksumur, Sleman 55281, Yogyakarta, Indonesia.

2)Departement of Biology Education, Faculty of Teacher Training and Education, Tadulako University. Jl. Soekarno Hatta No. KM. 9, Tondo, Mantikulore, Palu 94148, Central Sulawesi, Indonesia.

3)Laboratory of Genetics and Breeding, Faculty of Biology, Universitas Gadjah Mada. Jl. Teknika Selatan, Sekip Utara, Bulaksumur, Sleman 55281, Yogyakarta, Indonesia.

4)Laboratory of Entomology, Faculty of Biology, Universitas Gadjah Mada. Jl. Teknika Selatan, Sekip Utara, Bulaksumur, Sleman 55281, Yogyakarta, Indonesia.

5)Research Center for Biosystematics and Evolution, National Research and Innovation Agency (BRIN). Jl. Raya Jakarta-Bogor Km 46, Cibinong, West Java, Indonesia. email: rosichon.ubaidillah@brin.go.id.

* Corresponding author, email: hari.purwanto@ugm.ac.id.

Keywords:

Annotated catalog
bibliography
Indonesian
meliponini
stingless bees

Submitted:

19 August 2022

Accepted:

10 April 2023

Published:

17 July 2023

Editor:

Miftahul Ilmi

ABSTRACT

A catalog provides an index to previous studies in taxonomy, behavioral research, and pollination ecology, thus consolidating the existing knowledge in an accessible format. In this study, we explore the annotated catalog and bibliography of the Indonesian meliponini stingless bees (Hymenoptera, Apidae, Apinae, Meliponini). The catalog format is arranged based on Rasmussen (2008). All available literature was reviewed for compiling this catalog and bibliography. References to a Meliponini genus only were not included in the list of references. Cited references must have used a trackable specific epithet to have been included. In total, Indonesia has 52 recorded stingless bee species across the Indonesian archipelagoes of Sumatera (27 species), Java (13 species), Nusa Tenggara (1 species), Kalimantan (34 species), Sulawesi (8 species), Bali (1 species), Maluku (4 species), and Papua (12 species). After the data was updated, there was an increase in the number of stingless bee species in Indonesia, namely 46 species (before update) to 52 species (after update). An up-to-date, comprehensive taxonomic and biological catalog is fundamental to any comparative evolutionary, ecological, and behavioral research on any group of organisms.

Copyright: © 2023, J. Tropical Biodiversity Biotechnology (CC BY-SA 4.0)

INTRODUCTION

Stingless bees (Hymenoptera, Apidae, Apinae, Meliponini) are by far the largest group of eusocial bees on Earth, with more than 500 described (Rasmussen & Cameron 2010) and possibly 100 more undescribed species (Michener 2013). They outnumber honeybees in Indonesia by a factor of 50 (Apidae, Apini: 11 species) and make up twice as many species as the known bumble bees (Apidae, Bombini: about 250 species) (Michener 2007). Meliponini tribe is believed to have originated from the ancient Gondwana continent, which included tropical America, Africa, Southeast Asia, and Australia, more than 100 million years ago based on their pantropical range, (Sakagami 1982; Camargo & Pedro 1992). To date, most stingless bee species are found in the Neotropics, where they

exhibit remarkable diversity in their life cycles and taxonomic composition (more than 400 nominate taxa in 32 extant genera) (Camargo 2013).

The shortened wing venation, penicillum (a brush of long setae on the outer, apical side of the hind tibia), and vestige of a sting are several of the characteristics that immediately distinguish Meliponini from other tribes of the subfamily Apinae (Wille 1979, 1983; Michener 1990, 2000). The lack of an auricle on the hind basitarsus distinguishes Meliponini from other corbiculate tribes. The tribe's species exhibit considerable variation in could be omitted size, nesting location, and nest design (Michener 1974; Sakagami 1982). The morphologies of the two female castes, namely, the queen and laborer, differ drastically (Michener 1974; Wille 1979).

Stingless bees are important native plant pollinators in tropical and subtropical regions of the world (Heard 1999). They have a wide range of nesting biology ranging from exposed to underground colonies (Camargo & Pedro 2003; Roubik 2006; Rasmussen & Camargo 2008), create sizable perennial colonies with a sophisticated social organization (Michener 2007), and are frequently observed in their natural habitat (Roubik 2006). A current and thorough taxonomic and biological catalog is essential to any comparative evolutionary, ecological, and behavioral investigation of any group of organisms, in addition to a well-corroborated phylogeny. A catalog offers an index to early research on taxonomy, behavioral science, and pollination ecology, thus condensing the available knowledge to become accessible. Camargo and Pedro recently cataloged the diverse Neotropical fauna (2007: 391 spp.), and a systematic study of the Afrotropical stingless bees involved a fairly exhaustive bibliography (Eardley 2004: 26 spp. incl. Madagascar). Rasmussen (2008) catalog attempts to list the world's stingless bee fauna by treating the remaining Indo-Malayan/Australasian stingless bees (129 proposed species-group names, 89 currently accepted valid species). These methods are anticipated to rekindle scientific interest in this diverse group of bees, together with the recent molecular phylogenies of stingless bees (Rasmussen & Cameron 2007; Rasmussen 2008).

The distribution of stingless bees in the Indo-Malay/Australasian region stretches from India to the Solomon Island and from China (Yunnan, Hainan, Taiwan) (Wu 2000) to Australia (New South Wales). Schwarz (1937) suggested that the greater abundance of stingless bees in Thailand and Malaysia, including all of Borneo, is due to the abundance of resin-secreting trees (Dipterocarpaceae) and humid tropical climate, although most likely an array of factors are responsible for this concentration of species. Meliponini research in Indonesia has experienced an ever-diversifying range of interests and methods since the post-Sakagami era (1978) (Grüter 2020). Possible migration of stingless bees since the Paleocene is studied. Papers on Meliponini now span all modern apidology disciplines from taxonomy, evolutionary biology, ecology, ethology, agronomics, and physiology. In this study, we provide the annotated catalog and bibliography of the Indonesian Meliponini stingless bees (Hymenoptera, Apidae, Apinae, Meliponini) to elaborate on the current progress in meliponinie studies in Indonesia.

MATERIALS AND METHODS

The catalog format is arranged based on Rasmussen (2008) with modification. Subspecies are not recognized in the catalog; instead, genus-group and currently accepted species-group names are arranged alphabetically. Headings for genera-groups are in capital letters, bold, and italic. The list of distributional records is restricted to records could be omitted cited in

either taxonomic publications or faunal inventories. The literature has been updated until mid-2022. References are cited within these records, with a total of 109 papers. Most biological data pertaining to Meliponini are listed in the nearly complete stingless bee bibliography by Rasmussen (2008).

All available literature was reviewed for compiling this catalog and bibliography. References to a Meliponini genus only were not included in the list of references. Cited references must have used a trackable specific epithet to have been included. The institutional and collection acronyms used throughout the catalog follow Rasmussen (2008) when possible. For museum acronyms, curators and sources of information concerning the collection are listed in Table 1.

RESULTS AND DISCUSSION

Distribution of Stingless Bee Species Across the Indonesian Archipelagos

In total, Indonesia has 52 recorded stingless bee species across the Indonesian archipelagos of Sumatera, Java, Bali, Kalimantan, Sulawesi, Nusa Tenggara, Maluku, and Papua (Figure 1). Scattered records and undescribed species are found in collections for the remaining islands of Indonesia (Table 2).

Table 1. Museum acronyms, curators and sources of information concerning the collection are listed in parenthesis.

Museum acronyms	Curators and sources of information
AMNH	USA, New York, New York, American Museum of Natural History (Jerome G. Rozen, John S. Ascher)
AMS	Australia, New South Wales, Sydney, Australian Museum (David Britton, Max Beatson)
ANIC	Australia, Australian Capital Territory, Canberra City, CSIRO, Australian National Insect Collection (John La Salle, Nicole Fisher)
BMNH	United Kingdom, London, The Natural History Museum (David Notton)
BPBM	USA, Hawaii, Honolulu, Bernice P. Bishop Museum (Shepherd P. Myers) Calicut India, Kerala, Calicut University, Zoology Department
DEI	Germany, Müncheberg, Deutsches Entomologisches Institut im ZALF (Holger H. Dathe, Stephan Blank)
HNHM	Hungary, Budapest, Hungarian Natural History Museum (Sándor Csösz)
MNHN	France, Paris, Muséum National d'Histoire Naturelle (Claire Villemant)
MSNG	(Collezione Gribodo) Italy, Genova, Museo Civico di Storia Naturale "Giacomo Doria" (Fabio Penati)
MZB	Indonesia, Bogor, Museum Zoologicum Bogoriense (Yayuk R. Suhardjono)
OUMNH	(=Wilson Saunders collection) United Kingdom, Oxford, University Museum of Natural History (James Hogan)
QM	Australia, Queensland, South Brisbane, Queensland Museum
RMNH	Netherlands, Leiden, Nationaal Natuurhistorische Museum ("Naturalis") (Cornelius van Achterberg)
SEHU	Japan, Sapporo, Hokkaido University Museum, Systematic entomology (Masahiro Ohara)
SFS	Shōichi F. Sakagami's collection (see SEHU)
USNM	USA, Washington D.C., National Museum of Natural History, (formerly, United States National Museum) (David Furth, Brian Harris)
ZMHB	Germany, Berlin, Museum für Naturkunde der Humboldt-Universität (Frank Koch)
ZRC	Singapore, National University of Singapore, Raffles Museum of Biodiversity Research, Zoological Reference Collection (Lua Hui Kheng)

Table 2. List of stingless bee species described in Indonesia based on geographical region.

Genus	Species	Sumatera	Jawa	Nusa Tenggara	Kalimantan	Sulawesi	Bali	Maluku	Papua
<i>Austroplebeia</i> Moure	<i>cincta</i> (Mocsáry in Friese)								+
<i>Geniotrigona</i> Moure	<i>lactefasciata</i> (Cameron)				+				
	<i>thoracica</i> (Smith)	+			+				
<i>Heterotrigona</i> Schwarz	<i>erythrogastra</i> (Cameron)				+				
	<i>itama</i> (Cockerell)	+	+		+				
	<i>flaviventris</i> (Friese)								+
	<i>hobbyi</i> (Schwarz)				+				
	<i>keyensis</i> (Friese)								+
	<i>lamingtonia</i> (Cockerell)								+
	<i>planifrons</i> (Smith)								+
	<i>lieftincki</i> (Sakagami and Inoue)	+							+
	<i>moorei</i> (Schwarz)	+				+			
	<i>bakeri</i> (Cockerell)					+			
	<i>paradisaea</i> (Engel & Rasmussen)								+
	<i>taraxis</i> (Engel & Rasmussen)								+
<i>Homotrigona</i> Moure	<i>tricholoma</i> (Engel & Rasmussen)								+
	<i>aliceae</i> (Cockerell)	+							
	<i>anamitica</i> (Friese)								
	<i>fimbriata</i> (Smith)	+							+
	<i>canifrons</i> (Smith)	+							+
	<i>haematoptera</i> (Cockerell)								+
	<i>apicalis</i> (Smith)	+							+
	<i>binghami</i> (Schwarz)	+							+
	<i>vidua</i> (Lepeletier)	+							+
	<i>javanica</i> (Gribodo)		+	+					
	<i>latebaltata</i> (Cameron)					+			

Table 2. Contd.

Genus	Species	Sumatera	Jawa	Nusa Tenggara	Kalimantan	Sulawesi	Bali	Maluku	Papua
<i>Lisotrigona</i> Moure	<i>nitidiventris</i> (Smith)	+	+		+				
	<i>terminata</i> (Smith)	+	+		+				
	<i>trochanterica</i> (Cockerell)	+			+				
	<i>ventralis</i> (Smith)	+			+				
	<i>cacciae</i> (Nurse)	+			+				
<i>Papuatrigona</i> Michener and Sakagami	<i>atricornis</i> (Smith)								+
	<i>pendleburyi</i> (Schwarz)	+							
<i>Pariotrigona</i> Moure	<i>atripes</i> (Smith)	+			+				
	<i>collina</i> (Smith)	+			+				
<i>Tetragonula</i> Moure	<i>fuscibasis</i> (Cockerell)	+			+				
	<i>biroi</i> (Friese)		+		+				+
	<i>chlypearis</i> (Friese)				+			+	+
	<i>drescheri</i> (Schwarz)	+	+		+				
	<i>fuscobalteata</i> (Cameron)	+			+			+	
	<i>geissleri</i> (Cockerell)	+			+				
	<i>iridipennis</i> (Smith)		+		+				
	<i>laeviceps</i> (Smith)	+	+		+		+		+
	<i>melanocephala</i> (Gribodo)				+				
	<i>melina</i> (Gribodo)	+			+				
	<i>minanghabau</i> (Sakagami and Inoue)	+							
	<i>pagdeni</i> (Schwarz)								+
<i>reepeni</i> (Friese)	+			+					
<i>sapiens</i> (Cockerell)		+						+	
<i>sarawakensis</i> (Schwarz)		+		+					
<i>testaceitarsis</i> (Cameron)	+			+					
<i>Wallacetrigona</i> Engel and Rasmussen	<i>incisa</i> (Sakagami and Inoue)				+				
Total		27	13	1	34	8	1	4	12

Annotated Catalog and Bibliography of Indonesian Meliponini Stingless Bees

AUSTROPLEBEIA Moure, 1961

Austroplebeia cincta (Mocsáry in Friese, 1898)

Trigona cincta Friese, 1898: 431: **Holotype** (HNHM, worker): examined, “Friedrich- / Wilh.-hafen”, “N. Guinea / Biró 96”; **Type locality:** PAPUA NEW GUINEA “Neu-Guinea”.

Distribution: INDONESIA (Papua); AUSTRALIA; PAPUA NEW GUINEA.

References: Friese 1898; Kahono 2018.

GENIOTRIGONA Moure, 1961

Geniotrigona lacteifasciata (Cameron, 1902)

Trigona lacteifasciata Cameron, 1902: 131: **Holotype** (BMNH 17b.1132); **Type locality** MALAYSIA “Borneo” (unknown).

Trigona borneënsis Friese, 1933a: 46. Synonymy vide Schwarz (1939): **Lectotype** (ZMHB, worker); **Type locality:** INDONESIA “Sanggau (Borneo)”.

Trigona thoracica variety *lacteifasciata* Cameron; Schwarz, 1937: 317: examination of types of *T. thoracica* Smith and *T. lacteifasciata* Cameron.

Trigona thoracica variety *borneënsis* Friese; Schwarz, 1937: 328.

Geniotrigona lacteifasciata (Cameron); Moure, 1961: 213.

Distribution: INDONESIA (Kalimantan); MALAYSIA; SINGAPORE; THAILAND.

References: Cameron 1902; Friese 1933a; Schwarz 1937; Moure 1961; Smith 2012; Zubaidah et al. 2017; Kahono et al. 2018; Kerisna et al. 2019.

Geniotrigona thoracica (Smith, 1857)

Trigona ambusta Cockerell, 1918: 387. Synonymy vide Schwarz (1939): **Holotype** (BMNH 17b.1131); **Type locality:** MALAYSIA/SINGAPORE “Sandakan and Singapore”.

Trigona thoracica Smith, 1857: 50: **Type** (BMNH 17b.1181) (taxonomy); **Type locality:** SINGAPORE “Singapore”.

Distribution: INDONESIA (Kalimantan, Sumatera); BRUNEI; CAMBODIA; MALAYSIA; MYANMAR; SINGAPORE; THAILAND.

References: Smith 1857; Dalla Torre 1896; Cockerell 1918; Schwarz 1937; Schwarz 1939; Moure 1961; Sakagami 1975; Michener 1990; Smith 2012; Jaapar et al. 2016; Kahono et al. 2018; Samsudin et al. 2018; Tuksitha et al. 2018; Ascher et al. 2019; Sanjaya et al. 2019; Priawandiputra et al. 2020; Rosli et al. 2020; Syafrizal et al. 2020; Herwina et al. 2021; Rahmad et al. 2021; Ramly et al. 2021; Purwanto et al. 2022.

HETEROTRIGONA Schwarz, 1939

Heterotrigona erythrogastra (Cameron, 1902)

Trigona erythrogastra Cameron 1902: 129-130: **Holotype** (BMNH 17b.1130); **Type locality:** MALAYSIA “Sarawak (R. Shelford)”.

Trigona luteiventris Friese 1909 (“1908”): 354, 358: **Lectotype** (ZMHB, worker); **Type locality:** MALAYSIA/PHILIPPINES “Perak (Malaka)”; Palawan” (s).

Trigona sandacana Cockerell 1919: 242-243: **Holotype** (BMNH 17b.1129); **Type locality: MALAYSIA** “Sandakan, Borneo”.
Distribution: INDONESIA (Kalimantan); BRUNEI; MALAYSIA; PHILIPPINES.
References: Cameron 1902; Friese 1909; Cockerell 1919; Smith 2012; Kahono et al. 2018; Samsudin et al. 2018; Tuksitha et al. 2018; Rosli et al. 2020; Ramly et al. 2021.

***Heterotrigona itama* (Cockerell, 1918)**

Trigona itama Cockerell 1918: 387: **Holotype** (USNM 29471, worker); **Type locality: SINGAPORE** “Singapore” (unknown).
Trigona breviceps Cockerell 1919b: 244: **Holotype** (BMNH 17b.1123, worker); **Type locality: MALAYSIA** “Sandakan, Borneo”.
Distribution: INDONESIA (Java, Sumatera, Kalimantan, Sulawesi); MALAYSIA; SINGAPORE; THAILAND.
References: Cockerell 1918; Cockerell 1919b; Smith 2012; Syafrizal et al. 2014; Jaapar et al. 2016; Basari et al. 2018; Kahono et al. 2018; Samsudin et al. 2018; Tuksitha et al. 2018; Sanjaya et al. 2019; Febrianti et al. 2020; Priawandiputra et al. 2020; Rosli et al. 2020; Syafrizal et al. 2020; Kerisna et al. 2019; Trianto & Purwanto 2020a; Trianto & Purwanto 2020b; Arung et al. 2021; Herwina et al. 2021; Purwanto & Trianto 2021; Rahmad et al. 2021; Ramly et al. 2021; Purwanto et al. 2022; Suderajat et al. 2021; Trianto & Purwanto 2022; Saputra & Nurlina 2022.

***Heterotrigona flaviventris* (Friese, 1909)**

Trigona flaviventris Friese 1909 (“1908”): 354, 356, 357-358: **Lectotype** (ZMHB, worker); **Type locality: INDONESIA (PAPUA)** “Cyclopen-Gebirge”.
Distribution: INDONESIA (Papua).
References: Friese 1909; Kahono et al. 2018; Engel 2019.

***Heterotrigona hobbyi* (Schwarz, 1937)**

Trigona hobbyi Schwarz 1937: 283, 288, 298-300*, 328: **Holotype** (BMNH 17b.1118); **Type locality: MALAYSIA** “Sarawak: Mt. Dulit, 4000 feet, moss forest”.
Distribution: INDONESIA (Kalimantan); BRUNEI; MALAYSIA.
References: Schwarz 1937; Kahono et al. 2018; Engel 2019.

***Heterotrigona keyensis* (Friese, 1901)**

Trigona keyensis Friese 1901: 271: **Lectotype** (ZMHB, worker); **Type locality: INDONESIA** “Key-Eilanden (Amboina, Nederland India) durch H. Kuhn”.
Distribution: INDONESIA (Papua).
References: Friese 1901; Kahono et al. 2018; Engel 2019.

***Heterotrigona lamingtonia* (Cockerell, 1929)**

Trigona lamingtonia Cockerell 1929: 243: **Holotype** (AMS, worker); **Type locality: PAPUA NEW GUINEA** “Mt. Lamington”.
Distribution: INDONESIA (Papua); PAPUA NEW GUINEA.
References: Cockerell 1929; Kahono et al. 2018; Engel 2019.

***Heterotrigona planifrons* (Smith, 1865)**

Trigona planifrons Smith 1865: 93-94: **Holotype** (OUMNH, worker); **Type locality: INDONESIA** “New Guinea”.
Distribution: INDONESIA (Papua); MALAYSIA.

References: [Smith 1865](#); [Kahono et al. 2018](#); [Engel 2019](#).

***Heterotrigona lieftincki* (Sakagami & Inoue, 1987)**

Trigona (Trigonella) lieftincki Sakagami & Inoue 1987: 610, 611, 613-615, 617-624: **Holotype** (RMNH, not located, nor in SEHU); Paratypes (RMNH, 3 workers, 2 males); **Type locality:** INDONESIA “N.E. Sumatra, Tongkoh, probably Mt. Talamau (Pasaman)”.

Distribution: INDONESIA (Sumatera).

References: [Sakagami & Inoue 1987](#); [Kahono et al. 2018](#); [Priawandiputra et al. 2020](#).

***Heterotrigona moorei* (Schwarz, 1937)**

Trigona moorei Schwarz 1937: 283, 292, 321-322*, 328, plate 3, 4: **Holotype** (BMNH 17b.1124); 1 paratype (AMNH); **Type locality:** MALAYSIA “Sarawak: Mt. Dulit, R. Lejok, near sweat and water”.

Trigona (Tetragona) matsumurai Sakagami 1959: 120-121: **Holotype** (SEHU, worker); 1 paratype (SEHU); **Type locality:** SINGAPORE “Singapore”.

Distribution: INDONESIA (Sumatera, Kalimantan); MALAYSIA; SINGAPORE.

References: [Schwarz 1937](#); [Sakagami 1959](#); [Herwina et al. 2021](#); [Kahono et al. 2018](#); [Priawandiputra et al. 2020](#).

***Heterotrigona bakeri* (Cockerell, 1919)**

Trigona bakeri Cockerell 1919c: 78, 79: **Holotype** (USNM 29468, worker); **Type locality:** MALAYSIA “Penang Island”.

Distribution: INDONESIA (Kalimantan); CAMBODIA; MALAYSIA.

References: [Cockerell 1919c](#); [Smith 2012](#); [Syafrizal et al. 2020](#); [Arung et al. 2021](#).

***Heterotrigona taraxis* (Engel & Rasmussen, 2017)**

Heterotrigona taraxis Engel & Rasmussen 2017: 1-25: **Holotype** (AMNH); **Type locality:** INDONESIA “Papua”.

Distribution: INDONESIA (Papua); PAPUA NEW GUINEA.

References: [Engel & Rasmussen 2017](#); [Engel 2019](#).

***Heterotrigona tricholoma* (Engel & Rasmussen, 2017)**

Heterotrigona tricholoma Engel & Rasmussen 2017: 1-25: **Holotype** (AMNH); **Type locality:** INDONESIA “Papua”.

Distribution: INDONESIA; PAPUA NEW GUINEA.

References: [Engel & Rasmussen 2017](#); [Engel 2019](#).

***Heterotrigona paradisaea* (Engel & Rasmussen, 2017)**

Heterotrigona paradisaea Engel & Rasmussen 2017: 1-25: **Holotype** (AMNH); **Type locality:** INDONESIA “Papua”.

Distribution: INDONESIA (Papua); PAPUA NEW GUINEA.

References: [Engel & Rasmussen 2017](#).

HOMOTRIGONA Moure, 1961

***Homotrigona alicae* (Cockerell, 1929)**

Trigona alicae Cockerell 1929b: 139, 140: **Holotype** (BMNH 17b.1116) (comparative note, taxonomy); **Type locality:** THAILAND “Siam: On trail in jungle between Pahtoop mountain and Nan”.

Distribution: INDONESIA (Sumatera, Kalimantan); CAMBODIA; MALAYSIA; THAILAND; VIETNAM.

References: Cockerell 1929b; Smith 2012; Awang et al. 2018; Kahono et al. 2018.

***Homotrigona anamitica* (Friese, 1909)**

Trigona anamitica Friese 1909("1908"): 358-359, fig 15-4: **Lectotype** (ZMHB, worker): here designated, "Süd-Annam / Xom-Gom / Februar / H. Fruhstorfer", "Trigona / anamitica / 1904 Friese det. / Fr."; paralectotype (ZMHB (1)); **Type locality:** VIETNAM "Xom-Gom, SüdAnnam"

Trigona melanotricha Cockerell 1918: 386, 387: **Holotype** (BMNH 17b.1095); **Type locality:** MALAYSIA "Sandakan, Borneo".

Distribution: INDONESIA (Kalimantan); MALAYSIA; VIETNAM.

References: Friese 1909; Cockerell 1918; Smith 2012; Kahono et al. 2018.

***Homotrigona fimbriata* (Smith, 1857)**

Trigona fimbriata Smith 1857: 52: **Type** (BMNH 17b.1182); **Type locality:** SINGAPORE "Singapore".

Trigona flavistigma Cameron 1902: 130: **Holotype** (BMNH 17b.1097); **Type locality:** MALAYSIA "Kuching, Sarawak".

Melipona castanea Bingham 1903: vi: **Type** (BMNH 17b.1128); **Type locality:** THAILAND "Bukit Besar, Nawngchik. 1500 to 2500 feet".

Trigona versicolor Friese 1909("1908"): 358, 359, fig. 15-1: **Lectotype** (ZMHB, worker): here designated, "Tandjong / SO.-Kalimantan / coll.Speyer", "Trigona / versicolor / 1904 Friese det. / n. Fr.", "Type" (red label); **Type locality:** MALAYSIA "Malaka (Perak); "SO-Borneo (Tandjong)".

Distribution: INDONESIA (Kalimantan; Java, Sumatera); CAMBODIA; LAOS; MALAYSIA.

References: Smith 1857; Cameron 1902; Bingham 1903; Friese 1909; Smith 2012; Kahono et al. 2018; Samsudin et al. 2018; Awang et al. 2018; Ascher et al. 2019; Priawandiputra et al. 2020; Rosli et al. 2020; Syafrizal et al. 2020; Arung et al. 2021; Herwina et al. 2021.

***Homotrigona canifrons* (Smith, 1857)**

Trigona canifrons Smith 1857: 51: **Syntype** (OUMNH, 1 worker); additional putative type (BMNH 17b.1183); **Type locality:** MALAYSIA "Borneo (Sarawak)".

Trigona busara Cockerell 1918: 387: **Holotype** (USNM 29496, worker): examined, "Singapore / Coll. Baker", "9072", Type No. / 29496 / U.S.N.M.", "Trigona / busara / Ckll TYPE"; **Type locality:** MALAYSIA "Sandakan".

Distribution: INDONESIA (Kalimantan, Sumatera); AUSTRALIA; MALAYSIA; MYANMAR; SINGAPORE; SRI LANKA; THAILAND.

References: Smith 1857; Cockerell 1918; Samsudin et al. 2018; Awang et al. 2018; Priawandiputra et al. 2020; Herwina et al. 2021; Kahono et al. 2018; Ascher et al. 2019; Purwanto et al. 2022.

***Homotrigona haematoptera* (Cockerell, 1919)**

Trigona haematoptera Cockerell 1919b: 243: **Holotype** (BMNH 17b.1126); **Type locality:** MALAYSIA "Sandakan, Borneo".

Trigona haematoptera variety *dulitae* Schwarz 1937: 282, 283, 286, 291, 320-321*, 328, plate 2, 6: **Holotype** (BMNH 17b.1125); **Paratypes**

(AMNH, BMNH (8)); **Type locality: MALAYSIA** “Sarawak: Foot of Mt. Dulit, junction of rivers Tinjar and Lejok”.

Distribution: INDONESIA (Kalimantan); **MALAYSIA**.

References: Cockerell 1919b; Schwarz 1937; Kahono et al. 2018.

***Homotrigona apicalis* (Smith, 1857)**

Trigona apicalis Smith 1857: 51: **Holotype** (OUMNH); additional putative type (BMNH 17b.1188) (taxonomy); **Type locality: MALAYSIA** “Borneo (Sarawak)”.

Trigona hemileuca Cockerell 1929b: 140: **Holotype** (BMNH 17b.1098) (comparative note, taxonomy); **Type locality: THAILAND** “Siam: Nan”.

Trigona sericea Friese 1933a: 45-46: **Lectotype** (ZMHB, worker): here designated, "Kalimantan / Sanggau / 24- 7-32", "Trigona / sericea / 1925 Friese det. / Fr."; paralectotypes (ZMHB (5), DEI (4)) (taxonomy); **Type locality: MALAYSIA/INDONESIA** “Meliau (Borneo); Sanggau (Borneo)”.

Distribution: INDONESIA (Java, Sumatera, Kalimantan); **CAMBODIA; LAOS; MALAYSIA; MYANMAR; SINGAPORE; THAILAND; VIETNAM.**

References: Smith 1857; Cockerell 1929b; Friese 1933a; Jaapar et al. 2016; Samsudin et al. 2018; Awang et al. 2018; Priawandiputra et al. 2020; Herwina et al. 2021; Kahono et al. 2018; Purwanto et al. 2022.

***Homotrigona binghami* (Schwarz, 1937)**

Trigona apicalis variety *binghami* Schwarz 1937: 288, 300, 301, 303-304*, 328, plate 2, 5, 7: **Holotype** (BMNH 17b.1142); paratypes (AMNH, BMNH, USNM); **Type locality: MYANMAR** “Tenasserim: Dawnat Range”.

Distribution: INDONESIA (Java, Kalimantan); **MALAYSIA; MYANMAR.**

References: Schwarz 1937; Samsudin et al. 2018; Awang et al. 2018; Kerisna et al. 2019; Rosli et al. 2020; Herwina et al. 2021; Kahono et al. 2018.

***Homotrigona vidua* (Lepeletier de Saint Fargeau, 1836)**

Melipona vidua Lepeletier de Saint Fargeau 1836: 429: **Syntype** (MNHN, 1 worker): putative syntype examined, "Museum Paris / Bengale / Diard & Duvaucel 1815", "vidua", "Diard et Duvaucel", "type", "TYPE", "M. Vidua / Lep. S. Farg / Bengale". I consider this a true type: Alfred Duvaucel (1793-1825) and Pierre-Médard Diard (1794-1863) arrived on their first expedition to Kolkata, India, in January 1818 and spent years collecting in the Indo-Malayan region; **Type locality: INDONESIA/E TIMOR** “Ile de Timor”.

Distribution: INDONESIA (Java, Sumatera, Kalimantan); **INDIA; MALAYSIA; MYANMAR.**

References: Lepeletier de Saint Fargeau 1836; Awang et al. 2018; Kahono et al. 2018.

***LEPIDOTRIGONA* Schwarz, 1939**

***Lepidotrigona javanica* (Gribodo, 1891)**

Trigona javanica Gribodo 1891: 109: **Holotype** (MSNG, worker); **Type locality: INDONESIA** “Giava” (=Java”).

Distribution: INDONESIA (Java).

References: [Gribodo 1891](#); [Smith 2012](#); [Kahono et al. 2018](#).

***Lepidotrigona latebalteata* (Cameron, 1902)**

Trigona latebalteata Cameron 1902: 130-131: **Syntypes** (BMNH 17b.1084, 2 workers). The *terminata* species group; **Type locality:** MALAYSIA “Kuching, Sarawak”.

Distribution: INDONESIA (Kalimantan); MALAYSIA.

References: [Cameron 1902](#); [Smith 2012](#); [Kahono et al. 2018](#).

***Lepidotrigona nitidiventris* (Smith, 1857)**

Trigona nitidiventris Smith 1857: 50-51: **Type** (OUMNH (=Wilson Saunders collection)): **Type locality:** MALAYSIA “Malacca (Mount Ophir).”

Trigona fulvopilosella Cameron 1908: 193, 194: **Syntypes** (BMNH 17b.1101, 2 workers): **Type locality:** MALAYSIA “Kuching, May and October (John Hewitt)”.

Distribution: INDONESIA (Kalimantan, Java, Sumatera); BRUNEI; MALAYSIA; PHILIPPINES; THAILAND.

References: [Smith 1857](#); [Cameron 1908](#); [Smith 2012](#); [Kahono et al. 2018](#); [Samsudin et al. 2018](#); [Priawandiputra et al. 2020](#); [Herwina et al. 2021](#).

***Lepidotrigona terminata* (Smith, 1878)**

Trigona terminata Smith 1878: 169: **Type** (BMNH 17b.1100); **Type locality:** MYANMAR no precise locality, presumably “Maulmain, Tenasserim Provinces”.

Trigona fulvomarginata Cockerell 1919c: 78: **Holotype** (BMNH 17b.1083); **Type locality:** MALAYSIA “Penang”.

Distribution: INDONESIA (Sulawesi, Kalimantan, Java); BRUNEI; CAMBODIA; LAOS; MALAYSIA; MYANMAR; THAILAND; VIETNAM.

References: [Smith 1878](#); [Cockerell 1919c](#); [Smith 2012](#); [Syafrizal et al. 2014](#); [Azlan et al. 2016](#); [Rasmussen & Cameron 2010](#); [Jaapar et al. 2016](#); [Kahono et al. 2018](#); [Samsudin et al. 2018](#); [Kerisna et al. 2019](#); [Priawandiputra et al. 2020](#); [Rosli et al. 2020](#); [Suprianto et al. 2020](#); [Syafrizal et al. 2020](#); [Trianto & Purwanto 2020a](#); [Trianto & Purwanto 2020b](#); [Wicaksono et al. 2020](#); [Herwina et al. 2021](#); [Purwanto & Trianto 2021](#); [Rahmad et al. 2021](#); [Ramly et al. 2021](#); [Sayusti et al. 2021](#); [Purwanto et al. 2022](#); [Suderajat et al. 2021](#); [Trianto & Purwanto 2022](#).

***Lepidotrigona trochanterica* (Cockerell, 1920)**

Trigona trochanterica Cockerell 1920a: 115: **Holotype** (BMNH 17b.1102); **Type locality:** MALAYSIA “Sandakan, Borneo”.

Distribution: INDONESIA (Sumatera, Kalimantan); MALAYSIA.

References: [Cockerell 1920a](#); [Smith 2012](#); [Jaapar et al. 2016](#); [Kahono et al. 2018](#); [Priawandiputra et al. 2020](#).

***Lepidotrigona ventralis* (Smith, 1857)**

Trigona ventralis Smith 1857: 50: **Type** (BMNH 17b.1186); Mt. Ophir specimen is *latebalteata*; **Type locality:** MALAYSIA “Borneo (Sarawak)”.

Distribution: INDONESIA (Sumatera, Kalimantan, Java); BRUNEI; CAMBODIA; INDIA; LAOS; VIETNAM; MALAYSIA; MYANMAR; THAILAND; VIETNAM.

References: [Smith 1857](#); [Smith 2012](#); [Kahono et al. 2018](#); [Priawandiputra et al. 2020](#); [Herwina et al. 2021](#).

LISOTRIGONA Moure, 1961

***Lisotrigona cacciae* (Nurse, 1907)**

Melipona cacciae Nurse 1907: 619: Lectotype (BMNH 17b.1103, worker);
Type locality: INDIA “Hoshangabad, Central Provinces”.

Trigona scintillans Cockerell 1920a: 116: **Holotype** (BMNH 17b.1115);
Type locality: MALAYSIA “Sandakan, Borneo”.

Distribution: INDONESIA (Sumatera, Kalimantan); CAMBODIA;
LAOS; MALAYSIA; THAILAND; VIETNAM.

References: [Nurse 1907](#); [Smith 2012](#); [Kahono et al. 2018](#); [Priawandiputra et al. 2020](#).

PAPUATRIGONA Michener and Sakagami, 1990

***Papuatrigona atricornis* (Smith, 1865)**

Trigona atricornis Smith 1865: 94: **Holotype** (OUMNH, worker):
According to Baker (1993) the specimen is labeled " 'N' [New
Guinea (Allen); white disc] and 'Trigona atricornis' 'Smith'; **Type
locality:** INDONESIA (PAPUA) “New Guinea”.

Distribution: INDONESIA (Papua).

References: [Smith 1865](#); [Friese 1909](#); [Kahono et al. 2018](#); [Engel 2019](#).

PARIOTRIGONA Moure, 1961

***Pariotrigona pendleburyi* (Schwarz, 1939)**

Trigona (Hypotrigona) pendleburyi variety *klossi* Schwarz 1939a: 85, 94,
132*: **Holotype** (BMNH, no number); **Type locality:** MALAYSIA
“MALAYA. State of Selangor: Bukit Kutu, 200 feet”.

Trigona (Hypotrigona) pendleburyi Schwarz 1939a: 85, 86, 94, 130-132*:
Holotype (BMNH, no number); paratypes (BMNH (5)); **Type
locality:** MALAYSIA “Cameron Highlands, Rhododendron Hill,
5000 feet”.

Distribution: INDONESIA (Sumatera); MALAYSIA; THAILAND.

References: [Schwarz 1939a](#); [Smith 2012](#); [Kahono et al. 2018](#); [Priawandiputra et al. 2020](#).

TETRAGONULA Moure, 1961

***Tetragonula atripes* (Smith, 1857)**

Trigona atripes Smith 1857: 50: **Type** (OUMNH (=Wilson Saunders
collection)); **Type locality:** MALAYSIA “Malacca (Mt. Ophir)”.

Distribution: INDONESIA (Sumatera, Kalimantan); MALAYSIA;
MYANMAR; SINGAPORE; THAILAND.

References: [Smith 1857](#); [Smith 2012](#); [Kahono et al. 2018](#); [Ascher et al. 2019](#); [Priawandiputra et al. 2020](#).

***Tetragonula collina* (Smith, 1857)**

Trigona collina Smith 1857: 51-52: **Type** (OUMNH (=Wilson Saunders
collection)); **Type locality:** MALAYSIA “Malacca (Mount Ophir)”.

Trigona cambodiensis Cockerell 1926a: 224: **Holotype** (USNM 29470,
worker); **Type locality:** CAMBODIA “Angkov (=Angkor) Wat,
Cambodia”.

Distribution: INDONESIA (Sumatera, Kalimantan); BRUNEI; CAMBODIA; LAOS; MALAYSIA; MYANMAR; THAILAND; VIETNAM.

References: [Smith 1857](#); [Cockerell 1926a](#); [Smith 2012](#); [Azlan et al. 2016](#); [Kahono et al. 2018](#); [Samsudin et al. 2018](#); [Kerisna et al. 2019](#); [Priawandiputra et al. 2020](#); [Herwina et al. 2021](#).

***Tetragonula fuscibasis* (Cockerell, 1920)**

Trigona fuscibasis Cockerell 1920a: 115-116: **Holotype** (BMNH 17b.1082); **Type locality:** MALAYSIA "Sandakan, Borneo".

Distribution: INDONESIA (Sumatera, Kalimantan); BRUNEI; MALAYSIA.

References: [Cockerell 1920a](#); [Smith 2012](#); [Kustiawan et al. 2014](#); [Syafri-
zal et al. 2014](#); [Kahono et al. 2018](#); [Samsudin et al. 2018](#); [Priawandi-
putra et al. 2020](#).

***Tetragonula biroi* (Friese, 1898)**

Trigona birói Friese 1898: 428, 429: **Syntypes** (ZMHB, 2 workers): examined, "N. Guinea / Biró 96", "Friedrich- / Wilh.-hafen", "Trigona / biroi / det. Friese 1897" (1 worker); "Philippinen / Schadenberg", "Trigona / biroi / det. Friese 1897 / n.sp.", "Coll. / Friese" (1 worker); **Type locality:** PHILIPPINES "Philippinen (Schadenburg)".

Distribution: INDONESIA (Sulawesi, Papua, Moluccas, Kalimantan, Java, Sumatera); CAMBODIA; PAPUA NEW GUINEA; PHILIPPINES.

References: [Friese 1898](#); [Smith 2012](#); [Suriawanto et al. 2017](#); [Kahono et al. 2018](#); [Hasan et al. 2020](#); [Syafri-
zal et al. 2020](#); [Trianto & Purwan-
to 2020a](#); [Trianto & Purwanto 2020b](#); [Octaviani et al. 2020](#); [Her-
wina et al. 2021](#); [Purwanto & Trianto 2021](#); [Salatnaya et al. 2021](#); [Purwanto et al. 2022](#); [Trianto & Purwanto 2022](#).

***Tetragonula clypearis* (Friese, 1909)**

Trigona laeviceps variety clypearis Friese 1909("1908"): 356, 358, fig. 15-3: Unknown; **paralectotype** (ZMHB (1)): **Type locality:** INDONESIA (PAPUA) "Manikion".

Trigona wybenica Cockerell 1929d: 300: **Holotype** (USNM 54960, worker): examined; paratypes (BMNH (1), QM (3), ZMHB (1)) (common name (wyben), nest, taxonomy); **Type locality:** AUSTRALIA "Thursday island".

Distribution: INDONESIA (Papua, Sulawesi); AUSTRALIA; PHILIPPINES.

References: [Friese 1909](#); [Cockerell 1929c](#); [Smith 2012](#); [Kahono et al. 2018](#); [Salatnaya et al. 2021](#); [Sayusti et al. 2021](#).

***Tetragonula drescheri* (Schwarz, 1939)**

Trigona (Tetragona) sarawakensis variety drescheri Schwarz 1939a: 85, 93, 106-107*: **Holotype** (AMNH); paratype (AMNH (1)) (distribution, key to species, taxonomy); **Type locality:** INDONESIA "M. Java. South Banjoemas, Koebangkangkoeng".

Distribution: INDONESIA (Kalimantan, Java, Sumatera); BRUNEI; MALAYSIA.

References: [Schwarz 1939a](#); [Smith 2012](#); [Syafri-
zal et al. 2014](#); [Kahono et al. 2018](#); [Priawandiputra et al. 2020](#); [Purwanto & Trianto 2021](#); [Purwanto et al. 2022](#).

***Tetragonula fuscobalteata* (Cameron, 1908)**

Trigona atomella Cockerell 1919b: 243-244: **Holotype** (USNM 29467, worker): examined, "Island of / Penang / Baker", "Type No. / 29467 / U.S.N.M.", "Trigona / atomella / Ckll TYPE"); 2 paratypes (USNM); **Type locality:** MALAYSIA "Island of Penang".

Trigona erythrostoma Cameron 1908: 193-194: **Syntypes** (BMNH 17b.1113, 2 workers); **Type locality:** MALAYSIA "Kuching, Borneo".

Trigona fuscobalteata Cameron 1908: 193, 194: **Lectotype** (BMNH 17b.1112): Designated Moure 1961 (key to species, taxonomy); **Type locality:** MALAYSIA "Medang, Sarawak (Hewitt)".

Trigona pallidistigma Cameron 1908: 193, 195: **Syntypes** (BMNH 17b.1133, 2[?] workers); **Type locality:** MALAYSIA "Sarawak, Borneo".

Trigona pfeifferi Friese 1925: 41: **Lectotype** (AMNH, worker): here designated, "Brasil / Campinas", "Trigona / pfeifferi / Friese det. 25 / Fr.", "Typus" (orange label), "Heterotrigona / cf. fuscobalteata / (erroneous locality) / det. J.S.Ascher"; paralectotypes (DEI (3)); **Type locality:** UNCERTAIN "Campinas (Sao Paulo), S.-Brasil".

Trigona pygmaea Friese 1933b: 147: **Lectotype** (ZMHB, worker): here designated "O-Sumatra / Mandau / 7.1933", "Trigona / pygmaea / Fr. / 1933 Friese det. / n."; paralectotype (DEI (1), ZMHB (1)) (common name (kloeloet itam ketjid)); **Type locality:** INDONESIA "Beringin, in der Waldern oberhalb Mandau (Sumatra), v. Bengkalis".

Distribution: INDONESIA (Sulawesi, Kalimantan, Sumatera); AUSTRALIA; BRUNEI; CAMBODIA; MALAYSIA; PALAU ISLANDS; PHILIPPINES; THAILAND; UNCERTAIN.

References: Cockerell 1919b; Cameron 1908; Friese 1925; Friese 1933b; Rasmussen & Cameron 2010; Smith 2012; Suriawanto et al. 2017; Kahono et al. 2018; Samsudin et al. 2018; Kerisna et al. 2019; Syafrizal et al. 2020; Anaktototy et al. 2021; Arung et al. 2021; Herwina et al. 2021; Sayusti et al. 2021; Purwanto et al. 2022.

***Tetragonula geissleri* (Cockerell, 1918)**

Trigona geissleri Cockerell 1918: 385-386, 387: **Unknown:** Cockerell used a Friese manuscript name for his description (key to species, distribution, manuscript name of Friese, taxonomy, variation); **Type locality:** MALAYSIA "Sintang, North Borneo".

Trigona confusella Cockerell 1919b: 242: **Holotype** (USNM 40248) (taxonomy, previously identified as *T. geissleri* (in Cockerell 1918)); **Type locality:** SINGAPORE "Singapore".

Distribution: INDONESIA (Kalimantan, Sumatera); BRUNEI; LAOS; MALAYSIA; SINGAPORE; THAILAND.

References: Cockerell 1918; Cockerell 1919b; Smith 2012; Kahono et al. 2018; Samsudin et al. 2018; Herwina et al. 2021.

***Tetragonula iridipennis* (Smith, 1854)**

Trigona iridipennis Smith 1854: 413-414: **Holotype** (BMNH 17b.1114, worker): examined, "Type" (orange border), "iridipennis / Type Sm.", "B.M.TYPE / HYM. / 17B.1114", "Trigona / iridipennis / TYPE. Smith.", "Ceylon" (reverse side "53 / 23"). Citations for *iridipennis* are included in a broad sense, as species limits for this taxon is uncertain. To the same group belongs also *T. bengalensis*, *T. praeterita*, and *T. ruficornis*, as well as several undescribed species

(see Rasmussen & Cameron (2007)) (taxonomy); **Type locality:** SRI LANKA “Ceylon”.

Distribution: INDONESIA (Kalimantan, Java); CAMBODIA; INDIA; MYANMAR; PHILIPPINES; SRI LANKA; SRI LANKA; THAILAND.

References: Smith 1854; Smith 2012; Trianto & Purwanto 2020a; Trianto & Purwanto 2020b; Syafrizal et al. 2020; Trianto & Purwanto 2022.

***Tetragonula laeviceps* (Smith, 1857)**

Trigona laeviceps Smith 1857: 51: **Holotype** (OUMNH); **Type locality:** SINGAPORE “Singapore”.

Distribution: INDONESIA (Bali, Kalimantan, Sumatera, Java, Papua); AUSTRALIA; BRUNEI; CAMBODIA; INDIA; LAOS; MALAYSIA; MYANMAR; SINGAPORE; PAPUA NEW GUINEA; PHILIPPINES; SRI LANKA; THAILAND; VIETNAM.

References: Smith 1857; Thummajitsakul et al. 2008; Smith 2012; Syafrizal et al. 2014; Hasan et al. 2020; Jaapar et al. 2016; Putra et al. 2016; Suriawanto et al. 2017; Kahono et al. 2018; Kerisna et al. 2019; Sanjaya et al. 2019; Samsudin et al. 2018; Efin et al. 2019; Febrianti et al. 2020; Priawandiputra et al. 2020; Syafrizal et al. 2020; Trianto & Purwanto 2020a; Trianto & Purwanto 2020b; Arung et al. 2021; Atmowidi et al. 2021; Herwina et al. 2021; Purwanto & Trianto 2021; Rahmad et al. 2021; Suderajat et al. 2021; Purwanto et al. 2022; Trianto & Purwanto 2022.

***Tetragonula melanocephala* (Gribodo, 1893)**

Trigona melanocephala Gribodo 1893: 264: **Holotype** (MSNG, worker): The authentic holotype of this taxon is labeled “Bandjarmas” (? =Bandjarmasin, near Liangtelan) (F. Penati, pers. com.); **Type locality:** MALAYSIA “Liangtelan (Borneo)”.

Trigona testaceinerva Cameron 1908: 193, 195: **Type** (BMNH 17b.1109) (key to species, taxonomy); **Type locality:** MALAYSIA “Kuching, Borneo”.

Distribution: INDONESIA (Kalimantan); BRUNEI; MALAYSIA.

References: Gribodo 1893; Cameron 1908; Smith 2012; Zubaidah et al. 2017; Kahono et al. 2018; Purwanto et al. 2022.

***Tetragonula melina* (Gribodo, 1893)**

Trigona melina Gribodo 1893: 262-263, 264: **Syntypes** (MSNG, 3 workers; unknown depository, 2 workers): Two syntypes are labeled “Bandjarmas” (?=Bandjarmasin, near Liangtelan), while the third syntype carry no locality label (F. Penati, pers. com.); **Type locality:** MALAYSIA “Liangtelan (Borneo)”.

Distribution: INDONESIA (Sumatera, Kalimantan); BRUNEI; MALAYSIA; THAILAND.

References: Gribodo 1893; Smith 2012; Syafrizal et al. 2014; Priawandiputra et al. 2020; Jaapar et al. 2016.

***Tetragonula minangkabau* (Sakagami & Inoue, 1985)**

Trigona (Tetragonula) minangkabau Sakagami & Inoue 1985: 175, 176, 177, 178, 179, 180, 181, 184-186*, 187-188: **Holotype** (MZB, Hymn.0198, worker); paratypes (MZB (Hymn.0195-0197)); **Type locality:** INDONESIA “Lubuk Mintrun nr. Padang, Sumatera Barat”.

Distribution: INDONESIA (Sumatera); MALAYSIA. *Trigona* (*Tetragona*) *fuscobalteata* variety *pagdeni* Schwarz, 1939, by original designation.

References: Sakagami & Inoue 1985; Smith 2012; Kahono et al. 2018; Samsudin et al. 2018; Priawandiputra et al. 2020; Herwina et al. 2021.

***Tetragonula pagdeni* (Schwarz, 1939)**

Trigona (*Tetragona*) *fuscobalteata* variety *pagdeni* Schwarz 1939a: 85, 93, 96, 110-111*, 113: **Holotype** (USNM 53564, male): examined, "Nakon / SriTamarat / Siam 7/5/28", "HughSmith / coll", Type No. / 53564 / U.S.N.M.", "Holotype", "Trigona / fusco-balteata / var. pagdeni / H.F. Schwarz"; paratype (AMNH (1)); **Type locality:** THAILAND "SIAM.-Nakon Sri Tamarat".

Distribution: INDONESIA (Sulawesi); CAMBODIA; MALAYSIA; THAILAND.

References: Schwarz 1939a; Thummajitsakul et al. 2008; Rasmussen & Cameron 2010; Smith 2012.

***Tetragonula reepeni* (Friese, 1918)**

Trigona reepeni Friese 1918: 519-520: **Lectotype** (ZMHB, worker): here designated, "Malacca / Taip. Hills/ 2.1912 / Butt.-Reep.", "Trigona / reepeni / 1914 Friese det. / Fr.", "Type" (red label), "Coll. / Friese"; para- lectotypes (DEI (1), USNM (1), ZMHB (7)); **Type locality:** MALAYSIA "Taiping Hills (Upp. Perak) auf Malakka".

Trigona (*Tetragonula*) *latigenalis* Sakagami 1978: 166-194, 194-195*, 196, 227, 236, 237, 238, 247, plate 5: **Holotype** (SEHU); **Type locality:** MALAYSIA "Frasers Hill-b, Malaya".

Distribution: INDONESIA (Sumatera); MALAYSIA; THAILAND.

References: Friese 1918; Sakagami 1978; Smith 2012; Kahono et al. 2018; Priawandiputra et al. 2020; Syafrizal et al. 2020; Herwina et al. 2021.

***Tetragonula sapiens* (Cockerell, 1911)**

Trigona sapiens Cockerell 1911: 176: **Holotype** (ANIC, worker); **Type locality:** SOLOMON ISLANDS "Solomon Islands".

Distribution: INDONESIA (Sulawesi, Maluku, Papua, Java); AUSTRALIA; PHILIPPINES; SOLOMON ISLANDS.

References: Cockerell 1911; Wallace et al. 2008; Smith 2012; Suriawanto et al. 2017; Kahono et al. 2018; Salatnaya et al. 2021; Djakaria et al. 2020; Suhri et al. 2020; Trianto & Purwanto 2020a; Trianto & Purwanto 2020b; Anaktototy et al. 2021; Sayusti et al. 2021; Trianto & Purwanto 2022.

***Tetragonula sarawakensis* (Schwarz, 1937)**

Trigona sarawakensis Schwarz 1937: 283, 290, 313-315*, 316, 328, plate 2, 4: **Holotype** (BMNH 17b.1110); paratypes (AMNH, BMNH?); **Type locality:** MALAYSIA "Sarawak: Mt. Dulit, 4000 ft."

Distribution: INDONESIA (Kalimantan, Java); MALAYSIA; SINGAPORE; THAILAND.

References: Schwarz 1937; Smith 2012; Kahono et al. 2018; Syafrizal et al. 2020b; Trianto & Purwanto 2020a; Trianto & Purwanto 2020b; Arung et al. 2021; Sari et al. 2021; Purwanto & Trianto 2021; Trianto & Purwanto 2022.

***Tetragonula testaceitarsis* (Cameron, 1901)**

Trigona testaceitarsis Cameron 1901: 36: **Type** (BMNH 17b.1121); **Type locality: MALAYSIA** “Patani, Malay Peninsula”.

Distribution: INDONESIA (Kalimantan, Sumatera); MALAYSIA.

References: Cameron 1901; Syafrizal et al. 2020; Arung et al. 2021; Herwina et al. 2021; Sari et al. 2021.

WALLACETRIGONA Engel and Rasmussen, 2017

***Wallacetrigona incisa* (Sakagami & Inoue, 1989)**

Trigona incisa Sakagami & Inoue 1989: 605-610*, 614, 615, 617, 618, 619:

Holotype (RMNH); paratypes (RMNH, 6 workers; MBBJ, 1 worker; SFS, remaining); **Type locality: INDONESIA** “Modoinding Minahasa, N. Celebes, vi. 26-27, 1941, native collector, ded. F. Dupont” (3 workers, holotype, paratypes); “Todyamboe, 900m, C. Celebes” (3 workers); “Wuasa, Kab. Poso, Sulteng, Sulawesi” (9 workers); “Lorei Lindu Nat. Park, C. Sulawesi”.

Distribution: INDONESIA (Sulawesi, Kalimantan).

References: Sakagami & Inoue 1989; Smith 2012; Kustiawan et al. 2014; Syafrizal et al. 2014; Azlan et al. 2016; Saleng et al. 2016; Hasan et al. 2020; Kustiawan et al. 2021; Rasmussen et al. 2017; Kahono et al. 2018; Djakaria et al. 2020; Octaviani et al. 2020; Sayusti et al. 2021.

DISCUSSION

Indonesia has the highest diversity of stingless bee species in Asia (Kahono et al. 2018), but more thorough research on these insects are needed, particularly in terms of the adoption of sustainable meliponiculture systems. The literature has been updated up to mid-2022. References are cited within these records, with a total of 109 papers. Most biological data pertaining to Meliponini are listed in the nearly complete stingless bee bibliography by Rasmussen (2008). This publication provides updated data regarding the annotated catalog and bibliography of the Indonesian Meliponini stingless bees (Hymenoptera, Apidae, Apinae, Meliponini). First, our study showed 52 recorded stingless bee species across the Indonesian archipelagos. This information adds to the data on the number of stingless bees from a previous publication by Kahono et al. (2018) which recorded 46 species and Rasmussen (2008) which recorded 49 species of stingless bees in Indonesia. Second, this catalog provides up-to-date data regarding the distribution of Indonesian stingless bees. For example, Sulawesi Island is inhabited by three species of stingless bees (Kahono et al. 2018), but by mid-2022 eight stingless bee species had been recorded on the island. Third, there is the addition of data on new species of Indonesian stingless bee that have never been reported in the catalog Rasmussen (2008), namely *Heterotrigona paradisaea* (Engel & Rasmussen), *H. taraxis* (Engel & Rasmussen), and *H. tricholoma* (Engel & Rasmussen). Fourth, in addition to presenting data on the distribution of the Indonesian stingless bees, this catalog provides the type of specimen holding institutions, which would be of value to the reader.

AUTHOR CONTRIBUTION

M.T., searched the literatures and wrote the manuscript, T.A., H.P., and R.U. supervised the processes.

ACKNOWLEDGEMENTS

The first author was supported by LPDP (Indonesia Endowment Fund

for Education) for Doctoral Scholarship [KEP-308/LPDP/LPDP.3/2022].

CONFLICT OF INTEREST

The authors state that they do not have any conflicts of interest. However, the authors are responsible for the article's content and writing.

REFERENCES

- Anaktototy et al., 2021. Morfologi dan variasi morfometrik stingless bees di Kepulauan Maluku, Indonesia. *Jurnal Entomologi Indonesia*, 18(1), pp.10-22. doi: 10.5994/jei.18.1.10.
- Arung et al., 2021. Cytotoxicity effect of honey, bee pollen, and propolis from even stingless bees in some cancer cell lines. *Saudi Journal of Biological Science*, 28(12), pp.1-8. doi: 10.1016/j.sjbs.2021.08.017.
- Ascher et al., 2019. Bees of the Bukit Timah nature reserve and vicinity. *Gard. Bull. Singapore*, 71(Suppl 1), pp.245-271. doi: 10.26492/GBS71(SUPPL.1).2019-09.
- Atmowidi et al., 2021. Stingless Bees Pollination Increases Fruit Formation of Strawberry (*Fragaria x annanassa* Duch) and Melon (*Cucumis melo* L.). *Tropical Life Sciences Research*, 33(1), pp.43. doi: 10.21315/tlsr2022.33.1.3.
- Awang et al., 2018. Total flavonoids and phenolic contents of sticky and hard propolis from 10 species of Indo-Malayan stingless bees. *Malaysia Journal of Analytical Science*, 22(5), pp. 877-884. doi: 10.17576/mjas-2018-2205-15.
- Azlan et al., 2016. The successfull of affectiveness in the movement of *Trigona* spp. Colonies on the artificial nests at the prohibition forest of indigenous village of rumbio kampar regency. *Jom Faperta UR*, 3, pp.1-7.
- Basari et al., 2018. Food reward and distance influence the foraging pattern of stingless bee, *Heterotrigona itama*. *Insects*, 9(4), pp.1-10. doi: 10.3390/insects9040138.
- Bingham, C.T., 1903. Diagnoses of aceuleate Hymenoptera. In *Fasciculi Malayenses, Anthropological and Zoological Results of an Expedition to Perak and the Siamese Malay States, 1901-1902*. Zoology Vol. I (appendix). London: University Press of Liverpool.
- Camargo, J.M.F. & Pedro, S.R.M., 1992. Systematics, phylogeny and biogeography of the Meliponinae (Hymenoptera, Apidae): a mini-review. *Apidologie*, 23, pp.509-522. doi: 10.1051/apido:19920603.
- Camargo, J.M.F. & Pedro, S.R.M., 2003. *Sobre as relações filogenéticas de Trichotrigona Camargo & Moure (Hymenoptera, Apidae, Meliponini)*. In *Apoidea neotropica: Homenagem aos 90 anos de Jesus Santiago Moure*. Criciúma: Editora UNESC, pp.109-122.
- Camargo, J.M.F. & Pedro, S.R.M., 2007. Meliponini. In *Catalogue of bees (Hymenoptera, Apoidea) in the Neotropical region*. Curitiba (Paraná): Sociedade Brasileira de Entomologia, pp.272-578.
- Camargo, J.M.F., 2013. Historical biogeography of the Meliponini (Hymenoptera, Apidae, Apinae) of the Neotropical region. In *Pot-honey: a legacy of stingless bees*. Springer New York, pp.19-34.
- Cameron, P., 1901. On the Hymenoptera collected during the "Skeat Expedition" to the Malay Peninsula, 1899-1900. *Proceedings of the Zoological Society of London*, pp.16-44.

- Cameron, P., 1902. On the Hymenoptera collected by Mr. Robert Shelford at Sarawak, and on the Hymenoptera of the Sarawak museum. *Journal of the Straits Branch of the Royal Asiatic Society*, 37, pp.29-131.
- Cameron, P., 1908. On some bornean species of *Trigona* (Apidae). *The Entomologist*, 41, pp.192-195.
- Cockerell, T.D.A., 1911. The bees of the Solomon Islands. *Proceedings of the Linnean Society of New South Wales*, 36, pp.160-178.
- Cockerell, T.D.A., 1918. Descriptions and records of bees. —LXXX. *Annals and Magazine of Natural History*, 9(2), pp.384-390. doi: 10.1080/00222931808562381.
- Cockerell, T.D.A., 1919a. Descriptions and records of bees. —LXXXIII. *Annals and Magazine of Natural History*, 3, pp.118-125. doi: 10.1080/00222931908673805.
- Cockerell, T.D.A., 1919b. Descriptions and records of bees. —LXXXV. *Annals and Magazine of Natural History*, 3, pp.240-250. doi: 10.1080/00222931908673818.
- Cockerell, T.D.A., 1919c. The social bees of the Philippine Islands. *Philippine Journal of Science*, 14, pp.77-81. https://digitalcommons.usu.edu/bee_lab_co/609.
- Cockerell, T.D.A., 1920. Descriptions and records of bees. —LXXXVIII. *Annals and Magazine of Natural History*, 5, pp.113-119. doi: 10.1080/00222932008632346.
- Cockerell, T.D.A., 1926a. Descriptions and records of bees. —CXII. *Annals and Magazine of Natural History*, 18, 216-227. doi: 10.1080/00222932608633504.
- Cockerell, T.D.A., 1929a. Bees from the Australian region. *American Museum Novitates*, 346, pp.1-18. https://digitalcommons.usu.edu/bee_lab_co/761.
- Cockerell, T.D.A., 1929b. Descriptions and records of bees. —CXVII. *Annals and Magazine of Natural History*, 4, pp.132-141. https://digitalcommons.usu.edu/bee_lab_co/767.
- Cockerell, T.D.A., 1929c. Bees in the Queensland Museum. *Memoirs of the Queensland Museum*, 9, pp. 298-323. https://digitalcommons.usu.edu/bee_lab_co/648
- Dalla Torre, K.W.V., 1896. *Catalogus hymenopterorum hucusque descriptorum systematicus et synonymicus*. Vol. 10, Apidae (Anthophila). G. Engelmann, Leipzig, pp.643. doi: 10.5962/bhl.title.10348.
- Djakaria et al., 2020. Antioxidant and antibacterial activity of selected Indonesian honey against bacteria of acne. *Jurnal Kimia Sains dan Aplikasi*, 23(8), pp.267-275. doi: 10.14710/jksa.23.8.267-275.
- Eardley, C.D., 2004. Taxonomic revision of the African stingless bees (Apoidea: Apidae: Apinae: Meliponini). *African Plant Protection*, 10, pp.63-96. doi: 10.10520/EJC87785.
- Efin et al., 2019. Morphological characteristics & morphometric of stingless bee (Apidae: Hymenoptera) from Banten Province, Indonesia. *Biodiversitas*, 20(6), pp.1693-1698. doi: 10.13057/biodiv/d200627.
- Engel et al., 2019. A key to the genera and subgenera of stingless bees in Indonesia (Hymenoptera: Apidae). *Treubia*, 45, pp.65-84.
- Engel, M.S. & Rasmussen, C., 2017. A new subgenus of Heterotrigona from New Guinea (Hymenoptera: Apidae). *Journal of Melittology*, 73, pp.1-6. doi: 10.17161/jom.v0i73.6673.
- Engel, M.S., 2001. A monograph of the Baltic amber bees and evolution of the Apoidea (Hymenoptera). *Bulletin of the American Museum of Natural History*, 259, pp.1-192. <http://hdl.handle.net/2246/1437>.

- Febrianti et al., 2020. Bentuk pintu masuk sarang *Trigona* spp. di kawasan hutan mangrove surya perdana mandiri kelurahan setapak besar singkawang utara. *Jurnal Hutan Lestari*, 8(3), pp.620-627.
- Friese, H., 1898. Die Trigona-Arten Australiens. *Természetráji Füzetek*, 21(1), pp.427-431.
- Friese, H., 1901. Neue Arten der Bienengattung Trigona Jur. (Hym.). Zeitschrift für systematische Hymenopterologie und *Dipterologie*, 1, pp.265-271. <https://biostor.org/reference/145407>.
- Friese, H., 1909. Die Bienenfauna von Neu-Guinea. *Annales Historico-Naturales Musei Nationalis Hungarici*. Budapest: Természettudományi Múzeum évkönyve.
- Friese, H., 1918. Wissenschaftliche Ergebnisse einer Forschungsreise nach Ostindien, ausgeführt im Auftrage der Kgl. Preuß. Akademie der Wissenschaften zu Berlin von H. v. Buttel-Reepen. VII. Bienen aus Sumatra, Java, Malakka und Ceylon. Gesammelt von Herrn Prof. Dr. v. Buttel-Reepen in den Jahren 1911-1912. *Zoologische Jahrbücher, Abteilung für Systematik, Geographie und Biologie der Tiere*, 41, pp.489-520.
- Friese, H., 1925. Neue neotropischen Bienenarten, zugleich II. Nachtrag zur Bienenfauna von Costa Rica (Hym.). *Stettiner Entomologische Zeitung*, 86, pp. 1-41.
- Friese, H., 1933a. Neue Trigona-Arten von Borneo (Hym.). *Naturhistorisch Maandblad*, 22, pp.45-46.
- Friese, H., 1933b. Eine neue Trigona von Sumatra (Hymenoptera, Apidae). *Naturhistorisch Maandblad*, 22, pp.147
- Gribodo, G. 1893. Note imenotterologiche. Nota II. Nuovi generi e nuove specie di imenotteri antofili ed osservazioni sopra alcune specie già conosciute. *Bollettino della Società Entomologica Italiana, Genova*, 25, pp.248-287.
- Gribodo, G., 1891. Contribuzioni imenotterologiche sopra alcune specie nuove o poco conosciute di imenotteri antofili (Generi Ctenoplectra, Xylocopa, Centris, Trigona e Bombus). *Bollettino della Società Entomologica Italiana, Genova*, 23, pp.102-119.
- Grüter, C., 2020. *Stingless Bees*, Cham, Switzerland: Springer International Publishing. doi: 10.1007/978-3-030-60090-7.
- Hasan et al., 2020. Gambaran Umum *Trigona* spp. di Kabupaten Luwu Utara Provinsi Sulawesi Selatan. *Jurnal Matematika, Sains, dan Pembelajarannya*, 6(2), pp.121-124. doi: 10.31605/saintifik.v6i2.267.
- Heard, T.A., 1999a. The role of stingless bees in crop pollination. *Annual Review of Entomology*, 44, pp.183-206. doi: 10.1146/annurev.ento.44.1.183.
- Herwina et al., 2021. West Sumatran Stingless Bees (Hymenoptera: Apidae: Meliponini): What can be told from its Local Distribution. *Conf. Series: Earth and Environmental Science*, 754(1), pp.012084. doi: 10.1088/1755-1315/757/1/012084.
- Jaapar et al., 2016. The diversity and abundance of stingless bee (Hymenoptera: Meliponini) in Peninsular Malaysia. *Advances in Environmental Biology*, 10(9), pp.1-8.
- Kahono, et al., 2018. Social bees and the current status of beekeeping in Indonesia. In *Asian Beekeeping in the 21st Century*. Springer Verlag. doi: 10.1007/978-981-10-8222-1_13.
- Kerisna et al., 2019. Identification of *Trigona* spp. bee on Utilization Zone of Village Forest Menua Sadap Village, Embaloh Hulu District, Kapuas Hulu Regency. *Jurnal Tengkarwang*, 9, pp.82-91. doi: 10.26418/jt.v9i2.36184.

- Kustiawan et al., 2014. In vitro cytotoxicity of Indonesian stingless bee products against human cancer cell lines. *Asian Pasific Journal of Tropical Biomedicine*, 4(7), pp.549-556. doi: 10.12980/apjtb.4.2014apjtb-2013-0039.
- Kustiawan et al., 2017. Protective Effects of Indonesian Propolis Against Light Induced Retinal Damage. *International Journal of Toxicological and Pharmacological Research*, 9, pp.163-170. doi: 10.25258/ijtpr.v9i02.9054.
- Lepeletier de Saint Fargeau, A.L.M., 1836. Histoire naturelle des insectes. Hyménoptères. In. *Vol. 1, Librairie encyclopédique de Roret*. Paris. pp. 1-547. doi: 10.5962/bhl.title.9005.
- Michener, C.D., 1974. The social behavior of the bees. Cambridge, MA: Harvard University Press, xii+404.
- Michener, C.D., 1990. Classification of the Apidae (Hymenoptera). Appendix: *Trigona genalis* Friese, a hitherto unplaced New Guinea species. *University of Kansas Science Bulletin*, 54, pp.75-163.
- Michener, C.D., 2000. *The bees of the world*, Baltimore: Johns Hopkins University Press, xiv+[1]+913.
- Michener, C.D., 2007. *Lisotrigona* in Thailand, and the male of the genus (Hymenoptera: Apidae: Meliponini). *Journal of the Kansas Entomological Society*, 80, pp.130-135. <https://www.jstor.org/stable/25086370>.
- Michener, C.D., 2013. The Meliponini. In *Pot-honey: a legacy of stingless bees*. New York: Springer, pp.3-17. doi: 10.1007/978-1-4614-4960-7.
- Moure, J.S., 1961. A preliminary supra-specific classification of the old world meliponine bees (Hymenoptera, Apoidea). *Studia Entomologica*, 4, pp.181-242.
- Nurse, C.G., 1907. A new species of Indian wax-producing bee. *Journal of the Bombay Natural History Society*, 17(3), pp.619.
- Octaviani et al., 2020. Quality test comparison for Wallacetrigona incise and Tetragonula biroii honey in Mappedeceng District, North Luwu Regency, South Sulawesi Province. *Advances in Environmental Biology*, 14(10), pp.1-8. doi: 10.22587/aeb.2020.14.10.1.
- Priawandiputra et al., 2020. Lebah tanpa sengat (stingless bee) di Desa Perbatasan Hutan (Sumatera Selatan; 1st ed.). *ZSL Indonesia*, pp. 1-82.
- Purwanto et al., 2022. Stingless bees from meliponiculture in South Kalimantan, Indonesia. *Biodiversitas*, 23(3), pp.1254-1266. doi: 10.13057/biodiv/d230309.
- Purwanto, H. & Trianto, M., 2021. Species description, morphometric measurement and molecular identification of stingless bees (Hymenoptera: Apidae: meliponini) in meliponiculture industry in West Java Province, Indonesia. *Serangga*, 26(1), pp.13-33.
- Putra et al., 2016. Jenis Lebah *Trigona* (Apidae: Meliponinae) Pada Ketinggian Tempat Berbeda di Bali. *Jurnal Simbiosis*, 4(1), pp.6-9.
- Rahmad et al., 2021. Jenis Lebah Madu Dan Tanaman Sumber Pakan Pada Budi Daya Lebah Madu Di Hutan Produksi Subanjeriji, Kabupaten Muara Enim, Sumatera Selatan. *Jurnal Penelitian Kehutanan Faloak*, 5(1), pp.47-61. doi: 10.20886/jpkf.2021.5.1.47-61.
- Ramly et al., 2021. Physicochemical properties and mineral elements in honey from various species of Malaysian stingless bee. *Bioscience Research*, 18, pp.34-44. doi: 10.1016/j.jfca.2018.06.002.

- Rasmussen et al., 2017. A new genus of eastern hemisphere stingless bees (Hymenoptera: Apidae), with a key to the supraspecific groups of Indomalayan and Australasian Meliponini. *American Museum Novitates*, 2017(3888), pp.1-33. doi: 10.1206/3888.1.
- Rasmussen, C., & Camargo, J.M.F., 2008. A molecular phylogeny and the evolution of nest architecture and behavior in *Trigona* s.s. (Hymenoptera: Apidae: Meliponini). *Apidologie*, 39, pp.102–118. doi: 10.1051/apido:2007051.
- Rasmussen, C., & Cameron SA., 2007. A molecular phylogeny of the Old World stingless bees (Hymenoptera: Apidae: Meliponini) and the non-monophyly of the large genus *Trigona*. *Systematic Entomology*, 32, pp.26–39. doi: 10.1111/j.1095-8312.2009.01341.x.
- Rasmussen, C., & Cameron, S.A., 2010. Global stingless bee phylogeny supports ancient divergence, vicariance, and long distance dispersal. *Biol. J. Linn. Soc.*, 99, pp.206–232. doi: 10.1111/j.1095-8312.2009.01341.x.
- Rasmussen, C., 2008. *Molecular phylogeny of stingless bees: Insights into divergence times, biogeography, and nest architecture evolution (Hymenoptera: Apidae: Meliponini)*, University of Illinois at UrbanaChampaign,
- Rosli et al., 2020. Stingless Bee Honey: Evaluating Its Antibacterial Activity and Bacterial Diversity. *Insects*, 11(8), pp.500. doi: 10.3390/Insects11080500.
- Roubik, D.W., 2006. Stingless bee nesting biology. *Apidologie*, 37, pp.124–143. doi: 10.1051/apido:2006026.
- Sakagami, S.F. & Inoue, T., 1985. Taxonomic notes on three bicolorous *Tetragonula* stingless bees in Southeast Asia. *Kontyû*, 53, pp.174–189.
- Sakagami, S.F. & Inoue, T., 1987. Stingless bees of the genus *Trigona* (subgenus *Trigonella*) with notes on the reduction of spatha in male genitalia of the subgenus *Tetragonula* (Hymenoptera, Apidae). *Kontyû*, 55, pp.610–627. <http://dl.ndl.go.jp/info:ndljp/pid/10653539>.
- Sakagami, S.F. & Inoue, T., 1989. Stingless bees of the genus *Trigona* (subgen. *Geniotrigona*) (Hymenoptera, Apidae), with description of *T. (G.) incisa* sp.nov. from Sulawesi. *Japanese Journal of Entomology*, 57, pp.605–620. <http://dl.ndl.go.jp/info:ndljp/pid/10653869>.
- Sakagami, S.F., 1959. Stingless bees collected by Prof. S. Matsumura from Singapore (Hymenoptera, Apidae). *Insecta Matsumurana*, 22, pp.119–121. <http://hdl.handle.net/2115/9646>.
- Sakagami, S.F., 1975. Stingless bees (excl. *Tetragonula*) from the continental Southeast Asia in the collection of Bernice P. Bishop museum, Honolulu (Hymenoptera, Apidae). *Journal of the Faculty of Science, Hokkaido University, Series VI, Zoology*, 20, pp.49–76. <http://hdl.handle.net/2115/27593>.
- Sakagami, S.F., 1978. *Tetragonula* stingless bees of the continental Asia and Sri Lanka (Hymenoptera, Apidae). *Journal of the Faculty of Science Hokkaido University Series VI Zoology*, 21, pp.165–247.
- Sakagami, S.F., 1982. Stingless bees. In *Social insects*, Vol. 3. New York: Academic Press, pp.361–423. doi: 10.1051/apido:2006026.
- Salatnaya et al., 2021. Diversity, nest preferences, and forage plants of stingless bees (Hymenoptera: Apidae: Meliponini) from West Halmahera, North Moluccas, Indonesia. *Jurnal Ilmu Ternak dan Veteriner*, 26, pp.167–178. doi: 10.14334/jitv.v26i4.2896.

- Saleng et al., 2016. Uji Aktivitas Antibakteri Ekstrak Propolis Lebah *Trigona incisa* Terhadap Bakteri klebsiella *Pneumonia* dan *Staphylococcus aureus*. *Bioprospek*, 11, pp.42-48. doi: 10.30872/bp.v11i1.126.
- Samsudin et al., 2018. Taxonomic study on selected species of stingless bee (Hymenoptera: Apidae: Meliponini) in Peninsular Malaysia. *Serangga*, 23, pp.203-258. doi:
- Sanjaya et al., 2019. Study of The Habitat and Food Sources Kelulut Bees in the Area of Gunung Nyiut Nature Reserve at Pisak Village Bengkayang District. *Jurnal Hutan Lestari*, 7, pp.786-798. doi: 10.26418/jhl.v7i2.34072.
- Saputra, S.H. & Nurlina, S., 2022. Chemical Components, Pollen and Bioactivity of Stingless Honey Bee Kelulut (*Heterotrigona itama*) Meliponiculture from Samarinda East Kalimantan. *Conf. Series: Earth and Environmental Science*, pp.985. doi: 10.1088/1755-1315/985/1/012004.
- Sari et al., 2021. Aktivitas Antioksidan dan Antibakteri dari Ekstrak Bee Pollen Lebah Kelulut (*Tetragonula sarawakensis*). *Jurnal Riset Industri Hasil Hutan*, 13, pp.123-132. doi: 10.24111/jrihh.v13i2.7050.
- Sayusti et al., 2021. Stingless bees (Hymenoptera: Apidae) in South and West Sulawesi, Indonesia: Morphology, nest structure, and molecular characteristics. *Journal Apicultural Research*, 60(1), pp.143-156. doi: 10.1080/00218839.2020.1816272.
- Schwarz, H.F., 1937. Results of the Oxford University Sarawak (Kalimantan) expedition: Bornean stingless bees of the genus *Trigona*. *Bulletin of the American Museum of Natural History*, 73, pp.281-328.
- Schwarz, H.F., 1939. The Indo-Malayan species of *Trigona*. *Bulletin of the American Museum of Natural History*, 76, pp.83-141.
- Smith, D.R., 2012. Key to workers of Indo-Malayan stingless bees. In: Smith DR (eds). For use in the stingless bees. *Proceeding of the 11th International Conference of the Asian Apiculture Association Malaysia*.
- Smith, F., 1854. Catalogue of the Hymenopterous Insects in the Collection of the British Museum. Part II, Apidæ. *British Museum (Natural History) London*, pp. 197. doi: 10.5962/bhl.title.20858.
- Smith, F., 1857. Catalogue of the hymenopterous insects collected at Sarawak, Kalimantan; Mount Ophir, Malacca; and at Singapore, by A. R. Wallace. *Journal of the Proceedings of the Linnean Society Zoology*, 2, pp.42-88. doi: 10.1111/j.1096-3642.1857.tb01759.x.
- Smith, F., 1865. Descriptions of new species of Hymenopterous insects from the Islands of Sumatra, Sula, Gilolo, Salwatty, and New Guinea, collected by Mr. A.R. Wallace. *Journal of the Proceedings of the Linnean society Zoology*, 8, pp.61-94. doi: 10.1111/j.1096-3642.1865.tb02422.x.
- Smith, F., 1878. List of Hymenoptera obtained by Mr. Ossian Limborg east of Maulmain, Tenasserim provinces, during the months december 1876, january, march and april 1877, with descriptions of new species. *Journal of the Asiatic Society of Bengal (Physical Science)*, 47, pp.167-169. doi: 10.1111/j.1469-7998.1878.tb08027.x.
- Suderajat et al., 2021. The type of *Trigona* bee (Apidae: Meliponini) in three different habitat in South Sumatera. *Jurnal Biologi Tropis*, 21, pp.206-212. doi: 10.29303/jbt.v21i1.2461.
- Suhri et al., 2020. Pollen Collected by Stingless Bee *Tetragonula sapiens* Cockerell (Apidae: Meliponini) in Organic Farm Land. *The 6th International Conference on Biological Science ICBS*, pp.1-6. doi: 10.1063/5.0016393.

- Suprianto et al., 2020. Karakter morfologi dan analisis daerah conserved gen elongation factor 1a (EF1a) pada *Lepidotrigona terminata*. *Metamorfosa Journal of Biological Science*, 7, pp.30-39. doi: 10.24843/metamorfosa.2020.v07.i02.p05.
- Suriawanto et al., 2017. Nesting Sites Characteristics of Stingless Bees (Hymenoptera: Apidae) in Central Sulawesi, Indonesia. *Journal of Insect Biodiversity*, 5(10), pp.1-9. doi: 10.12976/jib/2017.5.10.
- Syafrizal et al., 2020. Diversity and honey properties of stingless bees from meliponiculture in East and North Kalimantan, Indonesia. *Biodiversitas*, 21(10), pp.4623-4630. doi: 10.13057/biodiv/d211021.
- Syafrizal, et al., 2014. Keragaman dan habitat lebah Trigona pada hutan sekunder tropis basah di Hutan Pendidikan Lempake, Samarinda, Kalimantan Timur. *Jurnal Teknologi Pertanian*, 9(1), pp.34-38.
- Thummajitsakul et al., 2008. Genetic diversity and population structure of Trigona pagdeni Schwarz in Thailand. *Apidologie*, 39(4), pp.446-455. doi: 10.1051/apido:2008026.
- Trianto M, Purwanto H. 2020a. Morphological characteristics and morphometrics of stingless bees (Hymenoptera: Meliponini) in Yogyakarta, Indonesia. *Biodiversitas*, 21(6), pp.2619-2628. doi: 10.13057/biodiv/d210633.
- Trianto, M. & Purwanto, H., 2020b. Molecular Phylogeny of Stingless Bees in the Special Region of Yogyakarta Revealed Using Partial 16S rRNA Mitochondrial Gene. *Buletin Peternakan*, 44(4), pp.186-93. doi: 10.21059/buletinpeternak.v44i4.55539.
- Trianto, M. & Purwanto, H., 2022. Diversity, abundance, and distribution patterns of stingless bees (Hymenoptera: Meliponini) in Yogyakarta, Indonesia. *Biodiversitas Journal of Biological Diversity*, 23(2), pp. 695-702. doi: 10.13057/biodiv/d230214.
- Tuksitha et al., 2018. Antioxidant and Antibacterial of Stingless Bees Honey from Kalimantan (Sarawak). *Journal of Asia Pasific Entomology*, 21(2), pp.563-570. doi: 10.13057/nusbiosci/n130213.
- Wallace et al., 2008. Standard yet unusual mechanisms of long-distance dispersal: seed dispersal of *Corymbia torelliana* by bees. *Diversity and Distributions*, 14(1), pp.87-94. doi: 10.1111/j.1472-4642.2007.00427.x.
- Wicaksono et al., 2020. Flight Activities and Pollen Load of *Lepidotrigona terminata* Smith (Apidae: Meliponinae). *HAYATI Journal of Biosciences*, 27, pp.97-106. doi: 10.4308/hjb.27.2.97.
- Wille, A., 1979. A comparative study of the pollen press and nearby structures in the bees of the family Apidae. *Revista de Biología Tropical*, 27, pp.217-222.
- Wille, A., 1983. Biology of the stingless bees. *Annual Review of Entomology*, 28, pp.41-64. doi: 10.1146/annurev.en.28.010183.000353.
- Wu, Y., 2000. [Original title in Chinese=Hymenoptera Melittidae Apidae]. In: *Fauna Sinica, Insecta*, 20, pp.1-442.
- Zubaidah et al., 2017. Ultrastructural comparison of three stingless bees species of Borneo. *Malaysian Journal of Microscopy*, 13, pp.8-16.